# MECHANISMS OF INJURY IN EXPERIMENTAL GLOMERULONEPHRITIS

Phoebe Elizabeth Halley Sharp

Imperial College London

Department of Medicine

Doctor of Philosophy

# Abstract

Proliferative glomerulonephritis (GN), seen in patients with Goodpasture's disease or systemic lupus erythematosus (SLE), is characterised by glomerular infiltration of macrophages and T cells as well as proliferation of intrinsic renal cells. Significant insights into the pathogenesis of GN have been obtained through the use of experimental rodent models, such as nephrotoxic nephritis (NTN). In this thesis I have investigated the role of two important immunological molecules in NTN: Fas ligand (FasL) and Fc gamma receptor IIB (FcγRIIB).

FasL is a well-known inducer of apoptosis in cells expressing its receptor Fas; however FasL also mediates non-apoptotic pro-inflammatory responses. FasL is widely expressed throughout the hematopoietic system but is also expressed within healthy and diseased kidney. I describe a novel role for FasL in the promotion of NTN independent from antibody and T cell responses. This pathological effect correlates with enhanced glomerular inflammation and appears to be dependent on FasL expression on both circulating leukocytes and intrinsic renal cells. Additionally, I have shown FasL-defective mesangial cells have impaired signalling through the IL-1R with a reduction in MCP-1 production.

FcγRIIB is the sole inhibitory Fc receptor for IgG and is involved in the negative regulation of B cells and cellular activation. FcγRIIB is widely expressed throughout the hematopoietic system but is also expressed on mesangial cells within the kidney. FcγRIIB deficiency greatly exacerbates NTN. Here I use cell-specific deletion to demonstrate the critical importance of FcγRIIB expressed on myeloid cells rather than B cells in the protection from NTN. Further to this, I highlight a role for FcγRIIB on intrinsic renal cells, possibly mesangial cells, in the protection from NTN. Overall, these data widen our knowledge on the pathogenesis of GN and open up possibilities for finding future novel treatments.

# Table of Contents

# Index of Figures

# Index of Tables

# Acknowledgements

I would like to start by thanking my supervisors, Dr. Ruth Tarzi, Professor Terry Cook and Professor Charles Pusey, for giving me the opportunity to do this Ph.D and for their guidance throughout the process, and Arthritis Research UK for the funding that allowed me to do the project. I would also like to thank Professor Sjef Verbeek and the members of his laboratory for their assistance during my trips to Leiden and my new supervisor, Professor Bill Cushley, for his support, advice and patience during the last year.

Big love to all members of the Renal laboratory, past and present, you were all amazing to work with and I had so much fun during the course of my Ph.D. An extra special mention must go to my laboratory family, Anisha, Anjli, Gurjeet, Ruth P., Sally, and Steve; who all looked after me and helped me with my consumption of unhealthy amounts of coffee, porridge and sweets. A massive thank you to the members of 310, Hazel, Phil and Jon; as well as all my other friends up in Glasgow. You have all been awesome. Thank you to Catherine; despite being on the other side of the world you have always been there for me.

Finally, I would like to thank my family, especially my Mum and Dad, for their endless love and support. I realise this has been just as hard for you as it has for me. Your belief in me has kept me going when I wanted to give up.

## Declaration of Originality

I hereby declare that the work presented in this thesis is my own, except where otherwise cited or acknowledged. No part of this thesis has been presented for any other degree.

## Copyright Declaration

# Published Material

Phoebe E.H. Sharp, Javier Martin-Ramirez, Sara M. Mangsbo, Peter Boross, Charles D. Pusey, H. Terrence Cook, J. Sjef Verbeek, and Ruth M. Tarzi. (2012) 'FcγRIIb on myeloid cells and intrinsic renal cells rather than B cells protects from nephrotoxic nephritis.' The Journal of Immunology.

Phoebe E.H. Sharp, Javier Martin-Ramirez, Sara M. Mangsbo, Peter Boross, John Reynolds, Jill Moss, Charles D. Pusey, H. Terence Cook, Ruth M. Tarzi, and J. Sjef Verbeek. (2012). 'Increased incidence of anti-GBM disease in Fc gamma receptor 2b deficient mice, but not mice with conditional deletion of Fcgr2b on either B cells or macrophages alone.' Molecular Immunology.

Ruth M. Tarzi, Phoebe E.H. Sharp, John P. McDaid, Liliane Fossati-Jimack, Paul E. Herbert, Charles D. Pusey, H. Terrence Cook, and Anthony N. Warrens. (2012). 'Mice with defective Fas ligand are protected from crescentic glomerulonephritis.' Kidney International.

# Abbreviations

| | |
|---|---|
| AAV | Anti-neutrophil cytoplasmic antibody-associated vascultitis |
| ABC | Avidin-biotin complex |
| ADCC | Antibody-dependent cell-mediated cytotoxicity |
| AECA | Anti-endothelial cell antibodies |
| AFU | Arbitrary fluorescence units |
| AICD | Activation-induced cell death |
| ALPS | Autoimmune lymphoproliferative syndrome |
| ANCA | Anti-neutrophil cytoplasmic antibody |
| APC | Antigen-presenting cell |
| AU | Arbitrary units |
| BcR | B cell receptor |
| BMDM | Bone marrow-derived macrophage |
| BMT | Bone marrow transplant |
| BN | Brown Norway |
| BP | Base pair |
| BSA | Bovine serum albumin |
| C | Complement |
| CBS | Central Biomedical Services |
| CFA | Complete Freund's adjuvant |
| CIA | Collagen-induced arthritis |
| CIDP | Chronic inflammatory demyelinating polyneuropathy |
| CR | Complement receptor |
| C.P.M | Counts per minute |
| DAB | 3,3'-Diaminobenzidine |

| | |
|---|---|
| DAF | Decay-accelerating factor |
| DcR | Decoy receptor |
| DD | Death domain |
| $ddH_2O$ | Double distilled $H_2O$ |
| DED | Death effector domain |
| $dH_2O$ | Distilled $H_2O$ |
| DISC | Death-inducing signalling complex |
| DN | Double negative |
| DTH | Delayed-type hypersensitivity |
| DTR | Diphtheria toxin receptor |
| DTx | Diphtheria toxin |
| D1-like-R | Dopamine type-1-like receptor |
| EAE | Experimental autoimmune encephalomyelitis |
| EAG | Experimental autoimmune glomerulonephritis |
| EAU | Experimental autoimmune uveitis |
| EAV | Experimental autoimmune vasculitis |
| ELISA | Enzyme-linked immunosorbent assay |
| ES | Embryonic stem |
| FADD | Fas-associated protein with death domain |
| FasL | Fas ligand |
| FcγR | Fc gamma receptor |
| FcγRIIB | Fc gamma receptor IIB |
| FcεR | Fc epsilon receptor |
| FcR | Fc receptor |
| FcRγ | Fc receptor gamma-chain |
| FCS | Foetal calf serum |

| | |
|---|---|
| GBM | Glomerular basement membrane |
| GCS | Glomerular cross section |
| G-CSF | Granulocyte colony-stimulating factor |
| *Gld* | Generalised lymphoproliferative disease |
| GlDH | Glutamate dehydrogenase |
| GN | Glomerulonephritis |
| GPI | Glycosylphosphatidylinositol |
| GPVI | Glycoprotein VI |
| Gy | Gray |
| $^{3}H$ | Tritium |
| HMEC | Human dermal microvascular endothelial cells |
| HRP | Horseradish peroxidase |
| HSV-1 | Herpes simplex virus-1 |
| H&E | Hematoxylin-eosin |
| ICAM | Intracellular adhesion molecule |
| ICOS-L | Inducible co-stimulatory molecule ligand |
| IFN | Interferon |
| Ig | Immunoglobulin |
| IL | Interleukin |
| IL-1R | Interleukin-1 receptor |
| iNOS | Inducible nitrous oxide synthase |
| IRI | Ischemia reperfusion injury |
| ITAM | Immunoreceptor tyrosine-based activation motif |
| ITIM | Immunoreceptor tyrosine-based inhibition motif |
| ITS | Insulin-transferrin-selenium |
| IVIG | Intravenous immunoglobulin |

| | |
|---|---|
| KC | Keratinocyte chemoattractant |
| LEW | Lewis |
| *Lpr* | Lymphoproliferative |
| $Lpr^{cg}$ | Lymphoproliferative complementing generalised lymphoproliferative disease |
| LPS | Lipopolysaccharide |
| LUMC | Leiden University Medical Centre |
| LysM | Lysozyme M |
| MAC | Membrane attack complex |
| MCP | Monocyte chemoattractant protein |
| M-CSF | Macrophage colony-stimulating factor |
| MEF | Mouse embryo fibroblasts |
| MHC | Major histocompatibility complex |
| MIF | Macrophage migration inhibition factor |
| MIP | Macrophage inflammatory protein |
| mMCP | Mouse mast cell protease |
| MMP | Matrix metalloproteinase |
| MPO | Myeloperoxidase |
| MR | Mannose receptor |
| MS | Multiple sclerosis |
| NADH | Nicotinamide adenine dinucleotide |
| NC | Non-collagenous |
| NF-κB | Nuclear factor kappa-B |
| NO | Nitrous oxide |
| NOD | Non-obese diabetic |
| NK | Natural killer |

| | |
|---|---|
| NS | Non-significant |
| NTN | Nephrotoxic nephritis |
| NTS | Nephrotoxic serum |
| OD | Optical density |
| PAS | Periodic acid-Schiff |
| PBS | Phosphate buffered saline |
| PCR | Polymerase chain reaction |
| $PIP_3$ | Phosphoinositide (3,4,5)-triphosphate |
| PI3K | Phosphoinositide 3-kinase |
| PLP | Paraformaldehyde lysine-periodate |
| PMA | Phorbol myrisate acetate |
| PMN | Polymorphonuclear neutrophil |
| PR3 | Proteinase 3 |
| qRT-PCR | Quantitative real-time polymerase chain reaction |
| QTL | Quantitative trait loci |
| RA | Rheumatoid arthritis |
| RBC | Red blood cell |
| RM2 | Reaction mixture 2 |
| ROR | Retinoid orphan receptor |
| ROS | Reactive oxygen species |
| sFas | Soluble Fas |
| sFasL | Soluble Fas ligand |
| SHIP | SH2-containing inositol-5'-phosphatase |
| SH2 | SRC homology domain 2 |
| siRNA | Small interfering RNA |
| SLE | Systemic lupus erythematosus |

| | |
|---|---|
| TAE | Tris-acetate-EDTA |
| $T_c$ | Cytotoxic T cell |
| TcR | T cell receptor |
| TdT | Terminal deoxynucleotidyl transferase |
| TGF | Transforming growth factor |
| $T_h$ | Helper T cell |
| THD | Tumour necrosis factor homology domain |
| TLR | Toll-like receptor |
| TMB | Tetramethylbenzidine |
| TNF | Tumour necrosis factor |
| TNFR | Tumour necrosis factor receptor |
| $T_{reg}$ | Regulatory T cell |
| TUNEL | Terminal deoxynucleotidyl transferase dUTP nick-end labelling |
| UUO | Unilateral ureteral obstruction |
| VEGF | Vascular endothelial growth factor |
| VFU | Visual fluorescence units |
| WKY | Wistar Kyoto |
| WT | Wild-type |

# CHAPTER 1

# Introduction

## 1.1 Overview

The work described in this thesis is a study of the pathogenesis of glomerulonephritis using the murine model, nephrotoxic nephritis (NTN). I have focused on the role of the death ligand, Fas ligand (FasL) and the inhibitory Fc receptor, Fc gamma receptor IIB (FcγRIIB), two key molecules in the modulation of the inflammatory immune response.

This introductory chapter begins with an overview of immune-mediated glomerulonephritis in humans and the description of three commonly employed animal models, including important pathological insights previously gained from their use. Evidence for the involvement of both humoral and cell-mediated mechanisms in the pathogenesis of glomerulonephritis, gained from studies using nephrotoxic nephritis, is then reviewed. Following this I go onto describe the structure, function and expression of FasL and Fc gamma receptors (FcγR), their roles in autoimmunity and inflammation, and observations from studies, in both humans and animals, supporting roles for both in glomerulonephritis. The chapter ends with the project hypotheses and aims.

The second chapter describes methods, followed by four results chapters, each divided into introduction, aim, experimental design, results, discussion and conclusion. Chapter 3 describes experiments comparing NTN in FasL-deficient mice with wild-type (WT) controls and *in vitro* studies looking at the differences between cultured FasL-deficient and WT splenocytes following stimulation with cytokines. In Chapter 4, I discuss how bone marrow chimeras were created to examine the role of FasL on circulating leukocytes and intrinsic renal cells *in vivo* together with *in vitro* studies looking at mesangial cell expression of FasL and differences between cultured FasL-deficient and WT mesangial cells, following stimulation with cytokines. Chapter 5 includes work from a collaboration in the Netherlands, looking at the role of FcγRIIB expressed by different cell lineages in NTN, compared to WT and FcγRIIB-deficient mice. Chapter 6 carries on this work comparing results from bone marrow transplant experiments between WT mice and complete FcγRIIB knockouts and

confirming expression of FcγRIIB on mesangial cells. The final chapter, Chapter 7, is a discussion of the limitations and future directions of all the work described.

## 1.2 Immunopathogenesis of immune glomerular disease

Proliferative glomerulonephritis (GN) is characterised histologically by glomerular hypercellularity caused by infiltration of circulating leukocytes (neutrophils, monocytes and T cells) into the glomerulus as well as proliferation of intrinsic renal cells (epithelial and mesangial cells). This hypercellularity is often accompanied by glomerular thrombosis, necrosis and the formation of crescents that may eventually lead to destruction of the glomerulus and rapid loss of renal function (Figure 1.1). Clinical features of proliferative GN include haematuria, proteinuria, hypoalbuminuria, hypertension and renal failure. Certain forms of proliferative GN can resolve, either spontaneously or with treatment, but most lead to long term scarring and are a significant cause of morbidity and mortality.

GN usually occurs secondary to antibody-mediated processes, cell-mediated processes, or both. When antibody-mediated processes predominate, and the immune deposits are on the outside of the basement membrane, injury is mediated by either non-complement fixing antibodies or by the complement C5b-9 attack complex without significant infiltration of circulating leukocytes or proliferation of intrinsic renal cells. GN can be classified depending on several factors, such as the clinical presentation of disease, the morphological changes within the glomerulus, or the immune mechanism causing the damage. The immunological categorisation of GN is based on the Gell-Coombs classification for hypersensitivity reactions that requires a pre-sensitised (immune) state of the host. Immune-mediated GN falls into three categories: GN caused by antibodies to intrinsic renal antigens (Type II hypersensitivity reaction), GN caused by deposition of immune complexes (Type III hypersensitivity reaction) and pauci-immune GN (related to anti-neutrophil cytoplasmic antibodies (ANCA) or Type IV delayed-type hypersensitivity (DTH) reaction), where few or no antibodies are deposited within the kidney. The general pathogenesis of each major group, along with examples of specific diseases, will be discussed in the following sections.

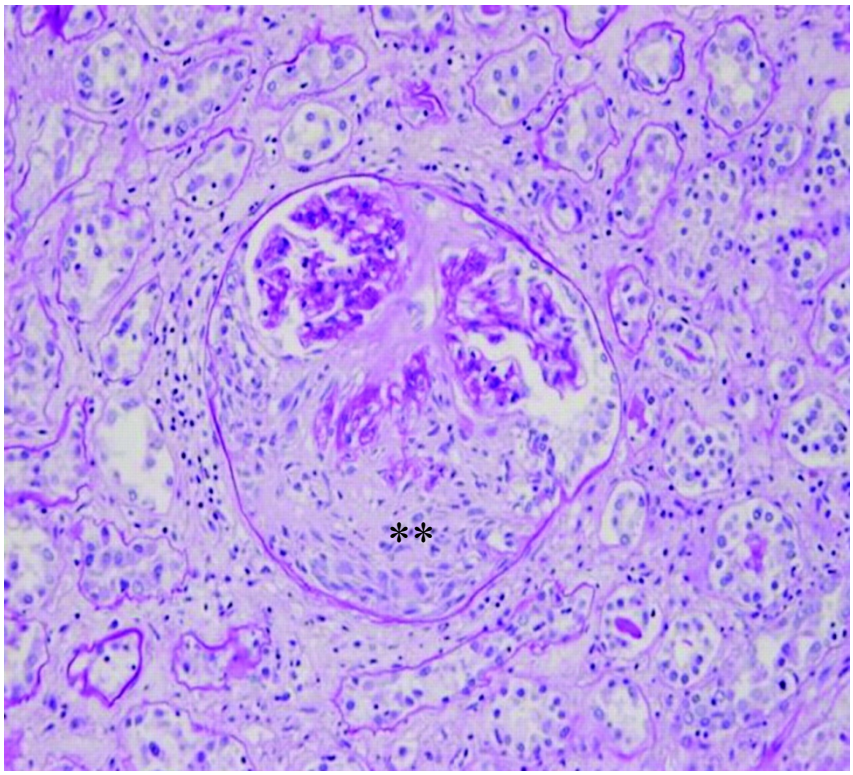


**Figure 1.1 Histopathological image of human crescentic glomerulonephritis.**

Periodic acid-Schiff (PAS) stain of a renal biopsy showing crescent formation (**) (Araki and Ogane, 2008). This image has been reproduced with the permission of the right holder, American Heart Association.

### 1.2.1 Antibodies to intrinsic renal antigens

Antibodies against endogenous antigens are referred to as autoantibodies and are generated following a loss of tolerance to self-antigens within the host. Goodpasture's, or anti-glomerular basement membrane (GBM) antibody disease, is a rare autoimmune disorder in which circulating autoantibodies are directed against the non-collagenous domain (NC1) of the $\alpha_3$ chain of type IV collagen found in the GBM of the kidney, lung, choroid plexus, retina and cochlea (Kalluri et al., 1991; Kalluri et al., 1995; Saus et al., 1988; Turner et al., 1992). The disease is characterised by rapidly progressive GN, with or without pulmonary haemorrhage. Rarely it follows a relapsing-remitting course. Immunofluorescence studies of diseased glomeruli reveal linear staining of immunoglobulin (Ig) G along the GBM.

Lerner *et al.* proved the pathogenic properties of anti-GBM antibodies using passive transfer experiments. Antibodies obtained from the kidneys of patients with Goodpasture's disease were infused into squirrel monkeys and found to induce GN (Lerner et al., 1967). As well as humoral immunity, cellular immunity has also been proven to play a role in disease pathogenesis. Auto-reactive T cells have been shown to contribute to anti-GBM disease with both $CD8^+$ and $CD4^+$ T cells, reactive to $\alpha_3$ (IV) collagen, being isolated from patients with the disease (Kalluri et al., 1997; Merkel et al., 1996; Salama et al., 2001). Regulatory $CD25^+$ T cells have been found to play a role in inhibiting the autoimmune response and may be responsible for re-establishing tolerance, perhaps explaining the single-hit nature of the disease (Salama et al., 2003).

### 1.2.2 Deposition of immune complexes

Immune complexes form when there is roughly a balance of antibodies to soluble antigens in the circulation, allowing extensive cross-linking. These soluble antigens can be either exogenous or endogenous. Exogenous antigens can include bacterial products (notably streptococcus which is the cause of post-infectious GN), hepatitis B or C viral antigens and malarial antigens. In diseases such as systemic lupus erythematosus (SLE) autoantibodies are generated against endogenous nuclear components, such as RNA, DNA and histones.

Cross-linking of antigens to antibodies causes the formation of large immune complexes. These immune complexes are difficult to clear and can deposit in vessel walls, such as those of the glomerulus, inducing an inflammatory response. The pattern of GN that

results following immune complex deposition depends upon the class of antibody involved and the location of the deposits. Immune complexes deposited in the mesangium, such as in lupus nephritis, cause mesangial proliferation, but they can also be deposited in the sub-epithelial or sub-endothelial compartments, causing basement membrane thickening or crescents, respectively. Some immune complex diseases, such as post-infectious GN, may resolve spontaneously; however many lead to renal scarring.

### 1.2.3 Pauci-immune glomerulonephritis

Pauci-immune GN differs from anti-GBM disease, lupus nephritis and post-infectious GN in that there is little or no deposition of immunoglobulin within the kidney. It is one feature of a group of rare systemic vasculitides, such as Wegener's granulomatosis, Churg-Strauss syndrome and microscopic polyangiitis, which are characterised by inflammation and necrosis of small blood vessels. In the kidney the disease is characterised by segmental necrosis of glomerular tufts, capillary rupture and bleeding into the Bowman's space, as well as accumulation and proliferation of monocytes and epithelial cells resulting in the formation of crescents (Harper and Savage, 2000).

The aetiology of these vasculitides is unknown. However, ANCA have been implicated in the pathogenesis (Falk and Jennette, 2002; Jennette et al., 1989). These antibodies are directed against components of azurophilic granules in neutrophils, in particular proteinase 3 (PR3) and myeloperoxidase (MPO), and ANCA titres have been found to correlate with human disease activity (Egner and Chapel, 1990; Jennette et al., 1989). Immunofluorescence of PR3-ANCA on normal neutrophils produces a typical cytoplasmic granular stain (c-ANCA) whereas MPO-ANCA produces a perinuclear-staining pattern (p-ANCA). The most direct *in vivo* evidence that ANCA are pathogenic in humans comes from a single case report of transplacental transfer of MPO-ANCA from a mother to a neonate, resulting in neonatal pulmonary haemorrhage and GN (Bansal and Tobin, 2004).

*In vitro* studies have shown that ANCA can activate monocytes, but not macrophages, and neutrophils primed with tumour necrosis factor (TNF)-α to express azurophilic granules on their surface. Binding of ANCA results in a respiratory burst, the release of reactive oxygen species (ROS), and secretion of pro-inflammatory cytokines (Charles et al., 1992; Falk et al., 1990). Complement has also recently been implicated as an amplifying loop in the

inflammation process. ANCA can bind either the MPO/PR3 ligands or FcγR on neutrophils resulting in activation. These neutrophils can then stimulate the complement alternative pathway, which in turn amplifies the neutrophil pro-inflammatory response (Halbwachs-Mecarelli et al., 2011). There is also a hypothesis that proposes ANCA can activate neutrophils by ligating FcγR. *In vitro* studies on human neutrophils, using specific monoclonal blocking antibodies, showed that blocking FcγRIIa prevented ANCA-induced respiratory burst, whereas blocking FcγRIIIb had no effect (Mulder et al., 1994; Porges et al., 1994). This could be due to activation-induced receptor shedding following FcγRIIIb engagement, Kocher *et al.* have shown that ANCA preferentially bind FcγRIIIb, almost 10-fold more than FcγRIIa (Kocher et al., 1998).

Cell-mediated immune responses are also involved. $CD4^+$ and $CD8^+$ T cells have been found in the kidneys of patients with pauci-immune GN (Bolton et al., 1987). PR3- and MPO-specific T cells have been identified in the peripheral blood of patients with vasculitides, and ANCA-associated vasculitis (AAV) patients have been found to have ANCA-specific memory helper T ($T_h$)-17 cells, suggesting T cells may mediate the effector stage of the immune response (Griffith et al., 1996a; Nogueira et al., 2010).

Despite the evidence suggesting a role for ANCA in pauci-immune GN, a small subgroup of patients (roughly 20%) remain persistently ANCA-negative. The pathogenesis of ANCA-negative pauci-immune GN is unknown, however neutrophils are still thought to play a central role (Chen et al., 2009). There is also some evidence to suggest that anti-endothelial cell antibodies (AECA) may be involved, although they are not always present in the sera of patients with ANCA-negative pauci-immune GN (Cong et al., 2008).

## 1.3 Experimental animal models of immune glomerular disease

Through clinical studies it has been possible to determine disease patterns in GN, as well as identify biomarkers of disease activity and injury; however it has been difficult to separate out disease effector mechanisms. In order to study the pathogenic mechanisms involved in GN, the development of animal models has been necessary. The development of gene targeting and transgenic technology in rodents in the past 20 years has facilitated investigation of the roles of individual molecules in disease, allowing a greater understanding of the cellular processes involved and the identification of possible therapeutic targets.

In the following sections, there are descriptions of three commonly used rodent models: nephrotoxic nephritis, experimental autoimmune glomerulonephritis and experimental autoimmune vasculitis. Their strengths, weaknesses and important pathological insights from their use are highlighted.

### 1.3.1 Nephrotoxic nephritis

Nephrotoxic nephritis (NTN) was one of the first experimental models used to look at immune-mediated glomerular injury and has been studied in a variety of species including rabbits, rats and mice, and in its most severe form is similar to human crescentic GN. The accelerated murine variant of this model has been used extensively in this thesis. NTN has two distinct phases, the heterologous phase and the autologous phase.

The heterologous phase refers to the glomerular injury and inflammation that results from the binding of the foreign antibody onto the GBM of the animal prior to the host adaptive immune response (Hammer and Dixon, 1963). The antibody is usually raised in rabbits or sheep immunised with GBM antigens and is called nephrotoxic serum (NTS). NTS is injected into the susceptible animal and binds to the GBM producing immediate inflammation with structural and functional damage. The model is characterised by a peak in neutrophil influx a few hours after injection and a peak in proteinuria within the first 24 hours. The model is dependent on the concentration of NTS injected. Following low doses of NTS the disease can resolve quickly, otherwise the autologous phase of the injury develops.

The autologous phase follows 5-7 days after the induction of the heterologous phase. It is characterised by the development of an immune response against the sheep or rabbit

antibodies that are deposited on the GBM with the development of autologous antibodies that become deposited in the glomerulus, and also a T cell response, leading to mixed proliferative and thrombotic injury. As the disease progresses further, it becomes difficult to differentiate between the effects of the heterologous antibody and the host immune response, but the two are considered separately as a theoretical concept.

These circulating host antibodies were thought either to represent an immune response to the heterologous antibody, deposited in the glomerular capillaries, or alternatively an immune response against glomerular antigens released following injury in the heterologous phase. Hammer and Dixon conducted a series of experiments looking at the development of the autologous phase. Firstly, they found rats tolerised at birth with the heterologous antibody did not develop the autologous phase and secondly, the autologous phase could be transferred to tolerised rats by passive transfer of rat anti-NTS antibodies. This suggests that the autologous phase is largely or entirely dependent on responses to the heterologous antibody (Hammer and Dixon, 1963).

In the accelerated model of NTN, the animals are pre-immunised against the heterologous immunoglobulin, which results in the autologous phase being initiated with the injection of NTS. This accelerated model is more reproducible and results in rapid injury. Studies using NTN have shed light on the involvement of many immune effectors in glomerulonephritis, including macrophages, T cells, complement, FcγR and intrinsic renal cells, as well as the release of pro- and anti-inflammatory cytokines. The factors effecting the development of NTN are described in detail in Section 1.4.

### 1.3.2 Experimental autoimmune glomerulonephritis

Experimental autoimmune glomerulonephritis (EAG) is a model in which GN is induced by immunisation with heterologous or homologous antigenic material from the GBM. Following immunisation, an autoimmune kidney disease develops with linear deposition of anti-GBM antibodies, similar to human anti-GBM disease. EAG was first described in the 1960's by Steblay, who immunised sheep with human collagenase-solubilised GBM in complete Freund's adjuvant (CFA) and observed a uniformly fatal crescentic GN (Steblay, 1962). This model has since been reproduced in susceptible strains of rats and mice by immunisation with preparations of bovine or rat GBM or, more recently, a

recombinant version of the rat α3 chain of type IV collagen (α3(IV)NC1) (Abbate et al., 1998).

Studies in susceptible strains of rat, such as Wistar Kyoto (WKY) and Brown Norway (BN), have provided good models of human disease and confirmed a role for both humoral and cell-mediated responses in the pathogenesis of disease. Reynolds *et al.* showed that passive transfer of eluted anti-GBM antibodies from the kidneys of WKY rats with EAG resulted in linear deposition of IgG on the GBM of both WKY and Lewis (LEW) rats. However, only the susceptible WKY strain developed crescentic GN, showing the importance of the inflammatory response to antibody deposition (Reynolds et al., 2006). A role for T cells in disease initiation has also been highlighted. Transfer of splenic $CD4^+$ T cells from EAG rats primed naïve recipients for disease (Reynolds et al., 1993) and transfer of *in vitro* activated $CD4^+$ T cells, from immunised rats, resulted in crescentic GN in the absence of IgG binding to the GBM, suggesting a direct role for T cells in glomerular injury (Wu et al., 2002).

Several mouse strains, such as SJL, DBA/1 and CD1, are susceptible to EAG but in mice the disease is less reproducible and takes longer to develop, which limits the possibility of functional susceptibility studies (Hopfer et al., 2003). However, studies of EAG in mice have confirmed a role for T cells in disease. T cell receptor-deficient mice ($TcR^{-/-}$), that do not express α/β or γ/δ TcR, do not develop disease following either immunisation with α3(IV)NC1 collagen or passive transfer of anti-α3(IV)NC1 antibodies generated in disease-susceptible mice (Kalluri et al., 1997). Dean *et al.* also demonstrated, using B cell-deficient mice (μ chain-deficient), that cell-mediated immunity is sufficient for the induction of EAG, but then went on to prove that humoral immunity alone is sufficient, as transfer of sera from EAG C57BL/6 mice to RAG-$1^{-/-}$ mice (lacking mature B and T cells) induced disease (Dean et al., 2005). Mice deficient in the inhibitory FcγRIIB are also susceptible to EAG. This supports the suggestion of a role for this receptor in maintaining immunological tolerance. FcγRIIB-deficient animals have generalised enhanced antibody responses and heightened inflammation in all antibody-mediated classes of hypersensitivity reactions (Nakamura et al., 2000).

### 1.3.3 Experimental autoimmune vasculitis

To study directly the role of ANCA in the pathogenesis of AAV, different mouse and rat models have been developed. Xiao *et al.* described one such mouse model in 2002 (Xiao et al., 2002a). Immunisation of MPO-deficient mice with mouse MPO in CFA produced an immune response against MPO. When splenocytes from these mice were transferred to RAG-$2^{-/-}$ mice, which lack mature B and T cells, or purified anti-MPO IgG was injected into RAG-$2^{-/-}$ or WT mice, the recipient mice developed severe necrotising and crescentic GN and pulmonary haemorrhage, remarkably similar to human AAV (Xiao et al., 2002a). The use of this model has highlighted a role for complement in pauci-immune GN. The development of crescentic GN, following anti-MPO antibodies, could be blocked by complement (C3) depletion (Xiao et al., 2007). Then, using the model in knockout mice lacking either C5, involved in both the classical pathway and alternative pathway, the classical pathway component C4, or the alternative pathway component factor B, it was found that $C5^{-/-}$ and factor $B^{-/-}$ mice were protected, suggesting a role for the alternative complement pathway in disease pathogenesis (Xiao et al., 2007). However, this model is not strictly autoimmune as it does not involve breaking tolerance and nor is the transfer of splenocytes a good example of pauci-immune GN because there is a moderate amount of glomerular IgG deposition.

In an alternative mouse model, $MPO^{-/-}$ mice were immunised with MPO before being irradiated and transplanted with MPO-positive bone marrow, resulting in the development of pauci-immune necrotising GN and pulmonary capillaritis, and indicating that bone marrow-derived cells are sufficient and necessary for induction of disease (Schreiber et al., 2006). Other studies using these models have also highlighted roles for TNF-α (Huugen et al., 2005), interleukin (IL)-17A (Gan et al., 2010), and primed neutrophils in pauci-immune GN (Schreiber et al., 2006; Xiao et al., 2005).

In the rat model of experimental autoimmune vasculitis (EAV), disease is induced in WKY rats by immunisation with purified human MPO in CFA. After 6 to 7 weeks, the rats developed high titres of ANCA, as well as a pauci-immune GN and lung haemorrhage (Little et al., 2005). This model has since been optimised, by using higher doses of human MPO and altering the adjuvant by addition of pertussis toxin and killed *Mycobacterium tuberculosis*, to produce a reliable, reproducible system (Little et al., 2009). Studies in this model have suggested TNF-α as a potential therapeutic target of AAV (Little et al., 2006).

As with MPO-ANCA, there are many *in vitro* observations to suggest a role for PR3-ANCA in the pathogenesis of AAV, but until recently a reliable animal model was not available. Immunisation of mice with human PR3 did not trigger an immune response and passive transfer of mouse PR3-specific polyclonal antibodies into WT mice did not induce renal or pulmonary disease (Pfister et al., 2004). However, Little *et al.* have found that by generating chimeric mice with a human immune system, human anti-PR3 autoantibodies were pathogenic and induced acute vasculitis (Little et al., 2011).

## 1.4 Pathogenesis of glomerulonephritis

### 1.4.1 Fc gamma receptors

For FcγR in GN please see Section 1.10.

### 1.4.2 Complement

The complement system comprises a number of small proteins circulating in the blood that 'complement' the ability of antibodies and phagocytic cells in clearing external pathogens. Complement components are generally synthesised by the liver as inactive pre-cursors that, following certain triggers, are cleaved by proteases to produce active proteins and start a sequential amplification cascade. Inappropriate complement activation is prevented in normal tissue by different soluble and membrane-bound inhibitors. However, unregulated activation has been implicated in various immune-mediated diseases, such as rheumatoid arthritis (RA) and multiple sclerosis (MS), and deposition of complement proteins in glomeruli is a common finding in human GN. Activation of complement mediates tissue damage via a number of mechanisms, including the generation of chemotactic anaphylatoxins, C3a and C5a, and by insertion of the membrane attack complex (MAC/C5b-9) into cells, which disrupts intracellular homeostasis leading to cell lysis and death.

Several studies have been performed to identify the importance of complement, and its different components, in the development of GN. Two initial studies looked at the roles of C3, a central component of the complement system, and C4, a member of the classical

pathway, using knockout mice. Deficiency in both C3 and C4 was found to protect mice from proteinuria and histological lesions; however Sheerin *et al.* found the degree of protection was greater in the C3-deficient animals. This suggests a pathogenic role for both the alternative and classical complement pathways in NTN (Hebert et al., 1998; Sheerin et al., 1997). Other studies have looked at proteins involved in controlling complement activation, showing how unregulated activation of complement also results in the initiation of renal damage. Decay-accelerating factor (DAF, CD55), CD59 and Factor H are inhibitory complement regulatory proteins. DAF is involved in inhibiting the activation of C3; CD59 prevents the formation of the terminal part of the complement system, C5-9b; Factor H regulates complement activation by possessing cofactor activity for the Factor I-mediated C3b cleavage, iC3b. Deficiency of DAF, CD59 or Factor H in mice exacerbated accelerated NTN with increased proteinuria and histological lesions (Pickering et al., 2002; Sogabe et al., 2001; Turnberg et al., 2003).

In contrast, complement may also play a protective role in GN. Humans and mice deficient in complement component C1q are both predisposed to developing SLE. The glomeruli of C1q-deficient mice induced with accelerated NTN developed severe thrombosis and had increased IgG deposits, infiltrating neutrophils and apoptotic cells when compared to age- and sex-matched WT control mice (Robson et al., 2001). These findings suggest a protective role for C1q in the clearance of immune complexes and apoptotic cells within the kidney.

### 1.4.3 Circulating leukocytes

#### 1.4.3.1 Neutrophils

Neutrophils are one of the first inflammatory cells to migrate to sites of inflammation where they play a critical role in driving acute inflammation by expressing and secreting cytokines, recruiting and activating other cells of the immune system, and by releasing proteolytic enzymes. During NTN, neutrophils have been shown to accumulate within the glomeruli immediately following the dose of NTS, with their influx peaking within the first few hours (Cochrane et al., 1965).

The role of neutrophils in NTN has been studied in mice using varying approaches. Schrijver *et al.* depleted mice of neutrophils by using total body irradiation and found that

after a low dose of NTS the mice were completely protected from albuminuria but when the dose was increased the albuminuria returned, although it was markedly reduced (Schrijver et al., 1990). This indicates that neutrophils play a key role in mediating albuminuria, but at higher doses of NTS other factors, such as complement, can induce disease directly. Kitching *et al.* used a different approach by inducing non-accelerated NTN in granulocyte colony-stimulating factor (G-CSF) deficient mice, which have low levels of circulating neutrophils. Following NTS injection these mice were protected from neutrophil infiltration and proteinuria (Kitching et al., 2002).

NTN has also been studied in *Beige* mice, deficient in neutrophil neutral proteinases. Compared to WT C57BL/6 mice, *Beige* mice had remarkably reduced levels of albuminuria despite a comparable influx of neutrophils following the injection of NTS (Feith et al., 1993; Schrijver et al., 1989). This led to the conclusion that neutrophil proteinases are important in mediating the glomerular damage that leads to proteinuria.

#### 1.4.3.2 T cells

The presence of T lymphocytes in human renal biopsies and their role in experimental animal models of GN has been well documented. T cells play a role in adaptive immunity by enhancing antibody production by B cells, by recruitment and activation of macrophages, and by mediating cellular cytotoxicity. Several experimental studies in animal models have demonstrated a role for T cells in GN. These have focused on the role of $CD4^+$ T cells, including their subsets $T_h1$, $T_h2$ and $T_h17$, and to a lesser extent the role of $CD8^+$ T cells. More recently, a role for regulatory T cells ($T_{reg}$) has also been explored.

##### 1.4.3.2.1 $CD4^+$ T cells

$CD4^+$ T cells are also known as helper T cells ($T_h$ cells) as they have no cytotoxic or phagocytic activity but instead activate or direct other immune cells. They are essential in determining B cell antibody class switching, activating $CD8^+$ cytotoxic T cells and maximising the activity of phagocytes such as macrophages. The prominent accumulation of $CD4^+$ T cells in crescentic GN provides evidence for a role for 'helper' T cells in driving crescentic injury.

The role of $CD4^+$ T cells in NTN was first explored using CD4-deficient mice. Compared to WT mice, $CD4^{-/-}$ mice showed only mild proliferative changes whilst crescents and proteinuria were absent (Tipping et al., 1998). To follow this up, NTN was then induced in knockout mice lacking major histocompatibility complex (MHC) Class II, which is required for antigen presentation to $CD4^+$ T cells. MHC Class $II^{-/-}$ mice were protected from developing glomerular crescents, $CD4^+$ T cell infiltration and renal injury, supporting the role of $CD4^+$ T cells in crescentic GN (Li et al., 1998).

$CD4^+$ T cells may be contributing to crescentic GN via two possible mechanisms. They may provide help to B cells to produce an autologous antibody response, or they may be causing direct damage by activating macrophages locally in the kidney – a DTH reaction. To assess whether DTH mechanisms play a role in glomerular crescent formation, T cell depletion was induced using CD4 or CD5 monoclonal antibodies, during the effector phase of NTN in rats. The humoral response was unaffected; however, there was a significant reduction in crescents, macrophage accumulation and proteinuria in the rats treated with anti-CD4 and anti-CD5 monoclonal antibodies compared to the rats treated with an isotype control (Huang et al., 1994).

The phenotype of $CD4^+$ T cells also plays an important factor in the development of NTN. There are three distinct subsets of $T_h$ cell, $T_h1$, $T_h2$ and $T_h17$, which mature from naïve T helper cells ($T_h0$) following activation by lineage-specific cytokines (Figure 1.2). As $T_h17$ cells were not identified until 2005, initial experiments only looked at the role of $T_h1$ and $T_h2$ cells. C57BL/6 mice demonstrate a predominant $T_h1$ immune response, driven by interferon (IFN)-γ and IL-12, which are important in directing a DTH response, activating macrophages and cytotoxic T cells and inducing IgG subclass switching. When induced with NTN, C57BL/6 mice develop a pronounced DTH response to the sheep IgG and severe crescentic GN with prominent T cell and macrophage infiltration (Huang et al., 1997c). In contrast, BALB/c mice are prone to a $T_h2$ response, which develops under the influence of IL-4 and IL-13 and is important in allergy, mast cell/IgE-mediated type hypersensitivity responses, and production of IgE and IgG with lower complement fixing capacity. When BALB/c mice were induced with NTN they did not develop a DTH response and had significantly less crescent formation and lymphocyte infiltration (Huang et al., 1997a). Further support that NTN is directed by a $T_h1$ response came from studies in mice deficient in the co-stimulatory molecules CD28, CD80 and CD86. Stimulation of CD80 or CD86 on antigen-presenting cells (APC) by CD28 on T cells can affect the polarisation of $CD4^+$ T cells towards a $T_h1$ or $T_h2$

profile, respectively. Mice deficient in CD28 and CD80 were completely protected from accelerated NTN, in contrast to mice deficient in CD86 that showed exacerbated glomerular injury and crescent formation (Nitta et al., 2003; Odobasic et al., 2005b).

The role of specific $T_h1/T_h2$ cytokines in the development of GN has also been explored. Mice deficient in IFN-γ, the IFN-γ receptor or IL-12 all show attenuation of renal injury compared to WT mice (Haas et al., 1995; Kitching et al., 1999a; Kitching et al., 2005), and neutralisation of IL-12 in C57BL/6 mice also attenuated crescent formation and cell-mediated injury (Kitching et al., 1999b). Conversely, mice deficient in IL-4 or IL-10 have an enhanced $T_h1$ response and develop severe crescentic GN with increased renal impairment, crescent formation and T cell and macrophage recruitment (Kitching et al., 1998; Kitching et al., 2000). By changing the balance of cytokines it is possible to alter the $T_h1/T_h2$ immune response and therefore influence the disease state. C57BL/6 mice treated with exogenous IL-4, IL-10 or a combination of both, either before or after injury was established, were protected from crescentic GN, with reduced crescent formation, proteinuria and renal impairment compared to untreated mice (Kitching et al., 1997; Tipping et al., 1997). Conversely, administration of IL-12 to BALB/c mice with GN induced a $T_h1$ response and crescent formation (Kitching et al., 1999b).

Since the identification of $T_h17$ cells in 2005 their role in NTN has been explored. $T_h17$ cells polarise in the presence of IL-6 and transforming growth factor (TGF)-β and play an important role in autoimmunity and the recruitment, activation and migration of neutrophils. Initial experiments looked at IL-23, involved in $T_h17$ cell expansion and survival, and IL-17, the main effector cytokine produced by $T_h17$ cells. One group found that both IL-23p19$^{-/-}$ and IL-17$^{-/-}$ mice were protected from nephritis compared to WT mice at day 10 (Paust et al., 2009). However, another group found that although IL-17$^{-/-}$ mice were protected from disease early on at day 6, by day 21 IL-17$^{-/-}$ and IL-23p19$^{-/-}$ mice had more severe disease than WT mice (Odobasic et al., 2011). Other experiments have looked at receptors important in the differentiation of CD4$^+$ T cells into $T_h17$ cells, such as the dopamine type 1-like receptor (D1-like-R) that is expressed on dendritic cells. Blocking this receptor with an antagonist inhibited IL-17 production and attenuated crescentic GN in mice with NTN (Okada et al., 2009). Another important receptor is retinoid orphan receptor (ROR)-γt, which is crucial for $T_h17$ effector cytokine secretion. RORγt$^{-/-}$ mice were protected from histological and functional renal injury with fewer glomerular crescents and lower albuminuria and serum urea compared to WT mice (Steinmetz et al., 2011). The discovery of

$T_h17$ cells has confounded our original understanding of the role of $T_h1$ cells in GN. In a mouse model of antigen-specific GN, $T_h1$ and $T_h17$ cells were both found to induce proliferative GN (Summers et al., 2009). Also, IL-12p35$^{-/-}$ mice developed less severe crescentic GN than WT mice and had a decreased $T_h1$ response but an increased $T_h17$ response (Odobasic et al., 2011).

Together these studies highlight roles for both $T_h1$ and $T_h17$ cells in crescentic GN. IFN-γ and IL-17A both contribute to early glomerular injury; however later on during the course of disease IL-17A attenuates crescentic GN by suppressing the $T_h1$ response, providing evidence that $T_h1$ and $T_h17$ cells counter-regulate each other (Odobasic et al., 2011).

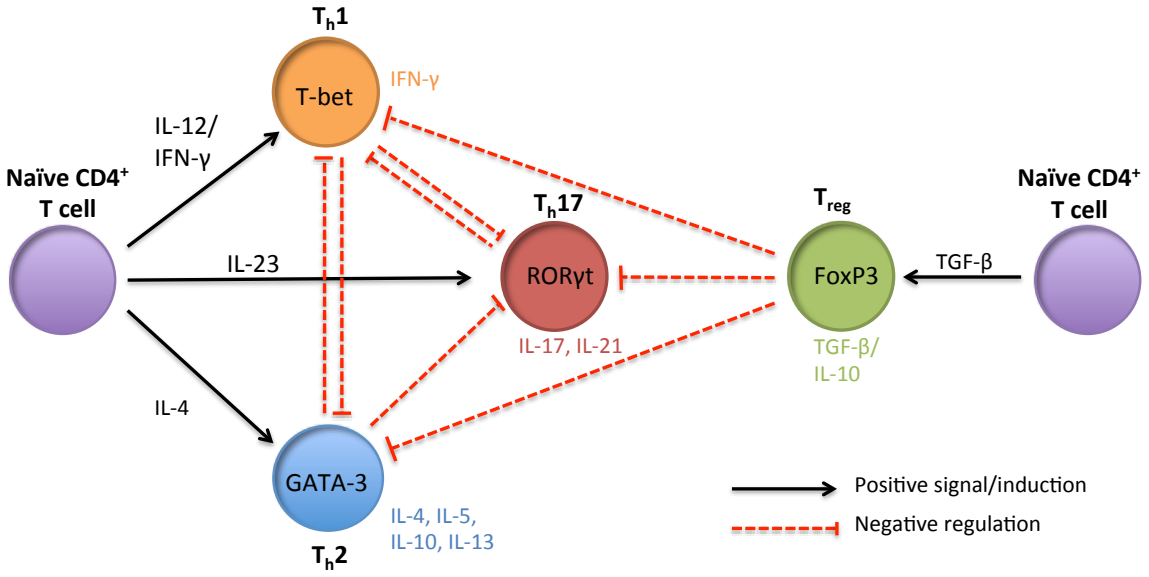


**Figure 1.2 The T helper cell subsets, $T_h1$, $T_h2$, $T_h17$ and $T_{reg}$.**

Following activation by antigen presenting cells, naïve $CD4^+$ T cells differentiate into $T_h1$, $T_h2$, $T_h17$ or $T_{reg}$ cells depending on the cytokine milieu. In the presence of IL-12 and IFN-γ $T_h$ cells differentiate into $T_h1$ cells, in the presence of IL-4 they differentiate into $T_h2$ cells, in the presence of IL-23 (following stimulation with IL-6 and TGF-β) they differentiate into $T_h17$ cells, and in the presence of TGF-β they differentiate into $T_{reg}$ cells. The phenotypes of $T_h1$ and $T_h2$ cells are stable; however there is considerable plasticity within $T_h17$ cells, which can convert to dual cytokine producing phenotypes under the right conditions (not shown in diagram). Each $T_h$ cell subset secrets a unique milieu of cytokines that work to regulate other cells of the immune system.

#### 1.4.3.2.2 $CD8^+$ T cells

The presence of $CD8^+$ T cells in glomeruli during GN has been demonstrated in both human biopsies and experimental animal models. $CD8^+$ T cells are also known as cytotoxic T cells ($T_c$) due to their ability to induce the death of infected, damaged or dysfunctional cells. $T_c$ express TcR that recognise specific antigenic peptides presented by Class I MHC molecules, present on the surface of all nucleated cells, as well as the CD8 glycoprotein. $CD8^+$ T cells are recognised as being cytotoxic once they become activated following antigen presentation.

The role of $CD8^+$ T cells in GN has been explored in both rats and mice with contrasting results being seen. Administration of an anti-CD8 antibody in the WKY rat models of EAG and NTN prevented the development of proteinuria and influx of macrophages (Huang et al., 1997b; Reynolds et al., 2002). However, CD8-deficient mice with NTN developed an accelerated, severe crescentic GN (Tipping et al., 1998), and TAP-1 knockout mice (TAP delivers peptides for presentation by Class I MHC molecules) with NTN developed similar GN to normal littermate controls (Li et al., 2000).

#### 1.4.3.2.3 Regulatory T cells

Regulatory T cells ($T_{reg}$) are a specialised subset of T cell that suppress the immune response of other cells, maintaining immune system homeostasis and tolerance to self-antigens. Naturally occurring $T_{reg}$ are made in the thymus and constitutively express CD4, CD25 and FoxP3. $CD4^+CD25^+$ T cells comprise around 5-10% of the peripheral $CD4^+$ T cell subpopulation in humans and mice. They exert their function by inhibiting the overactivation of dendritic cells and $T_h$ cells through the production of cytokines, such as IL-10 and TGF-β, and via MHC-class-II-mediated suppression of dendritic cell maturation. They can also stimulate macrophages and dendritic cells to produce indoleamine 2,3-dioxygenase, an enzyme that breaks down tryptophan through kynurenine pathway, which has an anti-proliferative effect on T cells.

Impairment of $T_{reg}$ function has been found to contribute to several autoimmune diseases, including GN, and the role of $T_{reg}$ in the mouse model of NTN has been explored. Transfer of $1x10^6$ $CD4^+CD25^+$ $T_{reg}$, purified from naïve mice, one day before administration of NTS, was found to dramatically decrease proteinuria, cell infiltration and glomerular damage compared to the transfer of $CD4^+CD25^-$ T cells, providing evidence for therapeutic

potential to control the onset and course of NTN. Tracking green fluorescent protein-transgenic $T_{reg}$ revealed a predominant migration towards secondary lymphoid organs, with an increase of $T_{reg}$ in the lymph nodes, which was regulated by the chemokine receptor CCR7 (Eller et al., 2010; Wolf et al., 2005). Paust *et al.* used DEREG mice, which express the diphtheria toxin (DTx) receptor under the control of the FoxP3 promoter, to selectively and efficiently deplete $T_{reg}$ by injection of DTx prior to induction of NTN. $T_{reg}$ depletion aggravated the course of NTN, increased systemic and renal IFN-γ, and increased recruitment of $T_h1$ cells into the kidney, without an effect on $T_h17$ cells, suggesting that $T_{reg}$ are important in controlling the $T_h1$ immune response during NTN (Paust et al., 2011).

#### 1.4.3.3 B cells

B lymphocytes are an essential component of the adaptive immune system where they play a central role in the humoral immune response. The principal functions of B cells are to produce antibodies against antigens, to act as APC, and to eventually develop into memory B cells. The development of the autologous phase of NTN is characterised by the presence of circulating host antibodies against the rabbit or sheep antigen deposited on the GBM, indicating a clear role for B cells in disease.

Li *et al.* investigated the role of B cells in NTN using mice with deletion of the μ immunoglobulin heavy chain (μ-chain deficient mice). Homozygous μ-chain deficient mice fail to develop mature B cells or produce immunoglobulin; however they have intact cell-mediated immunity. Following induction of NTN, both homozygous and heterozygous mice developed proliferative GN, with homozygous mice developing essentially the same degree of injury as heterozygous mice, despite the absence of circulating and deposited mouse antibody. The immunopathological features seen in the homozygous mice are similar to those seen in pauci-immune crescentic human GN. This study demonstrates that GN can develop independently of an antibody response as a result of DTH (Li et al., 1997).

#### 1.4.3.4 Macrophages

Accumulation of macrophages within the glomerulus and interstitium is a prominent feature of experimental models of GN, including autologous NTN (Nikolic-Paterson and Atkins, 2001). Macrophages are a heterogeneous population of cells predominantly

associated with phagocytosis. However, they exhibit a wide array of responses depending on their activation state. *In vitro* studies have identified four activation states of macrophages: the classical pathway, the alternative pathway, the type II pathway, and activation by apoptotic cells. Classically-activated macrophages are activated by two stimuli; IFN-γ and a microbial trigger e.g. lipopolysaccharide (LPS), and are involved in microbial killing and adaptive immunity. Classically-activated macrophages are found at sites of immune-mediated GN, especially during the initiation of immune responses (Erwig et al., 2000). Alternatively-activated macrophages are less well defined and develop after exposure to IL-4 and IL-13, produced by $T_h2$ cells. They are associated with resolution of inflammation by restricting self-damage and promoting repair. More recently the type II pathway has been proposed (Anderson and Mosser, 2002). Ligation of FcγR on activated macrophages in conjunction with an inflammatory stimulus, e.g. LPS, results in a macrophage with similar activity to the alternatively-activated macrophage; however they do not induce arginase production and preserve their ability to produce pro-inflammatory cytokines, e.g. TNF-α and IL-1 (Gerber and Mosser, 2001). Macrophages are also activated by apoptotic cells. Apoptotic cells express cell surface markers that allow recognition and phagocytosis by macrophages, to prevent the release of potentially toxic contents into the surrounding tissue. Phagocytosis of apoptotic cells has been well documented *in vivo* in experimental as well as clinical disease states. Macrophages involved in the removal of apoptotic cells develop an anti-inflammatory phenotype involved in controlling immunological responses (Wilson et al., 2004). However, it must be noted that these activation pathways have been defined through *in vitro* studies and are therefore unlikely to be as clear-cut *in vivo.*

A number of different strategies have been employed to address the role of macrophages in contributing to renal injury in animal models of GN. A few studies have looked at depleting circulating macrophages. One approach was the use of microencapsulated clodronate, which is taken up preferentially by macrophages, and is an effective method to deplete their numbers. Used in rats with accelerated NTN, it was found that it reduced glomerular macrophage influx and proteinuria, whilst there was no effect on glomerular T cell infiltration (Huang et al., 1997b). Another approach was the administration of anti-macrophage serum. Rabbits treated with anti-rabbit macrophage serum had reduced circulating monocytes and were protected from macrophage accumulation within the glomeruli and proteinuria (Holdsworth et al., 1981). Duffield *et al.* used transgenic mice modified to express the human diphtheria toxin receptor (DTR) under the control of the

CD11b promoter, CD11b-DTR. Injection of DTx through day 15 to 20 of crescentic GN allowed selective, specific ablation of renal inflammatory macrophages and reduced the number of glomerular crescents, improved renal function and reduced proteinuria (Duffield et al., 2005).

Adoptive transfer studies have further demonstrated that macrophages can induce proteinuria and mesangial cell proliferation. Rats were treated with cyclophosphamide two days before the injection of NTS to deplete leukocytes and then reconstituted with either bone marrow derived macrophages or a macrophage cell line, NR8383, 24 hours following the injection. Pre-treatment with cyclophosphamide prevented glomerular leukocyte accumulation, proteinuria, mesangial cell proliferation and hypercellularity in accelerated NTN, whilst adoptive transfer of macrophages into cyclophosphamide-treated rats reversed the protective role. The degree of renal injury correlated with the number of transferred glomerular macrophages (Ikezumi et al., 2003).

Other studies have focussed on targeting the cytokines involved in monocyte recruitment and macrophage activation. Blocking pro-inflammatory cytokines, such as IL-1, TNF-α and MIF (macrophage migration inhibition factor) was found to inhibit the accumulation and activation of both interstitial and glomerular macrophages and suppress renal injury in rats, due to their role in the upregulation of chemokines and leukocyte adhesion molecules within the kidney (Hruby et al., 1991; Lan et al., 1997a; Lan et al., 1993; Lan et al., 1997b; Tang et al., 1994). Direct blockade of chemokines, e.g. monocyte chemoattractant protein (MCP)-1 and RANTES, in mice with NTN was found to prevent proteinuria, crescent formation and leukocyte infiltration (Lloyd et al., 1997). Also, blocking leukocyte adhesion molecules, e.g. intercellular adhesion molecule (ICAM)-1 and osteopontin, in rats has proven effective in inhibiting renal macrophage infiltration and injury (Nishikawa et al., 1993; Yu et al., 1998). However, when NTN was induced in MCP-1 deficient mice, they were protected from tubular injury but not glomerular injury (Tesch et al., 1999).

Distinct macrophage phenotypes have been shown to contribute to kidney injury and repair in ischemia reperfusion. Classically-activated, pro-inflammatory macrophages are recruited into the kidney within the first 48 hours following injury. At the onset of repair these can then switch to an alternatively activated phenotype, promoting the resolution of inflammation (Lee et al., 2011). With regards to NTN, rats treated with IL-4 were found to have significantly reduced proteinuria and glomerular injury compared to untreated rats.

Treatment from the start of induction of NTN was associated with markedly decreased infiltration of macrophages, whereas delaying treatment until inflammation was established did not alter macrophage numbers, suggesting that the IL-4 may be acting to reduce macrophage activation (Cook et al., 1999).

Although these studies strongly support a role for macrophages in the pathogenesis of GN, it must be remembered that blockade of cytokines and chemokines not only alters the infiltration and activation of macrophages, but also other leukocytes that are involved in the progression of renal injury.

#### 1.4.3.5 Dendritic cells

The primary role of dendritic cells is antigen presentation. Dendritic cells exist in virtually all tissues, both lymphatic and non-lymphatic, where they perform sentinel functions and gather antigens for transport to the draining lymph nodes for T cell activation. An extensive network of dendritic cells has been identified in the tubulointerstitium of both healthy and inflamed murine kidneys, with dendritic cells accumulating around, but not within, the glomeruli during NTN (Kruger et al., 2004; Soos et al., 2006). Kidney dendritic cells have been shown to attenuate the early phase of NTN, by stimulating the production of IL-10 by $CD4^+$ T cells, and their depletion aggravates disease (Scholz et al., 2008). However, the phenotype and activation state of kidney dendritic cells changes during the course of non-accelerated NTN. Surface expression of CD40 and CD80, which have been shown to be involved in leukocyte recruitment and accumulation (Odobasic et al., 2005a; Odobasic et al., 2005b; Ruth et al., 2004), increased with progression of disease, whereas expression of inducible co-stimulatory molecule ligand (ICOS-L), that can induce IL-10 and is protective in NTN (Odobasic et al., 2006), decreased significantly (Hochheiser et al., 2011). Depletion of kidney dendritic cells during this later stage of disease was found to be protective rather than harmful (Hochheiser et al., 2011).

### 1.4.3.6 Mast cells

Mast cells are classically considered innate immune cells with a role in first-line defence against infection and also in allergic reactions. However, recent advances in autoimmunity research have suggested a role for mast cells in the pathogenic responses that exacerbate disease. Mast cells develop from $CD34^+$ bone marrow cells and circulate in the blood in an immature form until they set up residency in a particular tissue and mature. They are mainly found in tissues that form barriers between self and the environment, such as the skin, respiratory tract and gut, as well as being associated with blood vessels, lymphatic vessels and nerves. Activation of mast cells, via receptor binding, cell-cell contact or physical activators, causes them to release an array of preformed molecules that are stored in granules, such as ligands for T cells and B cells. Mast cells have been implicated in RA and MS, and more recently their role in GN has been explored, although the results are conflicting.

Initial experiments into the role of mast cells in GN made use of mast cell-deficient mice, $Kit^{W/Wv}$. Timoshanko *et al.* found that mast cell-deficient mice were protected from crescentic GN and had reduced DTH response following induction of non-accelerated NTN, and that adoptive transfer of mast cells to these mice restored susceptibility to similar levels as seen in WT mice (Timoshanko et al., 2006). However, independently of each other, Hochegger *et al.* and Kanamaru *et al.* found the contrary, as they observed that $Kit^{W/Wv}$ mice developed more severe proteinuria, glomerular damage and an increase in macrophage accumulation, following induction of accelerated NTN, when compared to WT ($Kit^{+/+}$) mice. In addition, reconstitution of mast cells in $Kit^{W/Wv}$ mice protected them from NTN (Hochegger et al., 2005; Kanamaru et al., 2006). Kanamaru *et al.* also went on to show that the protective role of mast cells was independent of the activating FcγR, as reconstitution of $Kit^{W/Wv}$ mice with $FcR\gamma^{-/-}$ mast cells still conferred protection (Kanamaru et al., 2006). Deterioration of renal function correlated with thick layers of subendothelial glomerular deposits, which were found to be rich in fibrin and type I collagen, in the $Kit^{W/Wv}$ mice, suggesting a deficiency in repair mechanisms. This was supported by a decrease in the activity of two crucial enzymes in the plasminogen/plasmin system. These results indicated that mast cells exert a protective role in accelerated NTN by mediating remodelling and repair (Kanamaru et al., 2006).

Interestingly, no mast cells were detected in the kidneys of WT mice or mast cell-reconstituted $Kit^{W/Wv}$ mice following induction of accelerated NTN, whereas they were following the induction of the non-accelerated disease model (Hochegger et al., 2005; Kanamaru et al., 2006; Timoshanko et al., 2006). Further investigation revealed an increase

in mast cells in the renal draining lymph nodes of the mice with accelerated NTN (Hochegger et al., 2005). These results suggest that during acute, accelerated disease mast cells act in the draining lymph nodes as immunoregulatory cells that can counteract injury and control repair; however, during chronic, non-accelerated disease, mast cells are contributory in mounting a $T_h1$-directed DTH immune response that promotes injury.

Recently, two groups have further explored the relationship between mast cells and $T_{reg}$, supporting the evidence that mast cells play a protective, immunoregulatory role during murine GN. Eller *et al.* found that transfer of $T_{reg}$ into WT animals almost completely prevented the development of glomerular damage and produced an increase of mast cells in the renal draining lymph nodes following induction of accelerated NTN, whereas transfer of $T_{reg}$ into mast cell-deficient mice resulted in no protective effects (Eller et al., 2011). Further to this they found that blocking the cytokine IL-9, known to be involved in mast cell recruitment and proliferation, or transferring $T_{reg}$ from IL-9-deficient mice, abrogated protection from NTN (Eller et al., 2011). Gan *et al.* found, following the induction of AAV as a result of autoimmunity to MPO, mast cell-deficient mice exhibited more severe focal necrotising GN, as well as increased anti-MPO $CD4^+$ T cells and enhanced DTH responses. Furthermore, the draining lymph nodes around the sites of immunisation had fewer $T_{reg}$ and reduced production of IL-10 in mice lacking mast cells (Gan et al., 2012). *Ex vivo*, mast cells were found to enhance $T_{reg}$ suppression through IL-10. Reconstitution of mast cell-deficient mice with IL-$10^{-/-}$ mast cells led to enhanced autoimmunity to MPO and greater disease severity when compared to reconstitution with IL-10-producing mast cells (Gan et al., 2012). Taken together, these results suggest that, in acute disease settings, there is a close interaction between mast cells and $T_{reg}$ in controlling $CD4^+$ T cell responses within the draining lymph nodes.

As well as using mast cell-deficient mice, GN has also been induced in mice deficient in mouse mast cell protease (mMCP)-4, the murine counterpart of human mast cell chymase. mMCP-4 is a mast cell-specific protease that is released from secretory granules and involved in tissue homeostasis. mMCP-$4^{-/-}$ mice were protected from accelerated NTN. During the heterologous stage of disease there was no difference between WT and mMCP-4-deficient mice, indicating that mast cells may exert protective functions in the initial stages but prolonged activation can result in damage further down the line (Scandiuzzi et al., 2010).

### 1.4.3 Intrinsic renal cells

As well as infiltrating leukocytes, intrinsic renal cells, within the glomerulus, also play a major role in the development of GN. The glomerulus is a capillary tuft surrounded by Bowman's capsule. The glomerular capillary wall consists of three main layers: a thin layer of fenestrated endothelial cells, the GBM, and podocytes. Located centrally within the glomerulus, between the capillary loops and the glomerular basement membrane, is the mesangium, which is made up of mesangial cells and their surrounding extracellular matrix. Lining the inside of the Bowman's capsule are parietal epithelial cells (Figure 1.3). Most of our knowledge on the role of intrinsic renal cells during GN comes from *in vitro* experiments; however, the generation of bone marrow chimeric mice has proved a useful tool to address this question using *in vivo* models of GN. Evidence for the role of mesangial cells, endothelial cells and podocytes in GN are discussed in the next few paragraphs.

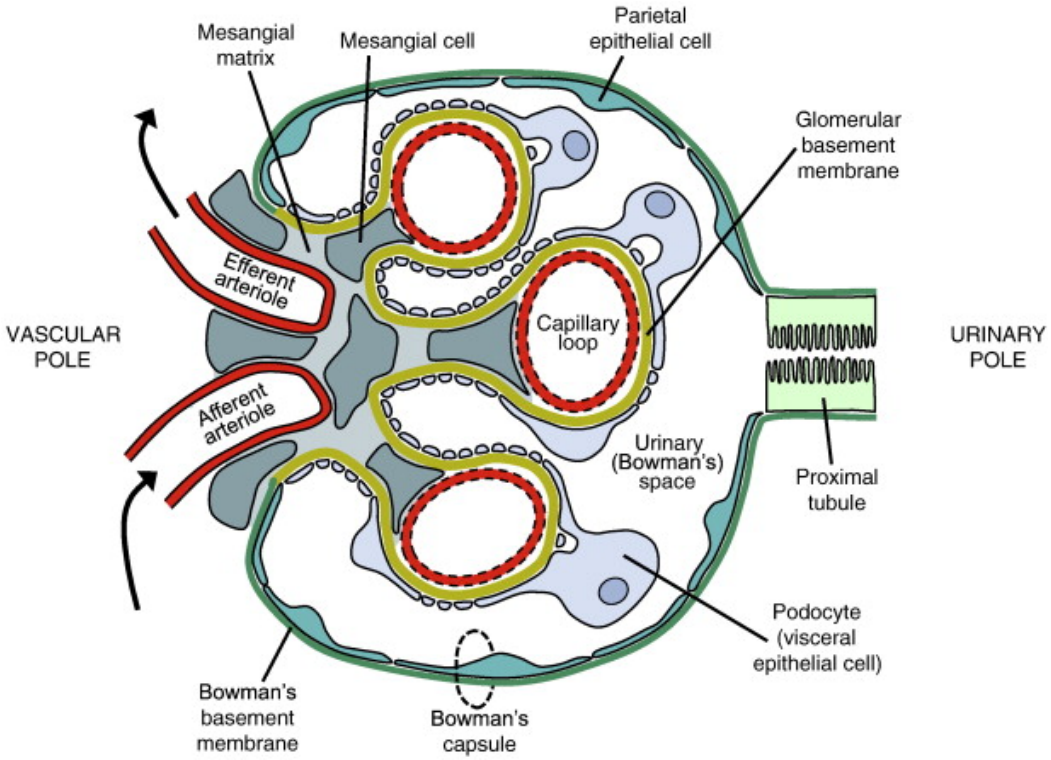


**Figure 1.3 Schematic representation of the glomerulus.**

Blood enters the glomerulus by the afferent arteriole and leaves by the efferent arteriole. Within the glomerulus, blood is filtered through the capillary wall, which consists of endothelial cells, the GBM, and podocytes, and urine collects in the urinary space (Bowman's space) where it is passed to the proximal tubule. Centrally within the glomerulus, among the glomerular capillaries, is the mesangium. Lining the inside of the Bowman's capsule are parietal epithelial cells (Leeuwis et al., 2010). This image has been reproduced with the permission of the rights holder, Elsevier.

#### 1.4.3.1 Mesangial cells

Mesangial cells are specialised pericytes, of mesenchymal origin, that have the characteristics of modified smooth muscle cells. The primary roles of mesangial cells are maintaining the structure of the glomerulus and controlling the glomerular filtration rate. They also modulate glomerular injury by generating mediators of inflammation and by phagocytosis of macromolecules and immune complexes (Schlondorff, 1987). Proliferation of mesangial cells and deposition of extracellular mesangial matrix are commonly observed in many forms of GN, such as IgA nephropathy and SLE. The precise role of mesangial cells in the pathogenesis of GN is still not fully understood.

Mesangial cells are thought to be involved in antigen presentation and co-stimulation. Resting mesangial cells do not express MHC Class II; however following stimulation with IFN-γ they start to express MHC Class II in a dose- and time-dependent manner. Furthermore, a combination of IFN-γ and TNF-α or IL-1β resulted in an enhanced induction of MHC Class II compared to IFN-γ alone. TNF-α and IL-1β, either alone or together, had no effect in enhancing MHC Class II (Martin et al., 1989). As mentioned in Section 1.4.3.2.1, MHC Class II-deficient mice are protected from crescentic GN, $CD4^+$ T cell infiltration and glomerular injury (Li et al., 1998). The role of intrinsic renal cell MHC Class II was further explored in accelerated NTN using MHC Class II chimeric mice. MHC Class II-deficient mice were transplanted with the bone marrow and thymus of WT animals. Despite having normal T and B cell populations and MHC Class II expression in secondary lymphoid organs they were protected from crescentic GN, $CD4^+$ T cell infiltration and glomerular injury. These data suggest a pivotal role for intrinsic renal cell MHC Class II interaction with $CD4^+$ T cells in the development of cell-mediated renal injury (Li et al., 1998).

Mesangial cells also express the co-stimulatory molecule CD40 that binds to CD154 on T cells and enhances their activation. $CD40^{-/-}$ mice do not develop immunity in response to sheep globulin and thus fail to develop effector responses in NTN. Transplantation of WT bone marrow into $CD40^{-/-}$ mice restored their ability to develop antigen-specific immune responses; however they had minimal T cell and macrophage influx and were protected from renal injury, suggesting a role for mesangial cell CD40 expression in the development of NTN (Ruth et al., 2003).

Mesangial cells can produce an array of cytokines and inflammatory mediators that are involved in glomerular injury. TNF-α, IFN-γ, IL-6 and IL-12 are pro-inflammatory

cytokines produced by mesangial cells and are important mediators in the development of GN (Bussolati et al., 1999; Gomez-Guerrero et al., 1994; Zoja et al., 1991). Bone marrow transplantation experiments have shown that intrinsic renal cell production of TNF-α, IFN-γ and IL-12 are required for full expression of murine crescentic GN (Timoshanko et al., 2002; Timoshanko et al., 2001; Timoshanko et al., 2003). TNF-α, IFN-γ and IgG aggregates have also been shown to induce mesangial cell expression of chemokines with specificity for monocyte/macrophage recruitment, such as M-CSF (macrophage colony-stimulating factor) and MCP-1 (Satriano et al., 1993; Zoja et al., 1991).

Mesangial cells also produce cytokines that can have anti-inflammatory effects within the kidney, such as IL-4 and IL-10. These cytokines act to alter the activation state of leukocytes, such as macrophages, to protect against glomerular damage. IL-4 and IL-10 are both potent inhibitors of the $T_h1$ response and inactivate the pro-inflammatory macrophage phenotype. *In vivo*, IL-10-deficient mice and IL-4-deficient mice were found to develop more severe NTN compared to WT mice (Kitching et al., 1998; Kitching et al., 2000), and administration of either IL-4, IL-10 or both to WT mice with NTN was found to attenuate disease (Kitching et al., 1997; Tipping et al., 1997).

#### 1.4.3.2 Endothelial cells

The glomerular endothelium is a highly fenestrated barrier and, unlike most fenestrated capillaries, its pores are not spanned by diaphragms. The fenestrations are 70-100 nm in diameter, constituting around 20-50% of the entire endothelial surface (Bulger et al., 1983), which allows for the free filtration of fluid, plasma solutes and proteins, but not red blood cells. Until recently, it was believed the endothelium did not contribute to the permselectivity of the glomerular barrier, due to the large size of the pores, so it has long been neglected as playing a role in proteinuria. However, lately, research has paid more attention to the endothelial surface layer (ESL), which is produced by, and surrounds, the endothelial cells. The ESL is of similar thickness to the GBM and has two elements, the glycocalyx, which refers to the covalently bonded plasma-membrane-bound part of the layer, and the cell coat, a larger, more loosely associated part of the layer. The ESL is composed of negatively charged glycoproteins, glycosaminoglycans and membrane-associated and secreted proteoglycans (Haraldsson et al., 2008).

Glomerular endothelial cells are difficult to culture, with the cellular phenotype being lost after a few passages. As well as this, the cell coat is easily disturbed, and therefore rather elusive. However, various studies have overcome these complications and more is being understood about the roles of these cells in GN. *In vivo,* disruption of the ESL with chondroitinase or hyaluronidase was found to increase the permeability of the glomerular capillary wall to albumin, but not neutral Ficoll, indicating a defect in charge selectivity (Dane et al., 2013; Jeansson and Haraldsson, 2006). Also, displacement of the cell coat in rats, using an injection of hypertonic sodium chloride in the left renal artery, increased fractional clearance of albumin 12-fold without morphological changes, compared to rats treated with isotonic sodium saline (Friden et al., 2011). These results are supported *in vitro,* in both primary and immortalised human glomerular endothelial cells, where treatment with puromycin aminonucleoside, neuraminidase or human heparanase reduced the thickness of the glycocalyx and caused an increase in albumin passage across the cell monolayers (Bjornson et al., 2005; Singh et al., 2007).

As well as contributing to the permselectivity of the glomerular filtration barrier, the ESL is also involved in the regulation of coagulation pathways and preventing leukocyte adhesion to the underlying endothelial cells. Disruption of the glycocalyx and subsequent exposure of the endothelial cells to pro-inflammatory molecules, such as TNF-α, IL-1 and MCP-1, leads to the expression of tissue factor, which is necessary for thrombosis formation (Dosquet et al., 1995; Grabowski and Lam, 1995; Kirchhofer et al., 1994). The glycocalyx houses endothelial cell adhesion molecules, such as P-selectin, ICAM-1, and VCAM-1. However, the thickness of the glycocalyx ranges from 0.2-0.5μm in capillaries and 2-3μm in small arteries, whereas P-selectin, the molecule that initiates leukocyte rolling, only extends 38nm from the cell surface (Reitsma et al., 2007).

Apoptotic endothelial cells have also been shown to contribute to thrombotic events due to increased adherence of platelets to the endothelium and their subsequent activation (Bombeli et al., 1999).

#### 1.4.3.3 Podocytes

Podocytes, or visceral epithelial cells, are pericyte-like cells found within the Bowman's capsule where they wrap around the glomerular capillaries and play a major role in establishing the selective permeability of the glomerular filtration barrier. Podocytes are highly differentiated, polarised cells with limited capability to undergo cell division. Mature podocytes consist of a cell body with major processes that branch into foot processes. Foot processes on adjacent podocytes form an interdigitating network, separated by a slit diaphragm, which can modulate the permeability of the filtration barrier through changes in morphology (Greka and Mundel, 2012).

Proteinuria is a hallmark of glomerular injury, with its severity acting to predict the progression of renal disease. Podocyte injury, due to damage of the actin cytoskeleton leading to a shortening of the foot processes and disruption of the slit diaphragm, is major cause of proteinuria in both human and experimental models of glomerular diseases. A number of inflammatory mediators, including cytokines, chemokines and growth factors, have been implicated in this process.

TNF-α and IL-1 have both been found to play an important role in proteinuria. Stimulation of podocytes with TNF-α and IL-1 activates NF-κB, resulting in the upregulation of pro-inflammatory cytokines (Brahler et al., 2012; Bruggeman et al., 2011). *In vitro,* podocytes with abrogated activation of NF-κB, via inhibition of NF-κB essential modulator (NEMO) or neutralisation of TNFR2, had a marked reduction in pro-inflammatory cytokine secretion following stimulation with TNF-α and IL-1, compared to WT podocytes (Brahler et al., 2012; Bruggeman et al., 2011). *In vivo*, mice with a podocyte-specific deletion of NEMO recovered much faster from GN, showing rapid remission of proteinuria and restoration of podocyte morphology compared to WT mice (Brahler et al., 2012).

Treatment with IFN-β has been found to reduce proteinuria in rats with NTN, Thy-1 nephritis and puromycin aminonucleoside nephrosis, without an effect on glomerular inflammation, suggesting IFN-β may have a direct effect on the glomerular filtration barrier (Satchell et al., 2007). *In vitro* studies, using human glomerular endothelial cell monolayers or podocyte monolayers, showed that treatment with IFN-β reduced permeability of the cell layer, thought to be due to increased integrity of intracellular junctions by upregulation of junctional adhesion molecules or resistance to their downregulation (Satchell et al., 2007).

Similar to mesangial cells, podocytes are thought to be involved in antigen presentation. Podocytes have been shown to express MHC Class I, MHC Class II and ICAM-1 in a model of necrotising crescentic GN *in vivo*, as well as following stimulation with IFN-γ *in vitro* (Coers et al., 1994). More recently, it has been shown that deletion of MHC Class II on podocytes only can protect from the induction of anti-GBM disease (Goldwich et al., 2013).

Podocytes are known to both secrete and respond to certain chemokines and cytokines. Podocytes have been found to release MCP-1 and IL-8 (CXCR1), suggesting they may actively participate in cell recruitment during GN (Huber et al., 2002; Natori et al., 1997), as well as IL-6 (Hughes et al., 2001). Podocytes are also a prominent source of TNF-α in human membranous nephritis (Neale et al., 1995) and are known to express the receptors for IL-4 and IL-13, the presence of which can disrupt cell function (Lai et al., 2007; Van Den Berg et al., 2000).

Podocytes have also been found to contribute to glomerular crescents, both in animal models of GN as well as human disease (Bariety et al., 2005; Le Hir et al., 2001; Moeller et al., 2004; Thorner et al., 2008). Originally, it was thought crescents were composed of parietal epithelial cells, monocytes/macrophages and myofibroblasts, with podocytes being excluded as participants due to the absence of podocyte markers. However, in a study to investigate the formation of crescents in mice, 6-10 days following induction of NTN podocytes were seen to bridge the gap between the glomerular tuft and Bowman's capsule, as well as detach from the GBM and infiltrate the parietal epithelial cells. During this process these podocytes appeared to lose their phenotypic markers (Le Hir et al., 2001). This observation was later confirmed in a NTN study in which podocytes were genetically tagged with β-galactosidase. Six days after induction of disease, kidney sections were enzymatically stained with X-gal and crescents were found to comprise 25-50% podocytes, despite the cells being negative for podocyte-specific antigens. Suggesting, that during NTN, podocytes undergo profound phenotypic changes (Moeller et al., 2004). Studies in human GN have also supported these observations (Bariety et al., 2005; Thorner et al., 2008).

## 1.5 Fas ligand

### 1.5.1 Introduction

The TNF superfamily is a growing family of cytokines that have varied and pleiotropic actions but share a common structural motif, the TNF homology domain (THD), which allows self-trimerisation and receptor binding. TNF-α was the first family member to be identified over 25 years ago and was named due to its ability to cause necrosis of tumours (Aggarwal et al., 1985). Since then 18 other members have been isolated and cloned. Fas ligand (FasL, CD95L) is the sixth member of the TNF superfamily and is best characterised for binding its receptor, Fas (APO-1, CD95), and causing apoptosis of the Fas-bearing cell.

FasL was first detected as the natural ligand for Fas in 1993 (Suda et al., 1993). Molecular cloning, purification and characterisation revealed FasL to be a heavily glycosylated, 40kDa, type-II transmembrane protein, with an intracellular N-terminus, an extracellular C-terminus and a single transmembrane domain, belonging to the TNF superfamily (Suda and Nagata, 1994; Suda et al., 1993). The N-terminal region of FasL has no signal sequence but the C-terminus contains the THD, a stretch of 150 amino acids with significant homology (20-25%) to the corresponding region in other TNF family members, such as TNF-α and TNF-β (lymphotoxin) (Nagata and Golstein, 1995; Suda et al., 1993). Biologically active FasL exists as a homotrimer (Suda and Nagata, 1994).

Fas was first identified by two independent groups in 1989 (Trauth et al., 1989; Yonehara et al., 1989). Purification and molecular cloning of Fas in the early 1990's highlighted its significant sequence homology to the members of the TNF receptor (TNFR) superfamily (Itoh et al., 1991; Oehm et al., 1992; Watanabe-Fukunaga et al., 1992b). Fas is a 45kDa, type-I membrane protein, with an intracellular C-terminus, extracellular N-terminus and a single transmembrane domain, belonging to the TNFR superfamily (Itoh et al., 1991; Oehm et al., 1992). All members of the TNFR superfamily have a well conserved (17-30%) N-terminal region that contains 2-6 tandem repeats of a cysteine-rich domain, of which Fas contains three (Itoh et al., 1991). The cytoplasmic domain of Fas is relatively abundant in charged amino acids but shows little homology to other members of the TNFR superfamily, except for a stretch of 80 amino acids, which are conserved in TNF-R1, known as the death domain (DD) due to its importance in cytotoxicity (Itoh and Nagata, 1993; Itoh et al., 1991;

Tartaglia et al., 1993). Similarly to FasL, Fas exists as a preassembled homotrimer (Chan et al., 2000; Papoff et al., 1999; Siegel et al., 2000).

In 1998 a second receptor for FasL was identified. Decoy receptor 3 (DcR3) contains four tandem cysteine-rich domains; however it lacks a transmembrane domain and is instead synthesised as a secreted, soluble protein. Fas and DcR3 both bind FasL with comparable affinities of 1.1nM and 0.8nM, respectively. DcR3 is thought to act as an immunomodulatory protein (Pitti et al., 1998).

Similarly to TNF-α, and other members of the TNF superfamily, FasL can be cleaved by a matrix metalloproteinase (MMP) to a soluble form (Kayagaki et al., 1995; Tanaka et al., 1995). Matrilysin (MMP7) cleaves FasL at the leucine residues in the site 'ELAELR', found between the transmembrane and trimerisation domains, to form a 26kDa protein (Powell et al., 1999; Vargo-Gogola et al., 2002). Soluble FasL (sFasL) retains its ability to form a trimeric structure and bind to the Fas receptor (Tanaka et al., 1995).

### 1.5.2 Fas-Fas ligand induced apoptosis

FasL, acting through Fas, is best characterised for inducing apoptosis in the Fas-bearing cell. How the binding of FasL to Fas initiates Fas activation is not completely known; however, the intracellular sequence of events following ligation are well documented. Initially, through homologous DD interactions, Fas recruits FADD, Fas-associated protein with death domain (MORT1) (Boldin et al., 1995; Chinnaiyan et al., 1995). The DD of FADD is located at the C-terminus, whilst the N-terminal region contains another protein-protein interaction domain, the death effector domain (DED). It is the DED that is responsible for downstream signal transduction, as it is required for the recruitment of procaspase-8 (MACH, FLICE), an aspartate–specific cysteine protease present in the cytoplasm as an inactive zymogen, which contains two DED at its N-terminus (Boldin et al., 1996; Muzio et al., 1996). This assembly of proteins has been named the death inducing signalling complex (DISC) and assembles within seconds after FasL engagement to Fas (Kischkel et al., 1995).

Following dimerisation at the DISC, procaspase-8 undergoes a conformational change that allows it to gain full enzymatic activity and leads to its autoproteolytic processing, releasing active caspase-8 into the cytoplasm (Medema et al., 1997). From here active

caspase-8 can now go on to cleave other caspases, leading to a ‘caspase cascade’ (Figure 1.4). Due to its position at the start of the cascade, caspase-8 is known as an initiator caspase. One of the lead effector caspases cleaved by caspase-8 is caspase-3. Caspase-3 is responsible for the cleavage of most of the proteins characteristic of apoptosis and the proteins involved in inducing the morphological changes observed during programmed cell death (Earnshaw et al., 1999).

Despite retaining its ability to trimerise and bind the Fas receptor, sFasL is a weak inducer of apoptosis. Naturally processed sFasL was 1000-fold less active at inducing apoptosis compared to membrane-bound FasL (Schneider et al., 1998) and comparisons of mice deficient in either membrane-bound FasL or sFasL showed that the membrane-bound form only is essential for Fas-induced apoptosis (O' Reilly et al., 2009). However, cross-linking of sFasL was found to restore its cytotoxic activity both *in vitro* and *in vivo* (Dupont and Warrens, 2007; Schneider et al., 1998). The precise functions of sFasL are still not fully understood, however it appears that cleavage of FasL into the soluble form may serve to downregulate FasL activity.

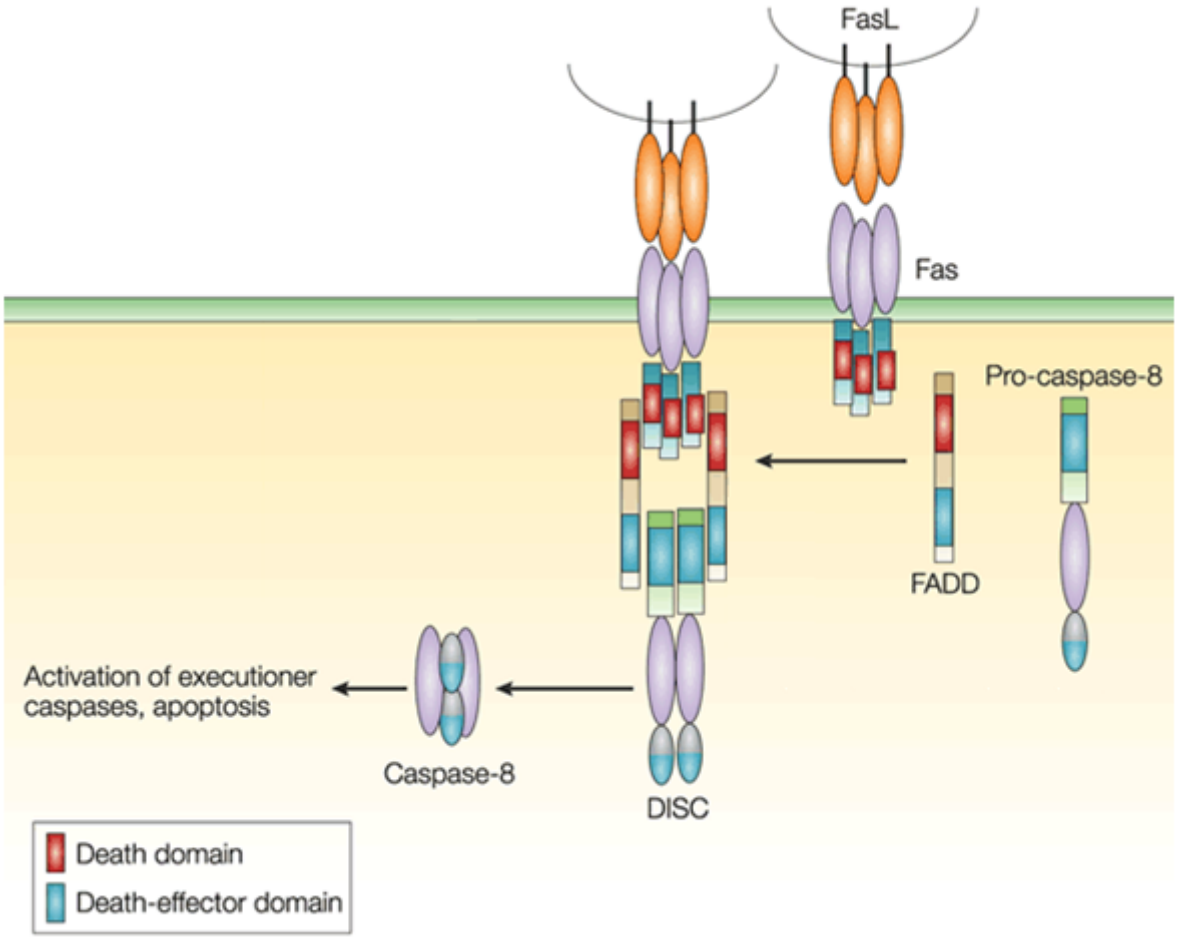


**Figure 1.4 Intracellular signalling events following ligation of Fas ligand to Fas.**

Fas ligand binds to Fas as a homotrimer and Fas recruits FADD, which in turn recruits procaspase-8 forming the DISC. Procaspase-8 is cleaved to its active form and activates the caspase cascade, resulting in death of the Fas-bearing cell (Green and Ferguson, 2001). This image has been reproduced with the permission of the rights holder, Macmillan Magazines.

### 1.5.3 Fas ligand expression

Fas expression is ubiquitous, so for this reason expression of FasL needs to be tightly controlled to regulate FasL-induced apoptosis. It was initially thought that FasL was predominantly expressed by lymphatic cells as FasL expression is inducible in T cells (Kasibhatla et al., 1998; Oshimi et al., 1996; Suda et al., 1995), natural killer (NK) cells (Montel et al., 1995), and B cells (Hahne et al., 1996; Tanner and Alfieri, 1999). However it has now become recognised that it is also expressed by myeloid cells, such as $CD8^+$ dendritic cells (Suss and Shortman, 1996) and mature, activated macrophages (Badley et al., 1996; Boyle et al., 2001; Dockrell et al., 1998; Kiener et al., 1997) and non-lymphoid tissues, such as the lung (Gochuico et al., 1998; Suda et al., 1995), small intestine (Bonfoco et al., 1998; Suda et al., 1995), and kidney in both humans (Tsukinoki et al., 2004) and mice (Lorz et al., 2000).

### 1.5.4 Fas ligand and immune privilege

Immunologically-privileged sites are defined as sites where an immune response is not initiated when antigen is introduced, thought to be because the sites concerned cannot tolerate the non-specific damage that may occur during an inflammatory response. These areas include the brain, testis, ovary, pregnant uterus and the anterior chamber of the eye. Although these sites have long been recognised as being immune privileged it was not until 1995 that this was associated with FasL.

In 1995, two independent groups identified expression of FasL in the eye and testis. Bellgrau *et al*. derived testis grafts from mice expressing functional FasL and those expressing defective FasL and transplanted them under the kidney capsule of allogenic animals. The grafts from mice with functional FasL survived indefinitely whereas the grafts expressing non-functional FasL were rejected. Polymerase chain reaction (PCR) analysis of isolated RNA showed FasL expression by testicular Sertoli cells (Bellgrau et al., 1995). Griffith *et al*. injected herpes simplex virus-type 1 (HSV-1 (KOS)) into the anterior chamber of the eye of WT mice and mice with non-functioning Fas or FasL. They observed extensive apoptosis of infiltrating neutrophils and lymphocytes in the eyes of WT mice but not in the mice with defective Fas-FasL signalling. To test whether this was due to defective FasL in the eye or because of a toxic effect from the inflammatory cells they created bone marrow

chimeras where mice with defective FasL were irradiated and reconstituted with bone marrow from WT mice. Following infection the mice still had an intense inflammatory response, proving that FasL is expressed in the eye during infection (Griffith et al., 1995). Following this they also analysed RNA isolated from the eye and other organs and showed that FasL is expressed by the eye, testis and spleen but not the heart or skin (Griffith et al., 1995; Griffith et al., 1996b). Both groups went on to conclude that non-hematopoietic cells at sites of immune privilege express FasL and are able to kill infiltrating leukocytes.

However, in 1997 Allison *et al*. created transgenic mice expressing FasL on islet β-cells and transplanted foetal pancreata under the kidney capsules of allogenic animals. This failed to protect the grafts from rejection and resulted in granulocytic infiltration into the pancreata, indicating that FasL expression alone may not be sufficient to establish immune privilege and demonstrating a pro-inflammatory function of FasL (Allison et al., 1997).

Features of immune privilege are also found within cancers, where it is known as ‘tumour evasion’ or ‘tumour counterattack’. Tumour cells express FasL to kill infiltrating leukocytes and are also resistant to Fas-mediated apoptosis which allows them to evade death (O'Connell et al., 1999a). FasL expression has been identified on many different cancers, including esophageal cancer, human breast cancer, and colon adenocarcinomas (O'Connell et al., 1999b; O'Connell et al., 1999c; O'Connell et al., 1998).

## 1.6 Fas ligand and autoimmunity

Our understanding of the roles of Fas and FasL come from studying mice with defective Fas-FasL signalling. Autoimmunity is seen both in animal models of Fas/FasL deficiency and in humans with autoimmune lymphoproliferative syndrome (ALPS), who carry mutations on the proteins involved in Fas-FasL signalling. Mouse models of FasL deficiency and ALPS are described in the following sections.

### 1.6.1 Mouse models of Fas ligand deficiency

#### 1.6.1.1 *Lpr*, *gld* and *lpr$^{cg}$* mice

Lymphoproliferative (*lpr*) and generalised lymphoproliferative disease (*gld*) are autosomal recessive, single gene mutations that both arose spontaneously and were first identified by the Jackson Laboratories. The *lpr* mutation first arose in the MRL mouse strain in 1977 and in 1984 the *gld* mutation was identified in the inbred mouse strain C3H/HeJ (Murphy and Roths, 1977; Roths et al., 1984). Genetic linkage studies pinpointed the *lpr* and *gld* mutations to chromosomes 19 and 1, respectively (Roths et al., 1984; Watanabe et al., 1991), and in the early 1990's Fas and FasL were mapped to the sites of the mutations (Takahashi et al., 1994; Watanabe-Fukunaga et al., 1992a). In *lpr* mice the mutated Fas gene contains an early transposable element that results in impaired transcription. However, expression of Fas is not completely inhibited, and full length Fas mRNA has been detected at very low levels in the liver and thymus of *lpr* mice (Adachi et al., 1993; Kobayashi et al., 1993). The *gld* mutation is caused by a point mutation in the C-terminus of the coding region for FasL. Expression of FasL is not inhibited and the full-length protein is synthesised and sent to the cell membrane; however the mutation changes a phenylalanine to a leucine that affects the ability of FasL to bind to Fas (Takahashi et al., 1994). A third mutation also exists, *lpr$^{cg}$* (*lpr* complementing *gld*), which was identified in 1990 in the CBA/KlJms (CBA) strain of mouse. *Lpr$^{cg}$* mice carry a point mutation in the cytoplasmic region of Fas that leads to the replacement of an isoleucine with an asparagine. This results in a conformational change in the fold of the DD and upsets the ability of Fas to bind its downstream adaptor protein, FADD, altering signalling through the receptor (Matsuzawa et al., 1990).

Homozygosity at any of the loci results in massive non-malignant lymphoproliferation, lymphadenopathy, splenomegaly, autoantibody production, including

anti-DNA antibodies, and the presence of mature peripheral double negative (DN) T cells, that express the TcR, CD3, and the B cell marker, B220, but are negative for CD4 and CD8. Genetic background plays a large role in the severity of autoimmunity seen in both *lpr* and *gld* mice. MRL mice are predisposed to autoimmune disease and develop late onset GN, dying within the second year of life. When combined with the *lpr* gene, this predisposition is accelerated, with 50% mortality at 5-6 months due to early onset, aggressive, and fatal renal disease. Intercrossing the *lpr* gene onto strains of mice with no predisposition to autoimmunity, such as C3H/HeJ, C57BL/6, and AKR/J, was found to shorten survival of the mice and induce autoantibodies; however GN was not seen until 13-16 months of age and was minimal (Kelley and Roths, 1985). The same phenomenon is also seen with the $lpr^{cg}$ and *gld* genes. Both were originally identified on strains of mice not predisposed to autoimmunity, CBA and C3H/HeJ, respectively. However, intercrossing these genetic mutations onto an MRL background accelerated the onset of GN in these mice (Kimura et al., 1992).

#### 1.6.1.2 Fas and Fas ligand knockout mice

FasL expression is not abolished in *gld* mice and there are reports that some residual activity may remain. Karray *et al.* created a FasL knockout mouse on a C57BL/6 background, using the Cre-*loxP*-based strategy, to investigate the *in vivo* functions of FasL. Germline deletion of FasL resulted in a severe phenotype with $FasL^{-/-}$ mice exhibiting extreme splenomegaly and lymphadenopathy associated with lymphocytic infiltration into multiple organs, and autoimmune disease with histological signs of GN. This accelerated phenotype led to premature death at 4 months of more than 50% of the homozygous mice. This is in stark contrast to the mild disease usually seen in *gld* mice on the same genetic background and shows that the expressed FasL in *gld* mice has a residual function (Karray et al., 2004).

To determine the cellular subset responsible for the prevention of autoimmunity in FasL-deficient mice, Mabrouk *et al.* created conditional knockouts lacking FasL on B cells, T cells and myeloid cells. Deletion of FasL on T cells or B cells resulted in a mild autoimmune syndrome, suggesting that FasL deficiencies in different cell types are likely to be additive, but FasL deficiency in myeloid cells did not result in an autoimmune phenotype. Loss of FasL on T cells also led to the accumulation of T cells, B cells and dendritic cells in the lymph nodes (Mabrouk et al., 2008). Similar results were seen when Fas was deleted from

specific cellular subsets. Deletion of Fas on T cells, B cells or T cells and B cells was insufficient for the pathogenesis of lymphoproliferative disease (Hao et al., 2004; Stranges et al., 2007).

#### 1.6.1.3 Membrane-bound versus soluble Fas ligand

Recently, O'Reilly *et al.* used gene targeting to create mice that selectively express either the membrane-bound form of FasL or sFasL, on a C57BL/6 background. Mice expressing the membrane-bound form of FasL appeared normal and their T cells readily killed target cells, whereas mice expressing sFasL only developed lymphadenopathy and hypergammaglobulinemia similar to *gld* mice. Interestingly, these mice also developed a severe SLE-like autoimmune kidney disease, which only rarely occurs in *gld* mice on the C57BL/6 background and tends to develop much later. It was hypothesised that this was because these mice produced excess sFasL that could bind to its receptor Fas and activate NF-κB (nuclear factor kappa-B), driving production of pro-inflammatory cytokines (O' Reilly et al., 2009).

### 1.6.2 Autoimmune lymphoproliferative syndrome

Autoimmune lymphoproliferative syndrome (ALPS) is a human disorder of lymphocyte homeostasis and immunological tolerance first described in 1967 by Canale and Smith (Canale and Smith, 1967). It is characterised by accumulation of benign lymphocytes, accompanied by splenomegaly and lymphadenopathy, hypergammaglobulinemia, autoimmunity, and the presence of mature peripheral DN T cells. In 1992, Sneller *et al.* investigated two similar patients with progressive lymphoproliferative disease and autoimmunity and found they had a high population of the usually rare peripheral DN T cells. Drawing comparisons between the phenotypes seen in the patients and the phenotypes seen in *lpr* and *gld* mice it was suggested that these patients had a human equivalent of the murine disease (Sneller et al., 1992). In the same year, mutations in Fas and FasL were identified as being the cause of the phenotypes seen in the *lpr* and *gld* mice, respectively (Takahashi et al., 1994; Watanabe-Fukunaga et al., 1992a), and shortly thereafter it was documented by two groups that mutations in Fas were responsible for the human disease (Fisher et al., 1995; Rieux-Laucat et al., 1995).

Subsequent studies of mutations in ALPS patients have shown that ALPS can result from mutations not only in the Fas gene but also in other molecules involved in apoptotic pathways, which are not limited to the Fas-FasL signalling pathway. To date there are five classifications of ALPS and four classifications of ALPS-related disorders, which incorporate mutations in caspase-8 or proteins involved in the mitochondrial apoptotic pathway (Oliveira et al., 2010).

Autoimmune phenomena are also frequent in ALPS patients, with circulating autoantibodies seen in around 90% of cases (Straus et al., 1999). However, the autoimmune aggression is largely directed at blood cells, with little report of other autoimmune disease such as GN, hepatitis, arthritis or colitis (Deutsch et al., 2004). ALPS patients have also been reported to have elevated levels of circulating IL-10 (Fuss et al., 1997; Lopatin et al., 2001; Magerus-Chatinet et al., 2009).

*In vitro* studies with T cells have shown that ALPS patients' $CD4^+DR^+$ T cells were shifted to a $T_h2$ phenotype with increased production of IL-4 and IL-5 but decreased levels of IFN-γ and IL-2 when compared to control cells. DN T cells were found to produce very low levels of cytokines. ALPS patients' monocytes/macrophages were also found to produce 30-fold less IL-12 than control individuals (Fuss et al., 1997). $T_h1$ cells and $T_h17$ cells are more sensitive to Fas-mediated apoptosis compared to $T_h2$ cells (Fang et al., 2010). In an environment where Fas-FasL signalling is defective, but not completely deleted, $T_h1$ cells are placed more at risk, allowing $T_h2$ cells to accumulate. This, along with decreased production of IL-12 by monocytes/macrophages, could play a part in ALPS patients having a skewed $T_h2$ response (Fuss et al., 1997).

### 1.6.3 Lymphocyte homeostasis

Homeostasis of a cell population is dependent on the rate of cell proliferation, cell differentiation and also cell death, occurring through apoptosis. Tight maintenance of immune system homeostasis is vital for controlling an immune response. *Lpr, gld* and *lpr$^{cg}$* mice, as well as ALPS patients, all develop progressive lymphadenopathy, which predominantly involves the accumulation of DN T cells but also the accumulation of regular $CD4^+$ and $CD8^+$ T cells and B cells. This led to the conclusion that Fas-FasL signalling plays a critical role in lymphocyte homeostasis.

Fas-FasL signalling has been shown to be involved in both the activation and deletion of T cells. *In vitro*, anti-Fas antibodies were found to co-stimulate freshly isolated human T lymphocytes, along with anti-CD3 antibodies, causing T cell proliferation and secretion of cytokines (Alderson et al., 1993). This is supported *in vivo*; T cell activation was defective in mice carrying a mutation in the downstream signalling molecule FADD (Kennedy et al., 1999; Newton et al., 1998; Walsh et al., 1998; Zhang et al., 1998). Following an immune response, activated T cells need to be removed to downregulate the inflammatory reaction and prevent irreversible damage from occurring. This is done by a process called activation-induced cell death (AICD). Chronic restimulation of the TcR sensitises T cells to FasL-induced apoptosis (Kabelitz et al., 1993). *In vitro,* ligation of Fas on activated human T cells, by either a monoclonal anti-Fas antibody or recombinant human FasL, resulted in apoptosis of the cells (Alderson et al., 1995), whilst *in vivo, lpr, gld,* and *lpr$^{cg}$* mice show reduced, but not completely absent, deletion of peripheral T cells (Bossu et al., 1993; Russell et al., 1993; Russell and Wang, 1993). Activated $CD8^+$ T cells can also undergo Fas-induced AICD (Miyawaki et al., 1992), although a Fas-independent mechanism also contributes to the deletion of these cells (Ramaswamy et al., 2009). However, the Fas-FasL pathway plays no part in thymic negative selection as self-reactive T cells are effectively deleted in the thymus of *lpr, gld, and lpr$^{cg}$* mice (Singer and Abbas, 1994; Zhang et al., 2005).

Fas signalling also regulates B cell and dendritic cell homeostasis. Fas-FasL signalling is dispensable for B cell development but important in mediating peripheral B cell tolerance because *lpr, gld,* and *lpr$^{cg}$* mice accumulate B cells and have elevated levels of autoantibodies (Cohen and Eisenberg, 1991; Fields et al., 2001; Fukuyama et al., 1998). Mice lacking Fas on their B cells only, develop characteristic lymphadenopathy, splenomegaly, high autoantibody titres and accumulate T cells in a similar manner to *lpr, gld,* and *lpr$^{cg}$* mice,

emphasising the role of Fas in maintaining peripheral B cell tolerance (Stranges et al., 2007). Dendritic cells are also eliminated through Fas-FasL apoptosis, and this may serve to down modulate antigen presentation. Accumulation of dendritic cells is seen in *lpr* mice and also human patients harboring caspase 10 mutations (Fields et al., 2001; Wang et al., 1999).

## 1.7 Fas ligand and inflammation

### 1.7.1 Evidence for a pro-inflammatory role of Fas ligand

As well as an immune regulatory role, ligation of Fas has also been shown to cause a pro-inflammatory response by activating transcription factors, which in turn leads to the production of cytokines and the recruitment and activation of immune cells. The pro-inflammatory effect of FasL on monocytes and macrophages has been researched extensively, but is still not fully understood. *In vivo,* injection of a membrane-bound cell-free form of FasL into the peritoneum of mice led to the rapid activation and subsequent demise of $Mac1^{high}$ resident peritoneal macrophages, as measured by an increase in gene expression of neutrophil chemotactic factors, IL-1β, macrophage inflammatory protein (MIP)-2, MIP-1α, and MIP-1β (Hohlbaum et al., 2001), whilst *in vitro,* Fas ligation on human monocytes and monocyte-derived macrophages resulted in the release of TNF-α and IL-8. Also, conditioned medium from Fas-activated monocytes and macrophages induced the directed migration of neutrophils in a chemotaxis assay (Park et al., 2003).

The induction of chemokine and cytokine synthesis by macrophages is due to the activation and nuclear translocation of the transcription factor NF-κB. Fas ligation on macrophages enhances NF-κB signalling through the IL-1 receptor (IL-1R) and toll-like receptor 4 (TLR4). IL-1R and TLR4 share a common adaptor protein, MyD88, which carries a DD sequence. Through homologous DD interactions, FADD associates with MyD88, sequestering it from IL-1R and TLR4 signalling. However, when FasL signals through Fas and FADD is required for DISC assembly, MyD88 is released for IL-1R and TLR4 signalling allowing activation of NF-κB (Altemeier et al., 2007; Bannerman et al., 2002; Ma et al., 2004).

More recently, FasL has been implicated in the activation of macrophages. Chakour *et al.* found that FasL and IFN-γ acted synergistically to activate bone marrow-derived macrophages (BMDM), as reflected by enhanced secretion of TNF-α, IL-6 and nitric oxide (NO) and the induction of their microbicidal activity. The presence of IL-4 decreased this synergy (Chakour et al., 2009). Fas signalling has also been shown to recruit and activate Syk kinase, leading to the activation of phosphoinositide 3-kinase (PI3K) and MMP-9 and ultimately the migration of peripheral blood myeloid cells (Letellier et al., 2010). In cultured dermal fibroblasts, signalling through Fas upregulated vascular endothelial growth factor (VEGF) and MCP-1 expression (Fujiwara et al., 2007).

As already mentioned, sFasL is a weak inducer of apoptosis, suggesting that cleavage of FasL from the membrane may serve to downregulate its apoptotic activity. However, this does not mean sFasL does not play an important role in the immune system as it has been shown to act as a potent chemoattractant for polymorphonuclear neutrophils (PMN). Using a recombinant soluble form of human FasL and a Boyden Chamber, Seino *et al.* found sFasL acted as a chemoattractant for both human and mouse PMN, and also HL-60 cells when differentiated into neutrophils or monocytes. This activity could be abolished using a neutralising anti-FasL monoclonal antibody. PMN derived from *lpr* mice, that express very few Fas molecules, did not respond to sFasL, whereas PMN derived from $lpr^{cg}$ mice responded normally (Seino et al., 1998). Two groups went on to conclude that FasL exerts its pro-inflammatory effects via neutrophil recruitment but not activation. Neutrophils exposed to sFasL did not display detectable changes in $Ca^{2+}$ and did not undergo superoxide production or exocytosis of primary or secondary granules (Dupont and Warrens, 2007; Ottonello et al., 1999). As well as having chemotactic activity, sFasL was also found to induce IL-6 and IL-8 gene expression in serum-starved human fibroblasts. Sensitisation of the gene-inducing activity by serum starvation correlated with NF-κB activation by sFasL (Ahn et al., 2001).

### 1.7.2 Evidence for a role of Fas ligand in inflammatory diseases

A few groups have concentrated on looking at the role of the Fas-FasL system in inflammatory diseases using well established animal models and either *lpr* or *gld* mice. In 1997, two groups simultaneously published results in the same journal that *lpr* and *gld* mice were resistant to the induction of experimental autoimmune encephalomyelitis (EAE), the T cell-dependent animal model of the autoimmune demyelinating disease MS. Despite EAE being a T cell-dependent model, the T cell responses of both *lpr* and *gld* mice were found to be unaffected when compared to WT mice, suggesting that the Fas-FasL system plays a critical role in disease development by mediating apoptosis within the target tissue (Sabelko et al., 1997; Waldner et al., 1997). One of the groups then went on to show, using adoptive transfer, that FasL was playing a dual role in the initiation and the recovery of EAE. Transfer of *gld* lymphocytes into WT mice was found to attenuate disease, suggesting a role for T cell FasL in disease initiation, however *gld* mice receiving WT lymphocytes developed prolonged clinical signs of disease, suggesting FasL expressed by cells of the central nervous system plays a role in disease recovery (Sabelko-Downes et al., 1999).

Research has also been conducted looking at the role of Fas/FasL in autoimmune diabetes using non-obese diabetic (NOD) mice. NOD-*lpr* mice are protected from developing autoimmune diabetes and adoptive transfer of lymphocytes from diabetic NOD mice into NOD-*lpr* mice failed to induce disease, suggesting that the Fas-FasL system might be critical for autoimmune β cell destruction in the pancreas (Chervonsky et al., 1997; Itoh et al., 1997). However, this was later disproved by two groups who found the Fas-FasL system played little role in β cell apoptosis (Allison and Strasser, 1998; Kim et al., 1999). In 2000, Kim *et al.* set about to solve the paradox and found that lymphocytes from NOD-*lpr* mice were constitutively expressing FasL and having a cytotoxic effect on the lymphocytes from the NOD mice. Blocking FasL with an anti-FasL antibody reversed the inhibition of disease following lymphocyte transfer, supporting the previous reports that FasL is not an effector molecule in autoimmune β cell destruction (Kim et al., 2000). This result has not stopped other groups looking at the role of FasL in autoimmune diabetes. Mohamood *et al.* found that NOD-*gld* mice were protected from developing disease and, by creating bone marrow chimeras with NOD-WT mice, that partial disruption of FasL protects from disease because inactivation of FasL in either the hematopoietic or non-hematopoietic compartment was sufficient for protection (Mohamood et al., 2007). Similar results were then demonstrated genetically in NOD-*gld*/+ mice, heterozygous for the FasL mutation. These mice were

protected from both autoimmune diabetes and T cell lymphoproliferation (Mohamood et al., 2007).

Other inflammatory diseases examined include experimental autoimmune uveitis (EAU), collagen-induced arthritis (CIA), inflammatory lung disease, experimental stroke, and spinal cord injury. *Gld* mice are protected from EAU; a T cell-mediated autoimmune disease, with FasL expression on cells of the immune system important for induction of disease. It was also noted that *lpr* and *gld* T cells, *in vitro*¸ responded less to antigen compared to WT T cells and produced less of a $T_h1$ response, as measured by IFN-γ production (Wahlsten et al., 2000).

CIA is a T cell-mediated, chronic inflammatory disease, bearing the hallmarks of RA. One feature of the disease that contributes to joint damage is synovial hyperplasia, which is thought to be due to an imbalance between the rates of cell proliferation and apoptosis. *Lpr* mice on a DBA/1 background are protected from CIA (Ma et al., 2004; Tu-Rapp et al., 2004). Interestingly, the mice still had elevated levels of the critical pro-inflammatory cytokine IL-1β in their joints; however there was inefficient activation of the IL-1R signalling pathway due to disruption of Fas signalling (Ma et al., 2004).

Both *lpr* and *gld* mice were protected from developing acute pulmonary damage in the animal model of IgG immune complex-induced lung injury. In WT lungs, there was a marked increase in Fas expression associated with the lung injury and striking evidence of activated caspase-3, which was diminished in inflamed lungs from *lpr* mice. Also, intra-tracheal administration of a monoclonal Fas-activating antibody in WT mice was found to induce production of MIP-2 and keratinocyte chemoattractant (KC) in bronchoalveolar lavage fluids. Levels of these chemokines in bronchoalveolar lavage fluids from *lpr* mice, following lung injury, were significantly lower compared to WT mice. These data together suggest that the Fas/FasL system regulates acute lung inflammation by positively affecting CXC-chemokine production and enhancing neutrophil influx and tissue damage (Neff et al., 2005).

Recently, the role of FasL in experimental stroke has been explored. Focal cerebral ischemia was induced for 2 hours by right middle cerebral artery occlusion in WT and *gld* mice. *Gld* mice showed profoundly reduced brain damage and improved neurological performance from 6 to 72 hours after ischemic stroke. The production of inflammatory cytokines was attenuated in the *gld* mice, as was the recruitment of neutrophils. In addition,

$CD8^+$ T cell numbers were also reduced and the $T_h1/T_h2$ balance was skewed towards a $T_h2$ response in both the brain and peripheral blood, offering further support that *gld* mice are predisposed towards a $T_h2$ response (Niu et al., 2011).

Expression of FasL can also be induced on myeloid cells in spinal cord injury, where it binds and stimulates Fas to activate PI3K and MMP-9 via recruitment and activation of Syk kinase. This leads to increased migration of inflammatory cells to the site of injury. Deletion of FasL on myeloid cells only greatly reduced the numbers of infiltrating neutrophils and macrophages in the injured spinal cord and led to functional recovery. However, deletion of Fas on neural cells did not lead to functional recovery, indicating that FasL on myeloid cells is important for cell migration and injury (Letellier et al., 2010).

### 1.7.3 Evidence for a role of Fas ligand in renal injury

Fas and FasL are both widely expressed throughout the kidney. Fas is constitutively expressed on mesangial and tubular cells, podocytes and fibroblasts, with upregulation occurring during inflammation (Sanchez-Nino et al., 2010), as well as on glomerular endothelial cells, with upregulation occurring following exposure to pro-inflammatory cytokines (Sata et al., 2000). FasL expression has been shown in both normal and injured kidneys in humans and mice. Normal expression of FasL in the kidney is by tubular epithelial cells; however during injury expression is upregulated within the glomerulus, with mesangial cells being a potential source (Lorz et al., 2000; Tsukinoki et al., 2004). Other possible sources of renal FasL are thought to be podocytes, endothelial cells and fibroblasts (Ortiz et al., 1999; Ross et al., 2005). Dual expression of both Fas and FasL could result in paracrine/autocrine cell death. However, on tubular cells for example, Fas and FasL are segregated from each other: Fas is restricted to the basolateral surface whilst FasL is sequestered to an intracellular compartment and the apical surface (Tan and Hunziker, 2003). This segregation is lost upon disruption of tight junctions by physical injury, ischemia or pro-inflammatory cytokines.

*In vivo,* FasL has been implicated as playing a pathogenic role in kidney injury. Following induction of ischemia-reperfusion injury (IRI), *gld* mice had significantly lower serum creatinine and fewer TNF-α-producing T lymphocytes in the kidneys and lymph nodes, compared to WT mice. Blockade of FasL in WT mice with a monoclonal antibody

protected them from IRI (Ko et al., 2011). Furthermore, transfer of *gld* splenocytes to WT mice attenuated IRI whereas transfer of WT splenocytes to *gld* mice enhanced injury, demonstrating that FasL expression on leukocytes mediates acute kidney injury (Ko et al., 2011). When studying obstruction-induced renal tubular cell apoptosis in a model of unilateral ureteral obstruction (UUO), it was found that IL-18 significantly increased the expression of FasL. Similarly, small interfering RNA (siRNA) knockdown of FasL significantly reduced IL-18-induced apoptosis (Zhang et al., 2011). In a model of cisplatin-induced nephropathy it was found blockade of FasL, with a monoclonal anti-FasL antibody, protected SCID-beige mice (lacking B cells, T cells and NK cells) from disease, suggesting expression of FasL by tubular epithelial cells is capable of causing apoptosis of neighbouring tubular cells (Linkermann et al., 2011). This was then supported *in vitro* by co-incubation of primary tubular cells with segments of thick ascending limb (Linkermann et al., 2011).

There is mounting evidence that FasL plays a role in GN, although the results are conflicting as to whether its role is pro-inflammatory or anti-inflammatory. *Lpr* and *gld* mice, when bred on permissive backgrounds, such as MRL, develop spontaneous autoimmunity and a lupus-like GN, suggesting a protective role for FasL (Izui et al., 1984). This has recently been attributed to the membrane-bound form of FasL. Mice bred to express sFasL only, on a C57BL/6 background, developed a lupus-like GN more severe than *gld* mice on the same background, whereas mice expressing membrane-bound FasL only appeared normal. The authors hypothesised that this result was seen due to a combination of the autoimmune phenomena, resulting from the deletion of membrane-bound FasL, and an increase in pro-inflammatory activity, caused by an increase in sFasL. However, it is not possible to compare directly these mice, as FasL activity is not completely abrogated in *gld* mice (O' Reilly et al., 2009). However, FasL also appears to play a damaging role in GN. Agonistic anti-Fas antibodies were found to induce glomerular cell apoptosis and injury in mice *in vivo* and treatment of lupus prone mice, NZB/W F1, with an anti-FasL monoclonal blocking antibody twice a week for 15 weeks, was found to prevent the development of lupus nephritis, although the mice had higher autoantibody titres (Gonzalez-Cuadrado et al., 1997; Nakajima et al., 2000).

Although conflicting, it must be noted that results from experiments using antibody blockade are not directly comparable to loss-of-function gene mutations present from birth. This is especially true with the Fas-FasL system, which plays a complicated dual-role in the regulation of autoimmunity and inflammation. The defect in apoptosis in the *gld* mice means

they are prone to developing spontaneous autoimmunity, due to the role of FasL in mediating lymphocyte homeostasis. The lack of functional FasL in these mice leads to an accumulation of B cells and T cells and an inability to maintain peripheral B cell tolerance (Stranges et al., 2007). It should be noted though, that this is strain dependent. In some strains, such as C57BL/6, compensatory systems are in place that can slow the onset or severity of autoimmunity; TNF-TNF receptor-mediated apoptosis has been shown to partially compensate for the Fas deletion in *lpr* mice on a C57BL/6 background (Zhou et al., 1996). In the lupus prone mice however, where FasL-dependent apoptosis of lymphocytes is intact, it appears FasL may be playing a pro-inflammatory role, either via its role in neutrophil recruitment or its role in IL-1 signalling (Nakajima et al., 2000).

## 1.8 Fc gamma receptors

### 1.8.1 Introduction

Fc receptors (FcR) are a family of cell surface molecules that bind the Fc part of the constant region of immunoglobulins and contribute to the protective functions of the immune system. They are mainly expressed on cells of haematopoietic lineage such as NK cells, macrophages, neutrophils, mast cells, dendritic cells, and B cells. Their cross-linking with immunoglobulins can initiate an array of cellular responses; phagocytosis, endocytosis, antibody-dependent cell-mediated cytotoxicity (ADCC), mast cell degranulation, immunomodulation of antibody responses, and lymphocyte proliferation.

Fc gamma receptors (FcγR) specifically bind the Fc portion of IgG. Based on genetic and structural analysis there are three classes of FcγR in humans and four classes in mice (Figure 1.5). The high affinity receptor, FcγRI (CD64), is capable of binding monomeric IgG (especially IgG2a) and the low affinity receptors, FcγRII (CD32) and FcγRIII (CD16), preferentially bind complexed IgG (Dijstelbloem et al., 2001). FcγRIV (CD16-2), which is only found in mice, is also a low affinity receptor that binds IgG2a and IgG2b with no affinity for IgG1 or IgG3 (Nimmerjahn et al., 2005).

The human FcγR system is more complex than the murine system. Mice express four different FcγRs: FcγRI, FcγRIIB, FcγRIII and FcγRIV; whereas humans express six: FcγRI, FcγRIIA, FcγRIIB, FcγRIIC, FcγRIIIA and FcγRIIIB (Radaev and Sun, 2002). In addition there are also several allelic variants for most of the human FcγR genes, with the exception of FcγRI and FcγRIIC (Nimmerjahn and Ravetch, 2008). Based on the sequence similarity in the extracellular portion of the FcγR, as well as the genomic localisation, FcγRI and FcγRIIB are homologous between mice and humans, whereas it appears mouse FcγRIV is most closely related to human FcγRIIIA and mouse FcγRIII is most closely related to human FcγRIIA. There are no murine equivalents to human FcγRIIC and FcγRIIIB (Nimmerjahn and Ravetch, 2006) (Figure 1.5).

Human and murine FcγR are structurally related. They are type I membrane proteins (although soluble molecules can occur through alternative splicing of FcγR transcripts or proteolysis), except for FcγRIIIB that is glycosylphosphatidylinositol **(**GPI)-anchored, and contain either two (FcγRII, FcγRIII and FcγRIV) or three (FcγRI) Ig-like domains in their

extracellular region. The third Ig-like domain of FcγRI is thought to be responsible for its increased affinity to bind monomeric IgG (Radaev and Sun, 2002).

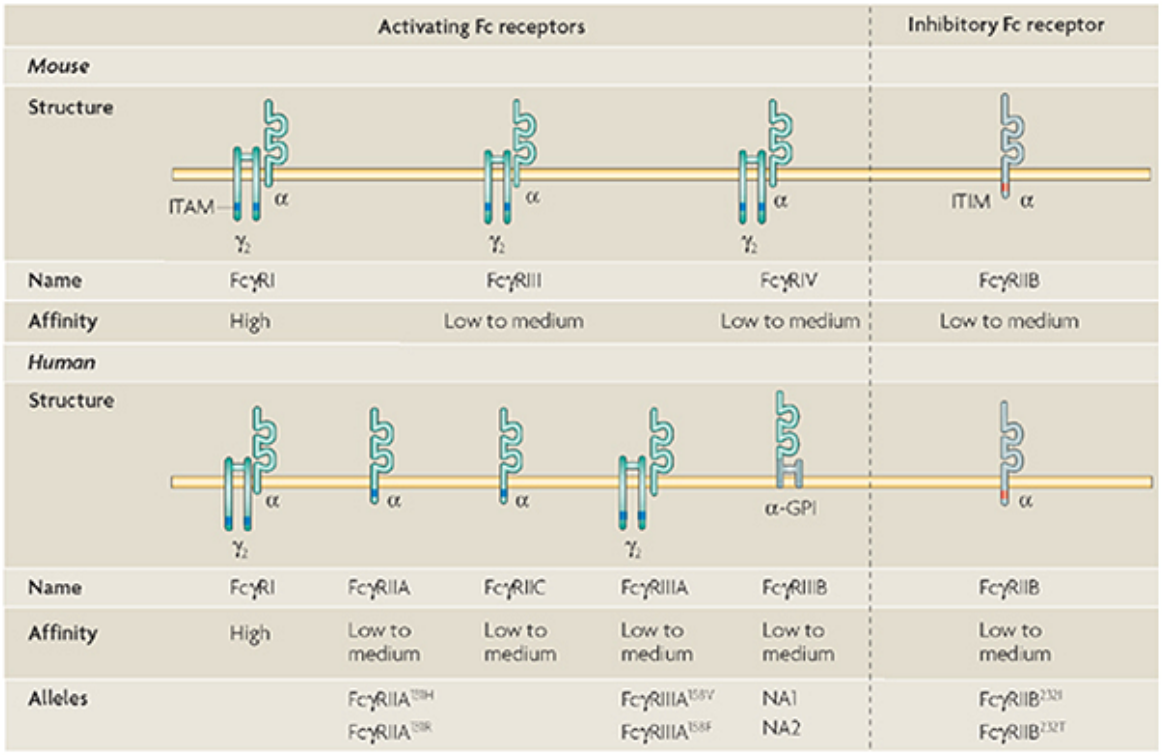


**Figure 1.5 Mouse and human Fc gamma receptors.**

Human and murine activating and inhibitory FcγR (Nimmerjahn and Ravetch, 2008). This image has been reproduced with the permission of the rights holder, Nature Publishing Group.

### 1.8.2 Fc gamma receptor signalling

FcγR can be functionally divided into activating receptors and inhibiting receptors. In humans the activating receptors are FcγRI, FcγRIIA, FcγRIIC, FcγRIIIA and FcγRIIIB, and in mice they are FcγRI, FcγRIII and FcγRIV. FcγRIIB is the sole inhibitory FcγR in both humans and mice. With the exception of FcγRIIIB, functional activating FcγR either contain an immunoreceptor tyrosine-based activation motif (ITAM), responsible for cell signalling, in their cytoplasmic tail (in humans FcγRIIA and FcγRIIC), or are associated with an ITAM containing non-covalently attached intracellular signal-transducing adaptor molecule, a FcR γ (FcRγ) chain (in humans FcγRI and FcγRIIIA and in mice FcγRI, FcγRIII and FcγRIV) (Cambier, 1995; Reth, 1989). FcγRIIIB is not associated with a FcRγ chain and does not contain an ITAM within its cytoplasmic tail, instead it is thought to act synergistically with other receptors, such as FcγRIIA, and use their signalling apparatus for signal transduction and cell activation (Unkeless et al., 1995; Wirthmueller et al., 1992). The inhibitory receptor, FcγRIIB, carries an immunoreceptor tyrosine-based inhibition motif (ITIM) within its cytoplasmic tail (Daeron et al., 1995). Activating and inhibitory FcγR are often co-expressed on cells and, when co-aggregated at the cell surface, the net signal to the cell depends upon the sum total of the activator and inhibitor signals. Expression of activating and inhibiting receptors is tightly controlled by the cytokine milieu surrounding the cell (Pricop et al., 2001; Radeke et al., 2002)

The ITAM is composed of a twice-repeated YxxL/I amino acid sequence flanking 7 variable residues (x represents any amino acid) (Reth, 1989). The ITAM has no intrinsic enzymatic activity; however, following receptor cross-linking by immune complexes, tyrosine phosphorylation of the ITAM is induced by SRC kinase family members. Phosphorylation of the ITAM generates SRC homology 2 (SH2) docking sites that recruit and activate members of the Syk-family of kinases. Syk can then activate various downstream targets, such as PI3K, which leads to the production of phosphatidylinositol (3,4,5)-triphosphate ($PIP_3$), a key product in the recruitment of further downstream molecules. The responses that result from FcγR signalling largely depends on the cell type involved, but they mainly fall into two main categories of activation or internalisation (Nimmerjahn and Ravetch, 2008; Ravetch and Bolland, 2001).

The ITIM is composed of a six amino acid sequence, S/I/V/LxYxxI/V/L, where x denotes any amino acid (Daeron et al., 1995; Muta et al., 1994). Following receptor cross-

linking to ITAM-bearing receptors by immune complexes, tyrosine phosphorylation of the ITIM is induced by SRC kinase family members. This phosphorylation results in the recruitment of phosphatases, such as SHIP (SH2-domain-contraining inositol polyphosphate 5' phosphatase), that interfere with the signalling pathways being stimulated by the phosphorylated ITAM, namely by hydrolysing $PIP_3$ (Nimmerjahn and Ravetch, 2006, 2008; Ravetch and Bolland, 2001).

### 1.8.3 Fc gamma receptor expression

The activating FcγR are widely expressed throughout the haematopoietic system. However not all cells express all activating FcγR. In humans, FcγRI is constitutively expressed by monocytes and macrophages and can be induced in neutrophils and eosinophils following stimulation with IFN-γ (Goulding et al., 1992; Valerius et al., 1990). FcγRIIA and FcγRIIC are expressed by myeloid cells. FcγRIIIA is found on NK cells, a subset of macrophages (Edwards et al., 1997), but is not present on the majority of circulating monocytes, however stimulation with TGF-β can induce expression during activation and maturation to macrophages *in vitro* (Wong et al., 1991). FcγRIIIB is expressed solely on neutrophils (Edwards et al., 1997). A similar picture is seen in mice. Monocytes and macrophages express FcγRI, FcγRIII and FcγRIV; dendritic cells express FcγRI and FcγRIII; neutrophils express FcγRIII and FcγRIV; and NK cells express FcγRIII (Nimmerjahn and Ravetch, 2008).

The inhibitory FcγR, FcγRIIB, is the most widely expressed, being found on most cells of myeloid and lymphoid lineage (with the exception of NK cells and T cells) where it is responsible for the negative regulation of activating FcγR. FcγRIIB is the only antibody-binding Fc receptor expressed on B cells where it plays a role in downregulating B cell activation, proliferation, and antibody secretion, as well as maintaining peripheral tolerance (Boross et al., 2011; Takai et al., 1996).

## 1.9 Functions of Fc gamma receptors

Binding of IgG to FcγR can initiate various functions, depending on the cell type and the balance of activating and inhibitory receptors being ligated. The overall organisation of human and murine FcγR is similar. The cellular distribution and signalling capacities of FcγR overlap between the two species, so by studying the murine receptors we can gain insight into the functions of their human counterparts. The generation of FcγR-deficient mice has made it possible to dissect the functions of FcγR *in vivo* and study the roles of these receptors in inflammation and autoimmunity. These functions can be classified into two major categories: regulation of cellular responses and uptake of immune complexes (Figure 1.6). The involvement of FcγR in each of these roles will be discussed in the following sections.

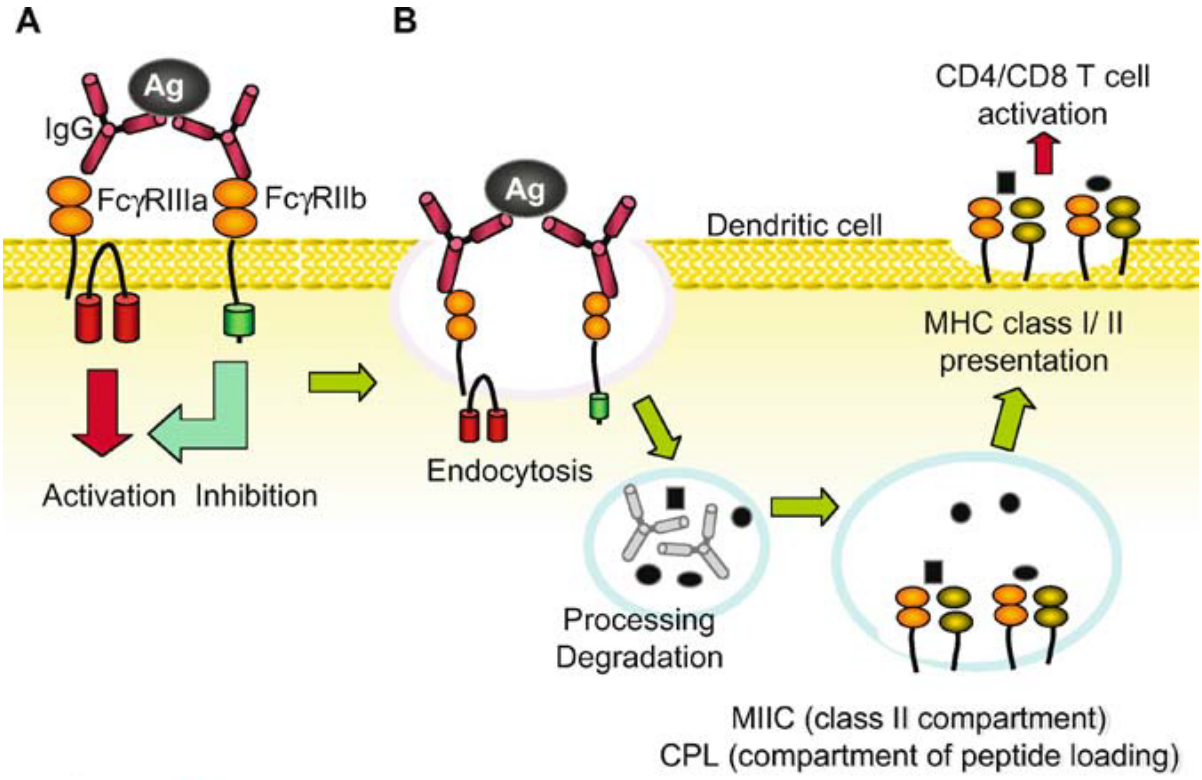


**Figure 1.6 Major functions of Fc gamma receptors.**

**(A)** Positive and negative regulation of cellular signalling. **(B)** Immune complex uptake for antigen presentation of clearance. Adapted from (Takai, 2005). This image has been reproduced with the permission of the rights holder, Springer Science + Business Media.

### 1.9.1 Regulation of cellular responses

Clustering of activating and inhibitory FcγR on the cell surface allows for the tight regulation of cell activation or suppression, which is critical for defence against IgG-complexed antigens. FcγR are expressed on most leukocytes, with the exception of T cells, allowing positive and negative regulation of both the adaptive and innate immune response. Co-aggregation of activating FcγR can lead to various cellular responses such as oxidative burst, cytokine release, and phagocytosis by macrophages, ADCC by NK cells, and degranulation of mast cells. FcγRIIB physiologically acts as a negative regulator. With the exception of NK cells, that only express activating FcγR, FcγRIIB acts to dampen the effects of immune complex-triggered activation.

The generation of single and multiple FcγR knockout mice has provided the opportunity to study the roles of FcγR *in vivo* and *in vitro* and dissect their specific functions in different cellular subsets. Initial studies into the functions of FcγR were done using FcRγ chain-deficient mice ($FcR\gamma^{-/-}$). These mice lack the γ chain necessary for signalling through activating FcγR and show an absence of surface expression of FcγRI, FcγRIII, FcγRIV and also the high-affinity IgE receptor, Fc epsilon receptor (FcεRI). Mast cell degranulation, seen in immediate hypersensitivity responses such as allergy, is initiated by IgE binding to FcεRI. In keeping with this, both cutaneous and systemic IgE-mediated anaphylaxis was found to be absent in $FcR\gamma^{-/-}$ mice (Takai et al., 1994). However, passive systemic anaphylaxis, following IgG stimulation was also attenuated, suggesting a role for FcγR in mast cell degranulation (Miyajima et al., 1997). Further studies, using single FcγR knockout mice, went on to show enhanced mast cell degranulation in $Fc\gamma RIIB^{-/-}$ mice and that FcγRIII, in particular, was responsible for IgG-mediated anaphylaxis rather than FcγRI (Hazenbos et al., 1996; Ioan-Facsinay et al., 2002; Ujike et al., 1999). Mast cells do not express FcγRIV.

Macrophages and monocytes from mice express all four classes of FcγR. Phagocytosis of antibody-coated particles was found to be inhibited in $FcR\gamma^{-/-}$ macrophages compared to WT macrophages, despite normal binding (Takai et al., 1994). However, macrophages from $Fc\gamma RI^{-/-}$ mice were found to have impaired binding of IgG2a-opsonised particles (Ioan-Facsinay et al., 2002) and macrophages from $Fc\gamma RIII^{-/-}$ mice were found to have impaired binding and phagocytosis of IgG1-opsonised particles (Hazenbos et al., 1996). As well as impaired binding of IgG2a-opsonised particles, ADCC was also decreased in $Fc\gamma RI^{-/-}$ macrophages (Ioan-Facsinay et al., 2002). In contrast, $Fc\gamma RIIB^{-/-}$ macrophages were

shown to have enhanced phagocytic activity of IgG2b-opsonised particles and, following FcγRIII cross-linking with a FcγRII/III specific antibody, calcium influx was also greatly increased compared to WT macrophages (Clynes et al., 1999). To date little work has been done on the role of FcγRIV on macrophages and monocytes in mice. FcγRIV binds IgG2a and IgG2b but not IgG1 or IgG3. This could explain in part why, in the absence of FcγRI, macrophages still have the capability to phagocytose IgG2a-opsonised particles.

NK cells have the capability to kill IgG-coated target cells by ADCC. FcγRIII is the sole FcR expressed by NK cells and therefore mediates all antibody dependent responses on these cells. As expected, ADCC was abolished in both FcRγ$^{-/-}$ mice (Takai et al., 1994) and FcγRIII$^{-/-}$ mice (Hazenbos et al., 1996).

As mentioned in Section 1.8.3, FcγRIIB is the only FcR expressed on B cells and its inhibitory function has best been demonstrated on these cells. FcγRIIB plays an important role in B cell regulation and survival. Cross-linking of the B cell receptor (BcR) with FcγRIIB by immune complexes activates a distinct ITIM-dependent pathway that inhibits B cell proliferation, maturation and the production of cytokines (Phillips and Parker, 1984). However, cross-linking of FcγRIIB in the absence of the BcR initiates a bim-dependent apoptosis pathway (Ashman et al., 1996; Pearse et al., 1999; Tzeng et al., 2005; Xiang et al., 2007). This mechanism allows FcγRIIB to maintain peripheral tolerance and delete self-reactive B cells. Immune complexes will preferentially aggregate FcγRIIB if the BcR has a low affinity for the antigen. In contrast, the BcR will preferentially bind immune complexes with high affinity cognate antigen, thus providing a survival signal (Pearse et al., 1999). Reduced expression of FcγRIIB can therefore promote B cell survival as well as lower their activation threshold. Studies using FcγRIIB-deficient mice have highlighted the importance of the receptor in B cell regulation. FcγRIIB$^{-/-}$ mice have hyper-reactive B cells that produce increased antibody titres in response to both thymus-dependent and thymus-independent antigens (Takai et al., 1996).

### 1.9.2 Uptake of immune complexes

Uptake of immune complexes by dendritic cells and macrophages is important for antigen presentation and immune complex clearance. Dendritic cells are the only APC capable of initiating adaptive immune responses. To do this they must first go through a differentiation process called 'maturation'. FcγR have been found to play a central role in dendritic cell maturation. Cross-linking of FcγR by immune complexes induced maturation of human dendritic cells *in vitro* (Banki et al., 2003; Boruchov et al., 2005). This affect was abolished in murine FcRγ$^{-/-}$ dendritic cells (Sedlik et al., 2003) but not in FcγRI$^{-/-}$ or FcγRIII$^{-/-}$ dendritic cells, suggesting both receptors are capable of inducing maturation (Sedlik et al., 2003). FcγRIV is also highly expressed in dendritic cells and likely to be involved in initiating their maturation (Nimmerjahn et al., 2005; Nimmerjahn and Ravetch, 2006). FcγRIIB expression on dendritic cells appears to be important in preventing inappropriate activation and controlling the degree of activation. Selective blockade of FcγRIIB resulted in spontaneous maturation of dendritic cells (Boruchov et al., 2005; Dhodapkar et al., 2005).

As well as maturation, FcγR are also involved in immune complex uptake and antigen presentation by dendritic cells. FcγR-mediated antigen uptake was found to enhance the antigen presentation of the dendritic cells, resulting in the activation of both CD4$^{+}$ and CD8$^{+}$ T cells (Amigorena and Bonnerot, 1999; Regnault et al., 1999). FcγRIIB controls the magnitude of this response. Dendritic cells from FcγRIIB$^{-/-}$ mice generate a stronger and longer-lasting immune response both *in vitro* and *in vivo* (Kalergis and Ravetch, 2002).

Following an antigen-antibody reaction, immune complexes need to be efficiently removed from circulation because their deposition in tissues and organs can set off reactions resulting in inflammation and tissue damage (Jancar and Sanchez Crespo, 2005; Mayadas et al., 2009). Deposition of immune complexes is a prominent feature of several autoimmune diseases, for example, SLE (Bagavant and Fu, 2009; Niederer et al., 2010).

Immune complex clearance is regulated by the mononuclear phagocyte system. Erythrocytes, in primates, or platelets, in non-primates, bind to immune complexes through their complement receptor 1 (CR1) and transport them to the liver or spleen. Once there, the immune complexes are removed from the erythrocytes by proteolytic cleavage of CR1 and internalised by tissue-resident phagocytes, with the erythrocytes returning to circulation (Cornacoff et al., 1983; Nardin et al., 1999).

The role of FcγR in this process has been highlighted both *in vivo* and *in vitro*. *In vivo*, blockade of murine FcγR with a monoclonal antibody inhibited the binding and internalisation of CR1-bound immune complexes (Kurlander et al., 1984) and *in vitro,* the application of anti-FcγRI antibody on U937 cells prevented recognition and transfer of erythrocyte CR1-bound immune complexes (Craig et al., 2000).

## 1.10 Fc gamma receptors in glomerulonephritis

Many forms of human GN, such as lupus nephritis and Goodpasture's disease, are characterised by deposition of immune complexes within the kidney, suggesting the involvement of FcγR. Further evidence for the involvement of FcγR in autoimmune diseases, and subsequently GN, comes from genetic studies of humans, rats, and autoimmune prone strains of mice, as well as the generation of different FcγR-deficient mice. The roles of activating and inhibiting FcγR in autoimmunity and GN are discussed in the following two sections.

### 1.10.1 Activating Fc gamma receptors

Initial studies to look at the roles of activating FcγR in GN were carried out in FcRγ$^{-/-}$ mice. FcRγ$^{-/-}$ mice were found to be protected from accelerated NTN with no glomerular crescents, thrombosis, proteinuria or renal failure and reduced leukocyte influx, despite producing a similar immune response to WT mice (Park et al., 1998; Suzuki et al., 1998). *In vitro* data from Radeke *et al.* showed that expression of FcγR was upregulated on mesangial cells following stimulation with IFN-γ and LPS (Radeke et al., 2002). However, results from bone marrow transplantation experiments performed between WT and FcRγ$^{-/-}$ mice showed that susceptibility to disease was entirely dependent on FcγR expression on circulating leukocytes (Tarzi et al., 2002).

However, using FcRγ$^{-/-}$ mice is not conclusive proof that activating FcγR are involved in immune-mediated nephritis because the FcRγ chain is the intracellular signalling subunit for more than just the FcγR, such as the collagen receptor glycoprotein VI (GPVI) (Berlanga et al., 2002). Development of mice lacking the α chains of specific FcγR has helped with

discovering which of the activating receptors are important. Deletion of FcγRIII was found to protect mice from the heterologous model of NTN (Coxon et al., 2001). This was initially explained by the heterologous phase of NTN being neutrophil-dependent since FcγRI is not expressed on neutrophils; however, this theory does not account for FcγRIV. To date, little research has been carried out on the role of FcγRIV in GN, although there are some suggestions that it works alongside FcγRIII in the manifestations of disease due to its selective affinity for IgG2a and IgG2b (Giorgini et al., 2008). In accelerated NTN, deletion of FcγRIII alone was not sufficient to protect from disease, suggesting roles for FcγRI and FcγRIV (Tarzi et al., 2003).

A link between FcγRIII and GN has also been found in rats and humans. WKY rats are highly susceptible to NTN and EAG when compared to other rat strains, such as LEW or BN. Injury and crescent formation in NTN are macrophage driven. Ten days following a single injection of NTS, WKY rats consistently develop NTN, whereas LEW, BN and Wistar show no crescent formation, no proteinuria and minimal glomerular macrophage infiltration. $F_1$ rats (WKY and LEW) show an intermediate phenotype and $F_2$ rats span the range of the parental strains (Aitman et al., 2006).

Aitman *et al.* carried out a genome wide screen for NTN susceptibility loci in the $F_2$ strain and found two major quantitative trait loci (QTL) on chromosomes 13 and 16, designated *Crgn1* and *Crgn2* respectively. Both loci were strongly linked to crescent formation and proteinuria, and *Crgn1* was also found to be linked to macrophage infiltration. *Crgn1* was found to contain several candidate genes, including the genes for FcγRII (*Fcgr2*) and FcγRIII (*Fcgr3*). Sequencing of *Fcgr2* revealed a point mutation, G388T, which changes codon 103 from arginine in LEW rats to leucine in WKY rats. Sequencing of *Fcgr3* revealed genomic rearrangement involving the *Fcgr3* locus. Further investigation showed that WKY rats had lost a rat-specific *Fcgr3* paralogue, *Fcgr3*-related sequence (*Fcgr3-rs*), which results in macrophage overactivity, inhibition of FcγRIII mediated phagocytosis, and susceptibility to GN. Studies in humans revealed that low copy number of *FCGR3B,* an orthologue of rat *Fcgr3*, was associated with GN in patients with SLE (Aitman et al., 2006). An explanation for the relationship between copy number variation of FcγRIIIB and SLE susceptibility is the reduced expression of FcγRIIIB on neutrophils and consequently the reduced clearance of immune complexes (Willcocks et al., 2008).

### 1.10.2 Inhibitory Fc gamma receptor

Several autoimmune disease-prone strains of mice, such as NZB, BXSB, MRL, and NOD, contain a polymorphism in the promoter region of the FcγRIIB gene that is absent in control mouse strains, for example BALB/c and C57BL/6. The autoimmune haplotype is associated with reduced cell surface expression of FcγRIIB on macrophages and activated B cells, and with hyperactive macrophages resembling those in FcγRIIB$^{-/-}$ mice (Pritchard et al., 2000). Over-expression of FcγRIIB on B cells, but not macrophages, was found to inhibit the development of spontaneous SLE (Brownlie et al., 2008). FcγRIIB deficiency in Mrl-MpJ mice was found to lead to autoimmunity with chronic B cell activation, serum reactivity to several autoantigens, and kidney pathology by 8 months of age (McGaha et al., 2008).

The outcome of FcγRIIB deficiency in control mice is strain-dependent. The 129/B6/FcγRIIB$^{-/-}$ strain was backcrossed for 12 generations onto both BALB/c and C57BL/6 strains. C57BL/6 FcγRIIB$^{-/-}$ mice were susceptible to spontaneous SLE with anti-DNA and anti-chromatin antibodies, and fatal autoimmune GN with a mean survival of 9 months, whereas BALB/c FcγRIIB$^{-/-}$ mice maintained tolerance and were resistant to autoimmunity. Autoimmunity was shown to be dependent on the loss of peripheral tolerance by FcγRIIB$^{-/-}$ B cells in the B6 background (Bolland and Ravetch, 2000). However, loss of FcγRIIB alone is not sufficient to induce autoimmunity. Boross *et al.* generated an FcγRIIB knockout strain, by gene targeting in B6-derived embryonic stem (ES) cells, and found that the mice did not develop spontaneous disease, but when the B6 FcγRIIB$^{-/-}$ mice were crossed with the autoimmune-prone *Yaa* B6 strain, the *Yaa* offspring did develop fatal lupus. These results indicate that FcγRIIB deficiency amplifies spontaneous autoimmunity determined by underlying autoimmune susceptibility loci (Boross et al., 2011). FcγRIIB$^{-/-}$ mice show enhanced antibody responses and are susceptible to EAG as well as accelerated NTN (Nakamura et al., 2000; Sharp et al., 2012; Suzuki et al., 1998). However, the conditional deletion of FcγRIIB on either B cells or myeloid cells did not increase incidence of EAG compared to FcγRIIB$^{-/-}$ mice (Sharp et al., 2012), although, it must be noted, deletion of FcγRIIB was insufficient on myeloid cells in this model.

To date, little work has been done on the role of FcγRIIB expressed by mesangial cells in GN. Two reports, one *in vivo* and one *in vitro*, have confirmed mesangial cell FcγRIIB expression and shown downregulation of the receptor during disease or following

IFN-γ and LPS stimulation (Ichii et al., 2008; Radeke et al., 2002). However, whether it plays a role in protection from injury has not been investigated.

## 1.11 Project hypothesis and aims

Due to the key roles of FasL and FcγRIIB in modulating the inflammatory immune response, loss of function of either, on certain genetic backgrounds, results in the development of severe autoimmune phenotypes. FasL and FcγRIIB are expressed on circulating leukocytes and intrinsic renal cells, such as mesangial cells, both of which are important in the development of GN. Therefore, I have investigated their role in accelerated NTN. My original hypothesis was that FasL plays a pro-inflammatory role in the induction of autoimmune GN and its absence would attenuate disease, whereas FcγRIIB plays an anti-inflammatory role and its absence would exacerbate disease. To test these hypotheses I tried to answer the following questions:

### 1.11.1 What is the role of Fas ligand in glomerulonephritis? Is there a difference between the immune responses of WT and *gld* mice?

Due to the conflicting arguments for the role of FasL in GN, due to its roles in the immune response, inflammation and apoptosis, I decided to start by investigating whether defective FasL, on a non-permissive background, was protective in accelerated NTN, a model similar to immune complex GN. To address this the disease model was induced in WT and *gld* mice on a C57BL/6 background and renal injury was assessed. The role of FasL in lymphocyte homeostasis is well documented, with *gld* and *lpr* mice, as well as ALPS patients, having overactive immune responses and a predisposition to autoimmunity. In light of this, I then investigated the immune response of *gld* mice compared to WT mice. To do this, I re-challenged pre-immunised WT and *gld* splenocytes with sheep IgG, CD3/CD28 beads or PMA & ionomycin and measured proliferation and cytokine production. The results are analysed and discussed in Chapter 3.

### 1.11.2 Is Fas ligand expression on infiltrating leukocytes or intrinsic renal cells more critical for disease development?

FasL is known to be expressed on circulating leukocytes and has been shown to be upregulated during renal injury, with mesangial cells being identified as a source within the glomerulus. Both infiltrating leukocytes and intrinsic renal cells have been shown to play key

roles in the development of GN. FasL expression on circulating leukocytes has been found to be the main driving force for disease in EAU and kidney IRI. However, in EAE, FasL was found to play a dual role in inflammation and recovery, with expression on both circulating leukocytes and cells of the central nervous system contributing to disease. Therefore I wanted to know whether FasL on intrinsic renal cells or infiltrating leukocytes plays a role in GN. This question is addressed in Chapter 4 by the creation of bone marrow chimeras expressing functional FasL on their circulating cells but not intrinsic renal cells, and *vice versa,* and then inducing accelerated NTN. These mice were compared to WT mice transplanted with WT bone marrow and *gld* mice transplanted with *gld* bone marrow. Defective FasL has also been shown to interrupt IL-1R signalling in macrophages, resulting in reduced production of MCP-1. As mesangial cells express FasL and also produce MCP-1, I decided to culture mesangial cells from WT and *gld* mice, stimulate them with IL-1β, and assess the differences in cytokine production.

### 1.11.3 What is the role of FcγRIIB in glomerulonephritis?

FcγRIIB-deficiency (FcγRIIB$^{-/-}$) has already been shown to aggravate accelerated NTN in mice, due to its role in negatively regulating the immune response. FcγRIIB is widely expressed on cells of both myeloid and lymphoid origin; however, its precise role on specific cell types in GN has not been determined. Therefore, to ascertain the role of FcγRIIB in accelerated NTN, my collaborators created floxed FcγRIIB mice on a C57BL/6 background and, using Cre recombinase under cell specific promoters, successfully deleted the expression of FcγRIIB on B cells, dendritic cells, mast cells, and myeloid cells. Accelerated NTN was induced and the mice compared to WT and FcγRIIB$^{-/-}$ mice.

### 1.11.4 Is FcγRIIB expressed by mesangial cells? Does mesangial cell FcγRIIB contribute to protection from accelerated NTN.

Intrinsic renal cells are known to express FcγRI and FcγRIII; however, neither were found to play a role in the development of GN in accelerated NTN. Data suggest that intrinsic renal cells, possibly mesangial cells, express FcγRIIB. To confirm this I cultured mesangial cells and measured expression using quantitative real-time PCR (qRT-PCR), following

stimulation with LPS, as well as direct immunofluorescence. To determine whether mesangial cell FcγRIIB plays a role in protecting mice from disease I generated bone marrow chimeras, expressing FcγRIIB on their circulating leukocytes but not on their intrinsic renal cells, and *vice versa*, and induced accelerated NTN. These mice were compared to WT mice transplanted with WT bone marrow and FcγRIIB$^{-/-}$ mice transplanted with FcγRIIB$^{-/-}$ bone marrow.

# CHAPTER 2

# Materials and Methods

## 2.1 Materials

### 2.1.1 Animals

#### 2.1.1.1 Fas ligand experiments

*Gld* mice, backcrossed to a C57BL/6 background for 10 generations, were kindly provided by Professor David Gray, University of Edinburgh, UK, or purchased from the Jackson Laboratory. Homozygous *gld* mice were then bred to provide experimental mice at Central Biomedical Services (CBS), Hammersmith Hospital. Mice used in this study were between 6-15 weeks of age. Control age- and sex-matched C57BL/6 WT mice were purchased from Charles River. All mice were housed with free access to food and water and were kept in a specific pathogen-free environment, according to institutional guidelines. Experiments were performed under the terms of a licence issued by the UK Home Office.

#### 2.1.1.2 FcγRIIB experiments

The FcγRIIB$^{-/-}$ mice, on a pure C57BL/6 background, were generated in Leiden University Medical Centre (LUMC) as previously described (Boross et al., 2011). The CD19Cre mice were kindly provided by Dr. Ari Waisman (Cologne) (Rickert et al., 1997). The Lysozyme MCre (LysMCre) mice were kindly provided by Dr. Bjorn Clausen (Amsterdam) (Clausen et al., 1999). The CD11cCre mice were kindly provided by Dr. Boris Reizis (New York) (Caton et al., 2007). The Mcpt5Cre mice were kindly provided by Dr. Axel Roers (Dresden) (Scholten et al., 2008). The cEBPαCre mice were kindly provided by Dr. Ivo Touw (Rotterdam) (Wolfler et al., 2010). All Cre mice were backcrossed to a C57BL/6 background for more than six generations prior to crossing onto the floxed background (pure C57BL/6). During the breeding heterozygous Cre mice, carrying the homozygous floxed FcγRIIB gene, were continuously intercrossed with homozygous floxed

FcγRIIB mice on a pure C57BL/6 background, to generate floxed/floxed x Cre heterozygote experimental animals. Age- and sex-matched floxed/floxed littermate controls were used as WT animals for the experiments. Mice were bred and housed in the animal facility, LUMC, Leiden, The Netherlands, and used between 6-15 weeks of age. Experiments involving mice with a cell-specific deletion of FcγRIIB were performed at LUMC in part by myself and by technicians in Leiden. Experiments were performed in accordance with the regulations of the ethics committee at LUMC. Analysis of serology and histology was performed at Imperial College London, UK.

FcγRIIB$^{-/-}$ mice, on a pure C57BL/6 background, for bone marrow transplant experiments were kindly provided by Professor Sjef Verbeek (Leiden) (Boross et al., 2011). Homozygous mice were bred to provide experimental mice at CBS, Hammersmith Hospital. Mice used in this study were between 6-15 weeks of age. Control age- and sex-matched C57BL/6 WT mice were purchased from Charles River. All mice were housed with free access to food and water and were kept in a specific pathogen free environment, according to institutional guidelines. Experiments were performed under the terms of a licence issued by the UK Home Office.

## 2.2 Methods

### 2.2.1 *In vivo* experiments

#### 2.2.1.1 Genotyping of *gld* mice by polymerase chain reaction

Genomic DNA was isolated from mouse tissue (usually an ear punch). Tissue samples were lysed overnight at 56°C in 100µl of cell lysis buffer containing 100µg/ml proteinase K (Sigma-Aldrich) (added immediately before use), with agitation. For PCR analysis, the DNA was diluted in three volumes of distilled $H_2O$ ($dH_2O$) and heat-inactivated at 75°C for 15 minutes. A 12µl PCR was carried out using a PTC-200 thermal cycler (MJ Research) and a single pair of FasL primers (Sigma-Aldrich). Primer sequences were provided by the Jackson Laboratory:

FasL forward: 5'CAAGACAATATTCCTGGTGCC-3'

FasL reverse: 5'CAATTTTGAGGAATCTAAGGCC-3'

Reagents, excluding the DNA template, were made up as a master mix sufficient for all samples and then aliquoted before adding the appropriate DNA template to each reaction tube. The reagents in each reaction tube are summarised in Table 2.1. Thermal cycling conditions involved initial denaturation at 94°C for 3 minutes, followed by 35 cycles of 94°C for 1 minute (denaturation), 55°C for 1 minute (primer annealing temperature) and 72°C for 1 minute (extension). A final extension step at 72°C for 2 minutes was incorporated to ensure the extension of all amplified products. Both the WT band and mutant band were 108 base pairs (bp).

| PCR Reagents | Volume (µl) |
|---|---|
| MilliQ water | 6.58 |
| 10x PCR buffer (Qiagen) | 1.20 |
| dNTP's (2.5mM) (Promega) | 0.96 |
| FasL forward primer (20µM) | 0.60 |
| FasL reverse primer (20µM) | 0.60 |
| Taq polymerase (5U/µl) (Qiagen) | 0.06 |
| DNA (5-20ng) | 2.00 |
| Final volume | 12.0 |

**Table 2.1 Chemical reagents for *gld* PCR.**

The PCR products were then digested using Stu I restriction endonuclease (New England BioLabs). The WT product contains a restriction digestion site that cleaves the DNA into an 88bp and 20bp product. The mutant product contains no cleavage site. A master mix sufficient for all samples was made and 6µl added to each PCR reaction tube and run on a thermal cycler for a minimum of 4 hours at 37°C. The reagents for the restriction digestion are summarised in Table 2.2.

| Restriction Digestion Reagents | Volume (µl) |
|---|---|
| 10x buffer (New England Biolabs) | 1.50 |
| MilliQ water | 3.75 |
| Stu I (10U/µl) (New England Biolabs) | 0.75 |

**Table 2.2 Chemical reagents for restriction digestion.**

The restriction digestion products were analysed by gel electrophoresis. 3g of agarose (Sigma-Aldrich) was dissolved in 100ml 1xTris Acetate EDTA (TAE), micro-waved for 3 minutes and 10µl of Sybr green nucleic acid gel stain (Sigma-Aldrich) added to stain the DNA. The gel was left at room temperature for 30 minutes to set. 15µl of each sample (diluted 1:6 in loading dye (Bioline)) was loaded. Hyperladder V (Bioline) was used to size PCR products. Samples were electrophoresed in 1x TAE at 150V for 2 hours. The DNA was visualised using a Gel Doc 1000 transilluminator (Bio-Rad) and photographed.

### 2.2.1.2 Genotyping of FcγRIIB$^{-/-}$ mice by polymerase chain reaction

Genomic DNA was isolated from mouse tissue as previously described (Section 2.2.1.1). For PCR analysis, the DNA was diluted in three volumes of $dH_2O$ and heat inactivated at 75°C for 15 minutes. A 25µl PCR was carried out using a thermal cycler and the following FcγRIIB primers (Sigma-Aldrich). Primer sequences were taken from Boross *et al.* (Boross et al., 2011).

CreRecPr1: 5'CCTTCATCTTTCCTGCCAAG-3'

CreRecPr6v2: 5'TCACACCAGCAACACCTCTC-3'

CreRecPr2: 5'AACACCAGCTGAGGGGTCT-3'

Reagents, excluding the DNA template, were made up as a master mix sufficient for all samples and then aliquoted before adding the appropriate DNA template to each reaction tube. The reagents in each reaction tube are summarised in Table 2.3. Thermal cycling conditions involved initial denaturation at 94°C for 2 minutes, followed by 20 cycles of a stepwise PCR at 94°C for 30 seconds (denaturation), a required annealing temperature at 65°C for 1 minute 30 seconds which decreased by 0.5°C with each cycle (ending at 55°C) and an extension temperature at 72°C for 1 minute 30 seconds. This was followed by 20 cycles at 94°C for 30 seconds (denaturation), an annealing temperature at 55°C for 1 minute 30 seconds and an extension temperature at 72°C for 1 minute 30 seconds. The final extension at 72°C for 5 minutes was incorporated to ensure the extension of all amplification products. The WT band was 359bp and the recombinant band 600bp. The PCR products were analysed by gel electrophoresis. 2g of agarose was dissolved in 100ml 1x TAE, micro-waved for 3 minutes and 10µl of Sybr green nucleic acid gel stain (Sigma-Aldrich) added to stain the DNA. The gel was left at room temperature to set. 15µl of each sample (diluted 1:6 in loading dye (Bioline)) was loaded. Hyperladder IV (Bioline) was used to size PCR products. Samples were electrophoresed in 1x TAE at 150V for 1 hour. The DNA was visualised using a Gel Doc 1000 transilluminator (Bio-Rad) and photographed.

| PCR reagents | Volume (µl) |
|---|---|
| MilliQ water | 14.65 |
| 10x PCR buffer (Qiagen) | 2.50 |
| dNTP's (2mM) (Promega) | 2.50 |
| $MgCl_2$ (50mM) (Qiagen) | 1.25 |
| CreRecPr1 (100ng/µl) | 1.00 |
| CreRecPr6v2 (100ng/µl) | 0.50 |
| CreRecPr2 (100ng/µl) | 0.50 |
| Taq polymerase (5U/µl) (Qiagen) | 0.10 |
| DNA (5-20ng) | 2.00 |
| Final volume | 25.00 |

**Table 2.3 Chemical reagents for FcγRIIB$^{-/-}$ PCR.**

### 2.2.13 Preparation of nephrotoxic serum

NTS was kindly prepared and characterised by Dr Ruth Tarzi. Briefly, lyophilised mouse GBM was made at 4°C. Mouse kidneys were blended through a series of sieves: 150µm, 106µm and 45µm, respectively, and washed through with cold phosphate buffered saline (PBS). Glomeruli were retained on the 45µm sieve. The recovered glomeruli were spun down at 700 x *g* for 5 minutes, washed twice and resuspended in cold PBS. The resuspended material was then sonicated at 8µm amplitude for 30-second bursts on ice, spun down at 200 x *g* for 15 minutes and washed twice with cold PBS. The sonicated glomeruli were then washed twice with cold, distilled water, spun down at 700 x *g* for 5 minutes and frozen in liquid nitrogen. The GBM was lyophilised overnight and the final product stored at -20°C.

Regal Group generated the sheep serum containing nephrotoxic antibody. Sheep were immunised with 5mg of mouse GBM subcutaneously at four sites in a 50:50 mix of saline and CFA (Sigma-Aldrich). This mixture was prepared by repeatedly mixing the solution between two glass syringes joined by a double-luer lock (Sigma-Aldrich). When fully homogenised, a droplet placed on water retained its form. Boost immunisations of 1mg of mouse GBM in a 50:50 mix of saline and incomplete Freund's adjuvant (IFA) (Sigma-Aldrich) were then given four times, at monthly intervals, in two subcutaneous and two intramuscular sites. The sheep was bled at monthly intervals, as well as terminally, and the serum pooled in order to enrich the antibody content.

To purify the nephrotoxic antibody, firstly the complement in the serum was inactivated at 56°C for 30 minutes. A 50% saturated ammonium sulphate solution was obtained by adding 315g/l of ammonium sulphate slowly to the serum with constant stirring. The globulins were left to precipitate for 5 hours at room temperature. Following precipitation, serum was spun twice at 12000 x *g* for 10 minutes. The supernatant was removed and the precipitate resuspended in a minimal volume of PBS, transferred to dialysis tubing and dialysed against a large volume (5 litres) of PBS at 4°C. The dialysis fluid was changed four times over 24 hours and the content of the dialysis tubing collected and centrifuged at 1000 x *g* for 10 minutes. The supernatant was retained and sterilised using a 0.2µm filter. Aliquots were stored at -80°C.

The concentration of sheep IgG was determined by radial immunodiffusion. 150µl of rabbit anti-sheep IgG (Sigma-Aldrich) was added to 10ml 1.2% agarose gel in PBS and a gel

was prepared on a 3-inch glass square. 5µl of nephrotoxic globulin (neat and dilutions) or serial dilutions of reagent grade sheep IgG (Sigma-Aldrich) were added to wells punched into the gel. The gel was incubated at 4°C overnight in a humidified chamber. The following day the gel was washed, fixed onto GelBond film (Cambrex), dried and stained with Coomassie brilliant blue (Sigma-Aldrich). The diameter of the rings was measured using a micrometer eyepiece and the concentration of IgG in the samples was then calculated by linear regression with reference to the standard curve. The concentration of sheep IgG was found to be 50mg/ml.

#### 2.2.1.4 Induction of accelerated nephrotoxic nephritis

Mice were immunised subcutaneously with 0.2mg of sheep IgG (Sigma-Aldrich) in a 50:50 mix of saline and CFA (Sigma-Aldrich). This mixture was prepared by repeatedly mixing the solution between two glass syringes joined by a double-luer lock (Sigma-Aldrich). When fully homogenised, a droplet placed on water retained its form. Five days after immunisation, the animals were injected with 200µl (diluted in 0.9% NaCl) sheep NTS via the tail vein. 1-15 days after NTS injection mice were humanely killed. Kidneys, spleen and blood, for serum, were harvested.

#### 2.2.1.5 Bone marrow transplantation

Same sex transplants were carried out. Donor bone marrow was harvested from the femur, tibia and humerus by cleaning off the muscle and hair and flushing out the marrow into RPMI 1640 medium (Gibco) containing 100U/ml penicillin, 100µg/ml streptomycin (Gibco), 10% fetal calf serum (FCS) (Biosera) and 1% L-glutamine (Gibco). Cells were spun down at 352 x *g* for 5 minutes and then resuspended and counted using a haemocytometer. The cells were centrifuged again and resuspended in media at a final concentration of $5x10^7$ cells/ml.

Recipient mice were irradiated in an IBL 637 irradiator at CBS, Hammersmith Hospital. The optimal irradiation dose used was 8 Gray (Gy) (Tarzi et al., 2002). Following irradiation, mice were injected with 200µl (10 million) bone marrow cells via the tail vein. During the following eight weeks the mice were housed in individually-ventilated cages with free access to acidified water and an autoclaved diet, according to institutional guidelines.

#### 2.2.1.6 Quantification of bone marrow reconstitution in blood by flow cytometry

Peripheral blood was taken via the tail vein into 5% EDTA from mice transplanted with the CD45.1 bone marrow allotype marker at 10 weeks post bone marrow transplantation. Red cells were lysed for 10 minutes at room temperature using 2ml of 1X FACS®lysing solution (BD Biosciences). Cells were spun down at 500 x *g,* 4°C for 5 minutes and the supernatant discarded. Cells were washed twice and resuspended in PBS-1% FCS. First cells were incubated with anti-mouse CD16/32 (eBioscience) in order to block FcγRII and FcγRIII (Table 2.4). Cells were then stained with FITC-labelled CD45.1 and APC-labelled CD45.2 (both BD Biosciences) (Table 2.4). Suitable isotype controls were used. Flow cytometry was performed using a FACScalibur flow cytometer (BD Bioscience) and analysed using FlowJo software (TreeStar).

| Antibody Specificity | Source | Host/Clone | Isotype | µg/test |
|---|---|---|---|---|
| ***Anti-mouse CD16/32 (blocking)*** | eBioscience | Rat/93 | IgG2a, λ | 0.5 |
| ***CD45.1-APC*** | BD Bioscience | A20 | IgG2a, κ | 1.0 |
| ***CD45.2-PE*** | BD Bioscience | 104 | IgG2a, κ | 1.0 |

**Table 2.4 Antibodies used for quantification of bone marrow reconstitution in the blood by flow cytometry.**

### 2.2.1.7 Quantification of bone marrow reconstitution in blood by polymerase chain reaction

DNA was isolated from 100µl of blood obtained from a terminal bleed. The blood was lysed overnight at 56°C in 500µl of blood lysis buffer containing 100µg/ml proteinase K (Sigma-Aldrich) (added immediately before use). To extract the DNA, 300µl of saturated NaCl and 200µl of chloroform was added to each sample and vortexed. Samples were centrifuged at high speed for 10 minutes and the supernatant (500µl) collected. 50µl 3M sodium acetate and 550µl of isopropanol were added to the supernatant and mixed gently before centrifuging at high speed for 10 minutes. A white pellet of DNA formed at the bottom of the tube. The supernatant was discarded and the pellet washed twice in 70% ethanol before resuspending in 20µl of double distilled (dd) $H_2O$.

For bone marrow transplants involving *gld* mice, a PCR was run as before (Section 2.2.1.1) but replacing the reverse FasL primer for an identical primer modified at the 5' end with a FAM label. All samples were run in duplicate. Following the PCR one of the duplicates was digested as before (Section 2.2.1.1). The samples were then run on a Genescan (Applied Biosystems). 15µl of ROX 400 marker (Applied Biosystems) was mixed with 1ml of formamide (Sigma-Aldrich) and 11µl was placed in every well of a 96-well plate. DNA was diluted 1:4 with dd$H_2O$ and 1µl was added to the ROX mixture. The plate was run on an ABI 3100 Automated Sequencer (Applied Biosystems) and results were exported to Genemapper software (Applied Biosystems) for analysis.

For bone marrow transplants involving FcγRIIB$^{-/-}$ mice, a PCR was run as before (Section 2.2.1.2).

### 2.2.1.8 Isolation of resident renal leukocytes for flow cytometric analysis

Eight weeks following bone marrow transplantation, mice were sacrificed and the kidneys were collected and sliced into six cubes using a scalpel. The kidneys were not perfused prior to harvesting. The kidneys were digested in RPMI 1640 medium (Gibco) containing 0.1% FCS (Biosera), 20mM HEPES (Gibco), 0.1% β-mercaptoethanol (Sigma-Aldrich), 1mM L-glutamine (Gibco), 100U/ml penicillin, 100µg/ml streptomycin (Gibco), 0.5mg/ml collagenase (Roche) and 100µg/ml DNAse I (Roche) for 25 minutes at 37°C in a shaking water bath. The kidneys were then blended using a syringe plunger and incubated for a further 15 minutes at 37°C in a shaking water bath. Following digestion the kidneys were filtered through a 100µm nylon mesh and washed in PBS containing 0.1% FCS.

### 2.2.1.9 Flow cytometry of resident renal leukocytes

Isolated kidney cell digests were counted and 3 million cells/well plated out in a V-bottom welled plate. First, cells were blocked with anti-mouse CD16/32 (eBioscience) to block Fc receptors. Cells were washed with PBS and stained with the following antibodies obtained from eBioscience: APC-labelled CD45.1, PE-labelled CD45.2, FITC-labelled F4/80 and PerCP Cy5.5-labelled CD11c (Table 2.5). Flow cytometry was performed using a FACScalibur flow cytometer (BD Biosciences) and analyzed using FlowJo software (TreeStar).

| Antibody Specificity | Source | Host/Clone | Isotype | µg/test (100µl) |
|---|---|---|---|---|
| ***Anti-mouse CD16/32 (blocking)*** | eBioscience | Rat/93 | IgG2a, λ | 0.5 |
| ***CD45.1-APC*** | eBioscience | A20 | IgG2a, κ | 1.0 |
| ***CD45.2-PE*** | eBioscience | 104 | IgG2a, κ | 1.0 |
| ***F4/80-FITC*** | eBioscience | Rat/BM8 | IgG2a, κ | 0.5 |
| ***CD11c-PerCP Cy5.5*** | eBioscience | Armenian Hamster/N418 | IgG | 0.25 |

**Table 2.5 Antibodies used for flow cytometry of isolated resident renal leukocytes.**

#### 2.2.1.10 Assessment of the systemic immune response to sheep IgG by enzyme-linked immunosorbent assay

Mouse anti-sheep IgG levels were measured in mouse serum collected at the end of the experiment by an enzyme-linked immunosorbent assay (ELISA). Nuncmaxisorp ELISA plates (Fisher Scientific) were coated overnight at 4°C with 100µg/ml sheep IgG (Sigma-Aldrich) diluted in PBS (Table 2.6). Plates were blocked with 3% bovine serum albumin (BSA) (Sigma-Aldrich) for 1 hour at 37°C. The plates were then washed three times with PBS/0.1% Tween 20 (Sigma-Aldrich) and 100µl of serum, diluted 1:500 and 1:1000 in 1% BSA/PBS, incubated for 1 hour at 37°C. Following washing, 100µl of alkaline phosphatase conjugated goat anti-mouse IgG (Fc specific) (Sigma-Aldrich) was incubated for 1 hour at 37°C (Table 2.6). Optical density (OD) at 405nm was measured on a EL800 ELISA plate reader (BioTek) using *p*-nitrophenyl phosphate as a substrate (Sigma-Aldrich).

For IgG subclass analysis, goat anti-mouse IgG1, 2b, 2c and 3 alkaline phosphatase conjugated antibodies (SouthernBiotech) were used for detection (Table 2.6). The OD at 405nm was measured as above.

| Antibody Specificity | Source | Host/Clone | Concentration (µg/ml) | Dilution Used |
|---|---|---|---|---|
| ***Sheep IgG (Coating)*** | Sigma-Aldrich | Sheep polyclonal | 100 | 1:100 |
| ***Mouse IgG (Fc specific) Alkaline Phosphatase*** | Sigma-Aldrich | Goat polyclonal | 1.0 | 1:1000 |
| ***Mouse IgG1 Alkaline Phosphatase*** | SouthernBiotech | Mouse IgG1 | - | 1:1000 |
| ***Mouse IgG2b Alkaline Phosphatase*** | SouthernBiotech | Mouse IgG2b | - | 1:1000 |
| ***Mouse IgG2c Alkaline Phosphatase*** | SouthernBiotech | Mouse IgG2c | - | 1:500 |
| ***Mouse IgG3 Alkaline Phosphatase*** | SouthernBiotech | Mouse IgG3 | - | 1:500 |

**Table 2.6 Antibodies used for the assessment of the systemic immune responses to sheep IgG.**

#### 2.2.1.11 Measurement of serum creatinine and serum urea

Serum creatinine and serum urea were kindly measured in the Department of Clinical Chemistry, Hammersmith Hospital by Mr John Meek. Serum urea was also measured using Urea/Ammonia kit (R-Biopharm) according to the manufacturer's protocol. Briefly, all samples were diluted 1:10 in PBS. One tablet of nicotinamide adenine dinucleotide (NADH) was dissolved in 1ml of oxoglutarate to make reaction mixture 2 (RM2). Into a 96-well Nuncmaxisorp ELISA plate (Fisher Scientific) 100µl of RM2, 2µl of urease, 200µl of $ddH_2O$ and 10µl of diluted sample were added per well to measure urea and ammonia. This was repeated in a second well but without the urease to measure ammonia only. After 5 minutes the plate was read at 340nm and 2µl of glutamate dehydrogenase (GLDH) was added to all wells. After 20 minutes the plate was read at 340nm using an EL800 ELISA plate reader (BioTek). Concentration of urea in the sample was calculated by comparison to a positive control of known concentration.

#### 2.2.1.12 Measurement of urine creatinine and urinary albumin/creatinine ratio

Individual 24-hour urine collections were performed using metabolic cages, in which the mice had free access to food and water. Urinary albumin concentration was measured by radial immunodiffusion. 150µl of rabbit anti-mouse albumin (Serotec) was added to 10ml 1.2% agarose gel in PBS and a gel was prepared on a 3-inch glass square. 5µl of sample or serial dilutions of a mouse albumin standard (Sigma-Aldrich) were added to wells punched into the gel. The gel was incubated at 4°C overnight in a humidified chamber. The following day the gel was washed, fixed onto GelBond film (Cambrex), dried and stained with Coomassie brilliant blue (Sigma-Aldrich). The diameters of the rings were measured using a micrometer eyepiece and the concentration of albumin in the samples then calculated by linear regression with reference to the standard curve.

Urine creatinine was kindly measured in the Department of Clinical Chemistry, Hammersmith Hospital by Mr John Meek. This was then used to calculate the urinary albumin/creatinine ratio.

#### 2.2.1.13 Processing of histological specimens

For light microscopy, half kidneys were fixed in neutral buffered formalin overnight or Bouin's solution (Sigma-Aldrich) for 2 hours, transferred to 70% ethanol and processed to paraffin blocks. 4μm sections were stained with periodic acid-Schiff (PAS) and hematoxylin-eosin (H&E) reagents (Leukocyte Biology, Biological Sciences, South Kensington).

For immunofluorescence, half kidneys were placed on corkboards and snap-frozen embedded in Cryomatrix (Thermo Fisher Scientific) using isopentane cooled with liquid nitrogen. The samples were stored at -80°C until use. For staining cell surface markers, half kidneys were first fixed with paraformaldehyde lysine periodate (PLP) at 4°C for 4 hours, washed overnight in 13% (w/v) sucrose in PBS and snap frozen as above in isopentane cooled in liquid nitrogen. 5μm kidney sections were cut using a cryostat (Bright) onto slides coated with Poly-L-lysine (Surgipath). After air-drying, slides were either stained or stored at -80°C.

#### 2.2.1.14 Immunofluorescence staining of frozen sections

Direct immunofluorescence was used to detect sheep and mouse IgG on sections of mouse kidney. Antibodies used for immunofluorescence staining are listed in Table 2.7. Sections were blocked with 20% serum from the species of the FITC-conjugated antibody for 30 minutes in order to block non-specific cross-reactivity. The primary antibodies were diluted in PBS, incubated on the sections for one hour at room temperature in a humidified chamber covered with aluminium foil. The sections were washed three times in PBS and mounted in AF1 solution (Citiflur).

| Antibody Specificity | Source | Host/Clone | Concentration (mg/ml) | Dilution Used |
|---|---|---|---|---|
| ***Sheep IgG FITC (Fc specific)*** | Sigma-Aldrich | Mouse IgG1/ Clone GT34 | 1.7 | 1:200 |
| ***Mouse IgG FITC (Fc specific)*** | Sigma-Aldrich | Goat polyclonal | 5.2 | 1:200 |

**Table 2.7 Antibodies for direct immunofluorescence (all FITC-conjugated).**

#### 2.2.1.15 CD45.1 and CD45.2 tissue staining

CD45.1 and CD45.2 were stained using the avidin-biotin complex (ABC) method. The antibodies used are listed in Table 2.8. 5μm sections of frozen kidney fixed in PLP were used. Mouse spleen was used as a positive control. Endogenous peroxidase was first blocked by submerging the slides in 0.3% hydrogen peroxide (VWR International Ltd.) for 10 minutes. The sections were rinsed in $ddH_2O$ and endogenous avidin and biotin were blocked. Avidin block (Vector Laboratories) was applied to the sections for 15 minutes, rinsed off in PBS then biotin block (Vector Laboratories) was applied to the sections for 15 minutes and rinsed off in PBS. The primary biotinylated antibody was then applied for two hours at room temperature in a humidified chamber. As a negative control, sections were stained with the primary antibody omitted and PBS used in its place. After 3 washes in PBS (5 minutes each) ExtrAvidin-Peroxidase (Sigma-Aldrich) was applied for 30 minutes at room temperature in a humidified chamber. After three washes in PBS, slides were submerged in 3,3'-diaminobenzidine (DAB) solution for two minutes then rinsed in $ddH_2O$. Slides were counterstained by immersion in filtered Harris' haematoxylin (CellPath Ltd) for 40 seconds and then rinsed in a sink water bath. Slides were dipped in 1% acid alcohol and rinsed in a sink water bath until the sections turned blue. Sections were dehydrated by serial immersion for 5 minutes each in 100% ethanol (x2) and xylene (x2). Finally, slides were wiped dry and mounted with DePex (BDH) and coverslips.

| Antibody Specificity | Source | Host/Clone | Concentration (mg/ml) | Dilution |
|---|---|---|---|---|
| **Primary Antibodies** | | | | |
| ***CD45.1-biotin*** | eBioscience | Mouse/A20 | 0.5 | 1:200 |
| ***CD45.2-biotin*** | eBioscience | Mouse/104 | 0.5 | 1:200 |
| **Secondary Antibody** | | | | |
| ***ExtrAvidin-Peroxidase*** | Sigma-Aldrich | - | 2.0-2.5 | 1:50 |

**Table 2.8 Antibodies used for CD45.1 and CD45.2 staining.**

#### 2.2.1.16 Immunoperoxidase staining for cell surface markers

Immunoperoxidase staining was used to detect macrophages (CD68), neutrophils (Gr-1) and $CD4^+$ T cells using the Polink-2 Plus HRP (horseradish peroxidase) Rat with DAB kit (New Market Scientific). The antibodies used are listed in Table 2.9. 5µm sections of frozen kidney fixed in PLP were used. Mouse spleen was used as a positive control. First, endogenous peroxidase was blocked by submerging the slides in 0.3% hydrogen peroxide (VWR International Ltd.) for 10 minutes. The sections were then rinsed in $ddH_2O$ and the primary antibody, diluted in PBS, applied for one hour at room temperature in a humidified chamber. As a negative control, sections were stained with the primary antibody omitted and PBS used in its place. After three washes in PBS (2 minutes each) two drops of Rat Antibody Enhancer (supplied in the Polink-2 kit) were applied to each section and incubated for 10 minutes at room temperature in a humidified chamber. After three washes in PBS (2 minutes each) 50µl of Polymer-HRP for Rat Antibody (supplied in the Polink-2 kit), made up an hour in advance containing 20% goat serum to adsorb out any cross-reactivity with goat immunoglobulin in the sections, was applied to each section and incubated for 10 minutes at room temperature in a humidified chamber. The slides were washed three times and the bound antibody detected with DAB. 1 drop of DAB chromagen was added per ml of DAB substrate (both supplied in the Polink-2 kit) and 50µl applied to the sections for two minutes. Sections were rinsed in a sink water bath. Slides were counterstained by immersion in filtered

Harris' haematoxylin (CellPath Ltd) for 40 seconds and then rinsed in a sink water bath. Slides were dipped in 1% acid alcohol and rinsed in a sink water bath until the sections turned blue. Sections were dehydrated by serial immersion for 5 minutes each in 100% ethanol (x2) and xylene (x2). Finally, slides were wiped dry and mounted with DePex (BDH) and coverslips.

| Antibody Specificity | Source | Host/Clone | Concentration (mg/ml) | Dilution |
|---|---|---|---|---|
| **Primary Antibodies** | | | | |
| ***CD68*** | Serotec | Rat FA11 | 1.0 | 1:200 |
| ***CD4*** | BD Biosciences | Rat Monoclonal GK1.5 (L3T4) | 0.5 | 1:200 |
| ***Gr-1*** | Serotec | Rat Monoclonal RB6-8C5 | 1.0 | 1:50 |
| **Secondary Antibody** | | | | |
| ***Rat HRP (Polink Kit)*** | Newmarket Scientific | Rat | Kit | Kit |

**Table 2.9 Antibodies used for immunoperoxidase staining.**

#### 2.2.1.17 Terminal deoxynucleotidyl transferase (TdT) dUTP nick end labelling (TUNEL)

Apoptotic cells were stained for on paraffin-embedded sections using the ApopTag Fluorescein Kit (Roche). Sections were de-paraffinised by serial immersions in xylene (x2) and 100% ethanol (x2) for 5 minutes each, then 95% ethanol and 70% ethanol for 3 minutes and finally PBS for 5 minutes. Antigen retrieval was performed to facilitate the reaction in fixed tissue, maximising the availability of the antigen, using 20µg/ml proteinase K (Sigma-Aldrich) diluted in PBS for 15 minutes at room temperature. The slides were then washed in PBS and equilibration buffer was applied to the specimens and incubated for at least 10 seconds at room temperature. Excess liquid was tapped off before applying working strength TdT enzyme, prepared by mixing 77µl of reaction buffer with 33µl of TdT enzyme, to each sample and incubated for 1 hour at 37°C in a humidified chamber. The specimens were covered with a piece of parafilm cut slightly larger than the specimen to assure even distribution of the reaction mixture and prevent loss due to evaporation during incubation. The labelling reaction was stopped by immersing the slides in stop/wash buffer for 10 minutes at room temperature, with gentle agitation for the first 15 seconds. The slides were rinsed in PBS, anti-digoxigenin conjugate applied and incubated for 30 minutes at room temperature in a humidified chamber in the dark. The slides were washed for a final time and mounted with Vectashield with DAPI (Vector Laboratories).

#### 2.2.1.18 Histological analyses

All microscope analysis and quantitative immunofluorescence was performed using an Olympus BX4 Microscope (Olympus Optical) at x250 magnification without knowledge of the samples identity.

#### 2.2.1.19 Quantitative immunofluorescence

Immunofluorescent sections were scored either using a quantitative visual fluorescence scale or Image Pro Plus software (Media Cybernetics). The fluorescence scale used is as follows: 0: no increase in fluorescence compared to the background; 1: minimal increase; 2: moderate fluorescence, 3: strong fluorescence and 4: very strong fluorescence. To quantitate using Image Pro Plus images of glomeruli were captured using a QImaging

Retiga 2000R Fast 1396 camera (QImaging). Glomeruli were outlined manually on the computer screen and the mean fluorescence intensity over each glomerulus was measured electronically. For each section 20 glomeruli were examined and the mean fluorescence intensity recorded. Where Image Pro Plus software was used results are expressed in arbitrary fluorescence units (AFU). Where the quantitative visual fluorescence scale was used results are expressed as visual fluorescence units (VFU).

#### 2.2.1.20 Glomerular and interstitial immunoperoxidase scoring

Glomerular macrophages ($CD68^+$), neutrophils ($Gr\text{-}1^+$) and $CD4^+$ T cells were counted on immunoperoxidase stained sections. Only cells inside glomeruli, defined by the Bowman's capsule were counted and 50 glomerular cross sections (gcs) were scored per kidney.

Interstitial macrophage and $CD4^+$ T cell staining were quantified using Image Pro Plus software (Media Cybernetics). A field of view of interstitium, free from glomeruli, was captured using a QImaging Retiga 2000R Fast 1396 camera (QImaging). The areas of positive staining were selected manually and measured electronically. For each section, five fields of view were selected, the mean area of positive staining calculated and multiplied by 100 to produce an arbitrary unit (AU).

#### 2.2.1.21 Glomerular damage

Glomerular thrombosis was assessed by scoring individual glomeruli on PAS-stained kidney sections for PAS positive material as follows: grade 0: no PAS positive material; grade 1: 0-25%; grade 2: 25-50%; grade 3: 50-75% and grade 4: 75-100%. 50 glomeruli were assessed per section and the mean glomeruli thrombosis score was calculated for each mouse. Glomerular crescents were defined as glomeruli containing two or more layers of cells in the Bowman's space. 50 glomeruli were counted per sample and the results converted to percentage crescents.

#### 2.2.1.22 Quantification of apoptotic cells

Apoptotic cells were counted on TUNEL stained sections. Only apoptotic cells inside glomeruli, defined by Bowman's capsule, were counted and thirty glomerular cross sections were scored per kidney.

#### 2.2.1.23 RNA extraction from whole kidney

Total RNA was extracted from snap frozen kidney. 1ml of TRIzol (Invitrogen) was added for every 25mg of tissue and the tissue was homogenised. Samples were transferred to a clean eppendorf tube and 200µl of chloroform added. The samples were shaken by hand and left at room temperature for 5 minutes. Samples were spun down in a microcentrifuge at 12000 x *g* for 15 minutes at 4°C. The clear aqueous phase was transferred to a clean eppendorf tube and 500µl of isopropanol added. Samples were stored at -20°C overnight. RNA was spun down at 12000 x *g* for 10 minutes at 4°C and the supernatant discarded. The RNA pellet was washed with 75% ethanol, spun down at 8000 x *g* for 8 minutes at 4°C and the ethanol removed. The RNA was air dried for 10 minutes, resuspended in 40µl RNase free water (Gibco) and heated at 55°C for 5 minutes. Total RNA concentration was determined using Nanodrop spectrophotometer (Labtech Int.) before being stored at -80°C.

#### 2.2.1.24 Quantitative real-time polymerase chain reaction

qRT-PCR was used to measure mRNA expression levels. The Brilliant II Sybr Green QRT-PCR Master Mix Kit, 1 Step (Agilent Technologies) was used following manufacturer's instructions. RNA was used at a final concentration of 5-10ng/µl and primers at 200nm. A 25µl reaction was carried out in a 96-well plate (Applied Biosystems). Reagents, excluding the RNA template, were made up as a master mix sufficient for all samples and then aliquoted before adding the appropriate RNA to each reaction well. The reagents in each tube are summarised in Table 2.10.

| qRT-PCR Reagents | Volume (µl) |
|---|---|
| 2x SYBR Green qRT-PCR master mix (Agilent Technologies) | 12.5 |
| Forward primer (200nM) | 0.5 |
| Reverse primer (200nM) | 0.5 |
| RT/RNase block enzyme mixture (Agilent Technologies) | 1.0 |
| RNA (125-250ng) | 1.00 |
| Final volume | 25.0 |

**Table 2.10 Chemical reagents for qRT-PCR.**

Plates were run on a Mastercycler ep Realplex$^2$ (Eppendorf). Cycling conditions involved a reverse transcription step at 50°C for 30 minutes, a 10 minute incubation at 95°C to fully activate the DNA polymerase, followed by 40 cycles of 95°C for 30 seconds (denaturation) and 60°C for 1 minute (primer annealing and extension). Cycle threshold (Ct) values, the number of cycles required for the fluorescent signal to cross to a set threshold, were determined for all genes analysed. Relative change in gene expression, normalised to GAPDH and compared to a control, was quantified using the comparative Ct method using the following equations.

Normalisation to GAPDH: $\Delta Ct = Ct_{GENE} - Ct_{GAPDH}$

Change in gene expression: $\Delta\Delta Ct = \Delta Ct_{SAMPLE} - \Delta Ct_{CONTROL}$

Relative change in gene expression (assuming 100% efficiency of both gene of interest and GAPDH): $2^{-\Delta\Delta Ct}$

Primers were designed in house and synthesised by Sigma-Aldrich. Tables 2.11 and 2.12 list the primers and sequences.

| Primers | Sequences |
|---|---|
| **GAPDH** | Forward 5’GGGTGTGAACCACGAGAAAT-3’ |
| | Reverse 5’GTCTTCTGGGTGGCAGTGAT-3’ |
| **MCP-1** | Forward 5’ATGCAGTTAATGCCCCACTC-3’ |
| | Reverse 5’TTCCTTATTGGGGTCAGCAC-3 |
| **iNOS** | Forward 5’AAGCCCCGCTACTACTCCAT-3' |
| | Reverse 5’AGCTGGAAGCCACTGACACT-3' |
| **TNF-α** | Forward 5’AGCCCACGTCGTAGCAAACCACCAA-3’ |
| | Reverse 5’ACACCCATTCCCTTCACAGAGCAAT-3’ |
| **IL-6** | Forward 5’ATGAACTCCTTCTCCACAAGCGC-3’ |
| | Reverse 5’GAAGAGCCCTCAGGCTGGACTG-3’ |
| **Arginase** | Forward 5’CGCCTTTCTCAAAAGGACAG-3’ |
| | Reverse 5’ACAGACCGTGGGTTCTTCAC-3’ |
| **Mannose Receptor** | Forward 5’GACCTTGGACTGAGCAAAGGGG-3’ |
| | Reverse 5’GACATGATGTCCTCAGGAGGACG-3’ |

**Table 2.11 Primer pairs and sequences used for qRT-PCR.**

| Primers | Sequences |
|---|---|
| **IFN-γ** | Forward 5’ATCTGGAGGAACTGGCAAAA-3’ |
| | Reverse 5’TTCAAGACTTCAAAGAGTCTGAGG-3’ |
| **IL-12p40** | Forward 5’GGAAGCACGGCAGCAGAATA-3' |
| | Reverse 5’AACTTGAGGGAGAAGTAGGAAT-3' |
| **IL-4** | Forward 5’ACAGGAGAAGGGACGCCAT-3' |
| | Reverse 5’GAAGCCCTACAGACGAGCTCA-3’ |
| **IL-10** | Forward 5’GGTTGCCAAGCCTTATCGGA-3’ |
| | Reverse 5’ACCTGCTCCACTGCCTTGCT-3’ |

**Table 2.12 Primer pairs and sequences used for qRT-PCR.**

### 2.2.2 *In vitro* experiments

#### 2.2.2.1 Mesangial cell purification and culture

For mesangial cell purification, kidneys were removed from WT, *gld* and FcγRIIB$^{-/-}$ mice and kept on ice in PBS supplemented with 100U/ml penicillin, 100µg/ml streptomycin (Gibco). The kidneys were blended using a syringe plunger and forced through a series of sterile sieves with successively smaller pore sizes of 150µm, 106µm and 45µm, respectively. Glomeruli were retained on the 45µm sieve. The recovered glomeruli were collected in a 15ml falcon tube, resuspended in cold PBS and spun down at 157 x *g* for 5 minutes at 4°C to remove any tubules. Glomeruli were digested with 380U/ml collagenase (Sigma-Aldrich) in PBS for 30 minutes at 37°C with gentle agitation. Following digestion, glomeruli were spun down at 225 x *g* for 5 minutes at 4°C, washed once with cold PBS and resuspended in RPMI 1640 medium (Gibco) supplemented with 20% fetal calf serum (FCS) (Biosera), 100U/ml penicillin, 100µg/ml streptomycin (Gibco), 2% L-glutamine and 1% ITS (insulin-transferrin-selenium) liquid (Sigma-Aldrich). Finally, glomeruli were plated in 25cm$^2$ culture flasks and cultured in humidified air at 37°C with 5% $CO_2$. Medium was changed every 2 to 3 days thereafter.

#### 2.2.2.2 Mesangial cell characterisation

Mesangial cells were characterised by their typical stellate morphology when subconfluent, while on becoming confluent they adopted the well-recognised elongated conformation. To exclude contamination with other cell types, immunofluorescence studies were carried out. 1x10$^5$ mesangial cells were added to an 8-welled chamber slide and incubated overnight at 37°C with 5% $CO_2$. The following day cells were washed in PBS and fixed in acetone for 10 minutes. Antibodies used for immunofluorescence staining are listed in Table 2.13. Cells were blocked for 30 minutes with 20% serum from the species of the antibodies used for 30 minutes in order to block non-specific cross-reactivity. The antibodies were diluted in PBS, placed on the cells and incubated for 1 hour at room temperature in a humidified chamber covered with aluminium foil. The cells were washed 3 times in PBS. Secondary antibodies were diluted in PBS, placed on the cells and incubated as above. The cells were washed 3 times in PBS and mounted in AF1 solution (Citiflur). Cells were

visualised using an Olympus BX4 microscope (Olympus Optical) at x250 magnification and images captured using a QImaging Retiga 2000R Fast 1396 camera (QImaging).

| Antibody Specificity | Source | Host/Clone | Dilution Used |
|---|---|---|---|
| ***Rabbit anti-myosin*** | Sigma-Aldrich | Rabbit polyclonal | 1:10 |
| ***Goat anti-rabbit IgG FITC*** | Sigma-Aldrich | Goat polyclonal | 1:50 |
| ***Mouse anti-pancytokeratin FITC*** | Sigma-Aldrich | Mouse monoclonal | 1:50 |

**Table 2.13 Antibodies used for mesangial cell characterisation.**

### 2.2.2.3 Mesangial cell passage

When the cultured mesangial cells reached 90-95% confluency, mesangial cell culture medium (Section 2.2.2.1) was aspirated with a sterile glass pipette. Cells were washed twice with 5ml (25cm$^2$ flask) or 10ml (75cm$^2$) of sterile PBS. 1ml (25cm$^2$ flask) or 3ml (75cm$^2$) of non-enzymatic cell dissociation buffer (Sigma-Aldrich) was added to each flask and incubated at 37°C for 30 minutes. The tissue flask was shaken briefly to enhance cell separation from the flask. The cell dissociation solution effect was quenched by adding 5 volumes of 20% FCS culture medium. Cells were then pelleted by centrifugation at 352 x *g* for 5 minutes at 4°C. Supernatant was aspirated with a sterile glass pipette. The cell pellet was resuspended in an adequate volume of mesangial cell culture medium and placed in a fresh culture flask. Mesangial cells were used between passages 8-12 for all experiments.

### 2.2.2.4 Mesangial cell freezing

Mesangial cells were dissociated from the flask when confluent (see Section 2.2.2.3). The cell pellet from a 75cm$^2$ flask was resuspended in 1ml of recovery cell culture freezing medium (Invitrogen) and transferred to a cryogenic vial (Corning). To slowly freeze the cells the cryogenic vial was wrapped in tissue and placed at -80°C. After 24 hours the cells were transferred to liquid nitrogen.

### 2.2.2.5 Mesangial cell thawing

A vial was taken from the liquid nitrogen and quickly thawed at 37°C in an incubator for 2 minutes. The cell suspension was transferred to a sterile 15ml falcon tube. 15ml of mesangial cell culture medium (Section 2.2.2.1) was added to the falcon tube and the cells were pelleted down by centrifugation at 352 x *g* for 5 minutes at 4°C. These cells were then resuspended in 15ml of mesangial cell culture medium, placed in a fresh 75cm$^2$ culture flask and incubated at 37°C with 5% $CO_2$.

### 2.2.2.6 Preparation of heat aggregated IgG

Sheep and mouse IgG (reagent grade, Sigma-Aldrich) were dissolved in sterile saline to a stock concentration of 10mg/ml. The dissolved solution was aliquoted into autoclaved sterile eppendorf tubes (500µl each) and then stored at -20°C. To prepare heat-aggregated IgG, defrosted aliquots of filtered IgG were heat-aggregated at 63°C for 20 minutes on a heat block followed by microcentrifugation at high speed for 5 minutes at 4°C to remove the insoluble aggregates. The soluble aggregated IgG was diluted to a final concentration of 100µg/ml with the appropriate culture medium. All the heat-aggregated IgG was prepared and used the same day.

### 2.2.2.7 Stimulation of mesangial cells

Mesangial cells from WT or *gld* mice were stimulated with LPS, cytokines or heat-aggregated mouse IgG. Briefly, 1x10$^6$ mesangial cells/well were cultured in complete RPMI 1640 mesangial cell culture medium for 24 hours in a flat-bottomed 6-well plate. Following this period, the medium was replaced with serum-free RPMI 1640 mesangial cell culture medium and incubated overnight to put the mesangial cells into quiescence. The next day, mesangial cells were stimulated with either 100µg/ml heat-aggregated mouse IgG, 10ng/ml recombinant IL-1β or TNF-α (R&D Systems), 10ng/ml LPS (Sigma-Aldrich) or left unstimulated in serum-free RPMI 1640 meangial cell culture medium. After 24 hours stimulation, supernatants were harvested and centrifuged at 10,600 x *g* for 5 minutes at 4°C to remove cellular contaminants. These supernatants were transferred to new tubes and either examined immediately or stored at -20°C.

### 2.2.2.8 RNA extraction from mesangial cells

500µl of TRIzol (Invitrogen) was added to $1x10^6$ mesangial cells, following stimulation, and left for 5 minutes at room temperature and then placed in an eppendorf. 100µl of chloroform was added and the samples shaken by hand and left at room temperature for 5 minutes. Samples were spun down in a microcentrifuge at 12000 x *g* for 15 minutes at 4°C. The clear aqueous phase was transferred to a clean eppendorf and 250µl of isopropanol was added. Samples were stored at -20°C overnight. RNA were spun down at 12000 x *g* for 10 minutes at 4°C and the supernatant discarded. The RNA pellet was washed with 75% ethanol, spun down at 8000 x *g* for 8 minutes at 4°C and the supernatant removed. The RNA was air-dried for 10 minutes, resuspended in 40µl RNase free water (Gibco) and heated at 55°C for 5 minutes before being stored at -80°C.

### 2.2.2.9 Mesangial cell expression of Fas ligand and FcγRIIB

Expression of FasL and FcγRIIB on mesangial cells was determined by qRT-PCR. Mesangial cells were stimulated as Section 2.2.2.7 and RNA extracted as Section 2.2.2.8. qRT-PCR was repeated as in Section 2.2.1.23. FasL and FcγRIIB primers were synthesised by Sigma-Aldrich and taken from Ho *et al.* and Ichii *et al.,* respectively (Ho et al., 2011; Ichii et al., 2008):

FasL forward 5'ACCCCCACTCAAGGTCCAT-3'

FasL reverse 5'CGAAGTACAACCCAGTTTCGT-3'

FcγRIIB forward 5'CTGAGGCTGAGAATACGATC-3'

FcγRIIB reverse 5'GTGGATCGATAGCAGAGAG-3'

Expression of FcγRIIB on mesangial cells was also determined by direct immunofluorescence. Briefly, WT and FcγRIIB$^{-/-}$ mesangial cells were washed in ice-cold PBS and cytospins were prepared. After allowing the slides to air dry, the cells were fixed in acetone for 10 minutes. FITC-labelled anti-FcγRIIB (clone 17.2) antibody was diluted in PBS

(1:50), applied to the sections and incubated for one hour at room temperature in a humidified chamber covered with aluminium foil. The sections were washed three times in PBS and mounted in AF1 solution (Citiflur). Cells were visualised using an Olympus BX4 microscope (Olympus Optical) at x250 magnification and images captured using a QImaging Retiga 2000R Fast 1396 camera (QImaging).

#### 2.2.2.10 Splenocyte culture

For splenocyte isolation, the spleen was removed and a single cell suspension created. The spleen was passed through a 100µm cell strainer and splenocytes resuspended in HL-1 serum-free splenocyte medium (Lonza Group Ltd.) containing 100U/ml penicillin, 100µg/ml streptomycin and L-glutamine (Gibco). Splenocytes were spun down at 626 x *g* for 10 minutes and resuspended in 1ml RBC lysis buffer. Red blood cells were lysed on ice for 5 minutes before making up the volume to 14mls with medium. Splenocytes were spun down at 157 x *g* for 10 minutes and resuspended in HL-1 serum-free splenocyte medium at a final concentration of $8x10^6$ splenocytes/ml.

#### 2.2.2.11 Stimulation of splenocytes

Splenocytes from WT and *gld* mice were stimulated with heat-aggregated sheep IgG. For proliferation assays, $2x10^5$ splenocytes/well were cultured in a round-bottomed 96-well plate in HL-1 serum-free splenocyte medium (Lonza Group Ltd.) (Section 2.2.2.10) in the presence of 100µg/ml heat-aggregated sheep IgG or CD3/CD28 beads (Invitrogen) at 37°C, 5% $CO_2$ for 72 hours. For cytokine assays, $4x10^6$ splenocytes/well were cultured in a flat-bottomed 24-well plate in HL-1 serum-free splenocyte medium (Lonza Group Ltd.) (Section 2.2.2.10) in the presence of 100µg/ml heat-aggregated sheep IgG or 100ng/ml phorbolmyristate acetate (PMA) (Sigma-Aldrich) and 500ng/ml ionomycin (Sigma-Aldrich) at 37°C, 5% $CO_2$. After stimulation for 72 hours, supernatants were harvested and centrifuged at 10,600 x *g* for 5 minutes at 4°C to remove cellular contaminant. Supernatants were transferred to fresh eppendorfs and either examined immediately or stored at -20°C.

#### 2.2.2.12 Proliferation of splenocytes

Following stimulation for 72 hours, 0.037MBq of tritiated ($^3$H) thymidine (PerkinElmer) was added to each well of splenocytes and incubated for a further 24 hours at 37°C, 5% $CO_2$. The radioactivity uptake was counted the following day using a 1450 MicroBetaTriLux liquid scintillation and luminescence counter (PerkinElmer).

#### 2.2.2.13 Cytokine assessment

Supernatants collected following stimulation of mesangial cells or splenocytes were analysed for cytokine production by ELISA. All kits, antibodies, standards and concentrations used are summarised in Table 2.14. IL-10 and IL-17 were both measured using R&D DuoSet ELISA Development kits (R&D Systems). Briefly, Nuncmaxisorp ELISA plates (Fisher Scientific) were coated with capture antibody overnight at room temperature. Plates were washed three times with PBS/0.1% Tween 20 (Sigma Aldrich) between each step. Plates were blocked with 1% BSA (Sigma-Aldrich) for 1 hour before adding 100µl of supernatant, diluted in 1% BSA/PBS, along with a standard curve of known concentration of cytokine and incubated for two hours at room temperature. Following this, the detection antibody was applied for two hours and then streptavidin-HRP, diluted 1:200, for 20 minutes, both at room temperature. Tetramethylbenzidine (TMB) substrate solutions A and B (Cambridge Bioscience) were mixed in equal volumes, incubated for 20 minutes before adding 1M $H_2SO_4$. Optical density was read at 450nm on a EL800 ELISA plate reader (BioTek).

IFN-γ, IL-4 and MCP-1 were measured using Ready-SET-Go ELISA kits (eBioscience). Briefly, Nuncmaxisorp ELISA plates (Fisher Scientific) were coated with capture antibody overnight at 4°C. Plates were washed five times with PBS/0.1% Tween 20 (Sigma-Aldrich) between each step. Plates were blocked with 1x assay diluent for 1 hour before adding 100µl of supernatant, diluted in 1x assay diluent, along with a standard curve of known concentrations of cytokine and incubated for two hours at room temperature. Following this the detection antibody was applied for one hour and then avidin-HRP, diluted 1:250, for 30 minutes, both at room temperature. 1x TMB substrate solution was incubated for 15 minutes before adding 1M $H_2SO_4$. Optical density was read at 450nm on an EL800 ELISA plate reader (BioTek).

| Antibody specificity | Source | Host | Working Concentration/ Range of Standards |
|---|---|---|---|
| **IL-10 ELISA** | | | |
| ***IL-10 Coating*** | R&D Systems | Rat polyclonal | 4.0µg/ml |
| ***IL-10 Biotinylated*** | R&D Systems | Goat polyclonal | 300ng/ml |
| ***Standard*** | R&D Systems | - | 15-2,000pg/ml |
| **IL-17 ELISA** | | | |
| ***IL-17 Coating*** | R&D Systems | Rat polyclonal | 2.0µ/ml |
| ***IL-17 Biotinylated*** | R&D Systems | Goat polyclonal | 400ng/ml |
| ***Standard*** | R&D Systems | - | 23-3,000pg/ml |
| **IFN-γ ELISA** | | | |
| ***IFN-γ Coating*** | eBioscience | - | 1:1000 |
| ***IFN-γ Biotinylated*** | eBioscience | - | 1:1000 |
| ***Standard*** | eBioscience | - | 15-2,000pg/ml |
| **IL-4 ELISA** | | | |
| ***IL-4 Coating*** | eBioscience | - | 1:250 |
| ***IL-4 Biotinylated*** | eBioscience | - | 1:250 |
| ***Standard*** | eBioscience | - | 4-500pg/ml |
| **MCP-1 ELISA** | | | |
| ***MCP-1 Coating*** | eBioscience | - | 1:250 |
| ***MCP-1 Biotinylated*** | eBioscience | - | 1:250 |
| ***Standard*** | eBioscience | - | 15-2,000pg/ml |

**Table 2.14 Antibodies used for detecting cytokines in supernatants by ELISA.**

## 2.3 Statistical analysis

All results reported in this document are expressed as median (range). Non-parametric tests of significance were applied throughout as it could not be assumed that the distribution of the data was Gaussian. For comparing two unpaired groups, the Mann-Whitney U-test was used, and for comparing three or more groups, the Kruskal-Wallis test was used, with Dunn's Multiple Comparisons test (p values given are from Dunn's test). A probability of less than 0.05 was considered significant. Statistical analysis was carried out using GraphPad Prism 5.04 (GraphPad Software).

## 2.4 Buffers and solutions

### 2.4.1 Polymerase chain reaction (PCR)

**Lysis buffer for tail/toe/ear**

100mM Tris-HCl (pH 8.5), 5mM EDTA, 0.2% SDS, 200mM NaCl and 100µg/ml proteinase K (added immediately before use).

**Lysis buffer for blood**

25mM TRIS (pH 8.0), 100mM NaCl, 1% SDS and 100µg/ml of proteinase K (added immediately before use).

**TAE buffer (50x)**

40mM Tris-acetate, 1mM EDTA (pH 8.0). For use in DNA electrophoresis, TAE buffer was diluted down to 1x with $dH_2O$.

### 2.4.2 Tissue fixation

**Neutral buffered formalin (pH 7.0)**

100ml formalin, full strength (37-40% formaldehyde), 6.5g $Na_2HPO_4$, 4g $NaH_2PO_4$ and 900ml $dH_2O$.

**Paraformaldehyde lysine periodate (PLP) fixative**

Lysine stock solution: 0.2M lysine monohydrochloride (3.65g/100ml) added to an equal volume of 0.1M disodium hydrogen orthophosphate (1.41g/100ml for anhydrous). The solution was adjusted to pH 7.4 and stored at 4°C.

4% Paraformaldehyde: paraformaldehyde was dissolved in $dH_2O$ (4g/100ml) with stirring at 60°C in a fume hood. The solution was cleared by adding a few drops of 1M NaOH and then stored at 4°C.

Immediately prior to use: 1 volume of 4% paraformaldehyde was added to 3 volumes of lysine stock solution and 10mM sodium metaperiodate (0.214g/100ml) was added.

### 2.4.3 Immunohistochemistry

**Phosphate buffered saline (PBS)**

137mM NaCl, 0.27mM KCl, 8.1mM $Na_2PO_4$, 1.5mM $KH_2PO_4$, adjusted to pH 7.2.

**3,3'-Diaminobenzidine (DAB) solution**

0.05% (w/v) DAB, 0.003 $H_2O_2$ in PBS (pH 7.5). Stored at -20°C.

**Acid Alcohol**

1% HCl mixed with 70% ethanol.

### 2.4.4 Tissue culture

**Red blood cell (RBC) lysis buffer**

4.17g $NH_4Cl$, 0.00185g EDTA, 0.5g $NaHCO_3$, 500ml sterile $ddH_2O$.

**Splenocyte medium**

HL-1 serum-free medium containing 100U/ml penicillin, 100µg/ml streptomycin and L-glutamine.

**Mesangial cell medium**

RPMI-1640 medium supplemented with 20% fetal calf serum, 100U/ml penicillin, 100U/ml streptomycin, 2% L-glutamine and 1% insulin-transferrin-selenium growth supplement (ITS liquid).

## 2.5 Suppliers and distributors

| | |
|---|---|
| Agilent Technologies UK Ltd. | Edinburgh, UK |
| Applied Biosystems/Life Technologies Corp. | Carlsbad, CA, USA |
| BD Biosciences | San Jose, CA, USA |
| BDH | Poole, UK |
| Bio-Rad Laboratories Ltd. | Hemel Hempstead, UK |
| Bioline Reagents Ltd. | London, UK |
| Biosera | Ringmer, UK |
| BioTek | Winooski, VT, USA |
| Bright Instrument Company Ltd. | Huntingdon, UK |
| Cambrex | East Rutherford, NJ, USA |
| Cambridge Bioscience Ltd. | Cambridge, UK |
| CellPath Ltd. | Powys, UK |
| Citiflur Ltd. | London, UK |
| Corning Incorporated | Corning, NY, USA |
| eBioscience | San Diego, CA, USA |
| Eppendorf | Hamburg, Germany |
| Fisher Scientific | Loughborough, UK |
| Gibco/Life Technologies Ltd. | Paisley, UK |
| GraphPad Software | San Diego, CA, USA |
| Invitrogen/Life Technologies Ltd. | Paisley, UK |
| Labtech International Ltd. | Ringmer, UK |
| Lonza Group Ltd. | Basle, Switzerland |
| Media Cybernetics, Inc. | Bethesda, MD, USA |
| MJ Research | Waltham, MA, USA |
| New England BioLabs, Inc. | Hitchin, UK |

| | |
|---|---|
| Newmarket Scientific Ltd. | Newmarket, UK |
| Olympus Optical | London, UK |
| Perkin Elmer, Inc. | Waltham, MA, USA |
| Promega | Southampton, UK |
| Qiagen Ltd. | Crawley, UK |
| QImaging | Surrey, BC, Canada |
| R&D Systems | Abingdon, UK |
| R-Biopharm Rhone Ltd. | Glasgow, UK |
| Regal Group | Surrey, UK |
| Roche | Basle, Switzerland |
| Serotec | Oxford, UK |
| Sigma-Aldrich Company Ltd. | Dorset, England |
| SouthernBiotech | Birmingham, AL, USA |
| Surgipath Europe Ltd. | Peterborough, UK |
| The Jackson Laboratory | Bar Harbor, ME, USA |
| Thermo Fisher Scientific | Waltham, MA, USA |
| TreeStar | Ashland, OR, USA |
| Vector Laboratories | Burlingame, CA, USA |
| VWR International Ltd. | Poole, UK |

# CHAPTER 3

# The Role of Fas Ligand in Accelerated Nephrotoxic Nephritis

## 3.1 Introduction

The identification of the FasL mutation in *gld* mice has facilitated the study of the role of FasL in different diseases. FasL has been found to play a detrimental role in EAE (Sabelko et al., 1997; Waldner et al., 1997), autoimmune diabetes (Chervonsky et al., 1997; Itoh et al., 1997; Mohamood et al., 2007), EAU (Wahlsten et al., 2000), acute lung injury (Neff et al., 2005), and experimental stroke (Niu et al., 2011). In addition to its role in inducing apoptosis, defects in FasL have been reported to cause a reduction in signalling through the IL-1R, TLR4 and NF-κB (Ahn et al., 2001; Altemeier et al., 2007; Bannerman et al., 2002; Ma et al., 2004) as well as affecting the chemoattractant properties of sFasL towards neutrophils (Dupont and Warrens, 2007; Ottonello et al., 1999; Seino et al., 1998).

The role of FasL in glomerulonephritis, however, is undefined. FasL has been shown to be expressed in both healthy and diseased kidneys in humans and mice, with expression being upregulated in the glomerulus during injury (Lorz et al., 2000; Tsukinoki et al., 2004). Treatment of lupus-prone mice with an anti-FasL monoclonal blocking antibody prevented the development of nephritis, compared to untreated mice despite the presence of autoantibodies (Nakajima et al., 2000). However, both *lpr* and *gld* mice bred on permissive backgrounds develop spontaneous autoimmunity and severe nephritis (Izui et al., 1984). This is the first study to address the role of FasL in experimental GN. Since both circulating leukocytes and intrinsic renal cells express FasL, it is well placed to modulate renal disease either by inducing apoptosis of infiltrating cells or initiating an inflammatory response.

The model I have used to investigate the role of FasL in GN is accelerated NTN. This is a model in which disease is induced following an immune response to an antibody (raised in sheep against GBM antigens) planted on the GBM. NTN depends on a $T_h1/T_h17$ predominant immune response and is widely used in C57BL/6 mice. Preliminary work by my supervisor demonstrated protection of *gld* mice from NTN. The aim of the work presented in this chapter is to confirm this protection and establish possible mechanisms.

My hypothesis was that FasL is required to initiate an inflammatory response and its absence will protect the mice from developing GN, either due to defects in the immune response, alterations in cytokine production or the reduction in apoptosis.

## 3.2 Aim

This first chapter of the thesis was an investigation of the role of FasL in the well-characterised model of NTN. The results were based on the assessment of disease in WT and *gld* mice. I also studied the differences in intra-renal cytokine production during NTN, as well as the differences in splenocyte proliferation and cytokine production, following stimulation with sheep IgG, CD3/CD28 beads, or PMA and ionomycin, to ask if defective FasL affects the immune response in *gld* mice.

## 3.3 Experimental design

The role of FasL in accelerated NTN was studied to elucidate its role in a model of immune-mediated GN and to obtain further insights into pathogenesis of the disease. Nephritis was induced in *gld* mice on a C57BL/6 background and age- and sex-matched WT C57BL/6 control mice. Assessment of disease was done by the following methods: (1) renal function was assessed by measuring albuminuria and serum urea; (2) renal morphology (severity of glomerular injury) was analysed in PAS-stained sections under light microscopy; (3) quantitation of kidney sections for infiltrating leukocytes was done by immunoperoxidase staining; and (4) immune responses were analysed by quantitation of sheep and mouse IgG deposition in the kidney and circulating levels of mouse anti-sheep IgG. Apoptotic cells and whole kidney mRNA cytokine and chemokine expression levels were also assessed. Since *gld* mice on a C57BL/6 background are susceptible to developing late onset autoimmunity with GN, baseline parameters were taken of unmanipulated *gld* and WT mice at 2 and 4 months.

To study the immune response, spleens were collected from mice either 7 days after immunisation with the antigen (sheep IgG) or at the termination of a day 10 NTN experiment

and splenocytes were isolated and stimulated with sheep IgG, CD3/CD28 beads, or PMA and ionomycin. Proliferation was assessed by $^{3}H$ thymidine uptake and cytokine production was measured in the supernatant by ELISA.

## 3.4 Results

### 3.4.1 Genotyping of *gld* mice using polymerase chain reaction

The genotype of *gld* mice was confirmed by PCR analysis and restriction digest. DNA was extracted from tail snips and amplified by PCR using FasL specific primers. Amplified DNA was digested using the restriction endonuclease StuI, resulting in bands of 88bp and 20bp for the WT product, although the 20bp band was too small to detect, and a single band of 108bp for the mutated allele. The presence of the 108bp and 88bp bands represented a heterozygote. A negative control without DNA was used to demonstrate the specificity of the assay (Figure 3.1).

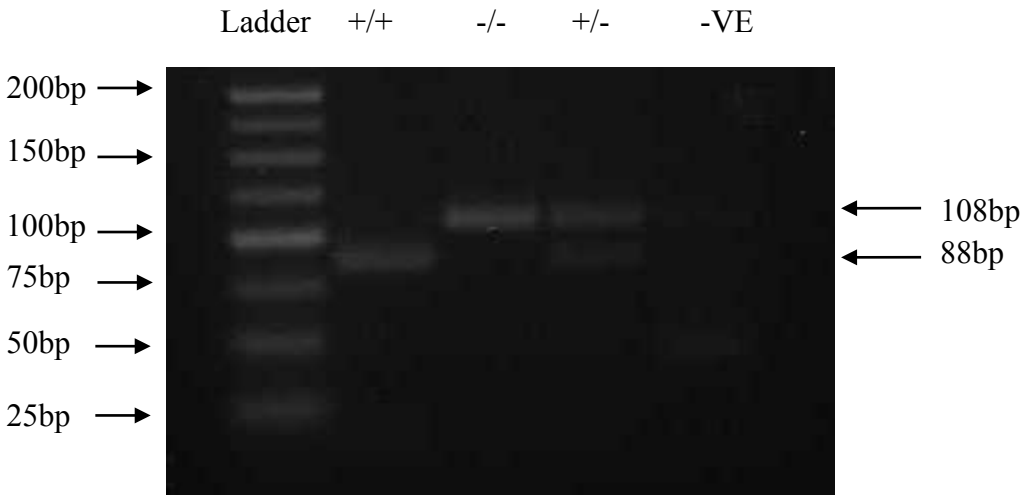


**Figure 3.1 PCR reactions of genomic DNA from WT and *gld* animals.**

Representative examples of WT (+/+), *gld* (-/-) and heterozygote (+/-) mice are shown here. The WT (+/+) mice show a band at 88bp, the *gld* (-/-) mice show a band at 108bp and the heterozygote (+/-) mice show bands at 108bp and 88bp. The negative control (-VE) has no bands.

### 3.4.2 Ageing *gld* mice on a C57BL/6 background developed glomerular immune complex deposition and mild renal dysfunction

Mice used in the NTN experiments were between 2-4 months of age. At 2 months, the *gld* mice showed no evidence of spontaneous renal disease, as assessed by the presence of glomerular crescents, thrombosis, IgG immune deposits and serum urea and creatinine, compared to WT C57BL/6 mice of the same age. At 4 months there was some granular IgG deposited in the glomeruli of the *gld* mice and elevated serum urea ($p=0.0037$). There was no significant difference in glomerular macrophage or $CD4^+$ T cell numbers between WT and *gld* mice at 2 and 4 months (Table 3.1). In view of these results, young mice, aged 6-8 weeks, were used for the NTN experiments.

| | **WT (2 months)** | ***Gld* (2 months)** | **WT (4 months)** | ***Gld* (4 months)** |
|---|---|---|---|---|
| **Deposited Glomerular Mouse IgG** | Negative | Negative | Negative | Granular |
| **Urinary Albumin/Creatinine (mg/mmol)** | 0.0057 (0.0044-0.0081) | 0.0064 (0.0052-0.036) | 0.012 (0.0079-0.017) | 0.012 (0.0067-0.020) |
| **Serum Creatinine (µmol/L)** | 49 (42-51) | 40 (36-44) | 43 (37-55) | 37 (33-41) |
| **Serum Urea (mmol/L)** | 9.4 (6.4-16) | 7.5 (5.3-8.7) | 7.2 (4.8-12) | 11** (11-14) |
| **Thrombosis Score** | 0.0 (0.0-0.0) | 0.0 (0.0-0.0) | 0.0 (0.0-0.0) | 0.0 (0.0-0.0) |
| **% Crescents** | 0.0 (0.0-0.0) | 0.0 (0.0-0.0) | 0.0 (0.0-0.0) | 0.0 (0.0-0.0) |
| **Macrophages/gcs** | 0.10 (0.020-1.1) | 0.12 (0.00-0.60) | 0.33 (0.10-0.56) | 0.49 (0.22-2.5) |
| **$CD4^+$ T cells/gcs** | 0.0 (0.0-0.48) | 0.020 (0.0-0.30) | 0.47 (0.18-0.62) | 0.54 (0.48-0.82) |

**Table 3.1 Baseline renal parameters of WT and *gld* mice at 2 and 4 months of age.**

For all groups n=8 and all results are expressed as median (range).

### 3.4.3 Preliminary data

Prior to the start of my PhD project, my supervisor performed some preliminary experiments inducing NTN in WT and *gld* mice, which are outlined in Table 3.2 and Table 3.3. In all experiments mice were pre-immunised with 0.2mg of sheep IgG in CFA and after five days 200µl (1:4 dilution) of NTS was administered via the tail vein. Three experiments were terminated on day 7 after the induction of NTN and demonstrated protection of *gld* mice from GN, with *gld* mice having significantly reduced glomerular thrombosis, crescents and serum creatinine compared to WT mice (Table 3.2 and Figure 3.2). Two further experiments were terminated 24 hours after the injection of NTS to measure neutrophil influx, with conflicting results. One experiment showed a reduction in neutrophil infiltration and reduced IgG deposition in the *gld* mice, whilst the other experiment showed no difference between the two groups (Table 3.3).

| | Experiment 1 | | Experiment 2 | | Experiment 3 | |
|---|---|---|---|---|---|---|
| **Genotype** | WT | *Gld* | WT | *Gld* | WT | *Gld* |
| **Mice** | 12 | 9 | 11 | 10 | 12 | 11 |
| **Sex** | M | M | M | M | M | M |
| **End Point (day)** | 7 | 7 | 7 | 7 | 7 | 7 |
| **Serum Anti-Sheep IgG** | Not done | Not done | 5.3* (2.6-19) | 9.0 (5.3-27) | Not done | Not done |
| **Deposited Glomerular Mouse IgG (AFU)** | 55* (35-72) | 65 (43-99) | 30 (23-38) | 35 (23-53) | 57 (41-79) | 54 (32-73) |
| **Urinary Albumin/Creatinine (mg/mmol)** | Not done | Not done | 16 (1.5-32) | 6.0 (0.0-32) | 7.0 (2.0-22) | 3.0 (0.0-31) |
| **Serum Creatinine (µmol/L)** | Not done | Not done | 78*** (56-112) | 38 (33-64) | 80*** (43-161) | 41 (34-59) |
| **Thrombosis Score** | 0.44** (0.0-0.8) | 0.0 (0.0-0.04) | 1.5*** (0.5-2.0) | 0.02 (0.0-1.0) | 2.0*** (0.1-2.7) | 0.0 (0.0-0.9) |
| **Crescents (%)** | 0.0 (0.0-0.0) | 0.0 (0.0-0.0) | 1.5*** (0.5-2.0) | 0.02 (0.0-1.0) | 4.0*** (0.0-16) | 0.0 (0.0-2.0) |
| **Macrophages/gcs** | 2.7 (0.4-4.3) | 1.9 (0.5-3.7) | 1.0 (0.5-1.3) | 1.6 (0.2-4.0) | Fixation problems | Fixation problems |

**Table 3.2 Preliminary data looking at NTN in WT and *gld* mice at day 7.**

M = male. All data represent the median (range). The data were analysed using the Mann-Whitney U-test (p*<0.05, p**<0.01, p***<0.001).

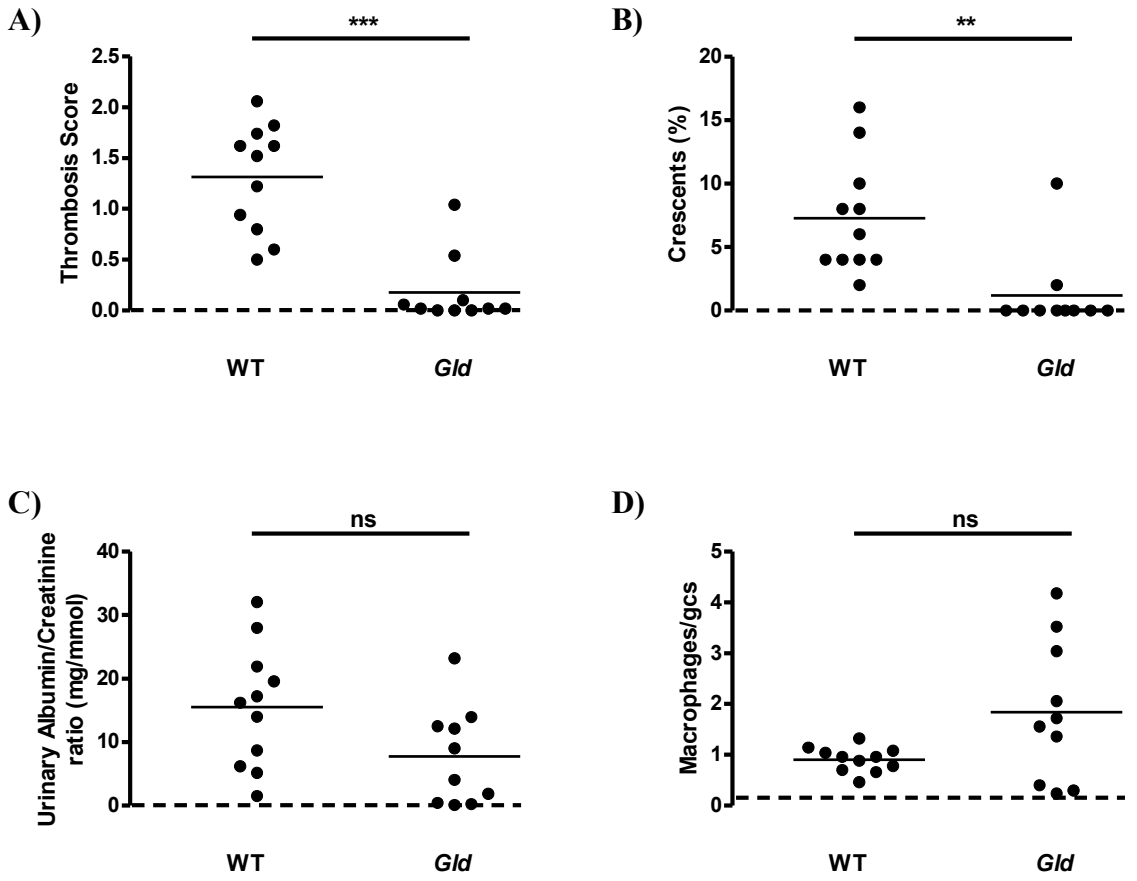


**Figure 3.2 Preliminary data looking at NTN in WT and *gld* mice at day 7.**

Crescents, thrombosis, urinary albumin/creatinine ratio and macrophages were compared in WT and *gld* mice 7 days after administration of NTS. WT mice had significantly more **(A)** thrombosis and **(B)** crescents, however there was no difference in **(C)** the urinary albumin/creatinine ratio and **(D)** glomerular macrophage infiltration in *gld* mice. All data represent individual values with the median. The data were analysed using the Mann-Whitney U-test (p**<0.01, p***<0.001). Dashed lines represent values for a group of normal WT mice.

| | Experiment 4 | | Experiment 5 | |
|---|---|---|---|---|
| **Genotype** | WT | *Gld* | WT | *Gld* |
| **Mice** | 10 | 9 | 14 | 7 |
| **Sex** | M | M | M | M |
| **End Point** | 24 hours | 24 hours | 24 hours | 24 hours |
| **Serum Anti-Sheep IgG** | 6.0** | 1.0 | Not done | Not done |
| | (1.0-10) | (0.2-7.6) | | |
| **Deposited Glomerular Mouse IgG (AFU)** | 84* | 42 | 55 | 47 |
| | (42-108) | (30-68) | (38-99) | (34-72) |
| **Deposited Glomerular Sheep IgG (AFU)** | 69 | 77 | 54 | 47 |
| | (47-79) | (55-94) | (40-68) | (34-72) |
| **Neutrophils/gcs** | 1.6* | 0.4 | 0.5 | 0.6 |
| | (0.2-3.1) | (0.1-3.2) | (0.1-1.5) | (0.28-1.1) |

**Table 3.3 Preliminary data looking at NTN in WT and *gld* mice 24 hours after induction of NTN.**

M = male. All data represent the median (range). The data were analysed using the Mann-Whitney U-test ($p^{*}<0.05$, $p^{**}<0.01$).

### 3.4.4 *Gld* mice are protected from developing glomerular crescents, thrombosis and renal failure

The results from the preliminary experiments raise questions about the mechanisms of protection of the *gld* mice from NTN. FasL is involved in the deletion of T cells at the end of the immune response (Kabelitz et al., 1993). In this context, although *gld* mice were protected from EAE initially (Sabelko et al., 1997; Waldner et al., 1997), one report showed worsening of EAE at later time points (Sabelko-Downes et al., 1999). Whilst EAE is a different model from NTN, we wanted to look at a later time point in the disease process to determine whether *gld* mice would develop worsening disease at a later stage. It is not possible to maintain mice for prolonged periods after the induction of NTN, as it can lead to severe renal failure. We therefore chose to investigate disease up to day 15. We also investigated mechanisms in more detail by assessing the immune response, cell infiltration, levels of apoptosis and intra-renal cytokines. The first part of this chapter details the results obtained at day 15 after the induction of NTN.

NTN was induced in WT and *gld* mice. Mice were pre-immunised with 0.2mg of sheep IgG in CFA and after five days 200µl (1:4 dilution) of NTS was administered via the tail vein. Twenty-two male animals were used (n=11 WT and n=11 *gld* mice) and mice were sacrificed on day 15.

To assess renal function, serum urea and albuminuria, expressed as a ratio of urinary albumin and creatinine, were measured in all mice. WT mice had reduced renal function as shown by significantly higher serum urea (29 (12-47) mmol/L) and albuminuria (5.3 (0.050-11) mg/mmol) compared to *gld* mice (serum urea: 16 (10-35) mmol/L, p=0.022; albuminuria: 0.025 (0.010-2.2) mg/mmol, p=0.0004) (Figure 3.3). Histological damage, in the form of glomerular crescents and thrombosis, was assessed in all mice on PAS-stained sections. WT mice had significantly more glomerular damage, shown by an increase in thrombosis (0.3 (0.00-1.6)) and glomerular crescents (16 (0.00-40) %) compared to *gld* mice (thrombosis: 0.020 (0.00-0.14), p=0.0023; crescents: 0.00 (0.00-2.0) %, p=0.0001) (Figure 3.4 and Figure 3.5).

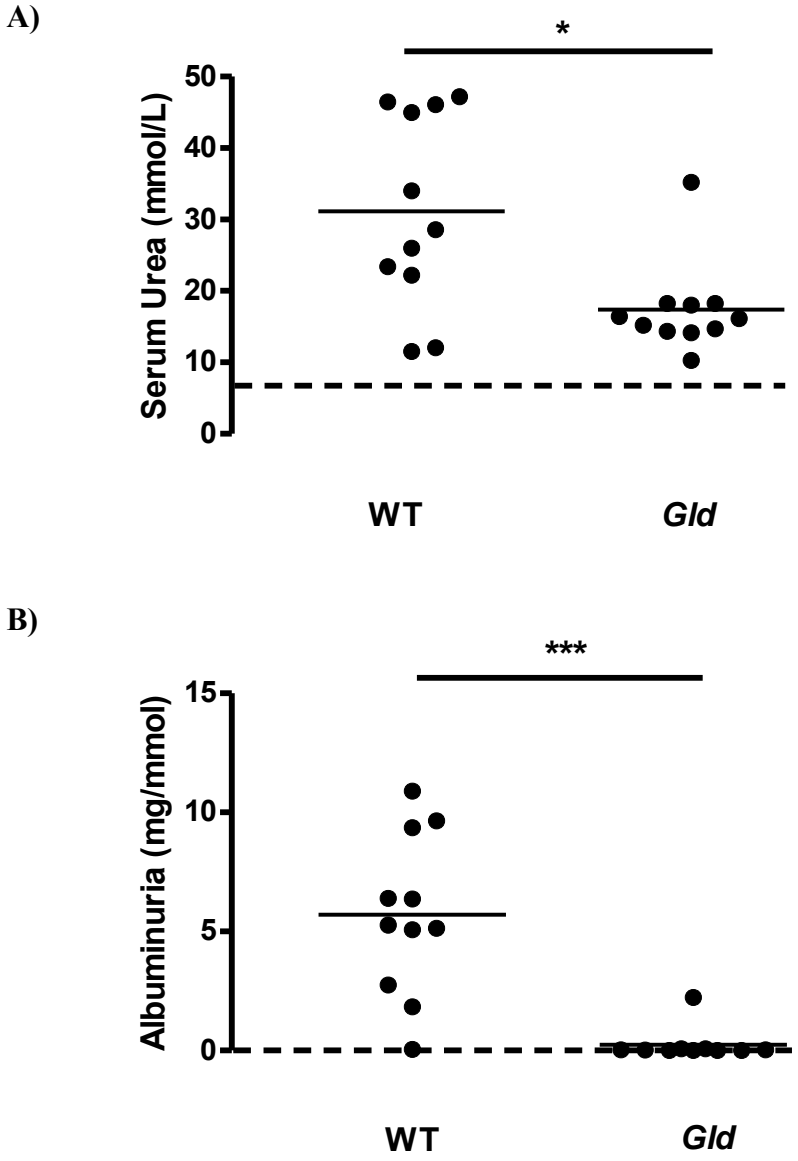


**Figure 3.3 Measurement of serum urea and urinary/albumin creatinine ratio in WT and *gld* mice with NTN at day 15.**

The level of serum urea and the urinary albumin/creatinine ratio was measured in WT and *gld* mice 15 days after administration of NTS. **(A)** WT mice had significantly higher levels of serum urea and **(B)** albuminuria compared to *gld* mice. All data represent individual values with the median. The data were analysed using the Mann-Whitney U-test ($p^{*}<0.05$, $p^{***}<0.001$). Dashed lines represent values for a group of normal WT mice.

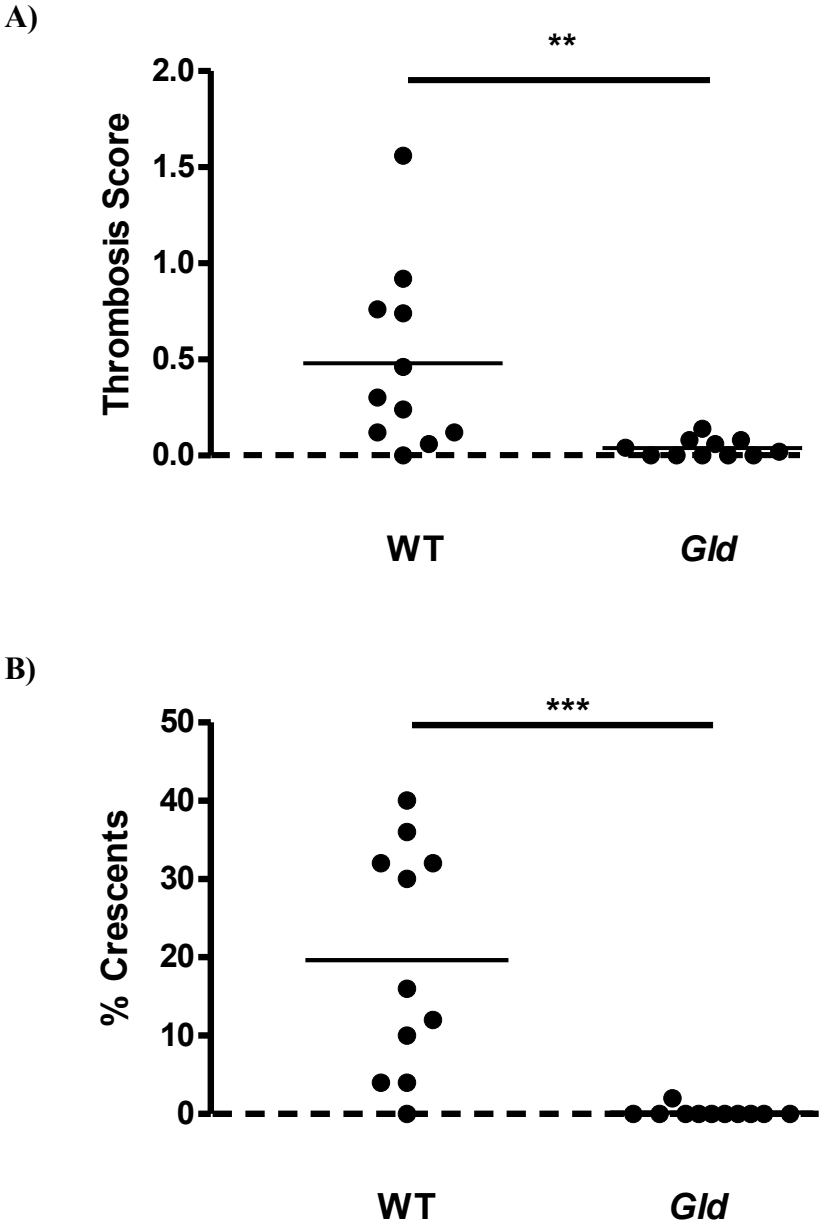


**Figure 3.4 Quantification of histologically abnormal glomeruli from WT and *gld* mice with NTN at day 15.**

**(A)** Thrombosis and **(B)** crescents scored on PAS-stained kidney sections from WT and *gld* mice day 15 post NTS injection. WT mice had significantly more damaged glomeruli than *gld* mice. All data represent individual values with the median. The data were analysed using Mann-Whitney U-test (p**<0.01 and p***<0.001). Dashed lines represent values for a group of normal WT mice.

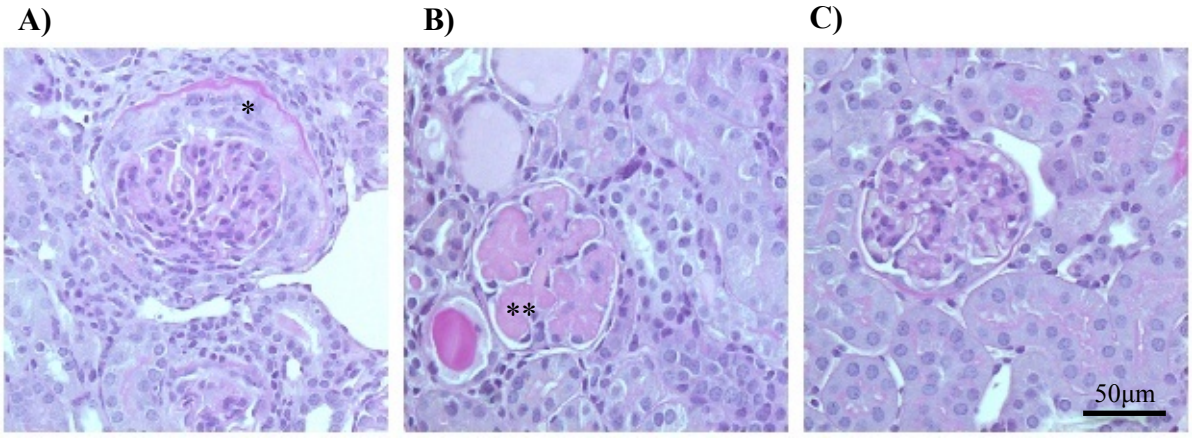


**Figure 3.5 PAS staining of kidneys from WT and *gld* mice.**

Representative PAS staining from **(A)** a WT mouse with a crescentic glomerulus, **(B)** a WT mouse with a thrombotic glomerulus and **(C)** a *gld* mouse with a healthy glomerulus, 15 days after administration of NTS. In the WT glomerulus **(*)** demonstrates crescent formation and **(**)** thrombosis.

### 3.4.5 There was no reduction in glomerular macrophage infiltration, but *gld* mice had fewer interstitial macrophages and glomerular and interstitial $CD4^+$ T cells

Kidney sections collected 15 days after administration of NTS from WT and *gld* mice were stained for macrophages (CD68) and $CD4^+$ T cells as a measure of inflammation (Figure 3.6 and Figure 3.8, respectively). There was no significant difference between glomerular macrophage infiltration between WT and *gld* mice (macrophages/gcs: WT 1.8 (0.24-4.7), *gld* 1.2 (0.36-4.1), p=0.43) (Figure 3.7 A); however, there were significantly fewer interstitial macrophages in *gld* mice (1.2 (0.56-3.3) arbitrary units (AU)) compared to WT mice (4.3 (0.29-12) AU, p=0.026) (Figure 3.7 B). *Gld* mice had significantly fewer glomerular T cells (0.19 (0.040-0.49) T cells/gcs) and interstitial T cells (0.10 (0.063-1.2) AU) than WT mice (T cells: 0.38 (0.12-1.1)/gcs, p=0.031; interstitial T cells: 0.57 (0.074-2.0) AU, p=0.026) (Figure 3.9 A and Figure 3.9 B, respectively).

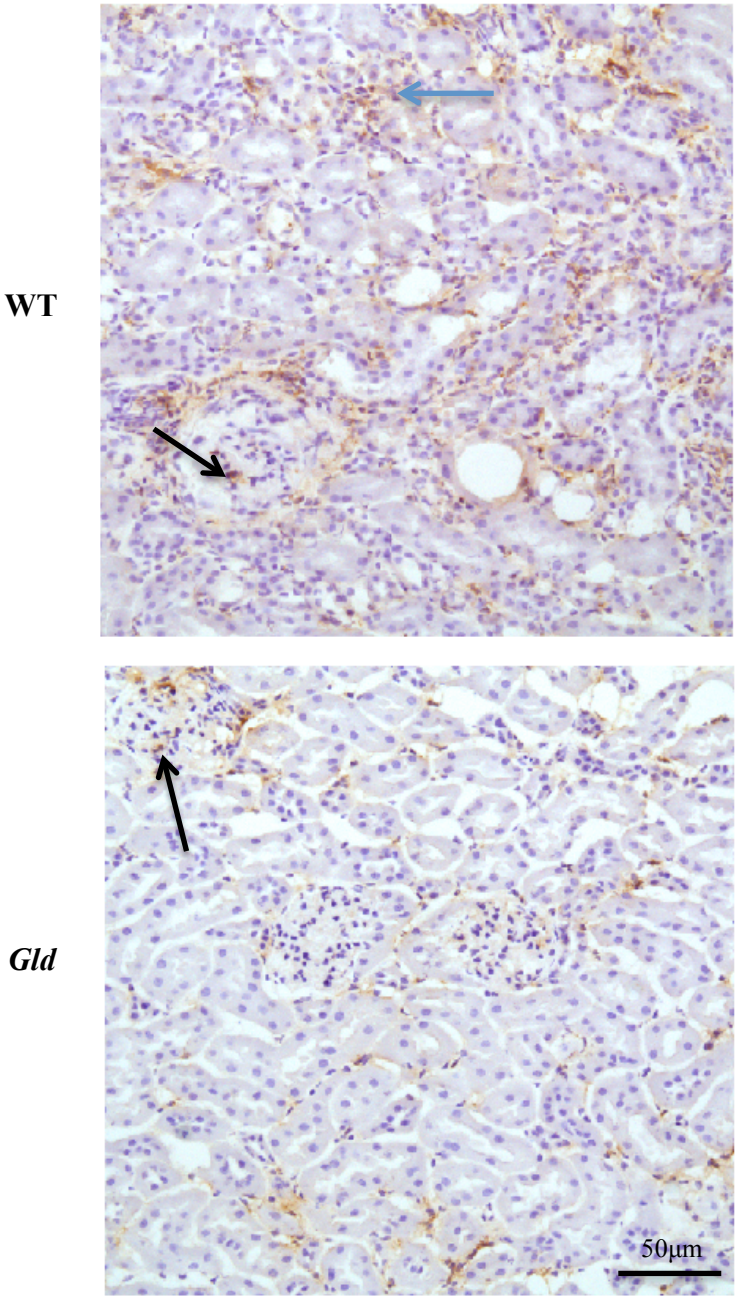


**Figure 3.6 Glomerular and interstitial macrophage infiltration in WT and *gld* mice with NTN at day 15.**

Immunohistochemistry for macrophages (CD68) on WT and *gld* mouse kidney sections at day 15. Black arrows highlight glomerular macrophages and the blue arrow highlights interstitial macrophages.

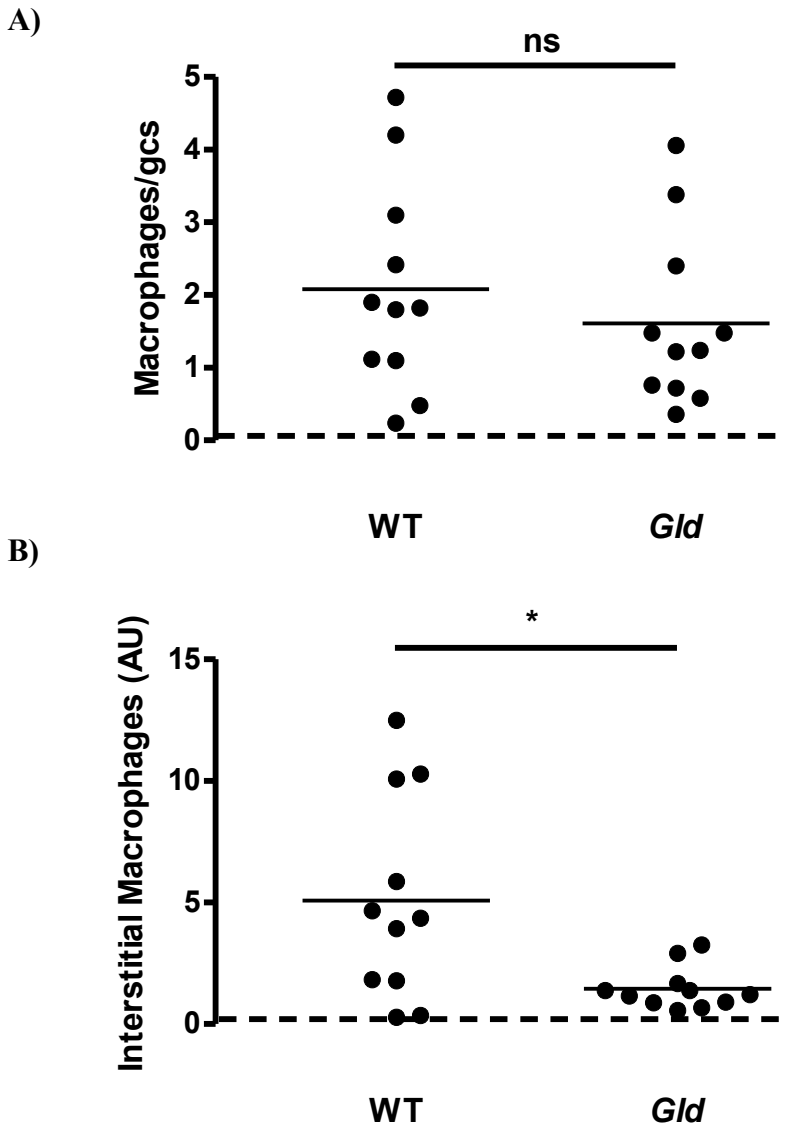


**Figure 3.7 Glomerular and interstitial macrophage infiltration in WT and *gld* mice with NTN at day 15.**

**(A)** Infiltration of macrophages/gcs (50 glomeruli scored per section) was measured. There was no significant difference in glomerular macrophage infiltration between WT and *gld* mice. **(B)** Interstitial macrophage infiltration (5 fields of view per section) was measured. There were significantly fewer interstitial macrophages in *gld* mice compared to WT mice. All data represent individual values with the median. The data were analysed using the Mann-Whitney U-test (ns= non-significant, p*<0.05). Dashed lines represent values for a group of normal WT mice.

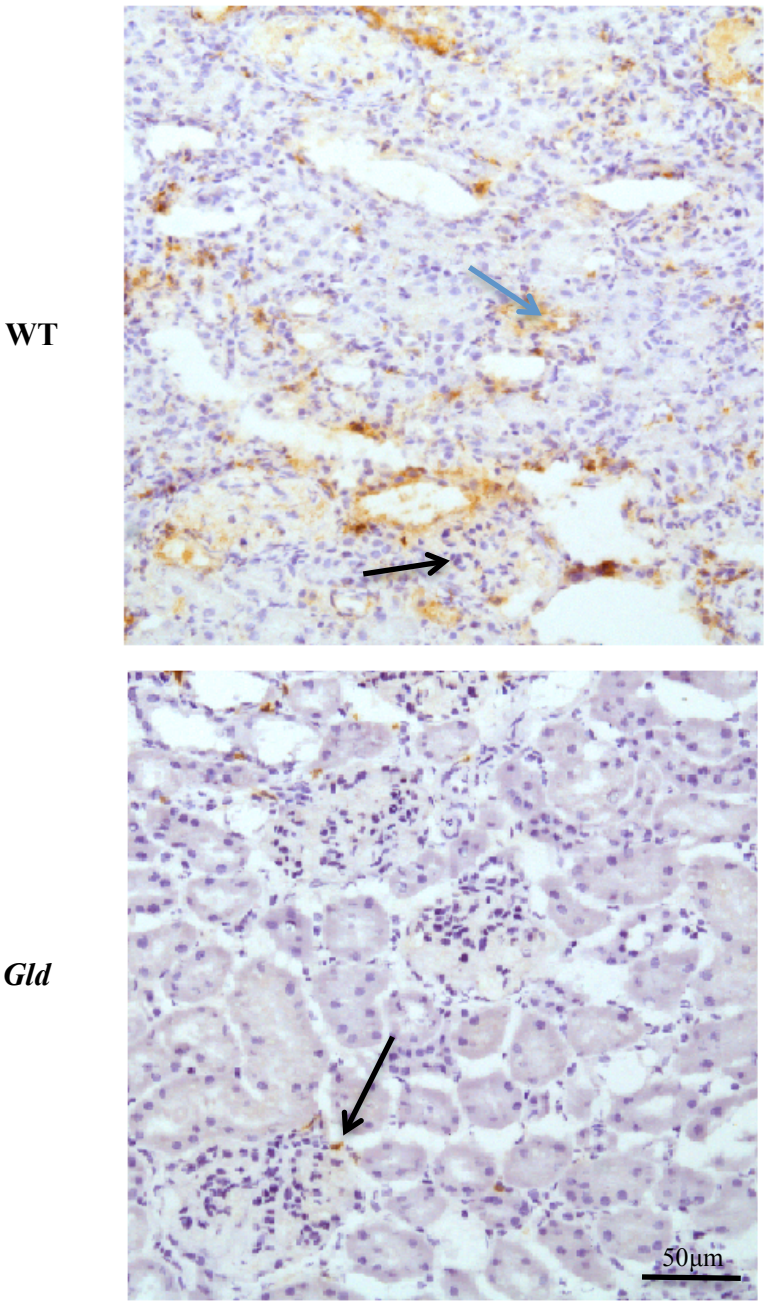


**Figure 3.8 Glomerular and interstitial CD4$^+$ T cell infiltration in WT and *gld* mice with NTN at day 15.**

Immunohistochemistry for T cells (CD4) on WT and *gld* mouse kidney sections at day 15. Black arrows highlight glomerular macrophages and the blue arrow highlights interstitial macrophages.

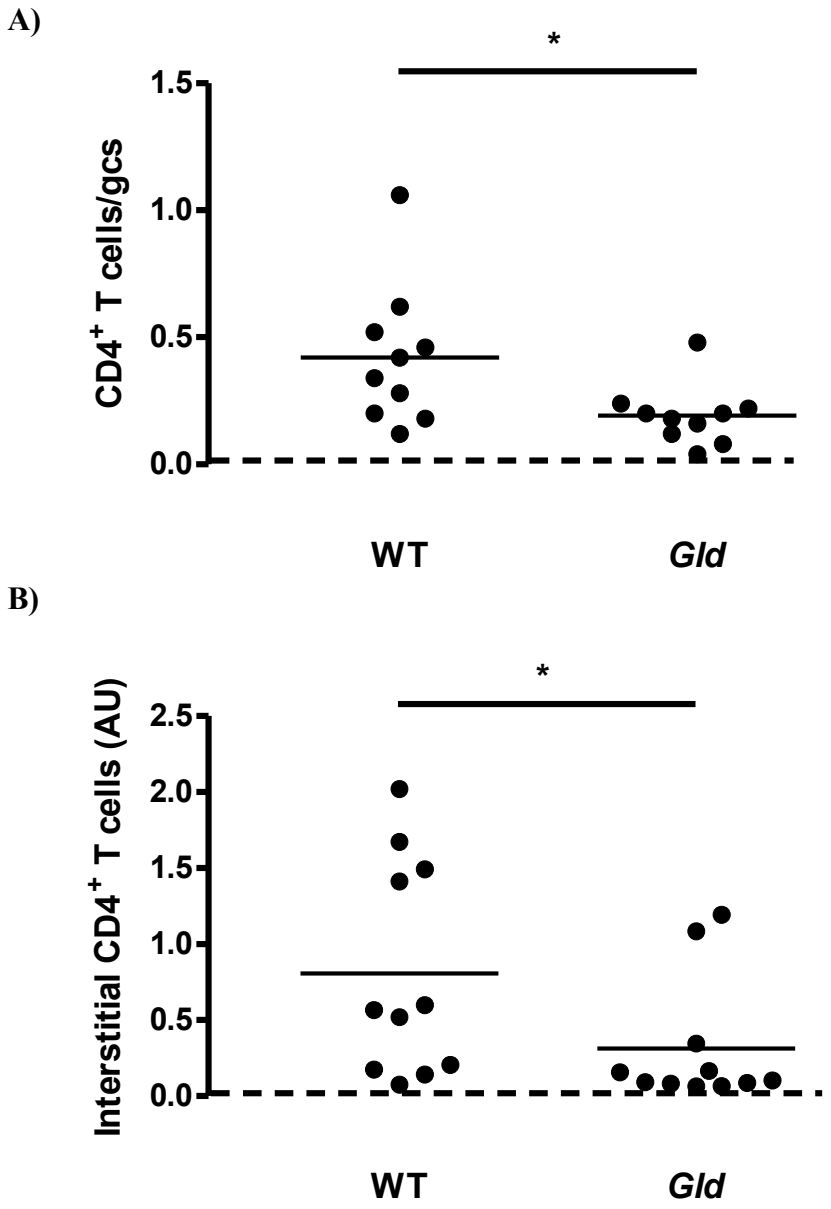


**Figure 3.9 Glomerular and interstitial CD4$^+$ T cell infiltration in WT and *gld* mice with NTN at day 15.**

**(A)** Infiltration of CD4$^+$ T cells/gcs (50 glomeruli scored per section) was measured. WT mice had significantly more glomerular CD4$^+$ T cells than *gld* mice. **(B)** Interstitial CD4$^+$ T cell infiltration (5 fields of view per section) was measured. WT mice had significantly more interstitial CD4$^+$ T cells than *gld* mice. All data represent individual values with the median. The data were analysed using the Mann-Whitney U-test ($p^*<0.05$). Dashed lines represent values for a group of normal WT mice.

### 3.4.6 There was no reduction in glomerular neutrophil infiltration in *gld* mice 24 hours after induction of NTN

NTN is characterised by an infiltration of glomerular neutrophils, within the first two hours, and sFasL has been shown to act as a potent chemoattractant for the migration of neutrophils to sites of inflammation (Dupont and Warrens, 2007; Letellier et al., 2010; Seino et al., 1998). To investigate whether FasL plays a role in neutrophil recruitment in NTN we induced disease in WT and *gld* mice and sacrificed them after 24 hours.

As the initial experiments performed to 24 hours had yielded conflicting results in terms of whether neutrophil infiltrate was reduced in *gld* mice, a third experiment was performed. NTN was induced, by pre-immunising with 0.2mg of sheep IgG in CFA and after five days administering 200µl (1:4 dilution) of NTS via the tail vein, in seventeen female mice (n=7 WT mice and n=10 *gld* mice). Female mice were used on this occasion due to availability of mice.

After 24 hours, there was no significant difference in the serum urea levels of WT and *gld* mice (WT 7.2 (6.4-9.4) mmol/L, *gld* 6.6 (5.5-8.9) mmol/L, p=0.31) (Figure 3.10). Kidney sections collected at the end of the experiment were PAS-stained and neutrophils counted by their distinctive morphology. There was no significant difference in glomerular neutrophil infiltrate between the two groups (neutrophils/gcs: WT 0.6 (0.08-2.4), *gld* 0.59 (0.04-3.0), p=0.66) (Figure 3.11).

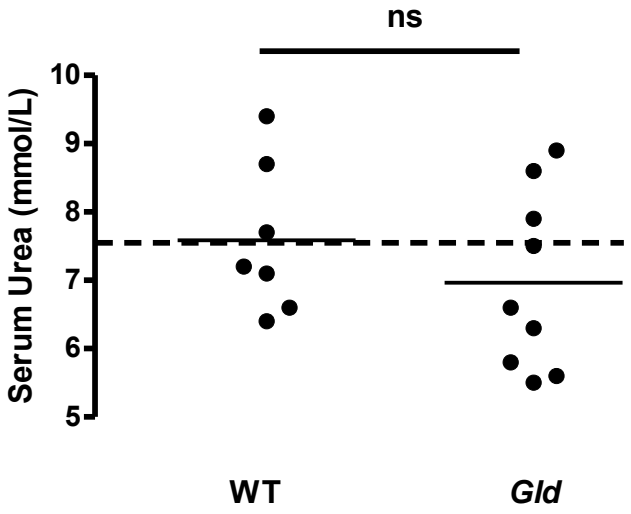


**Figure 3.10 Measurement of serum urea in WT and *gld* mice with NTN at 24 hours.**

Serum urea levels in WT and *gld* mice with NTN. There was no significant difference in levels of serum urea between WT and *gld* mice at 24 hours. All data represent individual values with the median. The data were analysed using the Mann-Whitney U-test (ns= non-significant). Dashed line represents values for a group of normal WT mice.

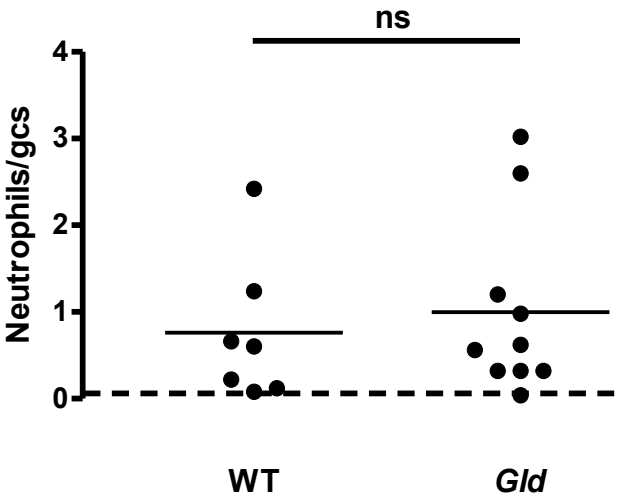


**Figure 3.11 Glomerular neutrophil infiltration in WT and *gld* mice with NTN at 24 hours.**

Infiltration of neutrophils/gcs (50 glomeruli scored per section) was measured. There was no significant difference in neutrophil infiltration between WT and *gld* mice. All data represent individual values with the median. The data were analysed using the Mann-Whitney U-test (ns= non-significant). Dashed line represents values for a group of normal WT mice.

### 3.4.7 Systemic immune responses

#### 3.4.7.1 Circulating mouse antibodies against sheep IgG

Although the IgG immune response appeared to be intact in the *gld* mice at the termination of the day 7 experiments, we confirmed this again at 24 hours and day 15, and also looked at the subclass responses. Certain subclasses of IgG, such as IgG2, have been reported to be more pathogenic than others in NTN (Robson et al., 2001).

Mouse serum, collected at the end of the experiments, was tested for the antigen-specific immune response against sheep IgG. At 24 hours (data shown from 24 hour experiment in Section 3.4.6), there was no significant difference in total circulating anti-sheep IgG, as measured by ELISA, between WT and *gld* mice (median optical density at 405nm (OD at 405nm): WT 1.3 (0.030-1.6), *gld* 1.2 (0.78-1.8), p=0.67) (Figure 3.12 A). However, at day 7 (see Table 3.2) and day 15, levels were significantly higher in the *gld* mice (results shown from day 15) (median OD at 405nm 1.8 (0.00-2.8)) compared to the WT mice (median OD at 405nm 0.33 (0.046-1.3), p=0.0039) (Figure 3.12 B). Levels of circulating anti-sheep IgG subclasses, IgG1, IgG2b, IgG2c, and IgG3, were measured at day 15. *Gld* mice had significantly higher titres of all subclasses (median OD at 405nm: IgG1 0.43 (0.011-0.60), IgG2b 0.20 (0.0060-0.66), IgG2c 0.50 (0.021-1.4), and IgG3 0.24 (0.00-3.0)) compared to WT mice (median OD at 405nm: IgG1 0.19 (0.060-0.49), p=0.0071; IgG2b 0.015 (0.0040-0.13), p=0.0022; IgG2c 0.028 (0.014-0.17), p=0.0006; IgG3 0.020 (0.0070-1.3), p=0.015) (Figure 3.13).

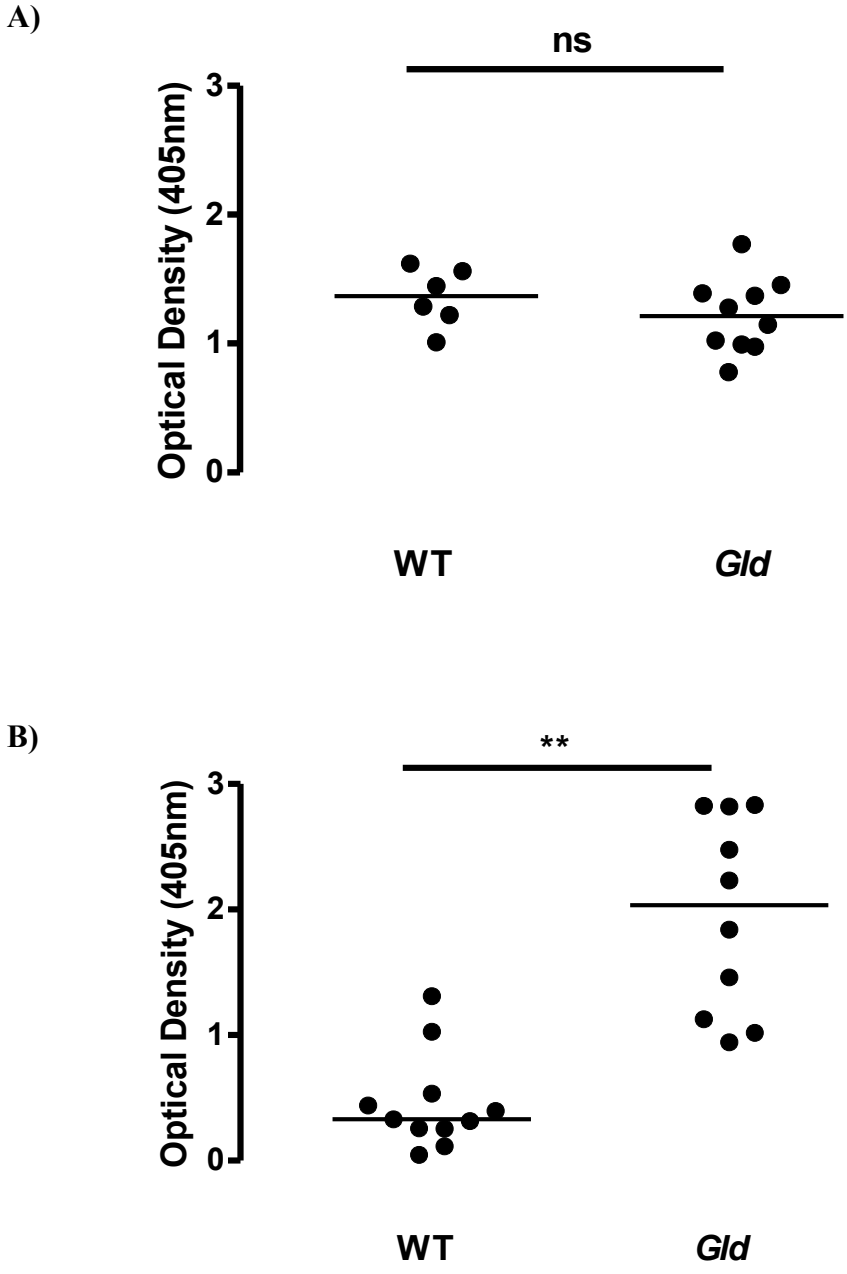


**Figure 3.12 Total circulating mouse anti-sheep IgG levels in WT and *gld* mice with NTN at 24 hours and day 15.**

The total circulating levels of mouse anti-sheep IgG were measured by ELISA. **(A)** The total circulating anti-sheep IgG levels were assessed in WT and *gld* mice at 24 hours and showed no difference. However, **(B)** *gld* mice had significantly higher titres at day 15 compared to WT mice. All data represent individual values with the median. The data were analysed using the Mann-Whitney U-test (ns= non-significant, p**<0.01).

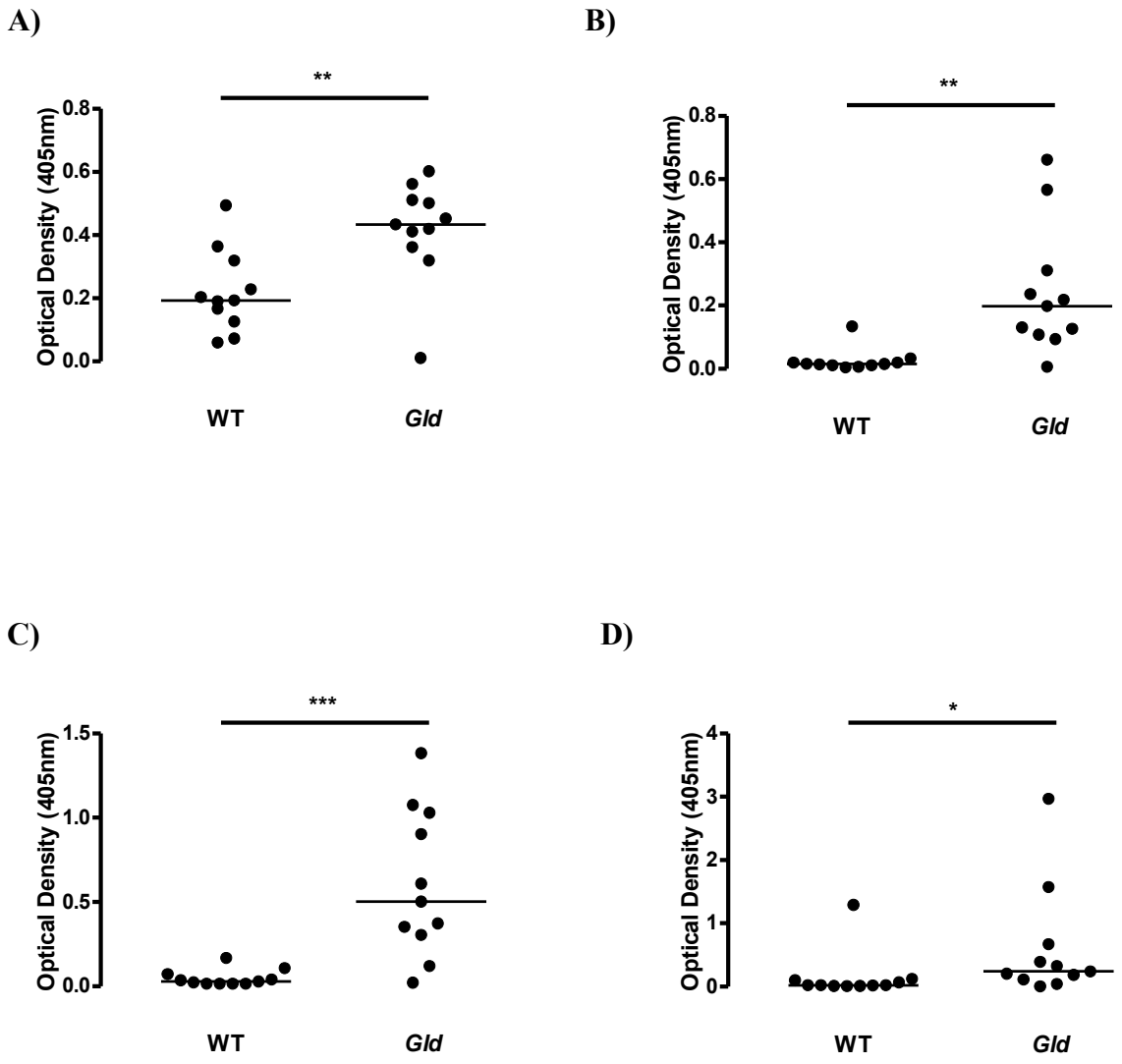


**Figure 3.13 Circulating mouse anti-sheep IgG1, IgG2b, IgG2c and IgG3 levels in WT and *gld* mice with NTN at day 15.**

The circulating levels of mouse anti-sheep IgG1, IgG2b, IgG2c and IgG3 were measured by ELISA. At day 15, *gld* mice had significantly higher titres of circulating **(A)** IgG1, **(B)** IgG2b, **(C)** IgG2c, and **(D)** IgG3 compared to WT mice. All data represent individual values with the median. The data were analysed using the Mann-Whitney U-test (p*<0.05, p**<0.01, p***<0.001).

#### 3.4.7.2 Deposited glomerular IgG

Frozen kidney sections from experiments were stained for deposited sheep IgG and mouse IgG by direct immunofluorescence on tissue taken at the end of the experiment. Total glomerular mouse IgG and sheep IgG were measured by quantitative immunofluorescence with the results expressed as arbitrary fluorescence units (AFU). Glomerular sheep IgG deposition was equivalent between WT and *gld* mice after 24 hours (data shown from experiment in Section 3.4.6) (WT 139 (98-153) AFU, *gld* 124 (31-147) AFU, p=0.67), 7 days (Table 3.2), and 15 days (WT 20 (14-32) AFU, *gld* 16 (10-32) AFU, p=0.13) (Figure 3.14 and Figure 3.15). There was no significant difference in glomerular mouse IgG deposition between WT and *gld* mice at 24 hours (data shown from experiment in Section 3.4.6) (WT 95 (0.00-135) AFU, *gld* 95 (0.00-170) AFU, p=0.96). However, at day 7 (Table 3.2) and day 15 there was significantly more mouse IgG deposited in the glomeruli of *gld* mice (results from day 15) (60 (53-79) AFU) compared to the WT mice (46 (32-58) AFU, p=0.0005) (Figure 3.16 and Figure 3.17).

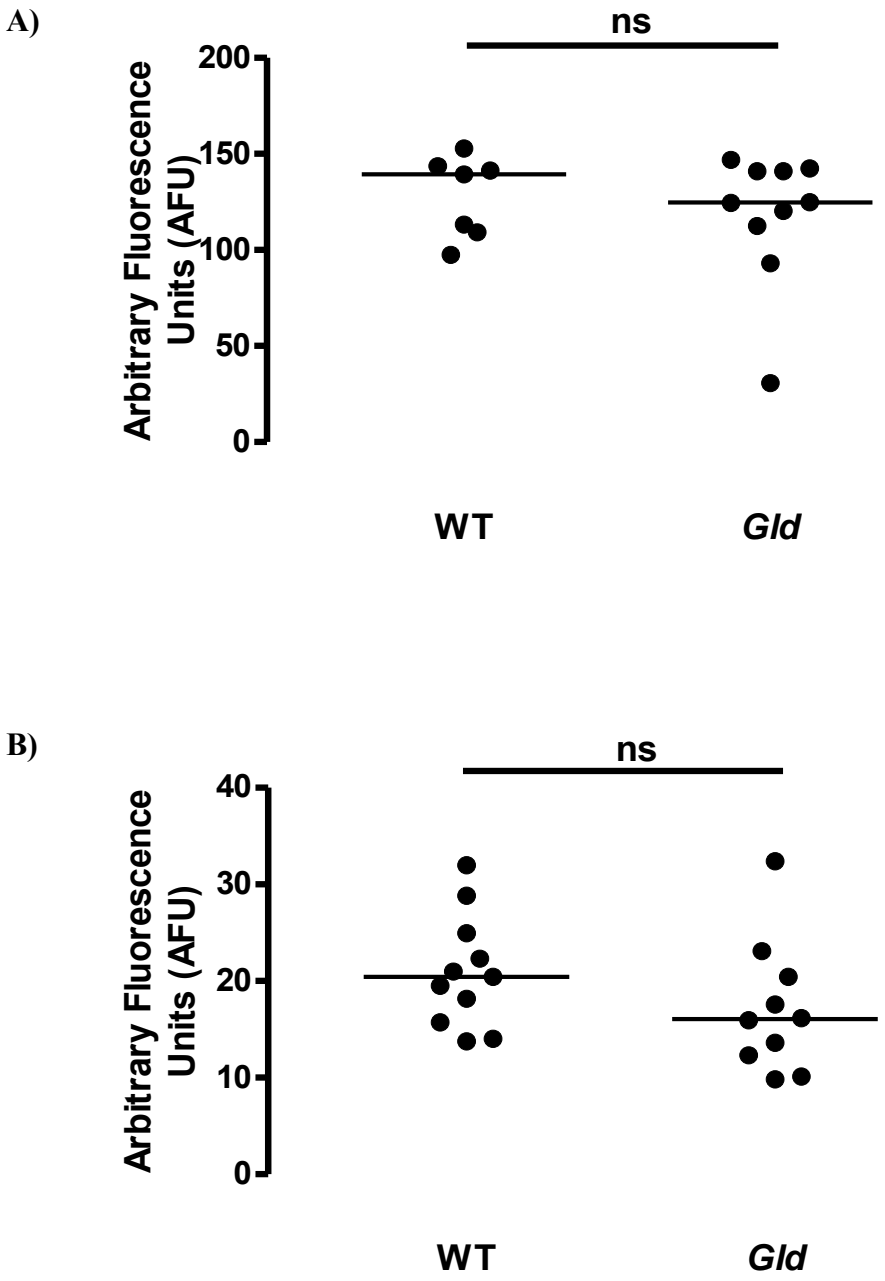


**Figure 3.14 Immunofluorescence for glomerular sheep IgG deposition in WT and *gld* mice with NTN at 24 hours and day 15.**

The relative median glomerular immunofluorescence was measured and expressed as arbitrary fluorescence units (AFU). There was no significant difference in deposited sheep IgG between WT and *gld* mice at **(A)** 24 hours and **(B)** day 15. All data represent individual values with the median. The data were analysed using the Mann-Whitney U-test (ns= non-significant).

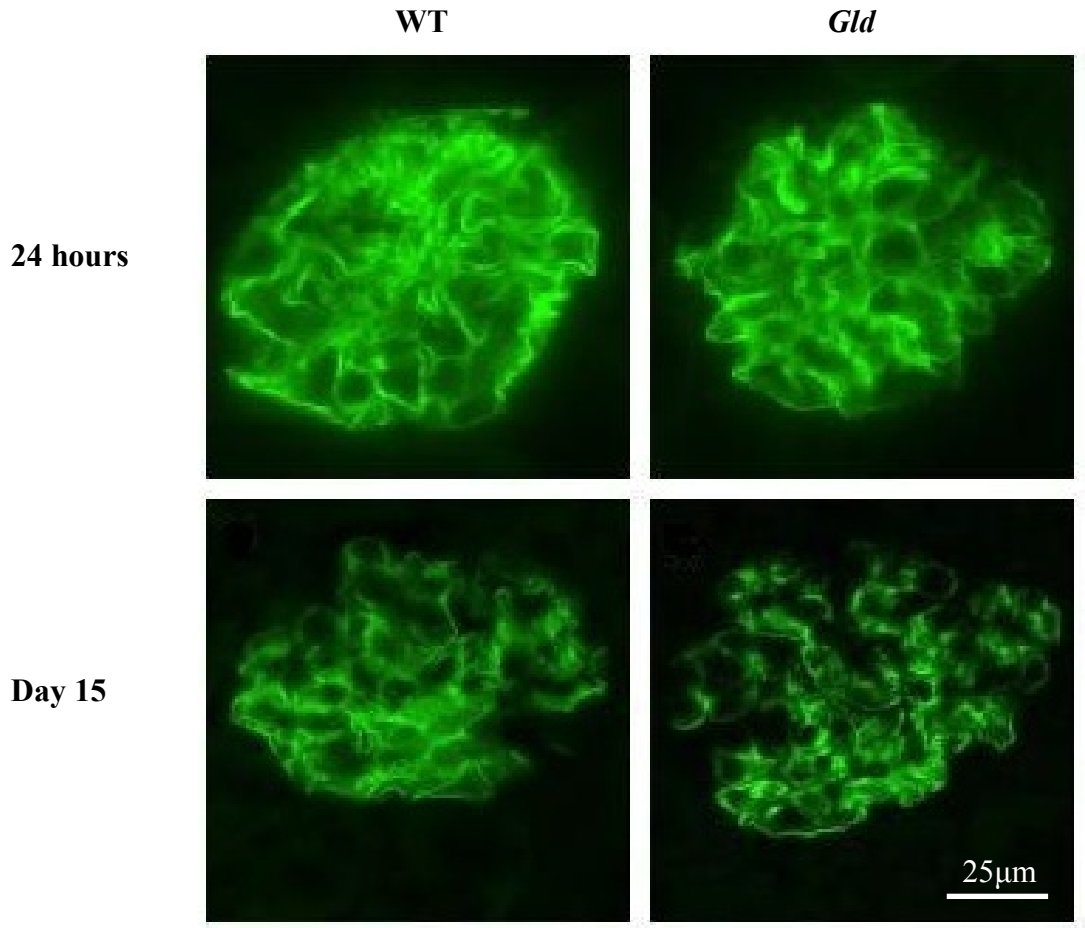


**Figure 3.15 Immunofluorescence for glomerular sheep IgG deposition in WT and *gld* mice with NTN, at 24 hours and day 15.**

Representative glomeruli from WT and *gld* mice showing sheep IgG deposition at 24 hours and day 15 after NTS injection. All images were taken using the same settings.

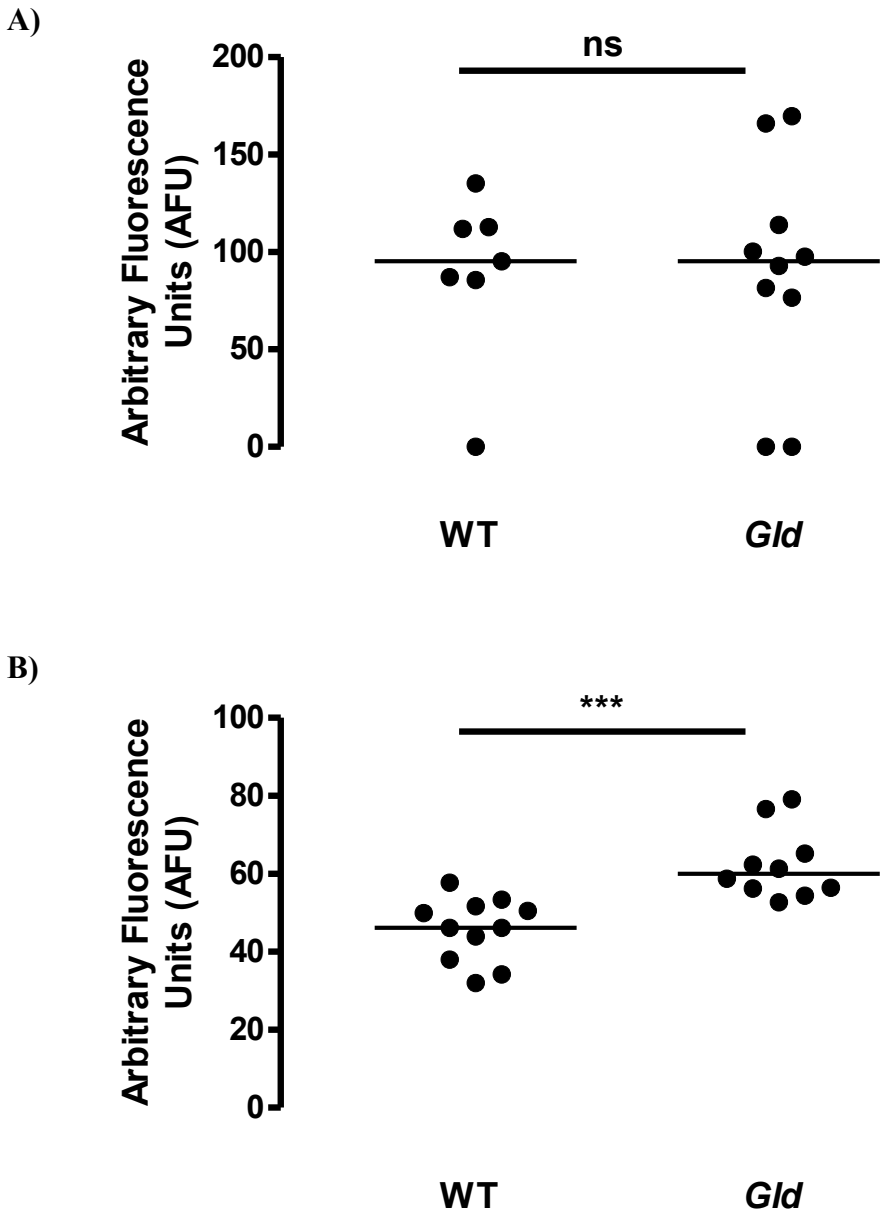


**Figure 3.16 Immunofluorescence for glomerular mouse IgG deposition in WT and *gld* mice with NTN, at 24 hours and day 15.**

The relative median glomerular immunofluorescence was measured and expressed as arbitrary fluorescence units (AFU). There was no significant difference in deposited mouse IgG between WT and *gld* mice at **(A)** 24 hours. At **(B)** day 15, *gld* mice had significantly more deposited glomerular mouse IgG than WT mice. All data represent individual values with the median. The data were analysed using the Mann-Whitney U-test (ns= non-significant, p***<0.001).

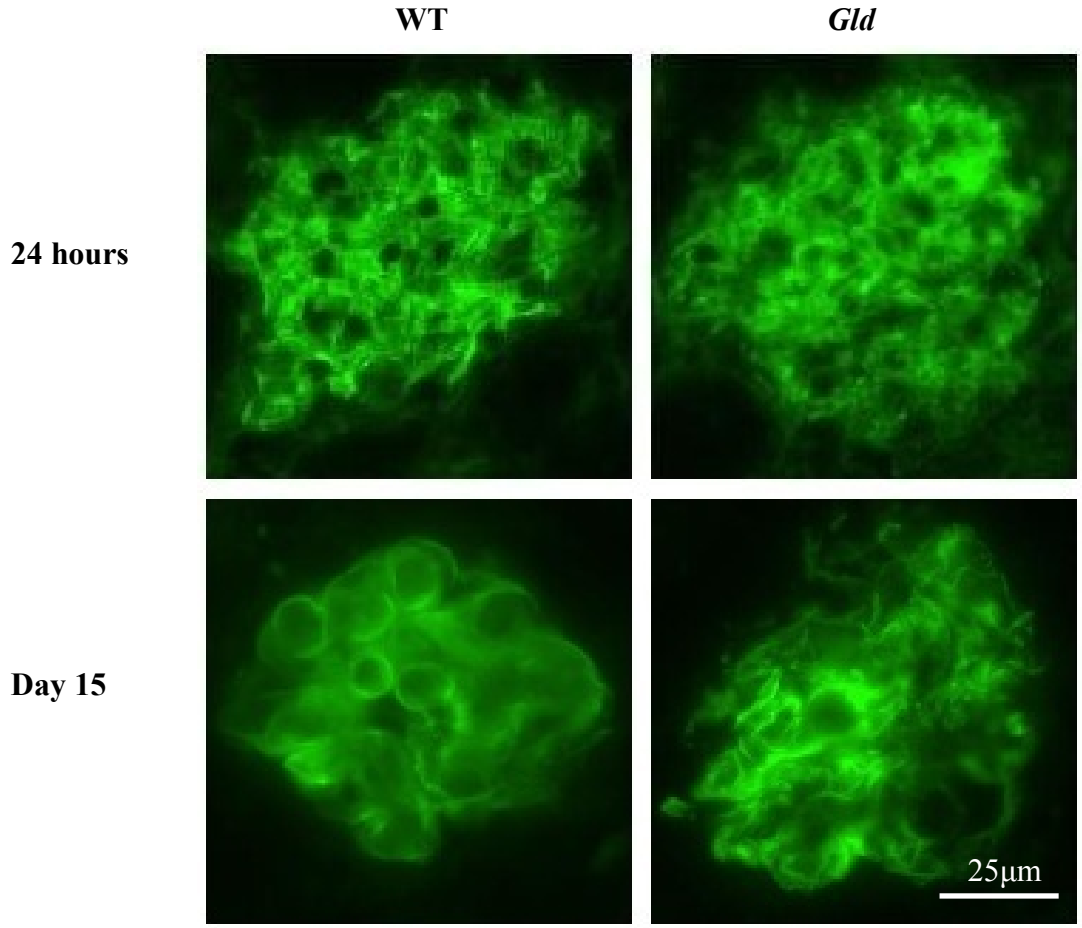


**Figure 3.17 Immunofluorescence for glomerular mouse IgG deposition in WT and *gld* mice with NTN, at 24 hours and day 15.**

Representative glomeruli from WT and *gld* mice showing mouse IgG deposition at 24 hours and day 15 after NTS injection. All images were taken using the same settings.

### 3.4.8 *Gld* mice have fewer glomerular apoptotic cells than WT mice

FasL is best characterised for inducing apoptosis through its receptor, Fas. However, as discussed in the introduction (Section 1.7), non-apoptotic functions are also postulated. In view of the involvement of FasL in apoptosis, it was important to quantitate the presence of apoptosis in the kidney in our model. Paraffin-fixed kidney sections from WT and *gld* mice (day 15) were stained for apoptosis by TUNEL (Figure 3.18 A). Apoptotic cells were counted in 30 glomeruli per cross section. *Gld* mice had significantly fewer apoptotic cells than WT mice per glomerular cross section (WT 0.2 (0.00-0.85)/gcs, *gld* 0.00 (0.00-0.00)/gcs, p=0.0009) (Figure 3.18 B).

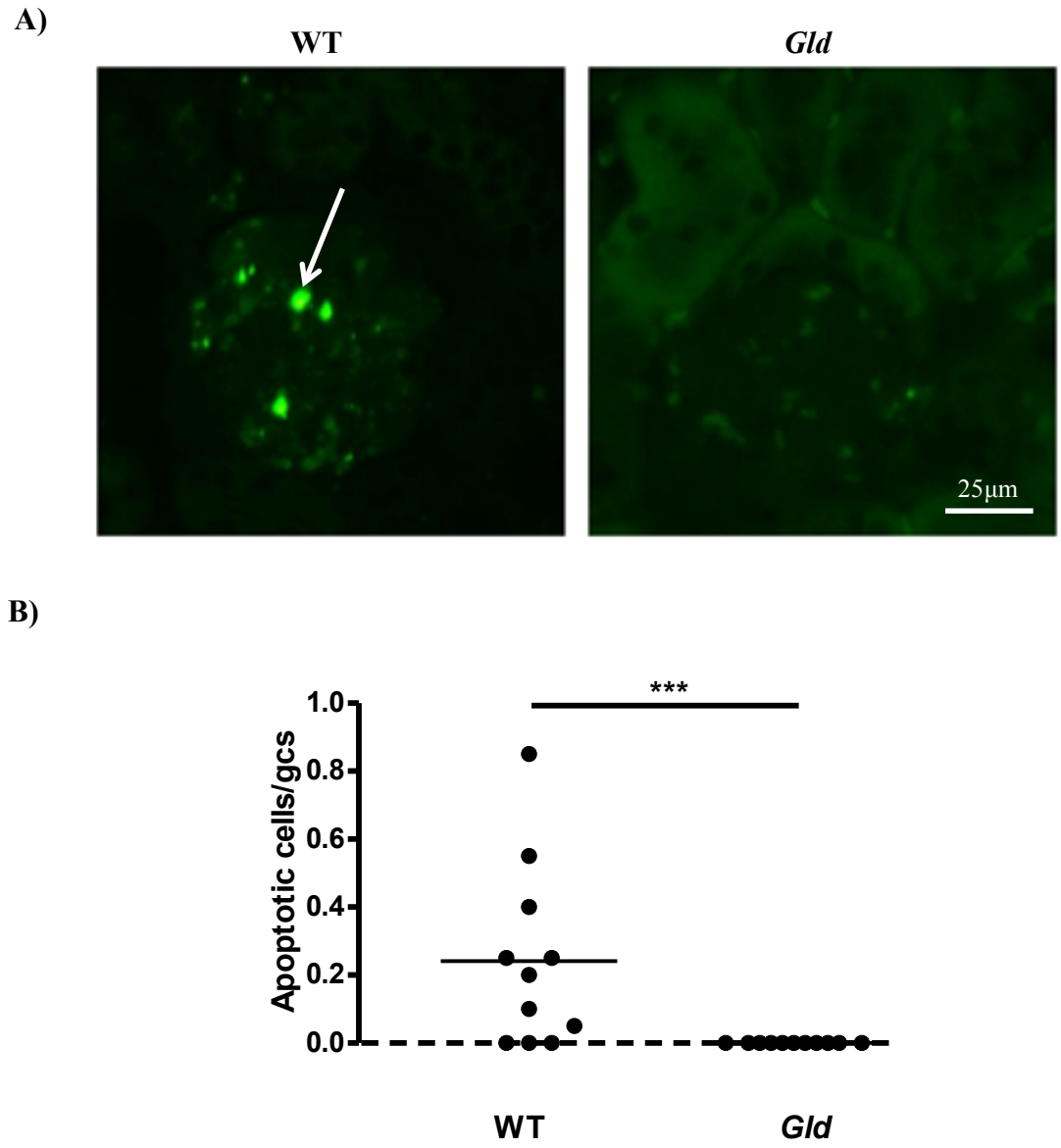


**Figure 3.18 Glomerular apoptotic cells in WT and *gld* mice with NTN were identified by TUNEL staining.**

**(A)** Representative TUNEL staining from WT and *gld* mice with NTN. Arrow highlighting an apoptotic cell. **(B)** The number of apoptotic cells per glomerular cross section (gcs) in WT and *gld* mice at day 15 post NTN induction. All data represent individual values with the median. The data were analysed using Mann-Whitney U-test (p***<0.001). Dashed line represents values for a group of normal WT mice.

### 3.4.9 mRNA expression of cytokines and other mediators

Previous data have shown that FasL is involved in the generation of pro-inflammatory cytokines (see Section 1.7.1) and can influence T cell phenotypes, and therefore the cytokine milieu (Section 1.6.2). To look at any possible differences between WT and *gld* mice, mRNA expression of cytokines, and other mediators, were measured by qRT-PCR. Whole kidney mRNA was extracted from frozen WT and *gld* kidneys from day 15 post NTS administration, as well as unmanipulated control mice. Mediators measured were: MCP-1, involved in the recruitment of macrophages; TNF-α and IL-6, pro-inflammatory cytokines secreted by macrophages; inducible nitrous oxide synthase (iNOS), arginase and mannose receptor (MR), markers of macrophage phenotype; IFN-γ and IL-12p40, $T_h1$ cytokines; and IL-4 and IL-10, $T_h2$ cytokines. Data represent relative expression, calculated using GAPDH as the housekeeping gene and an untreated WT mouse as the reference.

Post NTN, MCP-1 mRNA expression in whole kidney from WT mice was significantly greater compared to *gld* mice (MCP-1: WT 16 (0.45-111), *gld* 2.0 (0.50-5.1), p=0.0013), which is consistent with the overall increase in macrophages seen in the kidneys of WT mice. There was also a significant difference in iNOS expression, secreted by classically activated pro-inflammatory macrophages, with iNOS expression being higher in the WT mice than in the *gld* mice during disease (WT 1.2 (0.70-3.3), *gld* 0.56 (0.26-1.3), p=0.0031). Surprisingly, there was also a greater increase in MR expression in WT mice with NTN compared to *gld* mice with NTN (WT 9.9 (1.2-18), *gld* 2.0 (1.1-5.6), p=0.0043). MR is expressed by alternatively activated repair macrophages; the greater number of macrophages in the kidneys of the WT mice can account for this difference. There was no significant difference in TNF-α, IL-6 or arginase mRNA expression between WT and *gld* mice (TNF-α: WT 2.2 (0.11-20), *gld* 1.2 (0.41-5.1), p=0.32; IL-6: WT 2.4 (1.1-5.8), *gld* 1.1 (0.55-6.7), p=0.094; arginase: WT 43 (0.47-105), *gld* 16 (0.78-36), p=0.10) (Figure 3.19).

When measuring cytokines modulating T cell phenotypes, WT mice had greater expression of IFN-γ and IL-12p40 mRNA (IFN-γ 4.7 (0.56-14), IL-12p40 1.5 (0.41-3.6)) compared to *gld* mice (IFN-γ 1.7 (0.72-9.1), p=0.039; IL-12p40 0.40 (0.22-0.86) p=0.0005). IFN-γ and IL-12p40 are both $T_h1$ cytokines, associated with a pro-inflammatory response in NTN. However, there was no significant difference in expression of IL-4 and IL-10, $T_h2$ cytokines, between WT and *gld* mice (IL-4: WT 0.38 (0.10-0.60), *gld* 0.43 (0.15-1.1), p=0.22; IL-10: WT 0.72 (0.21-1.4), *gld* 0.57 (0.32-1.2), p=0.90) (Figure 3.20).

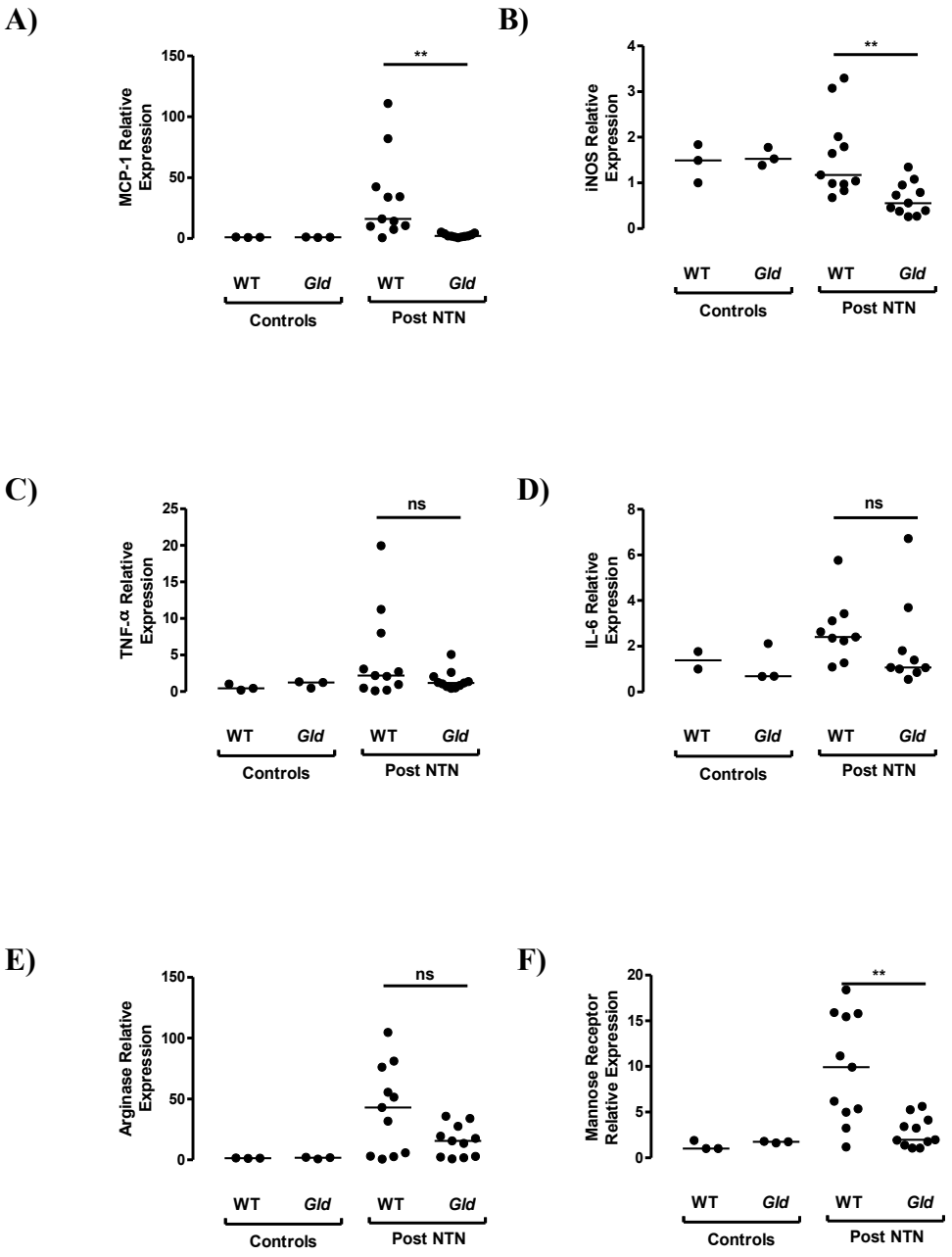


**Figure 3.19 Whole kidney mRNA expression of MCP-1, iNOS, TNF-α, IL-6, arginase and MR in WT and *gld* mice with NTN, at day 15.**

Relative expression of **(A)** MCP-1, **(B)** iNOS, **(C)** TNF-α, **(D)** IL-6, **(E)** arginase and **(F)** MR were measured in whole kidney mRNA extracts. WT mice had significantly greater mRNA expression of MCP-1 and MR, whilst *gld* mice had reduced expression of iNOS. There was no significant difference in mRNA expression of TNF-α, IL-6 and arginase. All data represent individual values with the median. The data were analysed using Mann-Whitney U-test (ns= non-significant, p**<0.01). Controls were unmanipulated age- and sex-matched mice.

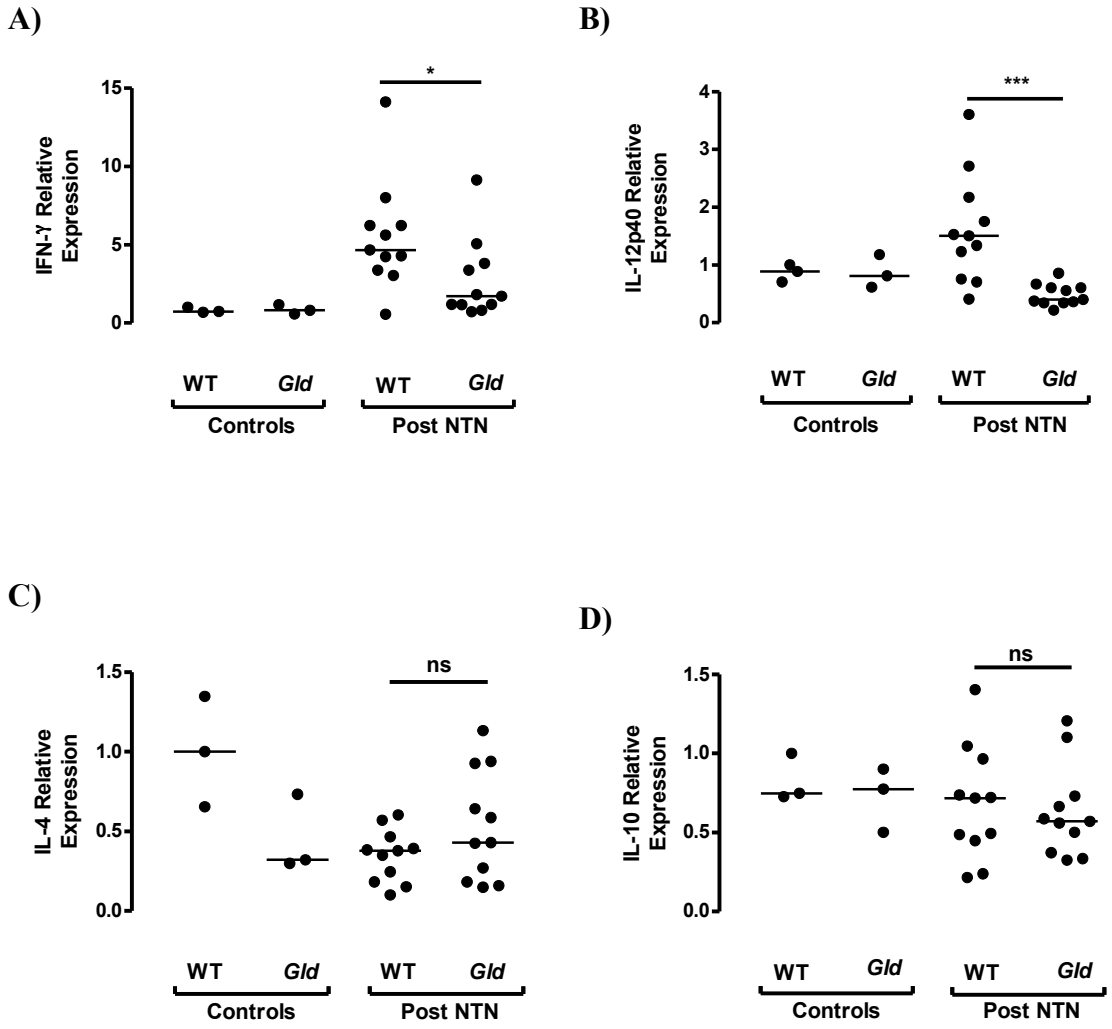


**Figure 3.20 Whole kidney mRNA expression of IFN-γ, IL-12p40, IL-4 and IL-10 in WT and *gld* mice with NTN, at day 15.**

Relative expression of **(A)** IFN-γ, **(B)** IL-12p40, **(C)** IL-4, and **(D)** IL-10 were measured in whole kidney mRNA extracts. WT mice had significantly greater mRNA expression of IFN-γ and IL-12p40 compared to *gld* mice. There was no significant difference in mRNA expression of IL-4 and IL-10. All data represent individual values with the median. The data were analysed using Mann-Whitney U-test (ns= non-significant, p*<0.05, p***<0.001). Controls were unmanipulated age- and sex-matched mice.

### 3.4.10 Renal expression of Fas ligand during NTN

To see if FasL was upregulated in the kidney during NTN, WT whole kidney mRNA was also assessed for expression of FasL, at day 15 post NTS administration, by qRT-PCR. FasL was detected in both healthy and diseased whole kidney, with an increase of expression during NTN (Figure 3.21).

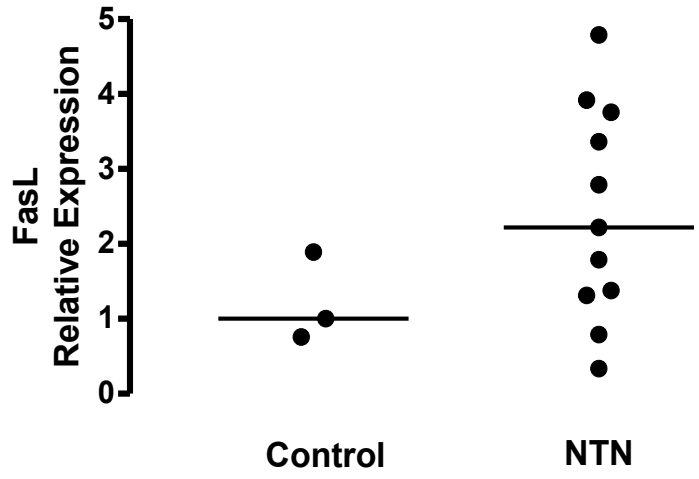


**Figure 3.21 Expression of Fas ligand in WT control and NTN whole kidney.**

Relative expression of FasL mRNA in whole kidney from unmanipulated WT mice (Control) and WT mice at day 15 NTN (NTN). All data represent individual values with the median.

### 3.4.11 Splenocyte proliferation

FasL is expressed on T cells and is involved in regulating the immune response by playing a role in T cell activation and proliferation (Alderson et al., 1993) as well as inducing apoptosis to terminate the response (Kabelitz et al., 1993). To investigate this further, in our model of NTN, splenocyte proliferation assays were carried out on splenocytes collected from WT and *gld* mice following pre-immunisation only (primary immune response) and at the termination (day 10) of a NTN experiment.

Initially, splenocytes were stimulated with CD3/CD28 beads, to compare maximal stimulation of the entire splenocyte population, at day 7 following pre-immunisation with sheep IgG. *Gld* splenocytes proliferated less in response to CD3/CD28 beads compared to WT splenocytes (counts per minute (c.p.m): WT 340200 (220300-402500), *gld* 212800 (68460-363500), p=0.023) (Figure 3.22).

To investigate antigen specific proliferation, following both pre-immunisation and at the termination (day 10) of a NTN experiment (histology data not shown but consistent with data from other experiments presented), WT and *gld* splenocytes were stimulated with 100μg/ml of sheep IgG. This was to gain better understanding of any differences there may be in the immune response both early on in the experiment, at the time the NTS is injected, and at the end of the NTN experiment. Following pre-immunisation only, *gld* splenocytes proliferated less in response to sheep IgG compared to WT splenocytes (c.p.m: WT 13000 (7791-21360), *gld* 8397 (1365-9589), p=0.0033) (Figure 3.23 A). However, following termination of the NTN experiment, there was no significant difference in splenocyte proliferation in response to sheep IgG between WT and *gld* mice (representative results of one of two experiments) (c.p.m: WT 8712 (1834-12670), *gld* 6222 (4613-12520), p=0.71) (Figure 3.23 B). These results suggest that a reduction in T cell-mediated immunity in the early phase of disease could be contributing to the protection of *gld* mice from developing NTN, although that result is only preliminary as it was only performed once at that time point.

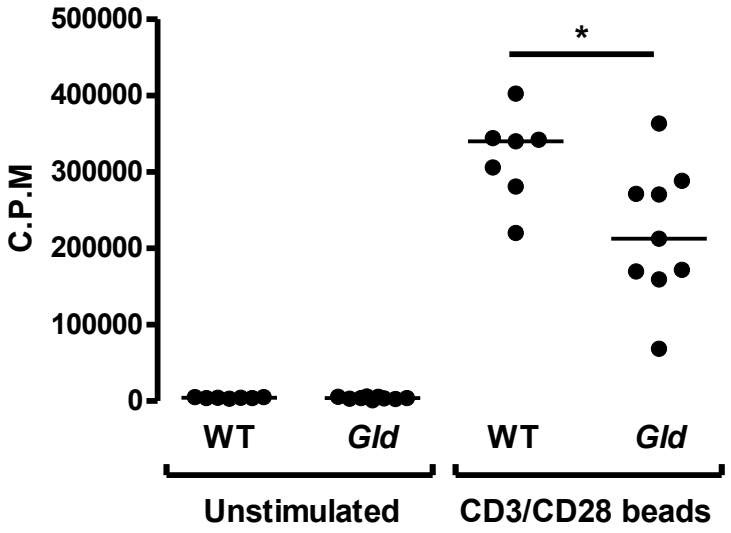


**Figure 3.22 Splenocyte proliferation following stimulation with CD3/CD28 beads.**

Splenocyte proliferation was assessed by measuring $^{3}H$ thymidine incorporation at 72 hours following stimulation with CD3/CD28 beads, after pre-immunisation only. WT splenocytes proliferated significantly more than *gld* splenocytes. All data represent individual values with the median. The data were analysed using Mann-Whitney U-test ($p^{*}<0.05$).

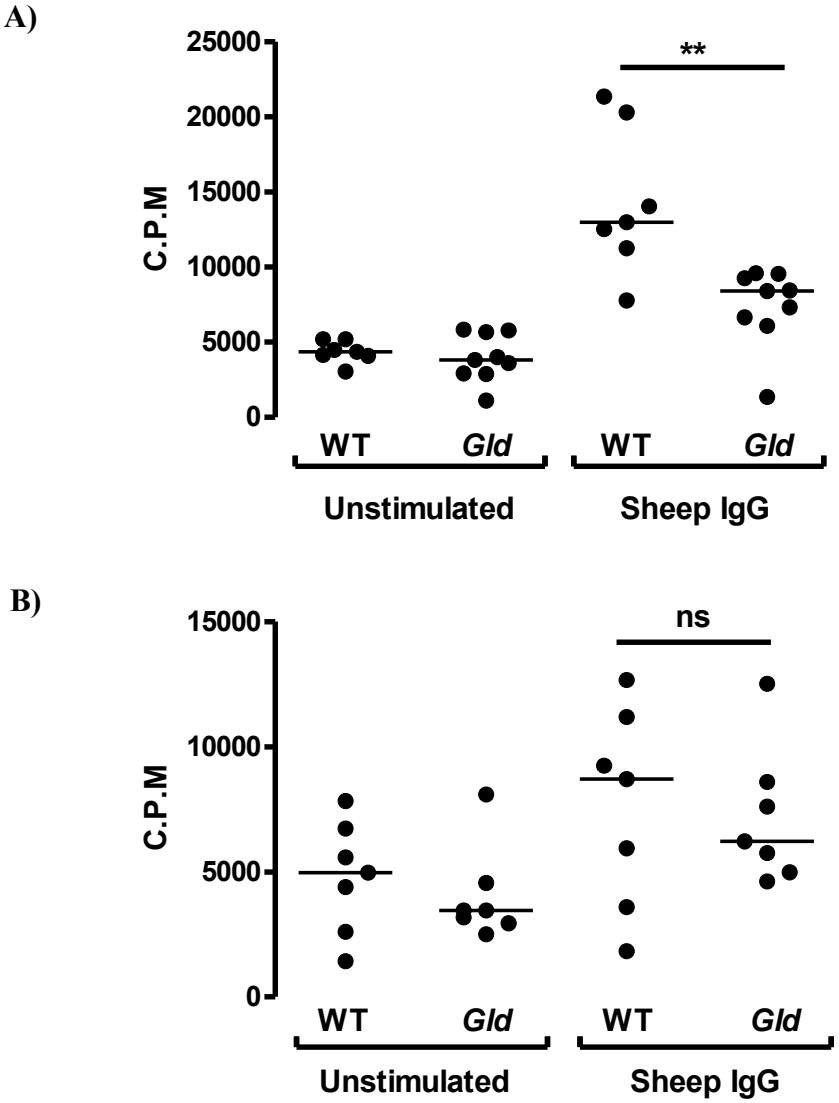


**Figure 3.23 Splenocyte proliferation following stimulation with 100µg/ml of sheep IgG.**

Splenocyte proliferation was assessed by measuring $^{3}$H thymidine incorporation at 72 hours following stimulation with 100µg/ml of aggregated sheep IgG. After **(A)** pre-immunisation only, WT splenocytes proliferated significantly more in response to sheep IgG than *gld* splenocytes, however **(B)** at the termination of the experiment, there was no significant difference in splenocyte proliferation in response to sheep IgG. All data represent individual values with the median. The data were analysed using Mann-Whitney U-test (ns= non-significant, p**<0.01).

### 3.4.12 Splenocyte cytokine production

NTN is thought to be driven by a $T_h1/T_h17$-deviated immune response; mice predisposed to a $T_h2$ immune response, such as BALB/c mice, are protected from disease (Holdsworth et al., 1999; Huang et al., 1997a; Summers et al., 2009). *Gld* mice and humans carrying mutations in Fas or FasL have been found to have a $T_h2$-deviated immune response (Fuss et al., 1997). To investigate whether the T cell responses of *gld* mice are deviated towards a $T_h2$ response in NTN we looked at cytokine production, following splenocyte stimulation, after pre-immunisation only.

Initially, splenocytes were stimulated with PMA and ionomycin to compare cytokine production of the entire splenocyte population. PMA and ionomycin were used as they are cheaper than CD3/CD28 beads and more splenocytes needed to be stimulated to produce enough cytokine for measuring by ELISA. There was a significant increase in IL-4 and IL-10 production by *gld* splenocytes (IL-4 46 (28-76) pg/ml; IL-10 446 (309-554) pg/ml) compared to WT splenocytes (IL-4 33 (27-42) pg/ml, p=0.042; IL-10 359 (303-440) pg/ml, p=0.042). There was no significant difference in IFN-γ production (WT 1609 (1040-2450) pg/ml, *gld* 1079 (886-2046) pg/ml, p=0.055) or IL-17 (WT 941 (626-1348) pg/ml, *gld* 648 (415-1101) pg/ml, p=0.11) although WT splenocytes trended towards producing more of a $T_h1/T_h17$ response compared to *gld* splenocytes (Figure 3.24).

To investigate antigen-specific proliferation, splenocytes from pre-immunised mice were stimulated with sheep IgG. There was no significant difference in IFN-γ production between WT and *gld* splenocytes (IFN-γ: WT 57 (38-1393) pg/ml, *gld* 75 (30-181) pg/ml, p=0.92) although there was a trend towards *gld* splenocytes producing less IL-17 (IL-17: WT 120 (41-246) pg/ml, *gld* 55 (27-194) pg/ml, p=0.071) (Figure 3.25). IL-4 and IL-10 were measured; however, levels were below the lower detection limit of the kit.

The greater production of IL-4 and IL-10 by the *gld* splenocytes after stimulation with PMA and ionomycin supports the reports from the literature that the overall T cell immune response in *gld* mice is predisposed to being $T_h2$. However, following antigen-specific stimulation, the pattern of cytokine production from the antigen-specific T cells does not support this hypothesis with regard to the immune response to sheep IgG as the IL-4 production was not increased in the *gld* splenocytes.

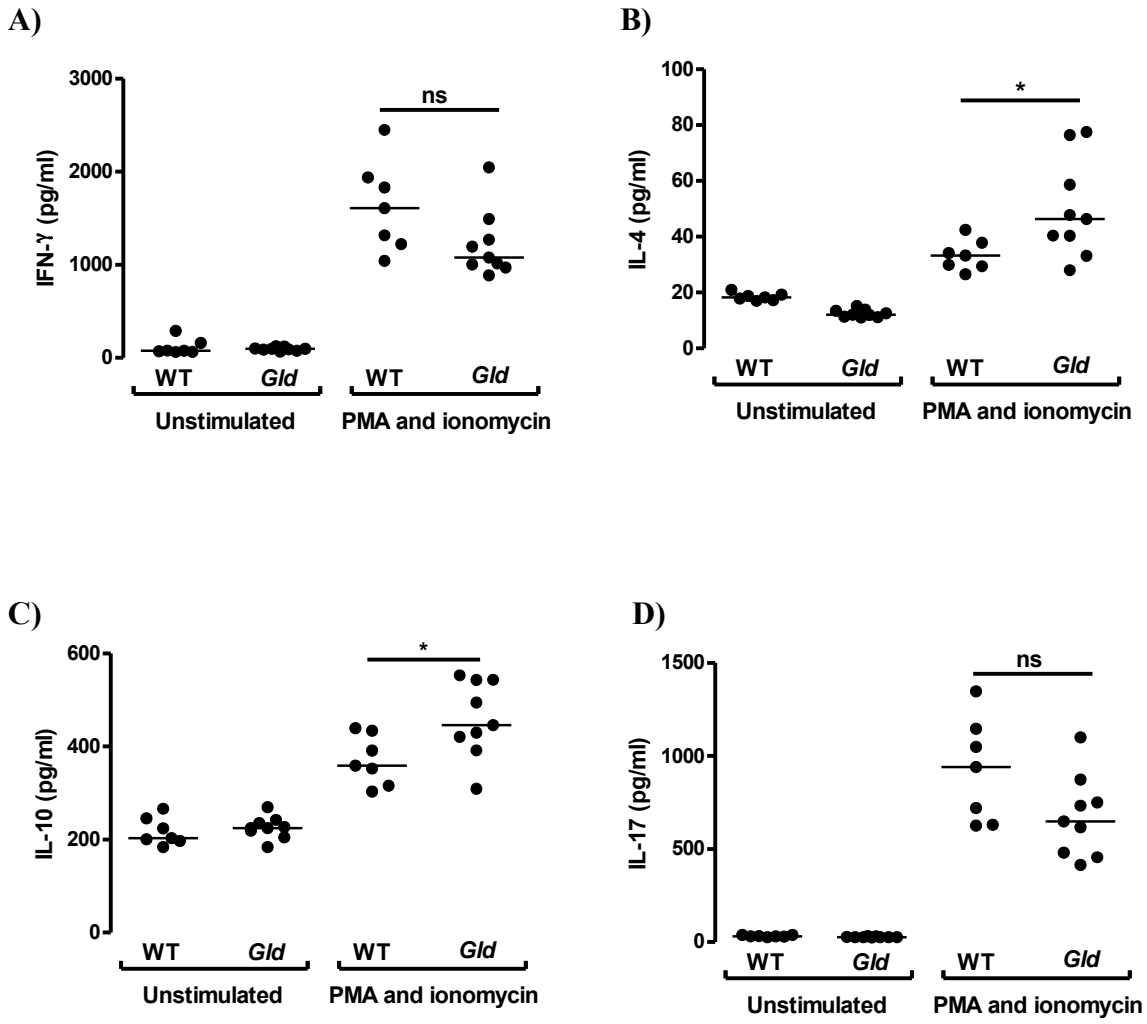


**Figure 3.24 Splenocyte cytokine release following stimulation with PMA and ionomycin.**

Splenocyte cytokine release into the supernatant was measured by ELISA at 72 hours following stimulation with PMA and ionomycin, after pre-immunisation only. **(A)** IFN-γ, **(B)** IL-4, **(C)** IL-10, and **(D)** IL-17. *Gld* splenocytes produced significantly more IL-4 compared to WT splenocytes. There was no significant difference with the other cytokines measured. All data represent individual values with the median. The data were analysed using Mann-Whitney U-test (ns= non-significant, p*<0.05).

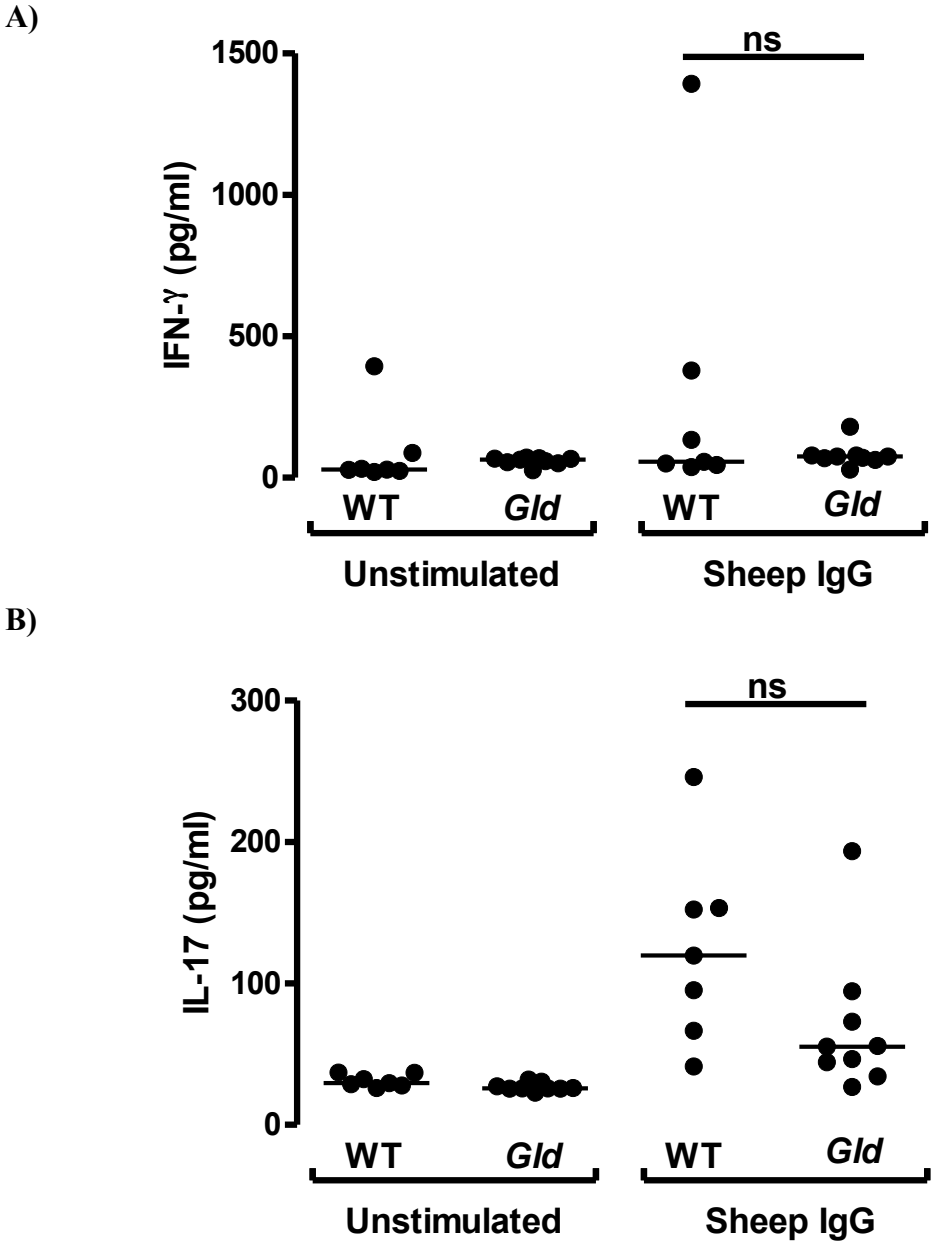


**Figure 3.25 Splenocyte cytokine release following stimulation with 100µg/ml of sheep IgG.**

Splenocyte cytokine release into the supernatant was measured by ELISA at 72 hours following stimulation with 100µg/ml of aggregated sheep IgG, after pre-immunisation only. **(A)** WT splenocytes produced significantly more IFN- γ than *gld* splenocytes and **(B)** trended towards producing more IL-17. All data represent individual values with the median. The data were analysed using Mann-Whitney U-test (ns= non-significant).

## 3.5 Discussion

The results in this chapter demonstrate that *gld* mice were strongly protected from renal injury and histological damage in accelerated NTN compared to WT counterparts, despite no reduction in systemic antibody response or deposited antibodies in the *gld* mice and similar levels of glomerular neutrophil and macrophage infiltration. Possible reasons for this protection are: (1) the reduction in immune response; *gld* mice showed a reduction in T cell-mediated systemic immunity in the early phase of disease, but not at the end of the experiment. (2) The reduction in apoptosis; *gld* mice had no glomerular apoptotic cells. Finally, (3) the reduction in cytokine production; *gld* mice had fewer glomerular and interstitial T cells and interstitial macrophages and reduced expression of pro-inflammatory cytokines, MCP-1 and iNOS, and $T_h1$ cytokines, IFN-γ and IL-12p40 in whole kidney compared to WT mice.

NTN is an animal model of crescentic GN that presents with histological damage similar to human crescentic nephritis. It is induced by targeting an immune response to the glomerulus by planting foreign antigen on the GBM. In accelerated NTN, pre-immunisation with sheep IgG primes the immune response for the injection of heterologous anti-GBM antibodies. The heterologous and host antibodies localise in the glomerulus where they induce glomerular damage via the activation of FcγR, an important link between the innate and adaptive immune response, which leads to the secretion of cytokines and the recruitment of leukocytes. In order to exclude an effect of FasL on priming of the immune response, the serum levels of antibodies to sheep IgG and deposition of immunoglobulins within the glomerulus were measured. There was no difference in the deposition of heterologous antibody (sheep anti-mouse GBM antibody) on the GBM between the two groups. However, at day 15, *gld* mice had increased deposition of autologous antibody (mouse anti-sheep IgG antibody) and higher circulating levels of total mouse anti-sheep IgG and the different IgG subclasses (IgG1, IgG2b, IgG2c and IgG3). This could be explained in part by the presence of proteinuria in the WT mice; however, defects in lymphocyte homeostasis in *gld* mice result in an accumulation of B cells which could also account for the increased immune response (Fukuyama et al., 1998). The fact that there was an increase in the immune response of *gld* mice, yet they showed fewer histological manifestations of injury, as highlighted by

reduced glomerular crescents and thrombosis, implies that it is possible to uncouple glomerular immunoglobulin deposition from glomerular damage. Other members of our laboratory have produced similar findings. MR-, FcRγ-, and FcγRIII-deficient mice were protected from developing renal disease yet mounted similar systemic immune responses to WT mice (Chavele et al., 2010; Tarzi et al., 2003). Whilst we consistently saw higher deposited and circulating antibody titres in the *gld* mice at the end of the experiment, there was some heterogeneity in antibody titres at 24 hours after injection of NTS. Two of the three experiments showed equivalent antibody titres between WT and *gld* mice, whilst the third experiment showed a reduction in the *gld* mice. There can be some variability in the immune response from one experiment to the next, but it is also possible that the effects of the *gld* mutation vary throughout the course of the experiment, with accumulation of more antigen-specific cells in the *gld* mice at later time points.

FasL is expressed on T cells, as well as myeloid cells, and is involved in regulating the immune response by playing a role in T cell activation (Alderson et al., 1993) and inducing apoptosis at the end of the immune response (Kabelitz et al., 1993). T cell-mediated systemic immunity was shown to be reduced in *gld* mice in the early phase of the disease and following non-specific stimulation with CD3/CD28 beads, supporting the hypothesis that FasL can function as an activator of T cells (Alderson et al., 1993). Coupled with the reduced numbers of $CD4^+$ T cells in the kidney, this could contribute to the protection of *gld* mice in the early phase of the experiment. However, similar to other groups' findings, we did not find a difference in T cell proliferation to antigen or antibody responses at the end of the experiment (Ma et al., 2004; Waldner et al., 1997) and this appeared to be a consistent finding. Despite this, the *gld* mice were protected both at day 7 and at later time points.

NTN is considered to be driven by a $T_h1/T_h17$-deviated immune response (Holdsworth et al., 1999; Summers et al., 2009). *Gld* mice, as well as patients with ALPS, have been shown to be skewed towards a $T_h2$ immune response (Fuss et al., 1997; Wahlsten et al., 2000). In keeping with this, cultured *gld* splenocytes produced significantly less IFN-γ (as well as slightly less IL-17) following stimulation with antigen, but this does not take into account the presence of DN T cells which do not produce cytokines. However, following non-specific stimulation with PMA and ionomycin, *gld* splenocytes were found to produce significantly more IL-4 as well as slightly increased levels of IL-10. Whole kidney mRNA expression of IFN-γ and IL-12p40 were also found to be reduced in *gld* mice, although there was no difference in expression of the $T_h2$ associated cytokines, IL-4 and IL-10. These

results cannot readily be directly related to a $T_h1$ immune response, as they do not take into account the greater number of $CD4^+$ T cells in WT mice or that IFN-γ and IL-12 are also produced by intrinsic renal cells (Timoshanko et al., 2002; Timoshanko et al., 2001). It is possible that a combination of the reduced overall T cell response and the predisposition to producing a $T_h2$ immune response contributes to protection from disease in the *gld* mice.

Aside from a small influx of neutrophils, there was no sign of renal dysfunction (increased serum urea) or inflammation (thrombosis, crescents) 24 hours after injection of NTS. This correlates with a time course study carried out previously by another member of the laboratory who showed that tubular and glomerular inflammation manifested around 48 hours following NTS injection (Chavele et al., 2010). In accelerated NTN, proteinuria starts to develop from day 1, getting progressively worse as the disease manifests, however urine collections were not carried out for the 24 hour experiment. NTN is characterised by an infiltration of glomerular neutrophils, within the first two hours, followed by macrophages. There was no reduction in glomerular neutrophil infiltration in *gld* mice at 24 hours in 2/3 of the experiments, where the immune response was equivalent between the groups, or in macrophage infiltration at day 7 and day 15. Soluble FasL has been shown to act as a potent chemoattractant for the migration of neutrophils and macrophages to sites of inflammation (Dupont and Warrens, 2007; Letellier et al., 2010; Seino et al., 1998), but my results indicate that in accelerated NTN sFasL does not play a major role in the recruitment of inflammatory cells to the glomerulus. Instead it is likely that other mechanisms, such as Fc receptors or complement-mediated events, are involved when immune complexes are deposited, as similar results were reported in both acute lung inflammation (Neff et al., 2005) and CIA (Ma et al., 2004).

Glomerular accumulation of macrophages is closely related to renal injury as the number of macrophages generally correlates with the severity of disease (Nikolic-Paterson and Atkins, 2001). However, other investigators in our laboratory have reported similar findings regarding the uncoupling of macrophage infiltration from injury. In the same model of NTN, $FcR\gamma^{-/-}$ and FcγRI/III-double deficient mice were protected from developing renal injury yet had similar numbers of glomerular macrophages, compared to WT mice (Tarzi et al., 2003). This suggests that the mechanisms of macrophage accumulation in immune-mediated GN may be different from the mechanisms of activation. Evidence supporting this idea comes from studies in rat models of crescentic GN. Treatment of rats with the cytokines IL-4 and IL-11 reduced glomerular crescent formation and proteinuria, by altering

macrophage activation, without reducing the glomerular accumulation of macrophages (Cook et al., 1999; Lai et al., 2001). It has been reported that FasL is involved in macrophage activation, acting synergistically with IFN-γ, to increase production of IL-6, NO and TNF-α. The presence of IL-4 was shown to decrease this synergy (Chakour et al., 2009). Interestingly I saw a significant reduction in IFN-γ expression in the whole kidney of *gld* mice, which combined with the lack of active FasL, suggests there could be a reduction in macrophage activation in the *gld* mice.

Interstitial macrophage infiltration is often thought to be a better marker of disease severity than glomerular infiltration in human GN (Nikolic-Paterson and Atkins, 2001). Although the initial insult in NTN is glomerular, damage to the integrity of the endothelium leads to proteinuria. Cytokines and chemokines can pass with the urine and across the tubular walls, causing local recruitment of macrophages to the interstitium. This can result in tubular injury and localised secretion of pro-inflammatory cytokines by the tubules. *Gld* mice were found to have very little glomerular damage, offering an explanation for the fact there were significantly fewer interstitial macrophages and dramatically reduced expression of MCP-1, a key chemokine in macrophage recruitment, compared to WT mice. MCP-1 expression occurs downstream of the IL-1R signalling pathway, of which there are multiple points of feedback and interaction with the Fas-FasL signalling pathway. Binding of FasL to Fas activates caspases, which process IL-1β for secretion, and frees the adaptor protein, MyD88, from FADD for signalling through the IL-1R (Ma et al., 2004). FasL signalling can also activate NF-κB for translocation into the nucleus (Xiao et al., 2002b). Both of these feedback points suggest defective FasL signalling can result in reduced MCP-1 expression. It would be interesting to stain for activated NF-κB in kidney sections and directly compare WT with *gld* mice following administration of NTN, to see if the lack of FasL has an effect on NF-κB activation in this model.

Macrophage phenotype has been shown to be important in kidney injury and repair (Lee et al., 2011). Surprisingly MR, a marker for the alternatively activated, repair macrophage, was upregulated in WT mice. Arginase expression, also a marker for alternatively activated macrophages, was upregulated slightly more in WT mice, although not significantly. However, it must be taken into account that WT mice had significantly more macrophages in the whole kidney than *gld* mice. iNOS expression in *gld* mice was downregulated compared to unmanipulated WT and *gld* mice, suggesting that the majority of macrophages in the *gld* mice are programmed to repair, whereas the macrophages in the WT

mice are both pro- and anti-inflammatory. There are a few possible explanations for the differences seen in macrophage phenotype between WT and *gld* mice. As already mentioned, FasL has been shown to act synergistically with IFN-γ in the activation of macrophages (Chakour et al., 2009). IFN-γ is involved in the classical pathway of macrophage activation, which results in a macrophage with a pro-inflammatory phenotype. The lack of functional FasL in the *gld* mice, along with the reduction in IFN-γ expression, could therefore result in fewer pro-inflammatory macrophages. As well as this, splenocytes from *gld* mice were found to produce greater amounts of IL-4 compared to WT splenocytes (following stimulation with CD3/CD28 beads) and there was an increase in IL-4 expression in the whole kidney of the *gld* mice (although not significant). IL-4, along with IL-13 (which was not measured), is involved in the alternative pathway of macrophage activation, resulting in an anti-inflammatory phenotype.

The use of whole kidney mRNA is not ideal when studying cytokine expression because it is not possible to identify which cells are expressing which cytokines. Indeed, as already mentioned, expression of IFN-γ and IL-12 are not limited to T cells, and iNOS and MR are not limited to macrophages. Mesangial cells have been shown to express iNOS and MR *in vitro,* following stimulation with immune complexes, and *in vivo,* during experimental GN (Chavele et al., 2010; Gomez-Guerrero et al., 2002). In an ideal situation, mRNA for analysis would be extracted from the cells of interest only, following cell isolation and purification.

*Gld* mice were dramatically protected from glomerular thrombosis compared to WT mice. Exposure of endothelial cells to pro-inflammatory molecules, such as TNF-α, IL-1 and MCP-1, leads to the expression of tissue factor, which is necessary for thrombosis formation (Dosquet et al., 1995; Grabowski and Lam, 1995; Kirchhofer et al., 1994). There was significant increase in expression of MCP-1 in the whole kidney of WT mice with NTN compared to *gld* mice and, although not significantly different, WT mice also expressed slightly more TNF-α. Both of these cytokines could possibly contribute to the greater incidence of thrombosis in these mice.

As well as initiation of tissue factor expression, TNF-α, along with IFN-γ, has been shown to upregulate expression of Fas on endothelial cells (Sata et al., 2000), leading to increased sensitivity to FasL induced apoptosis (Janin et al., 2002). Apoptotic endothelial cells have been shown to contribute to thrombotic events due to increased adherence of platelets to the endothelium and their subsequent activation (Bombeli et al., 1999). WT mice

were found to have significantly increased expression of IFN-γ following induction of NTN, which along with the presence of functional FasL, places them at greater risk of thrombosis compared to the *gld* mice.

One of the key roles of FasL is in inducing apoptosis. Apoptosis is a distinct mechanism of programmed cell death necessary for maintaining cellular homeostasis. Apoptosis can serve a dual role within inflammation. Deletion of cells can aid in the resolution of inflammation but inappropriate activation can cause cell damage that affects tissue function and remodelling (Baker et al., 1994; Savill, 1999; Sugiyama et al., 1996; Yang et al., 2001). It is not clear from our TUNEL staining which cells are undergoing apoptosis. It is likely both intrinsic renal cells and infiltrating leukocytes, although to fully determine this cells would need to be double-stained for fragmented DNA and cell specific markers, such as CD68, for macrophages, or CD4, for T cells.

In kidney IRI, apoptosis was suggested to be pro-inflammatory as blockade of FasL resulted in a reduction of apoptosis, inflammatory cytokine production and injury (Ko et al., 2011). In our model, there were no detectable glomerular apoptotic cells in *gld* mice. This could be due to the reduction in inflammation; however, another group in our laboratory found that MR-deficient mice have significantly more glomerular apoptotic cells than WT mice in the absence of inflammation, suggesting an anti-inflammatory role for apoptosis in NTN (Chavele et al., 2010). Due to the effects of the *gld* mutation on FasL function, a reduction in apoptotic cells would be expected; however a complete absence suggests that apoptosis is contributing to injury, similar to the effects seen in the IRI model, rather than repair, as none of the other pathways of apoptosis have been activated. Work looking at the effect of blocking caspase-3 in the rat in NTN solves the paradox. Caspase-3 is a central player in cellular apoptosis for both the extrinsic (death receptor-ligand) and intrinsic (mitochondrial) pathways. Inhibition of caspase-3 was found to reduce renal apoptosis, ameliorate inflammation and improve proteinuria (Yang et al., 2003). The dual roles of FasL in inducing apoptosis and inflammation make it difficult to dissect which is the cause and which is the effect. It would be interesting to study the role of FasL in a model of glomerulonephritis that requires apoptosis for repair, such as anti-Thy-1 nephritis in rats.

The presence of FasL was also studied in WT mice. FasL can be found in two forms, a membrane-bound form or a soluble form (sFasL). There was an upregulation of FasL mRNA expression in WT whole kidneys with NTN. Due to the nature of the mutation in *gld* mice, FasL is still expressed in full and does have some residual activity (Karray et al., 2004).

We did not look at expression of FasL in *gld* mice. It would be interesting to see if expression increases during NTN despite the ligand being mostly inactive. Due to the reduction in damage in *gld* mice it could be postulated that expression would stay the same. As mentioned before, the use of whole kidney does not allow us to determine which cells are expressing FasL. Possible sites of expression are infiltrating leukocytes, such as macrophages and T cells, or intrinsic renal cells, such as tubular epithelial cells and mesangial cells. Despite other groups publishing work showing the detection of FasL via immunoperoxidase staining (Lorz et al., 2000; Tsukinoki et al., 2004), our attempts to stain for FasL in WT kidney sections were unsuccessful. I also attempted to detect circulating sFasL in the serum of WT mice without success. It is likely the methods used were not sensitive enough and the levels of FasL present were below the levels of detection. As few as six molecules of FasL are sufficient to induce FasL-dependent cell death, which is well below protein detection level by methods such as ELISA, immunoperoxidase staining or Western blot (Holler et al., 2003).

Our results are in keeping with previous studies investigating the role of FasL in inflammatory diseases. *Gld* mice have been found to be protected from acute lung inflammation (Neff et al., 2005), EAE (Sabelko et al., 1997; Waldner et al., 1997), EAU (Wahlsten et al., 2000) and experimental stroke (Niu et al., 2011). A possible mechanism for protection in experimental stroke was proposed. Following injury the brains of WT mice showed high levels of sFasL and the *gld* mice had significantly decreased levels of infiltrating inflammatory cells suggesting that the chemotactic actions of FasL, rather than the apoptotic actions, and defects in the activation of transcription factors, are involved in the inflammation seen in this model (Niu et al., 2011).

Due to availability of mice and the regulations of the UK Home Office, both male and female mice were used in these experiments. Female mice are much more susceptible to NTN than male mice, however we did not find that differences in sex affected the outcome of the experiments. Most of these experiments were performed on male mice. However, one of the three 24 hours experiments (Section 3.4.6) and one experiment to day 10 (Section 3.4.11) were performed on female mice, with female *gld* mice still being protected from disease. In humans, there is a higher incidence of autoimmune disease in females compared to males (roughly 3:1). As well as genetic polymorphisms and environmental factors being involved, sex hormones also play a role in susceptibility. Castration of autoimmune prone NZB/NZW male mice was found to accelerate the onset of lupus-like disease, whereas ovariectomised female NZB/NZW mice given androgens had reduced lupus-like disease (Roubinian et al.,

1977). Although using different sexes in the experiments makes it difficult to compare directly the results seen, the results follow the same trend.

Our results showed a reduction in injury despite no reduction in the antibody responses and only a mild reduction in the T cell-mediated immune response of *gld* mice. There was reduced apoptosis in the *gld* kidney, but no reduction in glomerular macrophage or neutrophil infiltration. We saw a strong reduction in MCP-1 mRNA in the *gld* kidneys, suggesting that cytokine production may indeed be defective in these mice. To further investigate the role of FasL in GN I went on to perform bone marrow transplants to find out whether FasL expression on circulating leukocytes, or intrinsic renal cells, is involved in the development of disease. I also cultured mesangial cells for *in vitro* studies, to determine the mechanism by which defective FasL can protect from inflammation.

## 3.6 Conclusion

Since FasL has been implicated as an initiator of inflammation, I hypothesised that abnormalities in FasL signalling may play a critical role in the initiation of injury in accelerated NTN. At this point it can be concluded that the presence of FasL in the kidney does contribute to the development of disease. The mechanism through which FasL promotes disease may relate to T cell-mediated systemic immunity, but the defects seen in the *gld* T cell responses were transient. Cell activation or apoptosis, facilitated by FasL, may also contribute to disease. Unfortunately, the autoimmunity enhancing effects of FasL deficiency may prevent its use as a therapeutic treatment; however, this study has highlighted an important role of FasL in initiating inflammation. The next step was to investigate whether FasL expression on infiltrating leukocytes or resident renal cells is more critical for the development of disease.

# CHAPTER 4

# The Role of Fas Ligand on Circulating Leukocytes and Intrinsic Renal Cells in Accelerated Nephrotoxic Nephritis

## 4.1 Introduction

Infiltrating macrophages and T cells, as well as proliferating mesangial cells, play a central role in the development of GN in humans and mice. FasL has been shown to be expressed on activated macrophages and T cells (Dockrell et al., 1998; Suda et al., 1995), the tubular epithelium in healthy kidney (Lorz et al., 2000) and mesangial cells during renal injury (Tsukinoki et al., 2004). Since *gld* mice were protected from NTN, it was essential to investigate the importance of FasL in different subsets of cells that play a role in the development of GN. To do this, bone marrow chimeric mice were created with the *gld* gene in their bone marrow-derived cells but not their tissue cells, and *vice versa*. The susceptibility of these mice to accelerated NTN was compared to control WT mice transplanted with WT bone marrow and *gld* mice transplanted with *gld* bone marrow, respectively.

As well as causing defects in apoptosis, defective Fas-FasL signalling has also been shown to interfere with signalling through pathways that require the adapter protein MyD88, such as the IL-1R pathway and the TLR4 pathway (Altemeier et al., 2007; Bannerman et al., 2002; Ma et al., 2004). There was a significant reduction in MCP-1 expression in whole kidney from *gld* mice with NTN compared to WT mice. This can in part be explained by the reduction in interstitial macrophages in the *gld* mice; however, mesangial cells have also been shown to be a source of renal MCP-1 following stimulation with IL-1β and TNF-α (Zoja et al., 1991). Therefore it was of interest to culture mesangial cells from WT and *gld* mice and confirm FasL expression as well as compare cytokine expression following stimulation with IL-1β and TNF-α.

## 4.2 Aim

This part of the project was focused on answering whether FasL expression on resident renal cells or infiltrating cells (macrophages, T cells, NK cells) was more critical for the development of accelerated NTN. Mesangial cell expression of FasL was also assessed, as well as the differences in response to IL-1β and TNF-α stimulation between WT and *gld* mesangial cells *in vitro.*

## 4.3 Experimental design

In order to investigate if FasL expression on radioresistant renal cells or infiltrating leukocytes is more critical for the development of GN, bone marrow transplantation experiments were performed. A single dose of whole body gamma irradiation was used to ablate the bone marrow of both WT and *gld* mice. Immediately following irradiation, the mice received an intravenous injection of whole bone marrow. WT mice received bone marrow cells from *gld* mice (*gld*→WT) and *vice versa* (WT→*gld*). This resulted in WT mice with FasL-defective leukocytes and FasL expressing renal cells and *gld* mice with FasL expressing leukocytes and FasL-defective renal cells. As controls, WT mice were transplanted with WT bone marrow (WT→WT) and *gld* mice were transplanted with *gld* bone marrow (*gld*→*gld*). NTN was induced and disease was assessed in WT and *gld* chimeric mice as previously described (see Section 3.3).

To investigate directly FasL on mesangial cells, mesangial cells were isolated from WT and *gld* mice and cultured *in vitro.* WT mesangial cells were stimulated with LPS and assessed by qRT-PCR for FasL. Then WT and *gld* mesangial cells were assessed for differences in response to stimulation with pro-inflammatory cytokines (IL-1β and TNF-α) by measuring the MCP-1 levels released into the supernatant by ELISA.

## 4.4 Results

### 4.4.1 Bone marrow reconstitution

8Gy of irradiation was used, as previously optimised by Dr. Ruth Tarzi. The irradiated mice were intravenously injected with $1x10^7$ bone marrow cells harvested from the femur, tibia and humerus of donor sex-matched mice.

Bone marrow reconstitution was assessed by two methods. Firstly, WT mice (n=4) were transplanted with bone marrow marked with the allotype marker CD45.1 rather than CD45.2, the C57BL/6 allotype. Eight weeks post transplant blood was collected from these mice and stained for CD45.1 and CD45.2 for analysis by flow cytometry (mean % of CD45.1 positive cells of total cells: 92±0.083%) (Table 4.1 & Figure 4.1). Secondly, semi-quantitative PCR of DNA purified from mouse blood collected at the end of the experiment was performed as before (Section 3.4.1); however, the reverse primer was labelled with a fluorescent FAM marker. Following restriction digestion the products were run on a Genescan and the ratio of WT (88bp) versus mutant (108bp) product was calculated and compared to known mixtures of WT and *gld* DNA (0%, 5%, 10%, 25%, 50%, 75%, 90%, 95% and 100% WT DNA) (Figure 4.2).

| | CD45.1 | CD45.2 | BMT 1 | BMT 2 | BMT 3 | BMT 4 |
|---|---|---|---|---|---|---|
| $CD45.1^+$ cells | 85 | 0.24 | 84 | 88 | 65 | 66 |
| $CD45.2^+$ cells | 0 | 62 | 7.8 | 6.0 | 3.6 | 5.5 |
| $CD45.1^+CD45.2^+$ cells | 0 | 1.45 | 0.37 | 0.22 | 1.2 | 1.2 |
| % $CD45.1^+$ cells | 100 | 0.38 | 91 | 93 | 93 | 91 |

**Table 4.1 Flow cytometry data to assess reconstitution of donor bone marrow in chimeric mice.**

$CD45.1^+$ and $CD45.2^+$ cells in individual CD45.1, CD45.2 and chimeric mice (BMT (bone marrow transplant) 1-4).

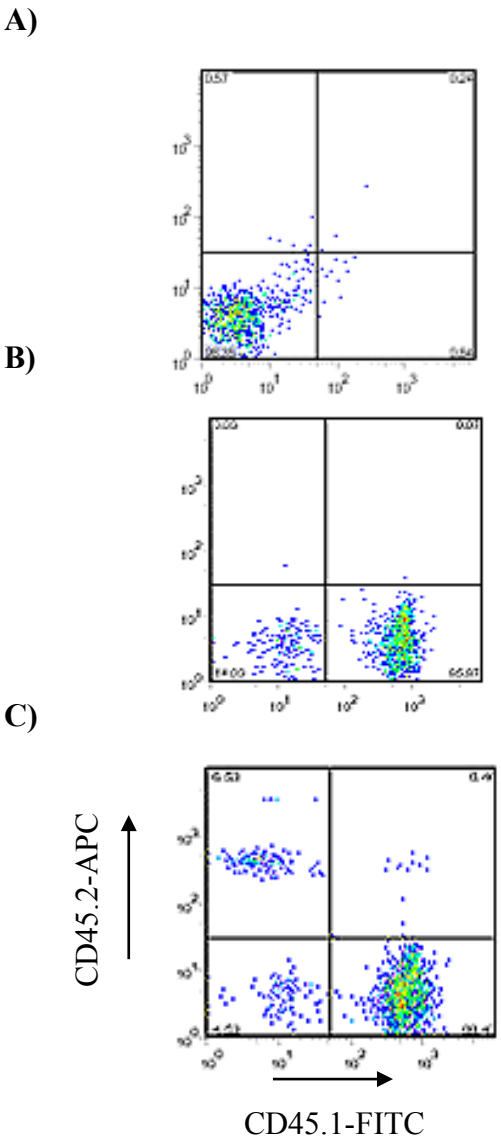


**Figure 4.1 Assessment of donor bone marrow reconstitution in chimeric mice by flow cytometry.**

Eight weeks post bone marrow transplant WT C57BL/6 mice transplanted with CD45.1 bone marrow were bled and the blood stained for CD45.1 and CD45.2 allotype markers. Upper left quadrant $CD45.2^+$ cells, lower right quadrant $CD45.1^+$ cells. **(A)** Unstained control, **(B)** $CD45.1^+$ mouse stained for $CD45.1^+$ cells and **(C)** WT $CD45.2^+$ mouse transplanted with $CD45.1^+$ cells double stained for $CD45.1^+$ and $CD45.2^+$ cells.

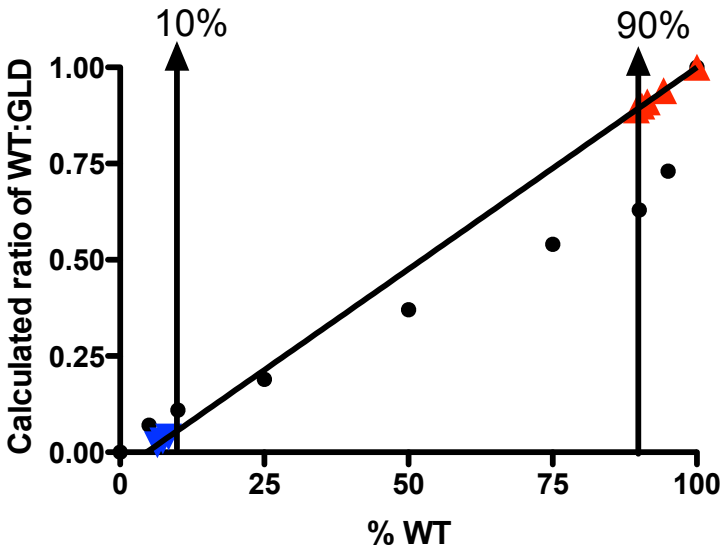


**Figure 4.2 Assessment of donor bone marrow reconstitution in chimeric mice by PCR.**

Different proportions of WT and *gld* DNA were mixed and subjected to PCR. Following restriction digestion the products were run on a Genescan and a standard curve of the percentage WT DNA compared to *gld* DNA plotted against the known calculated ratios of WT:*gld* DNA. In the same PCR reaction DNA from the two chimeric groups of mice were also run to examine the relative percentage of bone marrow reconstitution. In both groups (*gld* to WT transplanted mice represented by the blue downward triangles and WT to *gld* transplanted mice represented by the red upward triangles) reconstitution was greater than 90%.

### 4.4.2 Fas ligand from either bone marrow-derived or radioresistant intrinsic renal cells is sufficient to restore susceptibility to accelerated nephrotoxic nephritis

#### 4.4.2.1 Assessment of renal function in bone marrow transplanted mice with accelerated nephrotoxic nephritis

A cohort of *gld* mice (n=8) were transplanted with WT bone marrow and a cohort of WT mice (n=9) were transplanted with *gld* bone marrow. As controls, WT mice (n=8) were transplanted with WT bone marrow and *gld* mice (n=7) were transplanted with *gld* bone marrow. All mice used were males. The animals were left for nine weeks for bone marrow reconstitution to occur and then NTN was induced by pre-immunising the mice with 0.2mg of sheep IgG in CFA and after five days administering 200µl (1:4 dilution) of NTS via the tail vein. Mice were sacrificed at day 8 to allow significant differences in disease to develop without excessive suffering to the animals.

To assess kidney function serum urea and albuminuria, expressed as a ratio of urinary albumin/creatinine, were measured in all mice. The levels of serum urea were significantly lower in the *gld* mice transplanted with *gld* bone marrow compared to the *gld* mice transplanted with WT bone marrow (*gld*→*gld* 14 (10-20) mmol/L, WT→*gld* 37 (13-40) mmol/L, p=0.014), whereas there was no significant difference between the other groups (*gld*→WT 30 (11-41) mmol/L, WT→WT 34 (11-42) mmol/L) (Figure 4.3 A). *Gld* mice transplanted with *gld* bone marrow had a significantly lower urinary albumin/creatinine ratio (1.1 (0.00-6.9) mg/mmol) than *gld* mice transplanted with WT bone marrow (6.2 (3.3-9.1) mg/mmol, p=0.007) and WT mice transplanted with *gld* bone marrow (5.5 (0.020-7.7) mg/mmol, p=0.023). There was no significant difference in the urinary albumin/creatinine ratio between any of the groups with the WT mice transplanted with WT bone marrow (7.0 (0.020-12) mg/mmol) (Figure 4.3 B).

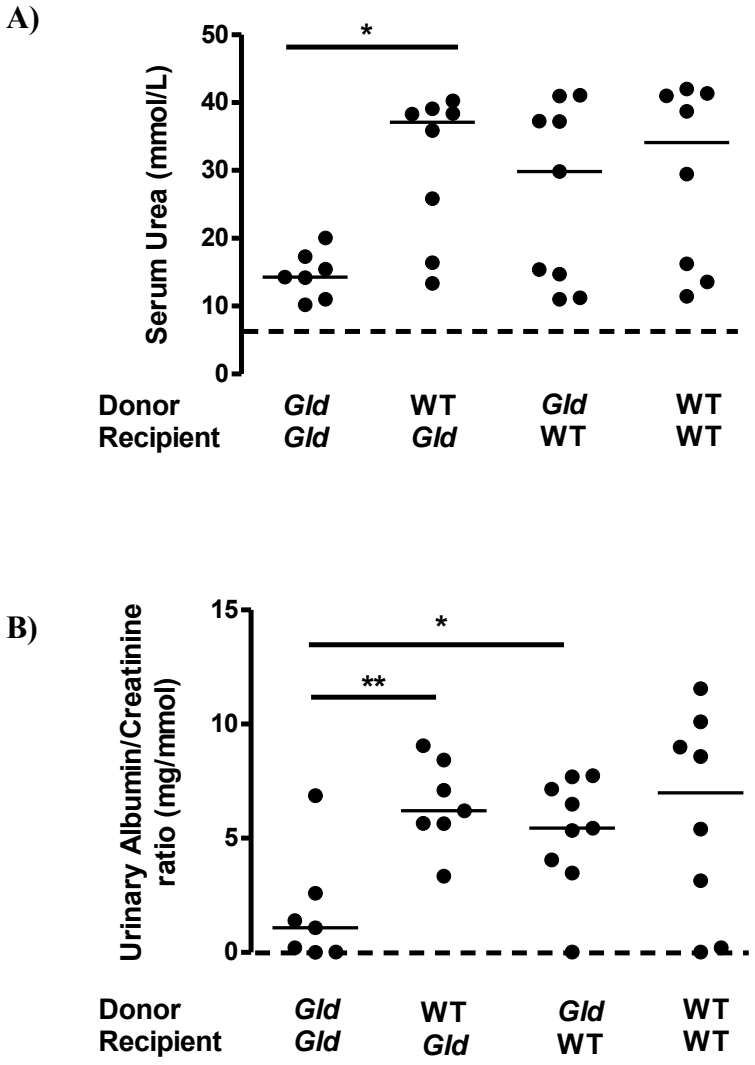


**Figure 4.3 Measurement of serum urea and urinary albumin/creatinine ratio in bone marrow transplanted mice with NTN.**

**(A)** Serum urea and **(B)** urinary albumin/creatinine ratio post NTS administration in bone marrow transplanted mice. *Gld* mice transplanted with *gld* bone marrow had significantly lower serum urea than *gld* mice transplanted with WT bone marrow. *Gld* mice transplanted with *gld* bone marrow had a significantly lower urinary albumin/creatinine ratio than WT mice transplanted with *gld* bone marrow and WT mice transplanted with *gld* bone marrow. There was no significant difference in urinary albumin/creatinine ratio between any of the other groups of mice. All data represent individual values with the median. The data were analysed using Mann-Whitney U-test ($p^{*}<0.05$, $p^{**}<0.01$). Dashed lines represent values for a group of normal WT mice.

#### 4.4.2.2 Renal histology of bone marrow transplanted mice with accelerated nephrotoxic nephritis

At day 8 after disease induction PAS-stained kidney sections were assessed for histological damage measured by glomerular thrombosis and crescents. *Gld* mice transplanted with *gld* bone marrow had significantly reduced susceptibility to glomerular thrombosis (0.00 (0.00-0.58)) and crescents (0.00 (0.00-0.00) %) compared to the other groups of mice (thrombosis: WT→*gld* 1.3 (0.060-3.3), p=0.0072; *gld*→WT 0.92 (0.004-2.1), p=0.0077; WT→WT 0.70 (0.00-1.6), p=0.029; crescents: WT→*gld* 5.0 (0.00-10) %, p=0.0074; WT→WT 2.0 (0.00-6.0) %, p=0.0071). There was no significant difference in crescents between the *gld* mice transplanted with *gld* bone marrow and the WT mice transplanted with *gld* bone marrow (*gld*→WT 0.00 (0.00-14) %) (Figure 4.4 and Figure 4.5).

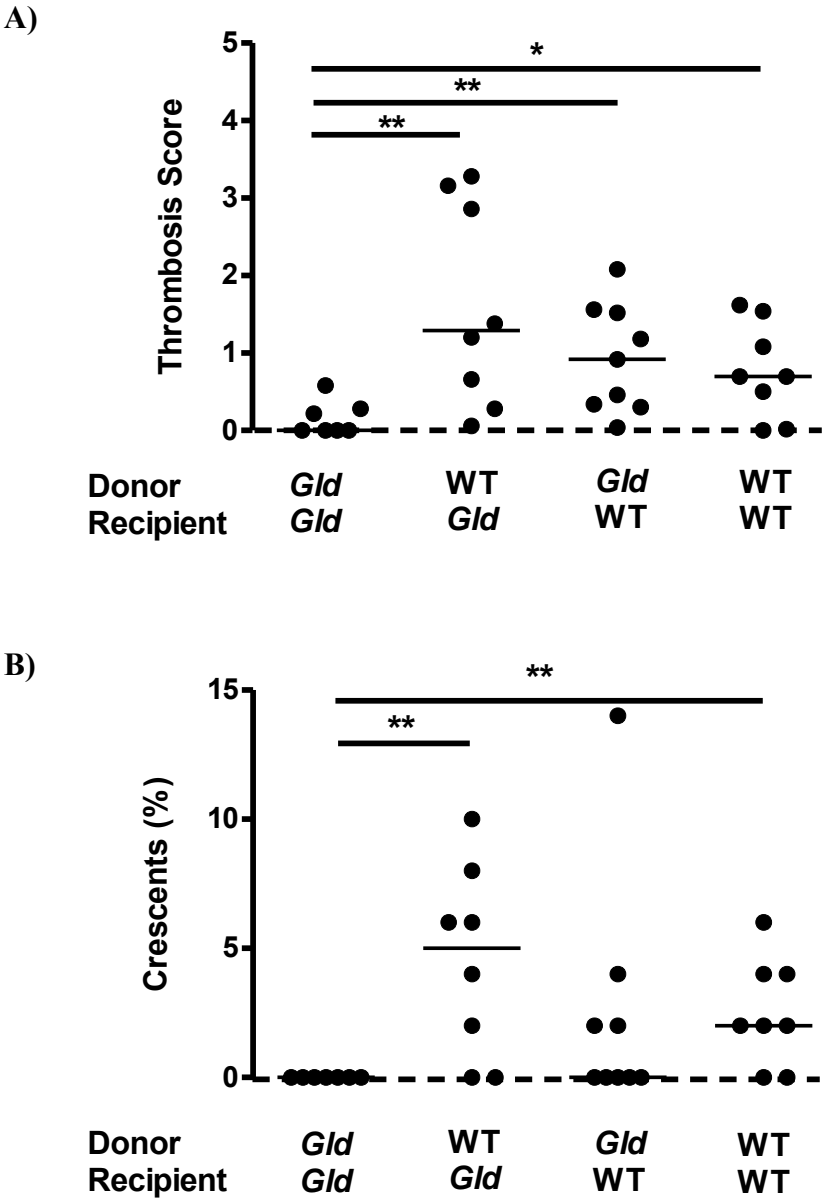


**Figure 4.4 Quantification of histologically abnormal glomeruli in bone marrow transplanted mice with NTN.**

**(A)** Thrombosis and **(B)** crescents in bone marrow transplanted mice on day 8, after NTN induction, scored on PAS-stained kidney sections. *Gld* mice that received *gld* bone marrow had less severely damaged glomeruli than the other groups of mice. All data represent individual values with the median. The data were analysed using Mann-Whitney U-test ($p^{*}<0.05$, $p^{**}<0.01$). Dashed lines represent values for a group of normal WT mice.

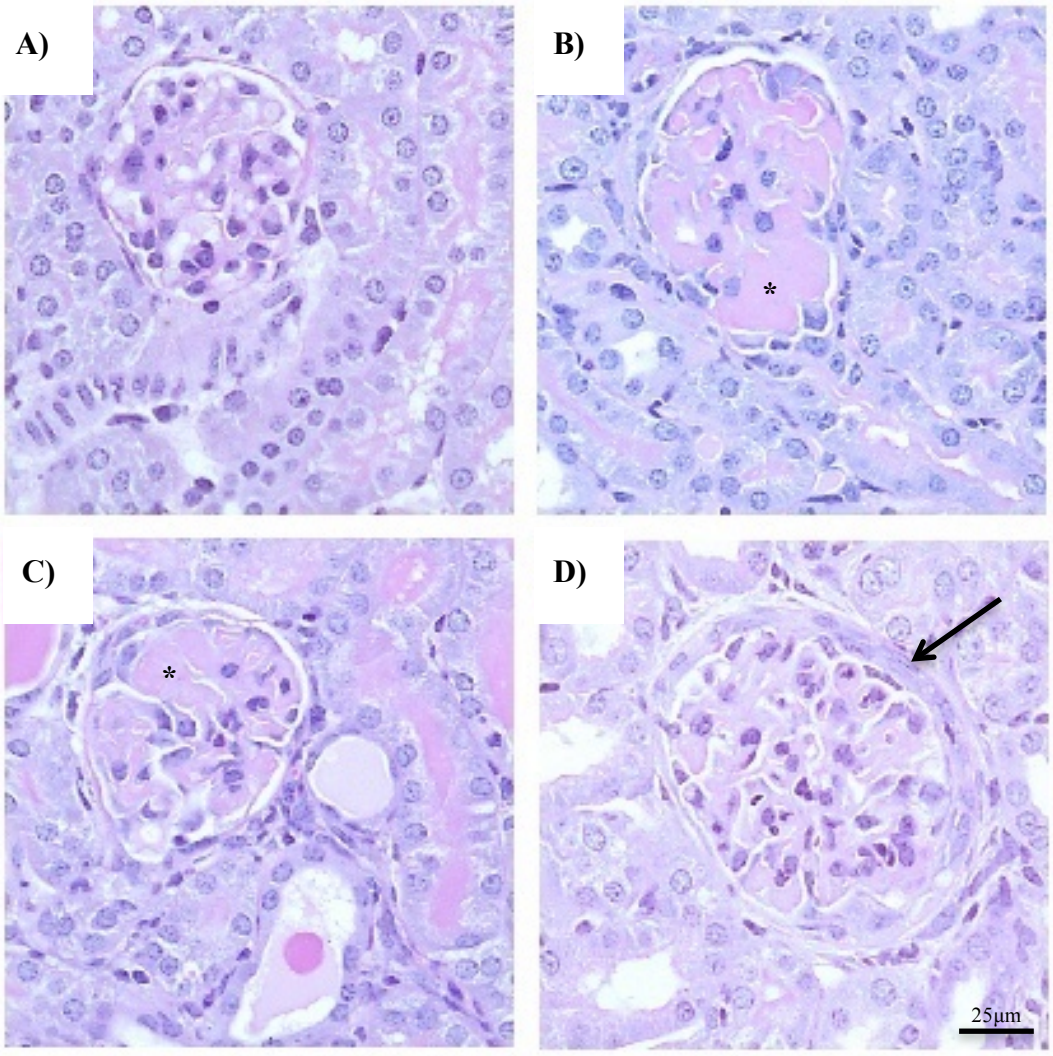


**Figure 4.5 PAS staining of kidneys from bone marrow transplanted mice with NTN.**

Representative PAS staining from a **(A)** *gld*→*gld* mouse showing a healthy glomerulus, **(B)** WT→*gld* mouse, showing a thrombotic glomerulus, **(C)** *gld*→WT mouse, showing a thrombotic glomerulus, and a **(D)** WT→WT mouse, showing a crescentic glomerulus, 8 days after administration of NTS. Arrow highlights crescent formation and asterisks (*) highlight thrombosis.

### 4.4.3 Infiltrating macrophages and T cells in bone marrow transplanted mice with accelerated nephrotoxic nephritis

As a measure of inflammation, frozen kidney sections were stained for macrophage and T cell infiltration at day 8 post NTS administration with anti-CD68 macrophage antibody (Figure 4.7) and anti-CD4 T cell antibody (Figure 4.8 A). *Gld* mice transplanted with *gld* bone marrow had fewer glomerular macrophages compared to WT mice transplanted with *gld* bone marrow (macrophages/gcs: *gld*→*gld* 0.74 (0.00-2.8), *gld*→WT 2.5 (1.1-4.6), p=0.023) but there was no significant difference between the other groups (macrophages/gcs: WT→*gld* 1.4 (0.52-2.6), WT→WT 1.8 (0.64-2.3)). There was no significant difference in glomerular T cell numbers between the four groups of mice (T cells/gcs: *gld*→*gld* 0.24 (0.12-0.62), WT→*gld* 0.22 (0.06-0.32), *gld*→WT 0.34 (0.16-0.54), WT→WT 0.23 (0.12-0.52). (Macrophages: Figure 4.6 A; T cells: Figure 4.8 B).

Interstitial macrophage numbers were measured quantitatively with the results being expressed in arbitrary units (AU). *Gld* mice transplanted with *gld* bone marrow had significantly fewer interstitial macrophages (0.49 (0.17-3.3) AU) compared to all other groups of mice (interstitial macrophages: WT→*gld* 3.4 (2.1-9.0) AU, p=0.0037; *gld*→WT 3.7 (0.83-9.9) AU, p=0.0052; WT→WT 7.1 (0.45-16.22) AU, p=0.0093). There was no significant difference between the other groups of transplanted mice (Figure 4.6 B).

These results, along with the reduced kidney function (Section 4.4.1) and increased glomerular damage (Section 4.4.2), suggest that the presence of active FasL on either infiltrating leukocytes or radioresistant intrinsic renal cells is enough to convey disease in this model of NTN. It was hypothesised that FasL on infiltrating leukocytes would play a role in the development of NTN; however, the active role of FasL on radioresistant intrinsic renal cells in NTN was unexpected. A second bone marrow transplant experiment was undertaken to confirm the result. A cohort of WT mice were transplanted with *gld* bone marrow and as controls WT mice were transplanted with WT bone marrow and *gld* mice were transplanted with *gld* bone marrow. Again, the presence of active FasL on radioresistant intrinsic renal cells was found to confer susceptibility to disease, with WT mice transplanted with *gld* bone marrow having reduced kidney function.

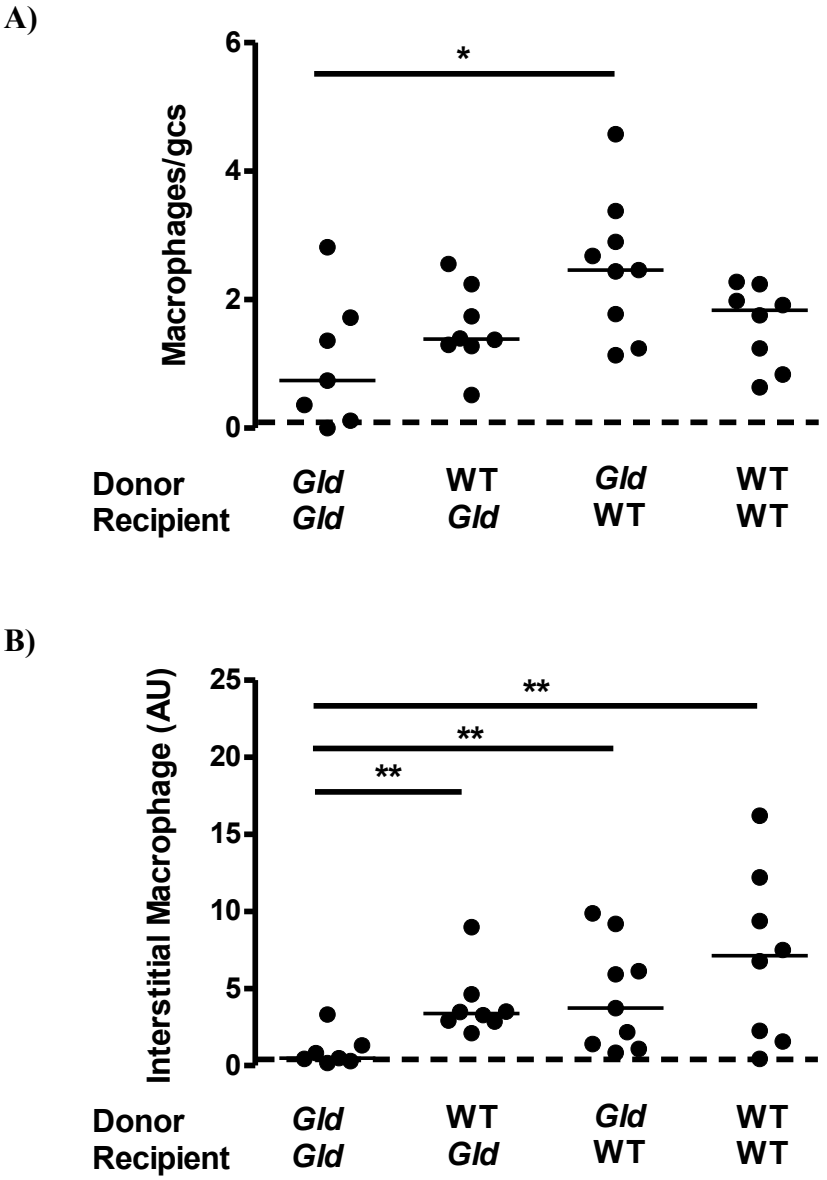


**Figure 4.6 Macrophage infiltration in bone marrow transplanted mice with NTN.**

Macrophage infiltration **(A)** per glomerular cross section (gcs) (50 glomeruli scored per cross section) and **(B)** in the interstitium (expressed as arbitrary units (AU) scored using 5 separate fields of view). *Gld* mice transplanted with *gld* bone marrow had significantly fewer glomerular macrophages than WT mice transplanted with *gld* bone marrow and interstitial macrophages compared to all other groups of mice. All data represent individual values with the median. The data were analysed using Mann-Whitney U-test ($p^{*}<0.05$, $p^{**}<0.01$). Dashed lines represent values for a group of normal WT mice.

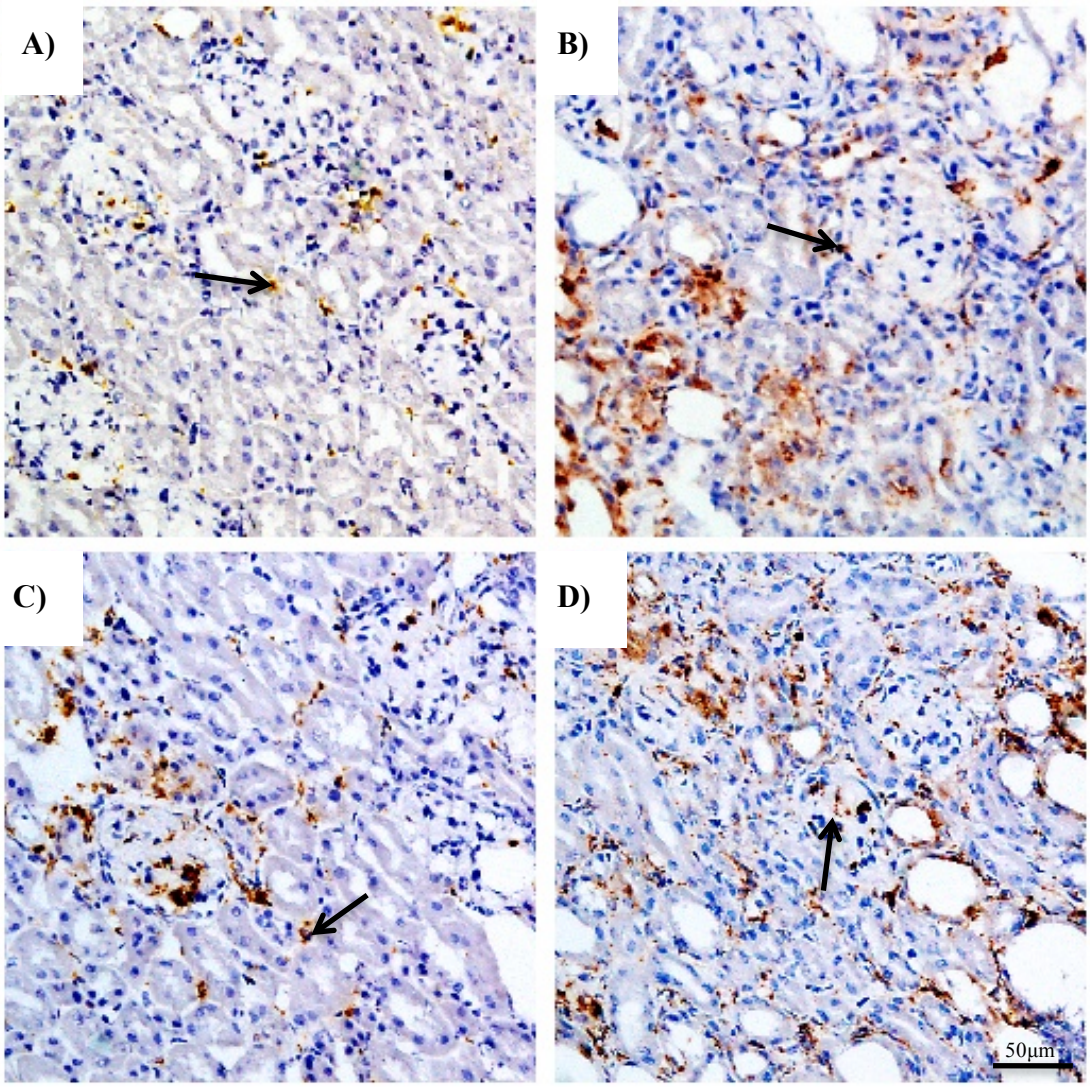


**Figure 4.7 Immunohistochemistry of glomerular and interstitial macrophage infiltration in bone marrow transplanted mice with NTN.**

Representative immunohistochemistry for macrophages (CD68) on **(A)** *gld→gld*, **(B)** WT→*gld,* **(C)** *gld*→WT and **(D)** WT→WT kidney sections. Arrows highlight macrophages.

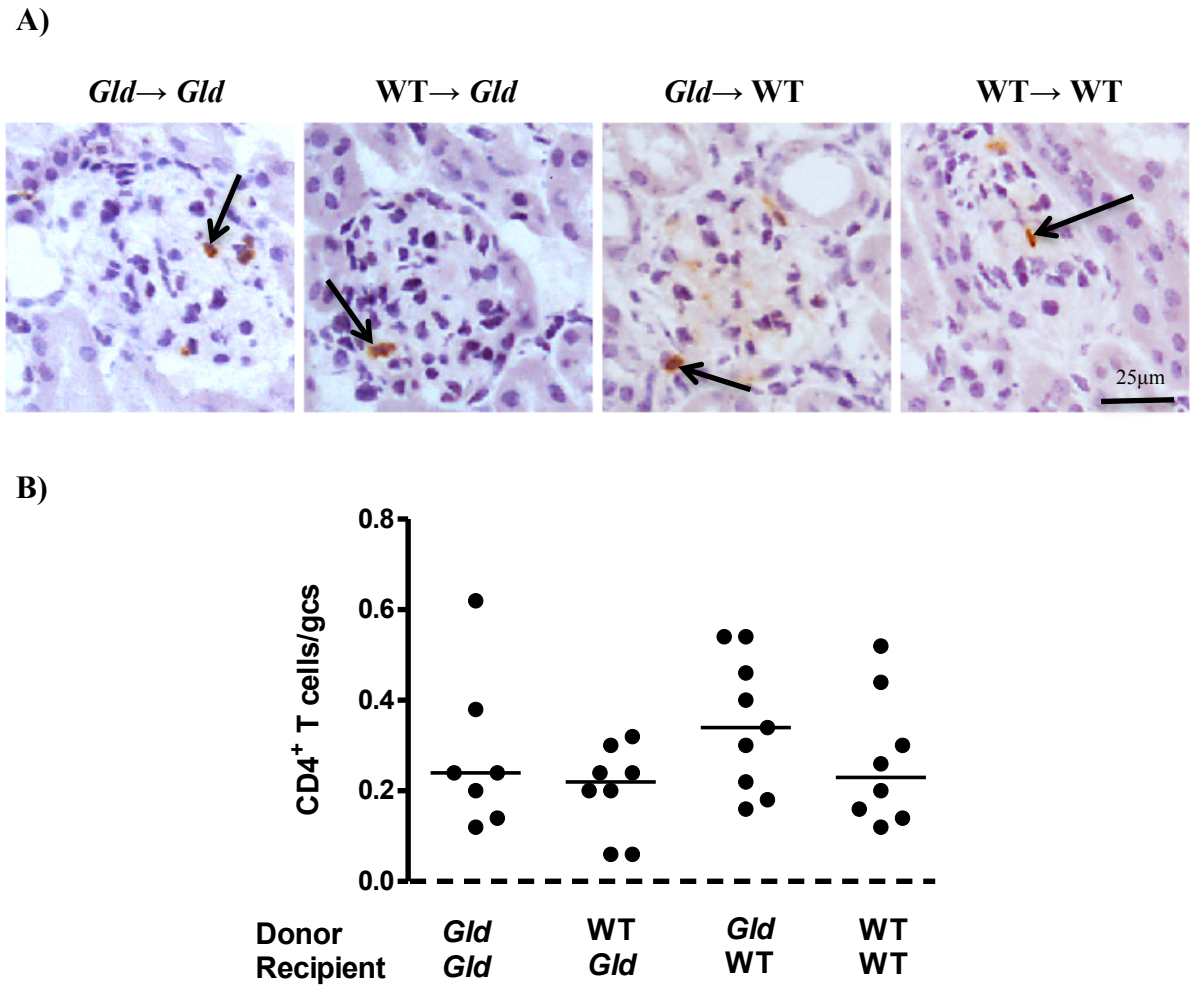


**Figure 4.8 Glomerular T cell infiltration in bone marrow transplanted mice with NTN.**

**(A)** Immunohistochemistry for T cells (CD4) on *gld*→*gld*, WT→*gld, gld*→WT and WT→WT kidney sections. Arrows highlight T cells. **(B)** T cell infiltration per glomerular cross section (gcs) (50 glomeruli scored per cross section). There was no statistical difference in glomerular T cell numbers between the different groups of mice. All data represent individual values with the median. The data were analysed using Mann-Whitney U-test. Dashed lines represent values for a group of normal WT mice.

### 4.4.4 Systemic immune responses

Mouse sera, collected at the end of the experiment, were tested for the antigen-specific immune response against sheep IgG. The circulating anti-sheep IgG levels were measured by ELISA (results expressed as median optical density at 405nm (OD 405nm)). WT and *gld* mice receiving *gld* bone marrow had slightly higher levels of circulating sheep IgG than mice receiving WT bone marrow (*gld*→*gld* vs. WT →*gld* p=0.040, *gld*→*gld* vs. WT→WT p=0.040, *gld*→WT vs. WT→WT p=0.051) (Table 4.2 and Figure 4.9). FasL is known to be involved in the deletion of B cells, which can result in elevated levels of autoantibodies. However, despite an increased immune response, *gld* mice transplanted with *gld* bone marrow had less disease, showing that antibody production is not the determining factor for heightened susceptibility to NTN.

Frozen kidney sections were stained for deposited sheep and mouse IgG by direct immunofluorescence on tissue taken at the end of the experiment (Figure 4.10 A and Figure 4.11 A, respectively). Glomerular total sheep IgG and mouse IgG were measured by semi-quantitative immunofluorescence, with results expressed as visual fluorescence units (VFU), and were equivalent between the different bone marrow transplanted groups. (Table 4.2, Figure 4.10 B and Figure 4.11 B, respectively).

| Donor | Recipient | Serum anti-sheep IgG (OD 405nm) | Deposited glomerular sheep IgG (VFU) | Deposited glomerular mouse IgG (VFU) |
|---|---|---|---|---|
| *Gld* | *Gld* | 0.54 (0.27-0.70) | 3.0 (2.0-4.0) | 3.0 (2.0-3.0) |
| WT | *Gld* | 0.37 (0.077-0.50) | 3.0 (2.0-3.0) | 3.0 (1.0-4.0) |
| *Gld* | WT | 0.63 (0.25-1.0) | 3.0 (2.0-4.0) | 3.0 (2.0-3.0) |
| WT | WT | 0.40 (0.25-0.60) | 3.0 (2.0-4.0) | 3.0 (2.0-3.0) |

**Table 4.2 Circulating anti-sheep IgG levels and deposited glomerular sheep and mouse IgG in bone marrow transplanted mice with NTN.**

All results are expressed as median (range).

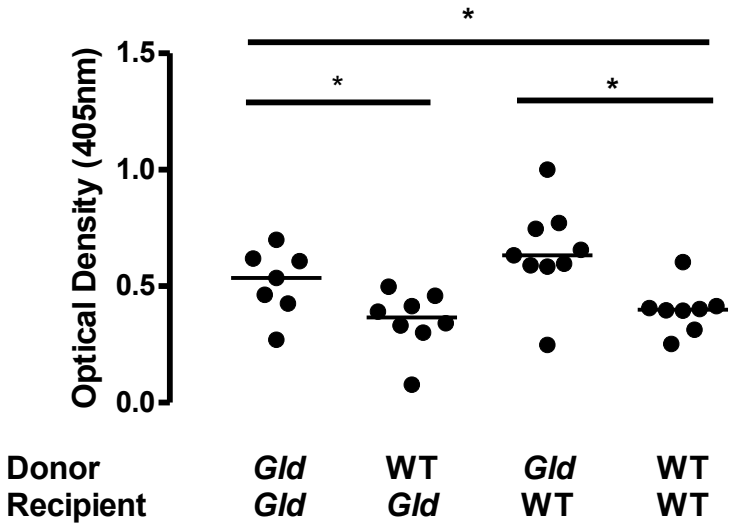


**Figure 4.9 Circulating mouse anti-sheep IgG levels in bone marrow transplanted mice with NTN.**

The circulating levels of mouse anti-sheep IgG were measured by ELISA. Mice transplanted with *gld* bone marrow had slightly elevated levels compared to mice transplanted with WT bone marrow. All data represent individual values with the median. The data were analysed using Mann-Whitney U-test ($p^*<0.05$).

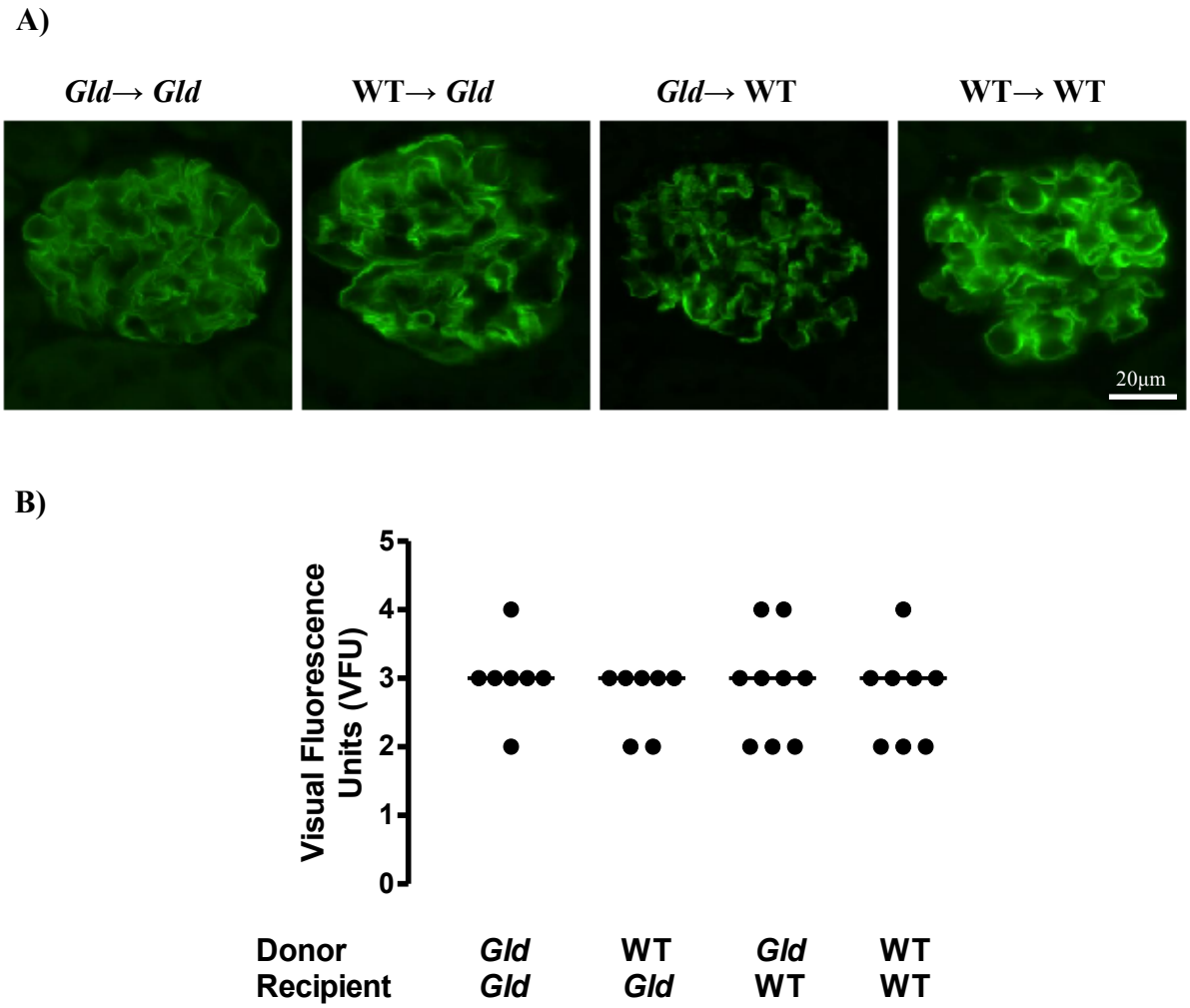


**Figure 4.10 Immunofluorescence of glomerular sheep IgG deposition in bone marrow transplanted mice with NTN.**

**(A)** Representative glomeruli from *gld*→*gld*, WT→*gld*, *gld*→WT and WT→WT mice showing sheep IgG deposition 8 days after NTS injection. All images were taken using the same settings. **(B)** Semi-quantitative analysis of glomerular immunofluorescence. There was no significant difference between the groups of mice. All data represent the individual values with the median. The data were analysed using the Mann-Whitney U-test.

**A)**

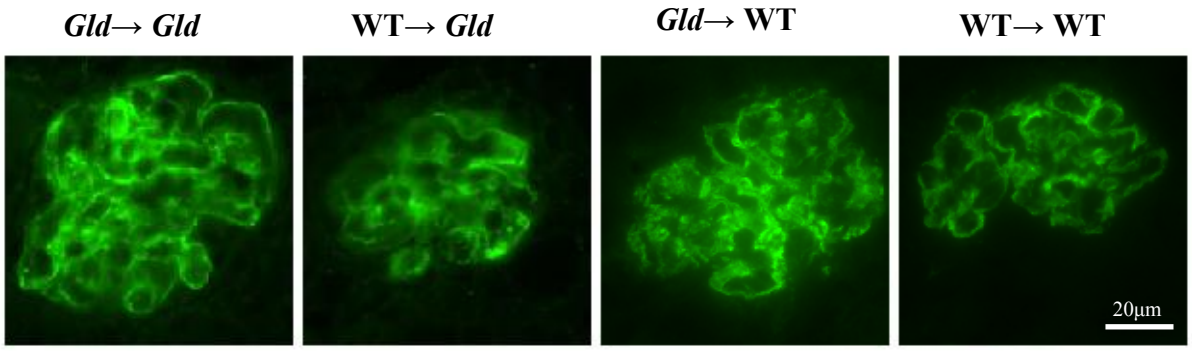


**B)**

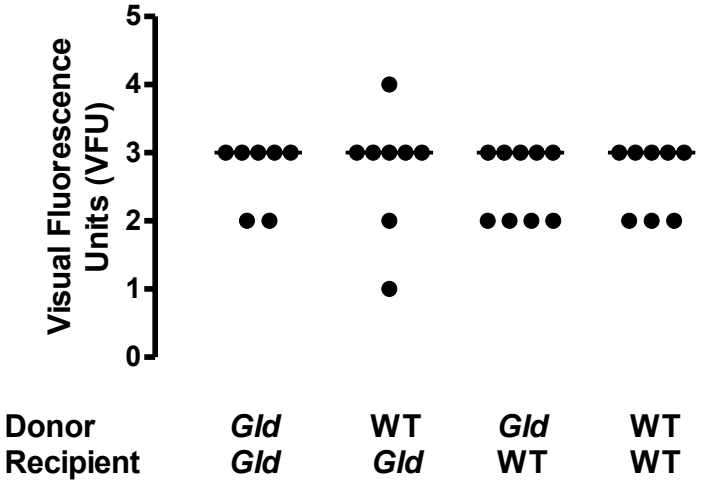


**Figure 4.11 Immunofluorescence of glomerular mouse IgG deposition in bone marrow transplanted mice with NTN.**

**(A)** Representative glomeruli from *gld*→*gld*, WT→*gld*, *gld*→WT and WT→WT mice showing mouse IgG deposition 8 days after NTS injection. All images were taken using the same settings. **(B)** Semi-quantitative analysis of glomerular immunofluorescence. There was no significant difference between the groups of mice. All data represent the individual values with the median. The data were analysed using the Mann-Whitney U-test.

### 4.4.5 Apoptotic cells in bone marrow transplanted mice with accelerated nephrotoxic nephritis

Due to the proposed dual role of FasL in apoptosis and inflammation and the stark differences seen between the numbers of apoptotic cells in WT and *gld* mice with NTN (Section 3.4.8), it was important to quantitate the presence of apoptosis in the kidney in our model following bone marrow transplant. Paraffin-fixed kidney sections were stained for apoptosis by TUNEL. Apoptotic cells were counted in 30 glomeruli per cross section. *Gld* mice transplanted with *gld* bone marrow had significantly fewer apoptotic cells per glomerular cross section than *gld* mice transplanted with WT bone marrow and WT mice transplanted with WT bone marrow (apoptotic cells/gcs: *gld*→*gld* 0.067 (0.00-0.17); *gld*→WT 0.53 (0.00-0.93), p=0.0079; WT→WT 0.37 (0.00-1.0), p=0.027). There was no significant difference between the other groups of mice (apoptotic cells/gcs: WT→*gld* 0.23 (0.033-0.80)). (Figure 4.12).

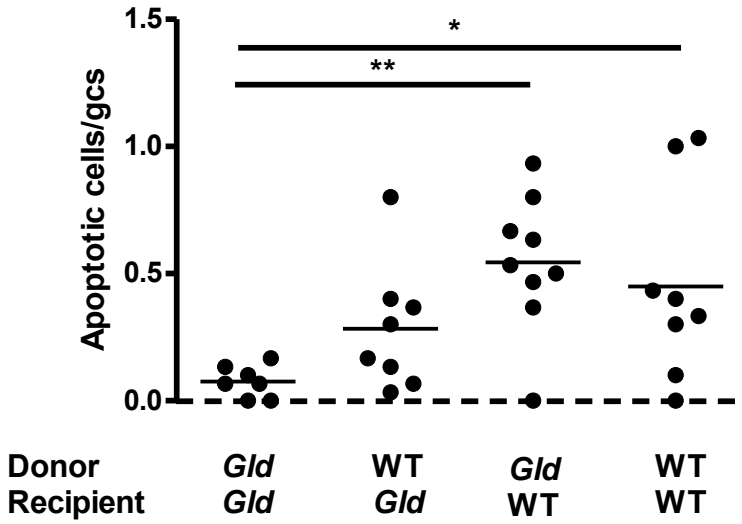


**Figure 4.12 Apoptotic cells in bone marrow transplanted kidneys with accelerated NTN were identified by TUNEL staining.**

Apoptotic cells per glomerular cross section (gcs) in WT and *gld* mice at day 8 post NTN induction. All data represent individual values with the median. The data were analysed using Mann-Whitney U-test ($p^{*}<0.05$, $p^{**}<0.01$). Dashed line represents values for a group of normal WT mice.

### 4.4.6 Renal expression of MCP-1 in bone marrow transplanted mice

MCP-1 is a key chemokine in glomerulonephritis, playing a role in macrophage recruitment. Expression of MCP-1 was found to be dramatically increased in WT mice compared to *gld* mice, following the induction of NTN (Section 3.4.9). To look at any possible differences in expression of MCP-1 between the bone marrow transplanted mice, whole kidney mRNA was extracted from frozen kidney of the four groups of mice and measured by qRT-PCR. Data represent relative expression, calculated using GAPDH as the housekeeping gene and a *gld* mouse transplanted with *gld* bone marrow with NTN as the reference.

*Gld* mice transplanted with *gld* bone marrow expressed significantly less renal MCP-1 (0.97 (0.64-3.6)) compared to *gld* mice transplanted with WT bone marrow (WT→*gld* 3.2 (1.1-13), p=0.021), WT mice transplanted with *gld* bone marrow (2.2 (0.52-11), p=0.044), and WT mice transplanted with WT bone marrow (7.7 (0.69-13), p=0.032). There was no significant difference between the other groups of mice. (Figure 4.13).

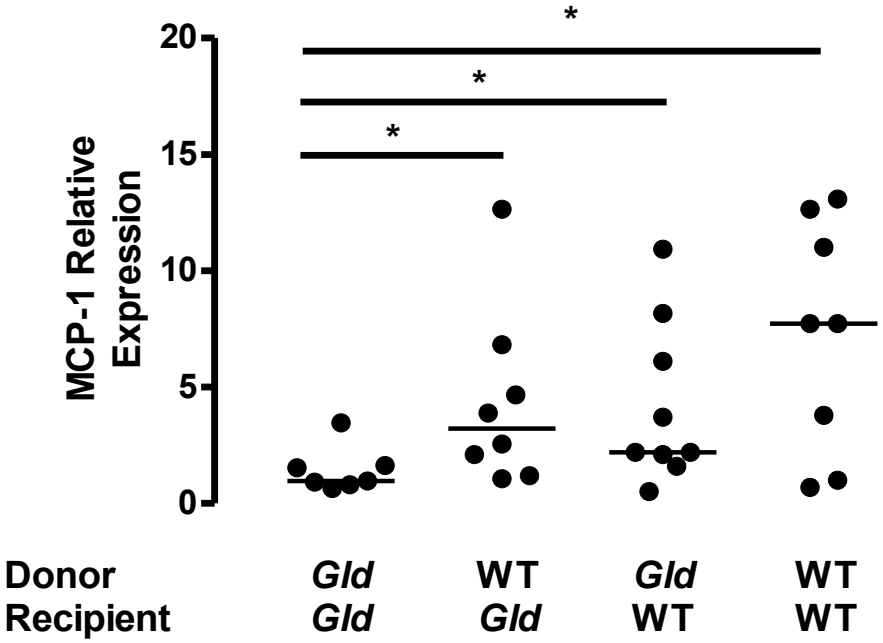


**Figure 4.13 Whole kidney mRNA expression of MCP-1 in bone marrow transplanted mice with NTN, at day 8.**

Expression of MCP-1 was measured in whole kidney mRNA extracts. *Gld* mice transplanted with *gld* bone marrow had significantly less MCP-1 expression than all other groups of mice. All data represent individual values with the median. The data were analysed using Mann-Whitney U-test ($p^* < 0.05$).

### 4.4.7 Fate of resident kidney leukocytes

To confirm that FasL expressed by intrinsic renal cells, in the *gld* mice transplanted with WT bone marrow, was the cause of disease susceptibility, and not due to a population of radioresistant leukocytes, we performed further bone marrow transplant experiments using $CD45.1^+$ and $CD45.2^+$ mice to assess chimerism of kidney leukocytes. C57BL/6 ($CD45.2^+$) mice (n=7) were transplanted with $CD45.1^+$ bone marrow. Ten weeks after transplant, blood was collected and kidney cells were dissociated and stained for $CD45.1^+$ and $CD45.2^+$ cells. In addition, kidney cells were stained for F4/80 and CD11c to assess tissue resident macrophages and dendritic cells. Staining was analysed by flow cytometry. The chimerism of resident kidney cells (total leukocytes: 88.9±0.61% $CD45.1^+$; macrophages ($CD11c^+F4/80^+$): 94.6±0.47% $CD45.1^+$ cells; dendritic cells ($CD11c^+F4/80^-$): 93.7±0.74% $CD45.1^+$ cells) was broadly similar to blood (total leukocytes: 93.2±0.70% $CD45.1^+$ cells) (Figure 4.14).

Frozen kidney sections were also collected and stained for CD45.1 and CD45.2. Sections from C57BL/6 (CD45.2) and CD45.1 mice were stained with both antibodies to demonstrate there was no cross reactivity between the antibodies (Figure 4.15). Sections were also collected from bone marrow transplanted mice without NTN and 8 days after the administration of NTS. The differences in $CD45.1^+$ and $CD45.2^+$ cell infiltrate were not formally quantified but, as can be seen in Figure 4.16, there are considerably more $CD45.1^+$ cells than $CD45.2^+$ cells in the bone marrow transplanted mice, both with and without NTN (Figure 4.16).

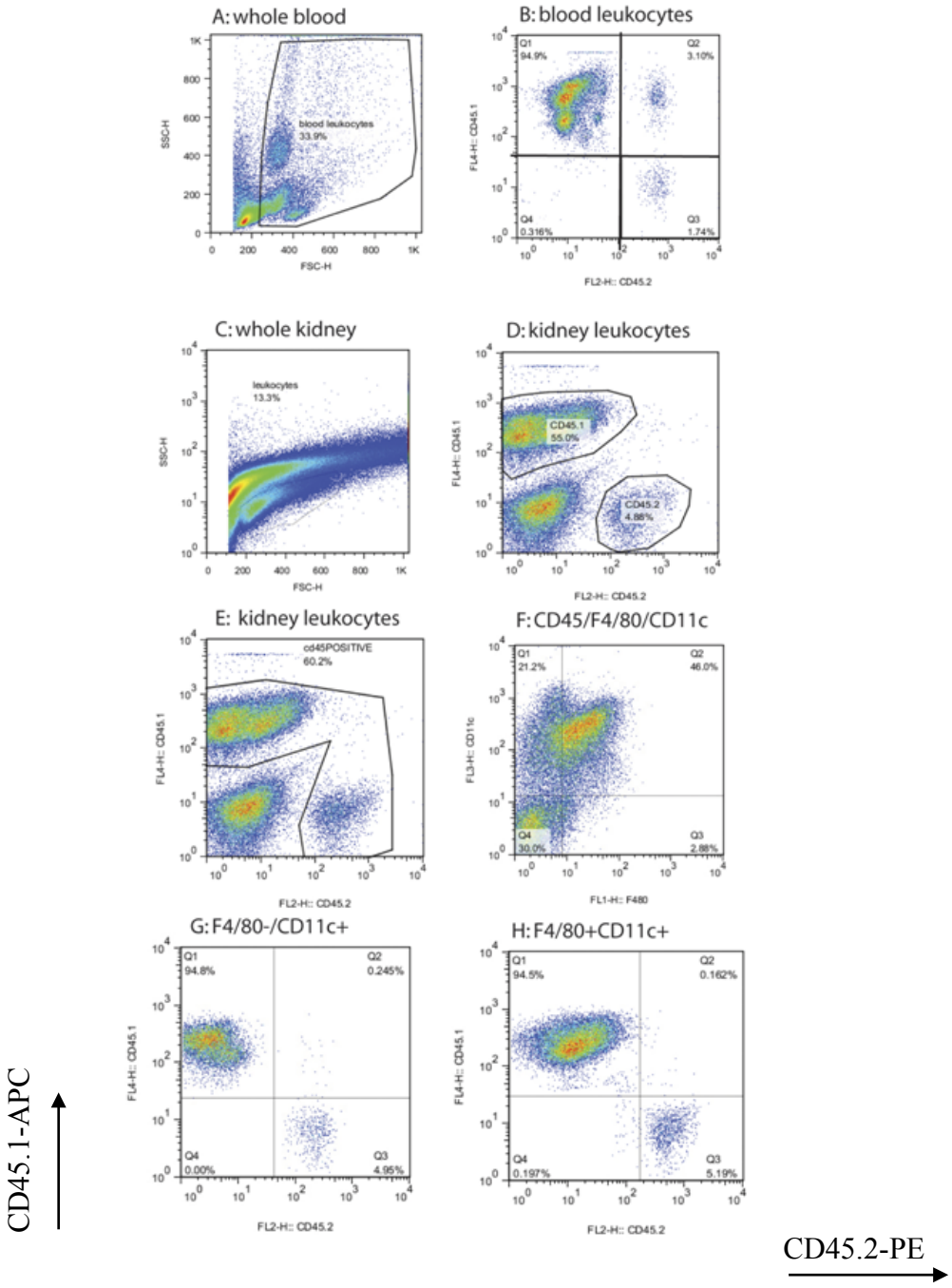


**Figure 4.14 Flow cytometry data to assess chimerism of resident kidney leukocytes following bone marrow transplantation.**

**(A-B)** Flow cytometry of blood taken at sacrifice; **(A)** whole blood and **(B)** $CD45^+$ leukocytes. The majority of circulating leukocytes are of donor (CD45.1) origin. **(C-H)** Flow cytometry of kidney lysates. **(C)** Whole kidney and **(D)** $CD45.1^+$ and $CD45.2^+$ kidney leukocytes (selected in C). **(E)** $CD45^+$ leukocytes were selected and plotted for **(F)** F4/80 and CD11c expression. **(G)** Dendritic cells ($CD11c^+F4/80^-$) and **(H)** macrophages ($CD11c^+F4/80^+$).

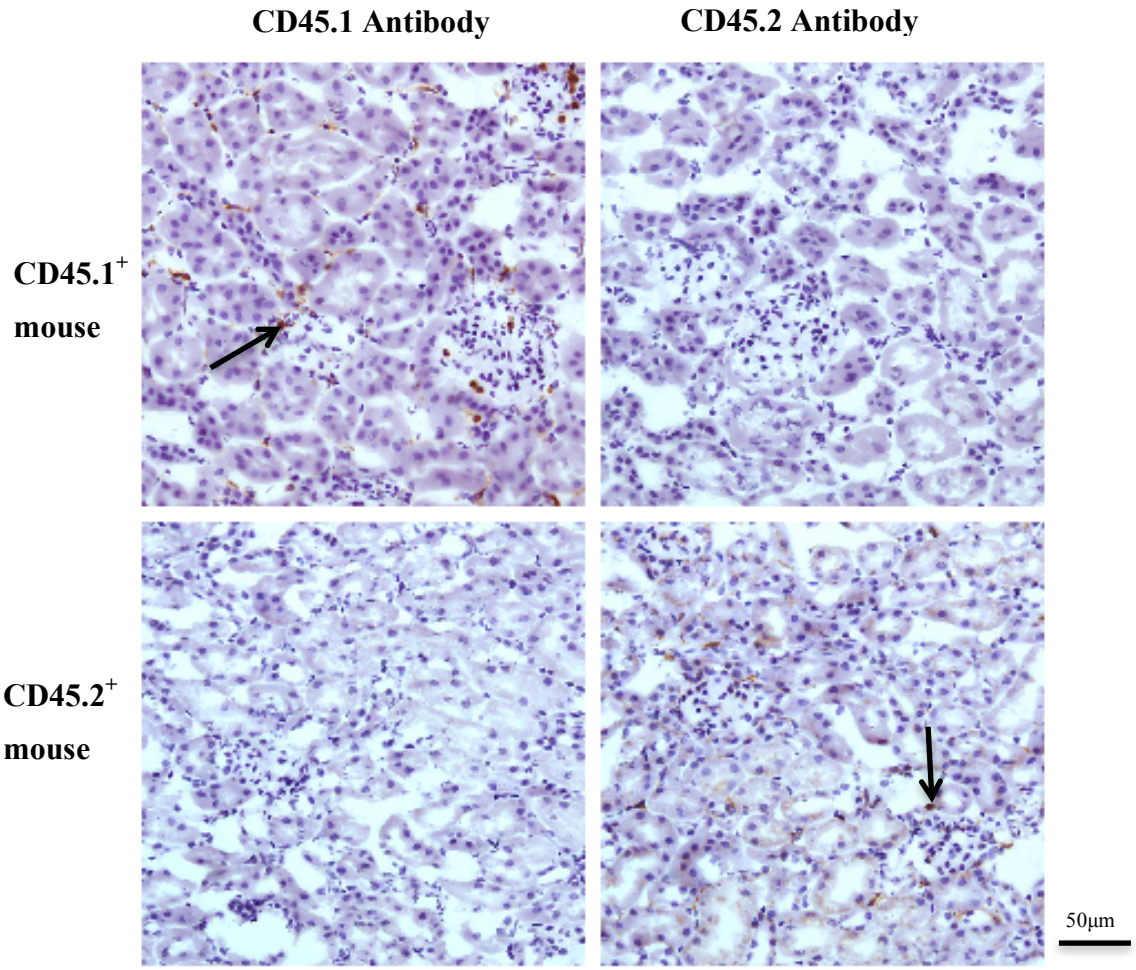


**Figure 4.15 CD45.1 and CD45.2 staining of frozen kidney sections from individual CD45.1$^+$ and CD45.2$^+$ mice.**

Frozen kidney sections from CD45.1$^+$ and CD45.2$^+$ mice were stained for CD45.1$^+$ and CD45.2$^+$ cells (brown staining). These images highlight that there is no cross-reactivity with the antibodies for the alternative allotype. Arrows highlight CD45$^+$ cells.

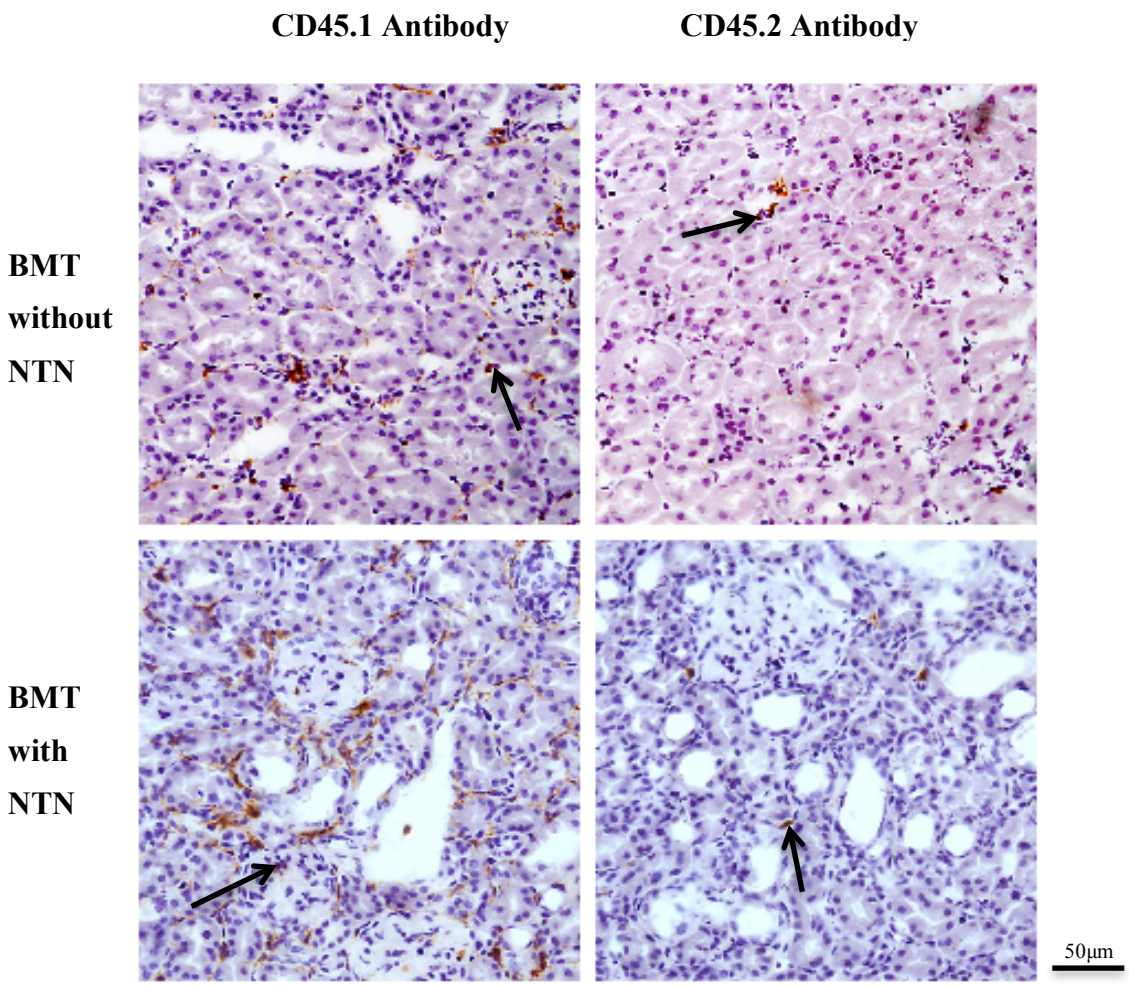


**Figure 4.16 CD45.1 and CD45.2 staining of frozen kidney sections from bone marrow transplanted (BMT) mice with and without NTN.**

Frozen kidney sections from bone marrow transplanted (BMT) mice, before and after the induction of NTN, were stained for $CD45.1^+$ and $CD45.2^+$ cells. The images highlight that the majority of $CD45^+$ cells (brown staining) following the bone marrow transplant are of donor, CD45.1, origin. Arrows highlight $CD45^+$ cells.

### 4.4.8 The role of Fas ligand on mesangial cells

Expression of FasL on intrinsic renal cells, specifically mesangial cells, has been previously reported (Lorz et al., 2000; Tsukinoki et al., 2004). Next we set out to confirm this by culturing both WT and *gld* mesangial cells and we investigated whether FasL deficiency has an effect on the IL-1R signalling pathway.

#### 4.4.8.1 Characterisation of mesangial cells and expression of Fas ligand

Mesangial cells were characterised by immunofluorescence studies and their characteristic stellate morphology. Mesangial cells were stained for myosin and pancytokeratin. As expected both WT and *gld* mesangial cells were positive for myosin and negative for pancytokeratin (Figure 4.17).

To confirm that cultured mesangial cells express FasL we used qRT-PCR. mRNA was extracted from unstimulated and LPS stimulated WT mesangial cells (LPS has been shown to upregulate FasL on mesangial cells (Tsukinoki et al., 2004)), using the TRIzol method, and amplified with FasL specific primers. FasL was detected from both the unstimulated and stimulated cells, with no difference in expression between both conditions (unstimulated cells 1.5 (0.99-2.0), stimulated cells 1.7 (1.6-2.0), p=0.42) (Figure 4.18).

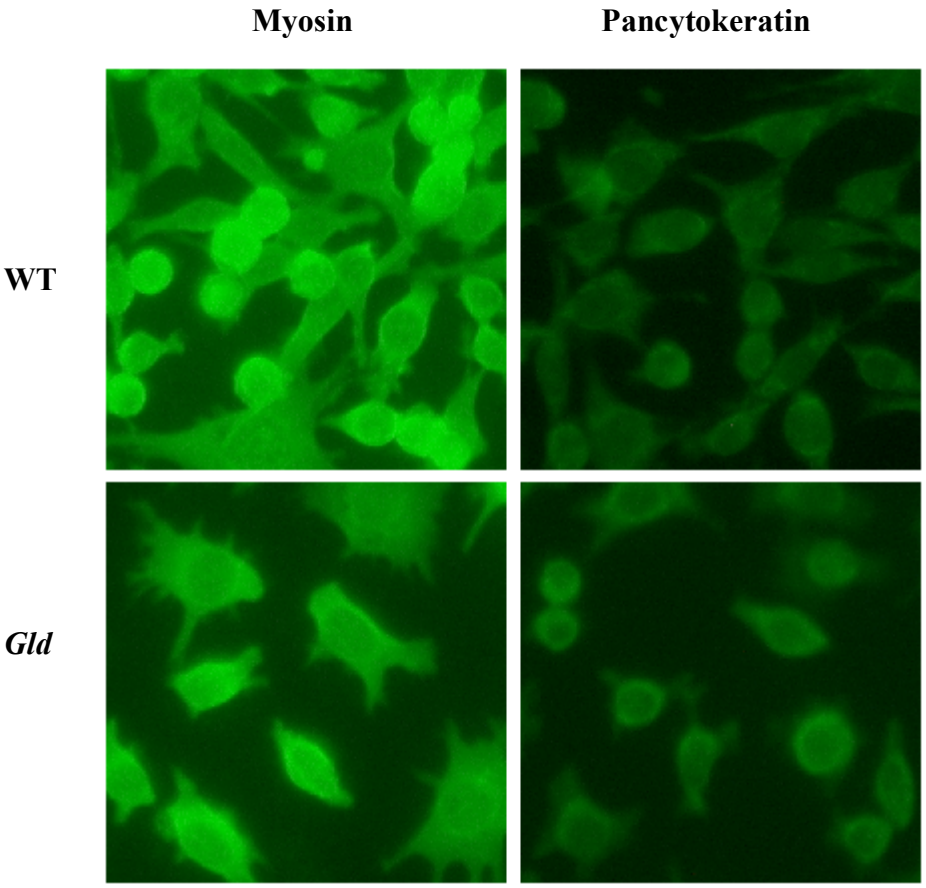


**Figure 4.17 Characterisation of WT and *gld* mesangial cells.**

WT and *gld* mesangial cells were stained for myosin and pancytokeratin, both were positive for myosin and negative for pancytokeratin.

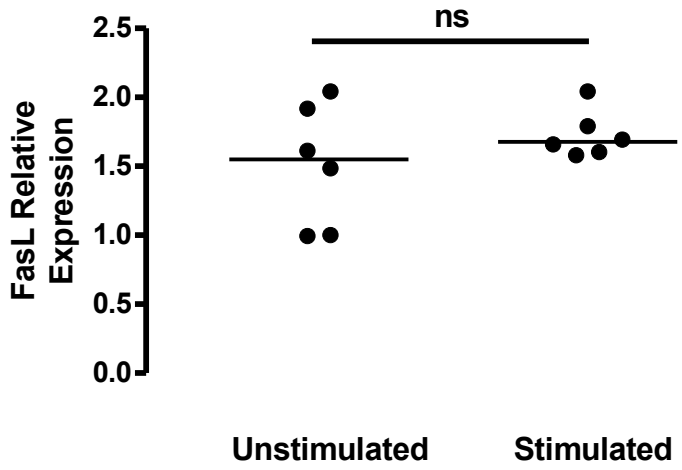


**Figure 4.18 Mesangial cell mRNA expression of Fas ligand following stimulation with LPS.**

Levels of mRNA expression of FasL were measured in mesangial cell mRNA extracts. There was no significant difference in FasL mRNA expression between unstimulated and LPS-stimulated WT mesangial cells. All data represent individual values with the median. The data were analysed using Mann-Whitney U-test (ns= non-significant).

#### 4.4.8.2 Fas ligand deficiency alters mesangial cell IL-1β dependent MCP-1 production, but not TNF-α dependent MCP-1 production

Defective FasL signalling has been previously reported to interrupt signalling through the IL-1R on macrophages, resulting in reduced expression of key cytokines and chemokines, such as MCP-1 (Altemeier et al., 2007; Bannerman et al., 2002; Ma et al., 2004). *Gld* mice transplanted with *gld* bone marrow were found to have reduced expression of MCP-1 compared to WT mice transplanted with *gld* bone marrow (Section 4.4.6), suggesting MCP-1 production by intrinsic renal cells could be affected by the defective FasL signalling.

To investigate a possible role for FasL on mesangial cells and provide further answers to the reduced expression of MCP-1 in the *gld* mice transplanted with *gld* bone marrow, WT and *gld* mesangial cells were stimulated with IL-1β and MCP-1 present in the supernatant measured by ELISA. The mesangial cells were also stimulated with TNF-α as a control, to rule out a generalised defect in cytokine signalling.

Under basal conditions, there was no significant difference in MCP-1 production between WT and *gld* mesangial cells (A: WT 103712 (89463-125951) pg/ml, *gld* 92467 (68109-104305) pg/ml; B: WT 26428 (22434-34073) pg/ml, *gld* 26266 (24258-32320) pg/ml) (Figure 4.19). *Gld* mesangial cells produced significantly less MCP-1 than WT mesangial cells when stimulated with IL-1β (representative results from one of five experiments: WT 235986 (177817-373759) pg/ml, *gld* 119380 (104418-150759) pg/ml, p=0.0022) (Figure 4.19 A), however there was no significant difference in MCP-1 production following stimulation with TNF-α (representative results from one of three experiments: WT 487867 (392922-565759) pg/ml, *gld* 460235 (431141-536649) pg/ml, p=0.48) (Figure 4.19 B).

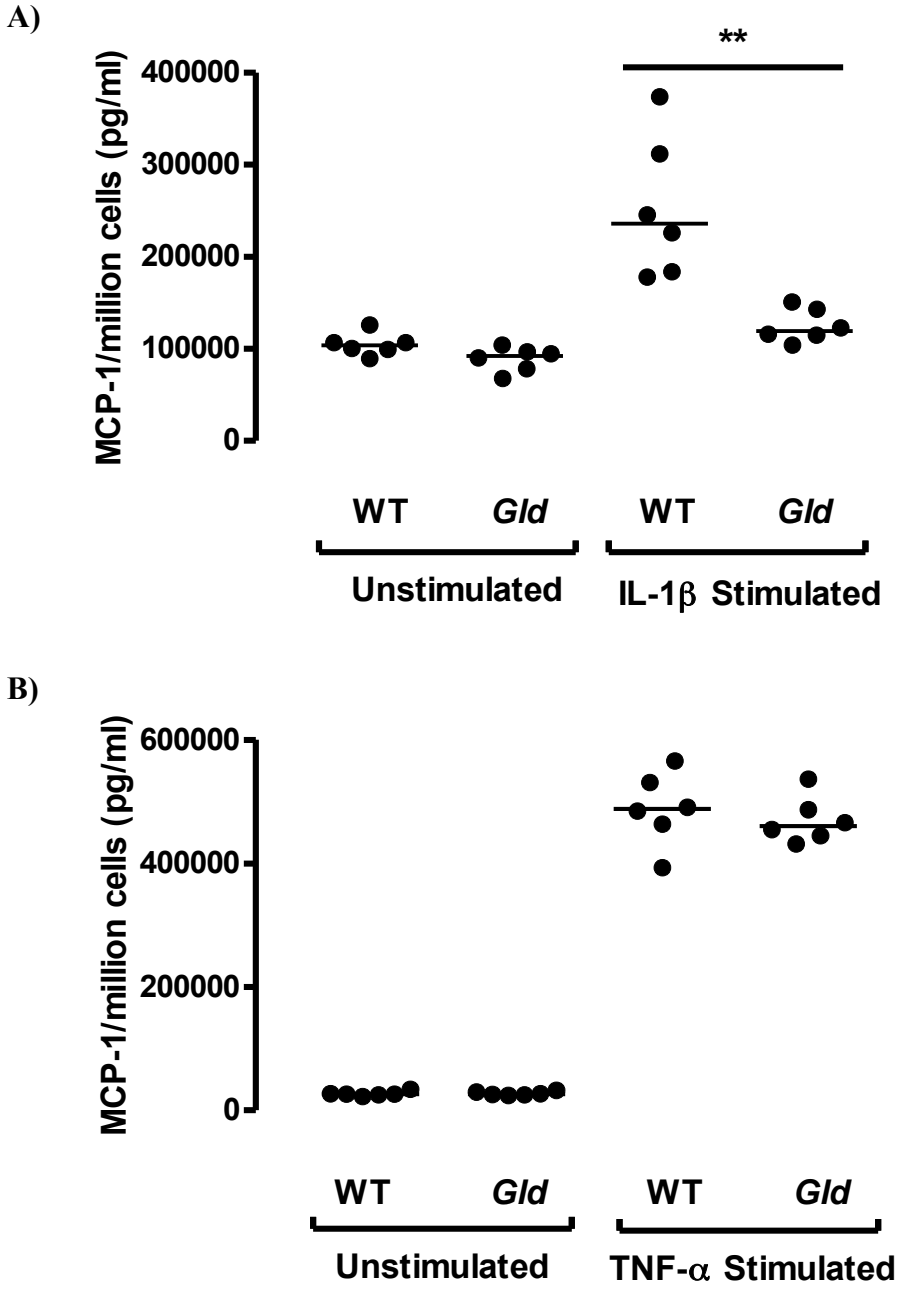


**Figure 4.19 MCP-1 production by mesangial cells following stimulation with IL-1β and TNF-α.**

MCP-1 measured in the supernatants of serum-starved WT and *gld* mesangial cells unstimulated or stimulated with **(A)** 10ng/ml of IL-1β (representative of five separate experiments) and **(B)** 10ng/ml of TNF-α (representative of three separate experiments). All data represent individual values with the median. The data were analysed using Mann-Whitney U-test (p**<0.01).

## 4.5 Discussion

The results shown in this chapter demonstrate that, in accelerated NTN, disease is dependent on FasL expression on either circulating leukocytes or resident radioresistant renal cells. The renal cells responsible for disease development could be mesangial cells since mesangial cell FasL expression has been shown to be upregulated during disease (Tsukinoki et al., 2004). However, we have not investigated the role of FasL on other cells in the kidney, such as tubular epithelial cells. There was no difference in deposited mouse IgG between the groups, but mice with a *gld* immune system had increased levels of total circulating mouse anti-sheep IgG compared to mice with a WT immune system. Glomerular macrophage and T cell infiltration was similar between the four groups. There was no significant difference in the number of apoptotic cells, although *gld* mice transplanted with *gld* bone marrow showed a trend towards having fewer apoptotic bodies than the other three groups. Finally, FasL expression was confirmed on WT mesangial cells and FasL-deficiency was shown to affect MCP-1 production via IL-1R signalling.

The generation of knockout animals has facilitated the study of deciphering the roles of diverse molecules in disease development. Mice deficient in several different cytokines, chemokines and receptors have been used to further our understanding of the pathogenesis of NTN; however, many of these molecules can be expressed by both circulating leukocytes and intrinsic renal cells, therefore the production of bone marrow chimeras has been utilised. Following lethal irradiation, the recipient's bone marrow is ablated allowing donor bone marrow, with a specific genetic alteration, to reconstitute in its place. This creates chimeras expressing different molecules, either normal or mutated, on their circulating leukocytes compared to tissue cells. Timoshanko *et al.* found that 8 weeks following bone marrow transplantation recipient circulating leukocytes were restored to baseline level with approximately 95% of cells being of donor origin, similar to our own findings (Timoshanko et al., 2002).

The failure of *gld* bone marrow to protect WT mice from disease suggests a role for FasL expressed by radioresistant renal cells in the development of NTN. Expression could either be by intrinsic renal cells, such as mesangial cells, or a population of radioresistant tissue resident leukocytes. However, following bone marrow transplantation, I found the

population of donor resident tissue leukocytes in the kidney to be similar to that seen in the circulation (~90% donor cells, 10% recipient cells). It should be noted that the kidneys were not perfused prior to cell isolation; this means some of the 10% of recipient cells found within the kidney could be cells from the circulation rather than resident tissue leukocytes. The lifespan of resident tissue leukocytes can range from days to weeks and at the end of their lifetime they are replenished by circulating cells. Therefore, it is highly likely that the population of resident tissue leukocytes would be of similar composition to the circulating leukocytes; this is supported by the immunostaining of $CD45.1^+$ and $CD45.2^+$ cells in the bone marrow transplanted mice. It is possible that FasL expressed by these remaining recipient circulating and resident tissue leukocytes is sufficient to induce NTN, but the lack of reduction of disease suggests that FasL expressed by intrinsic renal cells is the cause. This is in contrast to the results seen in previous experiments looking at FasL in kidney IRI and EAU; in both cases FasL expression by circulating cells was found to be responsible for susceptibility to disease (Ko et al., 2011; Wahlsten et al., 2000). Although, it should be noted that kidney IRI does not directly involve mesangial cells, but instead tubular cells. Therefore, it may be that FasL on mesangial cells plays more of a prominent role in NTN, accounting for the discrepancies between these two disease models. In addition, in the T cell dependent model of EAE, transfer of *gld* lymphocytes into WT mice attenuated disease, whereas transfer of WT lymphocytes into *gld* mice prolonged clinical signs of disease, suggesting FasL on hematopoietic cells is involved in initiating the inflammatory response and FasL on non-hematopoietic cells is necessary for disease recovery (Sabelko-Downes et al., 1999). However, this model cannot be directly compared to NTN as NTN cannot be passed on by T cell transfer.

At the end of the experiment we saw higher circulating antibody titres in the mice transplanted with *gld* bone marrow compared to the mice transplanted with WT bone marrow. As already mentioned, the defects in lymphocyte homeostasis in *gld* mice can result in an accumulation of B cells and autoantibodies. As there were increased antibody titres in the WT mice transplanted with *gld* bone marrow, this further supports the role for the expression of FasL on activated T cells in maintaining peripheral B cell numbers and, therefore, antibody titres (Stranges et al., 2007).

Mesangial cells are specialised pericytes located among the glomerular capillaries within the renal corpuscle. Mesangial cells have three primary functions: filtration, structural support and modulation of glomerular injury. The importance of mesangial cells in the

development of immune-mediated glomerular diseases has been extensively studied. Through previous studies using bone marrow chimeras it has been found that mesangial cell expression of CD40 is required for the development of NTN (Ruth et al., 2003), and the production of pro-inflammatory cytokines, such as TNF-α, IFN-γ and IL-12, by intrinsic renal cells is required for full expression of crescentic GN (Timoshanko et al., 2002; Timoshanko et al., 2001; Timoshanko et al., 2003).

There are a number of lines of evidence suggesting that mesangial cells express FasL. Upregulation of FasL mRNA and protein has been shown in whole kidney from mice with lupus nephritis and rats with immune complex proliferative GN (Lorz et al., 2000). Immunohistochemistry comparing normal and diseased kidneys from these examples highlighted *de novo* expression of FasL in the glomeruli during inflammation, which can be from either infiltrating leukocytes or mesangial cells (Lorz et al., 2000). In humans, FasL was shown to be upregulated in the glomerulus in lupus nephritis *in vivo* by immunohistochemistry, and FasL expression by mesangial cells was demonstrated *in vitro* following stimulation with IL-1β, LPS or IFN-γ (Tsukinoki et al., 2004). I have confirmed by qRT-PCR that mesangial cells *in vitro* express FasL. There was no significant difference in mesangial cell expression of FasL following stimulation with LPS. This could be because the cells were not stimulated with enough LPS or were not stimulated long enough for FasL expression to be upregulated.

*Gld* mesangial cells in culture had an attenuated response to IL-1β compared to WT mesangial cells, producing significantly less MCP-1. This is in keeping with results seen by other groups. Two groups reported a reduction in the production of NF-κB-dependent cytokines by macrophages with defective FasL signalling (Altemeier et al., 2007; Ma et al., 2004). Also, Bannerman *et al.* found that overexpression of FADD in human dermal microvascular endothelial cells (HMEC-1) blocked LPS and IL-1β NF-κB activation, whereas the absence of FADD in mouse embryo fibroblasts (MEF) enhanced NF-κB activity and the production of NF-κB-dependent cytokines (Bannerman et al., 2002). It is reasonable to assume that part of the effect seen in mesangial cells is due to the same interruption in the signalling pathway seen in the macrophages. That is, the defect in FasL signalling renders FADD free to sequester MyD88 away from the IL-1R signalling pathway. FasL signalling has also been shown to activate directly NF-κB (Ahn et al., 2001; Imamura et al., 2004). This too could account for the difference seen in MCP-1 production. My attempts to culture *gld* and WT BMDM and confirm the same result were unsuccessful due to the method of

culturing not being reproducible. These observations offer an explanation for the differences seen in levels of MCP-1 mRNA expression in the bone marrow transplanted mice. Relative expression of MCP-1 was determined using one of the *gld* mice transplanted with *gld* bone marrow as the reference. Ideally relative expression should have been determined using an untreated WT mouse as the reference, to compare accurately whether expression was increased in all groups of mice. However, the results show that MCP-1 production is significantly increased in all mice expressing functional FasL compared to the mice only expressing the mutated version. It would also be interesting to look at relative expression of other important modulators of inflammation, such as IL-1β, INF-γ and TNF-α.

Despite concentrating on the effects of the *gld* mutation on mesangial cells they are not the only intrinsic renal cells that express FasL. Glomerular endothelial cells, podocytes and tubular epithelial cells have been shown to be a source of FasL within the kidney, and therefore may contribute to susceptibility to NTN (Lorz et al., 2000; Ortiz et al., 1999; Ross et al., 2005). As previously mentioned (Section 1.4.3.2 and Section 3.5), endothelial cells have been found to contribute to thrombosis. Disruption of the glycocalyx exposes the endothelial cells to pro-inflammatory molecules, such as TNF-α, IL-1 and MCP-1, and leads to the formation of tissue factor (Dosquet et al., 1995; Grabowski and Lam, 1995; Kirchhofer et al., 1994). Also, podocyte injury is a major cause of proteinuria in both humans and mice. Stimulation of podocytes with TNF-α and IL-1 activates NF-κB, resulting in the upregulation of pro-inflammatory cytokines such as MCP-1 (Brahler et al., 2012; Bruggeman et al., 2011; Natori et al., 1997) and tubular epithelial cells have been shown to be the main source of renal MCP-1 during NTN, due to cytokines and chemokines exiting the glomerulus in the urine, following the initial glomerular injury, and causing localised injury and inflammation in the interstitium (Tesch et al., 1999). These data are in keeping with my results as I saw a reduction in thrombosis, proteinuria and interstitial macrophage infiltration in the *gld* mice transplanted with *gld* bone marrow compared to the WT mice transplanted with *gld* bone marrow. Taking into account the effect of the *gld* mutation on the IL-1R signalling pathway and MCP-1 production, it would be interesting to culture WT and *gld* glomerular endothelial cells, podocytes and tubular epithelial cells and compare differences in MCP-1 production as I have done with the mesangial cells. It would also be of interest to look at the production of other cytokines that are downstream of NF-κB. Direct activation of NF-κB via FasL signalling has been shown to induce the expression of the pro-inflammatory cytokines IL-6 and IL-8 (Ahn et al., 2001; Imamura et al., 2004), both of which have been shown to be

involved in kidney injury (Nechemia-Arbely et al., 2008; Niemir et al., 2004). Other important cytokines downstream of NF-κB include TNF-α and IL-12. These too are produced by intrinsic renal cells and are important in the development of GN (Timoshanko et al., 2001; Timoshanko et al., 2003).

As mentioned in Section 3.5, one of the key roles of FasL is in inducing apoptosis. Again it is unclear which cells are undergoing apoptosis. However, there were more apoptotic cells (although not always significantly different) in all groups of mice expressing functional FasL on either one or both cellular compartments compared to the *gld* mice transplanted with *gld* bone marrow, suggesting both circulating leukocytes and intrinsic renal cells are capable of inducing apoptosis. Apoptotic endothelial cells have been shown to contribute to thrombotic events due to increased adherence of platelets to the endothelium and their subsequent activation (Bombeli et al., 1999), which can lead us to assume that the apoptotic cells represent both infiltrating leukocytes and intrinsic renal cells. Within the interstitium, FasL on tubular epithelial cells has been shown to induce tubular epithelial cell 'fratricide' following cisplatin-induced kidney injury (Linkermann et al., 2011). This suggests that in the WT mice transplanted with *gld* bone marrow there is a possibility that neighbouring glomerular cells may be responsible for inducing apoptosis of each other.

Cleavage of FasL to its soluble form is thought to act to downregulate its apoptotic activity (Dupont and Warrens, 2007; O' Reilly et al., 2009; Schneider et al., 1998) and sFasL has been shown to play an important role in the activation of NF-κB and the production of pro-inflammatory cytokines (Ahn et al., 2001; O' Reilly et al., 2009). There are few studies looking at the role of sFasL in GN or kidney disease. One study by Perianayagam *et al.,* measured both sFasL and soluble Fas (sFas) in the serum of patients with chronic kidney failure and found serum sFas to be significantly higher in patients and those undergoing dialysis compared to healthy controls, whereas there was no difference in the levels of sFasL (Perianayagam et al., 2000). However, immunoblot analysis revealed large ~60kDa aggregates in the sera that could represent sFasL-sFas complexes, suggesting the method of detection of sFasL could not recognise sFasL bound to sFas (Perianayagam et al., 2000). Attempts to detect sFasL by ELISA in the serum of WT mice with NTN were unsuccessful due to the lower detection limits of the kit; however, it would be of interest to see if there is a correlation between levels of sFasL and severity of disease.

## 4.6 Conclusion

Based on these data, I can conclude that expression of FasL on circulating leukocytes or intrinsic renal cells can facilitate injury in accelerated NTN. My *in vitro* results looking at mesangial cells, as well as previous evidence present in the literature, suggest this is likely to be due to disrupted signalling through the IL-1R pathway as well as reduced direct activation of NF-κB by FasL. The result of this disrupted signalling affects the expression of pro-inflammatory cytokines, highlighted by the reduced levels of MCP-1 in the supernatant of *gld* mesangial cells, and therefore possibly the recruitment and activation of macrophages to the kidney during disease. This is the first study to show a role for intrinsic renal cell FasL in GN.

# CHAPTER 5

# The Role of Fc Gamma Receptor IIB in Accelerated Nephrotoxic Nephritis

## 5.1 Introduction

FcγRIIB is the only inhibitory FcγR in both humans and mice and is the most widely expressed, being found on cells of both myeloid and lymphoid origin, with the exception of T cells and NK cells. FcγRIIB plays an important role in the negative regulation of the activating FcγR and the BcR, controlling both the effector responses of myeloid cells as well as antibody production by B cells (Takai et al., 1996).

FcγRIIB$^{-/-}$ mice are more susceptible to the induction of CIA (Yuasa et al., 1999), inducible alveolitis (Clynes et al., 1999), EAG and NTN (Boross et al., 2011; Nakamura et al., 2000; Sharp et al., 2012; Suzuki et al., 1998). However, the cell types responsible for this are not known.

Autoimmune-prone mice show a reduced expression of FcγRIIB on both B cells and myeloid cells, with increased circulating autoantibody titres and hyperactive macrophages (Pritchard et al., 2000). In mice, overexpression of FcγRIIB on B cells resulted in a reduced immune response, earlier resolution of CIA, and reduced spontaneous SLE, whereas overexpression on macrophages had no effect on CIA except increased mortality after *Streptococcus pneumonia* infection (Brownlie et al., 2008). However, deletion of FcγRIIB from B cells alone did not increase susceptibility to EAG when compared to WT control mice, whereas FcγRIIB$^{-/-}$ mice were more susceptible, indicating that defects in FcγRIIB expression on both the B cell and myeloid compartment are required for full expression of disease (Sharp et al., 2012).

FcγRIIB$^{-/-}$ B cells have been shown to produce increased titres of antibody to T cell dependent antigens (Boross et al., 2011), but it is not known if this is sufficient in NTN to account for the increased disease in the FcγRIIB$^{-/-}$ mice. Macrophages deficient in FcγRIIB show enhanced phagocytic and calcium flux responses following FcγRIII crosslinking

(Clynes et al., 1999), suggesting NTN could be exacerbated in mice carrying a deletion of FcγRIIB in these cells.

Dendritic cells are involved in the immune response and their altered function is known to play a major role in autoimmunity. Selective blockade of FcγRIIB results in spontaneous maturation of dendritic cells (Boruchov et al., 2005; Dhodapkar et al., 2005) and dendritic cells from FcγRIIB$^{-/-}$ mice generate stronger and longer-lasting immune responses both *in vitro* and *in vivo* (Kalergis and Ravetch, 2002).

The presence of mast cells in the kidney tubulointerstitium has been associated with kidney fibrosis in human GN (Ehara and Shigematsu, 1998). However, in NTN, there are conflicting reports of the roles of mast cells. Timoshanko *et al.* found that mast cell-deficient Kit$^{W/W-v}$ mice were protected from non-accelerated NTN, with reduced glomerular crescent formation and reduced T cell and macrophage infiltration, but a similar immune response, compared to WT mice (Timoshanko et al., 2006). In contrast, Hochegger *et al.,* using the same strain of mice, found accelerated NTN was exacerbated (Hochegger et al., 2005). In a subsequent report, Eller *et al.* determined that, during accelerated NTN, mast cells were recruited to the renal draining lymph nodes by IL-9, produced by $T_{reg,}$ where they enhanced the immunosuppressive properties of the $T_{reg}$ (Eller et al., 2011). FcγRIIB$^{-/-}$ mice show enhanced mast cell degranulation (Ujike et al., 1999), therefore suggesting that the presence of FcγRIIB$^{-/-}$ mast cells in the kidney could exacerbate NTN. It is not know whether deletion of FcγRIIB on mast cells could modulate an effect on the immune response.

Cre-*loxP* recombination is a site-specific recombinase technology widely used to carry out deletions, insertions, translocations and inversions in the DNA of cells. Cre is a 38 kDa recombinase protein from bacteriophage P1 which recognises a *loxP* site, a 34bp sequence consisting of two 13bp inverted repeats separated by an 8bp asymmetric spacer region (Sauer, 1998). Two mouse lines are required for a conditional gene deletion. Firstly, a conventional transgenic mouse in which Cre is targeted to a tissue- or cell-specific promoter, and secondly, a mouse strain in which the target gene is flanked by two *loxP* sites in a direct orientation ("floxed" gene). Depending on the orientation of the *loxP* sites, crossing the mice can result in excision of the gene of interest, but only in the cells expressing Cre recombinase, therefore only inactivating the gene in the target tissue (Orban et al., 1992).

To further dissect the role of FcγRIIB on specific cell types in GN, mice with a cell-specific deletion of FcγRIIB in B cells, myeloid cells, dendritic cells, or mast cells were

created using the Cre-*loxP* system. This is the first study to look at the role of FcγRIIB in individual cell types in NTN.

## 5.2 Aim

This part of the thesis was an investigation of the role of the inhibitory FcγR, FcγRIIB, on specific cell lineages in accelerated NTN. The results were based on the assessment of disease in mice where FcγRIIB had been deleted in B cells, myeloid cells, dendritic cells or mast cells only compared to littermate WT controls and FcγRIIB-deficient mice.

## 5.3 Experimental design

To gain further insight into the role of FcγRIIB in immune-mediated GN, floxed FcγRIIB mice on a C57BL/6 background were generated by Professor Sjef Verbeek, LUMC, Leiden, The Netherlands, and crossed with mice expressing Cre recombinase under cell-specific promoters to delete FcγRIIB from specific cell lineages. Cre recombinase expression was driven by the CD19 promoter to delete FcγRIIB from B cells ($FcγRIIB_{CD19Cre}$ mice), the Lysozyme M promoter to delete FcγRIIB from macrophages and neutrophils ($FcγRIIB_{LysMCre}$ mice), the cEBPα promoter to delete FcγRIIB from myeloid cells (including macrophages, neutrophils, and dendritic cells) ($FcγRIIB_{cEBPαCre}$ mice), the CD11c promoter to delete FcγRIIB from dendritic cells ($FcγRIIB_{CD11cCre}$ mice) and the Mcpt5 promoter to delete FcγRIIB from mast cells ($FcγRIIB_{Mcpt5Cre}$ mice). Nephritis was induced in mice with the cell-specific deletion of FcγRIIB, and age- and sex-matched littermate WT and full knockout controls, at LUMC by Professor Sjef Verbeek using our NTS. Mice were monitored clinically and I travelled to LUMC to sacrifice the mice at the end of the experiments. Assessment of disease was carried out as previously described by myself at Imperial College London, UK (see Section 3.3).

## 5.4 Results

### 5.4.1 Genotyping of FcγRIIB$^{-/-}$ mice using polymerase chain reaction

The genotype of FcγRIIB$^{-/-}$ mice was confirmed by PCR analysis. DNA was extracted from tail snips and amplified by PCR using FcγRIIB specific primers. A band of 359bp was seen for the WT allele and 600bp for the targeted allele. The presence of both bands represented a heterozygote. A negative control, without DNA, was used to demonstrate the specificity of the assay (Figure 5.1).

Genotyping of mice carrying the cell-specific deletion of FcγRIIB was carried out in the laboratory of Professor Sjef Verbeek, LUMC (data not shown).

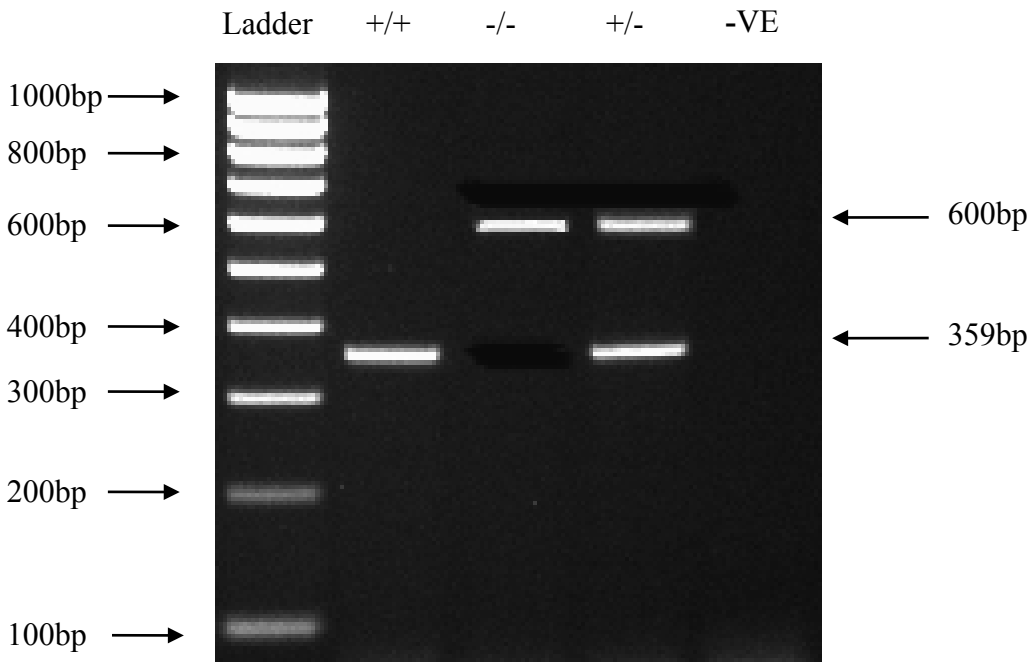


**Figure 5.1 PCR reactions of genomic DNA from WT and FcγRIIB$^{-/-}$ animals.**

Representative examples of WT (+/+), FcγRIIB$^{-/-}$ (-/-) and heterozygote (+/-) mice are shown here. The WT (+/+) mice show a band at 359bp, the FcγRIIB$^{-/-}$ (-/-) mice show a band at 600bp and the heterozygote (+/-) mice show bands at 359bp and 600bp. The negative control (-VE) has no bands.

### 5.4.2 Phenotyping of FcγRIIB cell-specific knockout mice using flow cytometry

The phenotype of FcγRIIB cell-specific knockout mice was confirmed by flow cytometric analysis of circulating leukocytes, resident splenic macrophages and dendritic cells, and peritoneal lavage sample mast cells from FcγRIIB$^{-/-}$ mice, FcγRIIB$_{CD19Cre}$ mice, FcγRIIB$_{CD11cCre}$ mice, FcγRIIB$_{Mcpt5Cre}$ mice, FcγRIIB$_{cEBPαCre}$ mice, FcγRIIB$_{LysMCre}$ mice, and WT C57BL/6 controls by Sara Mangsbo, LUMC.

To assess FcγRIIB expression on B cells, dendritic cells, macrophages, and neutrophils, heparinised whole blood or single cell suspensions obtained from the spleen were stained for CD19, B220 (both B cell markers), CD11c (dendritic cell marker), CD11b (macrophage marker when CD11c negative), Gr-1 (neutrophil marker), and FcγRIIB (clone Ly17.2) (Figure 5.2 A-C). To assess FcγRIIB expression on mast cells, peritoneal lavage samples were collected and stained for CD117, FcεR (both mast cell markers), and FcγRIIB (Figure 5.2 D).

FcγRIIB$_{CD19Cre}$ mice showed deletion of FcγRIIB from both circulating and splenic B cells comparable with FcγRIIB$^{-/-}$ mice, with no deletion from circulating neutrophils and monocytes or splenic macrophages (Figure 5.2 A). Deletion of FcγRIIB on circulating monocytes and neutrophils from FcγRIIB$_{cEBPαCre}$ mice was comparable with FcγRIIB$^{-/-}$ mice but, in the spleen, there was only, approximately, 50% deletion of FcγRIIB from macrophages and dendritic cells (Figure 5.2 B). Splenic dendritic cells from FcγRIIB$_{CD11cCre}$ mice had comparable deletion of FcγRIIB as dendritic cells from FcγRIIB$^{-/-}$ mice, with no deletion on splenic macrophages or B cells (Figure 5.2 C). FcγRIIB deletion in the FcγRIIB$_{Mcpt5Cre}$ mice was confined to mast cells, with no deletion from macrophages or dendritic cells (Figure 5.2 D).

Deletion of FcγRIIB on macrophages and neutrophils in FcγRIIB$_{LysMCre}$ mice was not fully effective. There was a 50% reduction in expression of FcγRIIB on circulating monocytes and an even smaller reduction on splenic macrophages. Expression of FcγRIIB on WT neutrophils was very low and was comparable with FcγRIIB$_{LysMCre}$ mice (data not shown, please see (Natori et al., 1997)). Therefore, to assess the role of FcγRIIB on macrophages and neutrophils, we decided to switch to using the FcγRIIB$_{cEBPαCre}$ mice, despite the deletion being less specific.

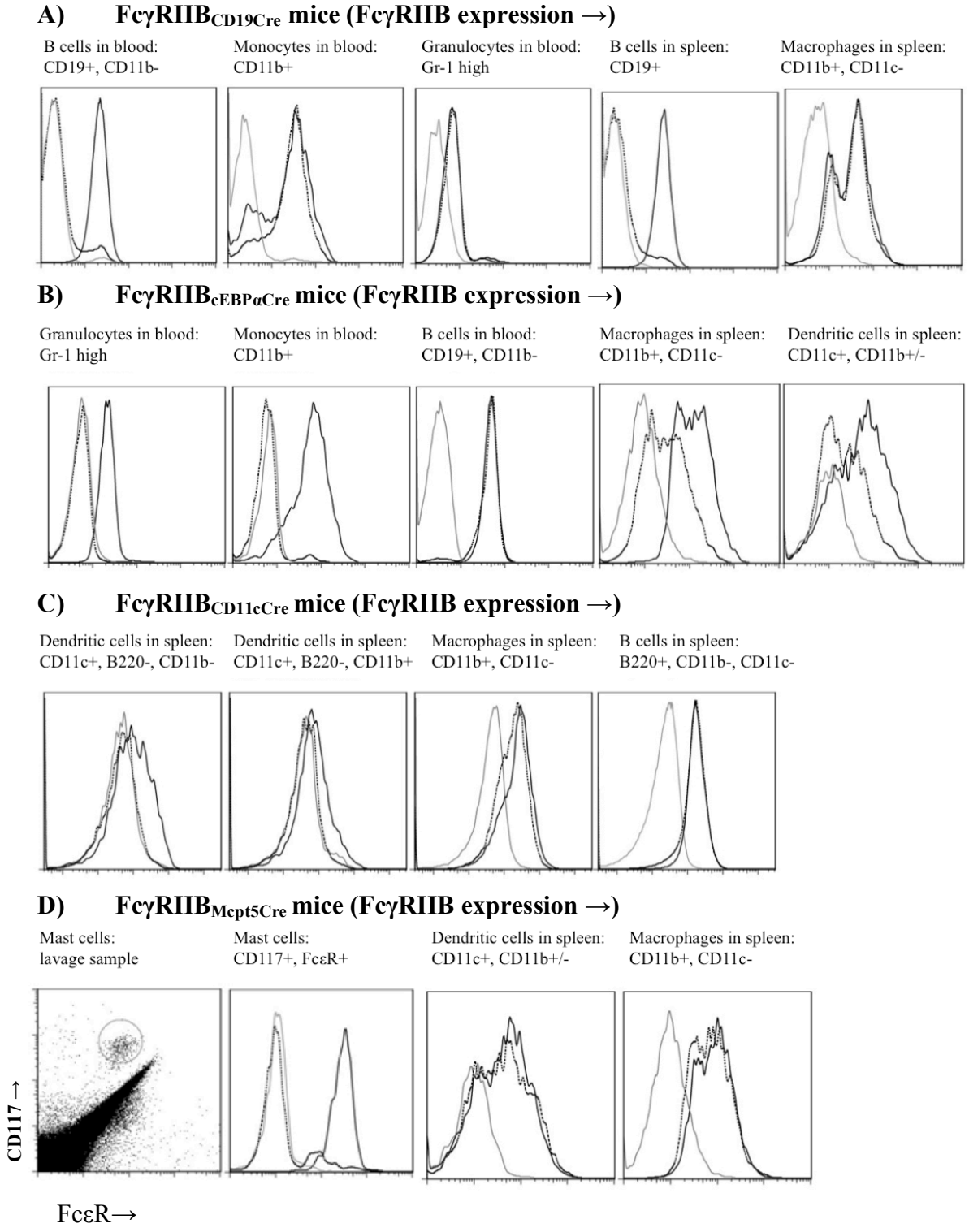


**Figure 5.2 Flow cytometry of blood, spleen and lavage cells for FcγRIIB expression in the cell-specific knockout mice.**

Deletion of FcγRIIB from **(A)** FcγRIIB$_{CD19Cre}$ mice, **(B)** FcγRIIB$_{cEBPαCre}$ mice, **(C)** FcγRIIB$_{CD11cCre}$ mice, and **(D)** FcγRIIB$_{Mcpt5Cre}$ mice compared to WT and FcγRIIB$^{-/-}$ mice showing cell specific deletion. Solid black line: WT mice. Dotted black line: cell-specific knockout mice. Solid grey line: FcγRIIB$^{-/-}$ mice.

### 5.4.3 Nephrotoxic nephritis in WT and FcγRIIB knockout mice

NTN was induced in three different experiments. In Experiment 1 NTN was induced in WT, FcγRIIB$^{-/-}$ and FcγRIIB$_{CD19Cre}$ mice, in Experiment 2 NTN was induced in WT, FcγRIIB$^{-/-}$, FcγRIIB$_{CD11cCre}$, FcγRIIB$_{Mcpt5Cre}$ and FcγRIIB$_{cEBPαCre}$ mice and in Experiment 3 NTN was induced in WT, FcγRIIB$_{CD19Cre}$ and FcγRIIB$_{cEBPαCre}$ mice. In addition, two other experiments were performed, one comparing FcγRIIB$_{CD19Cre}$ to WT and FcγRIIB$^{-/-}$ mice, with the same results to those shown, and another comparing WT and FcγRIIB$^{-/-}$ mice to FcγRIIB$_{LysMCre.}$ This latter experiment was flawed, due to the poor deletion of FcγRIIB on the myeloid cell compartment, but showed no increase in disease in FcγRIIB$_{LysMCre}$ mice compared to WT (data not shown). In all experiments, mice were pre-immunised with 0.2mg of sheep IgG in CFA and after five days 200μl of NTS was administered via the tail vein. In Experiment 1 and 2 a 1:20 dilution of NTS was used, in Experiment 3 a 1:10 dilution was used. In Experiment 1, 29 female animals were used (n=10 WT, n=10 FcγRIIB$^{-/-}$, and n=9 FcγRIIB$_{CD19Cre}$mice). In Experiment 2, 56 female animals were used (n=12 WT, n=11 FcγRIIB$^{-/-}$, n=10 FcγRIIB$_{CD11cCre}$, n=12 FcγRIIB$_{Mcpt5Cre}$, and n=11 FcγRIIB$_{cEBPαCre}$ mice). In Experiment 3, 23 female animals were used (n=7 WT, n=8 FcγRIIB$_{CD19Cre}$ and n=7 FcγRIIB$_{cEBPαCre}$ mice). Mice were monitored clinically and sacrificed when disease became too severe. Mice from Experiment 1 were sacrificed at day 5. In Experiment 2, FcγRIIB$^{-/-}$ mice were sacrificed at day 6 and the rest at day 8. Mice from Experiment 3 were sacrificed at day 7.

#### 5.4.3.1 FcγRIIB$^{-/-}$ mice are susceptible to renal failure, histological damage and increased glomerular macrophage infiltration, however deletion of FcγRIIB on B cells alone has no effect

In Experiment 1, a low dose of NTS (1:20) was administered to WT, FcγRIIB$^{-/-}$ and FcγRIIB$_{CD19Cre}$ mice on a pure C57BL/6 background to confirm that complete deletion of FcγRIIB exacerbates accelerated NTN and to assess whether expression of FcγRIIB on B cells alone is important in protection. Mice were sacrificed at day 5 after induction of NTN, because the mice with the full deletion of FcγRIIB started to show serious disease symptoms, including severe proteinuria.

To assess kidney function serum urea and albuminuria, expressed as a ratio of urinary albumin/creatinine, were measured in all mice. FcγRIIB$^{-/-}$ mice had significantly higher serum urea titres (105 (7.7-155) mmol/L) and albuminuria (9.8 (0.010-23) mg/mmol) compared to WT mice (serum urea: 7.9 (5.7-25) mmol/L, $p<0.01$; albuminuria: 0.085 (0.010-6.8) mg/mmol, $p<0.05$) and FcγRIIB$_{CD19Cre}$ mice (serum urea: 7.6 (6.3-29) mmol/L, $p<0.01$; albuminuria: 0.14 (0.010-13) mg/mmol, $p<0.05$) (Figure 5.3 A and Figure 5.3 B).

Histological damage, in the form of glomerular capillary thrombosis, was assessed on PAS-stained sections (Figure 5.4 A). FcγRIIB$^{-/-}$ mice had significantly more thrombotic glomeruli (2.2 (0.12-3.1)) compared to WT mice (0.00 (0.00-2.2), $p<0.001$) and FcγRIIB$_{CD19Cre}$ mice (0.040 (0.00-1.4), $p<0.01$) (Figure 5.4 B). There was no significant difference between WT and FcγRIIB$_{CD19Cre}$ mice.

Kidney sections collected at the termination of Experiment 1 were stained for macrophage (CD68) infiltration as a measure of inflammation (Figure 5.5 A). FcγRIIB$^{-/-}$ mice had significantly greater glomerular macrophage infiltration (8.3 (5.8-12)/gcs) compared to WT mice (2.1 (1.8-5.9)/gcs, $p<0.001$) and FcγRIIB$_{CD19Cre}$ mice (3.3 (1.7-10)/gcs, $p<0.05$) (Figure 5.5 B).

These results demonstrate that deletion of FcγRIIB on B cells alone is not sufficient to increase susceptibility to NTN compared to WT mice, whereas FcγRIIB$^{-/-}$ mice develop severe disease under the same conditions. This suggests the involvement of FcγRIIB on other cell types in the protection from NTN.

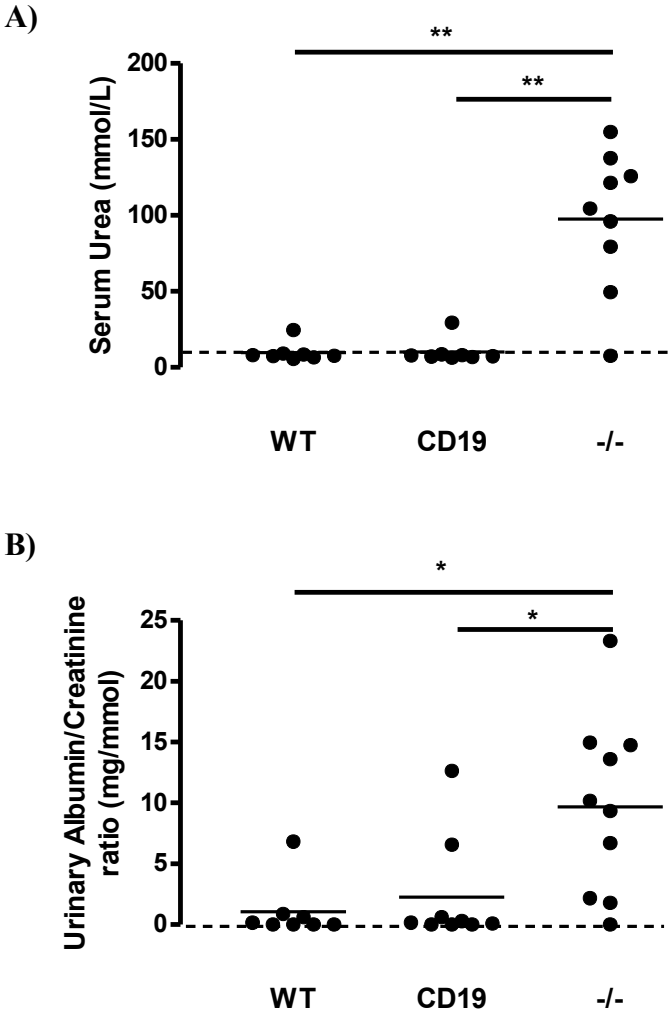


**Figure 5.3 Measurement of serum urea and urinary albumin/creatinine ratio in WT and FcγRIIB knockout mice with NTN, Experiment 1.**

**(A)** Serum urea and **(B)** urinary albumin/creatinine ratio were measured in WT and FcγRIIB knockout mice with NTN from Experiment 1. FcγRIIB$^{-/-}$ (-/-) mice had significantly higher serum urea and urinary albumin/creatinine ratio than WT and FcγRIIB$_{CD19Cre}$ (CD19) mice. All data represent individual values with the median. The data were analysed using Dunn's Multiple Comparison Test (p*<0.05, p**<0.01). Dashed lines represent values for a group of normal WT mice.

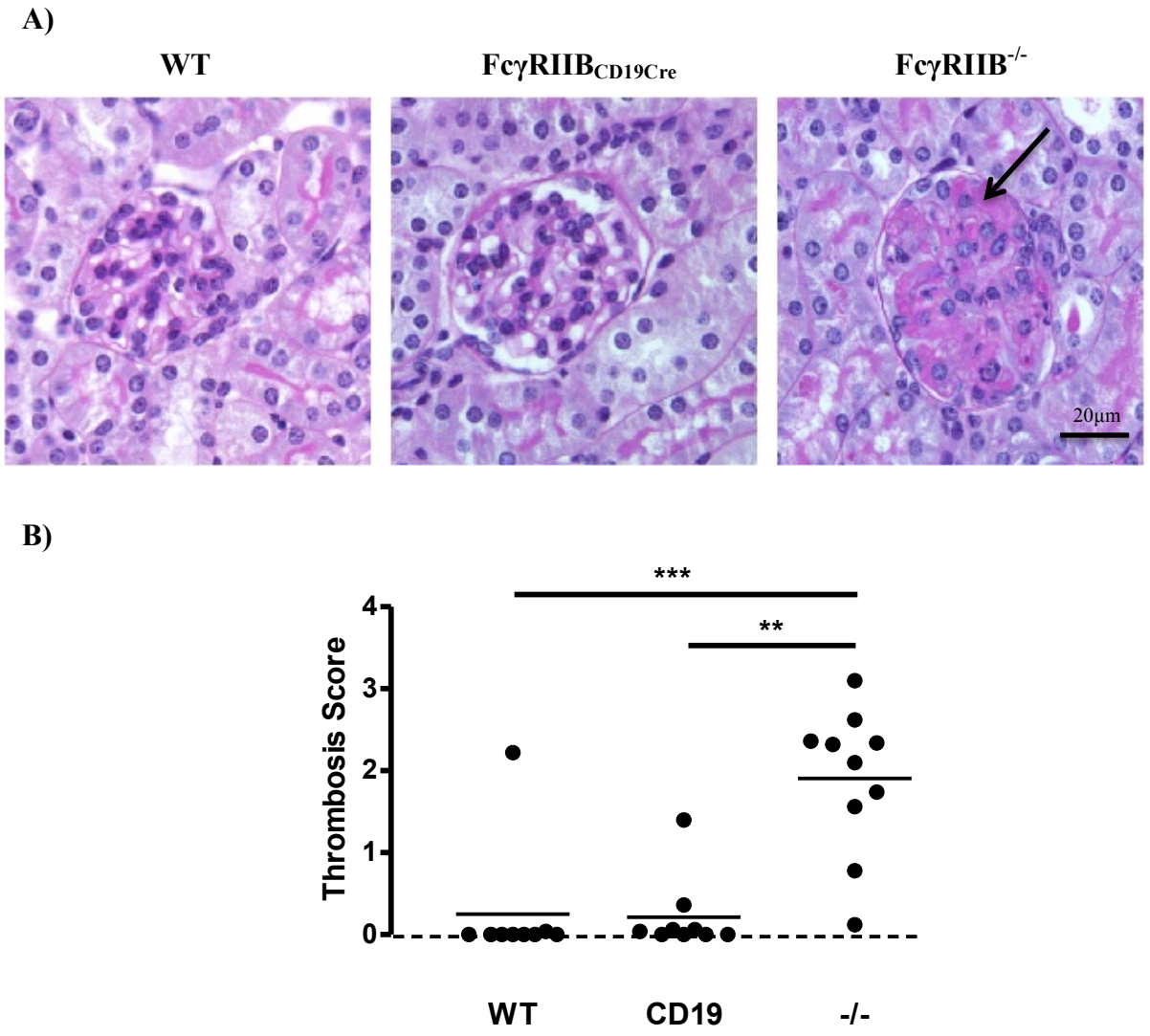


**Figure 5.4 Quantification of histologically abnormal glomeruli in WT and FcγRIIB knockout mice following induction of NTN, Experiment 1.**

**(A)** Representative PAS staining of glomeruli from WT, FcγRIIB$_{CD19Cre}$ and FcγRIIB$^{-/-}$ mice. Arrow highlights area of thrombosis in FcγRIIB$^{-/-}$ glomerulus. **(B)** Thrombosis score 5 days after the administration of NTS in WT mice and mice with a cell-specific deletion of FcγRIIB out 5 days after the administration of NTS. FcγRIIB$^{-/-}$ (-/-) mice had significantly more thrombotic glomeruli compared to WT and FcγRIIB$_{CD19Cre}$ (CD19) mice. All data represent individual values with the median. The data were analysed using Dunn's Multiple Comparison Test (p**<0.01, p***<0.001). Dashed line represents values for a group of normal WT mice.

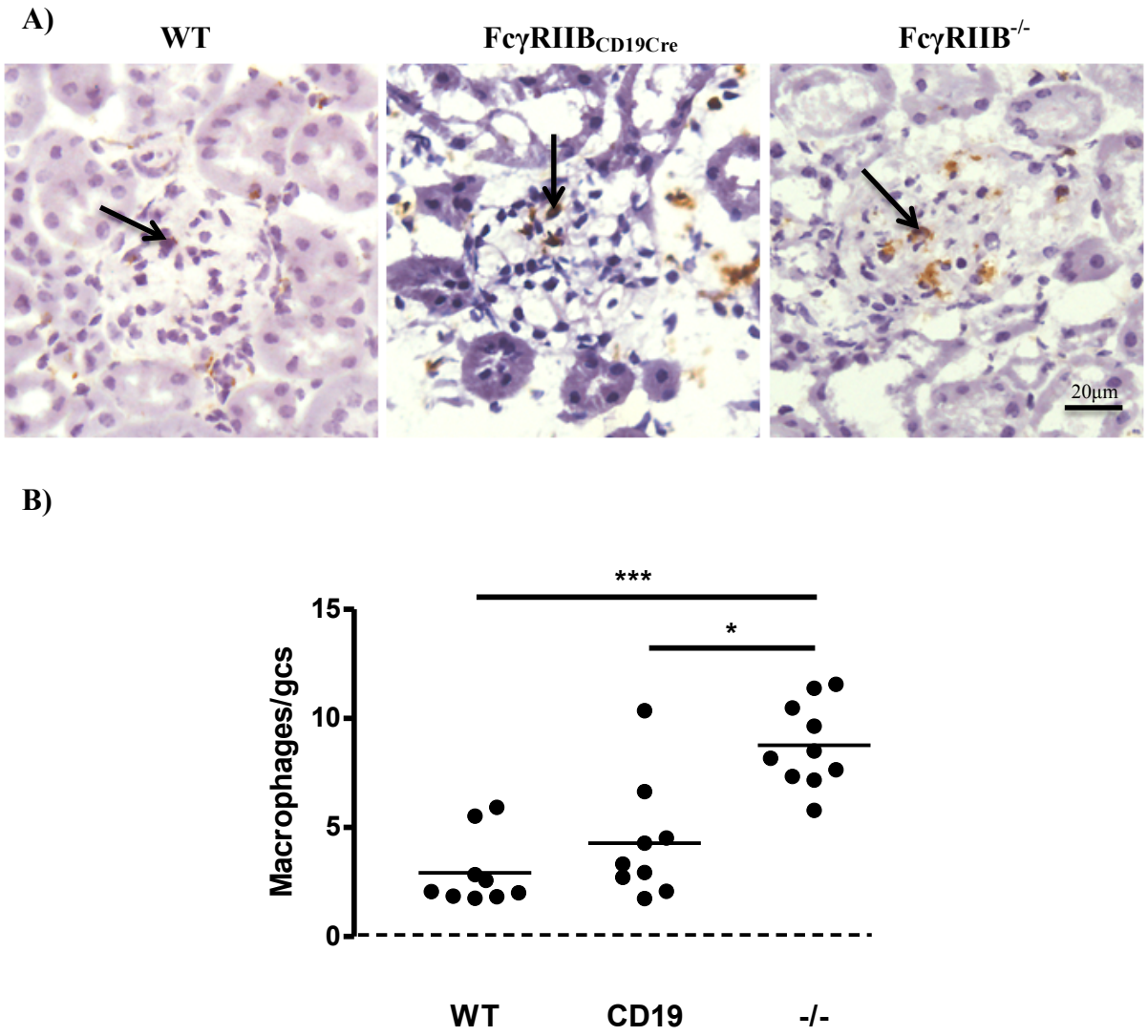


**Figure 5.5 Glomerular macrophage infiltration in WT and FcγRIIB knockout mice following induction of NTN, Experiment 1.**

**(A)** Immunohistochemistry for macrophages (CD68) on WT, FcγRIIB$_{CD19Cre,}$ and FcγRIIB$^{-/-}$ kidney sections. Arrows highlight macrophages. **(B)** Macrophage infiltration per glomerular cross section (50 glomeruli scored per section) from Experiment 1. FcγRIIB$^{-/-}$ (-/-) mice had significantly more infiltrating glomerular macrophages that WT and FcγRIIB$_{CD19Cre}$ (CD19) mice. All data represent individual values with the median. The data were analysed using Dunn's Multiple Comparison Test (p*<0.05, p***<0.001). Dashed line represents values for a group of normal WT mice.

### 5.4.3.2 FcγRIIB$^{-/-}$ had exacerbated disease compared to FcγRIIB$_{cEBP\alpha Cre}$ mice, FcγRIIB$_{CD11cCre}$ mice, and FcγRIIB$_{Mcpt5Cre}$ mice, when mild NTN was induced

Monocytes/macrophages, neutrophils, dendritic cells and mast cells have all been shown to play a role in the development of NTN and are known to express FcγRIIB. As the deletion of FcγRIIB on B cells alone had no effect on the susceptibility of mice to NTN the next step was to investigate the role of FcγRIIB on individual immune effector cells. In Experiment 2, a low dose of NTS (1:20) was administered to WT, FcγRIIB$_{CD11cCre,}$ FcγRIIB$_{Mcpt5Cre,}$ FcγRIIB$_{cEBP\alpha Cre}$ and FcγRIIB$^{-/-}$ mice on a pure C57BL/6 background to assess whether FcγRIIB expression by immune effector cells is important in protection from renal injury. FcγRIIB$^{-/-}$ mice were sacrificed at day 6 due to severe disease; all other mice were left till day 8 to allow disease to develop further.

To assess kidney function serum urea and albuminuria, expressed as a ratio of urinary albumin/creatinine, were measured in all mice. FcγRIIB$^{-/-}$ mice had significantly higher serum urea titres (131 (12-190) mmol/L) compared to WT mice (8.3 (6.9-12) mmol/L, $p<0.001$), FcγRIIB$_{CD11cCre}$ mice (9.5 (7.4-13) mmol/L, $p<0.05$) and FcγRIIB$_{cEBP\alpha Cre}$ mice (8.9 (7.8-12) mmol/L, $p<0.01$) but not FcγRIIB$_{Mcpt5Cre}$ mice (11 (8.2-14) mmol/L) (Figure 5.6 A). FcγRIIB$^{-/-}$ mice also had significantly higher levels of albuminuria (10 (0.013-28) mg/mmol) compared to WT mice (0.078 (0.014-0.85) mg/mmol, $p<0.05$) and FcγRIIB$_{CD11cCre}$ mice (0.019 (0.012-1.4) mg/mmol, $p<0.001$) but there was no significant difference between the other groups of mice (FcγRIIB$_{Mcpt5Cre}$ mice (0.15 (0.010-2.9) mg/mmol, FcγRIIB$_{cEBP\alpha Cre}$ mice (0.43 (0.010-8.5) mg/mmol) (Figure 5.6 B).

Histological damage, in the form of glomerular capillary thrombosis, was assessed in mice on PAS-stained sections (Figure 5.7 A). FcγRIIB$^{-/-}$ mice had significantly more thrombotic glomeruli (0.76 (0.020-1.1)) than WT mice (0.010 (0.00-0.22), $p<0.001$), FcγRIIB$_{CD11cCre}$ mice (0.00 (0.00-0.12), $p<0.001$) and FcγRIIB$_{cEBP\alpha Cre}$ mice (0.10 (0.00-0.40), $p<0.01$) but not FcγRIIB$_{Mcpt5Cre}$ mice (0.020 (0.00-0.20)) (Figure 5.7 B).

Kidney sections collected at the termination of Experiment 2 were stained for macrophage (CD68) and neutrophil (Gr-1) infiltration as a measure of inflammation (Figure 5.8 A and Figure 5.9 A, respectively). FcγRIIB$^{-/-}$ mice had a significantly greater glomerular macrophage infiltration (3.7 (1.0-4.9)/gcs) compared to WT mice (0.48 (0.080-1.1)/gcs, $p<0.01$), FcγRIIB$_{CD11cCre}$ mice (0.48 (0.18-2.2)/gcs, $p<0.05$), FcγRIIB$_{Mcpt5Cre}$ mice (0.18 (0.020-1.1)/gcs, $p<0.001$) and FcγRIIB$_{cEBP\alpha Cre}$ mice (0.30 (0.020-1.2)/gcs, $p<0.001$) (Figure

5.8 B). FcγRIIB$^{-/-}$ mice also had significantly more glomerular neutrophils (2.2 (0.94-2.8)/gcs) than WT mice (0.42 (0.10-0.70)/gcs, $p<0.001$), FcγRIIB$_{CD11cCre}$ mice (0.44 (0.32-0.74)/gcs, $p<0.01$), FcγRIIB$_{Mcpt5Cre}$ mice (0.50 (0.14-1.3)/gcs, $p<0.05$) and FcγRIIB$_{cEBP\alpha Cre}$ mice (0.45 (0.26-0.74)/gcs, $p<0.001$) (Figure 5.9 B).

These results demonstrate that, at a low dose of NTS, deletion of FcγRIIB on immune effector cells alone is not sufficient to increase susceptibility to NTN compared to WT mice, whereas FcγRIIB$^{-/-}$ mice develop severe disease under the same conditions. This indicates that no one cell type is able to reconstitute fully the increased disease susceptibility of the full gene deletion.

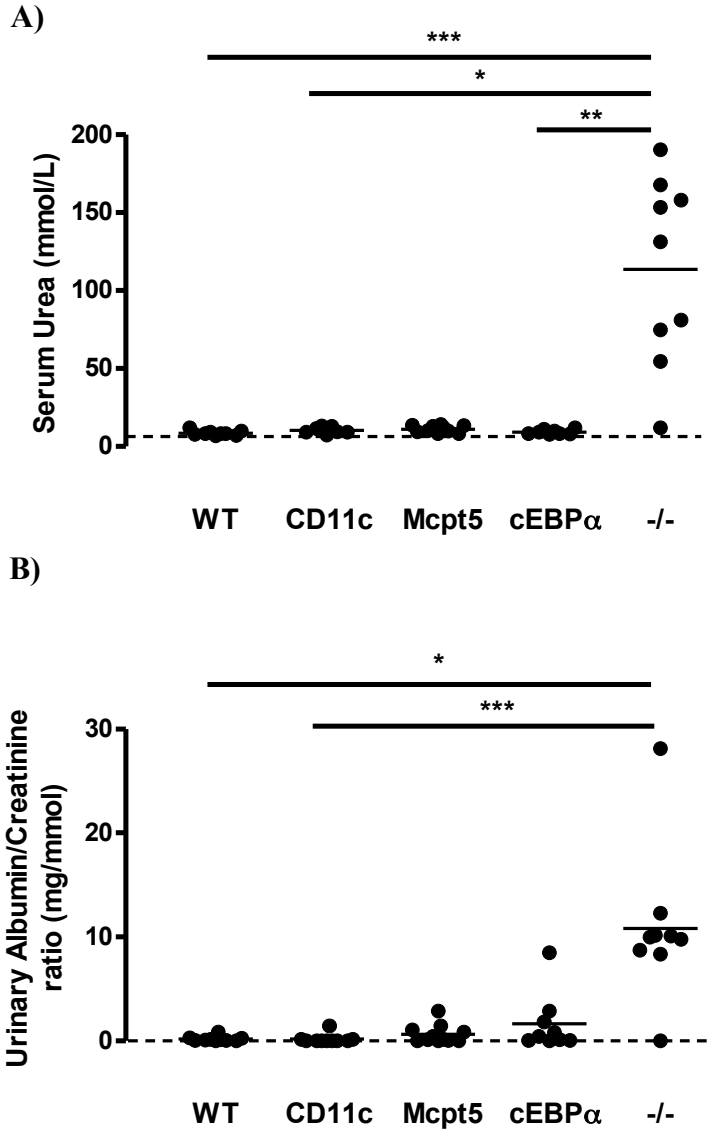


**Figure 5.6 Measurement of serum urea and urinary albumin/creatinine ratio in WT and FcγRIIB knockout mice with NTN, Experiment 2.**

**(A)** Serum urea and **(B)** urinary albumin/creatinine ratio were measured in WT and FcγRIIB knockout mice with NTN from Experiment 2. FcγRIIB$^{-/-}$ (-/-) mice had significantly higher serum urea than WT, FcγRIIB$_{CD11cCre}$ (CD11c) and FcγRIIB$_{cEBPαCre}$ (cEBPα) mice and significantly higher urinary albumin/creatinine ratio than WT and FcγRIIB$_{CD11cCre}$ mice (Mcpt5 = FcγRIIB$_{Mcpt5Cre}$). All data represent individual values with the median. The data were analysed using Dunn's Multiple Comparison Test (p*<0.05, p**<0.01, p***<0.001). Dashed lines represent values for a group of normal WT mice.

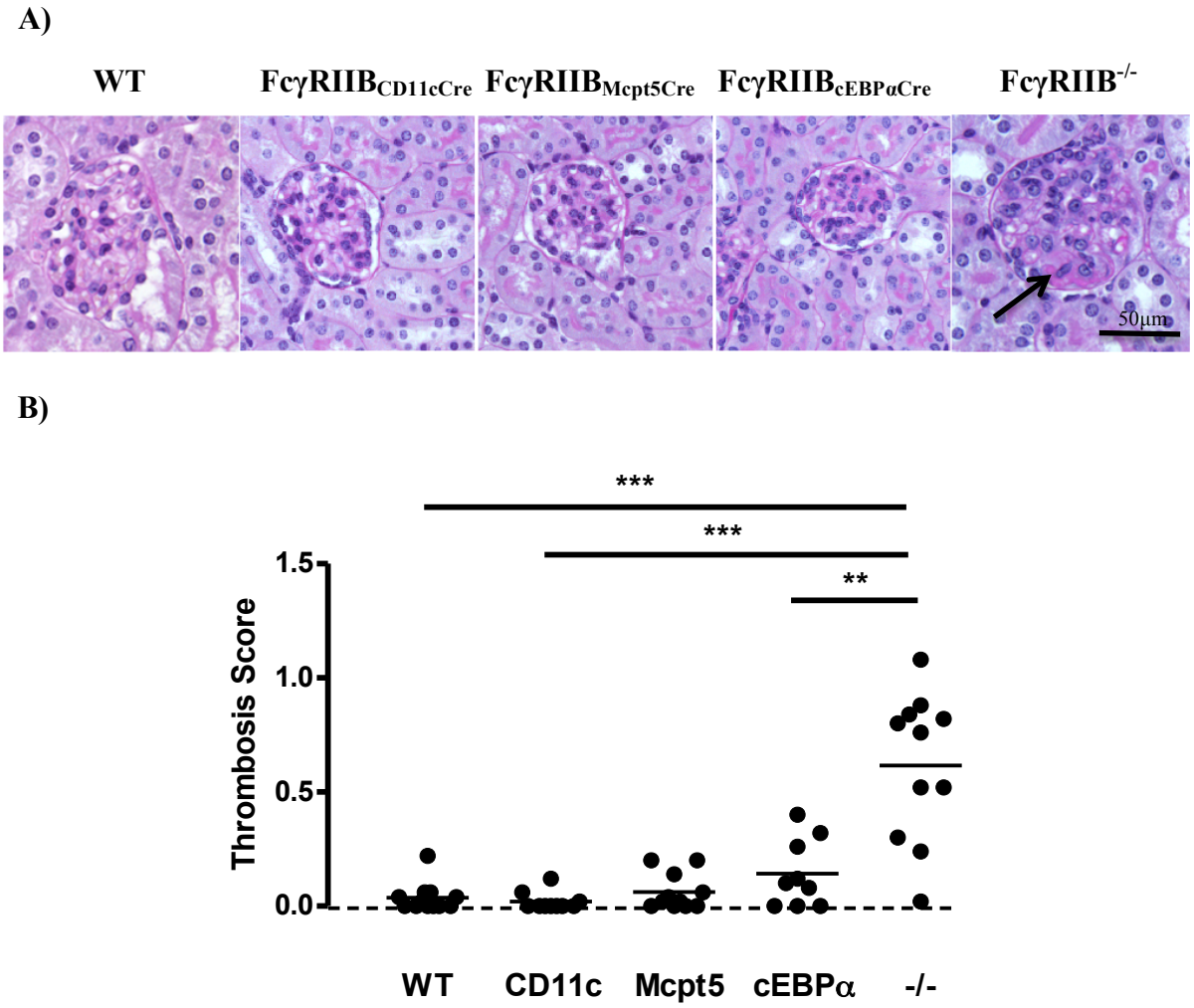


**Figure 5.7 Quantification of histologically abnormal glomeruli in WT and FcγRIIB knockout mice following induction of NTN, Experiment 2.**

**(A)** Representative PAS staining of glomeruli from WT, FcγRIIB$_{CD11cCre}$, FcγRIIB$_{Mcpt5Cre}$, FcγRIIB$_{cEBPαCre}$ and FcγRIIB$^{-/-}$ mice. Arrow highlights area of thrombosis in the FcγRIIB$^{-/-}$ glomerulus. **(B)** Thrombosis score 6 to 8 days after the administration of NTS in WT and FcγRIIB knockout mice. FcγRIIB$^{-/-}$ (-/-) mice had significantly more thrombotic glomeruli than WT, FcγRIIB$_{CD11cCre}$ (CD11c), and FcγRIIB$_{cEBPαCre}$ (cEBPα) mice (Mcpt5 = FcγRIIB$_{Mcpt5Cre}$). All data represent individual values with the median. The data were analysed using Dunn's Multiple Comparison Test (p**<0.01, p***<0.001). Dashed line represents values for a group of normal WT mice.

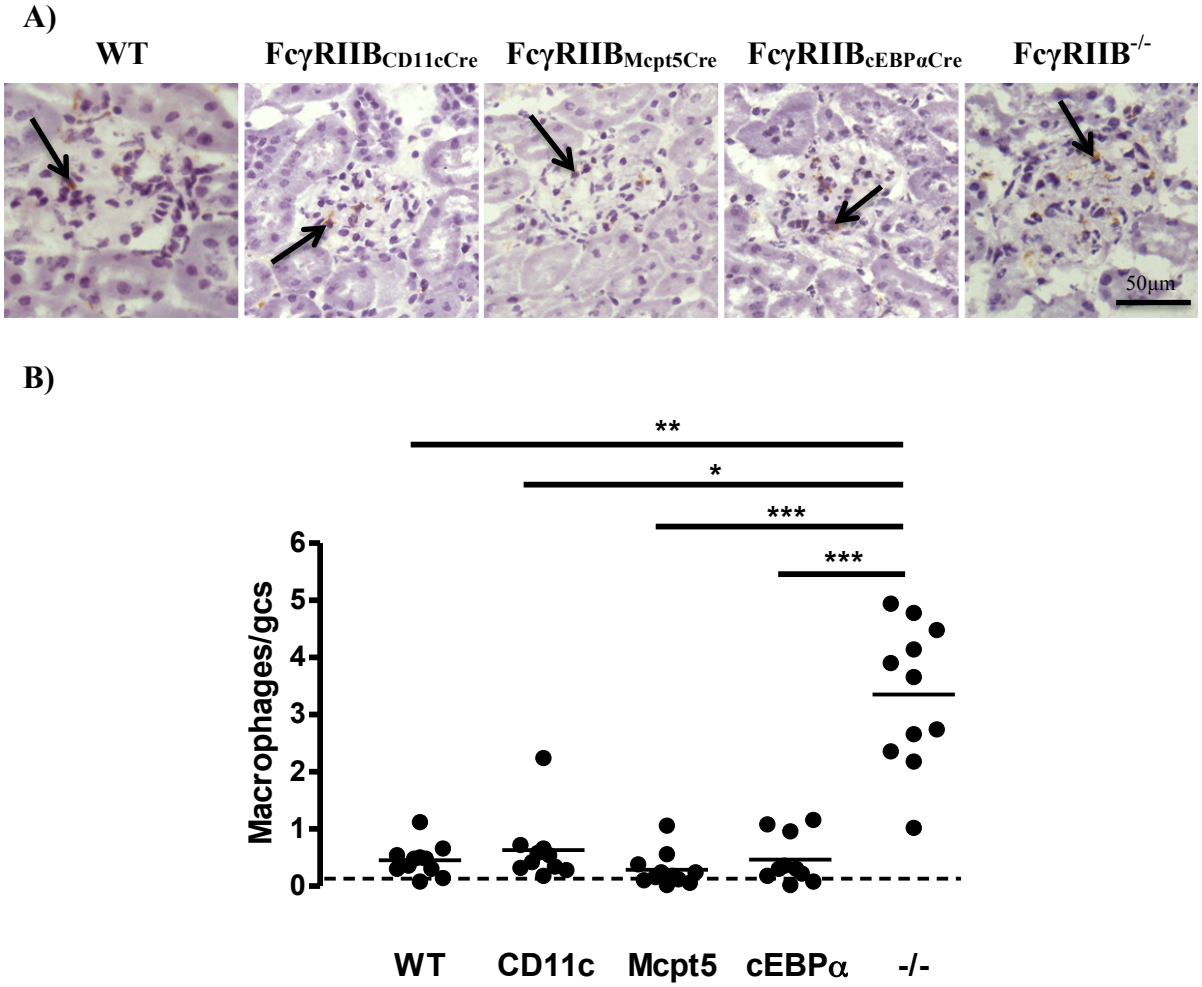


**Figure 5.8 Glomerular macrophage infiltration in WT and FcγRIIB knockout mice following induction of NTN, Experiment 2.**

**(A)** Immunohistochemistry for macrophages (CD68) on WT, FcγRIIB$_{CD11cCre,}$ FcγRIIB$_{Mcpt5Cre,}$ FcγRIIB$_{cEBPαCre}$ and FcγRIIB$^{-/-}$ sections. Arrows highlight macrophages. **(B)** Macrophage infiltration per glomerular cross section (gcs) (50 glomeruli scored per section) from Experiment 2. FcγRIIB$^{-/-}$ (-/-) mice had significantly more macrophages compared to all other groups of mice in both experiments (CD11c = FcγRIIB$_{CD11cCre}$, Mcpt5 = FcγRIIB$_{Mcpt5Cre}$, cEBPα = FcγRIIB$_{cEBPαCre}$). All data represent individual values with the median. The data were analysed using Dunn's Multiple Comparison Test (p*<0.05, p**<0.01, p***<0.001). Dashed line represents values for a group of normal WT mice.

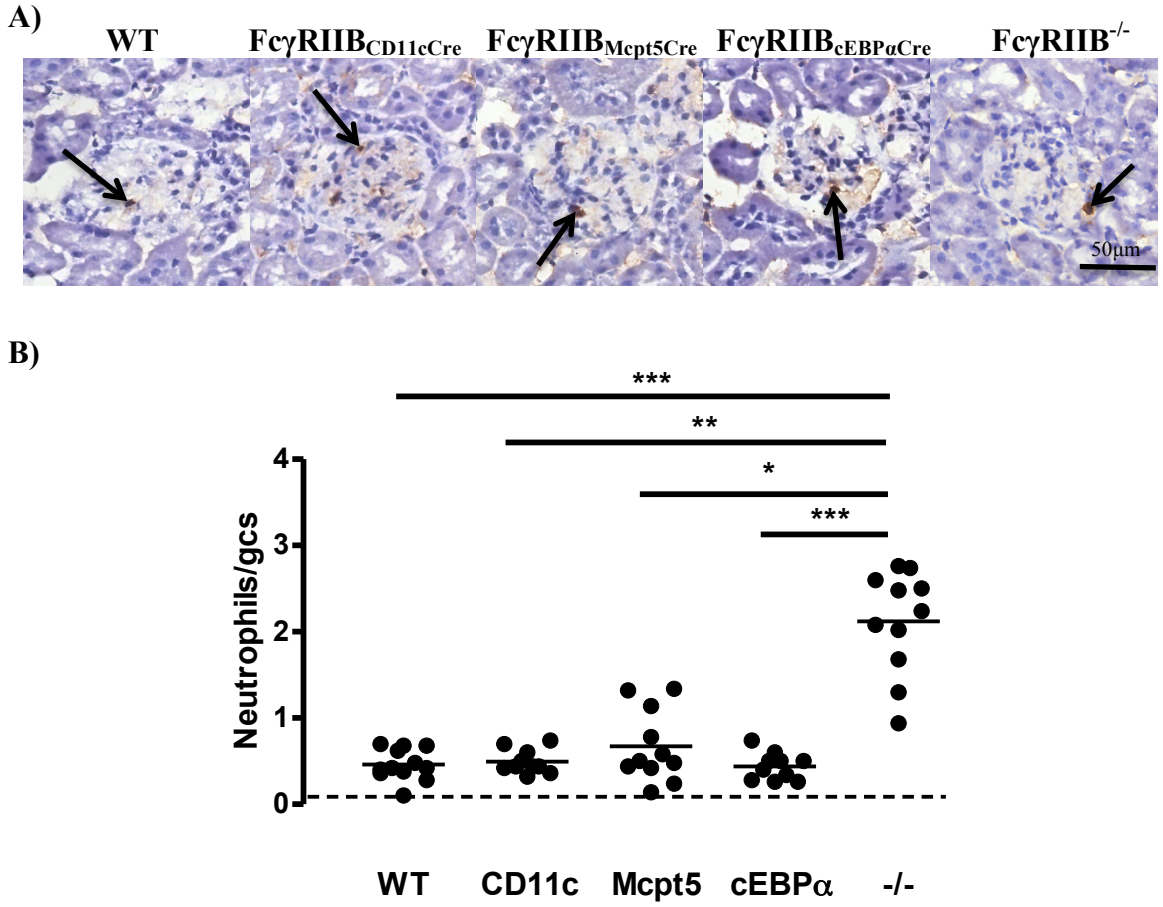


**Figure 5.9 Glomerular neutrophil infiltration in WT and FcγRIIB knockout mice following induction of NTN, Experiment 2.**

**(A)** Immunohistochemistry for neutrophils (Gr-1) on WT, FcγRIIB$_{CD11cCre,}$ FcγRIIB$_{Mcpt5Cre,}$ FcγRIIB$_{cEBPαCre}$ and FcγRIIB$^{-/-}$ kidney sections. Arrows highlight neutrophils. **(B)** Neutrophil infiltration per glomerular cross section (gcs) (50 glomeruli scored per section) from Experiment 2. FcγRIIB$^{-/-}$ (-/-) mice had significantly more glomerular neutrophils than all other groups of mice (CD11c = FcγRIIB$_{CD11cCre}$, Mcpt5 = FcγRIIB$_{Mcpt5Cre}$, cEBPα = FcγRIIB$_{cEBPαCre}$). All data represent individual values with the median. The data were analysed using Dunn's Multiple Comparison Test (p*<0.05, p**<0.01, p***<0.001). Dashed line represents values for a group of normal WT mice.

#### 5.4.3.3 Deletion of FcγRIIB on myeloid cells increases susceptibility to renal failure, histological damage and glomerular neutrophil infiltration compared to WT mice and deletion on B cells alone, following a higher dose of NTS

As FcγRIIB$^{-/-}$ mice are highly susceptible to developing NTN following a low dose of NTS, we decided to repeat the experiment using a higher dose of NTS (1:10) and omitting these mice in order to determine if FcγRIIB$_{cEBP\alpha Cre}$ and FcγRIIB$_{CD19Cre}$ mice would then become more susceptible to disease. In Experiment 3, nephritis was induced in the B cell and myeloid cell knockout mice, to dissect fully the role of FcγRIIB on B cells and immune effector cells, and compared to WT mice only. Mice were sacrificed at day 7-post induction of NTN because the FcγRIIB$_{cEBP\alpha Cre}$ mice started to show clinical signs of disease.

To assess kidney function serum urea and albuminuria, expressed as a ratio of urinary albumin/creatinine, were measured in all mice. FcγRIIB$_{cEBP\alpha Cre}$ mice had significantly higher levels of serum urea (48 (46-124) mmol/L) compared to FcγRIIB$_{CD19Cre}$ mice (8.1 (3.7-81) mmol/L, $p<0.05$) but not WT mice (12 (6.5-51) mmol/L) (Figure 5.10 A). FcγRIIB$_{cEBP\alpha Cre}$ mice also had significantly more albuminuria compared to FcγRIIB$_{CD19Cre}$ mice (FcγRIIB$_{cEBP\alpha Cre}$ 6.3 (3.1-16) mg/mmol, FcγRIIB$_{CD19Cre}$ 1.3 (0.010-3.3) mg/mmol, $p<0.01$) and WT mice (1.2 (0.05-4.8) mg/mmol, $p<0.05$) (Figure 5.10 B).

Histological damage, in the form of glomerular capillary thrombosis, was assessed in mice on PAS-stained sections (Figure 5.11 A). FcγRIIB$_{cEBP\alpha Cre}$ mice had significantly more thrombotic glomeruli (1.5 (0.78-2.9)) than both WT and FcγRIIB$_{CD19Cre}$ mice (thrombosis score: WT 0.20 (0.10-1.2), $p<0.05$; FcγRIIB$_{CD19Cre}$ mice 0.050 (0.00-1.3), $p<0.01$) (Figure 5.11 B).

Kidney sections collected at the termination of Experiment 3 were stained for macrophage (CD68) and neutrophil (Gr-1) infiltration as a measure of inflammation (Figure 5.12 A and Figure 5.13 A, respectively). There was no significant difference in glomerular macrophage numbers between the three groups of mice (macrophages/gcs: WT 1.3 (0.90-3.3), FcγRIIB$_{CD19Cre}$ 1.9 (0.74-3.3), FcγRIIB$_{cEBP\alpha Cre}$ 2.0 (1.4-6.1)) (Figure 5.12 B). However, FcγRIIB$_{cEBP\alpha Cre}$ mice had a significantly greater infiltration of glomerular neutrophils than WT mice (FcγRIIB$_{cEBP\alpha Cre}$ 1.5 (0.72-2.2)/gcs, WT 0.62 (0.32-1.1)/gcs, $p<0.05$) but there was no significant difference between the two groups with FcγRIIB$_{CD19Cre}$ mice (0.59 (0.23-1.7)/gcs) (Figure 5.13 B).

These results clearly demonstrate an important role for FcγRIIB on myeloid cells *in vivo* in NTN. However, taken with the results from Section 5.4.3.2, $Fc\gamma RIIB_{cEBP\alpha Cre}$ mice are not as susceptible to NTN as $Fc\gamma RIIB^{-/-}$ mice, suggesting other cell types may also play a protective role at a lower dose of NTS.

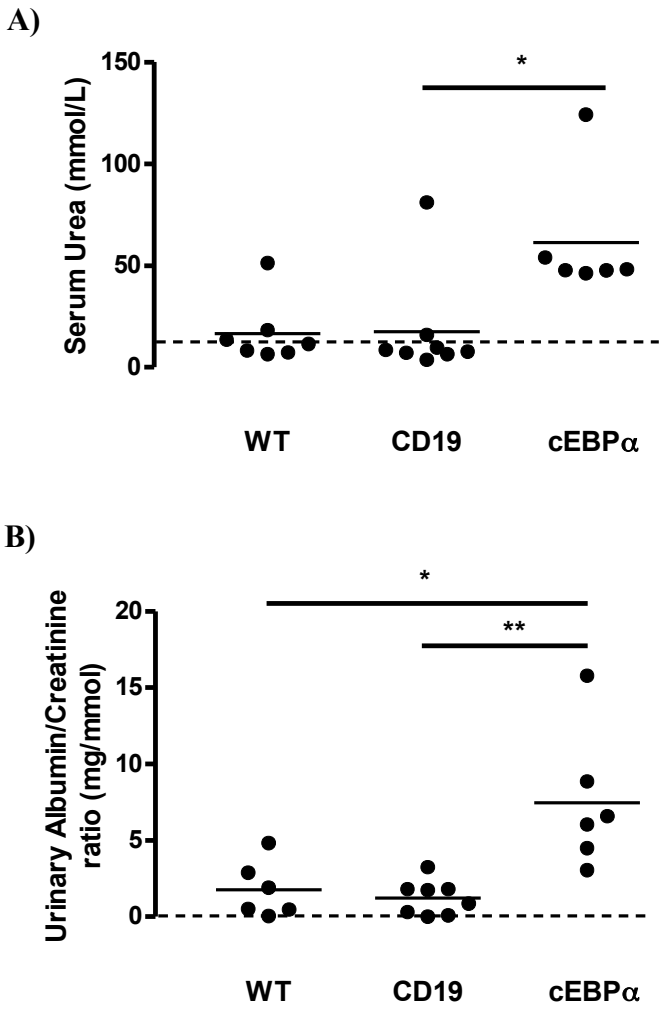


**Figure 5.10 Measurement of serum urea and urinary albumin/creatinine ratio in WT and FcγRIIB knockout mice with NTN, Experiment 3.**

**(A)** Serum urea and **(B)** urinary albumin/creatinine ratio were measured in WT and FcγRIIB knockout mice with NTN from Experiment 3. $FcγRIIB_{cEBPαCre}$ (cEBPα) mice had significantly higher serum urea than $FcγRIIB_{CD19Cre}$ (CD19) mice and urinary albumin/creatinine ratio than WT and $FcγRIIB_{CD19Cre}$ (CD19) mice and significantly lower serum albumin than WT and $FcγRIIB_{CD19Cre}$ mice. All data represent individual values with the median. The data were analysed using Dunn's Multiple Comparison Test ($p^*<0.05$, $p^{**}<0.01$). Dashed lines represent values for a group of normal WT mice.

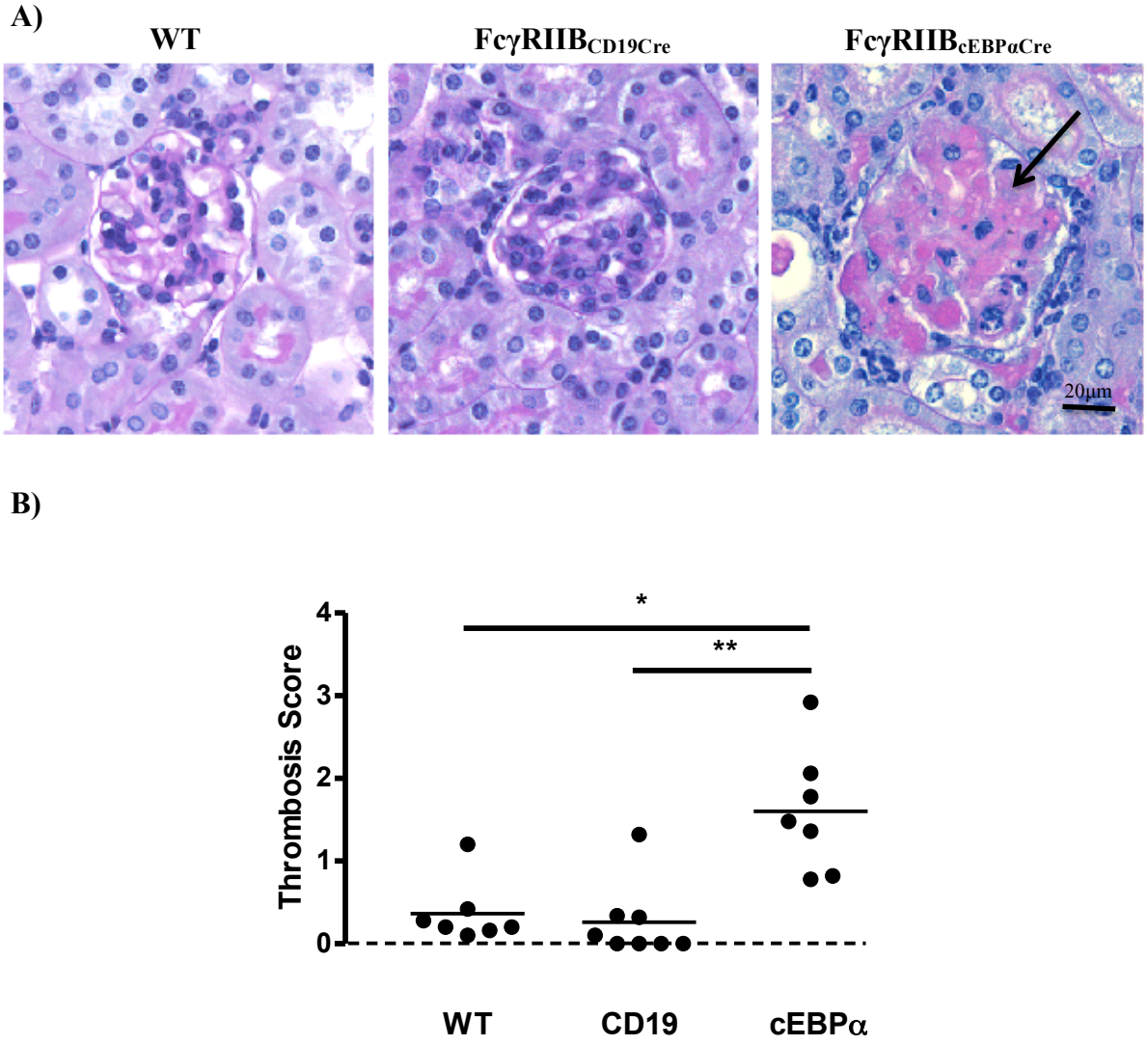


**Figure 5.11 Quantification of histologically abnormal glomeruli in WT and FcγRIIB knockout mice following induction of NTN, Experiment 3.**

**(A)** Representative PAS-stained of glomeruli from WT, FcγRIIB$_{CD19Cre}$ and FcγRIIB$_{cEBPαCre}$ mice. Arrow highlights area of thrombosis in FcγRIIB$_{cEBPαCre}$ glomerulus. **(B)** Thrombosis score in WT mice and mice with FcγRIIB conditionally knocked out 7 days after the administration of NTS. FcγRIIB$_{cEBPαCre}$ (cEBPα) mice had significantly more thrombotic glomeruli compared to WT and FcγRIIB$_{CD19Cre}$ (CD19) mice. All data represent individual values with the median. The data were analysed using Dunn's Multiple Comparison Test (p*<0.05, p**<0.01). Dashed line represents values for a group of normal WT mice.

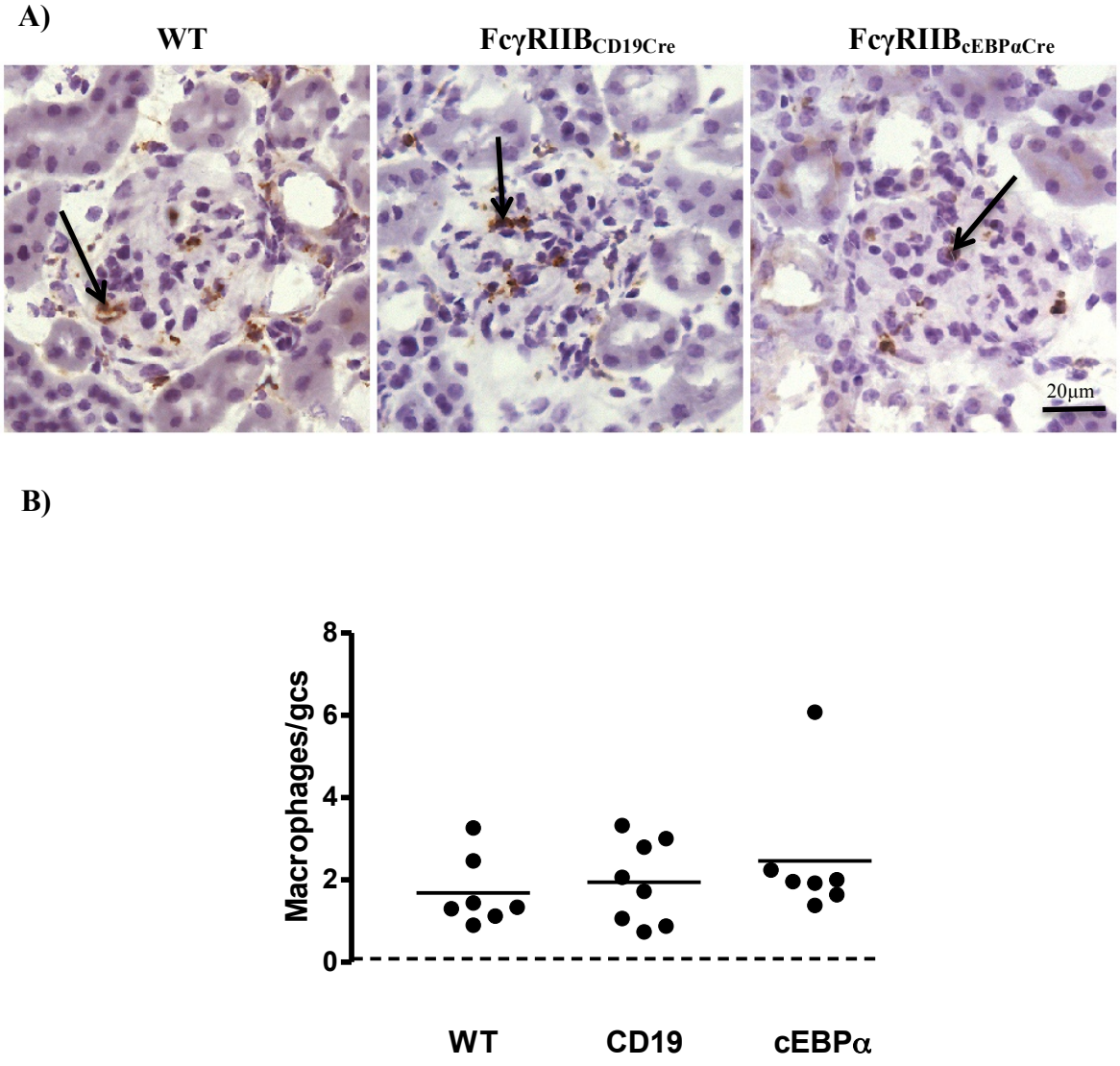


**Figure 5.12 Glomerular macrophage infiltration in WT and FcγRIIB knockout mice following induction of NTN, Experiment 3.**

**(A)** Immunohistochemistry for macrophages (CD68) on WT, FcγRIIB$_{CD19Cre,}$ and FcγRIIB$_{cEBPαCre}$ kidney sections. Arrows highlight macrophages. **(B)** Macrophage infiltration per glomerular cross section (gcs) (50 glomeruli scored per section) from Experiment 3. There was no significant difference between the three groups (CD19 = FcγRIIB$_{CD19Cre}$, cEBPα = FcγRIIB$_{cEBPαCre}$). All data represent individual values with the median. The data were analysed using Dunn's Multiple Comparison Test. Dashed line represents values for a group of normal WT mice.

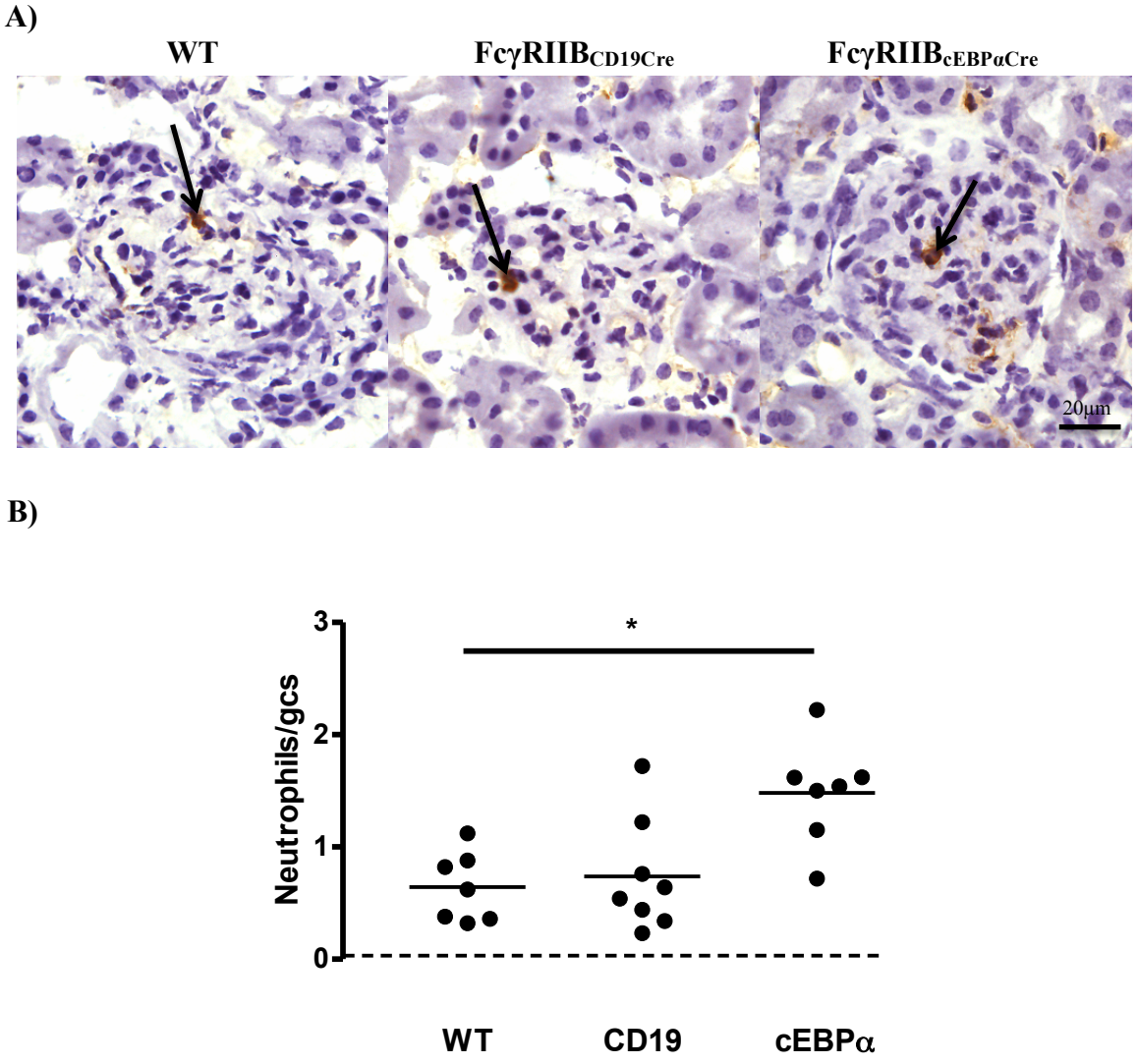


**Figure 5.13 Glomerular neutrophil infiltration in WT and FcγRIIB knockout mice following induction of NTN, Experiment 3.**

**(A)** Immunohistochemistry for neutrophils (Gr-1) on WT, FcγRIIB$_{CD19Cre}$ and FcγRIIB$_{cEBPαCre}$ kidney sections. Arrows highlight neutrophils. **(B)** Neutrophil infiltration per glomerular cross section (gcs) (50 glomeruli scored per section) from Experiment 3. FcγRIIB$_{cEBPαCre}$ (cEBPα) mice had significantly more glomerular neutrophils than WT mice (CD19 = FcγRIIB$_{CD19Cre}$). All data represent individual values with the median. The data were analysed using Dunn's Multiple Comparison Test ($p^*<0.05$). Dashed line represents values for a group of normal WT mice.

### 5.4.4 Systemic immune responses

The immune responses of the mice from all three experiments were assessed as before (Section 3.4.5). Circulating total mouse anti-sheep IgG levels were measured by ELISA. Despite having less disease, the FcγRIIB$_{CD19Cre}$ mice had higher circulating anti-sheep antibody titres, showing that increased antibody production is not the determining factor for heightened susceptibility to NTN. In Experiment 1, FcγRIIB$_{CD19Cre}$ mice had significantly higher levels of circulating antibodies compared to FcγRIIB$^{-/-}$ mice ($p<0.05$). In Experiment 2, FcγRIIB$_{CD11cCre}$ mice and FcγRIIB$_{Mcpt5Cre}$ mice had significantly higher levels of circulating antibodies compared to FcγRIIB$^{-/-}$ mice ($p<0.01$ for both). In Experiment 3, FcγRIIB$_{CD19Cre}$ mice had significantly higher circulating antibody titres compared to FcγRIIB$_{cEBP\alpha Cre}$ mice ($p<0.05$) (Table 5.1 and Figure 5.14).

Frozen kidney sections were stained for deposited sheep and mouse IgG by direct immunofluorescence on tissue taken at the end of the experiment. Total glomerular sheep and mouse IgG were measured by quantitative immunofluorescence with the results expressed as arbitrary fluorescence units (AFU) or visual fluorescence units (VFU) (depending upon availability of equipment at the time the experiments were run). There was no significant difference in glomerular sheep IgG deposition between any of the groups of mice in any of the experiments (Table 5.1, Figure 5.15 and Figure 5.16). In Experiment 1, FcγRIIB$^{-/-}$ mice had significantly greater deposition of mouse IgG compared to WT mice ($p<0.01$) and FcγRIIB$_{CD19Cre}$ mice ($p<0.01$). In Experiment 2, FcγRIIB$^{-/-}$ mice had significantly greater mouse IgG deposition compared to FcγRIIB$_{cEBP\alpha Cre}$ mice ($p<0.05$). There was no significant difference in deposited mouse IgG between any of the groups of mice in Experiment 3 (Table 5.1, Figure 5.17 and Figure 5.18).

| | Mouse | Serum anti-sheep IgG (OD 405nm) | Deposited glomerular sheep IgG | Deposited glomerular mouse IgG |
|---|---|---|---|---|
| **Experiment 1** | WT | 1.2 (0.12-1.5) | 101 (61-159) | 1055 (266-1236) |
| | $Fc\gamma RIIB_{CD19Cre}$ | 1.2 (1.0-1.4) | 63 (22-109) | 1111 (739-1502) |
| | $Fc\gamma RIIB^{-/-}$ | 0.95 (0.87-1.6) | 79 (0-147) | 1537 (1195-1840) |
| **Experiment 2** | WT | 0.80 (0.12-1.2) | 2.5 (1.0-3.0) | 1.8 (0.5-2.5) |
| | $Fc\gamma RIIB_{CD11cCre}$ | 0.91 (0.65-1.2) | 2.8 (1.0-3.0) | 1.8 (1.5-2.5) |
| | $Fc\gamma RIIB_{Mcpt5Cre}$ | 0.92 (0.66-1.0) | 2.0 (1.5-3.0) | 1.0 (0.5-2.5) |
| | $Fc\gamma RIIB_{cEBP\alpha Cre}$ | 0.83 (0.059-0.93) | 2.0 (1.0-3.0) | 1.0 (0.5-1.5) |
| | $Fc\gamma RIIB^{-/-}$ | 0.65 (0.21-0.76) | 2.5 (2.0-3.0) | 2.5 (0.5-3.0) |
| **Experiment 3** | WT | 1.0 (0.50-1.8) | 51 (35-73) | 97 (69-125) |
| | $Fc\gamma RIIB_{CD19Cre}$ | 1.6 (0.018-1.8) | 59 (38-118) | 114 (90-161) |
| | $Fc\gamma RIIB_{cEBP\alpha Cre}$ | 0.42 (0.0090-1.2) | 36 (24-86) | 114 (67-167) |

**Table 5.1 Circulating total mouse anti-sheep IgG levels and deposited glomerular sheep and mouse IgG in WT and FcγRIIB knockout mice with NTN.**

All results are expressed as median (range). Experiment 1 and Experiment 3, deposited glomerular sheep IgG and mouse IgG are represented as AFU. Experiment 2, deposited glomerular sheep and mouse IgG are represented as VFU.

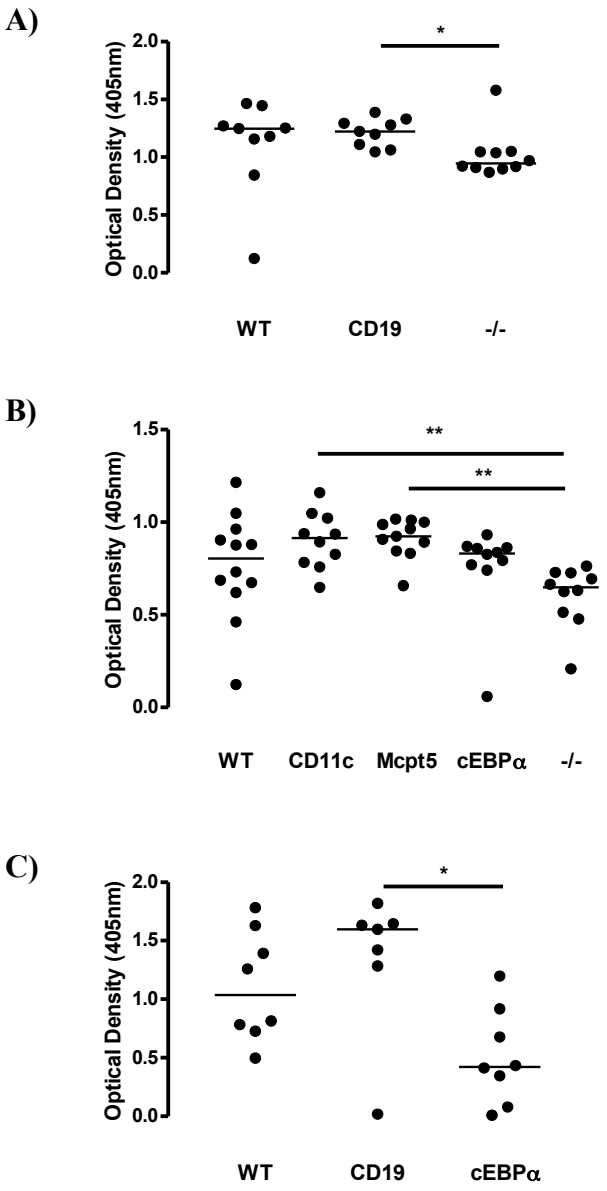


**Figure 5.14 Total circulating mouse anti-sheep IgG levels in WT and FcγRIIB knockout mice following induction of NTN.**

Circulating mouse anti-sheep IgG was measured by ELISA in **(A)** Experiment 1, **(B)** Experiment 2, and **(C)** Experiment 3. In Experiment 1 and Experiment 2, FcγRIIB$^{-/-}$ (-/-) mice had less circulating mouse anti-sheep IgG compared to FcγRIIB$_{CD19Cre}$ (CD19), FcγRIIB$_{Mcpt5Cre}$ (Mcpt5) and FcγRIIB$_{CD11cCre}$ (CD11c) mice. In Experiment 3, FcγRIIB$_{cEBPαCre}$ (cEBPα) mice had significantly less circulating mouse anti-sheep IgG compared to FcγRIIB$_{CD19Cre}$ mice. All data represent individual values with the median. The data were analysed using Dunn's Multiple Comparison Test (p*<0.05, p**<0.01).

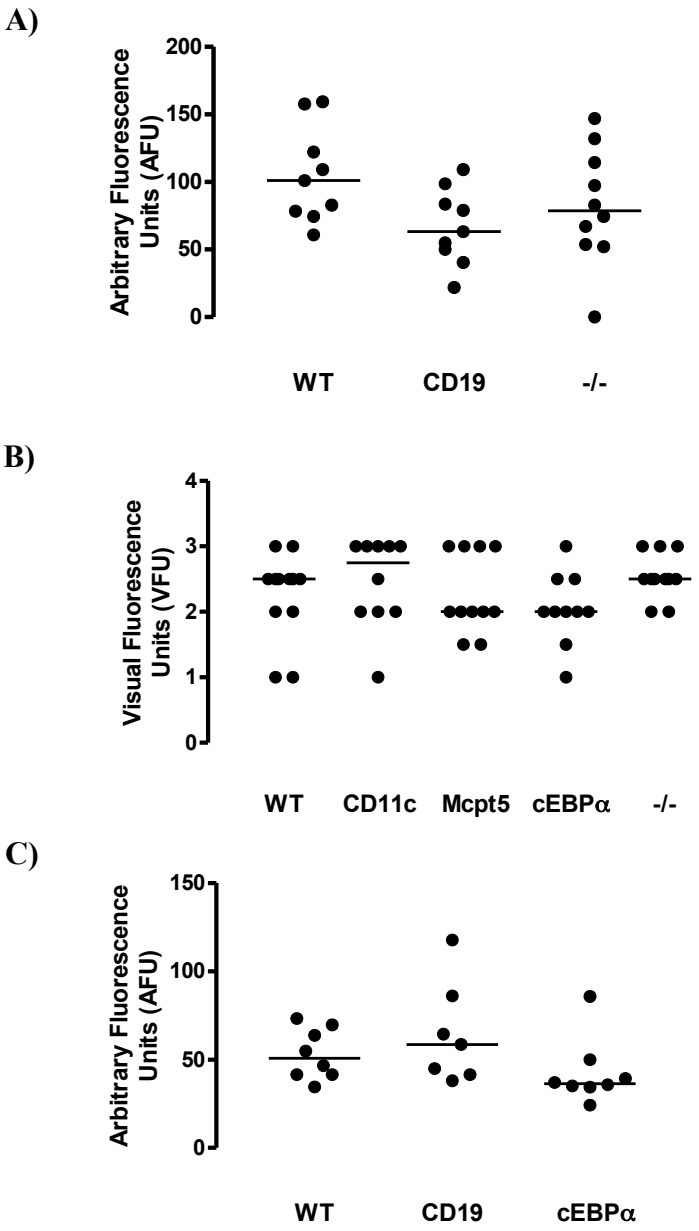


**Figure 5.15 Immunofluorescence for glomerular sheep IgG deposition in WT and FcγRIIB knockout mice following induction of NTN.**

The relative mean glomerular immunofluorescence was measured quantitatively, expressed as arbitrary fluorescence units (AFU), or semi-quantitatively, expressed as visual fluorescence units (VFU). There was no significant difference in deposited sheep IgG between any of the groups in **(A)** Experiment 1, **(B)** Experiment 2 or **(C)** Experiment 3 (CD19 = $Fc\gamma RIIB_{CD19Cre}$, cEBPα = $Fc\gamma RIIB_{cEBP\alpha Cre}$). All data represent individual values with the median. The data were analysed using Dunn's Multiple Comparison Test.

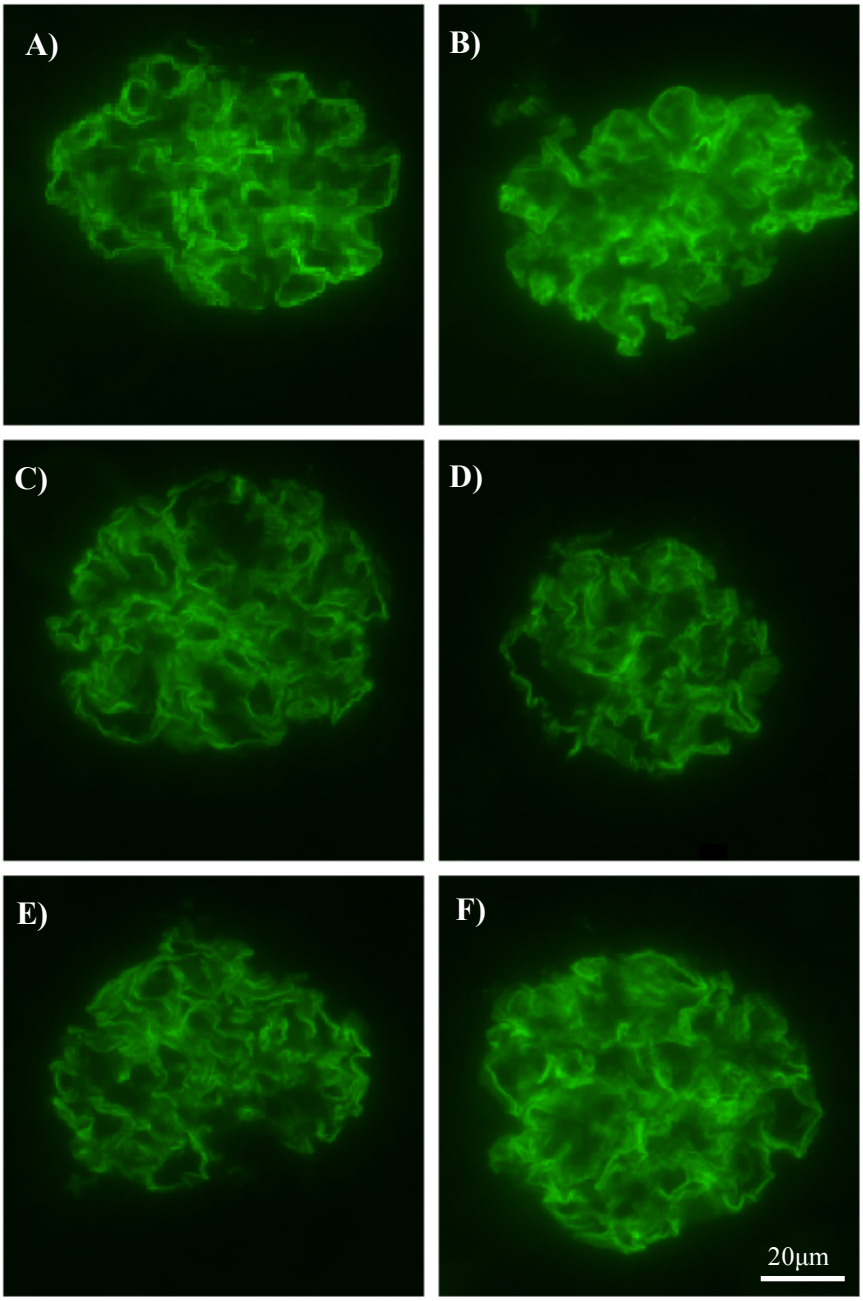


**Figure 5.16 Immunofluorescence for glomerular sheep IgG deposition in WT and FcγRIIB knockout mice from Experiment 1, Experiment 2, and Experiment 3.**

Representative glomeruli from **(A)** WT mice, **(B)** FcγRIIB$^{-/-}$ mice, **(C)** FcγRIIB$_{CD19Cre}$ mice, **(D)** FcγRIIB$_{cEBP\alpha Cre}$ mice, **(E)** FcγRIIB$_{CD11cCre}$ mice and **(F)** FcγRIIB$_{Mcpt5Cre}$ mice showing sheep IgG deposition. All images were taken using the same settings.

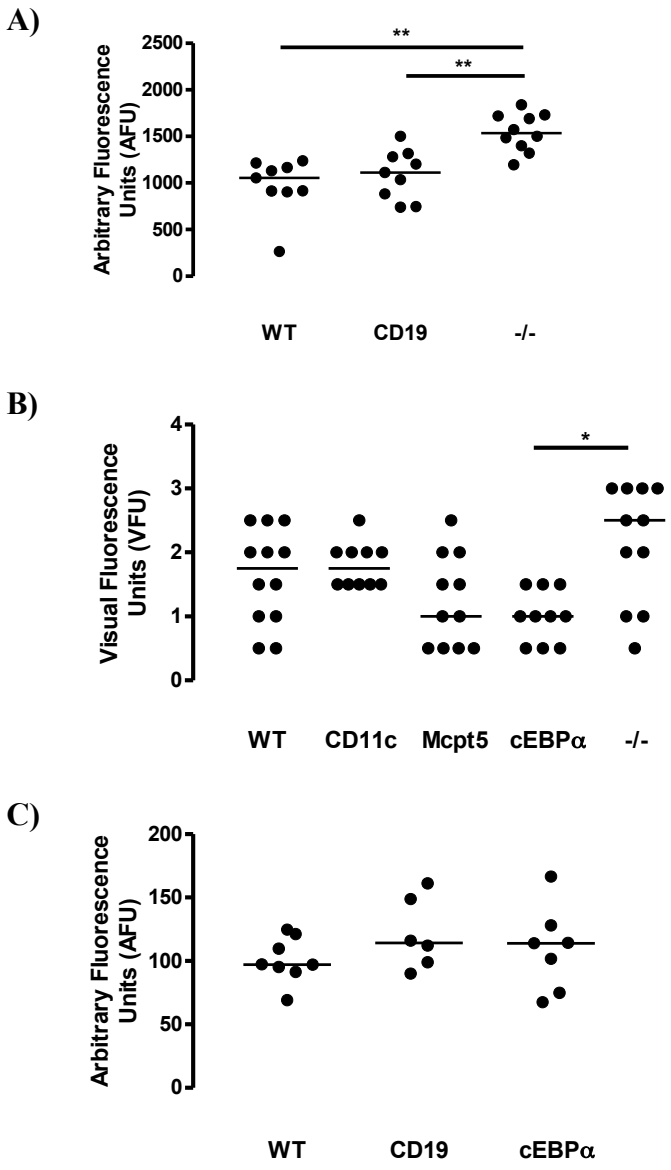


**Figure 5.17 Immunofluorescence for glomerular mouse IgG deposition in WT and FcγRIIB knockout mice following induction of NTN.**

The relative mean glomerular immunofluorescence was measured quantitatively, expressed as arbitrary fluorescence units (AFU), or semi-quantitatively, expressed as visual fluorescence units (VFU). FcγRIIB$^{-/-}$ (-/-) mice had more deposited mouse IgG compared to WT and FcγRIIB$_{CD19Cre}$ (CD19) mice in **(A)** Experiment 1 and FcγRIIB$_{cEBP\alpha Cre}$ (cEBPα) mice in **(B)** Experiment 2 (CD11c = FcγRIIB$_{CD11cCre}$, Mcpt5 = FcγRIIB$_{Mctp5Cre}$). There was no difference in deposited mouse IgG in **(C)** Experiment 3. All data represent individual values with the median. The data were analysed using Dunn's Multiple Comparison Test (p*<0.05, p**<0.01).

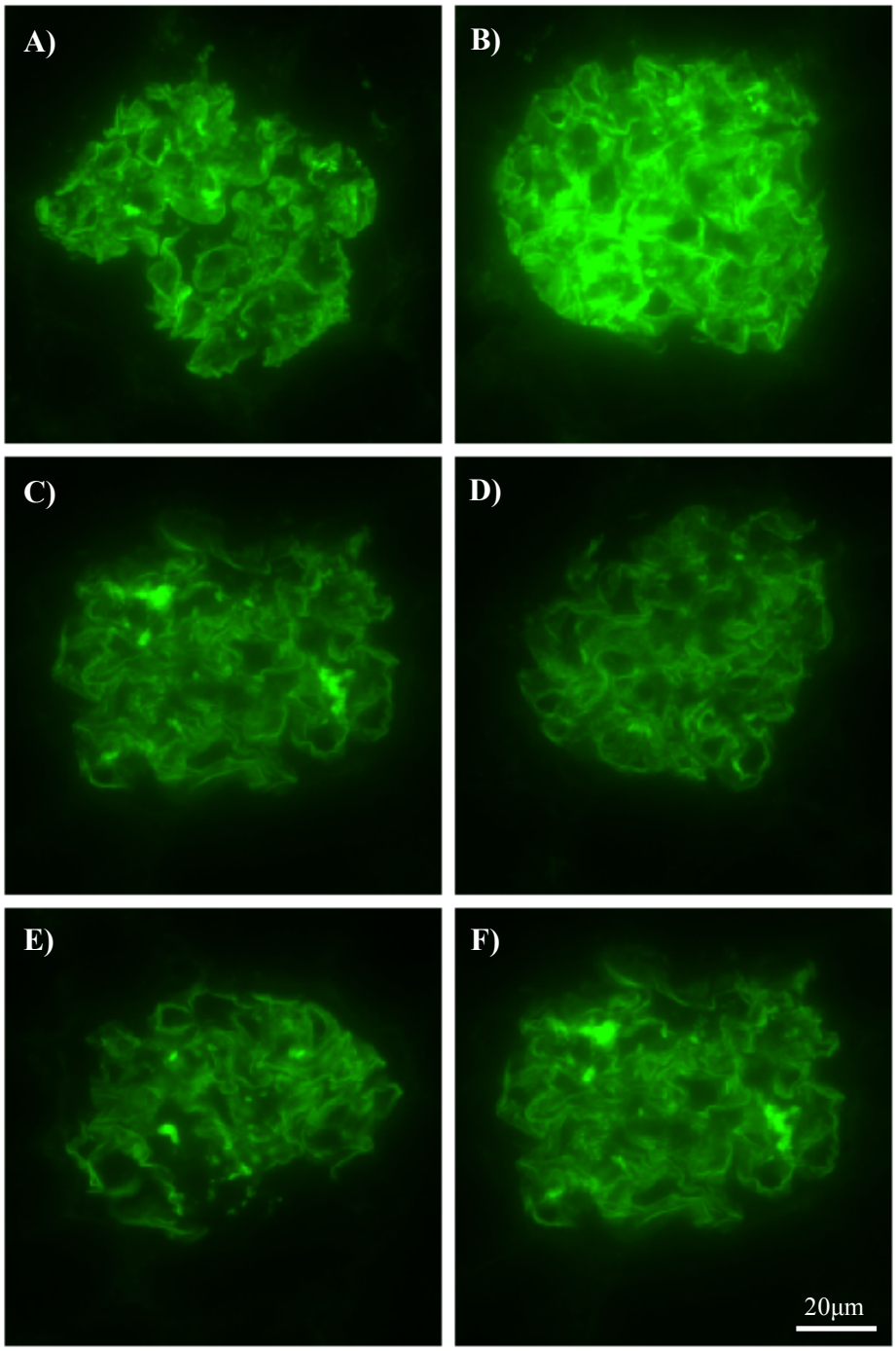


**Figure 5.18 Immunofluorescence for glomerular mouse IgG deposition in WT and FcγRIIB knockout mice from Experiment 1, Experiment 2, and Experiment 3.**

Representative glomeruli from **(A)** WT mice, **(B)** FcγRIIB$^{-/-}$ mice, **(C)** FcγRIIB$_{CD19Cre}$ mice, **(D)** FcγRIIB$_{cEBP\alpha Cre}$ mice, **(E)** FcγRIIB$_{CD11cCre}$ mice, and **(F)** FcγRIIB$_{Mcpt5Cre}$ mice showing mouse IgG deposition. All images were taken using the same settings.

### 5.4.5 mRNA expression of cytokines and other mediators

In Experiment 3, despite FcγRIIB$_{cEBP\alpha Cre}$ mice having increased susceptibility to NTN compared to WT and FcγRIIB$_{CD19Cre}$ mice, there was no significant difference in macrophage infiltration between the three groups. This suggests the differences seen may be due to increased macrophage activation in the FcγRIIB$_{cEBP\alpha Cre}$ mice. To investigate further the mechanism of injury, mRNA was extracted from whole kidney of WT, FcγRIIB$_{CD19Cre}$ and FcγRIIB$_{cEBP\alpha Cre}$ mice from Experiment 3. mRNA expression levels of cytokines and other mediators of macrophage activation were measured by qRT-PCR. Mediators measured were: MCP-1, involved in macrophage recruitment; TNF-α, produced by classically and alternatively activated macrophages; MR, a marker of alternatively activated macrophages; and IFN-γ, involved in the classically activated macrophage pathway. Data represent relative expression, calculated using GAPDH as the housekeeping gene and an untreated WT mouse as the reference.

Relative expression of MCP-1 in whole kidney from FcγRIIB$_{CD19Cre}$ mice (3.5 (2.4-13)) was significantly greater than FcγRIIB$_{cEBP\alpha Cre}$ mice (1.4 (0.6-3.7), $p<0.05$), there was no significant difference with WT mice (3.4 (0.54-6.1)). There was no significant difference in relative expression of TNF-α or MR between the three groups of mice (TNF-α: WT 1.2 (0.45-11), FcγRIIB$_{CD19Cre}$ 1.8 (0.48-3.9), FcγRIIB$_{cEBP\alpha Cre}$ 1.1 (0.60-2.7); MR: WT 0.86 (0.24-2.6), FcγRIIB$_{CD19Cre}$ 0.45 (0.35-1.2), FcγRIIB$_{cEBP\alpha Cre}$ mice 0.54 (0.38-1.8)). Although MR expression appeared to be slightly downregulated compared to control WT mice without NTN. IFN-γ expression was significantly greater in both WT mice (3.1 (2.2-13)) and FcγRIIB$_{CD19Cre}$ mice (3.3 (2.0-6.4)) compared to FcγRIIB$_{cEBP\alpha Cre}$ mice (0.85 (0.20-2.3), $p<0.01$ and $p<0.05$ respectively) (Figure 5.19). Therefore none of these markers were able to differentiate between the groups. It may be that the timepoint of analysis was late in the disease process, or that it is necessary to isolate glomeruli to assess the differences more specifically.

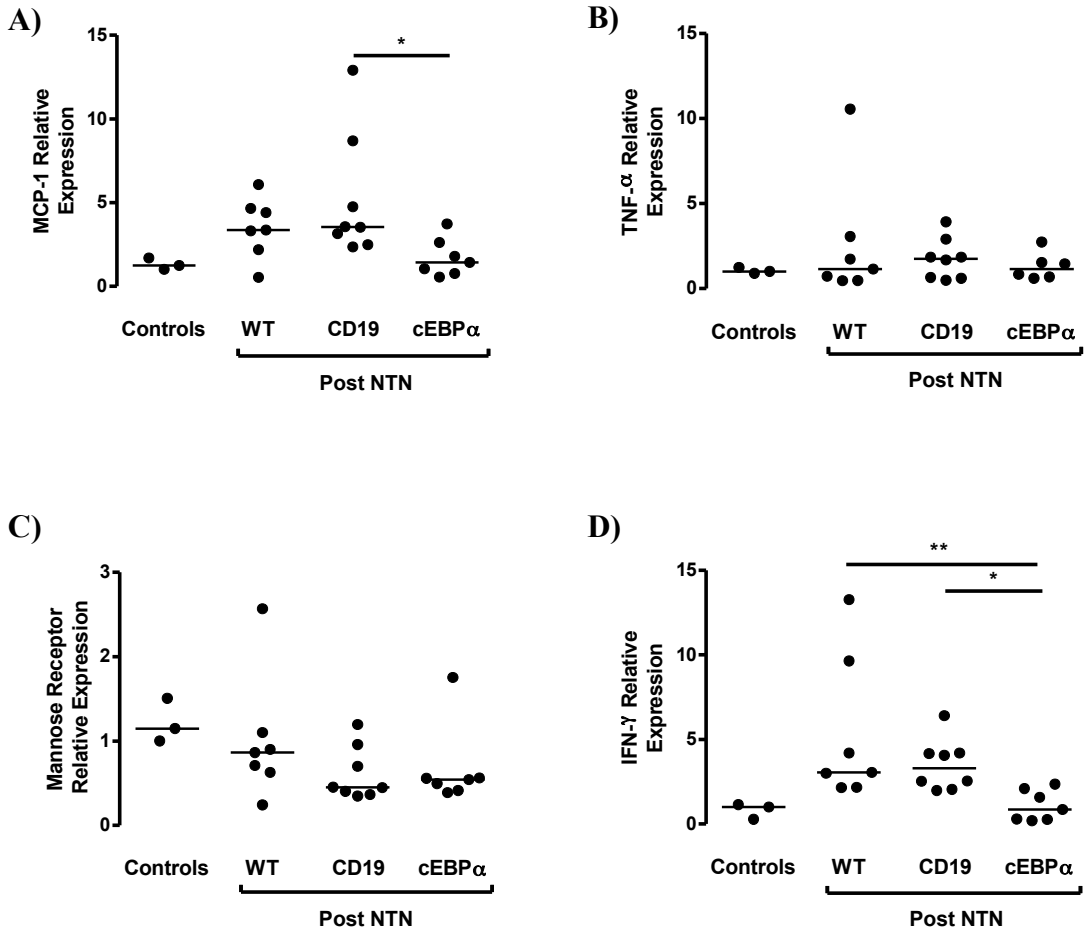


**Figure 5.19 Relative expression of MCP-1, TNF-α, MR and IFN-γ in whole kidney of WT, FcγRIIB$_{CD19Cre}$, and FcγRIIB$_{cEBPαCre}$ mice with NTN, Experiment 3.**

Relative expression of **(A)** MCP-1, **(B)** TNF-α, **(C)** MR and **(D)** IFN-γ were measured in whole kidney mRNA extracts. FcγRIIB$_{CD19Cre}$ (CD19) and WT mice had significantly greater expression of IFN-γ than FcγRIIB$_{cEBPαCre}$ (cEBPα) mice and FcγRIIB$_{CD19Cre}$ mice had significantly greater expression of MCP-1 than FcγRIIB$_{cEBPαCre}$ mice. There was no significant difference in the relative expression of TNF-α and MR. All data represent individual values with the median. The data were analysed using Dunn's Multiple Comparison Test ($p^{*}<0.05$, $p^{**}<0.01$).

## 5.5 Discussion

These results confirm that complete deletion of FcγRIIB from C57BL/6 mice causes exacerbated disease following the induction of accelerated NTN, as shown by increased renal dysfunction, histological damage, and cellular infiltration, compared to WT counterparts. Deletion of FcγRIIB from B cells, dendritic cells, mast cells or myeloid cells was not found to increase the incidence of accelerated NTN at a low dose of NTS, however we have then gone on to show at a higher dose of NTS that FcγRIIB expressed by myeloid cells, but not B cells, is important in protection from disease, despite an increased systemic antibody response in the $FcγRIIB_{CD19Cre}$ mice and similar levels of glomerular macrophage infiltration between WT, $FcγRIIB_{CD19Cre}$ and $FcγRIIB_{cEBPαCre}$ mice. There was no difference in deposited mouse IgG between the three groups; however $FcγRIIB_{cEBPαCre}$ mice had an increased glomerular neutrophil infiltration. These results indicate that FcγRIIB on myeloid cells is important in regulating myeloid cell activity in NTN and that expression of FcγRIIB on B cells, and raised antibody levels, are not important in the effector phase of GN in this model.

FcγRIIB is one of the most widely expressed FcγR, being found on most leukocytes, with the exception of T cells and NK cells. It functions as a negative regulator for activating receptors, such as the FcγR or BcR, and is also involved in immune complex uptake and antigen presentation, meaning it is a key player in regulating innate and adaptive immunity. The generation of mice carrying a cell-specific deletion, using cre-*loxP* recombination, has made it possible to decipher the precise roles of diverse molecules in different cell types in disease development. Using this technology, FcγRIIB was deleted from B cells, dendritic cells, mast cells and myeloid cells. The efficiency of the deletion was measured by flow cytometry by staining for FcγRIIB and specific cellular markers. There was good deletion of FcγRIIB from B cells, dendritic cells and mast cells. The myeloid cell knockout, using the cEBPα promoter, produced a good deletion from granulocytes and monocytes in the blood, however there was only partial deletion from macrophages and dendritic cells in the spleen. Within the haematopoietic system, cEBPα is exclusively expressed in early myeloid progenitors, making it a good target for creating myeloid cell knockouts (Akashi et al., 2000). $cEBPα^{-/-}$ mice were found to lack mature granulocytes, but not monocytes and macrophages, both circulating and in haematopoietic organs (Zhang et al., 1997). This suggests that cEBPα

is not essential for monocyte and macrophage maturation. It would be of interest to compare FcγRIIB expression on other tissue resident macrophages, such as resident renal macrophages, Kupffer cells in the liver and alveolar macrophages in the lung. The deletion of FcγRIIB on circulating monocytes and splenic macrophages in the $Fc\gamma RIIB_{LysMCre}$ mice was extremely poor (data not shown). Effective deletion of the target gene is dependent upon high-level expression of Cre in the cell type of interest, so it is possible that the levels of Cre generated by the Lysozyme M promoter were not sufficient. It has also been shown that Lysozyme M is not constitutively expressed in resident splenic macrophages (Keshav et al., 1991).

The increased severity of NTN in the $Fc\gamma RIIB^{-/-}$ mice on a pure C57BL/6 background supports previous work that FcγRIIB expression is an important factor in determining disease outcome and that the severity seen, following deletion, is not solely an effect of the 129-derived flanking sequences on Chromosome 1 (Boross et al., 2011; Sharp et al., 2012; Suzuki et al., 1998).

At both the lower and higher doses of NTS, in Experiment 1 and Experiment 3 respectively, there was no increase in susceptibility to NTN in mice with FcγRIIB deleted from their B cells compared to WT mice. FcγRIIB on B cells is involved in the negative regulation of the BcR, and therefore plays a key role in antibody production. $Fc\gamma RIIB^{-/-}$ mice have already been shown to have hyper-reactive B cells that produce increased antibody titres in response to both thymus-dependent and thymus-independent antigens both on the 129/B6 and the pure B6 background (Boross et al., 2011; Takai et al., 1996). Interestingly, $Fc\gamma RIIB^{-/-}$ mice had lower levels of circulating mouse anti-sheep IgG compared to $Fc\gamma RIIB_{CD19Cre}$ mice in Experiment 1 and $Fc\gamma RIIB_{CD11cCre}$ and $Fc\gamma RIIB_{Mcpt5Cre}$ mice in Experiment 2. This is likely due to the increase in glomerular damage, as these mice had severe levels of proteinuria. In Experiment 3, mice lacking FcγRIIB on B cells had increased circulating levels of total mouse anti-sheep IgG, that were significantly higher than myeloid cell knockouts but not the WT mice, most likely due to the wide range of antibody responses produced by the WT mice. There was no significant difference in antibody responses between the WT mice and the $Fc\gamma RIIB_{cEBP\alpha Cre}$ mice, although the WT mice trended towards having higher levels of circulating antibody. This can again be attributed to the wide range of antibody responses by the WT mice and the increased proteinuria in the myeloid cell knockout mice. Ideally, for a more accurate measure of immune response, circulating antibody should be studied before the onset of proteinuria.

Transgenic overexpression of FcγRIIB on B cells was associated with reduced severity of CIA and SLE in mice, and reduced anti-collagen titres (Brownlie et al., 2008). However, NTN is not an autoimmune model and it is possible that, in the situation of generating antibody to foreign antigen, the antibody response is already sufficient in WT mice to produce enough antibody to induce maximal nephritis. In contrast, in the situation of autoimmunity, such as SLE or EAG (Sharp et al., 2012) tolerance mechanisms exist to prevent excessive production of autoantibodies in WT mice. In this situation, the overproduction of antibody induced by the deficiency of FcγRIIB on B cells may be more critical in the generation of disease.

In addition, the levels of antibody themselves may not be a key determinant of NTN disease severity, as T cell responses are also important. This was highlighted in a study using mice lacking the μ immunoglobulin heavy chain gene. Homozygous μ-chain deficient mice fail to develop mature B cells or produce antibody but have intact cell-mediated immunity, whereas heterozygous μ-chain deficient mice demonstrate normal antibody responses. Following induction of NTN, there was no difference in the severity of renal injury between the two groups of mice, despite mouse immunoglobulin being absent from the serum and glomeruli of the homozygous mice, suggesting glomerular damage can occur independent of the humoral immune response to planted glomerular antigen (Li et al., 1997).

There was no significant difference in glomerular deposition of sheep IgG between any of the mice in the three experiments. However, FcγRIIB$^{-/-}$ had greater deposition of mouse IgG in glomeruli than WT and FcγRIIB$_{CD19Cre}$ mice in Experiment 1 and FcγRIIB$_{cEBP\alpha Cre}$ mice in Experiment 2. There was no significant difference in glomerular deposition of mouse IgG between the three groups of mice in Experiment 3. These results are difficult to interpret fully, due to the glomerular damage in the mice with more disease. However, FcγRIIB has been found to be involved in immune complex clearance by liver endothelial cells (Mousavi et al., 2007) and could be playing similar role within the glomerulus. This also provides a possible explanation for the lower levels of homologous antibody deposition in the FcγRIIB$_{CD19Cre}$ mice in Experiment 3, despite increased circulating titres.

At a higher dose of NTS, there was an increase in renal dysfunction (increased serum urea and increased albuminuria), neutrophil infiltration and glomerular injury (thrombosis) in the myeloid cell knockouts compared to WT and B cell knockouts, directly linking expression of FcγRIIB on myeloid cells to the development of GN. This supports previous

work looking at activating FcγR in accelerated NTN. Bergtold *et al.* generated transgenic FcRγ$^{-/-}$ mice expressing FcRγ on myeloid cells alone, under the control of the CD11b promoter. Induction of NTN resulted in severe disease in the WT mice whereas FcRγ$^{-/-}$ mice were protected. However, mice only expressing FcRγ on their myeloid cell compartment developed moderate disease, indicating that the presence of activating Fc receptors on CD11b-expressing cells is sufficient for NTN induction (Bergtold et al., 2006). In our recent publication, deletion of FcγRIIB on myeloid cells alone did not increase the incidence of EAG compared to full knockouts. However, first it must be noted that this publication used Cre expressed under the Lysozyme M promoter so there was only a 50% reduction of FcγRIIB expression on circulating monocytes and a smaller reduction in expression on circulating neutrophils and splenic macrophages (Sharp et al., 2012). Secondly, EAG is an autoimmune model of GN and it is necessary to break tolerance to induce disease. Therefore, it could be that FcγRIIB needs to be deleted from both the myeloid cells and B cells to increase susceptibility in EAG.

A small influx of neutrophils and macrophages into the glomerulus was seen in all three groups of mice. Mice lacking FcγRIIB on myeloid cells had a significantly greater neutrophil infiltration compared to WT and B cell knockouts; however, interestingly, there was no significant difference in macrophage infiltration. Neutrophils are one of the first inflammatory cells recruited to sites following the initiation of an immune reaction. FcγR are thought to play a role in neutrophil recruitment; FcRγ$^{-/-}$ and FcγRIII$^{-/-}$ mice both display strongly diminished recruitment of neutrophil effector cells during anti-GBM disease (Coxon et al., 2001). Therefore, FcγRIIB expression on neutrophils could be playing a role in the negative regulation of neutrophil recruitment.

Macrophages are known to be important effector cells in GN. Reduced surface expression of FcγRIIB on macrophages was associated with heightened responses following activatory FcγR cross-linking; including increased intracellular calcium flux, superoxide production, and pro-inflammatory cytokine release (Clatworthy and Smith, 2004; Pritchard et al., 2000). In a study looking at the role of FcγRIV in accelerated NTN, treatment with intravenous Ig (IVIG) was found to protect mice from developing renal pathology. Closer examination revealed IVIG induced on macrophages, but not neutrophils, upregulation of FcγRIIB and downregulation of FcγRIV. Additionally, the protective properties of IVIG were ablated in FcγRIIB$^{-/-}$ mice (Kaneko et al., 2006). The mechanism for IVIG protection has recently been determined. $T_h2$ cytokines, such as IL-4, are known to upregulate myeloid

expression of FcγRIIB (Pricop et al., 2001). The sialylated IgG component of human IVIG binds to a lectin receptor on dendritic cells, leading to secretion of IL-33. IL-33 in turn upregulates IL-4 secretion by basophils, leading to increased expression of FcγRIIB on myeloid cells (Anthony et al., 2011). These results support the importance of FcγRIIB on myeloid cells in the protection from GN. Therefore, a mechanism of action of IVIG may be the modulation of expression of FcγRIIB on myeloid cells.

Reduced expression of FcγRIIB on macrophages, leading to uncontrolled activation, could be involved in exacerbating GN in the myeloid cell knockouts. To determine if there was overactivation of macrophages in $FcγRIIB_{cEBPαCre}$ mice we analysed whole kidney mRNA levels for MCP-1, TNF-α, MR and IFN-γ. However, we did not find any significant increase in cytokines associated with the activation of macrophages in the myeloid cell knockout mice. As mentioned in Section 3.5, the use of whole kidney mRNA is not ideal to study cytokine expression levels because it is not possible to determine which cells are producing which cytokines. An alternative would be to isolate the glomeruli by sieving before mRNA analysis, or culture the glomeruli and measure cytokine secretion into the supernatant. Again though, from using whole glomeruli it would not be clear whether resident renal cells, such as mesangial cells, or infiltrating macrophages, are producing the cytokines or chemokines. To decipher fully the role of FcγRIIB on macrophages and neutrophils in GN, Cre would need to be downstream of more specific promoter.

At a low dose of NTS, there was no significant increase in susceptibility to renal dysfunction or inflammation in the mice with FcγRIIB deleted from dendritic cells, mast cells or myeloid cells compared to WT mice, whereas $FcγRIIB^{-/-}$ mice showed severe signs of disease. The presence of disease in the $FcγRIIB^{-/-}$ mice, as well as circulating anti-sheep IgG and deposited glomerular sheep and mouse IgG, suggests that expression of FcγRIIB by other circulating cells, and possibly intrinsic renal cells such as mesangial cells (Ichii et al., 2008; Radeke et al., 2002), can protect from NTN during mild disease.

As already mentioned, cEBPα is expressed in early myeloid cell progenitors. In the myeloid cell knockout mice this has lead to the deletion of FcγRIIB on a subset of splenic dendritic cells. Blockade of FcγRIIB on dendritic cells was found to result in their spontaneous maturation (Boruchov et al., 2005; Dhodapkar et al., 2005). Mature tissue-resident dendritic cells are potent APC and activators of T cells. Dendritic cells from $FcγRIIB^{-/-}$ mice were found to generate a stronger and longer lasting immune response (Kalergis and Ravetch, 2002). Therefore, the deletion of FcγRIIB on dendritic cells could be

contributing to the exacerbation of disease seen in these mice. To answer this question, it would be necessary to repeat the higher dose experiment in the mice with FcγRIIB expression under the control of the CD11c promoter. It would also be of interest to compare dendritic cell and T cell infiltration in the mice and to look more specifically at T cell responses by measuring both proliferation and cytokine production *in vitro.* This could help determine whether antigen presentation is enhanced by deletion of FcγRIIB on dendritic cells and whether this is contributing to the increased susceptibility to disease seen in FcγRIIB$^{-/-}$ mice.

Recently, mast cells have been implicated in GN, where they can exert either beneficial or detrimental effects, dependent on whether disease is acute or chronic, respectively. Mast cell-deficient mice were found to be protected from disease in non-accelerated NTN (Timoshanko et al., 2006); however, following induction of accelerated NTN or vasculitic GN, renal injury was exacerbated (Eller et al., 2011; Gan et al., 2012; Hochegger et al., 2005; Kanamaru et al., 2006). Both Eller *et al.* and Gan *et al.* have gone on to show that during acute disease mast cells migrate to the draining lymph nodes where they enhance immunosuppression by $T_{reg}$ (Eller et al., 2011; Gan et al., 2012), likely through the production of IL-10 (Gan et al., 2012). However, they disagree on which cells recruit which; Eller *et al.* claim IL-9 production by $T_{reg}$ recruits mast cells whereas Gan *et al.* believe IL-10 production by mast cells recruits $T_{reg}$ (Eller et al., 2011; Gan et al., 2012). It would be interesting to locate mast cells in our disease model and determine whether FcγRIIB$^{-/-}$ mast cells secrete IL-10 in GN to the same extent as WT mast cells. It is difficult to predict the outcome of FcγRIIB deletion on mast cells, as we cannot compare directly complete cell deletion with single receptor deletion. Mast cell degranulation is enhanced in FcγRIIB$^{-/-}$ mice, suggesting that accelerated NTN could be exacerbated in FcγRIIB$_{Mcpt5Cre}$ mice. We did not see an effect in the FcγRIIB$_{Mcpt5Cre}$ mice when a mild form of disease was induced in Experiment 2, but this experiment was performed only once and further work is required to optimise the disease induction.

As already shown, FcγRIIB$^{-/-}$ mice show enhanced macrophage recruitment compared to WT mice, whereas glomerular macrophage infiltration is similar between WT and FcγRIIB$_{cEBP\alpha Cre}$ mice. This suggests that FcγRIIB expression on macrophages is not involved in the recruitment of the cells to sites of inflammation. One of the key cytokines involved in the recruitment of macrophages is MCP-1, which can be produced by intrinsic renal cells (Zoja et al., 1991). Therefore, it could be that FcγRIIB on intrinsic renal cells is involved in

the negative regulation of cytokine production, and therefore macrophage recruitment, to the glomerulus during injury. It would be of interest to compare directly the macrophage recruitment properties of WT and FcγRIIB$^{-/-}$ mesangial cells using a cell migration assay.

A limitation of these experiments was that it was necessary to terminate some of the experiments at an earlier time point than planned after the induction of NTN due to the fact that the FcγRIIB$^{-/-}$ mice were highly susceptible to disease. Generally it is preferable to maintain mice for at least 7 days to allow the development of glomerular crescents. In all experiments mice were monitored closely and sacrificed if they were showing signs of ill health. The degree of proteinuria and GN generated is determined to an extent on operator dependent differences in the generation of the immunogen for preimmunisation and can be difficult to predict. In addition, prevalent immunogens in the environment of different animal facilities, which may differ at different times, can also influence the course of GN, and these experiments were performed at LUMC, whereas the rest of the experiments discussed in this thesis were performed at Imperial College London.

## 5.6 Conclusion

In conclusion, FcγRIIB$^{-/-}$ mice on a pure C57BL/6 background have exacerbated disease following induction of accelerated NTN compared to WT mice. Deletion of FcγRIIB on B cells alone was insufficient to demonstrate the phenotype at either a low or high dose of NTS. However, at a high dose of NTS, mice lacking FcγRIIB on myeloid cells had increased susceptibility to NTN compared with WT mice. This highlights the importance of FcγRIIB on myeloid cells in NTN. However, mice with myeloid cell deletion of FcγRIIB were not as susceptible to NTN as mice with full deletion of FcγRIIB. It is unclear whether this is because the Cre-mediated deletion on myeloid cells was not fully complete, or whether FcγRIIB on intrinsic renal cells is playing a role. This possibility is investigated in the next chapter of this thesis.

# CHAPTER 6

# The Role of Fc Gamma Receptor IIB on Circulating Leukocytes and Intrinsic Renal Cells in Accelerated Nephrotoxic Nephritis

## 6.1 Introduction

FcγRIIB is widely expressed, being found on most cells of the lymphatic system, where it negatively regulates the activating FcγR and BcR. However, expression of FcγRIIB is not limited to these cells, as it has also been found to be expressed on non-lymphoid tissue, such as mesangial cells in the kidney (Radeke et al., 2002). Results presented in Chapter 5 showed that FcγRIIB$^{-/-}$ mice were highly susceptible to renal injury following a low dose of NTS. However, mice lacking FcγRIIB only on myeloid cells were less susceptible to disease than mice with the full deletion. This suggests expression of FcγRIIB by other cells could play a role in protecting the mice from accelerated NTN. We have ruled out a role for FcγRIIB on B cells in disease. Therefore, it was essential to investigate the importance of FcγRIIB expressed by intrinsic renal cells in the development of GN. To do this we created bone marrow chimeric mice because a cell-specific promoter for mesangial cells is not available. To confirm the role of FcγRIIB on myeloid cells, FcγRIIB$^{-/-}$ mice transplanted with WT bone marrow were compared to control FcγRIIB$^{-/-}$ mice transplanted with FcγRIIB$^{-/-}$ bone marrow. To assess whether FcγRIIB expressed on intrinsic renal cells was important in protection from NTN, WT mice were transplanted with FcγRIIB$^{-/-}$ bone marrow and compared to WT mice transplanted with WT bone marrow. We also confirmed that mesangial cells express FcγRIIB.

## 6.2 Aim

The final chapter of this thesis was focused on assessing whether expression of FcγRIIB on intrinsic renal cells plays a role in protection from accelerated NTN or whether it is down to myeloid cell FcγRIIB expression alone. I also confirmed mesangial cell expression of FcγRIIB.

## 6.3 Experimental design

In order to investigate if FcγRIIB expression on intrinsic renal cells, as well as myeloid cells, plays a role in protection from accelerated NTN, bone marrow transplantation experiments were performed. A single dose of whole body gamma irradiation was used to ablate the bone marrow of WT and FcγRIIB$^{-/-}$ mice. Immediately following irradiation, the mice received an intravenous injection of whole bone marrow. WT mice received bone marrow cells from FcγRIIB$^{-/-}$ mice (FcγRIIB$^{-/-}$→WT) and *vice versa* (WT→FcγRIIB$^{-/-}$). This resulted in WT mice expressing FcγRIIB on their intrinsic renal cells but not on their circulating leukocytes and FcγRIIB$^{-/-}$ expressing FcγRIIB on their circulating leukocytes but not on their intrinsic renal cells. As controls, WT mice were transplanted with WT bone marrow (WT→WT) and FcγRIIB$^{-/-}$ mice were transplanted with FcγRIIB$^{-/-}$ bone marrow (FcγRIIB$^{-/-}$→FcγRIIB$^{-/-}$). NTN was induced and disease was assessed in WT and FcγRIIB$^{-/-}$ bone marrow chimeric mice as previously described (see Section 3.3).

To confirm expression of FcγRIIB on mesangial cells, mesangial cells were isolated from WT and FcγRIIB$^{-/-}$ mice and cultured *in vitro*. mRNA was extracted from unstimulated and stimulated WT and FcγRIIB$^{-/-}$ mesangial cells and FcγRIIB expression assessed by qRT-PCR. Mesangial cells were also stained with a FITC-labelled monoclonal antibody specific for FcγRIIB.

## 6.4 Results

### 6.4.1 Bone marrow reconstitution

8Gy of irradiation was used, as previously optimised by Dr. Ruth Tarzi. The irradiated mice were intravenously injected with $1x10^7$ bone marrow cells harvested from the femur, tibia and humerus of donor sex-matched mice.

Bone marrow reconstitution was assessed by semi-quantitative PCR of DNA purified from blood taken at the end of the experiment. By mixing different concentrations of WT and FcγRIIB$^{-/-}$ DNA, I determined that the WT band could be determined if it constituted 5% or more of the total DNA, whereas the FcγRIIB$^{-/-}$ band could be detected if it constituted 25% or more of the total DNA (Figure 6.1). The greater sensitivity of the PCR for the WT band is likely to be because this band is shorter (359bp) in comparison to the FcγRIIB$^{-/-}$ band (600bp). Generally, shorter bands are favoured in amplification in competitive PCR reactions.

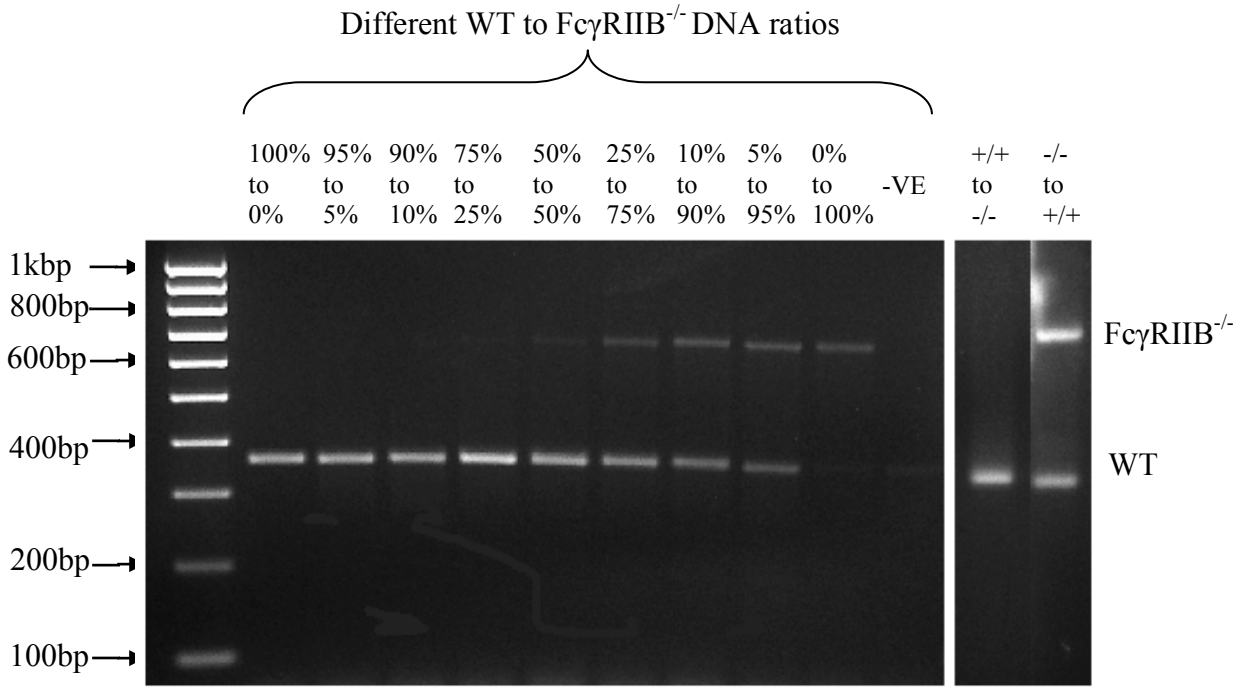


**Figure 6.1 Assessment of bone marrow reconstitution in chimeric mice by PCR.**

Different proportions of WT and FcγRIIB$^{-/-}$ DNA were mixed and subjected to PCR as described in Section 2.2.1.2. The WT band is 359bp and the FcγRIIB$^{-/-}$ band is 600bp. Note that the limit of detection of the WT band was 5% whereas the limit of detection of the FcγRIIB$^{-/-}$ band was 25%. In the same PCR reaction DNA from the two chimeric groups of mice were also run to examine the relative percentage of bone marrow reconstitution. In the WT to FcγRIIB$^{-/-}$ transplanted mice there was only the WT band indicating that the reconstitution was >75% (lane labelled +/+ to -/-). In the FcγRIIB$^{-/-}$ to WT transplanted mice both bands were detected, however the signal from the FcγRIIB$^{-/-}$ band was stronger, indicating that the reconstitution was also greater than >95% (lane labelled -/- to +/+).

### 6.4.2 Nephrotoxic nephritis in WT and FcγRIIB$^{-/-}$ bone marrow chimeric mice

The experiments performed are detailed in Table 6.1. In Experiments 1 and 2 male mice were used, and identical experiments were repeated in female mice in Experiments 3 and 4. Mice of both sexes were used due to the availability of mice and the requirements of the UK Home Office. After irradiation, bone marrow reconstitution was allowed to occur for 9 weeks before the induction of NTN. The female mice developed more disease than the male mice and needed to be sacrificed at an earlier time point after the injection of NTS (Table 6.1).

In Experiments 1 and 3, we determined whether the presence of FcγRIIB on intrinsic renal cells would protect from NTN by comparing WT mice transplanted with FcγRIIB$^{-/-}$ bone marrow with FcγRIIB$^{-/-}$ mice transplanted with FcγRIIB$^{-/-}$ bone marrow. In Experiments 2 and 4, we determined whether the absence of FcγRIIB on intrinsic renal cells would exacerbate disease in WT mice.

| | Sex | Donor | Recipient | Number transplanted | Sacrificed (Day) |
|---|---|---|---|---|---|
| **Experiment 1** | Male | FcγRIIB$^{-/-}$ | WT | 11 | 14 |
| | | FcγRIIB$^{-/-}$ | FcγRIIB$^{-/-}$ | 10 | |
| **Experiment 2** | Male | WT | FcγRIIB$^{-/-}$ | 12 | 12 |
| | | WT | WT | 10 | |
| **Experiment 3** | Female | FcγRIIB$^{-/-}$ | WT | 9 | 7* |
| | | FcγRIIB$^{-/-}$ | FcγRIIB$^{-/-}$ | 8 | |
| **Experiment 4** | Female | WT | FcγRIIB$^{-/-}$ | 6 | 7 |
| | | WT | WT | 10 | |

**Table 6.1 Summary of bone marrow transplant experiments in WT and FcγRIIB$^{-/-}$ mice.**

* One mouse in the FcγRIIB$^{-/-}$ group of mice transplanted with FcγRIIB$^{-/-}$ bone marrow was found dead at day 4, and another four in the same group sacrificed at day 5 due to renal disease. One mouse in the WT group transplanted with FcγRIIB$^{-/-}$ bone marrow was sacrificed at day 5. The remaining mice were sacrificed at day 7.

### 6.4.3 Mice with full deletion of FcγRIIB are more susceptible to NTN than WT mice transplanted with FcγRIIB$^{-/-}$ bone marrow, suggesting a role for FcγRIIB on intrinsic renal cells in protecting from disease

In Experiment 1, a low dose of NTS (1:20) was administered to WT and FcγRIIB$^{-/-}$ male mice transplanted with FcγRIIB$^{-/-}$ bone marrow. Whilst it is not always possible to control the severity of disease in this model, owing to the variations in the disease induced, a low dose was chosen so that only mild disease was induced, as otherwise the effect of the deletion of FcγRIIB on myeloid cells may have masked any protection from FcγRIIB on intrinsic renal cells.

PAS-stained kidney sections (Figure 6.2) were assessed for histological damage measured by glomerular capillary thrombosis and crescents. Transplantation of FcγRIIB$^{-/-}$ bone marrow into WT mice led to less susceptibility to thrombosis and crescents compared to FcγRIIB$^{-/-}$ mice transplanted with FcγRIIB$^{-/-}$ bone marrow (thrombosis: FcγRIIB$^{-/-}$→ FcγRIIB$^{-/-}$ 0.47 (0.16-1.3), FcγRIIB$^{-/-}$→WT 0.00 (0.00-0.12), p<0.0001; crescents: FcγRIIB$^{-/-}$ →FcγRIIB$^{-/-}$ 4.0 (0.00-18) %, FcγRIIB$^{-/-}$→WT 0.00 (0.00-0.00) %, p=0.0041) (Figure 6.3 A and Figure 6.3 B).

Twenty-four hour urine collections were obtained prior to sacrificing the animals and albuminuria was measured, expressed as a urinary albumin/creatinine ratio. Transplantation of FcγRIIB$^{-/-}$ bone marrow into WT mice led to less susceptibility to albuminuria when compared to FcγRIIB$^{-/-}$ mice transplanted with FcγRIIB$^{-/-}$ bone marrow (FcγRIIB$^{-/-}$ →FcγRIIB$^{-/-}$ 10 (0.36-18) mg/mmol, FcγRIIB$^{-/-}$→WT 0.026 (0.010-1.3) mg/mmol, p=0.0004) (Figure 6.4 A). Mouse sera collected at the end of the experiment were assessed for levels of serum urea. FcγRIIB$^{-/-}$ mice transplanted with FcγRIIB$^{-/-}$ bone marrow had significantly higher levels of serum urea compared to WT mice transplanted with FcγRIIB$^{-/-}$ bone marrow (FcγRIIB$^{-/-}$→FcγRIIB$^{-/-}$ 23 (12-40) mmol/L, FcγRIIB$^{-/-}$→WT 15 (12-23) mmol/L, p=0.045) (Figure 6.4 B).

Frozen kidney sections were stained for macrophage and neutrophil infiltration as a measure of inflammation at day 14 post NTS administration with anti-CD68 (macrophage) antibody (Figure 6.5 A) and anti-Gr-1 (neutrophil) antibody (Figure 6.6 A). FcγRIIB$^{-/-}$ mice transplanted with FcγRIIB$^{-/-}$ bone marrow had significantly more glomerular macrophages compared to WT mice transplanted with FcγRIIB$^{-/-}$ bone marrow (macrophages/gcs: FcγRIIB$^{-/-}$→FcγRIIB$^{-/-}$ 1.6 (0.64-3.1), FcγRIIB$^{-/-}$→WT 0.60 (0.12-1.7), p=0.0083) (Figure

6.5 B). There was no significant difference in glomerular neutrophil infiltration between either group of bone marrow transplanted mice (neutrophils/gcs: FcγRIIB$^{-/-}$→FcγRIIB$^{-/-}$ 0.71 (0.40-1.1), FcγRIIB$^{-/-}$→WT 0.78 (0.32-1.2, p=0.92) (Figure 6.6 B).

In Experiment 3, using female mice, a low dose of NTS (1:20) was again administered. On this occasion, the disease was more severe and unfortunately one of the nine FcγRIIB$^{-/-}$ mice transplanted with FcγRIIB$^{-/-}$ bone marrow was found dead at day 4 and 4/9 had to be killed at day 5, whereas only 1/8 WT mouse transplanted with FcγRIIB$^{-/-}$ bone marrow had to be killed at day 5. The rest of the mice were killed on day 7. Consistent with the results in Experiment 1, and allowing for the fact that there was no histology on one mouse that died early, there was a trend to more glomerular thrombosis in the FcγRIIB$^{-/-}$ mice transplanted with FcγRIIB$^{-/-}$ bone marrow compared to the WT mice transplanted with FcγRIIB$^{-/-}$ bone marrow (thrombosis score: FcγRIIB$^{-/-}$→FcγRIIB$^{-/-}$ 1.6 (0.28-3.0), FcγRIIB$^{-/-}$ →WT 0.34 (0.004-3.2), p=0.07) and there was a tendency to increased serum urea in the FcγRIIB$^{-/-}$ mice transplanted with FcγRIIB$^{-/-}$ bone marrow where serum was available (FcγRIIB$^{-/-}$→FcγRIIB$^{-/-}$ 49 (40-50) mmol/l, FcγRIIB$^{-/-}$→WT 20 (7.9-50) mmol/l, p=0.13).

These results from both Experiment 1 and Experiment 3 suggest that, in addition to expression of FcγRIIB on myeloid cells, FcγRIIB on intrinsic renal cells may also play a role in protection from NTN as the disease was worse in FcγRIIB$^{-/-}$ mice transplanted with FcγRIIB$^{-/-}$ bone marrow. Whilst these experiments were not performed concurrently, these results also highlight that female mice are much more susceptible to disease compared to their male counterparts.

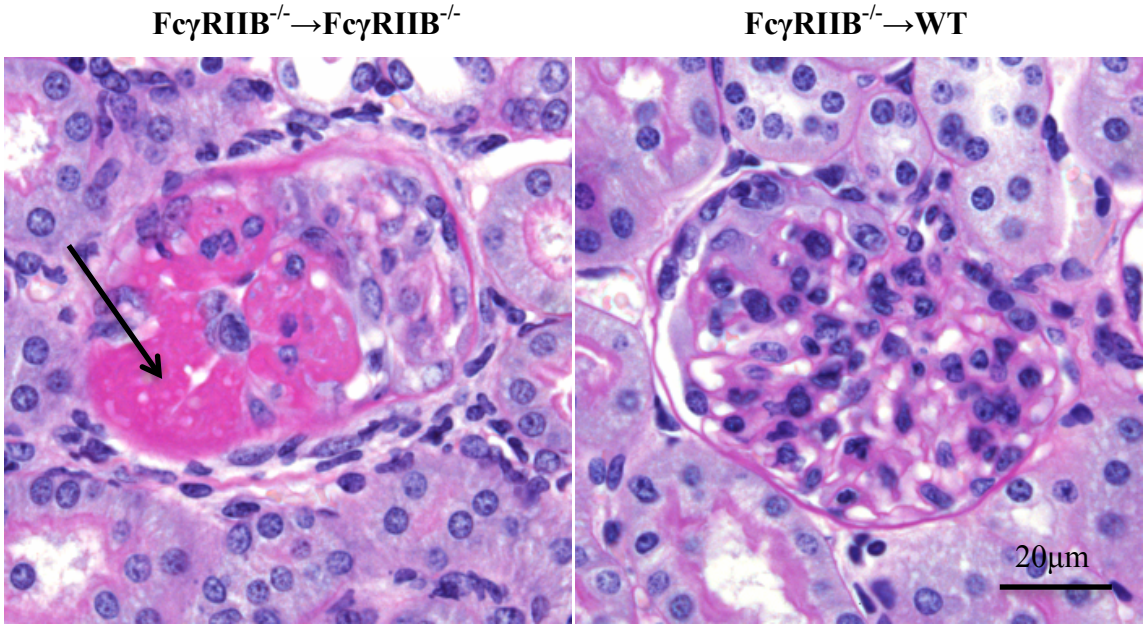


**Figure 6.2 PAS staining of kidneys from bone marrow transplanted mice with NTN, Experiment 1.**

Representative PAS staining: FcγRIIB$^{-/-}$→FcγRIIB$^{-/-}$mouse showing a thrombosed, crescentic glomerulus (arrow highlights area of thrombosis) and a FcγRIIB$^{-/-}$→WT mouse showing a healthy glomerulus.

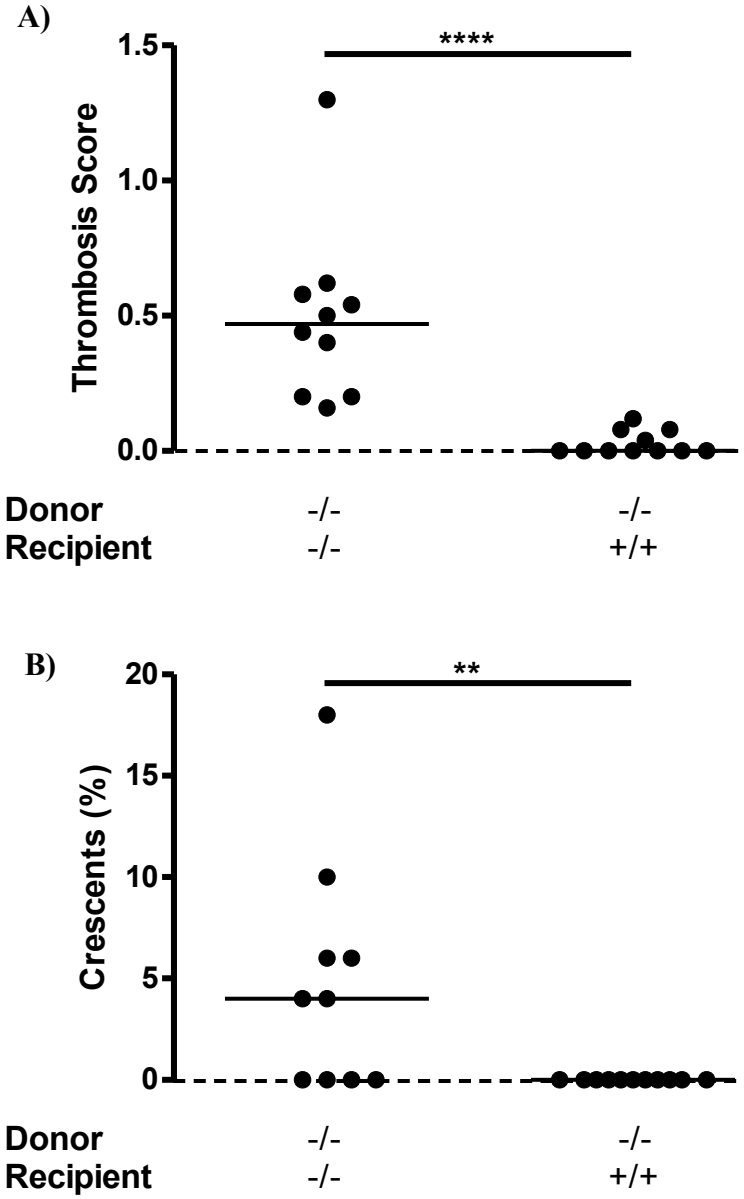


**Figure 6.3 Quantification of histologically abnormal glomeruli in bone marrow transplanted mice with NTN, Experiment 1.**

**(A)** Thrombosis and **(B)** crescents in bone marrow transplanted mice after NTN induction scored on PAS-stained kidney sections. FcγRIIB$^{-/-}$ mice that received FcγRIIB$^{-/-}$ bone marrow had more severely damaged glomeruli than WT mice receiving FcγRIIB$^{-/-}$ bone marrow (+/+ = WT, -/- = FcγRIIB$^{-/-}$). All data represent individual values with the median. The data were analysed using Mann-Whitney U-test (p**<0.01, p****<0.0001). Dashed line represents values for a group of normal WT mice.

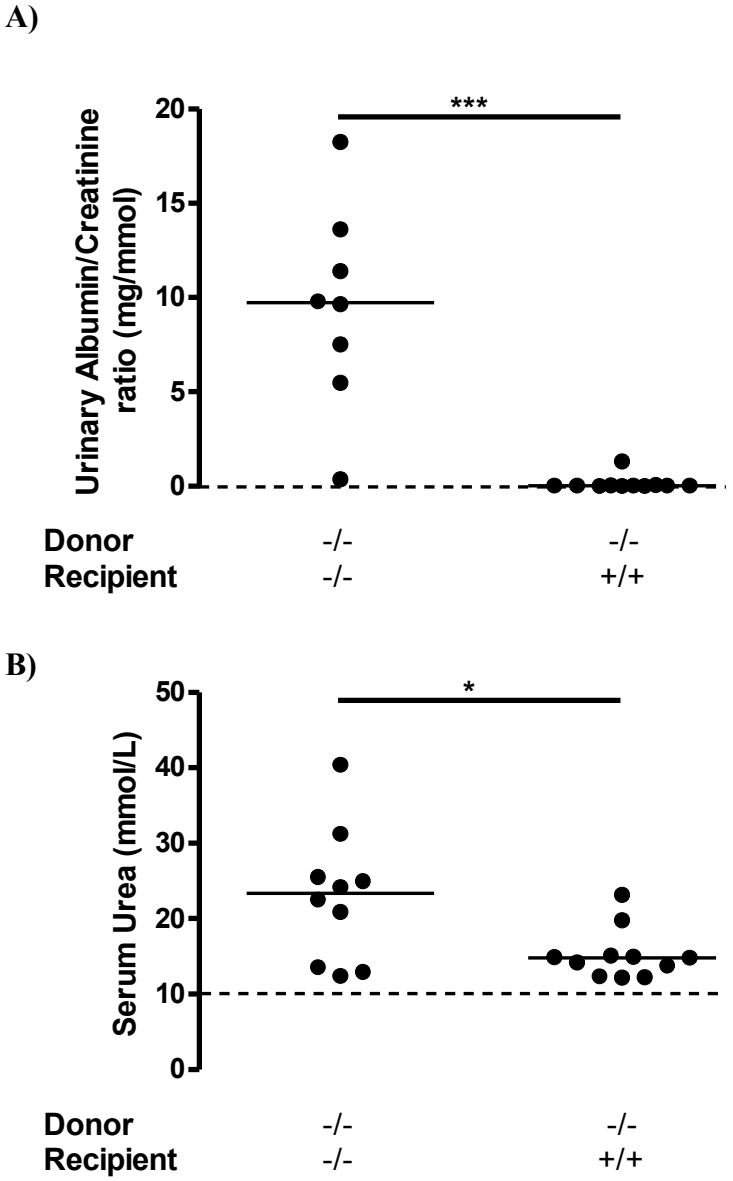


**Figure 6.4 Measurement of urinary albumin/creatinine ratio and serum urea in bone marrow transplanted mice with NTN, Experiment 1.**

**(A)** Urinary albumin/creatinine ratio and **(B)** serum urea titres following administration of NTS to bone marrow transplanted mice. FcγRIIB$^{-/-}$ mice transplanted with FcγRIIB$^{-/-}$ bone marrow had a wider range of values for both urinary albumin/creatinine ratio and serum urea, with exacerbated disease compared to WT mice transplanted with FcγRIIB$^{-/-}$ bone marrow (+/+ = WT, -/- = FcγRIIB$^{-/-}$). All data represent individual values with the median. The data were analysed using Mann-Whitney U-test ($p^{*}<0.05$, $p^{***}<0.001$). Dashed line represents values for a group of normal WT mice.

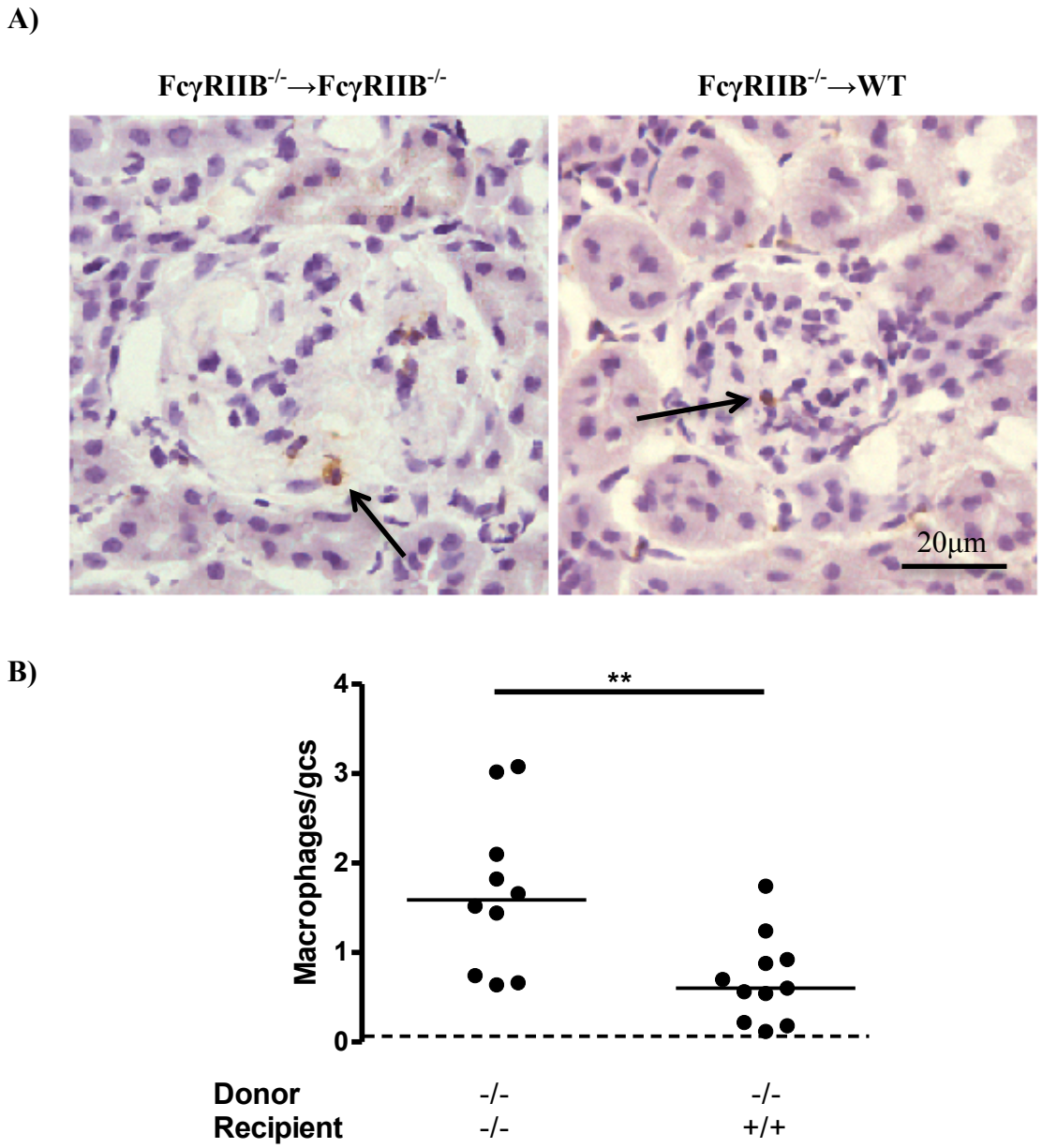


**Figure 6.5 Glomerular macrophage infiltration in bone marrow transplanted mice with NTN, Experiment 1.**

**(A)** Immunohistochemistry for macrophages (CD68) on FcγRIIB$^{-/-}$→ FcγRIIB$^{-/-}$ and FcγRIIB$^{-/-}$→WT kidney sections. Arrows highlight macrophages. **(B)** Macrophage infiltration per glomerular cross section (gcs) (50 glomeruli scored per cross section). FcγRIIB$^{-/-}$ mice transplanted with FcγRIIB$^{-/-}$ bone marrow had significantly more glomerular macrophages than WT mice transplanted with FcγRIIB$^{-/-}$ bone marrow (+/+ = WT, -/- = FcγRIIB$^{-/-}$). All data represent individual values with the median. The data were analysed using Mann-Whitney U-test (p**<0.01). Dashed line represents values for a group of normal WT mice.

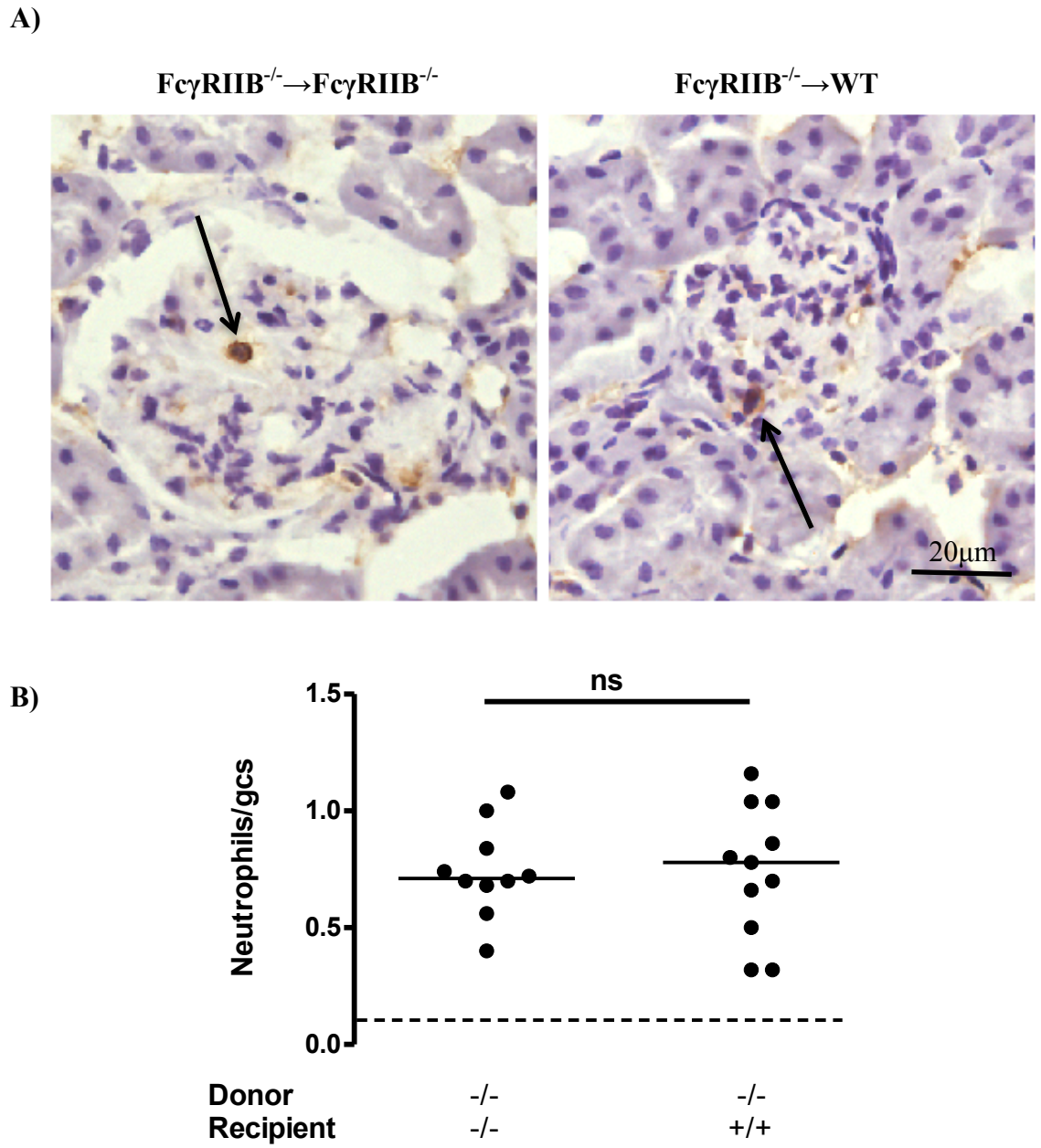


**Figure 6.6 Glomerular neutrophil infiltration in bone marrow transplanted mice with NTN, Experiment 1.**

**(A)** Immunohistochemistry for neutrophils (Gr-1) on FcγRIIB$^{-/-}$→FcγRIIB$^{-/-}$ and FcγRIIB$^{-/-}$ →WT kidney sections. Arrows highlight neutrophils. **(B)** Neutrophil infiltration per glomerular cross section (gcs) (50 glomeruli scored per cross section). There was no significant difference in neutrophil infiltration between the groups of mice (+/+ = WT, -/- = FcγRIIB$^{-/-}$). All data represent individual values with the median. The data were analysed using Mann-Whitney U-test (ns= non-significant). Dashed line represents values for a group of normal WT mice.

### 6.4.4 There is not enough evidence to show that deletion of FcγRIIB on intrinsic renal cells alone can exacerbate disease

In Experiment 2, the same dose of NTS (1:20) was administered to WT and FcγRIIB$^{-/-}$ male mice transplanted with WT bone marrow as in Experiment 1, to induce mild disease and to further assess the role of FcγRIIB on intrinsic renal cells or circulating leukocytes.

PAS-stained kidney sections were assessed for histological damage measured by glomerular capillary thrombosis and crescents (Figure 6.7). FcγRIIB$^{-/-}$ mice transplanted with WT bone marrow did not have exacerbated disease compared to WT mice transplanted with WT bone marrow (thrombosis: WT→FcγRIIB$^{-/-}$ 0.00 (0.00-0.30), WT→WT 0.00 (0.00-0.00), p=0.086; crescents: WT→FcγRIIB$^{-/-}$ 0.00 (0.00-2.0) %, WT→WT 0.00 (0.00-4.00) %, p=0.66) (Figure 6.8 A and Figure 6.8 B), despite the deletion of FcγRIIB on intrinsic renal cells.

Twenty-four hour urine collections were obtained prior to sacrificing the animals and albuminuria was measured, expressed as a urinary albumin/creatinine ratio. FcγRIIB$^{-/-}$ mice transplanted with WT bone marrow had significantly higher levels of albuminuria compared to WT mice transplanted with WT bone marrow (WT→FcγRIIB$^{-/-}$ 0.003 (0.0044-1.5) mg/mmol, WT→WT 0.0043 (0.0030-0.0098) mg/mmol, p=0.0072) (Figure 6.9 A), although most of the mice did not show significant albuminuria. Mouse sera samples collected at the end of the experiment were assessed for levels of serum urea. Surprisingly, in view of the lack of histological injury or albuminuria, WT mice transplanted with WT bone marrow had significantly higher serum urea compared to FcγRIIB$^{-/-}$ mice transplanted with WT bone marrow (WT→FcγRIIB$^{-/-}$ 6.4 (5.2-11) mmol/L, WT→WT 10 (7.3-12) mmol/L, p=0.005) (Figure 6.9 B). This anomalous result is unexplained, although the samples were not measured in our laboratory but in the clinical biochemistry department.

Frozen kidney sections were stained for macrophage and neutrophil infiltration at day 12 post NTS administration with anti-CD68 (macrophage antibody) (Figure 6.10 A) and anti-Gr-1 (neutrophil) antibody (Figure 6.11 A). FcγRIIB$^{-/-}$ mice transplanted with WT bone marrow had significantly more glomerular macrophages than WT mice transplanted with WT bone marrow (macrophages/gcs: WT→FcγRIIB$^{-/-}$ 0.30 (0.040-2.1), WT→WT 0.060 (0.00-0.72), p=0.0050) (Figure 6.10 B). There was no significant difference in glomerular neutrophil infiltration between either groups of bone marrow transplanted mice at this point, but neutrophil infiltration would be expected to be greater earlier in the course of disease

(neutrophils/gcs: WT→FcγRIIB$^{-/-}$ 0.76 (0.34-2.2), WT→WT 0.060 0.88 (0.16-1.7), p=0.64) (Figure 6.11 B).

In Experiment 4, using female mice, all mice were sacrificed on day 7 as the disease was more severe than in Experiment 2. As was found in Experiment 2, FcγRIIB$^{-/-}$ mice transplanted with WT bone marrow had significantly increased albuminuria (2.6 (0.0072-13) mg/mmol) compared with WT mice transplanted with WT bone marrow (0.032 (0.0029-1.5) mg/mmol, p=0.036) and there was a non-significant tendency towards increased glomerular capillary thrombosis (FcγRIIB$^{-/-}$ →WT 0.2 (0.0-1.0), WT→WT 0.060 (0.0-0.20), p=0.06). There was no significant difference in the macrophage infiltration between the groups and, unfortunately, we did not obtain enough serum from 2/6 FcγRIIB$^{-/-}$ mice transplanted with WT bone marrow to measure serum urea, so there were not enough samples for statistical analysis.

Therefore, whilst Experiment 1 and 3 showed evidence of a protective effect of FcγRIIB$^{-/-}$ on intrinsic renal cells, we were unable to demonstrate a clear exacerbation of disease in FcγRIIB$^{-/-}$ mice transplanted with WT bone marrow, other than a mild increase in albuminuria which was found in both Experiment 2 and Experiment 4, but no other statistically significant effects were consistently demonstrated.

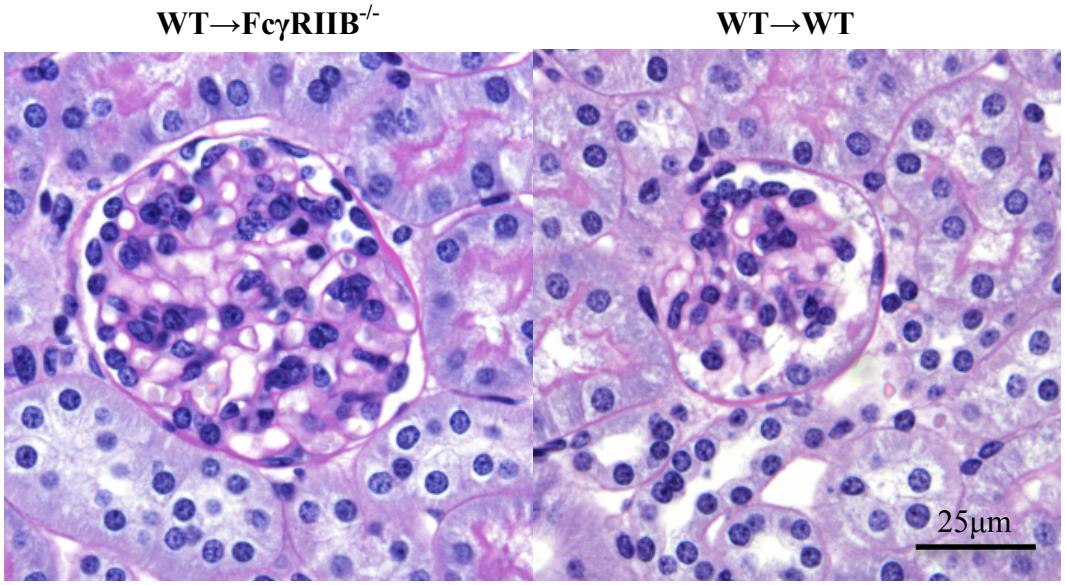


**Figure 6.7 PAS staining of kidneys from bone marrow transplanted mice with NTN, Experiment 2.**

Representative PAS staining: a WT→FcγRIIB$^{-/-}$ mouse and a WT→WT mouse, showing healthy glomeruli.

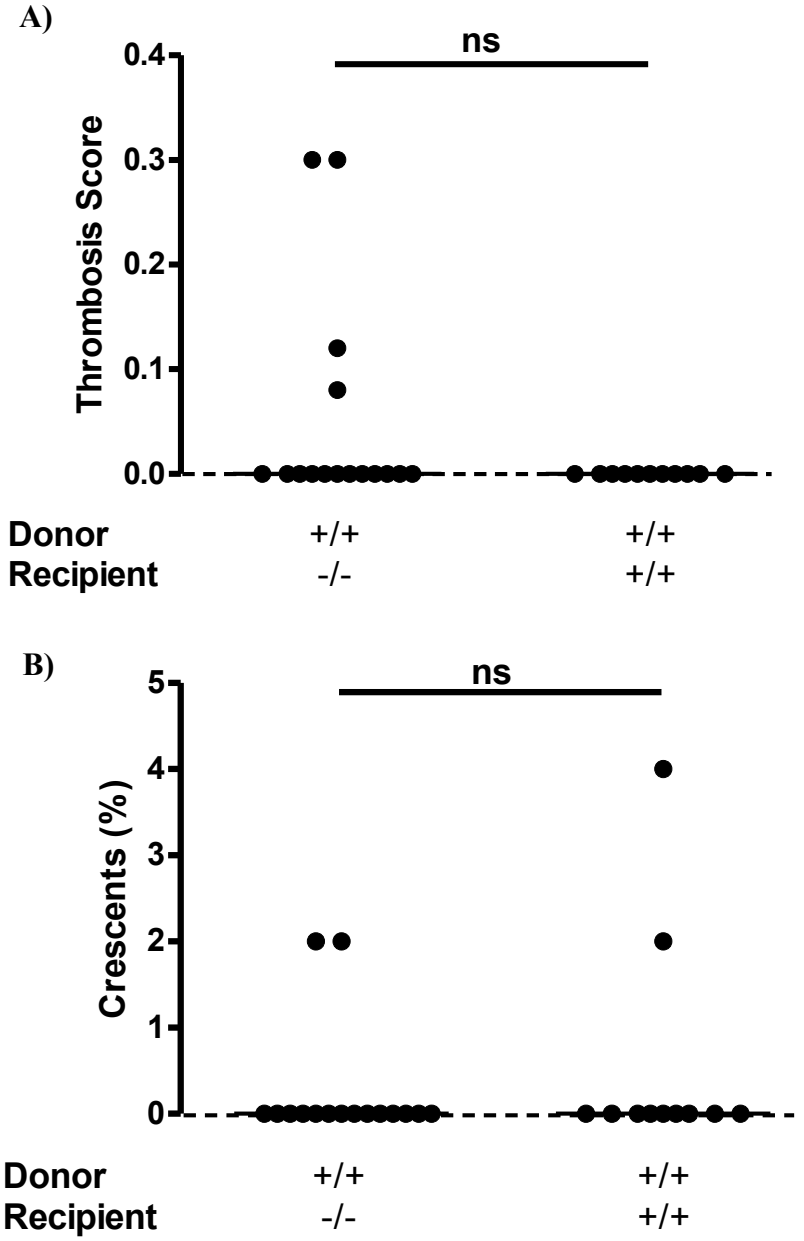


**Figure 6.8 Quantification of histologically abnormal glomeruli in bone marrow transplanted mice with NTN, Experiment 2.**

**(A)** Thrombosis and **(B)** crescents in bone marrow transplanted mice after NTN induction scored on PAS-stained kidney sections. There was no significant difference between the groups of mice (+/+ = WT, -/- = FcγRIIB$^{-/-}$). All data represent individual values with the median. The data were analysed using Mann-Whitney U-test (ns= non-significant). Dashed line represents values for a group of normal WT mice.

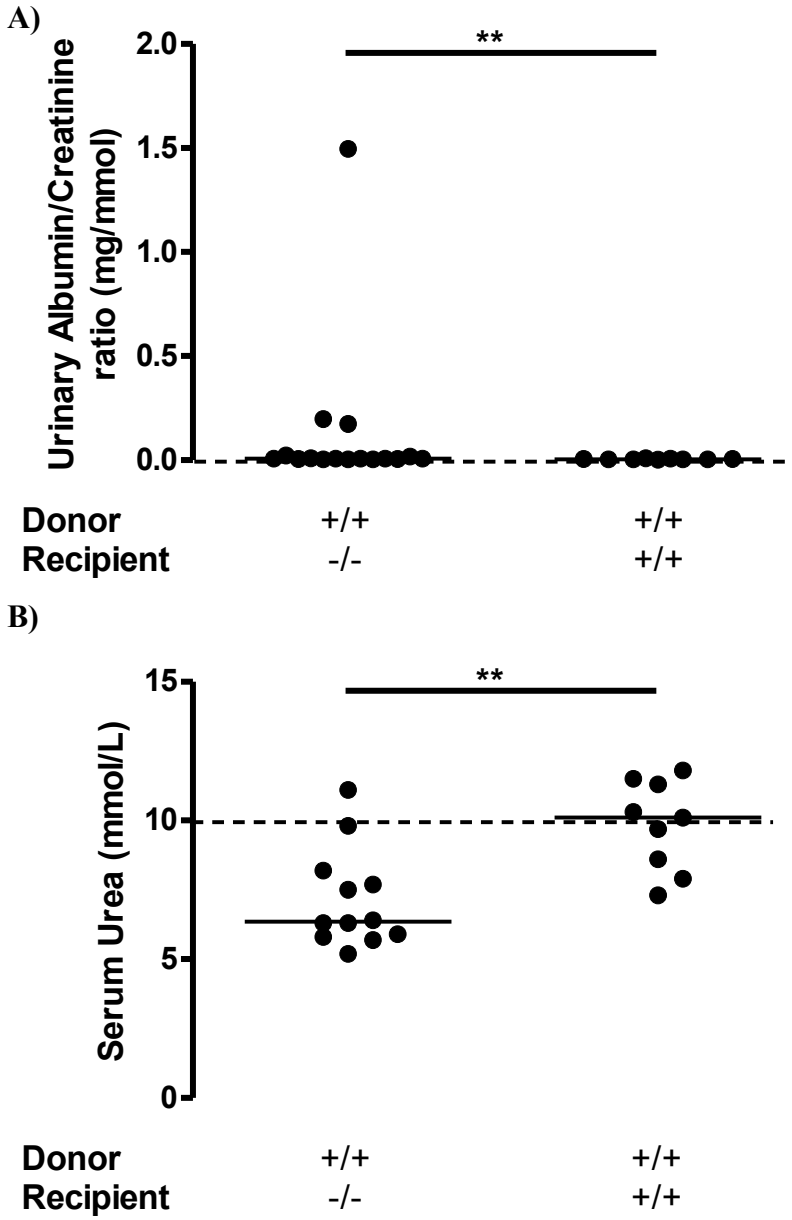


**Figure 6.9 Measurement of urinary albumin/creatinine ratio and serum urea in bone marrow transplanted mice with NTN, Experiment 2.**

**(A)** Urinary albumin/creatinine ratio and **(B)** serum urea levels following administration of NTS to bone marrow transplanted mice. FcγRIIB$^{-/-}$ mice transplanted with WT bone marrow had a significantly higher urinary albumin/creatinine ratio and significantly lower serum urea than WT mice transplanted with WT bone marrow (+/+ = WT, -/- = FcγRIIB$^{-/-}$). All data represent individual values with the median. The data were analysed using Mann-Whitney U-test (p**<0.01). Dashed line represents values for a group of normal WT mice.

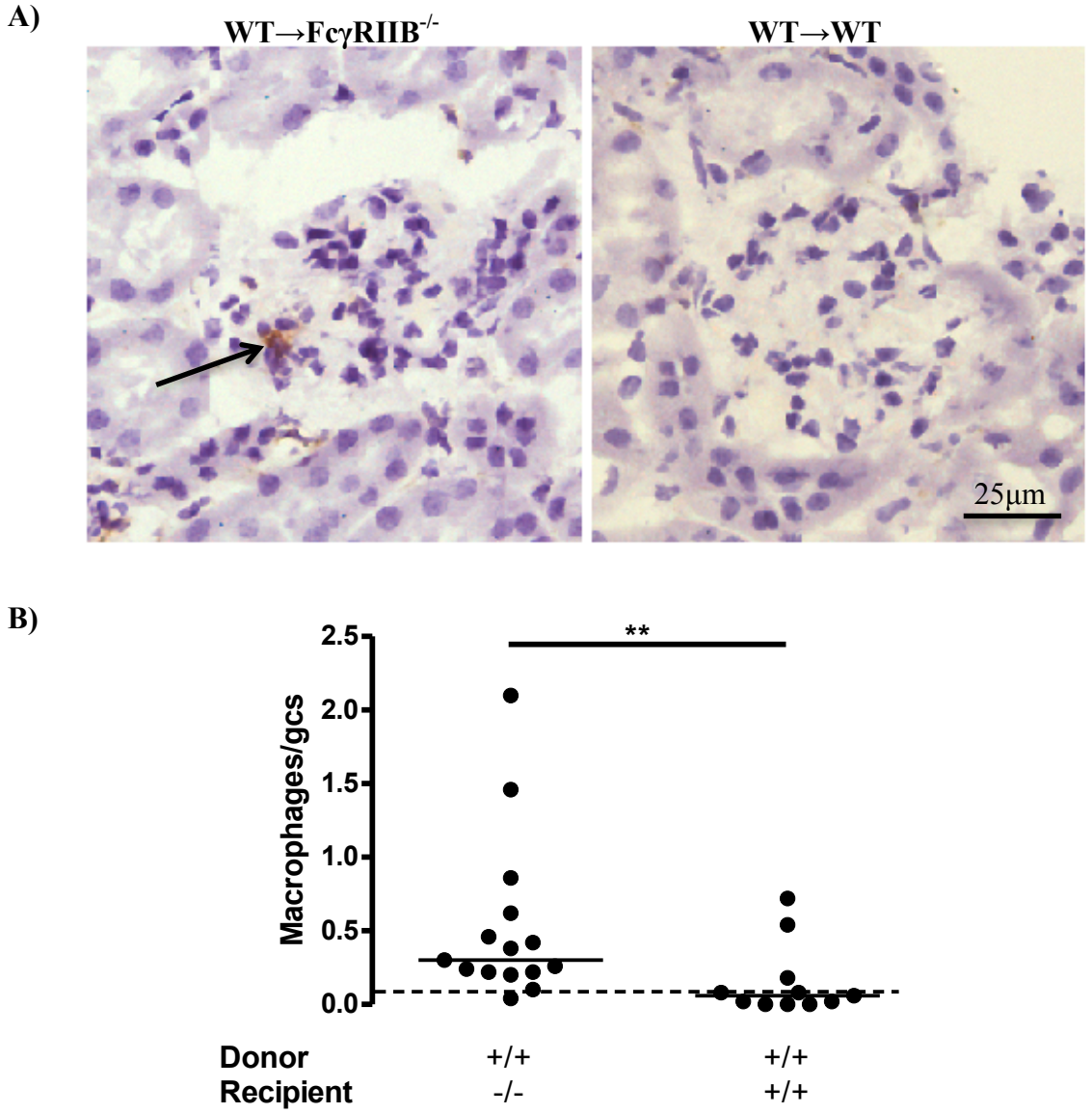


**Figure 6.10 Glomerular macrophage infiltration in bone marrow transplanted mice with NTN, Experiment 2.**

**(A)** Immunohistochemistry for macrophages (CD68) on WT→FcγRIIB$^{-/-}$ and WT→WT kidney sections. Arrow highlights macrophage. **(B)** Macrophage infiltration per glomerular cross section (gcs) (50 glomeruli scored per cross section). FcγRIIB$^{-/-}$ mice transplanted with WT bone marrow had significantly more glomerular macrophages than WT mice transplanted with WT bone marrow (+/+ = WT, -/- = FcγRIIB$^{-/-}$). All data represent individual values with the median. The data were analysed using Mann-Whitney U-test (p**<0.01). Dashed line represents values for a group of normal WT mice.

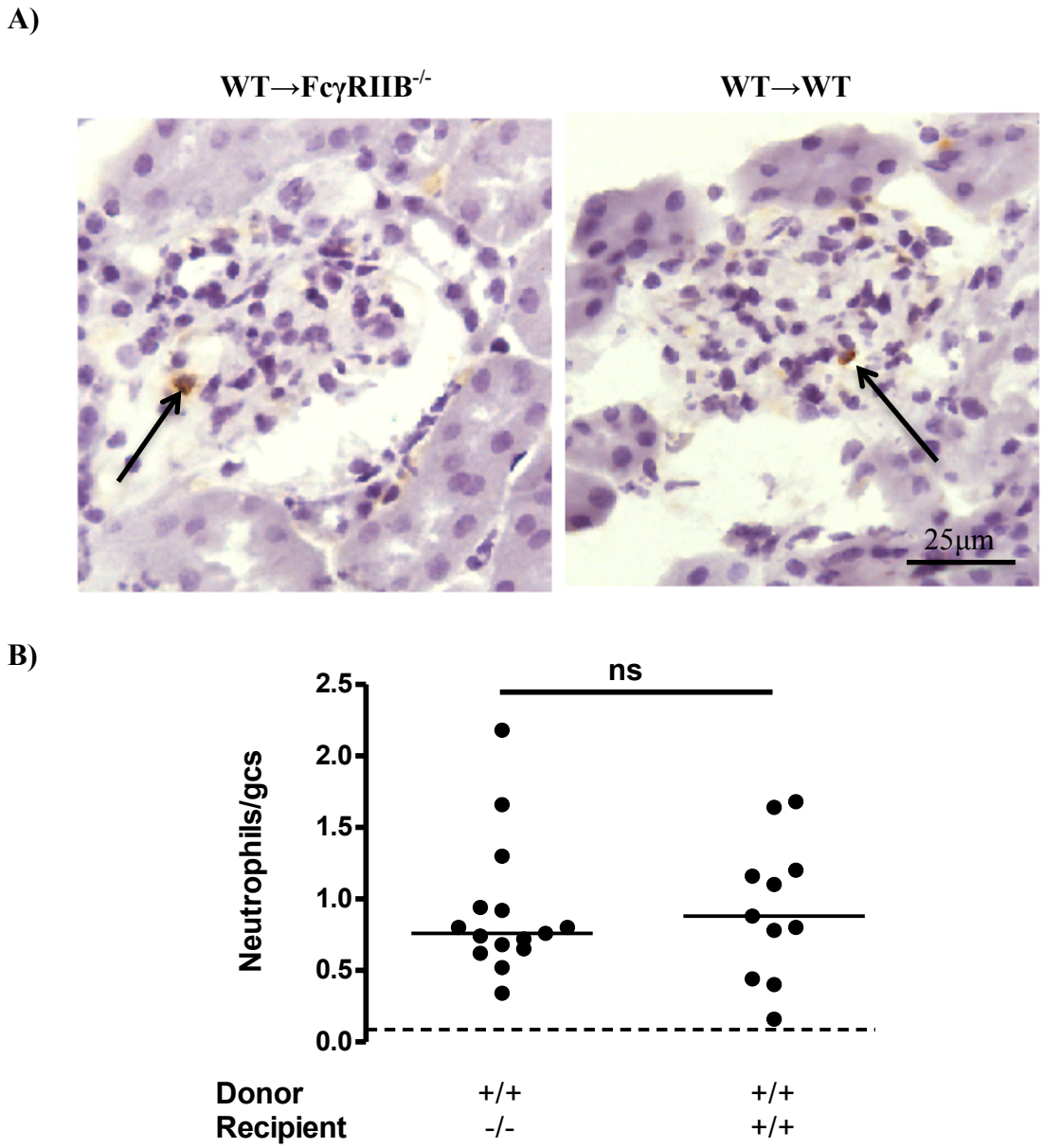


**Figure 6.11 Glomerular neutrophil infiltration in bone marrow transplanted mice with NTN, Experiment 2.**

**(A)** Immunohistochemistry for neutrophils (Gr-1) on WT→FcγRIIB$^{-/-}$ and WT→WT kidney sections. Arrows highlight neutrophils. **(B)** Neutrophil infiltration per glomerular cross section (gcs) (50 glomeruli scored per cross section). There was no significant difference in neutrophil infiltration between the groups of mice in each experiment (+/+ = WT, -/- = FcγRIIB$^{-/-}$). All data represent individual values with the median. The data were analysed using Mann-Whitney U-test (ns= non-significant). Dashed line represents values for a group of normal WT mice.

### 6.4.5 Systemic immune responses of bone marrow transplanted mice

Mouse serum, collected at the end of the experiments, was tested for the antigen-specific immune response against sheep IgG. The circulating mouse anti-sheep IgG levels were measured by ELISA (results expressed as median optical density at 405nm (OD 405nm)). In Experiment 1, FcγRIIB$^{-/-}$ mice receiving FcγRIIB$^{-/-}$ bone marrow had significantly less circulating mouse anti-sheep IgG than FcγRIIB$^{-/-}$ mice receiving WT bone marrow (FcγRIIB$^{-/-}$→FcγRIIB$^{-/-}$ vs. FcγRIIB$^{-/-}$→WT p=0.043) despite the fact that they had more renal disease. This is possibly explained by prolonged proteinuria with leakage of immunoglobulin into the urine. In Experiment 2, WT mice receiving WT bone marrow had significantly less circulating mouse anti-sheep IgG than WT mice receiving FcγRIIB$^{-/-}$ bone marrow (WT→FcγRIIB$^{-/-}$ vs. WT→WT p=0.048). However, this is of uncertain significance as there was no difference in deposited glomerular IgG between the two groups (Table 6.2 and Figure 6.12).

Frozen kidney sections were stained for deposited sheep and mouse IgG by direct immunofluorescence on tissue taken at the end of the experiment (Figure 6.13 A, Figure 6.14. A, Figure 6.15A, and Figure 6.16 A). Total glomerular sheep and mouse IgG were measured by quantitative immunofluorescence with the results expressed as arbitrary fluorescence units (AFU) or visual fluorescence units (VFU) (depending upon availability of equipment at the time the experiments were run). In Experiment 1, there was no significant difference between deposited sheep IgG (FcγRIIB$^{-/-}$→FcγRIIB$^{-/-}$ vs. FcγRIIB$^{-/-}$→WT p=0.28) (Figure 6.13 B) but there was significantly less deposited mouse IgG in FcγRIIB$^{-/-}$ mice transplanted with FcγRIIB$^{-/-}$ bone marrow (FcγRIIB$^{-/-}$→FcγRIIB$^{-/-}$ vs. FcγRIIB$^{-/-}$→WT p=0.032). This could be due to increased glomerular damage in these mice (Figure 6.15 B). In Experiment 2, there was no significant difference between the two groups for deposited sheep IgG (WT→FcγRIIB$^{-/-}$ vs. WT→WT p=0.54) (Figure 6.14 B) or mouse IgG (WT→FcγRIIB$^{-/-}$ vs. WT→WT p=0.54) (Figure 6.16 B).

| | Donor | Recipient | Serum anti-sheep IgG (OD 405nm) | Glomerular deposited sheep IgG (AFU) | Glomerular deposited mouse IgG (AFU) |
|---|---|---|---|---|---|
| **Experiment 1** | FcγRIIB$^{-/-}$ | FcγRIIB$^{-/-}$ | 2.1 (1.2-2.5) | 27 (16-75) | 24 (17-32) |
| | FcγRIIB$^{-/-}$ | WT | 2.4 (1.9-2.6) | 30 (18-90) | 30 (11-40) |
| **Experiment 2** | WT | FcγRIIB$^{-/-}$ | 2.1 (1.8-2.7) | 3.0 (1.0-3.0) | 115 (62-170) |
| | WT | WT | 1.9 (1.5-2.3) | 3.0 (2.0-3.0) | 97 (66-212) |

**Table 6.2 Deposited glomerular sheep and mouse IgG and circulating anti-sheep IgG levels in bone marrow transplanted mice with NTN.**

All results are expressed as median (range).

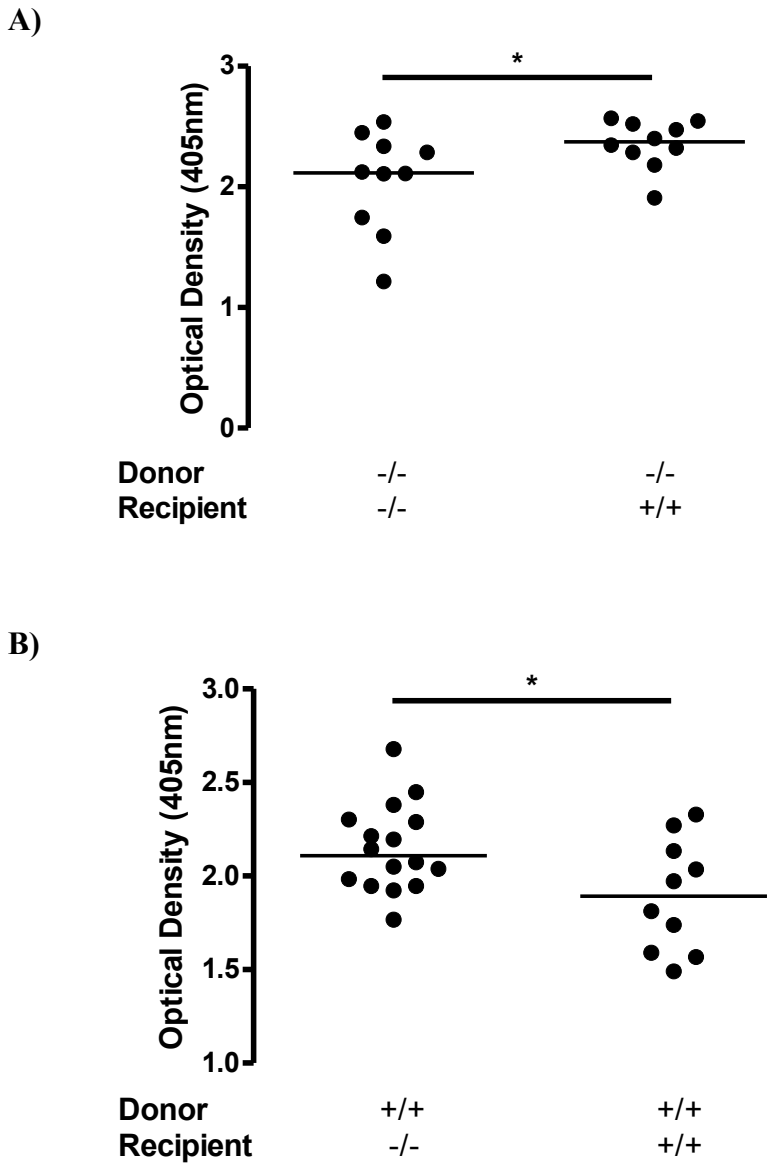


**Figure 6.12 Circulating mouse anti-sheep IgG levels in bone marrow transplanted mice with NTN, Experiment 1 and Experiment 2.**

Circulating mouse anti-sheep IgG was measured in **(A)** Experiment 1 and **(B)** Experiment 2 by ELISA. In Experiment 1, WT mice transplanted with FcγRIIB$^{-/-}$ bone marrow had slightly elevated levels of circulating mouse anti-sheep IgG compared to FcγRIIB$^{-/-}$ mice transplanted with FcγRIIB$^{-/-}$ bone marrow. In Experiment 2, FcγRIIB$^{-/-}$ mice transplanted with WT bone marrow, had slightly elevated levels of circulating mouse anti-sheep IgG compared to WT mice transplanted with WT bone marrow (+/+ = WT, -/- = FcγRIIB$^{-/-}$). All data represent individual values with the median. The data were analysed using Mann-Whitney U-test ($p^*<0.05$).

**A)**

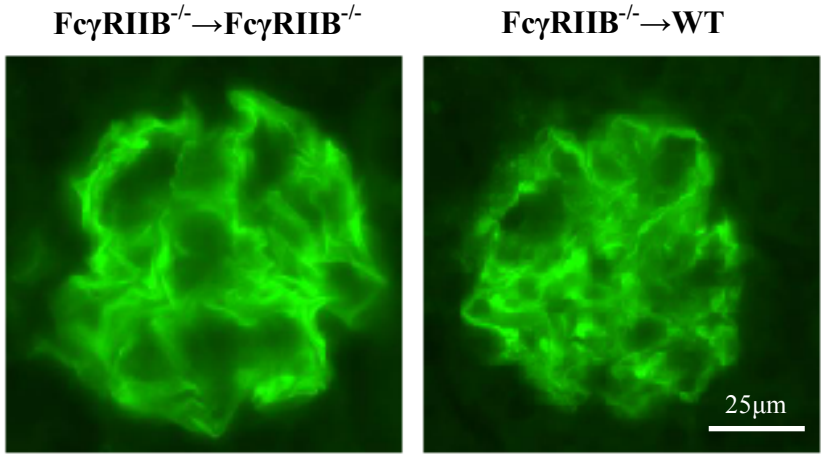


**B)**

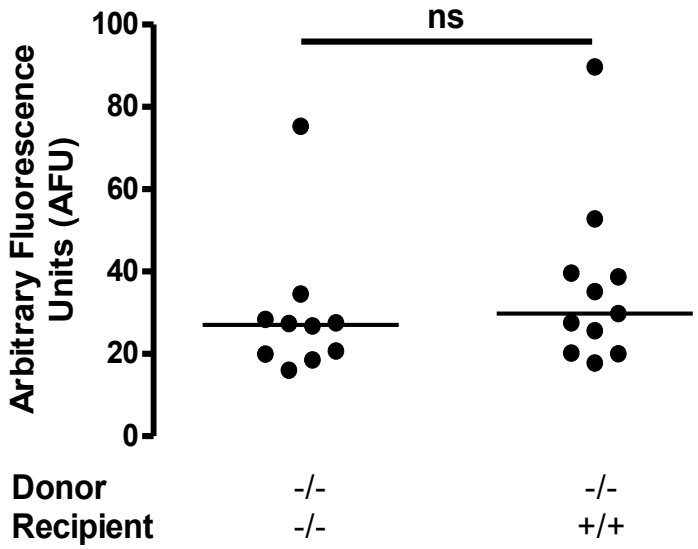


**Figure 6.13 Immunofluorescence for glomerular sheep IgG deposition in bone marrow transplanted mice with NTN, Experiment 1.**

**(A)** Representative glomeruli from FcγRIIB$^{-/-}$→FcγRIIB$^{-/-}$ mice and FcγRIIB$^{-/-}$→WT mice showing sheep IgG deposition. All images were taken using the same settings. **(B)** Relative mean glomerular immunofluorescence was measured quantitatively and expressed as arbitrary fluorescence units (AFU). There was no significant difference in deposited sheep IgG between the mice (+/+ = WT, -/- = FcγRIIB$^{-/-}$). All data represent individual values with the median. The data were analysed using Mann-Whitney U-test (ns= non-significant).

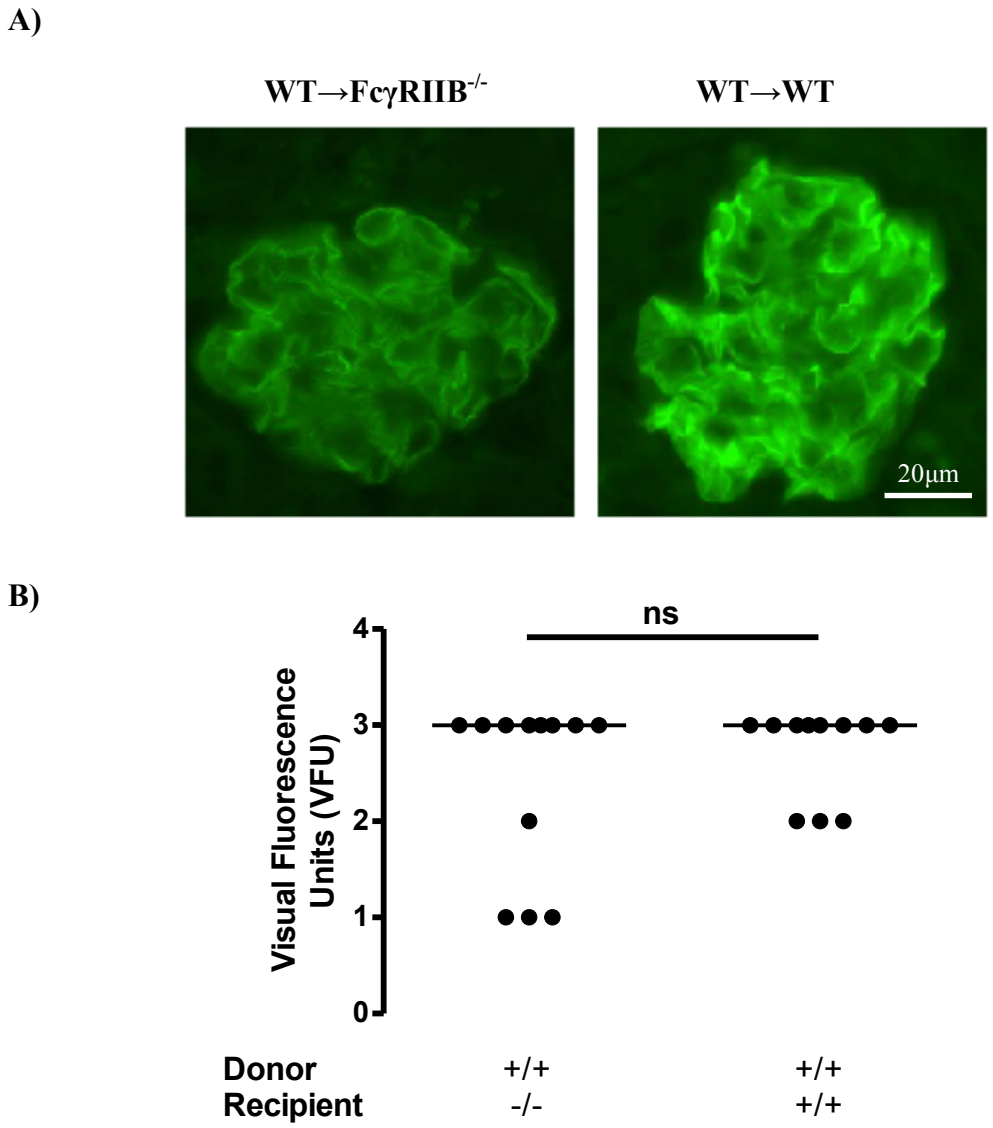


**Figure 6.14 Immunofluorescence for glomerular sheep IgG deposition in bone marrow transplanted mice with NTN, Experiment 2.**

**(A)** Representative glomeruli from WT→FcγRIIB$^{-/-}$ mice and WT→WT mice showing sheep IgG deposition. All images were taken using the same settings. **(B)** Relative mean glomerular immunofluorescence was measured quantitatively and expressed as visual fluorescence units (VFU). FcγRIIB$^{-/-}$ mice transplanted with WT bone marrow had significantly less deposited sheep IgG compared to WT mice transplanted with WT bone marrow (+/+ = WT, -/- = FcγRIIB$^{-/-}$). All data represent individual values with the median. The data were analysed using Mann-Whitney U-test (ns= non-significant).

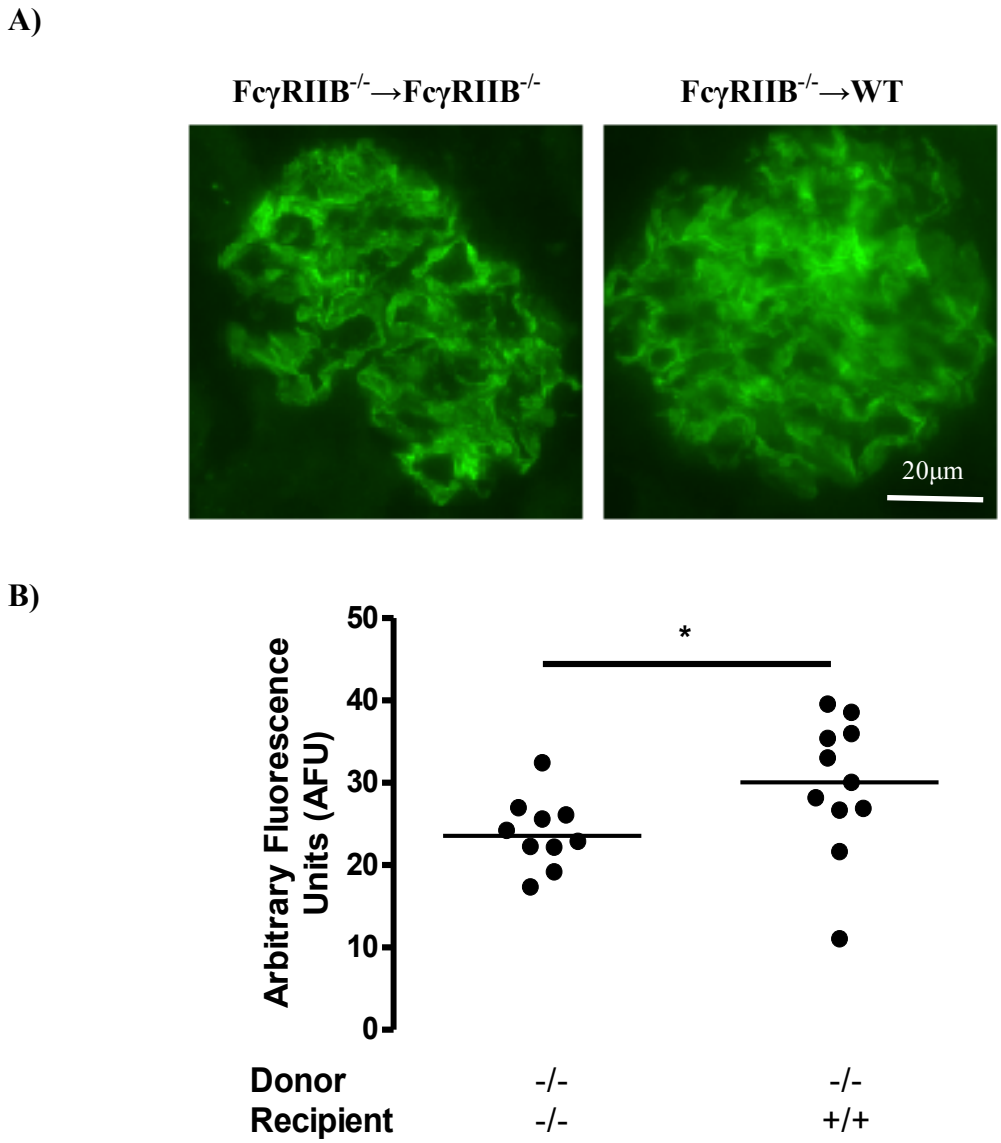


**Figure 6.15 Immunofluorescence for glomerular mouse IgG deposition in bone marrow transplanted mice with NTN, Experiment 1.**

**(A)** Representative glomeruli from FcγRIIB$^{-/-}$→FcγRIIB$^{-/-}$ mice and FcγRIIB$^{-/-}$→WT mice showing mouse IgG deposition. All images were taken using the same settings. **(B)** Relative mean glomerular immunofluorescence was measured quantitatively and expressed as arbitrary fluorescence units (AFU). FcγRIIB$^{-/-}$ mice transplanted with FcγRIIB$^{-/-}$ bone marrow had significantly less deposited mouse IgG than WT mice transplanted with FcγRIIB$^{-/-}$ bone marrow (+/+ = WT, -/- = FcγRIIB$^{-/-}$). All data represent individual values with the median. The data were analysed using Mann-Whitney U-test ($p^*<0.05$).

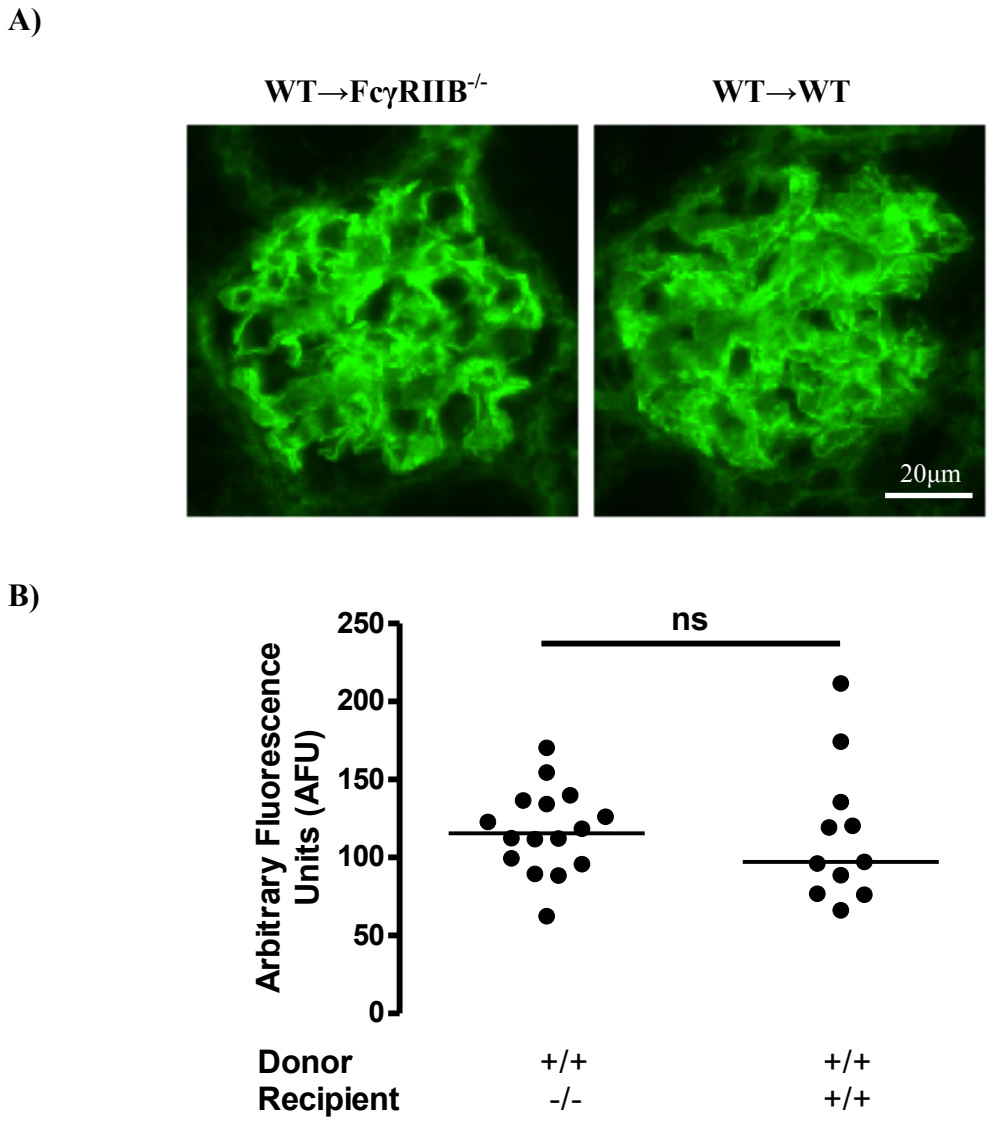


**Figure 6.16 Immunofluorescence for glomerular mouse IgG deposition in bone marrow transplanted mice with NTN, Experiment 2.**

**(A)** Representative glomeruli from WT→FcγRIIB$^{-/-}$ mice and WT→WT mice showing mouse IgG deposition. All images were taken using the same settings. **(B)** Relative mean glomerular immunofluorescence was measured quantitatively and expressed as arbitrary fluorescence units (AFU). There was no significant difference in deposited mouse IgG between the two groups (+/+ = WT, -/- = FcγRIIB$^{-/-}$). All data represent individual values with the median. The data were analysed using Mann-Whitney U-test (ns= non-significant).

### 6.4.6 Characterisation of mesangial cells and expression of FcγRIIB

Expression of FcγRIIB on intrinsic renal cells, specifically mesangial cells, has been previously reported (Radeke et al., 2002). Next we set out to confirm this by culturing both WT and FcγRIIB$^{-/-}$ mesangial cells.

WT and FcγRIIB$^{-/-}$mesangial cells were characterised by immunofluorescence studies and their characteristic stellate morphology. Mesangial cells were stained for myosin and pancytokeratin. As expected, WT and FcγRIIB$^{-/-}$ mesangial cells were positive for myosin and negative for pancytokeratin (Figure 6.17).

To confirm expression of FcγRIIB by cultured mesangial cells we used qRT-PCR and direct immunofluorescence. A FITC-labelled anti-FcγRIIB (clone Ly17.2) antibody was used on cytospins. WT mesangial cells were positive for FcγRIIB whereas FcγRIIB$^{-/-}$ mesangial cells were negative (Figure 6.18). For the qRT-PCR, mRNA was extracted from unstimulated and LPS stimulated WT mesangial cells (LPS has been shown to alter FcγRIIB expression (Radeke et al., 2002)) and unstimulated FcγRIIB$^{-/-}$ mesangial cells using the TRIzol method. mRNA was amplified with FcγRIIB specific primers. FcγRIIB was detected from both the unstimulated and stimulated mesangial cells, with no significant difference in expression following stimulation (unstimulated WT mesangial cells 2.2 (1.0-2.5), stimulated WT mesangial cells 3.7 (3.5-5.7), p=0.10) (Figure 6.19). FcγRIIB was not detected in the FcγRIIB$^{-/-}$ mesangial cells.

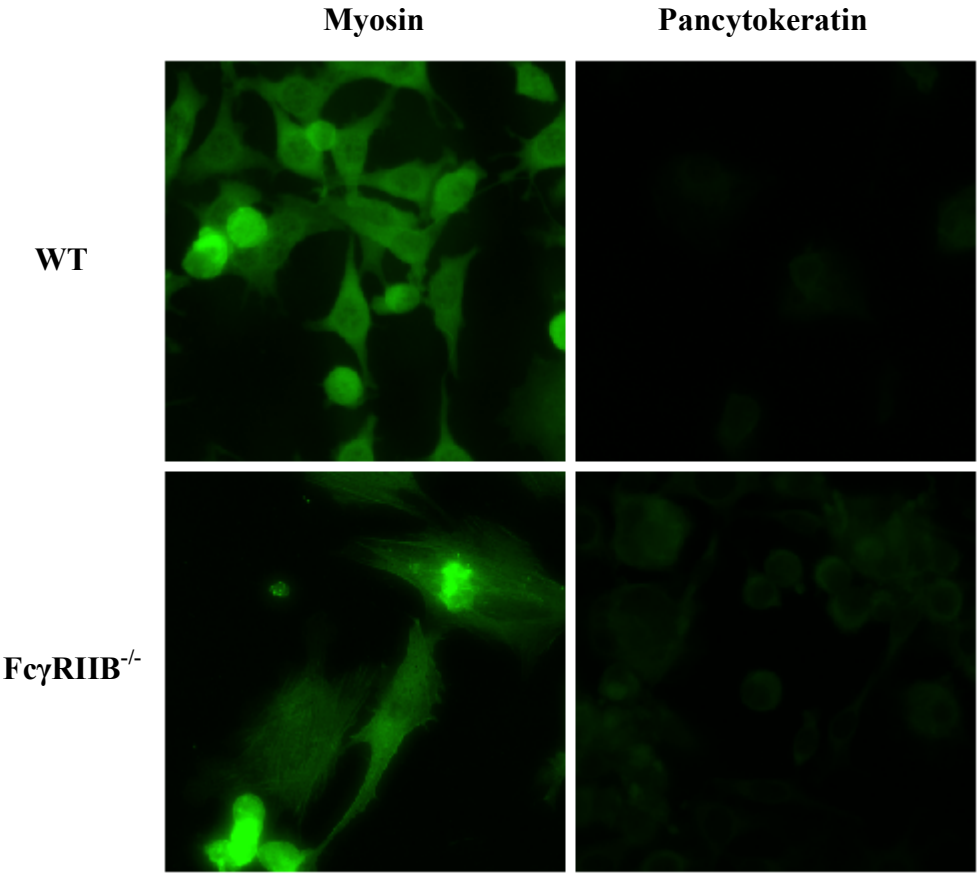


**Figure 6.17 Characterisation of WT and FcγRIIB$^{-/-}$ mesangial cells.**

WT and FcγRIIB$^{-/-}$ mesangial cells were stained for myosin and pancytokeratin; both were positive for myosin and negative for pancytokeratin.

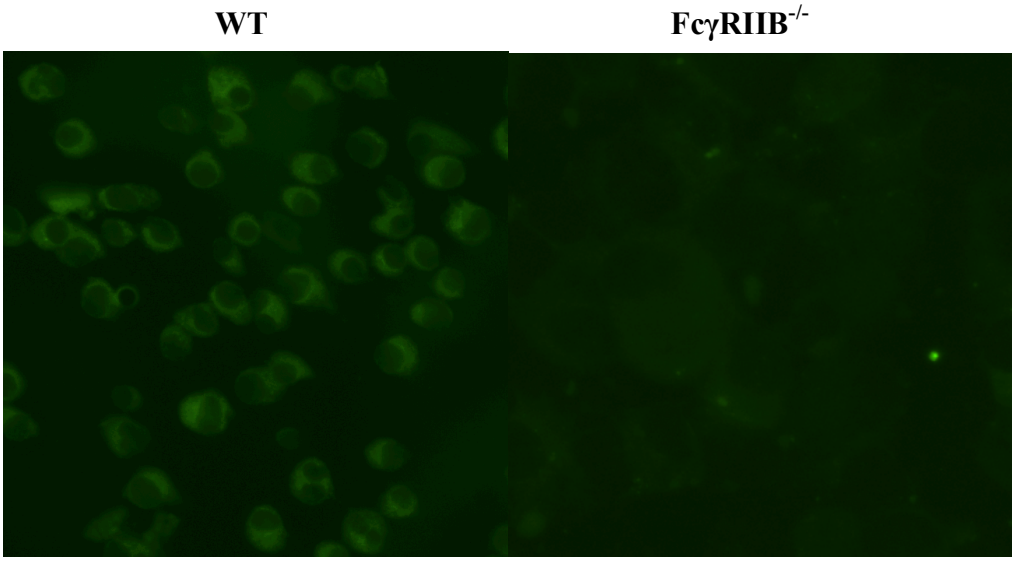


**Figure 6.18 Direct immunofluorescence for FcγRIIB on mesangial cells.**

WT and FcγRIIB$^{-/-}$ mesangial cells were stained for FcγRIIB. WT mesangial cells were positive for FcγRIIB whereas FcγRIIB$^{-/-}$ mesangial cells were negative.

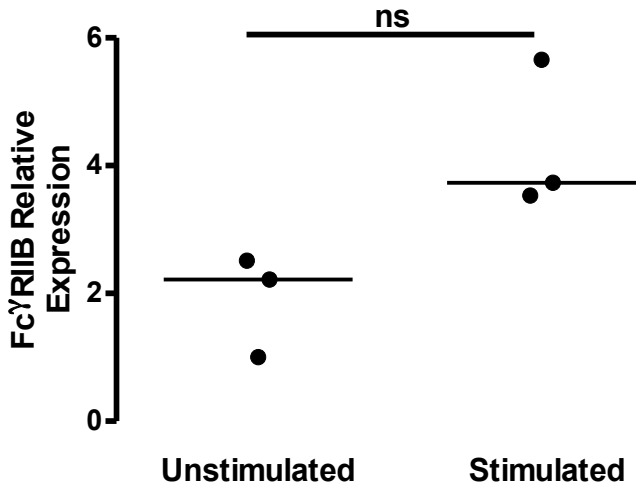


**Figure 6.19 Mesangial cell mRNA expression of FcγRIIB following stimulation with LPS.**

Levels of mRNA expression of FcγRIIB were measured in mesangial cell mRNA extracts. There was no significant difference in FcγRIIB mRNA expression between unstimulated and LPS stimulated WT mesangial cells. All data represent individual values with the median. The data were analysed using Mann-Whitney U-test (ns= non-significant).

## 6.5 Discussion

The results here show that FcγRIIB expressed on radioresistant renal cells plays a role in protection from NTN, as measured by reduced serum urea, reduced albuminuria and reduced glomerular thrombosis and crescent formation in the WT mice transplanted with FcγRIIB$^{-/-}$ bone marrow compared to the FcγRIIB$^{-/-}$ mice transplanted with FcγRIIB$^{-/-}$ bone marrow in Experiment 1 and this is supported by the need to sacrifice more of the FcγRIIB$^{-/-}$ mice transplanted with FcγRIIB$^{-/-}$ bone marrow early in Experiment 3. A possible candidate for renal cell expression of FcγRIIB is the mesangial cell (Radeke et al., 2002). However, deletion of FcγRIIB from intrinsic renal cells alone does not appear to play a major role in exacerbating injury; following induction of mild disease we did not see a large difference between FcγRIIB$^{-/-}$ mice transplanted with WT bone marrow compared to WT mice transplanted with WT bone marrow, within the limitations of the experimental model.

There was a greater infiltration of macrophages into the glomerulus in the mice lacking FcγRIIB on their intrinsic renal cells in both Experiment 1 and Experiment 2; however, glomerular neutrophil infiltration was similar between the groups of mice. At the day 12-14 timepoints neutrophil infiltration is not as prominent as it might be earlier in the course of the disease. To examine neutrophil infiltration fully we would need to look at an earlier timepoint, for example 2-24 hours after injection of NTS. There was slightly less circulating mouse anti-sheep IgG and deposited mouse IgG in the FcγRIIB$^{-/-}$ mice transplanted with FcγRIIB$^{-/-}$ bone marrow than the WT mice transplanted with FcγRIIB$^{-/-}$ bone marrow in Experiment 1, possibly due to the increased proteinuria and glomerular damage. Ideally we should have looked for the presence of immunoglobulin in the urine by ELISA. In Experiment 2, despite an increase in circulating antibody in FcγRIIB$^{-/-}$ mice transplanted with WT bone marrow there was no difference in deposited mouse IgG and no major increase in disease compared to WT mice transplanted with WT bone marrow.

Intrinsic renal cells, such as mesangial cells, have been shown to express both the activating and inhibitory FcγR (Radeke et al., 2002; Uciechowski et al., 1998). Activation of cultured mesangial cells, via their FcγR has been shown to induce the secretion of pro-inflammatory cytokines such as MCP-1 (Uciechowski et al., 1998) and TNF-α (Gomez-Guerrero et al., 1994) which led to the hypothesis that FcγR on intrinsic renal cells play a role in glomerular inflammation. However, by using bone marrow chimeras, a role for activating

FcγR in both accelerated NTN and lupus nephritis (using NZB x NZW mice) has been excluded (Bergtold et al., 2006; Tarzi et al., 2002). To determine whether intrinsic renal cell expression of FcγRIIB plays a role in protecting mice from NTN, we created bone marrow chimeras by transplanting FcγRIIB$^{-/-}$ bone marrow into WT mice and comparing them to FcγRIIB$^{-/-}$ mice transplanted with FcγRIIB$^{-/-}$ bone marrow. We also performed the reciprocal experiment by transplanting WT bone marrow into WT mice and FcγRIIB$^{-/-}$ mice.

In contrast to the results obtained above looking at activating FcγR on intrinsic renal cells, WT mice transplanted with FcγRIIB$^{-/-}$ bone marrow were protected from developing renal disease compared to FcγRIIB$^{-/-}$ mice transplanted with FcγRIIB$^{-/-}$ bone marrow, highlighting a role for intrinsic renal cell FcγRIIB expression in the protection from NTN. On the reverse, whilst there was no significant increase in renal histology, FcγRIIB$^{-/-}$ mice transplanted with WT bone marrow had a mild increase in glomerular macrophage infiltration and albuminuria compared to WT mice transplanted with WT bone marrow. In both experiments there was a good deletion (~75-95%) of recipient circulating cells; however, the PCR method used to measure reconstitution is biased towards shorter products, and therefore not sensitive enough to detect FcγRIIB$^{-/-}$ DNA when it constitutes less than 25% of the total DNA. Ideally we should have confirmed chimerism using FACS (see Chapter 4), but as we followed the same protocol as before we can be confident chimerism is likely to be high. It could be argued that radioresistant resident renal macrophages and dendritic cells could be remaining within the kidney and contributing to the protective effects seen in the WT mice transplanted with FcγRIIB$^{-/-}$ bone marrow. However, by creating bone marrow chimeras expressing different copies of the CD45 allotype (CD45.1 and CD45.2), we have previously shown that resident tissue cells within the kidney are mostly replaced following bone marrow transplantation to the same degree as the circulating cells (Tarzi et al., 2011). There was a small population of recipient macrophages and dendritic cells left in the kidney and we cannot exclude that these have a role; however, these results suggest a role for intrinsic renal cell expression of FcγRIIB in protection from GN. Whilst it may be that FcγRIIB expressed on intrinsic renal cells is sufficient to protect from disease, its absence alone is not sufficient to exacerbate disease.

As already mentioned, despite intrinsic renal cells expressing activating FcγRs, they do not play a role in the development of accelerated NTN (Tarzi et al., 2002). This further supports our observation that deletion of FcγRIIB from intrinsic renal cells alone is not enough to exacerbate disease. However, if FcγRIIB expression on intrinsic renal cells plays a

role in protecting from renal injury, this suggests a possibility for cross-talk between FcγRIIB and other receptors. Recently, a negative regulatory interaction has been suggested between FcγRIIB and the C5a receptor via dectin-1 (Karsten et al., 2012). Highly galactosylated IgG1 immune complexes promote the association of FcγRIIB with dectin-1, resulting in phosphorylation of SHIP and spleen tyrosine kinase, respectively. This then inhibits the phosphorylation of ERK1/2 downstream of the C5a receptor, blocking C5a effector functions *in vitro* and inflammatory responses *in vivo* (Karsten et al., 2012). IgG1 is a significant component of the murine immune response (data not shown). In order to determine whether this pathway could be important in NTN we would need to determine whether dectin-1 is expressed on mesangial cells, the galactosylation status of the NTS, as well as the galactosylation status of the murine IgG.

Also, in accelerated NTN, MR-deficient mice were protected from developing renal injury (Chavele et al., 2010). MR is a prototypic marker of alternatively activated macrophages; however, it is also known to be expressed by mesangial cells (Linehan et al., 1999) and has been found to interact with FcγR by binding the mannose residues found on immunoglobulins (Chavele et al., 2010). MR on mesangial cells was found to enhance FcγR responses, with increased production of pro-inflammatory cytokines, such as IFN-γ, IL-1 and TNF-α, as well as chemokines, for example MCP-1. $MR^{-/-}$ mice were also found to have fewer infiltrating glomerular macrophages (Chavele et al., 2010). Therefore it is a possibility that if MR can enhance the effects of immunoglobulin binding to FcγR, interaction with FcγRIIB may well dampen the effects.

We, and others (Radeke et al., 2002), have shown expression of FcγRIIB by mesangial cells suggesting a possible role for mesangial cell FcγRIIB in NTN. Although there was no significant difference, we found FcγRIIB expression to increase slightly in growth arrested mesangial cells following stimulation with LPS. This is similar to the result seen by Radeke *et al.*, who found minimal change in FcγRIIB expression following LPS stimulation alone (Radeke et al., 2002). Unfortunately, due to the difficulties in culturing mesangial cells, we were not able to study directly the effects of FcγRIIB-deficiency on the cells in culture. However, it would be of interest to compare cytokine and chemokine production in WT and $FcγRIIB^{-/-}$ cells following stimulation with IgG.

Although mesangial cells have been shown to express FcγRIIB, this does not mean mesangial cells are the only site of FcγRIIB expression within the glomerulus. Recently, podocytes have been found to play a role in GN (Cook et al., 2011). Therefore, it is of

importance, to further investigate sites of FcγRIIB expression within both healthy and diseased kidney. If other cells are found to express FcγRIIB it would be of interest to culture these cells and compare them with WT cells to see if FcγRIIB deficiency is found to have an effect.

A small influx of macrophages and neutrophils was measured in the glomeruli of all mice from both experiments. Interestingly, there was no significant difference in glomerular neutrophil accumulation between the two groups of mice in each experiment. In Experiment 1, all circulating cells were FcγRIIB-deficient, whereas in Experiment 2, all circulating cells expressed FcγRIIB. This further supports the hypothesis in Chapter 5 that expression of FcγRIIB on neutrophils is involved in their recruitment to the glomerulus and subsequent activation. On the contrary, in both Experiment 1 and Experiment 2, mice deficient in FcγRIIB on their intrinsic renal cells had a greater influx of glomerular macrophages compared to mice expressing FcγRIIB on intrinsic renal cells. Taken with the observations in Chapter 5, that FcγRIIB$^{-/-}$ mice have an increase in glomerular macrophage accumulation compared to WT mice and FcγRIIB$_{cEBP\alpha Cre}$ mice, this suggests that expression of FcγRIIB on intrinsic renal cells, rather than the macrophages themselves, is important in macrophage recruitment to the glomerulus. To further support this it would be useful to repeat the bone marrow transplant experiments comparing WT mice transplanted with FcγRIIB$^{-/-}$ bone marrow and WT mice transplanted with WT bone marrow. Again, it would also be interesting to compare directly MCP-1 production by WT and FcγRIIB$^{-/-}$ mesangial cells following stimulation to see if there is a significant decrease in expression in the FcγRIIB-deficient cells.

In Experiment 2, the WT mice transplanted with WT bone marrow had slightly elevated levels of serum urea than the FcγRIIB$^{-/-}$ mice transplanted with WT bone marrow. This is despite the mice having no signs of thrombosis. Nevertheless, the urea readings of both groups were within the normal limits when compared to a group of WT mice, which suggests that this finding is not indicative of renal disease in the WT mice transplanted with WT bone marrow. A possible explanation could be that the WT mice transplanted with WT bone marrow were slightly larger than the FcγRIIB$^{-/-}$ mice transplanted with WT bone marrow. Usually the mice are weighed at the start of the experiment, but this was an omission on this occasion. However, no size difference was noted during the experiments and their dates of birth were almost identical.

Due to availability of mice and the regulations of the UK Home Office, Experiments 1 and 2 were performed on male mice, whereas Experiments 3 and 4 were performed on female mice. Female mice are much more susceptible to NTN than male mice, and therefore it was necessary to terminate the experiments in female mice earlier on. In humans, there is a higher incidence of autoimmune disease in females compared to males (roughly 3:1). As well as genetic polymorphisms and environmental factors being involved, sex hormones also play a role in susceptibility. Castration of autoimmune prone NZB/NZW male mice was found to accelerate the onset of lupus-like disease, whereas ovariectomised female NZB/NZW mice given androgens had reduced lupus-like disease (Roubinian et al., 1977). Although using different sexes in the experiments makes it difficult to compare directly the results seen, the results follow the same trend. Ideally, if time had allowed, both sets of experiments would be repeated in both sexes.

To try and understand fully the role of FcγRIIB in NTN, both on circulating leukocytes and intrinsic renal cells, it would be of interest to transplant bone marrow from $Fc\gamma RIIB_{cEBP\alpha Cre}$ mice into $Fc\gamma RIIB^{-/-}$ mice. This will create mice lacking FcγRIIB on intrinsic renal cells and myeloid cells which can then be compared to WT mice and complete FcγRIIB knockout mice to see if disease is as exacerbated when FcγRIIB is missing from both cellular compartments.

## 6.6 Conclusion

In conclusion, expression of FcγRIIB by either circulating leukocytes or intrinsic renal cells is sufficient to protect mice from the onset of accelerated NTN at a low dose of NTS. This is likely due to the role of FcγRIIB in negatively regulating cell activation of myeloid cells and possibly negatively regulating cytokine and chemokine production by mesangial cells, as we and others have shown mesangial cells to express FcγRIIB in culture. However, based on the results presented in Chapter 5, when a higher dose of NTS is administered, effector cell activation can override the protective properties of FcγRIIB on intrinsic renal cells. This is the first study to show a role for intrinsic renal cell FcγRIIB expression in GN. Given the similarities between human and murine FcγR and that FcγR have been implicated in human GN, it is likely that these results have relevance for human disease.

# CHAPTER 7

# General Discussion

## 7.1 Summary of results

In Chapter 3, I showed that *gld* mice were strongly protected from accelerated NTN compared to WT mice, which could possibly be due to the reduction in T cell meditated immunity, reduction in apoptosis or reduction in pro-inflammatory cytokine production. This represents a novel role for FasL in the promotion of GN.

In Chapter 4, I performed bone marrow transplants from WT mice to *gld* mice and *vice versa* in order to investigate the relative contribution of FasL expressed on circulating leukocytes and intrinsic renal cells in the development of disease. With this experiment I was able to show that in the model of accelerated NTN, disease is dependent on FasL expression by either subset of cells. I also went on to confirm expression of FasL by WT mesangial cells and showed that signalling through the IL-1R is defective in the absence of FasL.

In Chapter 5, I investigated the role of FcγRIIB expression on different subsets of circulating leukocytes in accelerated NTN. I confirmed that complete deletion of FcγRIIB renders mice highly susceptible to renal injury and found expression of FcγRIIB on myeloid cells, but not B cells, plays an important role in protecting the mice from disease.

In Chapter 6, I used bone marrow transplants to investigate the role of FcγRIIB on circulating leukocytes and intrinsic renal cells in accelerated NTN. Interestingly, I found that expression of FcγRIIB on intrinsic renal cells does play a role in conferring protection from disease.

## 7.2 Thesis limitations

### 7.2.1 Limitations of using knockout mice

Through advances in genetic engineering it is now possible to generate mice with either an overexpression or deletion of an individual gene of interest from the entire organism or within individual cell subsets and tissues. This has provided us with a tool with which to study individual molecules in disease models *in vivo,* whilst avoiding the disadvantages of using pharmacological compounds, such as non-specific effects or a limited ability to reach target tissues. However, this does not mean genetic engineering is without limitations. For example, following loss of gene function it is possible that previously redundant pathways may be activated to compensate, therefore altering the results. Also, about 15% of gene knockouts are developmentally lethal and cannot grow into adult mice. There are also issues with incomplete deletion of the gene of interest in cell-specific knockouts, as seen in the $Fc\gamma RIIB_{LysMCre}$ mice. Technically the *gld* mouse is not a real knockout mouse. The *gld* mutation does not affect expression of FasL, but instead the ability of FasL to bind Fas (Takahashi et al., 1994). FasL-knockout mice, generated on a C57BL/6 background, were found to have a severe phenotype, with histological signs of GN, compared to *gld* mice on the same background. This accelerated phenotype led to the premature death of more than 50% of the homozygous mice at 4 months (Karray et al., 2004), highlighting that there is some residual activity of FasL in the *gld* mice.

Genetic background also needs to be considered when using genetically-engineered mice. In NTN, genetic background has been found to play an important role in regulating the development of disease (Huang et al., 1997c). Most knockout mice, including the original $Fc\gamma RIIB^{-/-}$ mice, are created from 129/Sv ES cells. Following genetic modification the ES cells are implanted into a C57BL/6 blastocyst to generate chimeric 129/Sv/C57BL/6 mice. Backcrossing these mice onto pure C57BL/6 mice produces mice in which both copies of the gene (one on each chromosome) are deleted in all tissues. Further backcrossing onto the C57BL/6 background for 8-10 generations produces mice with >99% C57BL/6 genotype; however there is always a variable region immediately surrounding the deleted gene that is 129/Sv. Bygrave *et al.,* have shown that epistatic interactions between genes from 129 and C57BL/6 genomes can promote an autoimmune phenotype (Bygrave et al., 2004). This is seen in $Fc\gamma RIIB^{-/-}$ mice. $Fc\gamma RIIB^{-/-}$ mice created using 129/Sv ES cells were found to develop spontaneous lupus, whereas $Fc\gamma RIIB^{-/-}$ mice made by gene-targeting in B6-derived ES cells

exhibited a hyperactive phenotype but failed to develop autoimmunity (Boross et al., 2011). Genetic background also affects the *gld* mutation. The *gld* mutation arose spontaneously in the inbred mouse strain C3H/HeJ, which has no predisposition to autoimmunity (Roths et al., 1984). When crossed to a C57BL/6 background, *gld* mice develop autoantibodies but GN is not seen until 13-16 months and is minimal (Kelley and Roths, 1985). However, intercrossing *gld* mice onto the MRL background results in accelerated onset of GN (Kimura et al., 1992).

### 7.2.2 Limitations of the accelerated nephrotoxic nephritis model

The murine model of accelerated NTN is well established and has been used extensively to define the roles of macrophages, T cells and other immune pathways in GN and to test novel therapeutic strategies. Although NTN is not an autoimmune model, it is suitable for looking at effector responses, which would be similar in an immune complex disease, such as lupus nephritis. One drawback is the variability in disease induction. The degree of proteinuria and GN generated is determined to an extent by operator dependent differences. When inducing NTN problems can arise with the pre-immunisation, such as the preparation of the immunogen, and the NTS injection, which is difficult to administer. Also, different batches of NTS can vary widely, due to differing concentrations of sheep IgG, and, in addition, prevalent immunogens in the environment of different animal facilities, which may differ at different times, can also influence the course of GN. Therefore, mice with similar genetic backgrounds can present with widely differing disease phenotypes. To avoid any possible differences, all mice in any one experiment were immunised at the same time with the same preparation of sheep IgG in CFA and the same preparation of NTS was used in all experiments in each of the projects. With the exception of the experiments in Chapter 5 that were performed at LUMC, all experiments were performed at Imperial College London. Therefore, in order to analyse data, I have compared results from individual experiments.

## 7.3 Hypothesis of the involvement of Fas ligand and Fc gamma receptor IIB in nephrotoxic nephritis

### 7.3.1 The role of Fas ligand in nephrotoxic nephritis

The *in vivo* data presented in this thesis suggest that FasL expression is critical for GN development in the model of accelerated NTN. More specifically, expression of FasL on either intrinsic renal cells or circulating leukocytes is sufficient to convey protection. The *in vitro* data on mesangial cells demonstrate a possible mechanism by which FasL-deficiency protects from disease development. In both WT and *gld* mice, immunisation with sheep IgG in CFA causes the production of an immune response. Administration of NTS localises deposition of sheep IgG, and subsequently mouse IgG, to the glomerulus. This leads to the activation of FcγR, recruitment of leukocytes, and the production of pro-inflammatory cytokines, such as IFN-γ, IL-1β and TNF-α, as well as chemokines, such as MCP-1. Within the WT kidney FasL binding to Fas, either on intrinsic renal cells or infiltrating leukocytes, induces inflammation by activating NF-κB and caspases, which leads to the secretion of IL-1β. IL-1β can then activate IL-1R, in either a paracrine or autocrine fashion, leading to the production of MCP-1 that works to recruit macrophages to the glomerulus and activate them. In *gld* mice, in the absence of FasL signalling, there is a possible reduction in NF-κB and caspase activation causing a reduction in IL-1β secretion and IL-1R activation. MyD88 and FADD are both adaptor proteins downstream of the IL-1R and Fas signalling pathways, respectively. In the absence of signalling through Fas, FADD associates with MyD88 through their death domains, retaining MyD88 in the cytoplasm away from the IL-1R pathway. This, taken together with the reduction in IL-1R activation, causes an overall reduction in MCP-1 production and possibly the activation of macrophages recruited to the glomerulus.

### 7.3.2 The role of FcγRIIB in nephrotoxic nephritis

The *in vivo* data presented in this thesis suggest that FcγRIIB expression is critical for protection from GN in the model of accelerated NTN. More specifically, FcγRIIB expressed on myeloid cells, with a contribution from intrinsic renal cell FcγRIIB, was important for protection. In WT and FcγRIIB$^{-/-}$ mice, immunisation with sheep IgG in CFA causes the production of an immune response. Administration of NTS localises deposition of sheep IgG, and subsequently mouse IgG, to the glomerulus. This leads to the activation of FcγR, recruitment of leukocytes, and the production of pro-inflammatory cytokines, such as IFN-γ, IL-1β and TNF-α, as well as chemokines, such as MCP-1. A proposed mechanism is expression of FcγRIIB on myeloid cells, such as macrophages, monocytes, neutrophils and possibly dendritic cells and mast cells, works to regulate their cellular activation and control their inflammatory response. In addition, FcγRIIB on neutrophils is involved in their recruitment to the site of inflammation. Within the kidney, FcγRIIB expressed on intrinsic renal cells is also involved in protection from NTN by possibly regulating the activation of mesangial cells and being involved in the recruitment of macrophages to the glomerulus.

## 7.4 Further questions arising from this Thesis

The results presented in this thesis raise further questions about the roles of FasL and FcγRIIB in accelerated NTN and in order to answer them further experiments need to be performed.

### 7.4.1 Is macrophage activation affected by Fas ligand deficiency?

Macrophage accumulation within the glomerulus is closely related to renal injury (Nikolic-Paterson and Atkins, 2001); however, glomerular macrophage infiltration still occurred in *gld* mice and *gld* mice transplanted with *gld* bone marrow, despite these mice being protected from NTN. This suggests that macrophage activation and phenotype, rather than numbers, determine disease outcome. Two studies, in rats, support this (Cook et al., 1999; Lai et al., 2001). Further to this, FasL has been implicated as playing a role in macrophage activation (Chakour et al., 2009). Therefore, it is important to study the activation status of *gld* macrophages compared to WT macrophages. This can be done *in vitro* and *in vivo*. Firstly, WT and *gld* BMDM can be cultured and stimulated with IFN-γ or IL-4, to induce pro- and anti-inflammatory phenotypes, respectively. ELISA can then be used to measure the secretion of cytokines and other mediators of inflammation, such as iNOS, IL-6, MR, and TNF-α. However, this would only tell us about the behaviour of macrophages *in vitro* and would not necessarily be representative of macrophages *in vivo.* Alternatively, to study macrophage phenotype *in vivo*, NTN would need to be induced in WT and *gld* mice, the macrophages isolated from the kidney by cell sorting, RNA extracted and markers for pro- or anti-inflammatory phenotypes measured by qRT-PCR.

### 7.4.2 Does downregulating Fas ligand with siRNA in mesangial cells replicate the knockout phenotype?

In culture, *gld* mesangial cells had an attenuated response to IL-1β compared to WT mesangial cells, producing significantly less MCP-1. A different way of proving that this is due to FasL-deficiency would be to use WT mesangial cells and to knockdown FasL expression with siRNA specific for the FasL gene. The success of the knock down can be

measured at the RNA and protein level, as well as functionally by stimulating with TNF-α or IL-1β and assessing MCP-1 production.

### 7.4.3 What are the differences in downstream signalling pathways in *gld* mesangial cells compared to WT mesangial cells?

The *gld* mutation has been suggested to disrupt the activation of NF-κB and caspases downstream of IL-1β by FADD sequestering MyD88 away from the signalling pathway (Bannerman et al., 2002). This can be confirmed *in vitro* by measuring NF-κB and caspase 1 activation of IL-1β-stimulated mesangial cells by western blotting. It would also be of interest to stimulate the *gld* mesangial cells with both IL-1β and FasL to see if this restores NF-κB and caspase 1 activation back to WT levels. Staining kidney sections from WT and gld mice with NTN for the activated molecules can support these results *in vivo*. To further explore the role of FADD and MyD88 in this process, immunoprecipitation of FADD from WT and *gld* mesangial cells stimulated with IL-1β can be carried out and MyD88 association measured by western blot.

### 7.4.4 Do other intrinsic renal cells express Fas ligand? Does Fas ligand on these cells play a role in NTN?

*In vitro* we have concentrated on the effects of FasL deficiency on mesangial cells. However, glomerular endothelial cells, podocytes and tubular epithelial cells have also been shown to express FasL within the kidney (Linkermann et al., 2011; Lorz et al., 2000; Ortiz et al., 1999; Ross et al., 2005) as well as be potential sources of MCP-1 (Natori et al., 1997; Tesch et al., 1999). It would be of interest to investigate the effect of *gld* mutation on these different renal cells, to compare MCP-1 production with WT cells following IL-1β and TNF-α stimulation, as well as NF-κB and caspase activation. It would also be interesting to further investigate the role of FasL on the individual cells within NTN. If possible, it would be interesting to knockout FasL in either glomerular endothelial cells, podocytes or tubular epithelial cells and, following induction of NTN, see if there is a reduction in either thrombosis, proteinuria, or interstitial macrophage infiltration, respectively.

### 7.4.5 What role does Fas ligand induced apoptosis play in NTN?

Overall, our data suggest that, following the induction of NTN, a reduction in the pro-inflammatory effect of FasL is responsible for protection in *gld* mice. However, this does not address whether the reduction in apoptosis is also contributing to protection. To answer this we would need to look at a model of nephritis that requires apoptosis for repair, such as anti-Thy-1 nephritis in the rats (Shimizu et al., 1995). To do this, one would need to induce anti-Thy-1 nephritis and block the effects of FasL with a blocking antibody. It could be hypothesised that blocking FasL would render the rats more susceptible to renal injury compared to untreated rats, as apoptosis plays an important part in kidney remodelling in this disease model.

### 7.4.6 Does soluble Fas ligand play a role in NTN? Is it responsible for the pro-inflammatory effects seen?

Cleavage of FasL into its soluble form is thought to act to downregulate its apoptotic activity (Dupont and Warrens, 2007; O' Reilly et al., 2009; Schneider et al., 1998) and sFasL has been shown to play a role in the production of pro-inflammatory cytokines (Ahn et al., 2001; O' Reilly et al., 2009). To date, little work has been done looking at the role of sFasL in GN. Unfortunately, we were unable to detect sFasL in the serum of WT mice, as it would have been interesting to see if the levels of circulating sFasL increase during disease. It would also have been of interest to measure levels of sFasL in the urine of healthy and diseased mice. An alternative method of studying the role of sFasL in NTN would be to induce NTN in mice expressing either the membrane-bound form of FasL or the soluble form only (O' Reilly et al., 2009). This would also give us further insight into whether the reduction in apoptosis or the pro-inflammatory effects of FasL play a greater role in protection from NTN, as mice expressing sFasL only developed a severe SLE-like autoimmune kidney disease whereas the mice expressing membrane-bound FasL only appeared normal (O' Reilly et al., 2009).

### 7.4.7 Does FcγRIIB deficiency result in macrophage overactivation during NTN?

FcγRIIB$_{cEBP\alpha Cre}$ mice show increased renal dysfunction despite similar numbers of glomerular infiltrating macrophages compared to WT mice. Reduced surface expression of FcγRIIB on macrophages has been associated with their overactivation following cross-linking of activating FcγR (Clatworthy and Smith, 2004; Jiang et al., 2000; Pritchard et al., 2000). To determine whether infiltrating macrophages are overactivated in FcγRIIB$_{cEBP\alpha Cre}$ mice, a similar technique could be employed as mentioned in Section 7.4.1. One would need to induce NTN in WT, FcγRIIB$_{cEBP\alpha Cre}$, and FcγRIIB$^{-/-}$ mice, isolate the macrophages from the kidney by cell sorting, extract RNA, and measure the production of pro-inflammatory cytokines, such as IL-1β, IFN-γ, MCP-1 and TNF-α, by qRT-PCR.

### 7.4.8 What is the role of FcγRIIB on dendritic cells, mast cells, macrophages, and neutrophils in NTN?

At a low dose of NTS, deletion of FcγRIIB on dendritic cells, mast cells or myeloid cells alone did not exacerbate disease. However, following a higher dose of NTS, mice carrying the deletion of FcγRIIB on myeloid cells showed signs of severe renal dysfunction, due to the increased dose of heterologous antibody to glomerular antigens inducing a greater immune response, which could overcome the protective effects of FcγRIIB expressed on other cell types. As well as deleting FcγRIIB on macrophages and neutrophils, the myeloid cell knockout mice are also deficient in FcγRIIB on dendritic cells, and possibly mast cells, although we did not stain for this. Therefore, it is possible that FcγRIIB expressed on dendritic cells and mast cells is contributing to protection from NTN. FcγRIIB on dendritic cells is thought to play a role in dendritic cell maturation and antigen presentation (Boruchov et al., 2005; Dhodapkar et al., 2005). Therefore, it would also be important to investigate whether T cell responses are modified by loss of FcγRIIB on dendritic cells. To answer these questions it would be necessary to repeat the experiment with the FcγRIIB$_{CD11cCre}$ and FcγRIIB$_{Mcpt5Cre}$ mice using the higher dose of NTS. To understand fully the role of FcγRIIB on macrophages and neutrophils in NTN an alternative promoter would need to be used with complete deletion of FcγRIIB from all subsets of cells.

### 7.4.9 Does FcγRIIB deficiency affect the production of cytokines by mesangial cells? Does FcγRIIB on mesangial cells interact with other receptors?

Our data suggest a role for intrinsic renal cell expression of FcγRIIB in the protection from NTN. We, and others, have shown that mesangial cells, in culture, express FcγRIIB (Radeke et al., 2002). To further understand the role of FcγRIIB on mesangial cells in NTN it would be of interest to culture WT and FcγRIIB$^{-/-}$mesangial cells, stimulate them with IgG immune complexes, and measure cytokine secretion into the supernatant by ELISA. Activating FcγR expressed on intrinsic renal cells do not contribute to the development of NTN (Tarzi et al., 2002), therefore it is possible FcγRIIB may be negatively regulating other receptors expressed on the surface of mesangial cells. To test this, WT mesangial cells could be incubated with IgG immune complexes and the cell lysates immunoprecipitated with anti-FcγRIIB and analysed for possible protein interactions, such as MR, by Western blot.

### 7.4.10 What role does FcγRIIB play in cellular recruitment?

Our data suggest FcγRIIB may be involved in the recruitment of leukocytes to the glomerulus. FcγRIIB expressed on intrinsic renal cells appears to play a role in the recruitment of macrophages, whereas neutrophil recruitment appears to be dependent on FcγRIIB expressed on the neutrophils themselves. To support this hypothesis, *in vitro* cell migration assays could be employed. WT and FcγRIIB$^{-/-}$ mesangial cells could be cultured with WT and FcγRIIB$^{-/-}$ BMDM or PMN. Alternatively; it would be of interest to repeat the four groups in the bone marrow transplant experiments at the same time to compare directly cellular infiltration into the glomerulus.

### 7.4.11 Is FcγRIIB expressed by other cells in the kidney and does it contribute to protection from NTN?

Although we have concentrated on mesangial cell expression of FcγRIIB, this does not mean mesangial cells are the only intrinsic renal cells expressing the receptor. It would be interesting to culture other WT intrinsic renal cells, such as tubular epithelial cells or podocytes, and look at FcγRIIB expression by qRT-PCR (gene expression level), Western blot or direct immunofluorescence on cytospins (protein expression level). WT cells found to

express FcγRIIB could then be compared to FcγRIIB-deficient cells by stimulating with IgG and measuring cytokine secretion into the supernatant by ELISA.

### 7.4.12 Can the phenotype of FcγRIIB$^{-/-}$ mice be restored by the deletion of FcγRIIB on intrinsic renal cells and myeloid cells?

Deletion of FcγRIIB on intrinsic renal cells or myeloid cells alone does not restore the extreme phenotype seen in FcγRIIB$^{-/-}$ mice, following induction of accelerated NTN. It would be interesting to transplant bone marrow from FcγRIIB$_{cEBP\alpha Cre}$ mice into FcγRIIB$^{-/-}$ mice, to delete FcγRIIB in both cellular compartments, and compare the severity of disease to FcγRIIB$^{-/-}$ mice. This would give us further insight into the mechanism of protection offered by FcγRIIB expression.

## 7.5 The role of Fas ligand and Fc gamma receptor IIB in other nephritis models

The NTN model has been widely employed to study the pathogenesis of autoimmune GN. However, there are drawbacks to using NTN. Firstly, NTN has a characteristic thrombotic phenotype that is not representative of human pathology. Secondly, NTN is not a real autoimmune model of GN as it does not require tolerance to be broken. For these reasons, and in order to understand fully the roles of FasL and FcγRIIB in autoimmune renal diseases, it would be useful to study other nephritis models such as EAG and EAV.

### 7.5.1 The role of Fas ligand and FcγRIIB in a murine model of experimental autoimmune glomerulonephritis

EAG is the murine model of human anti-GBM disease and is induced by immunisation with purified non-collagenous domain of $\alpha_3$ chain type IV collagen in CFA (Dean et al., 2005), the target antigen in human disease. We have already looked at the role of FcγRIIB in EAG and found mice carrying the full deletion of FcγRIIB were highly susceptible to developing disease. However, deletion of FcγRIIB on B cells or myeloid cells alone did not increase susceptibility of the mice to developing nephritis (Sharp et al., 2012). The role of FasL in EAG has not currently been investigated. From my observations that *gld* mice are protected from NTN one hypothesis is that *gld* mice would be protected from EAG. However, EAG is an autoimmune model and *gld* mice develop autoimmune renal disease later on in life, so the FasL defect could be found to enhance disease. To test this *gld* and WT mice could be immunised with purified $\alpha_3$ chain of type IV collagen and the disease assessed.

### 7.5.2 The role of Fas ligand and FcγRIIB in a murine model of ANCA-associated vasculitis

EAV is an experimental model of human AAV. MPO and PR3 are thought to be the two main target antigens for the disease and various models have been developed against these. The findings that FasL deficiency protects mice from NTN but FcγRIIB deficiency increases susceptibility to NTN and EAG imply that both FasL and FcγRIIB may play a role in induction of AAV. It can be hypothesised that EAV would be aggravated in FcγRIIB$^{-/-}$

mice. However, the effects of the *gld* mutation on the development of EAV are unclear. Judging by the results seen with the model of EAE, the effects may be complicated. The model of MPO vasculitis is passive, suggesting the mice may be protected. To test both these hypotheses, a model of EAV could be induced in *gld* or FcγRIIB$^{-/-}$ mice, either by transfer of anti-MPO antibodies (Xiao et al., 2002a) or injection of purified MPO in CFA (Little et al., 2005; Little et al., 2009), and the resulting vasculitis compared to WT mice.

## 7.6 The role of Fas ligand and Fc gamma receptor IIB in other inflammatory diseases

The role of FasL in models of inflammatory diseases is well established. Through the use of *gld* and *lpr* mice, FasL has been shown to play a role in acute lung inflammation (Neff et al., 2005), autoimmune diabetes (Chervonsky et al., 1997; Itoh et al., 1997; Mohamood et al., 2007), CIA (Ma et al., 2004; Tu-Rapp et al., 2004), EAE (Sabelko et al., 1997; Sabelko-Downes et al., 1999; Waldner et al., 1997), EAU (Wahlsten et al., 2000), experimental stroke (Niu et al., 2011), and spinal cord injury (Letellier et al., 2010).

The role of FcγRIIB in other inflammatory diseases has also been investigated. FcγRIIB$^{-/-}$ mice show exacerbated disease when induced with CIA (Boross et al., 2011; Yuasa et al., 1999), allergic airway inflammation (Dharajiya et al., 2010), and patients with chronic inflammatory demyelinating polyneuropathy (CIDP), an autoimmune disease similar to MS, were found to have consistently lower levels of FcγRIIB expression on naïve B cells and a failed to upregulate or maintain upregulation on memory B cells (Tackenberg et al., 2009).

## 7.7 Therapeutic approach to glomerulonephritis using Fas ligand and Fc gamma receptor IIB

### 7.7.1 Current therapeutic approach for glomerulonephritis

Current treatment of GN is through the use of steroids and immunosuppressive drugs. Although effective, they also have non-specific side effects and their continued use has detrimental effects on the patient's health, resulting in the patients suffering from infections and malignancies. Ideally, rather than targeting the entire immune system, therapeutic drugs would target specific pathways or components of pathways. The most effective way to target molecules and control them is the application of antibodies. Two currently available treatments for autoimmune diseases are infliximab, an anti-TNF-α antibody, and rituximab, an anti-CD20 antibody. However, even these drugs are not without their problems; the use of infliximab and rituximab comes with risks (Hadjinicolaou et al., 2012; Rosenblum and Amital, 2011).

### 7.7.2 Fas ligand and FcγRIIB as new therapeutic targets

Unfortunately, due to the autoimmunity-enhancing effects of FasL deficiency, the use of anti-FasL blocking antibodies may be more detrimental than beneficial as a treatment for GN in humans, unless it is possible to determine the exact pathway by which FasL deficiency offers protection. However, the *in vivo* data represented in this thesis suggest that FcγRIIB may be a novel therapeutic target for treatment of GN. Since FcγRIIB deficiency on myeloid cells is associated with exacerbated disease and treatment of macrophages with IVIG upregulates FcγRIIB expression (Kaneko et al., 2006; Tackenberg et al., 2009), this study offers further insight into the anti-inflammatory properties of IVIG for the treatment of autoimmune diseases (Anthony et al., 2008).

This project is all an original work. My study is the first report linking FasL expression on intrinsic renal cells and FcγRIIB expression on intrinsic renal cells and myeloid cells to the development of GN. I have shown that *gld* mice are completely protected from accelerated NTN, but expression of FasL on either circulating leukocytes or intrinsic

renal cells is enough to result in disease. I have also shown that FasL deficiency on mesangial cells results in impaired signalling through the IL-1R, resulting in reduced expression of MCP-1. Conversely, I have shown FcγRIIB expression on myeloid cells and intrinsic renal cells plays a role in protection from NTN.

# References

Abbate, M., Kalluri, R., Corna, D., Yamaguchi, N., McCluskey, R.T., Hudson, B.G., Andres, G., Zoja, C., and Remuzzi, G. (1998). Experimental Goodpasture's syndrome in Wistar-Kyoto rats immunized with alpha3 chain of type IV collagen. Kidney Int *54*, 1550-1561.

Adachi, M., Watanabe-Fukunaga, R., and Nagata, S. (1993). Aberrant transcription caused by the insertion of an early transposable element in an intron of the Fas antigen gene of lpr mice. Proc Natl Acad Sci U S A *90*, 1756-1760.

Aggarwal, B.B., Kohr, W.J., Hass, P.E., Moffat, B., Spencer, S.A., Henzel, W.J., Bringman, T.S., Nedwin, G.E., Goeddel, D.V., and Harkins, R.N. (1985). Human tumor necrosis factor. Production, purification, and characterization. J Biol Chem *260*, 2345-2354.

Ahn, J.H., Park, S.M., Cho, H.S., Lee, M.S., Yoon, J.B., Vilcek, J., and Lee, T.H. (2001). Non-apoptotic signaling pathways activated by soluble Fas ligand in serum-starved human fibroblasts. Mitogen-activated protein kinases and NF-kappaB-dependent gene expression. J Biol Chem *276*, 47100-47106.

Aitman, T.J., Dong, R., Vyse, T.J., Norsworthy, P.J., Johnson, M.D., Smith, J., Mangion, J., Roberton-Lowe, C., Marshall, A.J., Petretto, E.*, et al.* (2006). Copy number polymorphism in Fcgr3 predisposes to glomerulonephritis in rats and humans. Nature *439*, 851-855.

Akashi, K., Traver, D., Miyamoto, T., and Weissman, I.L. (2000). A clonogenic common myeloid progenitor that gives rise to all myeloid lineages. Nature *404*, 193-197.

Alderson, M.R., Armitage, R.J., Maraskovsky, E., Tough, T.W., Roux, E., Schooley, K., Ramsdell, F., and Lynch, D.H. (1993). Fas transduces activation signals in normal human T lymphocytes. J Exp Med *178*, 2231-2235.

Alderson, M.R., Tough, T.W., Davis-Smith, T., Braddy, S., Falk, B., Schooley, K.A., Goodwin, R.G., Smith, C.A., Ramsdell, F., and Lynch, D.H. (1995). Fas ligand mediates activation-induced cell death in human T lymphocytes. J Exp Med *181*, 71-77.

Allison, J., Georgiou, H.M., Strasser, A., and Vaux, D.L. (1997). Transgenic expression of CD95 ligand on islet beta cells induces a granulocytic infiltration but does not confer immune privilege upon islet allografts. Proc Natl Acad Sci U S A *94*, 3943-3947.

Allison, J., and Strasser, A. (1998). Mechanisms of beta cell death in diabetes: a minor role for CD95. Proc Natl Acad Sci U S A *95*, 13818-13822.

Altemeier, W.A., Zhu, X., Berrington, W.R., Harlan, J.M., and Liles, W.C. (2007). Fas (CD95) induces macrophage proinflammatory chemokine production via a MyD88-dependent, caspase-independent pathway. Journal of Leukocyte Biology *82*, 721-728.

Amigorena, S., and Bonnerot, C. (1999). Fc receptors for IgG and antigen presentation on MHC class I and class II molecules. Semin Immunol *11*, 385-390.

Anderson, C.F., and Mosser, D.M. (2002). A novel phenotype for an activated macrophage: the type 2 activated macrophage. J Leukoc Biol *72*, 101-106.

Anthony, R.M., Kobayashi, T., Wermeling, F., and Ravetch, J.V. (2011). Intravenous gammaglobulin suppresses inflammation through a novel T(H)2 pathway. Nature *475*, 110-113.

Anthony, R.M., Nimmerjahn, F., Ashline, D.J., Reinhold, V.N., Paulson, J.C., and Ravetch, J.V. (2008). Recapitulation of IVIG anti-inflammatory activity with a recombinant IgG Fc. Science *320*, 373-376.

Araki, T., and Ogane, K. (2008). Images in cardiovascular medicine. Rupture of infected splenic artery aneurysm secondary to infective endocarditis. Circulation *118*, 684-686.

Ashman, R.F., Peckham, D., and Stunz, L.L. (1996). Fc receptor off-signal in the B cell involves apoptosis. J Immunol *157*, 5-11.

Badley, A.D., McElhinny, J.A., Leibson, P.J., Lynch, D.H., Alderson, M.R., and Paya, C.V. (1996). Upregulation of Fas ligand expression by human immunodeficiency virus in human macrophages mediates apoptosis of uninfected T lymphocytes. J Virol *70*, 199-206.

Bagavant, H., and Fu, S.M. (2009). Pathogenesis of kidney disease in systemic lupus erythematosus. Curr Opin Rheumatol *21*, 489-494.

Baker, A.J., Mooney, A., Hughes, J., Lombardi, D., Johnson, R.J., and Savill, J. (1994). Mesangial cell apoptosis: the major mechanism for resolution of glomerular hypercellularity in experimental mesangial proliferative nephritis. J Clin Invest *94*, 2105-2116.

Banki, Z., Kacani, L., Mullauer, B., Wilflingseder, D., Obermoser, G., Niederegger, H., Schennach, H., Sprinzl, G.M., Sepp, N., Erdei, A*., et al.* (2003). Cross-linking of CD32 induces maturation of human monocyte-derived dendritic cells via NF-kappa B signaling pathway. J Immunol *170*, 3963-3970.

Bannerman, D.D., Tupper, J.C., Kelly, J.D., Winn, R.K., and Harlan, J.M. (2002). The Fas-associated death domain protein suppresses activation of NF-kB by LPS and IL-1βετα. The Journal of Clinical Investigation *109*, 419-425.

Bansal, P.J., and Tobin, M.C. (2004). Neonatal microscopic polyangiitis secondary to transfer of maternal myeloperoxidase-antineutrophil cytoplasmic antibody resulting in neonatal pulmonary hemorrhage and renal involvement. Ann Allergy Asthma Immunol *93*, 398-401.

Bariety, J., Bruneval, P., Meyrier, A., Mandet, C., Hill, G., and Jacquot, C. (2005). Podocyte involvement in human immune crescentic glomerulonephritis. Kidney Int *68*, 1109-1119.

Bellgrau, D., Gold, D., Selawry, H., Moore, J., Franzusoff, A., and Duke, R.C. (1995). A role for CD95 ligand in preventing graft rejection. Nature *377*, 630-632.

Bergtold, A., Gavhane, A., D'Agati, V., Madaio, M., and Clynes, R. (2006). FcR-bearing myeloid cells are responsible for triggering murine lupus nephritis. J Immunol *177*, 7287-7295.

Berlanga, O., Tulasne, D., Bori, T., Snell, D.C., Miura, Y., Jung, S., Moroi, M., Frampton, J., and Watson, S.P. (2002). The Fc receptor gamma-chain is necessary and sufficient to initiate signalling through glycoprotein VI in transfected cells by the snake C-type lectin, convulxin. Eur J Biochem *269*, 2951-2960.

Bjornson, A., Moses, J., Ingemansson, A., Haraldsson, B., and Sorensson, J. (2005). Primary human glomerular endothelial cells produce proteoglycans, and puromycin affects their posttranslational modification. Am J Physiol Renal Physiol *288*, F748-756.

Boldin, M.P., Goncharov, T.M., Goltsev, Y.V., and Wallach, D. (1996). Involvement of MACH, a novel MORT1/FADD-interacting protease, in Fas/APO-1- and TNF receptor-induced cell death. Cell *85*, 803-815.

Boldin, M.P., Varfolomeev, E.E., Pancer, Z., Mett, I.L., Camonis, J.H., and Wallach, D. (1995). A novel protein that interacts with the death domain of Fas/APO1 contains a sequence motif related to the death domain. The Journal of Biological Chemistry *270*, 7795-7798.

Bolland, S., and Ravetch, J.V. (2000). Spontaneous autoimmune disease in Fc(gamma)RIIB-deficient mice results from strain-specific epistasis. Immunity *13*, 277-285.

Bolton, W.K., Innes, D.J., Jr., Sturgill, B.C., and Kaiser, D.L. (1987). T-cells and macrophages in rapidly progressive glomerulonephritis: clinicopathologic correlations. Kidney Int *32*, 869-876.

Bombeli, T., Schwartz, B.R., and Harlan, J.M. (1999). Endothelial cells undergoing apoptosis become proadhesive for nonactivated platelets. Blood *93*, 3831-3838.

Bonfoco, E., Stuart, P.M., Brunner, T., Lin, T., Griffith, T.S., Gao, Y., Nakajima, H., Henkart, P.A., Ferguson, T.A., and Green, D.R. (1998). Inducible nonlymphoid expression of Fas ligand is responsible for superantigen-induced peripheral deletion of T cells. Immunity *9*, 711-720.

Boross, P., Arandhara, V.L., Martin-Ramirez, J., Santiago-Raber, M.L., Carlucci, F., Flierman, R., van der Kaa, J., Breukel, C., Claassens, J.W., Camps, M.*, et al.* (2011). The inhibiting Fc receptor for IgG, FcgammaRIIB, is a modifier of autoimmune susceptibility. J Immunol *187*, 1304-1313.

Boruchov, A.M., Heller, G., Veri, M.C., Bonvini, E., Ravetch, J.V., and Young, J.W. (2005). Activating and inhibitory IgG Fc receptors on human DCs mediate opposing functions. J Clin Invest *115*, 2914-2923.

Bossu, P., Singer, G.G., Andres, P., Ettinger, R., Marshak-Rothstein, A., and Abbas, A.K. (1993). Mature CD4+ T lymphocytes from MRL/lpr mice are resistant to receptor-mediated tolerance and apoptosis. J Immunol *151*, 7233-7239.

Boyle, J.J., Bowyer, D.E., Weissberg, P.L., and Bennett, M.R. (2001). Human blood-derived macrophages induce apoptosis in human plaque-derived vascular smooth muscle cells by Fas-ligand/Fas interactions. Arterioscler Thromb Vasc Biol *21*, 1402-1407.

Brahler, S., Ising, C., Hagmann, H., Rasmus, M., Hoehne, M., Kurschat, C., Kisner, T., Goebel, H., Shankland, S., Addicks, K.*, et al.* (2012). Intrinsic proinflammatory signaling in podocytes contributes to podocyte damage and prolonged proteinuria. Am J Physiol Renal Physiol *303*, F1473-1485.

Brownlie, R.J., Lawlor, K.E., Niederer, H.A., Cutler, A.J., Xiang, Z., Clatworthy, M.R., Floto, R.A., Greaves, D.R., Lyons, P.A., and Smith, K.G. (2008). Distinct cell-specific control of autoimmunity and infection by FcgammaRIIb. J Exp Med *205*, 883-895.

Bruggeman, L.A., Drawz, P.E., Kahoud, N., Lin, K., Barisoni, L., and Nelson, P.J. (2011). TNFR2 interposes the proliferative and NF-kappaB-mediated inflammatory response by podocytes to TNF-alpha. Lab Invest *91*, 413-425.

Bulger, R.E., Eknoyan, G., Purcell, D.J., 2nd, and Dobyan, D.C. (1983). Endothelial characteristics of glomerular capillaries in normal, mercuric chloride-induced, and gentamicin-induced acute renal failure in the rat. J Clin Invest *72*, 128-141.

Bussolati, B., Mariano, F., Biancone, L., Foa, R., David, S., Cambi, V., and Camussi, G. (1999). Interleukin-12 is synthesized by mesangial cells and stimulates platelet-activating

factor synthesis, cytoskeletal reorganization, and cell shape change. Am J Pathol *154*, 623-632.

Bygrave, A.E., Rose, K.L., Cortes-Hernandez, J., Warren, J., Rigby, R.J., Cook, H.T., Walport, M.J., Vyse, T.J., and Botto, M. (2004). Spontaneous autoimmunity in 129 and C57BL/6 mice-implications for autoimmunity described in gene-targeted mice. PLoS biology *2*, E243.

Cambier, J.C. (1995). New nomenclature for the Reth motif (or ARH1/TAM/ARAM/YXXL). Immunol Today *16*, 110.

Canale, V.C., and Smith, C.H. (1967). Chronic lymphadenopathy simulating malignant lymphoma. J Pediatr *70*, 891-899.

Caton, M.L., Smith-Raska, M.R., and Reizis, B. (2007). Notch-RBP-J signaling controls the homeostasis of CD8- dendritic cells in the spleen. J Exp Med *204*, 1653-1664.

Chakour, R., Allenbach, C., Desgranges, F., Charmoy, M., Mauel, J., Garcia, I., Launois, P., Louis, J., and Tacchini-Cottier, F. (2009). A new function of the Fas-FasL pathway in macrophage activation. Journal of Leukocyte Biology *86*, 81-90.

Chan, F.K., Chun, H.J., Zheng, L., Siegel, R.M., Bui, K.L., and Lenardo, M.J. (2000). A domain in TNF receptors that mediates ligand-independent receptor assembly and signaling. Science *288*, 2351-2354.

Charles, L.A., Falk, R.J., and Jennette, J.C. (1992). Reactivity of antineutrophil cytoplasmic autoantibodies with mononuclear phagocytes. J Leukoc Biol *51*, 65-68.

Chavele, K.M., Martinez-Pomares, L., Domin, J., Pemberton, S., Haslam, S.M., Dell, A., Cook, H.T., Pusey, C.D., Gordon, S., and Salama, A.D. (2010). Mannose receptor interacts with Fc receptors and is critical for the development of crescentic glomerulonephritis in mice. J Clin Invest *120*, 1469-1478.

Chen, M., Kallenberg, C.G., and Zhao, M.H. (2009). ANCA-negative pauci-immune crescentic glomerulonephritis. Nat Rev Nephrol *5*, 313-318.

Chervonsky, A.V., Wang, Y., Wong, F.S., Visintin, I., Flavell, R.A., Janeway, C.A., Jr., and Matis, L.A. (1997). The role of Fas in autoimmune diabetes. Cell *89*, 17-24.

Chinnaiyan, A.M., O'Rourke, K., Tewari, M., and Dixit, V.M. (1995). FADD, a novel death domain-containing protein, interacts with the death domain of Fas and initiates apoptosis. Cell *81*, 505-512.

Clatworthy, M.R., and Smith, K.G. (2004). FcgammaRIIb balances efficient pathogen clearance and the cytokine-mediated consequences of sepsis. J Exp Med *199*, 717-723.

Clausen, B.E., Burkhardt, C., Reith, W., Renkawitz, R., and Forster, I. (1999). Conditional gene targeting in macrophages and granulocytes using LysMcre mice. Transgenic Res *8*, 265-277.

Clynes, R., Maizes, J.S., Guinamard, R., Ono, M., Takai, T., and Ravetch, J.V. (1999). Modulation of immune complex-induced inflammation in vivo by the coordinate expression of activation and inhibitory Fc receptors. J Exp Med *189*, 179-185.

Cochrane, C.G., Unanue, E.R., and Dixon, F.J. (1965). A Role of Polymorphonuclear Leukocytes and Complement in Nephrotoxic Nephritis. J Exp Med *122*, 99-116.

Coers, W., Brouwer, E., Vos, J.T., Chand, A., Huitema, S., Heeringa, P., Kallenberg, C.G., and Weening, J.J. (1994). Podocyte expression of MHC class I and II and intercellular

adhesion molecule-1 (ICAM-1) in experimental pauci-immune crescentic glomerulonephritis. Clin Exp Immunol *98*, 279-286.

Cohen, P.L., and Eisenberg, R.A. (1991). Lpr and gld: single gene models of systemic autoimmunity and lymphoproliferative disease. Annu Rev Immunol *9*, 243-269.

Cong, M., Chen, M., Zhang, J.J., Hu, Z., and Zhao, M.H. (2008). Anti-endothelial cell antibodies in antineutrophil cytoplasmic antibodies negative pauci-immune crescentic glomerulonephritis. Nephrology (Carlton) *13*, 228-234.

Cook, H.T., Singh, S.J., Wembridge, D.E., Smith, J., Tam, F.W., and Pusey, C.D. (1999). Interleukin-4 ameliorates crescentic glomerulonephritis in Wistar Kyoto rats. Kidney Int *55*, 1319-1326.

Cook, H.T., Tarzi, R., D'Souza, Z., Laurent, G., Lin, W.C., Aitman, T.J., Mechta-Grigoriou, F., and Behmoaras, J. (2011). AP-1 transcription factor JunD confers protection from accelerated nephrotoxic nephritis and control podocyte-specific Vegfa expression. Am J Pathol *179*, 134-140.

Cornacoff, J.B., Hebert, L.A., Smead, W.L., VanAman, M.E., Birmingham, D.J., and Waxman, F.J. (1983). Primate erythrocyte-immune complex-clearing mechanism. J Clin Invest *71*, 236-247.

Coxon, A., Cullere, X., Knight, S., Sethi, S., Wakelin, M.W., Stavrakis, G., Luscinskas, F.W., and Mayadas, T.N. (2001). Fc gamma RIII mediates neutrophil recruitment to immune complexes. a mechanism for neutrophil accumulation in immune-mediated inflammation. Immunity *14*, 693-704.

Craig, M.L., Bankovich, A.J., McElhenny, J.L., and Taylor, R.P. (2000). Clearance of anti-double-stranded DNA antibodies: the natural immune complex clearance mechanism. Arthritis Rheum *43*, 2265-2275.

Daeron, M., Latour, S., Malbec, O., Espinosa, E., Pina, P., Pasmans, S., and Fridman, W.H. (1995). The same tyrosine-based inhibition motif, in the intracytoplasmic domain of Fc gamma RIIB, regulates negatively BCR-, TCR-, and FcR-dependent cell activation. Immunity *3*, 635-646.

Dane, M.J., van den Berg, B.M., Avramut, M.C., Faas, F.G., van der Vlag, J., Rops, A.L., Ravelli, R.B., Koster, B.J., van Zonneveld, A.J., Vink, H.*, et al.* (2013). Glomerular endothelial surface layer acts as a barrier against albumin filtration. Am J Pathol *182*, 1532-1540.

Dean, E.G., Wilson, G.R., Li, M., Edgtton, K.L., O'Sullivan, K.M., Hudson, B.G., Holdsworth, S.R., and Kitching, A.R. (2005). Experimental autoimmune Goodpasture's disease: a pathogenetic role for both effector cells and antibody in injury. Kidney Int *67*, 566-575.

Deutsch, M., Tsopanou, E., and Dourakis, S.P. (2004). The autoimmune lymphoproliferative syndrome (Canale-Smith) in adulthood. Clin Rheumatol *23*, 43-44.

Dharajiya, N., Vaidya, S.V., Murai, H., Cardenas, V., Kurosky, A., Boldogh, I., and Sur, S.A. (2010). FcgammaRIIb inhibits allergic lung inflammation in a murine model of allergic asthma. PLoS One *5*, e9337.

Dhodapkar, K.M., Kaufman, J.L., Ehlers, M., Banerjee, D.K., Bonvini, E., Koenig, S., Steinman, R.M., Ravetch, J.V., and Dhodapkar, M.V. (2005). Selective blockade of inhibitory Fcgamma receptor enables human dendritic cell maturation with IL-12p70

production and immunity to antibody-coated tumor cells. Proc Natl Acad Sci U S A *102*, 2910-2915.

Dijstelbloem, H.M., van de Winkel, J.G., and Kallenberg, C.G. (2001). Inflammation in autoimmunity: receptors for IgG revisited. Trends Immunol *22*, 510-516.

Dockrell, D.H., Badley, A.D., Villacian, J.S., Heppelmann, C.J., Algeciras, A., Ziesmer, S., Yagita, H., Lynch, D.H., Roche, P.C., Leibson, P.J.*, et al.* (1998). The expression of Fas Ligand by macrophages and its upregulation by human immunodeficiency virus infection. J Clin Invest *101*, 2394-2405.

Dosquet, C., Weill, D., and Wautier, J.L. (1995). Cytokines and thrombosis. Journal of cardiovascular pharmacology *25 Suppl 2*, S13-19.

Duffield, J.S., Tipping, P.G., Kipari, T., Cailhier, J.F., Clay, S., Lang, R., Bonventre, J.V., and Hughes, J. (2005). Conditional ablation of macrophages halts progression of crescentic glomerulonephritis. Am J Pathol *167*, 1207-1219.

Dupont, P.J., and Warrens, A.N. (2007). Fas ligand exerts its pro-inflammatory effects via neutrophil recruitment but not activation. Immunology *120*, 133-139.

Earnshaw, W.C., Martins, L.M., and Kaufmann, S.H. (1999). Mammalian caspases: structure, activation, substrates, and functions during apoptosis. Annu Rev Biochem *68*, 383-424.

Edwards, J.C., Blades, S., and Cambridge, G. (1997). Restricted expression of Fc gammaRIII (CD16) in synovium and dermis: implications for tissue targeting in rheumatoid arthritis (RA). Clin Exp Immunol *108*, 401-406.

Egner, W., and Chapel, H.M. (1990). Titration of antibodies against neutrophil cytoplasmic antigens is useful in monitoring disease activity in systemic vasculitides. Clin Exp Immunol *82*, 244-249.

Ehara, T., and Shigematsu, H. (1998). Contribution of mast cells to the tubulointerstitial lesions in IgA nephritis. Kidney Int *54*, 1675-1683.

Eller, K., Weber, T., Pruenster, M., Wolf, A.M., Mayer, G., Rosenkranz, A.R., and Rot, A. (2010). CCR7 deficiency exacerbates injury in acute nephritis due to aberrant localization of regulatory T cells. J Am Soc Nephrol *21*, 42-52.

Eller, K., Wolf, D., Huber, J.M., Metz, M., Mayer, G., McKenzie, A.N., Maurer, M., Rosenkranz, A.R., and Wolf, A.M. (2011). IL-9 production by regulatory T cells recruits mast cells that are essential for regulatory T cell-induced immune suppression. J Immunol *186*, 83-91.

Erwig, L.P., Stewart, K., and Rees, A.J. (2000). Macrophages from inflamed but not normal glomeruli are unresponsive to anti-inflammatory cytokines. Am J Pathol *156*, 295-301.

Falk, R.J., and Jennette, J.C. (2002). ANCA are pathogenic--oh yes they are! J Am Soc Nephrol *13*, 1977-1979.

Falk, R.J., Terrell, R.S., Charles, L.A., and Jennette, J.C. (1990). Anti-neutrophil cytoplasmic autoantibodies induce neutrophils to degranulate and produce oxygen radicals in vitro. Proc Natl Acad Sci U S A *87*, 4115-4119.

Fang, Y., Yu, S., Ellis, J.S., Sharav, T., and Braley-Mullen, H. (2010). Comparison of sensitivity of Th1, Th2, and Th17 cells with Fas-mediated apoptosis. J Leukoc Biol.

Feith, G.W., Assmann, K.J., Bogman, M.J., van Gompel, A.P., Schalkwijk, J., and Koene, R.A. (1993). Lack of albuminuria in the early heterologous phase of anti-GBM nephritis in beige mice. Kidney Int *43*, 824-827.

Fields, M.L., Sokol, C.L., Eaton-Bassiri, A., Seo, S., Madaio, M.P., and Erikson, J. (2001). Fas/Fas ligand deficiency results in altered localization of anti-double-stranded DNA B cells and dendritic cells. J Immunol *167*, 2370-2378.

Fisher, G.H., Rosenberg, F.J., Straus, S.E., Dale, J.K., Middleton, L.A., Lin, A.Y., Strober, W., Lenardo, M.J., and Puck, J.M. (1995). Dominant interfering Fas gene mutations impair apoptosis in a human autoimmune lymphoproliferative syndrome. Cell *81*, 935-946.

Friden, V., Oveland, E., Tenstad, O., Ebefors, K., Nystrom, J., Nilsson, U.A., and Haraldsson, B. (2011). The glomerular endothelial cell coat is essential for glomerular filtration. Kidney Int *79*, 1322-1330.

Fujiwara, M., Suemoto, H., Muragaki, Y., and Ooshima, A. (2007). Fas-mediated upregulation of vascular endothelial growth factor and monocyte chemoattractant protein-1 expression in cultured dermal fibroblasts: role in the inflammatory response. J Dermatol *34*, 99-109.

Fukuyama, H., Adachi, M., Suematsu, S., Miwa, K., Suda, T., Yoshida, N., and Nagata, S. (1998). Transgenic expression of Fas in T cells blocks lymphoproliferation but not autoimmune disease in MRL-lpr mice. J Immunol *160*, 3805-3811.

Fuss, I.J., Strober, W., Dale, J.K., Fritz, S., Pearlstein, G.R., Puck, J.M., Lenardo, M.J., and Straus, S.E. (1997). Characteristic T helper 2 T cell cytokine abnormalities in autoimmune lymphoproliferative syndrome, a syndrome marked by defective apoptosis and humoral autoimmunity. J Immunol *158*, 1912-1918.

Gan, P.Y., Steinmetz, O.M., Tan, D.S., O'Sullivan, K.M., Ooi, J.D., Iwakura, Y., Kitching, A.R., and Holdsworth, S.R. (2010). Th17 cells promote autoimmune anti-myeloperoxidase glomerulonephritis. J Am Soc Nephrol *21*, 925-931.

Gan, P.Y., Summers, S.A., Ooi, J.D., O'Sullivan, K.M., Tan, D.S., Muljadi, R.C., Odobasic, D., Kitching, A.R., and Holdsworth, S.R. (2012). Mast cells contribute to peripheral tolerance and attenuate autoimmune vasculitis. J Am Soc Nephrol *23*, 1955-1966.

Gerber, J.S., and Mosser, D.M. (2001). Reversing lipopolysaccharide toxicity by ligating the macrophage Fc gamma receptors. J Immunol *166*, 6861-6868.

Giorgini, A., Brown, H.J., Lock, H.R., Nimmerjahn, F., Ravetch, J.V., Verbeek, J.S., Sacks, S.H., and Robson, M.G. (2008). Fc gamma RIII and Fc gamma RIV are indispensable for acute glomerular inflammation induced by switch variant monoclonal antibodies. J Immunol *181*, 8745-8752.

Gochuico, B.R., Miranda, K.M., Hessel, E.M., De Bie, J.J., Van Oosterhout, A.J., Cruikshank, W.W., and Fine, A. (1998). Airway epithelial Fas ligand expression: potential role in modulating bronchial inflammation. Am J Physiol *274*, L444-449.

Goldwich, A., Burkard, M., Olke, M., Daniel, C., Amann, K., Hugo, C., Kurts, C., Steinkasserer, A., and Gessner, A. (2013). Podocytes are nonhematopoietic professional antigen-presenting cells. J Am Soc Nephrol *24*, 906-916.

Gomez-Guerrero, C., Lopez-Armada, M.J., Gonzalez, E., and Egido, J. (1994). Soluble IgA and IgG aggregates are catabolized by cultured rat mesangial cells and induce production of TNF-alpha and IL-6, and proliferation. J Immunol *153*, 5247-5255.

Gomez-Guerrero, C., Lopez-Franco, O., Suzuki, Y., Sanjuan, G., Hernandez-Vargas, P., Blanco, J., and Egido, J. (2002). Nitric oxide production in renal cells by immune complexes: Role of kinases and nuclear factor-kappaB. Kidney Int *62*, 2022-2034.

Gonzalez-Cuadrado, S., Lorz, C., Garcia del Moral, R., O'Valle, F., Alonso, C., Ramiro, F., Ortiz-Gonzalez, A., Egido, J., and Ortiz, A. (1997). Agonistic anti-Fas antibodies induce glomerular cell apoptosis in mice in vivo. Kidney Int *51*, 1739-1746.

Goulding, N.J., Knight, S.M., Godolphin, J.L., and Guyre, P.M. (1992). Increase in neutrophil Fc gamma receptor I expression following interferon gamma treatment in rheumatoid arthritis. Ann Rheum Dis *51*, 465-468.

Grabowski, E.F., and Lam, F.P. (1995). Endothelial cell function, including tissue factor expression, under flow conditions. Thromb Haemost *74*, 123-128.

Green, D.R., and Ferguson, T.A. (2001). The role of Fas ligand in immune privilege. Nat Rev Mol Cell Biol *2*, 917-924.

Greka, A., and Mundel, P. (2012). Cell biology and pathology of podocytes. Annual review of physiology *74*, 299-323.

Griffith, M.E., Coulthart, A., and Pusey, C.D. (1996a). T cell responses to myeloperoxidase (MPO) and proteinase 3 (PR3) in patients with systemic vasculitis. Clin Exp Immunol *103*, 253-258.

Griffith, T.S., Brunner, T., Fletcher, S.M., Green, D.R., and Ferguson, T.A. (1995). Fas ligand-induced apoptosis as a mechanism of immune privilege. Science *270*, 1189-1192.

Griffith, T.S., Yu, X., Herndon, J.M., Green, D.R., and Ferguson, T.A. (1996b). CD95-induced apoptosis of lymphocytes in an immune privileged site induces immunological tolerance. Immunity *5*, 7-16.

Haas, C., Ryffel, B., and Le Hir, M. (1995). Crescentic glomerulonephritis in interferon-gamma receptor deficient mice. J Inflamm *47*, 206-213.

Hadjinicolaou, A.V., Nisar, M.K., Parfrey, H., Chilvers, E.R., and Ostor, A.J. (2012). Non-infectious pulmonary toxicity of rituximab: a systematic review. Rheumatology (Oxford) *51*, 653-662.

Hahne, M., Renno, T., Schroeter, M., Irmler, M., French, L., Bornard, T., MacDonald, H.R., and Tschopp, J. (1996). Activated B cells express functional Fas ligand. Eur J Immunol *26*, 721-724.

Halbwachs-Mecarelli, L., Camous, L., Bigot, S., Roumenina, L., Brachemi, S., Fremeaux-Bacchi, V., and Lesavre, P. (2011). Neutrophils and complement activate each other: an inflammation amplification loop enhanced further by ANCA. Clinical and Experimental Immunology *164*, 146-146.

Hammer, D.K., and Dixon, F.J. (1963). Experimental glomerulonephritis. II. Immunologic events in the pathogenesis of nephrotoxic serum nephritis in the rat. J Exp Med *117*, 1019-1034.

Hao, Z., Hampel, B., Yagita, H., and Rajewsky, K. (2004). T cell-specific ablation of Fas leads to Fas ligand-mediated lymphocyte depletion and inflammatory pulmonary fibrosis. J Exp Med *199*, 1355-1365.

Haraldsson, B., Nystrom, J., and Deen, W.M. (2008). Properties of the glomerular barrier and mechanisms of proteinuria. Physiological reviews *88*, 451-487.

Harper, L., and Savage, C.O. (2000). Pathogenesis of ANCA-associated systemic vasculitis. J Pathol *190*, 349-359.

Hazenbos, W.L., Gessner, J.E., Hofhuis, F.M., Kuipers, H., Meyer, D., Heijnen, I.A., Schmidt, R.E., Sandor, M., Capel, P.J., Daeron, M.*, et al.* (1996). Impaired IgG-dependent anaphylaxis and Arthus reaction in Fc gamma RIII (CD16) deficient mice. Immunity *5*, 181-188.

Hebert, M.J., Takano, T., Papayianni, A., Rennke, H.G., Minto, A., Salant, D.J., Carroll, M.C., and Brady, H.R. (1998). Acute nephrotoxic serum nephritis in complement knockout mice: relative roles of the classical and alternate pathways in neutrophil recruitment and proteinuria. Nephrol Dial Transplant *13*, 2799-2803.

Ho, J.Q., Asagiri, M., Hoffmann, A., and Ghosh, G. (2011). NF-kappaB potentiates caspase independent hydrogen peroxide induced cell death. PLoS One *6*, e16815.

Hochegger, K., Siebenhaar, F., Vielhauer, V., Heininger, D., Mayadas, T.N., Mayer, G., Maurer, M., and Rosenkranz, A.R. (2005). Role of mast cells in experimental anti-glomerular basement membrane glomerulonephritis. Eur J Immunol *35*, 3074-3082.

Hochheiser, K., Engel, D.R., Hammerich, L., Heymann, F., Knolle, P.A., Panzer, U., and Kurts, C. (2011). Kidney Dendritic Cells Become Pathogenic during Crescentic Glomerulonephritis with Proteinuria. J Am Soc Nephrol *22*, 306-316.

Hohlbaum, A.M., Gregory, M.S., Ju, S.T., and Marshak-Rothstein, A. (2001). Fas ligand engagement of resident peritoneal macrophages in vivo induces apoptosis and the production of neutrophil chemotactic factors. J Immunol *167*, 6217-6224.

Holdsworth, S.R., Kitching, A.R., and Tipping, P.G. (1999). Th1 and Th2 T helper cell subsets affect patterns of injury and outcomes in glomerulonephritis. Kidney Int *55*, 1198-1216.

Holdsworth, S.R., Neale, T.J., and Wilson, C.B. (1981). Abrogation of macrophage-dependent injury in experimental glomerulonephritis in the rabbit. Use of an antimacrophage serum. The Journal of clinical investigation *68*, 686-698.

Holler, N., Tardivel, A., Kovacsovics-Bankowski, M., Hertig, S., Gaide, O., Martinon, F., Tinel, A., Deperthes, D., Calderara, S., Schulthess, T.*, et al.* (2003). Two adjacent trimeric Fas ligands are required for Fas signaling and formation of a death-inducing signaling complex. Mol Cell Biol *23*, 1428-1440.

Hopfer, H., Maron, R., Butzmann, U., Helmchen, U., Weiner, H.L., and Kalluri, R. (2003). The importance of cell-mediated immunity in the course and severity of autoimmune anti-glomerular basement membrane disease in mice. FASEB J *17*, 860-868.

Hruby, Z.W., Shirota, K., Jothy, S., and Lowry, R.P. (1991). Antiserum against tumor necrosis factor-alpha and a protease inhibitor reduce immune glomerular injury. Kidney Int *40*, 43-51.

Huang, X.R., Holdsworth, S.R., and Tipping, P.G. (1994). Evidence for delayed-type hypersensitivity mechanisms in glomerular crescent formation. Kidney Int *46*, 69-78.

Huang, X.R., Holdsworth, S.R., and Tipping, P.G. (1997a). Th2 responses induce humorally mediated injury in experimental anti-glomerular basement membrane glomerulonephritis. J Am Soc Nephrol *8*, 1101-1108.

Huang, X.R., Tipping, P.G., Apostolopoulos, J., Oettinger, C., D'Souza, M., Milton, G., and Holdsworth, S.R. (1997b). Mechanisms of T cell-induced glomerular injury in anti-

glomerular basement membrane (GBM) glomerulonephritis in rats. Clin Exp Immunol *109*, 134-142.

Huang, X.R., Tipping, P.G., Shuo, L., and Holdsworth, S.R. (1997c). Th1 responsiveness to nephritogenic antigens determines susceptibility to crescentic glomerulonephritis in mice. Kidney Int *51*, 94-103.

Huber, T.B., Reinhardt, H.C., Exner, M., Burger, J.A., Kerjaschki, D., Saleem, M.A., and Pavenstadt, H. (2002). Expression of functional CCR and CXCR chemokine receptors in podocytes. J Immunol *168*, 6244-6252.

Hughes, A.K., Stricklett, P.K., and Kohan, D.E. (2001). Shiga toxin-1 regulation of cytokine production by human glomerular epithelial cells. Nephron *88*, 14-23.

Huugen, D., Xiao, H., van Esch, A., Falk, R.J., Peutz-Kootstra, C.J., Buurman, W.A., Tervaert, J.W., Jennette, J.C., and Heeringa, P. (2005). Aggravation of anti-myeloperoxidase antibody-induced glomerulonephritis by bacterial lipopolysaccharide: role of tumor necrosis factor-alpha. Am J Pathol *167*, 47-58.

Ichii, O., Konno, A., Sasaki, N., Endoh, D., Hashimoto, Y., and Kon, Y. (2008). Altered balance of inhibitory and active Fc gamma receptors in murine autoimmune glomerulonephritis. Kidney Int *74*, 339-347.

Ikezumi, Y., Hurst, L.A., Masaki, T., Atkins, R.C., and Nikolic-Paterson, D.J. (2003). Adoptive transfer studies demonstrate that macrophages can induce proteinuria and mesangial cell proliferation. Kidney Int *63*, 83-95.

Imamura, R., Konaka, K., Matsumoto, N., Hasegawa, M., Fukui, M., Mukaida, N., Kinoshita, T., and Suda, T. (2004). Fas ligand induces cell-autonomous NF-kappaB activation and interleukin-8 production by a mechanism distinct from that of tumor necrosis factor-alpha. J Biol Chem *279*, 46415-46423.

Ioan-Facsinay, A., de Kimpe, S.J., Hellwig, S.M., van Lent, P.L., Hofhuis, F.M., van Ojik, H.H., Sedlik, C., da Silveira, S.A., Gerber, J., de Jong, Y.F.*, et al.* (2002). FcgammaRI (CD64) contributes substantially to severity of arthritis, hypersensitivity responses, and protection from bacterial infection. Immunity *16*, 391-402.

Itoh, N., Imagawa, A., Hanafusa, T., Waguri, M., Yamamoto, K., Iwahashi, H., Moriwaki, M., Nakajima, H., Miyagawa, J., Namba, M.*, et al.* (1997). Requirement of Fas for the development of autoimmune diabetes in nonobese diabetic mice. J Exp Med *186*, 613-618.

Itoh, N., and Nagata, S. (1993). A novel protein domain required for apoptosis. Mutational analysis of human Fas antigen. The Journal of Biological Chemistry

*268*, 10932-10937.

Itoh, N., Yonehara, S., Ishii, A., Yonehara, M., Mizushima, S., Sameshima, M., Hase, A., Seto, Y., and Nagata, S. (1991). The polypeptide encoded by the cDNA for human cell surface antigen Fas can mediate apoptosis. Cell *66*, 233-243.

Izui, S., Kelley, V.E., Masuda, K., Yoshida, H., Roths, J.B., and Murphy, E.D. (1984). Induction of various autoantibodies by mutant gene lpr in several strains of mice. J Immunol *133*, 227-233.

Jancar, S., and Sanchez Crespo, M. (2005). Immune complex-mediated tissue injury: a multistep paradigm. Trends Immunol *26*, 48-55.

Janin, A., Deschaumes, C., Daneshpouy, M., Estaquier, J., Micic-Polianski, J., Rajagopalan-Levasseur, P., Akarid, K., Mounier, N., Gluckman, E., Socie, G.*, et al.* (2002). CD95

engagement induces disseminated endothelial cell apoptosis in vivo: immunopathologic implications. Blood *99*, 2940-2947.

Jeansson, M., and Haraldsson, B. (2006). Morphological and functional evidence for an important role of the endothelial cell glycocalyx in the glomerular barrier. Am J Physiol Renal Physiol *290*, F111-116.

Jennette, J.C., Wilkman, A.S., and Falk, R.J. (1989). Anti-neutrophil cytoplasmic autoantibody-associated glomerulonephritis and vasculitis. Am J Pathol *135*, 921-930.

Jiang, Y., Hirose, S., Abe, M., Sanokawa-Akakura, R., Ohtsuji, M., Mi, X., Li, N., Xiu, Y., Zhang, D., Shirai, J.*, et al.* (2000). Polymorphisms in IgG Fc receptor IIB regulatory regions associated with autoimmune susceptibility. Immunogenetics *51*, 429-435.

Kabelitz, D., Pohl, T., and Pechhold, K. (1993). Activation-induced cell death (apoptosis) of mature peripheral T lymphocytes. Immunol Today *14*, 338-339.

Kalergis, A.M., and Ravetch, J.V. (2002). Inducing tumor immunity through the selective engagement of activating Fcgamma receptors on dendritic cells. J Exp Med *195*, 1653-1659.

Kalluri, R., Danoff, T.M., Okada, H., and Neilson, E.G. (1997). Susceptibility to anti-glomerular basement membrane disease and Goodpasture syndrome is linked to MHC class II genes and the emergence of T cell-mediated immunity in mice. J Clin Invest *100*, 2263-2275.

Kalluri, R., Gunwar, S., Reeders, S.T., Morrison, K.C., Mariyama, M., Ebner, K.E., Noelken, M.E., and Hudson, B.G. (1991). Goodpasture syndrome. Localization of the epitope for the autoantibodies to the carboxyl-terminal region of the alpha 3(IV) chain of basement membrane collagen. J Biol Chem *266*, 24018-24024.

Kalluri, R., Wilson, C.B., Weber, M., Gunwar, S., Chonko, A.M., Neilson, E.G., and Hudson, B.G. (1995). Identification of the alpha 3 chain of type IV collagen as the common autoantigen in antibasement membrane disease and Goodpasture syndrome. J Am Soc Nephrol *6*, 1178-1185.

Kanamaru, Y., Scandiuzzi, L., Essig, M., Brochetta, C., Guerin-Marchand, C., Tomino, Y., Monteiro, R.C., Peuchmaur, M., and Blank, U. (2006). Mast cell-mediated remodeling and fibrinolytic activity protect against fatal glomerulonephritis. J Immunol *176*, 5607-5615.

Kaneko, Y., Nimmerjahn, F., Madaio, M.P., and Ravetch, J.V. (2006). Pathology and protection in nephrotoxic nephritis is determined by selective engagement of specific Fc receptors. J Exp Med *203*, 789-797.

Karray, S., Kress, C., Cuvellier, S., Hue-Beauvais, C., Damotte, D., Babinet, C., and Levi-Strauss, M. (2004). Complete loss of Fas ligand gene causes massive lymphoproliferation and early death, indicating a residual activity of gld allele. J Immunol *172*, 2118-2125.

Karsten, C.M., Pandey, M.K., Figge, J., Kilchenstein, R., Taylor, P.R., Rosas, M., McDonald, J.U., Orr, S.J., Berger, M., Petzold, D.*, et al.* (2012). Anti-inflammatory activity of IgG1 mediated by Fc galactosylation and association of FcgammaRIIB and dectin-1. Nat Med *18*, 1401-1406.

Kasibhatla, S., Brunner, T., Genestier, L., Echeverri, F., Mahboubi, A., and Green, D.R. (1998). DNA damaging agents induce expression of Fas ligand and subsequent apoptosis in T lymphocytes via the activation of NF-kappa B and AP-1. Mol Cell *1*, 543-551.

Kayagaki, N., Kawasaki, A., Ebata, T., Ohmoto, H., Ikeda, S., Inoue, S., Yoshino, K., Okumura, K., and Yagita, H. (1995). Metalloproteinase-mediated release of human Fas ligand. J Exp Med *182*, 1777-1783.

Kelley, V.E., and Roths, J.B. (1985). Interaction of mutant lpr gene with background strain influences renal disease. Clin Immunol Immunopathol *37*, 220-229.

Kennedy, N.J., Kataoka, T., Tschopp, J., and Budd, R.C. (1999). Caspase activation is required for T cell proliferation. J Exp Med *190*, 1891-1896.

Keshav, S., Chung, P., Milon, G., and Gordon, S. (1991). Lysozyme is an inducible marker of macrophage activation in murine tissues as demonstrated by in situ hybridization. J Exp Med *174*, 1049-1058.

Kiener, P.A., Davis, P.M., Starling, G.C., Mehlin, C., Klebanoff, S.J., Ledbetter, J.A., and Liles, W.C. (1997). Differential induction of apoptosis by Fas-Fas ligand interactions in human monocytes and macrophages. J Exp Med *185*, 1511-1516.

Kim, S., Kim, K.A., Hwang, D.Y., Lee, T.H., Kayagaki, N., Yagita, H., and Lee, M.S. (2000). Inhibition of autoimmune diabetes by Fas ligand: the paradox is solved. J Immunol *164*, 2931-2936.

Kim, Y.H., Kim, S., Kim, K.A., Yagita, H., Kayagaki, N., Kim, K.W., and Lee, M.S. (1999). Apoptosis of pancreatic beta-cells detected in accelerated diabetes of NOD mice: no role of Fas-Fas ligand interaction in autoimmune diabetes. Eur J Immunol *29*, 455-465.

Kimura, M., Ogata, Y., Shimada, K., Wakabayashi, T., Onoda, H., Katagiri, T., and Matsuzawa, A. (1992). Nephritogenicity of the lprcg gene on the MRL background. Immunology *76*, 498-504.

Kirchhofer, D., Tschopp, T.B., Hadvary, P., and Baumgartner, H.R. (1994). Endothelial cells stimulated with tumor necrosis factor-alpha express varying amounts of tissue factor resulting in inhomogenous fibrin deposition in a native blood flow system. Effects of thrombin inhibitors. J Clin Invest *93*, 2073-2083.

Kischkel, F.C., Hellbardt, S., Behrmann, I., Germer, M., Pawlita, M., Krammer, P.H., and Peter, M.E. (1995). Cytotoxicity-dependent APO-1 (Fas/CD95)-associated proteins form a death-inducing signalling complex (DISC) with the receptor. EMBO J *14*, 5579-5588.

Kitching, A.R., Holdsworth, S.R., and Tipping, P.G. (1999a). IFN-gamma mediates crescent formation and cell-mediated immune injury in murine glomerulonephritis. J Am Soc Nephrol *10*, 752-759.

Kitching, A.R., Ru Huang, X., Turner, A.L., Tipping, P.G., Dunn, A.R., and Holdsworth, S.R. (2002). The requirement for granulocyte-macrophage colony-stimulating factor and granulocyte colony-stimulating factor in leukocyte-mediated immune glomerular injury. J Am Soc Nephrol *13*, 350-358.

Kitching, A.R., Tipping, P.G., and Holdsworth, S.R. (1999b). IL-12 directs severe renal injury, crescent formation and Th1 responses in murine glomerulonephritis. Eur J Immunol *29*, 1-10.

Kitching, A.R., Tipping, P.G., Huang, X.R., Mutch, D.A., and Holdsworth, S.R. (1997). Interleukin-4 and interleukin-10 attenuate established crescentic glomerulonephritis in mice. Kidney Int *52*, 52-59.

Kitching, A.R., Tipping, P.G., Mutch, D.A., Huang, X.R., and Holdsworth, S.R. (1998). Interleukin-4 deficiency enhances Th1 responses and crescentic glomerulonephritis in mice. Kidney Int *53*, 112-118.

Kitching, A.R., Tipping, P.G., Timoshanko, J.R., and Holdsworth, S.R. (2000). Endogenous interleukin-10 regulates Th1 responses that induce crescentic glomerulonephritis. Kidney Int *57*, 518-525.

Kitching, A.R., Turner, A.L., Wilson, G.R., Semple, T., Odobasic, D., Timoshanko, J.R., O'Sullivan, K.M., Tipping, P.G., Takeda, K., Akira, S.*, et al.* (2005). IL-12p40 and IL-18 in crescentic glomerulonephritis: IL-12p40 is the key Th1-defining cytokine chain, whereas IL-18 promotes local inflammation and leukocyte recruitment. J Am Soc Nephrol *16*, 2023-2033.

Ko, G.J., Jang, H.R., Huang, Y., Womer, K.L., Liu, M., Higbee, E., Xiao, Z., Yagita, H., Racusen, L., Hamad, A.R.*, et al.* (2011). Blocking Fas ligand on leukocytes attenuates kidney ischemia-reperfusion injury. J Am Soc Nephrol *22*, 732-742.

Kobayashi, S., Hirano, T., Kakinuma, M., and Uede, T. (1993). Transcriptional repression and differential splicing of Fas mRNA by early transposon (ETn) insertion in autoimmune lpr mice. Biochem Biophys Res Commun *191*, 617-624.

Kocher, M., Edberg, J.C., Fleit, H.B., and Kimberly, R.P. (1998). Antineutrophil cytoplasmic antibodies preferentially engage Fc gammaRIIIb on human neutrophils. J Immunol *161*, 6909-6914.

Kruger, T., Benke, D., Eitner, F., Lang, A., Wirtz, M., Hamilton-Williams, E.E., Engel, D., Giese, B., Muller-Newen, G., Floege, J.*, et al.* (2004). Identification and functional characterization of dendritic cells in the healthy murine kidney and in experimental glomerulonephritis. J Am Soc Nephrol *15*, 613-621.

Kurlander, R.J., Ellison, D.M., and Hall, J. (1984). The blockade of Fc receptor-mediated clearance of immune complexes in vivo by a monoclonal antibody (2.4G2) directed against Fc receptors on murine leukocytes. J Immunol *133*, 855-862.

Lai, K.W., Wei, C.L., Tan, L.K., Tan, P.H., Chiang, G.S., Lee, C.G., Jordan, S.C., and Yap, H.K. (2007). Overexpression of interleukin-13 induces minimal-change-like nephropathy in rats. J Am Soc Nephrol *18*, 1476-1485.

Lai, P.C., Cook, H.T., Smith, J., Keith, J.C., Jr., Pusey, C.D., and Tam, F.W. (2001). Interleukin-11 attenuates nephrotoxic nephritis in Wistar Kyoto rats. J Am Soc Nephrol *12*, 2310-2320.

Lan, H.Y., Bacher, M., Yang, N., Mu, W., Nikolic-Paterson, D.J., Metz, C., Meinhardt, A., Bucala, R., and Atkins, R.C. (1997a). The pathogenic role of macrophage migration inhibitory factor in immunologically induced kidney disease in the rat. J Exp Med *185*, 1455-1465.

Lan, H.Y., Nikolic-Paterson, D.J., Zarama, M., Vannice, J.L., and Atkins, R.C. (1993). Suppression of experimental crescentic glomerulonephritis by the interleukin-1 receptor antagonist. Kidney Int *43*, 479-485.

Lan, H.Y., Yang, N., Metz, C., Mu, W., Song, Q., Nikolic-Paterson, D.J., Bacher, M., Bucala, R., and Atkins, R.C. (1997b). TNF-alpha up-regulates renal MIF expression in rat crescentic glomerulonephritis. Mol Med *3*, 136-144.

Le Hir, M., Keller, C., Eschmann, V., Hahnel, B., Hosser, H., and Kriz, W. (2001). Podocyte bridges between the tuft and Bowman's capsule: an early event in experimental crescentic glomerulonephritis. J Am Soc Nephrol *12*, 2060-2071.

Lee, S., Huen, S., Nishio, H., Nishio, S., Lee, H.K., Choi, B.S., Ruhrberg, C., and Cantley, L.G. (2011). Distinct macrophage phenotypes contribute to kidney injury and repair. J Am Soc Nephrol *22*, 317-326.

Leeuwis, J.W., Nguyen, T.Q., Dendooven, A., Kok, R.J., and Goldschmeding, R. (2010). Targeting podocyte-associated diseases. Advanced drug delivery reviews *62*, 1325-1336.

Lerner, R.A., Glassock, R.J., and Dixon, F.J. (1967). The role of anti-glomerular basement membrane antibody in the pathogenesis of human glomerulonephritis. J Exp Med *126*, 989-1004.

Letellier, E., Kumar, S., Sancho-Martinez, I., Krauth, S., Funke-Kaiser, A., Laudenklos, S., Konecki, K., Klussmann, S., Corsini, N.S., Kleber, S.*, et al.* (2010). CD95-ligand on peripheral myeloid cells activates Syk kinase to trigger their recruitment to the inflammatory site. Immunity *32*, 240-252.

Li, S., Holdsworth, S.R., and Tipping, P.G. (1997). Antibody independent crescentic glomerulonephritis in mu chain deficient mice. Kidney Int *51*, 672-678.

Li, S., Holdsworth, S.R., and Tipping, P.G. (2000). MHC class I pathway is not required for the development of crescentic glomerulonephritis in mice. Clin Exp Immunol *122*, 453-458.

Li, S., Kurts, C., Kontgen, F., Holdsworth, S.R., and Tipping, P.G. (1998). Major histocompatibility complex class II expression by intrinsic renal cells is required for crescentic glomerulonephritis. J Exp Med *188*, 597-602.

Linehan, S.A., Martinez-Pomares, L., Stahl, P.D., and Gordon, S. (1999). Mannose receptor and its putative ligands in normal murine lymphoid and nonlymphoid organs: In situ expression of mannose receptor by selected macrophages, endothelial cells, perivascular microglia, and mesangial cells, but not dendritic cells. J Exp Med *189*, 1961-1972.

Linkermann, A., Himmerkus, N., Rolver, L., Keyser, K.A., Steen, P., Brasen, J.H., Bleich, M., Kunzendorf, U., and Krautwald, S. (2011). Renal tubular Fas ligand mediates fratricide in cisplatin-induced acute kidney failure. Kidney Int *79*, 169-178.

Little, M.A., Al-Ani, B., Ren, S.Y., Al-Nuaimi, H., Alpers, C.E., Savage, C., and Duffield, J.S. (2011). Human anti-PR3 ANCA recapitulate systemic vasculitis in mice with a humanized immune system. Clinical and Experimental Immunology *164*, 124-124.

Little, M.A., Bhangal, G., Smyth, C.L., Nakada, M.T., Cook, H.T., Nourshargh, S., and Pusey, C.D. (2006). Therapeutic effect of anti-TNF-alpha antibodies in an experimental model of anti-neutrophil cytoplasm antibody-associated systemic vasculitis. J Am Soc Nephrol *17*, 160-169.

Little, M.A., Smyth, C.L., Yadav, R., Ambrose, L., Cook, H.T., Nourshargh, S., and Pusey, C.D. (2005). Antineutrophil cytoplasm antibodies directed against myeloperoxidase augment leukocyte-microvascular interactions in vivo. Blood *106*, 2050-2058.

Little, M.A., Smyth, L., Salama, A.D., Mukherjee, S., Smith, J., Haskard, D., Nourshargh, S., Cook, H.T., and Pusey, C.D. (2009). Experimental autoimmune vasculitis: an animal model of anti-neutrophil cytoplasmic autoantibody-associated systemic vasculitis. Am J Pathol *174*, 1212-1220.

Lloyd, C.M., Minto, A.W., Dorf, M.E., Proudfoot, A., Wells, T.N., Salant, D.J., and Gutierrez-Ramos, J.C. (1997). RANTES and monocyte chemoattractant protein-1 (MCP-1) play an important role in the inflammatory phase of crescentic nephritis, but only MCP-1 is involved in crescent formation and interstitial fibrosis. J Exp Med *185*, 1371-1380.

Lopatin, U., Yao, X., Williams, R.K., Bleesing, J.J., Dale, J.K., Wong, D., Teruya-Feldstein, J., Fritz, S., Morrow, M.R., Fuss, I.*, et al.* (2001). Increases in circulating and lymphoid tissue interleukin-10 in autoimmune lymphoproliferative syndrome are associated with disease expression. Blood *97*, 3161-3170.

Lorz, C., Ortiz, A., Justo, P., Gonzalez-Cuadrado, S., Duque, N., Gomez-Guerrero, C., and Egido, J. (2000). Proapoptotic Fas ligand is expressed by normal kidney tubular epithelium and injured glomeruli. J Am Soc Nephrol *11*, 1266-1277.

Ma, Y., Liu, H., Tu-Rapp, H., Thiesen, H.-J., Ibrahim, S.M., Cole, S.M., and Pope, R.M. (2004). Fas ligation on macrophages enhances IL-1R1-Toll-like receptor 4 signalling and promotes chronic inflammation. Nature Immunology *5*, 380-387.

Mabrouk, I., Buart, S., Hasmim, M., Michiels, C., Connault, E., Opolon, P., Chiocchia, G., Levi-Strauss, M., Chouaib, S., and Karray, S. (2008). Prevention of autoimmunity and control of recall response to exogenous antigen by Fas death receptor ligand expression on T cells. Immunity *29*, 922-933.

Magerus-Chatinet, A., Stolzenberg, M.C., Loffredo, M.S., Neven, B., Schaffner, C., Ducrot, N., Arkwright, P.D., Bader-Meunier, B., Barbot, J., Blanche, S.*, et al.* (2009). FAS-L, IL-10, and double-negative CD4- CD8- TCR alpha/beta+ T cells are reliable markers of autoimmune lymphoproliferative syndrome (ALPS) associated with FAS loss of function. Blood *113*, 3027-3030.

Martin, M., Schwinzer, R., Schellekens, H., and Resch, K. (1989). Glomerular mesangial cells in local inflammation. Induction of the expression of MHC class II antigens by IFN-gamma. J Immunol *142*, 1887-1894.

Matsuzawa, A., Moriyama, T., Kaneko, T., Tanaka, M., Kimura, M., Ikeda, H., and Katagiri, T. (1990). A new allele of the lpr locus, lprcg, that complements the gld gene in induction of lymphadenopathy in the mouse. J Exp Med *171*, 519-531.

Mayadas, T.N., Tsokos, G.C., and Tsuboi, N. (2009). Mechanisms of immune complex-mediated neutrophil recruitment and tissue injury. Circulation *120*, 2012-2024.

McGaha, T.L., Karlsson, M.C., and Ravetch, J.V. (2008). FcgammaRIIB deficiency leads to autoimmunity and a defective response to apoptosis in Mrl-MpJ mice. J Immunol *180*, 5670-5679.

Medema, J.P., Scaffidi, C., Kischkel, F.C., Shevchenko, A., Mann, M., Krammer, P.H., and Peter, M.E. (1997). FLICE is activated by association with the CD95 death-inducing signaling complex (DISC). EMBO J *16*, 2794-2804.

Merkel, F., Kalluri, R., Marx, M., Enders, U., Stevanovic, S., Giegerich, G., Neilson, E.G., Rammensee, H.G., Hudson, B.G., and Weber, M. (1996). Autoreactive T-cells in Goodpasture's syndrome recognize the N-terminal NC1 domain on alpha 3 type IV collagen. Kidney Int *49*, 1127-1133.

Miyajima, I., Dombrowicz, D., Martin, T.R., Ravetch, J.V., Kinet, J.P., and Galli, S.J. (1997). Systemic anaphylaxis in the mouse can be mediated largely through IgG1 and Fc gammaRIII. Assessment of the cardiopulmonary changes, mast cell degranulation, and death associated with active or IgE- or IgG1-dependent passive anaphylaxis. J Clin Invest *99*, 901-914.

Miyawaki, T., Uehara, T., Nibu, R., Tsuji, T., Yachie, A., Yonehara, S., and Taniguchi, N. (1992). Differential expression of apoptosis-related Fas antigen on lymphocyte subpopulations in human peripheral blood. J Immunol *149*, 3753-3758.

Moeller, M.J., Soofi, A., Hartmann, I., Le Hir, M., Wiggins, R., Kriz, W., and Holzman, L.B. (2004). Podocytes populate cellular crescents in a murine model of inflammatory glomerulonephritis. J Am Soc Nephrol *15*, 61-67.

Mohamood, A.S., Guler, M.L., Xiao, Z., Zheng, D., Hess, A., Wang, Y., Yagita, H., Schneck, J.P., and Hamad, A.R.A. (2007). Protection from Autoimmune Diabetes and T-cell Lymphoproliferation Induced by FasL Mutation Are Differentially Regulated and Can Be Uncoupled Pharmacologically. The American Journal of Pathology *171*, 97-106.

Montel, A.H., Bochan, M.R., Hobbs, J.A., Lynch, D.H., and Brahmi, Z. (1995). Fas involvement in cytotoxicity mediated by human NK cells. Cell Immunol *166*, 236-246.

Mousavi, S.A., Sporstol, M., Fladeby, C., Kjeken, R., Barois, N., and Berg, T. (2007). Receptor-mediated endocytosis of immune complexes in rat liver sinusoidal endothelial cells is mediated by FcgammaRIIb2. Hepatology *46*, 871-884.

Mulder, A.H., Heeringa, P., Brouwer, E., Limburg, P.C., and Kallenberg, C.G. (1994). Activation of granulocytes by anti-neutrophil cytoplasmic antibodies (ANCA): a Fc gamma RII-dependent process. Clin Exp Immunol *98*, 270-278.

Murphy, E.D., and Roths, J.B. (1977). Single Gene Model for Massive Lymphoproliferation with Autoimmunity in New Mouse Strain Mrl. Fed Proc *36*, 1246-1246.

Muta, T., Kurosaki, T., Misulovin, Z., Sanchez, M., Nussenzweig, M.C., and Ravetch, J.V. (1994). A 13-amino-acid motif in the cytoplasmic domain of Fc gamma RIIB modulates B-cell receptor signalling. Nature *368*, 70-73.

Muzio, M., Chinnaiyan, A.M., Kischkel, F.C., O'Rourke, K., Schevchenko, A., Ni, J., Scaffidi, C., Bretz, J.D., Zhang, M., Gentz, R*., et al.* (1996). FLICE, a novel FADD homologous ICE/CED-3-like protease, is recruited to the CD95 (Fas/Apo-1) death-inducing signalling complex. Cell *85*, 817-827.

Nagata, S., and Golstein, P. (1995). The Fas death factor. Science *267*, 1449-1456.

Nakajima, A., Hirai, H., Kayagaki, N., Yoshino, S., Hirose, S., Yagita, H., and Okumura, K. (2000). Treatment of lupus in NZB/W F1 mice with monoclonal antibody against Fas ligand. J Autoimmun *14*, 151-157.

Nakamura, A., Yuasa, T., Ujike, A., Ono, M., Nukiwa, T., Ravetch, J.V., and Takai, T. (2000). Fcgamma receptor IIB-deficient mice develop Goodpasture's syndrome upon immunization with type IV collagen: a novel murine model for autoimmune glomerular basement membrane disease. J Exp Med *191*, 899-906.

Nardin, A., Lindorfer, M.A., and Taylor, R.P. (1999). How are immune complexes bound to the primate erythrocyte complement receptor transferred to acceptor phagocytic cells? Mol Immunol *36*, 827-835.

Natori, Y., Natori, Y., Nishimura, T., Yamabe, H., Iyonaga, K., Takeya, M., and Kawakami, M. (1997). Production of monocyte chemoattractant protein-1 by cultured glomerular epithelial cells: inhibition by dexamethasone. Exp Nephrol *5*, 318-322.

Neale, T.J., Ruger, B.M., Macaulay, H., Dunbar, P.R., Hasan, Q., Bourke, A., Murray-McIntosh, R.P., and Kitching, A.R. (1995). Tumor necrosis factor-alpha is expressed by

glomerular visceral epithelial cells in human membranous nephropathy. Am J Pathol *146*, 1444-1454.

Nechemia-Arbely, Y., Barkan, D., Pizov, G., Shriki, A., Rose-John, S., Galun, E., and Axelrod, J.H. (2008). IL-6/IL-6R axis plays a critical role in acute kidney injury. J Am Soc Nephrol *19*, 1106-1115.

Neff, T.A., Guo, R.-F., Neff, S.B., Sarma, J.V., Speyer, C.L., Gao, H., Bernacki, K.D., Huber-Lang, M., McGuire, S., Hoesel, L.M.*, et al.* (2005). Relationship of Acute Lung Inflammation Injury to Fas/FasL System. American Journal of Pathology *166*, 685-694.

Newton, K., Harris, A.W., Bath, M.L., Smith, K.G., and Strasser, A. (1998). A dominant interfering mutant of FADD/MORT1 enhances deletion of autoreactive thymocytes and inhibits proliferation of mature T lymphocytes. EMBO J *17*, 706-718.

Niederer, H.A., Clatworthy, M.R., Willcocks, L.C., and Smith, K.G. (2010). FcgammaRIIB, FcgammaRIIIB, and systemic lupus erythematosus. Ann N Y Acad Sci *1183*, 69-88.

Niemir, Z.I., Stein, H., Ciechanowicz, A., Olejniczak, P., Dworacki, G., Ritz, E., Waldherr, R., and Czekalski, S. (2004). The in situ expression of interleukin-8 in the normal human kidney and in different morphological forms of glomerulonephritis. Am J Kidney Dis *43*, 983-998.

Nikolic-Paterson, D.J., and Atkins, R.C. (2001). The role of macrophages in glomerulonephritis. Nephrology, dialysis, transplantation *16 Suppl 5*, 3-7.

Nimmerjahn, F., Bruhns, P., Horiuchi, K., and Ravetch, J.V. (2005). FcgammaRIV: a novel FcR with distinct IgG subclass specificity. Immunity *23*, 41-51.

Nimmerjahn, F., and Ravetch, J.V. (2006). Fcgamma receptors: old friends and new family members. Immunity *24*, 19-28.

Nimmerjahn, F., and Ravetch, J.V. (2008). Fcgamma receptors as regulators of immune responses. Nat Rev Immunol *8*, 34-47.

Nishikawa, K., Guo, Y.J., Miyasaka, M., Tamatani, T., Collins, A.B., Sy, M.S., McCluskey, R.T., and Andres, G. (1993). Antibodies to intercellular adhesion molecule 1/lymphocyte function-associated antigen 1 prevent crescent formation in rat autoimmune glomerulonephritis. J Exp Med *177*, 667-677.

Nitta, K., Horita, S., Ogawa, S., Matsumoto, M., Hara, Y., Okano, K., Hayashi, T., Abe, R., and Nihei, H. (2003). Resistance of CD28-deficient mice to autologous phase of anti-glomerular basement membrane glomerulonephritis. Clin Exp Nephrol *7*, 104-112.

Niu, F.N., Zhang, X., Hu, X.M., Chen, J., Chang, L.L., Li, J.W., Liu, Z., Cao, W., and Xu, Y. (2011). Targeted mutation of Fas ligand gene attenuates brain inflammation in experimental stroke. Brain Behav Immun.

Nogueira, E., Hamour, S., Sawant, D., Henderson, S., Mansfield, N., Chavele, K.M., Pusey, C.D., and Salama, A.D. (2010). Serum IL-17 and IL-23 levels and autoantigen-specific Th17 cells are elevated in patients with ANCA-associated vasculitis. Nephrol Dial Transplant *25*, 2209-2217.

O' Reilly, L.A., Tai, L., Lee, L., Kruse, E.A., Grabow, S., Fairlie, W.D., Haynes, N.M., Tarlinton, D.M., Zhang, J.-G., Belz, G.T.*, et al.* (2009). Membrane-bound Fas ligand only is essential for Fas-induced apoptosis. Nature *461*, 659-663.

O'Connell, J., Bennett, M.W., O'Sullivan, G.C., Collins, J.K., and Shanahan, F. (1999a). The Fas counterattack: cancer as a site of immune privilege. Immunol Today *20*, 46-52.

O'Connell, J., Bennett, M.W., O'Sullivan, G.C., Collins, J.K., and Shanahan, F. (1999b). Resistance to Fas (APO-1/CD95)-mediated apoptosis and expression of Fas ligand in esophageal cancer: the Fas counterattack. Dis Esophagus *12*, 83-89.

O'Connell, J., Bennett, M.W., O'Sullivan, G.C., O'Callaghan, J., Collins, J.K., and Shanahan, F. (1999c). Expression of Fas (CD95/APO-1) ligand by human breast cancers: significance for tumor immune privilege. Clin Diagn Lab Immunol *6*, 457-463.

O'Connell, J., Bennett, M.W., O'Sullivan, G.C., Roche, D., Kelly, J., Collins, J.K., and Shanahan, F. (1998). Fas ligand expression in primary colon adenocarcinomas: evidence that the Fas counterattack is a prevalent mechanism of immune evasion in human colon cancer. J Pathol *186*, 240-246.

Odobasic, D., Gan, P.Y., Summers, S.A., Semple, T.J., Muljadi, R.C., Iwakura, Y., Kitching, A.R., and Holdsworth, S.R. (2011). Interleukin-17A promotes early but attenuates established disease in crescentic glomerulonephritis in mice. Am J Pathol *179*, 1188-1198.

Odobasic, D., Kitching, A.R., Semple, T.J., and Holdsworth, S.R. (2006). Inducible co-stimulatory molecule ligand is protective during the induction and effector phases of crescentic glomerulonephritis. J Am Soc Nephrol *17*, 1044-1053.

Odobasic, D., Kitching, A.R., Semple, T.J., Timoshanko, J.R., Tipping, P.G., and Holdsworth, S.R. (2005a). Glomerular expression of CD80 and CD86 is required for leukocyte accumulation and injury in crescentic glomerulonephritis. J Am Soc Nephrol *16*, 2012-2022.

Odobasic, D., Kitching, A.R., Tipping, P.G., and Holdsworth, S.R. (2005b). CD80 and CD86 costimulatory molecules regulate crescentic glomerulonephritis by different mechanisms. Kidney Int *68*, 584-594.

Oehm, A., Behrmann, I., Falk, W., Pawlita, M., Maier, G., Klas, C., Li-Weber, M., Richards, S., Dhein, J., Trauth, B.C.*, et al.* (1992). Purification and molecular cloning of the APO-1 cell surface antigen, a member of the tumor necrosis factor/nerve growth factor receptor superfamily. Sequence identity with the Fas antigen. J Biol Chem *267*, 10709-10715.

Okada, H., Inoue, T., Hashimoto, K., Suzuki, H., and Matsushita, S. (2009). D1-like receptor antagonist inhibits IL-17 expression and attenuates crescent formation in nephrotoxic serum nephritis. Am J Nephrol *30*, 274-279.

Oliveira, J.B., Bleesing, J.J., Dianzani, U., Fleisher, T.A., Jaffe, E.S., Lenardo, M.J., Rieux-Laucat, F., Siegel, R.M., Su, H.C., Teachey, D.T.*, et al.* (2010). Revised diagnostic criteria and classification for the autoimmune lymphoproliferative syndrome (ALPS): report from the 2009 NIH International Workshop. Blood *116*, e35-40.

Orban, P.C., Chui, D., and Marth, J.D. (1992). Tissue- and site-specific DNA recombination in transgenic mice. Proc Natl Acad Sci U S A *89*, 6861-6865.

Ortiz, A., Lorz, C., and Egido, J. (1999). The Fas ligand/Fas system in renal injury. Nephrol Dial Transplant *14*, 1831-1834.

Oshimi, Y., Oda, S., Honda, Y., Nagata, S., and Miyazaki, S. (1996). Involvement of Fas ligand and Fas-mediated pathway in the cytotoxicity of human natural killer cells. J Immunol *157*, 2909-2915.

Ottonello, L., Tortolina, G., Amelotti, M., and Dallegri, F. (1999). Soluble Fas ligand is chemotactic for human neutrophilic polymorphonuclear leukocytes. J Immunol *162*, 3601-3606.

Papoff, G., Hausler, P., Eramo, A., Pagano, M.G., Di Leve, G., Signore, A., and Ruberti, G. (1999). Identification and characterization of a ligand-independent oligomerization domain in the extracellular region of the CD95 death receptor. J Biol Chem *274*, 38241-38250.

Park, D.R., Thomsen, A.R., Frevert, C.W., Pham, U., Skerrett, S.J., Kiener, P.A., and Liles, W.C. (2003). Fas (CD95) induces proinflammatory cytokine responses by human monocytes and monocyte-derived macrophages. The Journal of Immunology *170*, 6209-6216.

Park, S.Y., Ueda, S., Ohno, H., Hamano, Y., Tanaka, M., Shiratori, T., Yamazaki, T., Arase, H., Arase, N., Karasawa, A.*, et al.* (1998). Resistance of Fc receptor- deficient mice to fatal glomerulonephritis. J Clin Invest *102*, 1229-1238.

Paust, H.J., Ostmann, A., Erhardt, A., Turner, J.E., Velden, J., Mittrucker, H.W., Sparwasser, T., Panzer, U., and Tiegs, G. (2011). Regulatory T cells control the Th1 immune response in murine crescentic glomerulonephritis. Kidney Int.

Paust, H.J., Turner, J.E., Steinmetz, O.M., Peters, A., Heymann, F., Holscher, C., Wolf, G., Kurts, C., Mittrucker, H.W., Stahl, R.A.*, et al.* (2009). The IL-23/Th17 axis contributes to renal injury in experimental glomerulonephritis. J Am Soc Nephrol *20*, 969-979.

Pearse, R.N., Kawabe, T., Bolland, S., Guinamard, R., Kurosaki, T., and Ravetch, J.V. (1999). SHIP recruitment attenuates Fc gamma RIIB-induced B cell apoptosis. Immunity *10*, 753-760.

Perianayagam, M.C., Murray, S.L., Balakrishnan, V.S., Guo, D., King, A.J., Pereira, B.J., and Jaber, B.L. (2000). Serum soluble Fas (CD95) and Fas ligand profiles in chronic kidney failure. J Lab Clin Med *136*, 320-327.

Pfister, H., Ollert, M., Frohlich, L.F., Quintanilla-Martinez, L., Colby, T.V., Specks, U., and Jenne, D.E. (2004). Antineutrophil cytoplasmic autoantibodies against the murine homolog of proteinase 3 (Wegener autoantigen) are pathogenic in vivo. Blood *104*, 1411-1418.

Phillips, N.E., and Parker, D.C. (1984). Cross-linking of B lymphocyte Fc gamma receptors and membrane immunoglobulin inhibits anti-immunoglobulin-induced blastogenesis. J Immunol *132*, 627-632.

Pickering, M.C., Cook, H.T., Warren, J., Bygrave, A.E., Moss, J., Walport, M.J., and Botto, M. (2002). Uncontrolled C3 activation causes membranoproliferative glomerulonephritis in mice deficient in complement factor H. Nat Genet *31*, 424-428.

Pitti, R.M., Marsters, S.A., Lawrence, D.A., Roy, M., Kischkel, F.C., Dowd, P., Huang, A., Donahue, C.J., Sherwood, S.W., Baldwin, D.T.*, et al.* (1998). Genomic amplification of a decoy receptor for Fas ligand in lung and colon cancer. Nature *396*, 699-703.

Porges, A.J., Redecha, P.B., Kimberly, W.T., Csernok, E., Gross, W.L., and Kimberly, R.P. (1994). Anti-neutrophil cytoplasmic antibodies engage and activate human neutrophils via Fc gamma RIIa. J Immunol *153*, 1271-1280.

Powell, W.C., Fingleton, B., Wilson, C.L., Boothby, M., and Matrisian, L.M. (1999). The metalloproteinase matrilysin proteolytically generates active soluble Fas ligand and potentiates epithelial cell apoptosis. Curr Biol *9*, 1441-1447.

Pricop, L., Redecha, P., Teillaud, J.L., Frey, J., Fridman, W.H., Sautes-Fridman, C., and Salmon, J.E. (2001). Differential modulation of stimulatory and inhibitory Fc gamma receptors on human monocytes by Th1 and Th2 cytokines. J Immunol *166*, 531-537.

Pritchard, N.R., Cutler, A.J., Uribe, S., Chadban, S.J., Morley, B.J., and Smith, K.G. (2000). Autoimmune-prone mice share a promoter haplotype associated with reduced expression and function of the Fc receptor FcgammaRII. Curr Biol *10*, 227-230.

Radaev, S., and Sun, P. (2002). Recognition of immunoglobulins by Fcgamma receptors. Mol Immunol *38*, 1073-1083.

Radeke, H.H., Janssen-Graalfs, I., Sowa, E.N., Chouchakova, N., Skokowa, J., Loscher, F., Schmidt, R.E., Heeringa, P., and Gessner, J.E. (2002). Opposite regulation of type II and III receptors for immunoglobulin G in mouse glomerular mesangial cells and in the induction of anti-glomerular basement membrane (GBM) nephritis. J Biol Chem *277*, 27535-27544.

Ramaswamy, M., Cleland, S.Y., Cruz, A.C., and Siegel, R.M. (2009). Many checkpoints on the road to cell death: regulation of Fas-FasL interactions and Fas signaling in peripheral immune responses. Results Probl Cell Differ *49*, 17-47.

Ravetch, J.V., and Bolland, S. (2001). IgG Fc receptors. Annu Rev Immunol *19*, 275-290.

Regnault, A., Lankar, D., Lacabanne, V., Rodriguez, A., Thery, C., Rescigno, M., Saito, T., Verbeek, S., Bonnerot, C., Ricciardi-Castagnoli, P.*, et al.* (1999). Fcgamma receptor-mediated induction of dendritic cell maturation and major histocompatibility complex class I-restricted antigen presentation after immune complex internalization. J Exp Med *189*, 371-380.

Reitsma, S., Slaaf, D.W., Vink, H., van Zandvoort, M.A., and oude Egbrink, M.G. (2007). The endothelial glycocalyx: composition, functions, and visualization. Pflugers Archiv : European journal of physiology *454*, 345-359.

Reth, M. (1989). Antigen Receptor Tail Clue. Nature *338*, 383-384.

Reynolds, J., Albouainain, A., Duda, M.A., Evans, D.J., and Pusey, C.D. (2006). Strain susceptibility to active induction and passive transfer of experimental autoimmune glomerulonephritis in the rat. Nephrol Dial Transplant *21*, 3398-3408.

Reynolds, J., Norgan, V.A., Bhambra, U., Smith, J., Cook, H.T., and Pusey, C.D. (2002). Anti-CD8 monoclonal antibody therapy is effective in the prevention and treatment of experimental autoimmune glomerulonephritis. J Am Soc Nephrol *13*, 359-369.

Reynolds, J., Sallie, B.A., Syrganis, C., and Pusey, C.D. (1993). The role of T-helper lymphocytes in priming for experimental autoimmune glomerulonephritis in the BN rat. J Autoimmun *6*, 571-585.

Rickert, R.C., Roes, J., and Rajewsky, K. (1997). B lymphocyte-specific, Cre-mediated mutagenesis in mice. Nucleic Acids Res *25*, 1317-1318.

Rieux-Laucat, F., Le Deist, F., Hivroz, C., Roberts, I.A., Debatin, K.M., Fischer, A., and de Villartay, J.P. (1995). Mutations in Fas associated with human lymphoproliferative syndrome and autoimmunity. Science *268*, 1347-1349.

Robson, M.G., Cook, H.T., Botto, M., Taylor, P.R., Busso, N., Salvi, R., Pusey, C.D., Walport, M.J., and Davies, K.A. (2001). Accelerated nephrotoxic nephritis is exacerbated in C1q-deficient mice. J Immunol *166*, 6820-6828.

Rosenblum, H., and Amital, H. (2011). Anti-TNF therapy: safety aspects of taking the risk. Autoimmun Rev *10*, 563-568.

Ross, M.J., Martinka, S., D'Agati, V.D., and Bruggeman, L.A. (2005). NF-kappaB regulates Fas-mediated apoptosis in HIV-associated nephropathy. J Am Soc Nephrol *16*, 2403-2411.

Roths, J.B., Murphy, E.D., and Eicher, E.M. (1984). A new mutation, *gld*, that produces lymphoproliferation and autoimmunity in C3H/HeJ mice. The Journal of Experimental Medicine *159*, 1-20.

Roubinian, J.R., Papoian, R., and Talal, N. (1977). Androgenic hormones modulate autoantibody responses and improve survival in murine lupus. J Clin Invest *59*, 1066-1070.

Russell, J.H., Rush, B., Weaver, C., and Wang, R. (1993). Mature T cells of autoimmune lpr/lpr mice have a defect in antigen-stimulated suicide. Proc Natl Acad Sci U S A *90*, 4409-4413.

Russell, J.H., and Wang, R. (1993). Autoimmune gld mutation uncouples suicide and cytokine/proliferation pathways in activated, mature T cells. Eur J Immunol *23*, 2379-2382.

Ruth, A.J., Kitching, A.R., Li, M., Semple, T.J., Timoshanko, J.R., Tipping, P.G., and Holdsworth, S.R. (2004). An IL-12-independent role for CD40-CD154 in mediating effector responses: studies in cell-mediated glomerulonephritis and dermal delayed-type hypersensitivity. J Immunol *173*, 136-144.

Ruth, A.J., Kitching, A.R., Semple, T.J., Tipping, P.G., and Holdsworth, S.R. (2003). Intrinsic renal cell expression of CD40 directs Th1 effectors inducing experimental crescentic glomerulonephritis. J Am Soc Nephrol *14*, 2813-2822.

Sabelko, K.A., Kelly, K.A., Nahm, M.H., Cross, A.H., and Russell, J.H. (1997). Fas and Fas ligand enhance the pathogenesis of experimental allergic encephalomyelitis, but are not essential for immune privilege in the central nervous system. J Immunol *159*, 3096-3099.

Sabelko-Downes, K.A., Cross, A.H., and Russell, J.H. (1999). Dual role for Fas ligand in the initiation of and recovery from experimental allergic encephalomyelitis. J Exp Med *189*, 1195-1205.

Salama, A.D., Chaudhry, A.N., Holthaus, K.A., Mosley, K., Kalluri, R., Sayegh, M.H., Lechler, R.I., Pusey, C.D., and Lightstone, L. (2003). Regulation by CD25+ lymphocytes of autoantigen-specific T-cell responses in Goodpasture's (anti-GBM) disease. Kidney Int *64*, 1685-1694.

Salama, A.D., Chaudhry, A.N., Ryan, J.J., Eren, E., Levy, J.B., Pusey, C.D., Lightstone, L., and Lechler, R.I. (2001). In Goodpasture's disease, CD4(+) T cells escape thymic deletion and are reactive with the autoantigen alpha3(IV)NC1. J Am Soc Nephrol *12*, 1908-1915.

Sanchez-Nino, M.D., Benito-Martin, A., Goncalves, S., Sanz, A.B., Ucero, A.C., Izquierdo, M.C., Ramos, A.M., Berzal, S., Selgas, R., Ruiz-Ortega, M.*, et al.* (2010). TNF superfamily: a growing saga of kidney injury modulators. Mediators of inflammation *2010*.

Sata, M., Suhara, T., and Walsh, K. (2000). Vascular endothelial cells and smooth muscle cells differ in expression of Fas and Fas ligand and in sensitivity to Fas ligand-induced cell death: implications for vascular disease and therapy. Arterioscler Thromb Vasc Biol *20*, 309-316.

Satchell, S.C., Buchatska, O., Khan, S.B., Bhangal, G., Tasman, C.H., Saleem, M.A., Baker, D.P., Lobb, R.R., Smith, J., Cook, H.T.*, et al.* (2007). Interferon-beta reduces proteinuria in experimental glomerulonephritis. J Am Soc Nephrol *18*, 2875-2884.

Satriano, J.A., Hora, K., Shan, Z., Stanley, E.R., Mori, T., and Schlondorff, D. (1993). Regulation of monocyte chemoattractant protein-1 and macrophage colony-stimulating factor-1 by IFN-gamma, tumor necrosis factor-alpha, IgG aggregates, and cAMP in mouse mesangial cells. J Immunol *150*, 1971-1978.

Sauer, B. (1998). Inducible gene targeting in mice using the Cre/lox system. Methods *14*, 381-392.

Saus, J., Wieslander, J., Langeveld, J.P., Quinones, S., and Hudson, B.G. (1988). Identification of the Goodpasture antigen as the alpha 3(IV) chain of collagen IV. J Biol Chem *263*, 13374-13380.

Savill, J. (1999). Regulation of glomerular cell number by apoptosis. Kidney Int *56*, 1216-1222.

Scandiuzzi, L., Beghdadi, W., Daugas, E., Abrink, M., Tiwari, N., Brochetta, C., Claver, J., Arouche, N., Zang, X., Pretolani, M.*, et al.* (2010). Mouse mast cell protease-4 deteriorates renal function by contributing to inflammation and fibrosis in immune complex-mediated glomerulonephritis. J Immunol *185*, 624-633.

Schlondorff, D. (1987). The glomerular mesangial cell: an expanding role for a specialized pericyte. FASEB J *1*, 272-281.

Schneider, P., Holler, N., Bodmer, J.L., Hahne, M., Frei, K., Fontana, A., and Tschopp, J. (1998). Conversion of membrane-bound Fas(CD95) ligand to its soluble form is associated with downregulation of its proapoptotic activity and loss of liver toxicity. J Exp Med *187*, 1205-1213.

Scholten, J., Hartmann, K., Gerbaulet, A., Krieg, T., Muller, W., Testa, G., and Roers, A. (2008). Mast cell-specific Cre/loxP-mediated recombination in vivo. Transgenic Res *17*, 307-315.

Scholz, J., Lukacs-Kornek, V., Engel, D.R., Specht, S., Kiss, E., Eitner, F., Floege, J., Groene, H.J., and Kurts, C. (2008). Renal dendritic cells stimulate IL-10 production and attenuate nephrotoxic nephritis. J Am Soc Nephrol *19*, 527-537.

Schreiber, A., Xiao, H., Falk, R.J., and Jennette, J.C. (2006). Bone marrow-derived cells are sufficient and necessary targets to mediate glomerulonephritis and vasculitis induced by anti-myeloperoxidase antibodies. J Am Soc Nephrol *17*, 3355-3364.

Schrijver, G., Bogman, M.J., Assmann, K.J., de Waal, R.M., Robben, H.C., van Gasteren, H., and Koene, R.A. (1990). Anti-GBM nephritis in the mouse: role of granulocytes in the heterologous phase. Kidney Int *38*, 86-95.

Schrijver, G., Schalkwijk, J., Robben, J.C., Assmann, K.J., and Koene, R.A. (1989). Antiglomerular basement membrane nephritis in beige mice. Deficiency of leukocytic neutral proteinases prevents the induction of albuminuria in the heterologous phase. J Exp Med *169*, 1435-1448.

Sedlik, C., Orbach, D., Veron, P., Schweighoffer, E., Colucci, F., Gamberale, R., Ioan-Facsinay, A., Verbeek, S., Ricciardi-Castagnoli, P., Bonnerot, C.*, et al.* (2003). A critical role for Syk protein tyrosine kinase in Fc receptor-mediated antigen presentation and induction of dendritic cell maturation. J Immunol *170*, 846-852.

Seino, K., Iwabuchi, K., Kayagaki, N., Miyata, R., Nagaoka, I., Matsuzawa, A., Fukao, K., Yagita, H., and Okumura, K. (1998). Chemotactic activity of soluble Fas ligand against phagocytes. J Immunol *161*, 4484-4488.

Sharp, P.E., Martin-Ramirez, J., Boross, P., Mangsbo, S.M., Reynolds, J., Moss, J., Pusey, C.D., Cook, H.T., Tarzi, R.M., and Verbeek, J.S. (2012). Increased incidence of anti-GBM disease in Fcgamma receptor 2b deficient mice, but not mice with conditional deletion of Fcgr2b on either B cells or myeloid cells alone. Mol Immunol *50*, 49-56.

Sheerin, N.S., Springall, T., Carroll, M.C., Hartley, B., and Sacks, S.H. (1997). Protection against anti-glomerular basement membrane (GBM)-mediated nephritis in C3- and C4-deficient mice. Clin Exp Immunol *110*, 403-409.

Shimizu, A., Kitamura, H., Masuda, Y., Ishizaki, M., Sugisaki, Y., and Yamanaka, N. (1995). Apoptosis in the repair process of experimental proliferative glomerulonephritis. Kidney Int *47*, 114-121.

Siegel, R.M., Frederiksen, J.K., Zacharias, D.A., Chan, F.K., Johnson, M., Lynch, D., Tsien, R.Y., and Lenardo, M.J. (2000). Fas preassociation required for apoptosis signaling and dominant inhibition by pathogenic mutations. Science *288*, 2354-2357.

Singer, G.G., and Abbas, A.K. (1994). The fas antigen is involved in peripheral but not thymic deletion of T lymphocytes in T cell receptor transgenic mice. Immunity *1*, 365-371.

Singh, A., Satchell, S.C., Neal, C.R., McKenzie, E.A., Tooke, J.E., and Mathieson, P.W. (2007). Glomerular endothelial glycocalyx constitutes a barrier to protein permeability. J Am Soc Nephrol *18*, 2885-2893.

Sneller, M.C., Straus, S.E., Jaffe, E.S., Jaffe, J.S., Fleisher, T.A., Stetler-Stevenson, M., and Strober, W. (1992). A novel lymphoproliferative/autoimmune syndrome resembling murine lpr/gld disease. J Clin Invest *90*, 334-341.

Sogabe, H., Nangaku, M., Ishibashi, Y., Wada, T., Fujita, T., Sun, X., Miwa, T., Madaio, M.P., and Song, W.C. (2001). Increased susceptibility of decay-accelerating factor deficient mice to anti-glomerular basement membrane glomerulonephritis. J Immunol *167*, 2791-2797.

Soos, T.J., Sims, T.N., Barisoni, L., Lin, K., Littman, D.R., Dustin, M.L., and Nelson, P.J. (2006). CX3CR1+ interstitial dendritic cells form a contiguous network throughout the entire kidney. Kidney Int *70*, 591-596.

Steblay, R.W. (1962). Glomerulonephritis induced in sheep by injections of heterologous glomerular basement membrane and Freund's complete adjuvant. J Exp Med *116*, 253-272.

Steinmetz, O.M., Summers, S.A., Gan, P.Y., Semple, T., Holdsworth, S.R., and Kitching, A.R. (2011). The Th17-defining transcription factor RORgammat promotes glomerulonephritis. J Am Soc Nephrol *22*, 472-483.

Stranges, P.B., Watson, J., Cooper, C.J., Choisy-Rossi, C.M., Stonebraker, A.C., Beighton, R.A., Hartig, H., Sundberg, J.P., Servick, S., Kaufmann, G.*, et al.* (2007). Elimination of antigen-presenting cells and autoreactive T cells by Fas contributes to prevention of autoimmunity. Immunity *26*, 629-641.

Straus, S.E., Sneller, M., Lenardo, M.J., Puck, J.M., and Strober, W. (1999). An inherited disorder of lymphocyte apoptosis: the autoimmune lymphoproliferative syndrome. Ann Intern Med *130*, 591-601.

Suda, T., and Nagata, S. (1994). Purification and characterization of the Fas-ligand that induces apoptosis. The Journal of Experimental Medicine *179*, 873-879.

Suda, T., Okazaki, T., Naito, Y., Yokota, T., Arai, N., Ozaki, S., Nakao, K., and Nagata, S. (1995). Expression of the Fas ligand in cells of T cell lineage. J Immunol *154*, 3806-3813.

Suda, T., Takahashi, T., Golstein, P., and Nagata, S. (1993). Molecular cloning and expression of the Fas ligand, a novel member of the tumor necrosis factor family. Cell *75*, 1169-1178.

Sugiyama, H., Kashihara, N., Makino, H., Yamasaki, Y., and Ota, A. (1996). Apoptosis in glomerular sclerosis. Kidney Int *49*, 103-111.

Summers, S.A., Steinmetz, O.M., Li, M., Kausman, J.Y., Semple, T., Edgtton, K.L., Borza, D.B., Braley, H., Holdsworth, S.R., and Kitching, A.R. (2009). Th1 and Th17 cells induce proliferative glomerulonephritis. J Am Soc Nephrol *20*, 2518-2524.

Suss, G., and Shortman, K. (1996). A subclass of dendritic cells kills CD4 T cells via Fas/Fas-ligand-induced apoptosis. J Exp Med *183*, 1789-1796.

Suzuki, Y., Shirato, I., Okumura, K., Ravetch, J.V., Takai, T., Tomino, Y., and Ra, C. (1998). Distinct contribution of Fc receptors and angiotensin II-dependent pathways in anti-GBM glomerulonephritis. Kidney Int *54*, 1166-1174.

Tackenberg, B., Jelcic, I., Baerenwaldt, A., Oertel, W.H., Sommer, N., Nimmerjahn, F., and Lunemann, J.D. (2009). Impaired inhibitory Fcgamma receptor IIB expression on B cells in chronic inflammatory demyelinating polyneuropathy. Proc Natl Acad Sci U S A *106*, 4788-4792.

Takahashi, T., Tanaka, M., Brannan, C.I., Jenkins, N.A., Copeland, N.G., Suda, T., and Nagata, S. (1994). Generalized lymphoproliferative disease in mice, caused by a point mutation in the Fas ligand. Cell *76*, 969-976.

Takai, T. (2005). Fc receptors and their role in immune regulation and autoimmunity. J Clin Immunol *25*, 1-18.

Takai, T., Li, M., Sylvestre, D., Clynes, R., and Ravetch, J.V. (1994). FcR gamma chain deletion results in pleiotrophic effector cell defects. Cell *76*, 519-529.

Takai, T., Ono, M., Hikida, M., Ohmori, H., and Ravetch, J.V. (1996). Augmented humoral and anaphylactic responses in Fc gamma RII-deficient mice. Nature *379*, 346-349.

Tan, K.H., and Hunziker, W. (2003). Compartmentalization of Fas and Fas ligand may prevent auto- or paracrine apoptosis in epithelial cells. Experimental cell research *284*, 283-290.

Tanaka, M., Suda, T., Takahashi, T., and Nagata, S. (1995). Expression of the functional soluble form of human fas ligand in activated lymphocytes. EMBO J *14*, 1129-1135.

Tang, W.W., Feng, L., Vannice, J.L., and Wilson, C.B. (1994). Interleukin-1 receptor antagonist ameliorates experimental anti-glomerular basement membrane antibody-associated glomerulonephritis. J Clin Invest *93*, 273-279.

Tanner, J.E., and Alfieri, C. (1999). Epstein-Barr virus induces Fas (CD95) in T cells and Fas ligand in B cells leading to T-cell apoptosis. Blood *94*, 3439-3447.

Tartaglia, L.A., Ayres, T.M., Wong, G.H., and Goeddel, D.V. (1993). A novel domain within the 55 kd TNF receptor signals cell death. Cell *74*, 845-853.

Tarzi, R.M., Davies, K.A., Claassens, J.W., Verbeek, J.S., Walport, M.J., and Cook, H.T. (2003). Both Fcgamma receptor I and Fcgamma receptor III mediate disease in accelerated nephrotoxic nephritis. The American journal of pathology *162*, 1677-1683.

Tarzi, R.M., Davies, K.A., Robson, M.G., Fossati-Jimack, L., Saito, T., Walport, M.J., and Cook, H.T. (2002). Nephrotoxic nephritis is mediated by Fcgamma receptors on circulating leukocytes and not intrinsic renal cells. Kidney International *62*, 2087-2096.

Tarzi, R.M., Sharp, P.E., McDaid, J.P., Fossati-Jimack, L., Herbert, P.E., Pusey, C.D., Cook, H.T., and Warrens, A.N. (2011). Mice with defective Fas ligand are protected from crescentic glomerulonephritis. Kidney Int.

Tesch, G.H., Schwarting, A., Kinoshita, K., Lan, H.Y., Rollins, B.J., and Kelley, V.R. (1999). Monocyte chemoattractant protein-1 promotes macrophage-mediated tubular injury, but not glomerular injury, in nephrotoxic serum nephritis. J Clin Invest *103*, 73-80.

Thorner, P.S., Ho, M., Eremina, V., Sado, Y., and Quaggin, S. (2008). Podocytes contribute to the formation of glomerular crescents. J Am Soc Nephrol *19*, 495-502.

Timoshanko, J.R., Holdsworth, S.R., Kitching, A.R., and Tipping, P.G. (2002). IFN-gamma production by intrinsic renal cells and bone marrow-derived cells is required for full expression of crescentic glomerulonephritis in mice. J Immunol *168*, 4135-4141.

Timoshanko, J.R., Kitching, A.R., Holdsworth, S.R., and Tipping, P.G. (2001). Interleukin-12 from intrinsic cells is an effector of renal injury in crescentic glomerulonephritis. J Am Soc Nephrol *12*, 464-471.

Timoshanko, J.R., Kitching, A.R., Semple, T.J., Tipping, P.G., and Holdsworth, S.R. (2006). A pathogenetic role for mast cells in experimental crescentic glomerulonephritis. J Am Soc Nephrol *17*, 150-159.

Timoshanko, J.R., Sedgwick, J.D., Holdsworth, S.R., and Tipping, P.G. (2003). Intrinsic renal cells are the major source of tumor necrosis factor contributing to renal injury in murine crescentic glomerulonephritis. J Am Soc Nephrol *14*, 1785-1793.

Tipping, P.G., Huang, X.R., Qi, M., Van, G.Y., and Tang, W.W. (1998). Crescentic glomerulonephritis in CD4- and CD8-deficient mice. Requirement for CD4 but not CD8 cells. Am J Pathol *152*, 1541-1548.

Tipping, P.G., Kitching, A.R., Huang, X.R., Mutch, D.A., and Holdsworth, S.R. (1997). Immune modulation with interleukin-4 and interleukin-10 prevents crescent formation and glomerular injury in experimental glomerulonephritis. Eur J Immunol *27*, 530-537.

Trauth, B.C., Klas, C., Peters, A.M., Matzku, S., Moller, P., Falk, W., Debatin, K.M., and Krammer, P.H. (1989). Monoclonal antibody-mediated tumor regression by induction of apoptosis. Science *245*, 301-305.

Tsukinoki, T., Sugiyama, H., Sunami, R., Kobayashi, M., Onoda, T., Maeshima, Y., Yamasaki, Y., and Makino, H. (2004). Mesangial cell Fas ligand: upregulation in human lupus nephritis and NF-kappaB-mediated expression in cultured human mesangial cells. Clin Exp Nephrol *8*, 196-205.

Tu-Rapp, H., Hammermuller, A., Mix, E., Kreutzer, H.J., Goerlich, R., Kohler, H., Nizze, H., Thiesen, H.J., and Ibrahim, S.M. (2004). A proinflammatory role for Fas in joints of mice with collagen-induced arthritis. Arthritis Res Ther *6*, R404-414.

Turnberg, D., Botto, M., Warren, J., Morgan, B.P., Walport, M.J., and Cook, H.T. (2003). CD59a deficiency exacerbates accelerated nephrotoxic nephritis in mice. J Am Soc Nephrol *14*, 2271-2279.

Turner, N., Mason, P.J., Brown, R., Fox, M., Povey, S., Rees, A., and Pusey, C.D. (1992). Molecular cloning of the human Goodpasture antigen demonstrates it to be the alpha 3 chain of type IV collagen. J Clin Invest *89*, 592-601.

Tzeng, S.J., Bolland, S., Inabe, K., Kurosaki, T., and Pierce, S.K. (2005). The B cell inhibitory Fc receptor triggers apoptosis by a novel c-Abl family kinase-dependent pathway. J Biol Chem *280*, 35247-35254.

Uciechowski, P., Schwarz, M., Gessner, J.E., Schmidt, R.E., Resch, K., and Radeke, H.H. (1998). IFN-gamma induces the high-affinity Fc receptor I for IgG (CD64) on human glomerular mesangial cells. Eur J Immunol *28*, 2928-2935.

Ujike, A., Ishikawa, Y., Ono, M., Yuasa, T., Yoshino, T., Fukumoto, M., Ravetch, J.V., and Takai, T. (1999). Modulation of immunoglobulin (Ig)E-mediated systemic anaphylaxis by low-affinity Fc receptors for IgG. J Exp Med *189*, 1573-1579.

Unkeless, J.C., Shen, Z., Lin, C.W., and DeBeus, E. (1995). Function of human Fc gamma RIIA and Fc gamma RIIIB. Semin Immunol *7*, 37-44.

Valerius, T., Repp, R., Kalden, J.R., and Platzer, E. (1990). Effects of IFN on human eosinophils in comparison with other cytokines. A novel class of eosinophil activators with delayed onset of action. J Immunol *145*, 2950-2958.

Van Den Berg, J.G., Aten, J., Chand, M.A., Claessen, N., Dijkink, L., Wijdenes, J., Lakkis, F.G., and Weening, J.J. (2000). Interleukin-4 and interleukin-13 act on glomerular visceral epithelial cells. J Am Soc Nephrol *11*, 413-422.

Vargo-Gogola, T., Crawford, H.C., Fingleton, B., and Matrisian, L.M. (2002). Identification of novel matrix metalloproteinase-7 (matrilysin) cleavage sites in murine and human Fas ligand. Arch Biochem Biophys *408*, 155-161.

Wahlsten, J.L., Gitchell, H.L., Chan, C.C., Wiggert, B., and Caspi, R.R. (2000). Fas and Fas ligand expressed on cells of the immune system, not on the target tissue, control induction of experimental autoimmune uveitis. J Immunol *165*, 5480-5486.

Waldner, H., Sobel, R.A., Howard, E., and Kuchroo, V.K. (1997). Fas- and FasL-Deficient Mice Are Resistant to Induction of Autoimmune Encephalomyelitis. The Journal of Immunology *159*, 3100-3103.

Walsh, C.M., Wen, B.G., Chinnaiyan, A.M., O'Rourke, K., Dixit, V.M., and Hedrick, S.M. (1998). A role for FADD in T cell activation and development. Immunity *8*, 439-449.

Wang, J., Zheng, L., Lobito, A., Chan, F.K., Dale, J., Sneller, M., Yao, X., Puck, J.M., Straus, S.E., and Lenardo, M.J. (1999). Inherited human Caspase 10 mutations underlie defective lymphocyte and dendritic cell apoptosis in autoimmune lymphoproliferative syndrome type II. Cell *98*, 47-58.

Watanabe, T., Sakai, Y., Miyawaki, S., Shimizu, A., Koiwai, O., and Ohno, K. (1991). A Molecular Genetic Linkage Map of Mouse Chromosome 19, Including the *lpr*, *ly-44* and *Tdt* genes. Biochemical Genetics *29*, 325-335.

Watanabe-Fukunaga, R., Brannan, C.I., Copeland, N.G., Jenkins, N.A., and Nagata, S. (1992a). Lymphoproliferation disorder in mice explained by defects in Fas antigen that mediates apoptosis. Nature *356*, 314-317.

Watanabe-Fukunaga, R., Brannan, C.I., Itoh, N., Yonehara, S., Copeland, N.G., Jenkins, N.A., and Nagata, S. (1992b). The cDNA structure, expression, and chromosomal assignment of the mouse Fas antigen. J Immunol *148*, 1274-1279.

Willcocks, L.C., Lyons, P.A., Clatworthy, M.R., Robinson, J.I., Yang, W., Newland, S.A., Plagnol, V., McGovern, N.N., Condliffe, A.M., Chilvers, E.R.*, et al.* (2008). Copy number of FCGR3B, which is associated with systemic lupus erythematosus, correlates with protein expression and immune complex uptake. J Exp Med *205*, 1573-1582.

Wilson, H.M., Walbaum, D., and Rees, A.J. (2004). Macrophages and the kidney. Curr Opin Nephrol Hypertens *13*, 285-290.

Wirthmueller, U., Kurosaki, T., Murakami, M.S., and Ravetch, J.V. (1992). Signal transduction by Fc gamma RIII (CD16) is mediated through the gamma chain. J Exp Med *175*, 1381-1390.

Wolf, D., Hochegger, K., Wolf, A.M., Rumpold, H.F., Gastl, G., Tilg, H., Mayer, G., Gunsilius, E., and Rosenkranz, A.R. (2005). CD4+CD25+ regulatory T cells inhibit experimental anti-glomerular basement membrane glomerulonephritis in mice. J Am Soc Nephrol *16*, 1360-1370.

Wolfler, A., Danen-van Oorschot, A.A., Haanstra, J.R., Valkhof, M., Bodner, C., Vroegindeweij, E., van Strien, P., Novak, A., Cupedo, T., and Touw, I.P. (2010). Lineage-instructive function of C/EBPalpha in multipotent hematopoietic cells and early thymic progenitors. Blood *116*, 4116-4125.

Wong, H.L., Welch, G.R., Brandes, M.E., and Wahl, S.M. (1991). IL-4 antagonizes induction of Fc gamma RIII (CD16) expression by transforming growth factor-beta on human monocytes. J Immunol *147*, 1843-1848.

Wu, J., Hicks, J., Borillo, J., Glass, W.F., 2nd, and Lou, Y.H. (2002). CD4(+) T cells specific to a glomerular basement membrane antigen mediate glomerulonephritis. J Clin Invest *109*, 517-524.

Xiang, Z., Cutler, A.J., Brownlie, R.J., Fairfax, K., Lawlor, K.E., Severinson, E., Walker, E.U., Manz, R.A., Tarlinton, D.M., and Smith, K.G. (2007). FcgammaRIIb controls bone marrow plasma cell persistence and apoptosis. Nat Immunol *8*, 419-429.

Xiao, H., Heeringa, P., Hu, P., Liu, Z., Zhao, M., Aratani, Y., Maeda, N., Falk, R.J., and Jennette, J.C. (2002a). Antineutrophil cytoplasmic autoantibodies specific for myeloperoxidase cause glomerulonephritis and vasculitis in mice. J Clin Invest *110*, 955-963.

Xiao, H., Heeringa, P., Liu, Z., Huugen, D., Hu, P., Maeda, N., Falk, R.J., and Jennette, J.C. (2005). The role of neutrophils in the induction of glomerulonephritis by anti-myeloperoxidase antibodies. Am J Pathol *167*, 39-45.

Xiao, H., Schreiber, A., Heeringa, P., Falk, R.J., and Jennette, J.C. (2007). Alternative complement pathway in the pathogenesis of disease mediated by anti-neutrophil cytoplasmic autoantibodies. Am J Pathol *170*, 52-64.

Xiao, S., Jodo, S., Sung, S.S., Marshak-Rothstein, A., and Ju, S.T. (2002b). A novel signaling mechanism for soluble CD95 ligand. Synergy with anti-CD95 monoclonal antibodies for apoptosis and NF-kappaB nuclear translocation. J Biol Chem *277*, 50907-50913.

Yang, B., Johnson, T.S., Haylor, J.L., Wagner, B., Watson, P.F., El Kossi, M.M., Furness, P.N., and El Nahas, A.M. (2003). Effects of caspase inhibition on the progression of experimental glomerulonephritis. Kidney Int *63*, 2050-2064.

Yang, B., Johnson, T.S., Thomas, G.L., Watson, P.F., Wagner, B., and Nahas, A.M. (2001). Apoptosis and caspase-3 in experimental anti-glomerular basement membrane nephritis. J Am Soc Nephrol *12*, 485-495.

Yonehara, S., Ishii, A., and Yonehara, M. (1989). A cell-killing monoclonal antibody (anti-Fas) to a cell surface antigen co-downregulated with the receptor of tumor necrosis factor. J Exp Med *169*, 1747-1756.

Yu, X.Q., Nikolic-Paterson, D.J., Mu, W., Giachelli, C.M., Atkins, R.C., Johnson, R.J., and Lan, H.Y. (1998). A functional role for osteopontin in experimental crescentic glomerulonephritis in the rat. Proc Assoc Am Physicians *110*, 50-64.

Yuasa, T., Kubo, S., Yoshino, T., Ujike, A., Matsumura, K., Ono, M., Ravetch, J.V., and Takai, T. (1999). Deletion of fcgamma receptor IIB renders H-2(b) mice susceptible to collagen-induced arthritis. J Exp Med *189*, 187-194.

Zhang, D.E., Zhang, P., Wang, N.D., Hetherington, C.J., Darlington, G.J., and Tenen, D.G. (1997). Absence of granulocyte colony-stimulating factor signaling and neutrophil development in CCAAT enhancer binding protein alpha-deficient mice. Proc Natl Acad Sci U S A *94*, 569-574.

Zhang, H., Hile, K.L., Asanuma, H., Vanderbrink, B., Franke, E.I., Campbell, M.T., and Meldrum, K.K. (2011). IL-18 mediates proapoptotic signaling in renal tubular cells through a Fas ligand-dependent mechanism. Am J Physiol Renal Physiol *301*, F171-178.

Zhang, J., Cado, D., Chen, A., Kabra, N.H., and Winoto, A. (1998). Fas-mediated apoptosis and activation-induced T-cell proliferation are defective in mice lacking FADD/Mort1. Nature *392*, 296-300.

Zhang, Y., Rosenberg, S., Wang, H., Imtiyaz, H.Z., Hou, Y.J., and Zhang, J. (2005). Conditional Fas-associated death domain protein (FADD): GFP knockout mice reveal FADD is dispensable in thymic development but essential in peripheral T cell homeostasis. J Immunol *175*, 3033-3044.

Zhou, T., Edwards, C.K., 3rd, Yang, P., Wang, Z., Bluethmann, H., and Mountz, J.D. (1996). Greatly accelerated lymphadenopathy and autoimmune disease in lpr mice lacking tumor necrosis factor receptor I. J Immunol *156*, 2661-2665.

Zoja, C., Wang, J.M., Bettoni, S., Sironi, M., Renzi, D., Chiaffarino, F., Abboud, H.E., Van Damme, J., Mantovani, A., Remuzzi, G.*, et al.* (1991). Interleukin-1 beta and tumor necrosis factor-alpha induce gene expression and production of leukocyte chemotactic factors, colony-stimulating factors, and interleukin-6 in human mesangial cells. Am J Pathol *138*, 991-1003.

# Appendix 1 Summary of Permission for Third Party Copyright Works

| Item | Source of Work | Copyright Holder & Year | Permission | Date Granted | Licence Number |
|---|---|---|---|---|---|
| **Figure 1.1** | Circulation (2008), vol 118, 684-686 | © 2008 American Heart Association, Inc. | ✓ | 25 Sept 2013 | 3236000683151 |
| **Figure 1.3** | Advanced Drug Delivery Reviews, (2010), vol 62, 1325-1336 | © 2010 Elsevier Limited | ✓ | 25 Sept 2013 | 323600090375 |
| **Figure 1.4** | Nature Reviews Molecular Cell Biology (2001), vol 2, 917-924 | © 2001 Macmillan Magazines Ltd | ✓ | 25 Sept 2013 | 3236000843460 |
| **Figure 1.5** | Nature Reviews Immunology (2008), vol 8, 34-37 | © 2008 Nature Publishing Group | ✓ | 25 Sept 2013 | 3236001017045 |
| **Figure 1.6** | Journal of Clinical Immunology (2005), vol 25, 1-18 | © 2005 Springer Science + Business Media, Inc. | ✓ | 25 Sept 2013 | 3236001127602 |

| Item | Source of Work | Copyright Holder & Year | Permission | Date Granted | Licence Number |
|---|---|---|---|---|---|
| **Appendix 2a** | Kidney International (2012), vol 81, 170-178 | © 2012 International Society of Nephrology | Author withholds copyright | N/A | N/A |
| **Appendix 2b** | Molecular Immunology (2012), vol 50, 49-56 | © 2012 Elsevier Limited | ✓ | 25 Sept 2013 | 3236010269623 |
| **Appendix 2c** | Journal of Immunology (2012), vol 190, 340-348 | © 2012 The American Association of Immunologists, Inc. | ✓ | 25 Sept 2013 | Granted by Gene Bailey, Senior Editorial Manager |

# Appendix 2 Published Papers

**Appendix 2a Mice with defective Fas ligand are protected from crescentic glomerulonephritis.**

**Appendix 2b Increased incidence of anti-GBM disease in Fcgamma receptor 2b deficient mice, but not mice with conditional deletion of Fcgr2b on either B cells or myeloid cells alone.**

**Appendix 2c FcγRIIB on myeloid cells and intrinsic renal cells rather than B cells protects from nephrotoxic nephritis.**

http://www.kidney-international.org



# Mice with defective Fas ligand are protected from crescentic glomerulonephritis

Ruth M. Tarzi[1], Phoebe E.H. Sharp[1], John P. McDaid[1], Liliane Fossati-Jimack[1], Paul E. Herbert[1], Charles D. Pusey[1], H. Terence Cook[1] and Anthony N. Warrens[1]

[1]*Renal Section, Department of Medicine, Hammersmith Campus, Imperial College London, London, UK*

**Fas ligand is a well-known inducer of apoptosis in cells expressing its receptor Fas; it also prevents autoimmunity by inducing apoptosis of activated T cells. However, Fas ligand also mediates non-apoptotic functions involving inflammatory cell migration and cytokine responses. We sought here to study the role of Fas ligand in nephrotoxic nephritis, a model of crescentic glomerulonephritis, using generalized lymphoproliferative disorder (GLD) mice on a C57BL/6 background, which have defective Fas ligand and display only mild autoimmunity. These mice were significantly protected from glomerular crescent formation, glomerular thrombosis, renal impairment, and albuminuria 15 days after the induction of glomerulonephritis in comparison with wild-type mice. There were a reduced number of apoptotic cells in the glomeruli of nephritic GLD mice but no defect in their antibody responses or splenocyte proliferation at 15 days following the induction of glomerulonephritis. Bone marrow transplantation from wild-type mice restored disease susceptibility to GLD mice; however, wild-type mice were not protected when transplanted with bone marrow from GLD mice. Mesangial cells express Fas ligand *in vitro*, and these cells isolated from GLD mice produced lower amounts of monocyte chemoattractive protein-1 following interleukin-1 stimulation compared with cells from wild-type mice. Thus, Fas ligand-defective mice are protected from nephrotoxic nephritis, a disease in which both circulating and intrinsic renal cells appear to have a role.**

*Kidney International* (2012) **81,** 170–178; doi:10.1038/ki.2011.319; published online 14 September 2011

KEYWORDS: apoptosis; cytokines; glomerulonephritis; mesangial cells

**Correspondence:** *Ruth M. Tarzi, Renal Section, Hammersmith Campus, Imperial College London, Du Cane Road, London W12 0NN, UK. E-mail: r.tarzi@imperial.ac.uk*

**Received 30 January 2011; revised 6 July 2011; accepted 19 July 2011; published online 14 September 2011**

Fas ligand (FasL, CD95L) belongs to the tumor necrosis factor (TNF) family, and has a well-characterized role in inducing apoptosis in target cells by crosslinking the receptor, Fas (CD95), on the cell surface.[1] Deficiency of FasL can lead to autoimmunity in humans and mice on certain genetic backgrounds, due to the lack of activation-induced cell death of T lymphocytes.[2] However, paradoxically, deficiency of FasL has also been associated with protection from inflammation. FasL is involved in apoptosis of mesangial cells by macrophages.[3] Non-apoptotic functions of FasL including cell survival and migration, nuclear factor kappa B activation, and cytokine release are increasingly recognized.[4,5] Soluble FasL has been implicated in chemotaxis of neutrophils and monocytes.[6–8] FasL also has been implicated in facilitating the release of cytokines such as monocyte chemoattractive protein (MCP)-1, interleukin (IL)-6, and IL-12 in response to IL-1 and Toll-like receptor 4 stimulation.[9–11]

FasL is expressed in the kidney in human glomerulonephritis and animal models of glomerulonephritis,[12,13] but its functional effects are not known. We therefore set out to determine the role of FasL in nephrotoxic nephritis and to determine the relative roles of FasL expression on circulating and intrinsic renal cells.

Generalized lymphoproliferative disorder (GLD) mice have a defective form of FasL with a point mutation in the extracellular region of FasL,[2,14] affecting the binding of the protein to Fas. On permissive genetic backgrounds (for example, MRL), GLD mice developed lymphadenopathy, splenomegaly, and autoimmunity. However, in other strains (for example, C57BL/6), a defective Fas/FasL system induced autoantibodies, but only mild glomerulonephritis.[15] We have used mice on a C57BL/6 background for these studies.

## RESULTS

### GLD mice on a C57BL/6 background developed glomerular immune complex deposition, but no significant renal damage during the time course of the NTN experiments

Mice used in the nephrotoxic nephritis (NTN) experiments were between 2 and 4 months of age. We therefore investigated GLD mice of these ages for evidence of spontaneous renal disease. At 2 months, histology and immunofluorescence of the GLD mice were normal. At 4 months, there was some granular immunoglobulin (Ig)G

deposited in the glomeruli, but the kidneys were histologically normal (Supplementary Figure S1 online). There was no albuminuria or renal dysfunction in any of the groups and no significant difference in glomerular macrophage numbers between GLD and WT at 2 and 4 months (Table 1). There were no crescents or glomerular thrombosis in unmanipulated wild-type (WT) and GLD mice at 2 and 4 months.

### GLD mice were protected from renal injury in NTN

Nephrotoxic nephritis was induced in GLD mice and WT C57BL/6 controls. Mice were killed at Day 8 and Day 15 after the induction of disease (Figures 1 and 2 (Day 15) and Supplementary Figure S2 online (Day 8)). FasL-defective GLD mice were strongly protected from renal injury compared with WT mice, in terms of glomerular thrombosis ($P<0.01$), glomerular crescents ($P<0.001$), albuminuria ($P<0.001$), serum albumin ($P<0.001$), and serum urea ($P<0.01$). TUNEL staining revealed lower numbers of glomerular apoptotic cells in the GLD than in the WT mice ($P<0.001$; Figure 1f).

### There was no reduction in glomerular neutrophil or macrophage infiltration, but interstitial inflammation was reduced in GLD mice

Despite protection from injury, the GLD mice had a macrophage infiltrate in the glomeruli that was not significantly different from WT nephritic mice (median 1.86 versus 1.24 CD68-positive cells/glomerular cross-section in WT versus GLD, not significant; Figures 2 and 3a). In contrast, in the interstitial regions, there was a reduction in the macrophage infiltration in the GLD mice compared with WT ($P<0.01$, Figures 2 and 3b). This was mirrored by reduced MCP-1 mRNA in whole-kidney mRNA extracts at Day 15 (Figure 3c, $P<0.001$). At 24 h after injection of nephrotoxic serum, there was no significant difference in the glomerular neutrophil infiltrate between WT and GLD mice (Figure 3d), although there was a wide range, possibly because of the transient nature of the neutrophil population.

### Antibody and T-cell responses to the nephritogenic antigen

To determine the mechanism for the protection of disease, the systemic and local immune responses were analyzed. Murine IgG deposited in glomeruli was quantified at Day 1, Day 8, and Day 15 after the induction of disease. Compared with WT, there was a delay in the glomerular antibody deposition in GLD mice, as there was significantly less in GLD glomeruli at Day 1 ($P<0.01$), no difference at Day 8 and more mouse IgG ($P<0.01$) deposited at Day 15 after induction of disease (Figure 4a). Similarly, in terms of circulating mouse anti-sheep IgG, there was no significant difference between WT and GLD at Day 1, but relative to WT, there was significantly more circulating anti-sheep IgG at Day 8 and Day 15 in the GLD mice ($P<0.05$ and $P<0.01$, respectively; Figure 4b).

Splenocyte proliferation to sheep IgG was determined after preimmunization only (primary immune response) and in a separate experiment at the termination (Day 10). There was reduced splenocyte proliferation to antigen in the GLD mice after preimmunization alone (Figure 5a); however, by

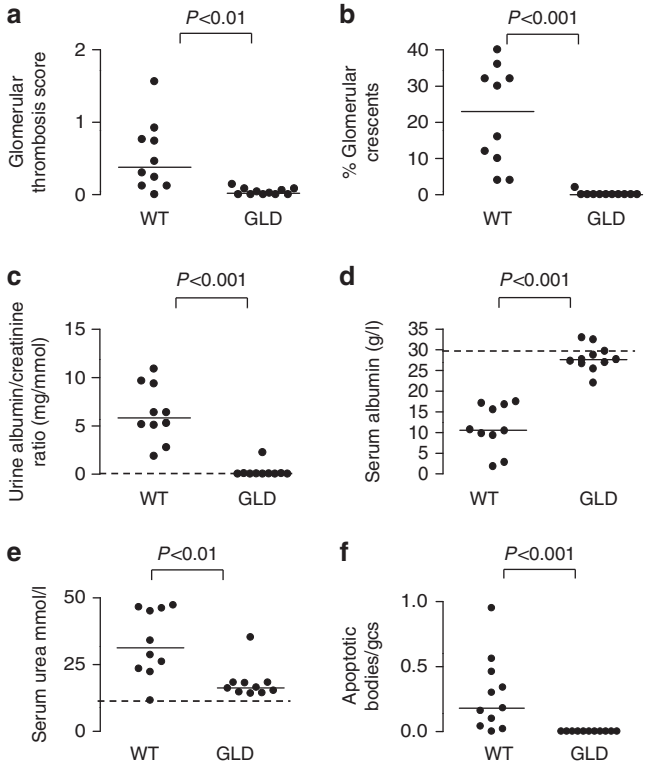


**Figure 1 | Functional and histological parameters at Day 15 after induction of nephrotoxic nephritis (NTN) in wild-type (WT) and generalized lymphoproliferative disorder (GLD) mice.** (**a**) Glomerular thrombosis score, (**b**) percentage glomerular crescents, (**c**) urinary albumin/creatinine ratio (mg/mmol), (**d**) serum albumin (g/l), (**e**) serum urea (mmol/l), (**f**) apoptotic bodies/gcs. Dashed lines represent values for a group of normal WT mice. gcs, glomerular cross-section.

**Table 1 | Control data: unmanipulated mice**

| | WT (*n*=8) | GLD (*n*=8) | WT (*n*=8) | GLD (*n*=8) |
|---|---|---|---|---|
| Age (in months) | 2 | 2 | 4 | 4 |
| Glomerular mouse IgG | Negative | Negative | Negative | Granular |
| Serum urea (mmol/l) | 9.4 (7.7–11.6) | 7.5 (5.8–8.4) | 7.2 (6.8–8.9) | 11.3 (11.1–12.9) |
| Serum creatinine (μmol/l) | 49.0 (45.5–50.0) | 39.5 (37.0–42.5) | 42.5 (38.0–49.0) | 37.0 (35.0–41.0) |
| Macrophages/gcs | 0.1 (0.02–0.19) | 0.12 (0–0.56) | 0.33 (0.24–0.044) | 0.49 (0.34–0.54) |
| Urinary albumin/creatinine ratio (mg/mmol) | 0.01 (0.01–0.01) | 0.01 (0.01–0.01) | 0.01 (0.01–0.01) | 0.01 (0.01–0.01) |

Abbreviations: gcs, glomerular cross-section; GLD, generalized lymphoproliferative disorder; IgG, immunoglobulin G; WT, wild-type.

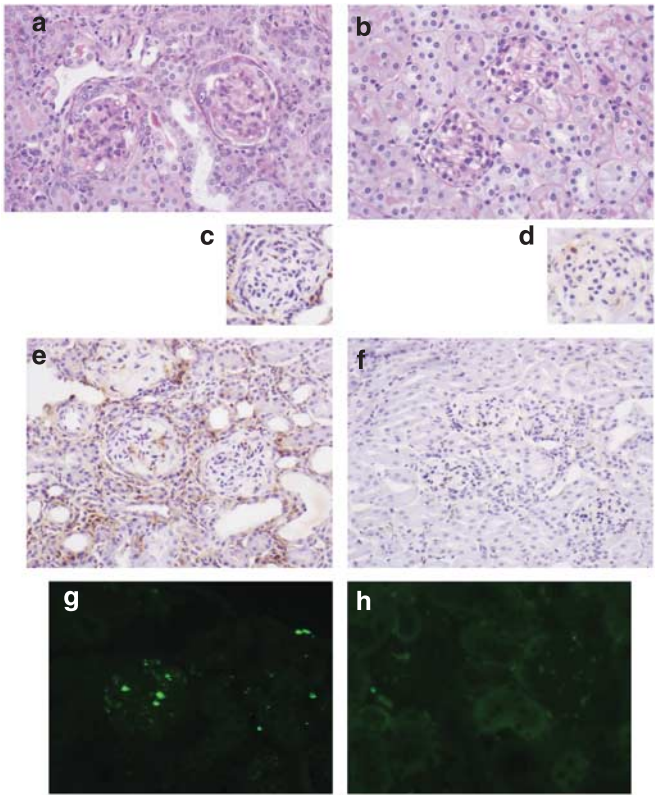


**Figure 2 | Histology at Day 15 after induction of nephrotoxic nephritis (NTN).** (**a**) Periodic acid-Schiff-stained wild-type (WT) kidney section showing glomerular hypercellularity, and a glomerular crescent; (**b**) generalized lymphoproliferative disorder (GLD) kidney at Day 15 after induction of NTN showing mild glomerular hypercellularity only. (**c**, **e**) Immunoperoxidase staining for CD68 in WT kidney showing interstitial and glomerular macrophage infiltration. (**d**, **f**) Immunoperoxidase staining for CD68 in GLD kidney showing glomerular, but little interstitial, macrophage infiltration. Apoptotic bodies were present in WT glomeruli (**g**) but absent from GLD glomeruli by TUNEL staining (**h**).

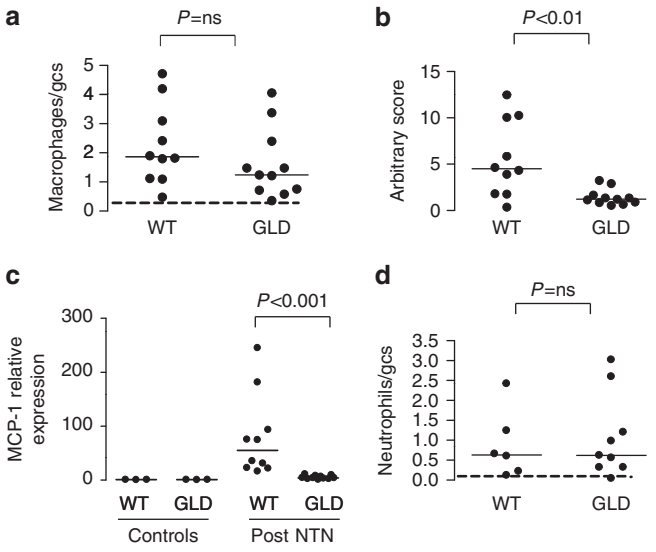


**Figure 3 | Day 15 after induction of NTN.** (**a**) CD68-positive macrophages/glomerular cross-section (gcs); (**b**) CD68-positive macrophage interstitial infiltration assessed by image analysis; (**c**) relative expression of MCP-1 mRNA in GLD and WT mice post nephrotoxic nephritis (NTN) compared with control wild-type (WT) and generalized lymphoproliferative disorder (GLD) mice; (**d**) neutrophils/gcs 24 h after induction of NTN. Dashed lines represent values for a group of normal WT mice. MCP, monocyte chemoattractive protein; ns, not significant.

the end of the experiment, the proliferation was equal between WT and GLD (Figure 5b). Analysis of cytokines produced by splenocytes after preimmunization and re-challenge with sheep IgG *in vitro* showed reduced interferon gamma (IFN-γ) production by GLD splenocytes ($P<0.05$) and a tendency to a reduced IL-17A production ($P=0.09$; Figure 5a). In the Day-10 experiment, the supernatant IFN-γ production was below the limit for detection by the enzyme-linked immunosorbent assay (ELISA). The IL-4 production by splenocytes in response to sheep IgG was barely above the detection limit of the assay, and not significantly different between the two groups. Therefore, there was a defect in T-cell responses early in the phase of the disease, although this was not evident at Day 10 post NTN.

To investigate this further, intrarenal T cells and cytokines were analyzed. There was a reduction in CD4-positive T-cell infiltration in the GLD mice at Day 15 after induction of NTN (median 0.38 (interquartile range 0.19–0.57) CD4-positive T cells/glomerular cross-section in the WT mice versus 0.19 (0.1–0.23) CD4+ cells/glomerular cross-section in the GLD mice; Figure 6a). In parallel with this observation, we saw reduced mRNA for IFN-γ in the kidneys of the nephritic GLD mice ($P<0.05$, Figure 6b). IL-4 mRNA was downregulated in nephritic kidneys compared with non-diseased kidneys, and there was no significant difference between WT and GLD nephritic mice (Figure 6c). mRNA for IL-12p40, a component of IL-12 and IL-23, was significantly reduced in the GLD kidneys compared with WT nephritic kidneys ($P<0.001$, Figure 6d). Taken together, there was a moderate reduction in the systemic T-cell response at an early stage of NTN, but not at later.

### Fas ligand derived from either bone marrow-derived or radioresistant intrinsic renal cells was sufficient to restore susceptibility to NTN

Bone marrow transplant experiments were conducted to compare the role of bone marrow-derived and radioresistant cell expression of FasL. GLD mice were transplanted with WT bone marrow and WT mice were transplanted with GLD bone marrow, as well as isografts performed as controls. To assess reconstitution of circulating leukocytes, mice were transplanted with bone marrow marked with the allotype marker CD45.1 rather than CD45.2, the C57BL/6 allotype. A median of 92.2% (range 90.9–93.4%) of CD45-positive circulating leukocytes were of CD45.1 donor origin, as opposed to the recipient CD45.2 cells in peripheral blood at 8 weeks after bone marrow transplantation (Supplementary

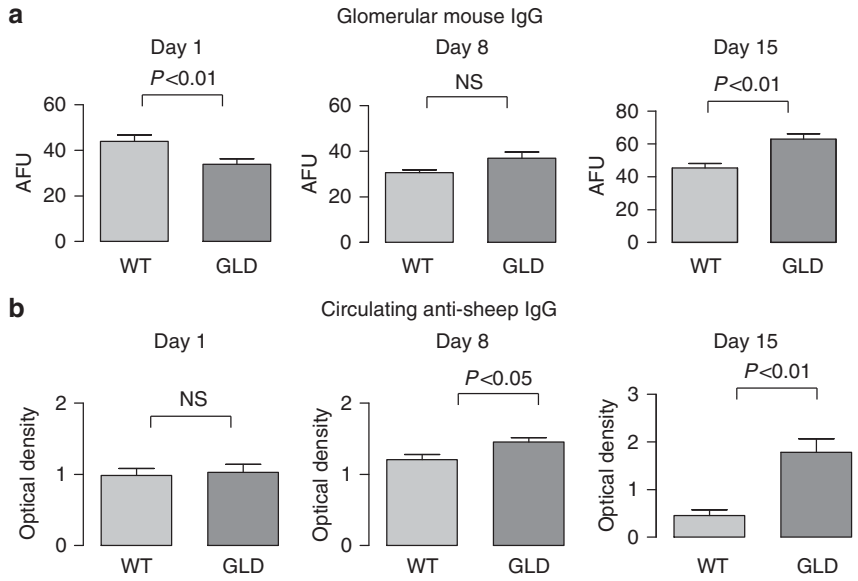


**Figure 4 | Deposited and circulating immunoglobulin (Ig)G responses in WT and GLD mice after the induction of nephrotoxic nephritis (NTN).** (**a**) Quantification of deposited glomerular mouse IgG at Day 1, Day 8, and Day 15 after induction of NTN (minimum $n = 7$/group). (**b**) Enzyme-linked immunosorbent assay (ELISA) for serum total sheep IgG (1:1000 dilution) at Day 1, Day 8, and Day 15 after induction of nephrotoxic serum. AFU, arbitrary fluorescence units; GLD, generalized lymphoproliferative disorder; NS, not significant; WT, wild type.

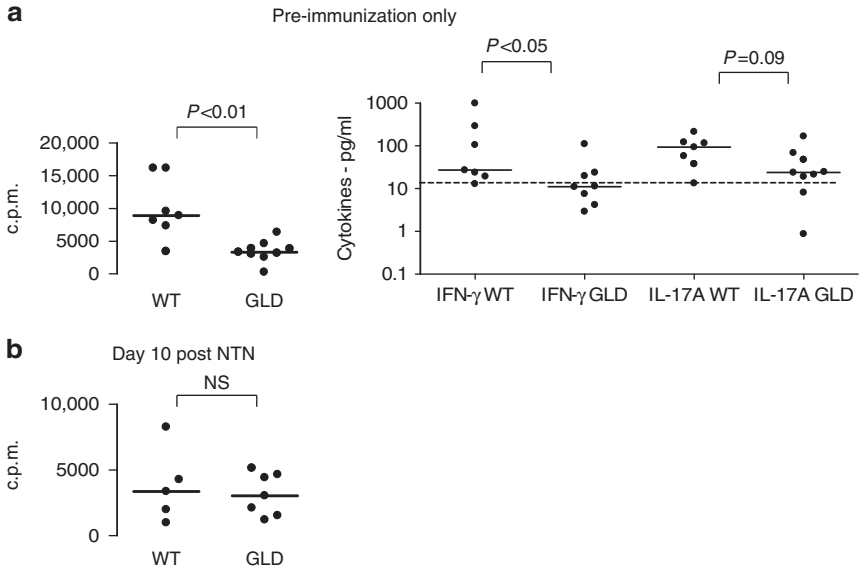


**Figure 5 | Splenocyte $^3$H thymidine incorporation at 72 h after exposure to 100 mcg/ml sheep IgG (left panels), and cytokine release into supernatant (right hand panel) after exposure to sheep IgG *in vitro*.** (**a**) Splenocytes collected 7 days after immunization alone, without injection of nephrotoxic serum; (**b**) splenocytes collected at 10 days after induction of nephrotoxic nephritis with preimmunization and nephrotoxic serum. c.p.m., counts per minute; GLD, generalized lymphoproliferative disorder; IgG, immunoglobulin G; IFN, interferon; IL, interleukin; NS, not significant; NTN, nephrotoxic nephritis; WT, wild type.

Figure S3 online). Semiquantitative PCR of DNA extracted from whole blood at the termination of the experiments was compared with a standard curve of known mixtures of WT and GLD DNA. More than 95% of DNA extracted from circulating blood was of donor origin in both the WT to GLD and the GLD to WT transplants (not shown).

Ten weeks post bone marrow transplantation, mice were induced with NTN, and were killed at Day 8 after the injection of nephrotoxic serum. WT bone marrow restored disease susceptibility, as GLD mice transplanted with WT bone marrow had more renal damage than GLD mice transplanted with GLD bone marrow ($P < 0.05$ for glomerular thrombosis, crescents, serum urea, and urinary albumin/creatinine ratios; Figure 7a–d). As noted in previous experiments, there was no significant difference in the glomerular macrophage infiltrate between any of the groups,

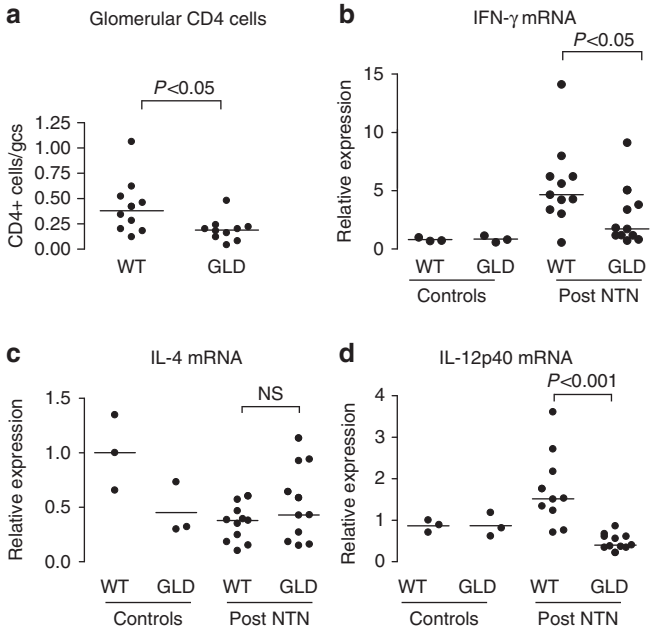


**Figure 6 | Intrarenal T-cell infiltration and intrarenal cytokine mRNA at Day 15 after induction of nephrotoxic nephritis.** (**a**) CD4-positive T cells/gcs; (**b**) relative expression of IFN-γ mRNA between wild-type (WT) and, generalized lymphoproliferative disorder (GLD) mice at Day 15 post nephrotoxic nephritis (NTN); (**c**) relative expression of interleukin (IL)-4 mRNA; (**d**) relative expression of IL-12p40 mRNA. WT and GLD controls refer to unmanipulated age-matched control mice. gcs, glomerular cross-section; NS, not significant.

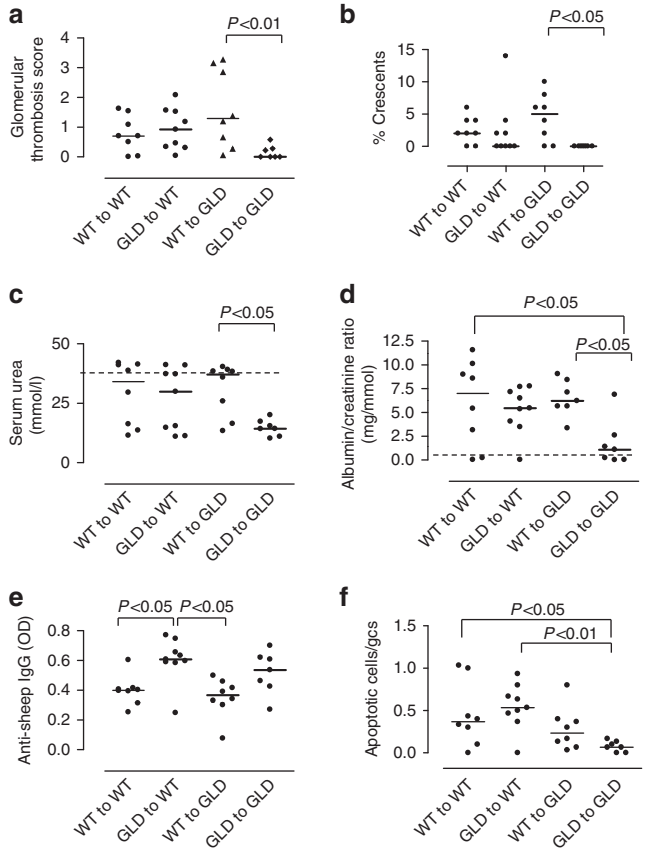


**Figure 7 | Nephrotoxic nephritis in bone marrow-transplanted mice at Day 8 after induction of NTN.** (**a**) Glomerular thrombosis score; (**b**) percentage glomerular crescents; (**c**) serum urea (mmol/l); (**d**) urinary albumin/creatinine ratio (mg/mmol); (**e**) Enzyme-linked immunosorbent assay (ELISA) for serum anti-sheep immunoglobulin (Ig)G; (**f**) apoptotic bodies/glomerular cross-section. Dashed lines refer to normal values for a group of control wild-type (WT) mice. gcs, glomerular cross-section; NTN, nephrotoxic nephritis; OD, optical density.

but there were reduced interstitial macrophages, only in the GLD to GLD transplants (not shown). Only the GLD to GLD transplants had reduced levels of glomerular apoptosis (Figure 7f).

However, our results suggest that FasL expression by radioresistant cells in the kidney is also sufficient to induce renal injury in NTN, as WT mice transplanted with GLD bone marrow were not protected from NTN as compared with WT mice transplanted with WT bone marrow (Figure 7). To determine whether there was chimerism of resident kidney leukocytes post bone marrow transplantation, C57BL/6 (CD45.2) mice were transplanted with CD45.1 bone marrow using the same protocol. Ten weeks later, kidney cells were dissociated, stained for CD45.1, CD45.2, F4/80, and CD11c, and analyzed by flow cytometry ($n=7$). The chimerism of resident kidney cells was broadly similar to blood with total leukocytes median 88% (range 87.3–91.8%), CD11c + F4/80 + 95.4 (92.3–95.6), and CD11c + F4/80 − 93.4% (90.7–96.3%), Supplementary Figure S3 online. These results suggest a role for intrinsic renal cell FasL in NTN pathogenesis.

### FasL mRNA increases in the kidney during NTN, and is expressed by cultured mesangial cells

mRNA for FasL was increased in whole-kidney lysates after the development of NTN, indicating that FasL in the kidney itself could have a local effect (Figure 8a); however, the mRNA results cannot distinguish whether this is originating from circulating or intrinsic renal cells. We therefore assessed the expression of FasL on mesangial cells, cultured overnight in the presence of a metalloproteinase inhibitor to inhibit cleavage to soluble FasL. By flow cytometry, we could detect FasL on 18.4% of the cultured mesangial cells using a FasFc conjugate, compared with 1.96% positive cells with the secondary antibody alone (Figure 8b). As defective FasL signaling has been associated with reduced responses to IL-1, we then examined MCP-1 secretion by WT and GLD mesangial cells after stimulation with IL-1 or TNF-α. There was significantly reduced MCP-1 secretion by GLD mesangial cells after stimulation with IL-1 but not TNF-α (representative results from one of five experiments for IL-1 and three experiments for TNF-α are shown in Figure 8c and d).

## DISCUSSION

Our results show that FasL mutant (GLD) mice on a C56BL/6 background were strongly protected from histological and

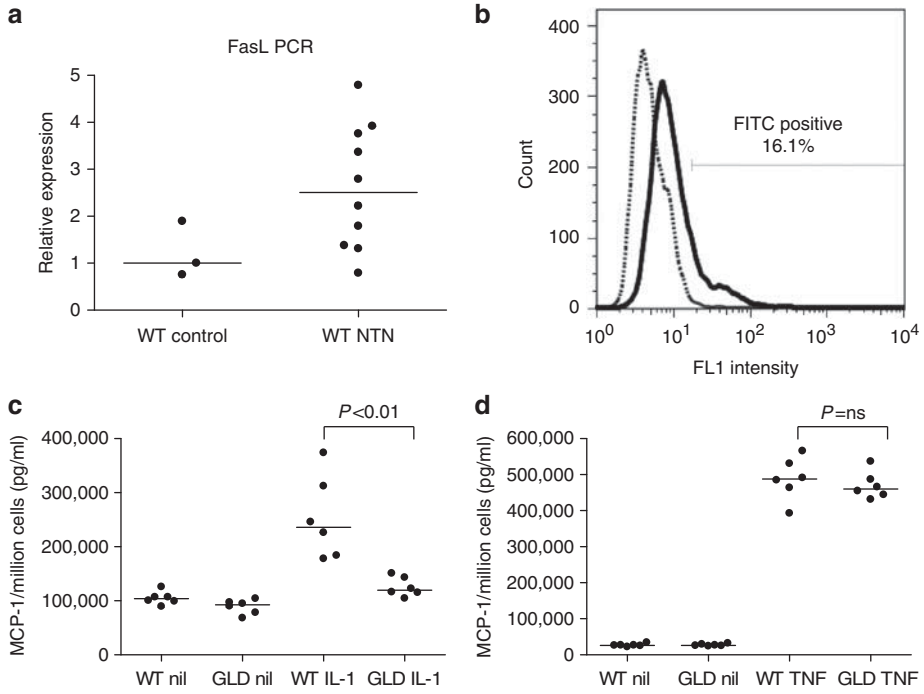


**Figure 8 | Expression of Fas ligand (FasL) in the kidney and analysis of functional effects of generalized lymphoproliferative disorder (GLD) mutation in mesangial cells.** (**a**) Relative expression of FasL mRNA in whole kidney in unmanipulated wild-type (WT) mice (WT control) and WT mice at Day 15 after the induction of nephrotoxic nephritis (NTN) (WT NTN). (**b**) Flow cytometry for FasL on cultured mesangial cells. Dotted line: fluorescein isothiocyanate (FITC)-conjugated antihuman immunoglobulin (Ig)G secondary antibody only; black line, recombinant FasFc protein ((Fas conjugated to human Fc) plus secondary antibody). (**c**) Monocyte chemoattractive protein (MCP)-1 measured in supernatant of serum-starved mesangial cells unstimulated, or stimulated with 10 ng/ml interleukin (IL)-1 (representative results from five separate experiments). (**d**) MCP-1 levels measured in supernatants of serum-starved mesangial cells unstimulated, or stimulated with 10 ng/ml tumor necrosis factor (TNF)-α (representative of three separate experiments). ns, not significant.

functional renal injury, using the nephrotoxic nephritis model of glomerulonephritis. T-cell-mediated systemic immunity was reduced in the early phase of the disease, which may have contributed to protection from injury. However, the bone marrow transplant results did not support an exclusive role for FasL expressed by circulating cells in mediating injury, making it less likely that differences in the immune response are completely responsible for the protection of GLD mice from glomerulonephritis. We showed expression of FasL in the kidney in NTN, and our results would suggest that local expression of FasL in the kidney by circulating or intrinsic renal cells can facilitate injury in this model.

GLD mice have been found to be protected from a number of models of injury.[10,16–19] Similar to our findings, T-cell proliferation to antigen was not reduced at the end of the experiments in either collagen-induced arthritis[10] or experimental allergic encephalomyelitis.[18] In these models, the immune response at earlier stages of disease was not examined.

A Th2-deviated immune response protects from murine nephrotoxic nephritis.[20] Th2-deviated immune responses have been found in human patients with Fas and FasL mutations causing autoimmune lymphoproliferative syndrome.[11] We noted significantly increased IL-4 production by GLD splenocytes after polyclonal stimulation (data not shown). However, we could not demonstrate enhanced antigen-specific Th2 responses systemically or in the kidney, and thus this mechanism is unlikely to explain protection from disease in our model.

Interestingly, there was no reduction in glomerular macrophage or neutrophil infiltration into glomeruli in GLD mice with NTN. Although FasL is involved in migration of neutrophils[6,7] and macrophages[8] to inflammatory sites, FasL does not have a major role in the entry of inflammatory cells to glomeruli in this model. It is likely that other mechanisms such as Fc receptor- or complement-mediated events have a larger role in models in which immune complexes are deposited.

It is striking that the glomerular injury and subsequent interstitial injury and inflammation was markedly reduced, despite the lack of reduction in glomerular macrophage infiltration. This suggests that in the absence of functional FasL, the ability of the cells to induce glomerular damage was reduced. We saw reduced apoptotic bodies in the kidneys of the GLD mice induced with NTN. FasL induces apoptosis of cells, including mesangial cells.[3] The reduction in apoptosis may be responsible for protection from injury. An alternative possibility is that the presence of FasL in the glomerulus is involved in cell activation. Indeed, FasL has been reported to function synergistically with IFN-γ to enhance macrophage activation.[21] In addition, FasL can activate the intracellular

mediator nuclear factor kappa B, a key transcription factor for inflammatory responses,[22] and facilitates signaling through the IL-1 receptor.[10] Binding of FasL to Fas activates caspases, which process IL-1β for secretion.

Transplantation of WT bone marrow to GLD mice was sufficient to restore susceptibility to NTN, indicating that expression of FasL by circulating cells was sufficient to induce NTN. However, transplantation of GLD bone marrow to WT mice did not protect from disease, despite good deletion of circulating WT bone marrow-derived cells. There were some (~10%) WT circulating and intrinsic renal cells present in these bone marrow transplants, and we cannot exclude the possibility that these are sufficient to induce disease. However, a lack of reduction of disease does suggest that there is a source of FasL from radioresistant cells in the kidney that is permissive for the development of NTN. This is in contrast to results from similar experiments conducted in experimental allergic encephalomyelitis and uveitis, where FasL expressed on circulating cells was responsible for protection from disease.[19,23] We confirm that mesangial cells *in vitro* express FasL. FasL on intrinsic renal cells is functional, as there is a previous report of a functional role for FasL expression by tubular cells in inducing apoptosis of surrounding tubular cells in a model of cisplatin-induced acute tubular necrosis.[24] A role for FasL on intrinsic renal cells in glomerulonephritis has not been previously shown. GLD mesangial cells had attenuated responses to IL-1-β in terms of the production of MCP-1 *in vitro*, consistent with previous reports in other cell types expressing FasL.[10,25] There was a large reduction in mRNA for MCP-1 in the GLD kidneys, consistent with this finding, and a large reduction in macrophages in the interstitium, which may indicate that similar mechanisms operate to regulate MCP-1 production in the interstitial compartment. MCP-1 is involved in cell activation and chemotaxis.[26]

The autoimmunity-enhancing effects of FasL blockade may preclude its use as a therapeutic agent. However, this study highlights the importance of FasL in renal injury and highlights a possible role for intrinsic renal cell FasL expression in the pathogenesis of glomerulonephritis.

## MATERIALS AND METHODS

### Mice

GLD mice on a C57BL/6 background were purchased from Jackson Laboratory (Maine, ME) and bred in-house, and C57BL/6 WT mice were purchased from Harlan (Blackthorn, UK). Animal experiments were conducted according to the institutional and the UK Home Office guidelines. Mice were genotyped using a protocol available on the Jackson Laboratory website. Experimental groups were matched for sex and age.

### Induction of nephrotoxic nephritis

Sheep anti-mouse nephrotoxic globulin was prepared as described previously.[27] The endotoxin content of the nephrotoxic globulin was undetectable, measured using a Biowhittaker 1000-QCL LPS assay kit (Biowhittaker, Walkersville, MD). Mice were immunized intraperitoneally with 0.2 mg of sheep IgG in a 50:50 mix of saline and complete Freund's adjuvant (Sigma Chemical, St Louis, MO). Five days later, 0.2 ml of nephrotoxic globulin was injected intravenously. Mice were monitored clinically and the experiments were terminated if the mice were showing signs of the disease.

### Histological studies and quantitative immunofluorescence

Glomerular crescents and thrombosis were scored on samples fixed in Bouin's solution and stained with periodic acid-Schiff, by an observer blinded to the experimental group. Glomerular thrombosis was assessed by scoring individual glomeruli for periodic acid-Schiff-positive material as follows: grade 0: no periodic acid-Schiff-positive material; grade 1: 0–25% of glomerular cross-section periodic acid-Schiff positive; grade 2: 25–50%; grade 3: 50–75%; grade 4: 75–100%. Fifty glomeruli were scored per kidney. Glomerular crescents were defined as glomeruli containing two or more layers of cells in Bowman's space.

Glomerular mouse and sheep IgG were visualized by direct immunofluorescence on frozen kidney sections using fluorescein isothiocyanate-conjugated goat anti-mouse IgG (Fc-specific) and fluorescein isothiocyanate-conjugated monoclonal mouse anti-sheep IgG clone GT34 (Sigma, Dorset, UK). To quantify immunofluorescence, sections were examined at ×40 magnification using an Olympus BX4 fluorescence microscope (Olympus Optical, London, UK) and a Photonic Science Colour Coolview camera (Photonic Science, Robertsbridge, UK). Samples from each experiment were stained on the same occasion and measured together. Images of the sections were captured using Image Pro (MediaCybernetics, Bethesda, MD) and the total pixel intensity for each glomerulus was measured and averaged for 20 glomeruli per section.

For cell markers, kidneys were fixed in periodate-lysine-paraformaldehyde. Sections of 5 μm were stained for macrophages with FA11 (monoclonal rat anti-mouse CD68, Serotec, Oxford, UK) or CD4 cells (GK1.5, BDPharmingen, Oxford, UK), and developed using the Polink-2 plus HRP rat detection kit (Newmarket Scientific, Newmarket, UK). Macrophages and T cells in 50 glomeruli/sample were counted and averaged to obtain cells/glomerular per cross-section. For interstitial macrophage infiltration, five high-power fields per kidney were photographed. The proportion of the pictures with brown peroxidise pigmentation was calculated using the ImagePro software (MediaCybernetics) and averaged for the five high-power fields. All slides from a single experiment were analyzed simultaneously TUNEL staining was used to detect apoptotic cells on formalin-fixed sections of mouse kidney using the ApopTag Fluorescein Kit (Qbiogene, Carlsbad, CA).

### Quantitative RT-PCR

Total RNA was extracted from whole kidneys using the TRIzol method. Real-time qRT-PCR was performed on an ABI 7500 Sequence Detection System (Applied Biosystems, Warrington, UK) using Brilliant II SYBR Green qRT-PCR Master Mix, 1 Step (Stratagene, Cambridge, UK). RNA was used at a final concentration of 5–10 ng/μl and all samples were run in duplicates. Results were exported to the 7500 Fast System SDS software (Applied Biosystems), and $C_t$ values were determined for all the genes analyzed. The relative expression levels, normalized to *GAPDH* gene expression, were determined by using the $2^{-\Delta\Delta Ct}$ method. The following primers were used: MCP-1 forward: 5′-ATGCAGTTAATGCCC CACTC-3′; MCP-1 reverse: 5′-AGCTGGAAGCCACTGACACT-3′; GAPDH forward: 5′-GGGTGTGAACCACGAGAAAT-3′; GAPDH reverse: 5′-GTCTTCTGGGTGGCAGTGAT-3′; IFN-γ forward: 5′-GCA

TCTTGGCTTTGCAGCTC-3′; IFN-γ reverse: 5′-CGACTCC TTTTCCGCTTCCT-3′; IL-4 forward: 5′-ACAGGAGAAGGGACGC CAT-3′; IL-4 reverse: 5′-GAAGCCCTACAGACGAGCTCA; IL-12-p40 forward: 5′-GGAAGCACGGCAGCAGAATA-3′; IL-12-p40 reverse: 5′-AACTTGAGGGAGAAGTAGGAAT-3′; FasL forward: 5′-ACCCCCACTCAAGGTCCAT-3′; FasL reverse: 5′-CGAAGTAC AACCCAGTTTCGT-3′.

### Serum urea, albumin, and urinary albumin/creatinine ratio

Serum urea and urinary creatinine were measured in the Department of Clinical Chemistry, Imperial College Healthcare NHS Trust. Serum albumin was measured using the AssayMax mouse albumin ELISA kit (AsssayPro, St Charles, MO). Albuminuria was assessed by radial immunodiffusion against a rabbit anti-mouse albumin (Biogenesis, Poole, UK), as previously described.[27]

### Circulating antibody and T-cell immune responses

Serum mouse anti-sheep IgG levels were measured by sandwich ELISA as previously described.[27] Detecting antibody for IgG (γ-chain specific) was obtained from Sigma. Samples were tested in duplicate at 1:500 and 1:1000 dilutions. Background fluorescence in uncoated wells was subtracted, and normal serum from unimmunized mice served as a control.

For splenocyte proliferation assays, single-cell suspensions were created and red cells were lysed. Cells were cultured at $1 \times 10^6$ cells/ml for 72 h in HL1 serum-free medium (Lonza, Basel, Switzerland), in the presence or absence of 100 ng/ml heat-aggregated sheep IgG, or 100 ng/ml phorbol myristate acetate plus ionomycin (500 ng/ml) as a positive control. At 72 h, 1 μCi/well $^3$H thymidine was added for 24 h before assessing splenocyte proliferation using standard procedures and a Wallac 1450 microbeta counter (Perkin Elmer, Waltham, MA). Supernatants collected at 72 h were assayed for IL-4 and IFN-γ using ELISA kits, according to the manufacturer's instructions (eBioscience, Hatfield, UK), and IL-17alpha (R&D Systems, Minneapolis, MN). Lower limits for detection were 1, 15, and 15 pg/ml.

### Bone marrow chimeras

Chimeric mice were made by irradiation with a dose of 8 Gy and reconstituted with $10 \times 10^6$ donor bone marrow cells. Nephritis experiments were conducted at 10 weeks after this. Confirmation of chimerism was obtained using PCR on DNA extracted from 0.1 ml blood obtained at the terminal bleed. PCR was performed as recommended on the Jackson laboratory website, except that the reverse primer was labeled with the fluorescent marker 6-carboxy-fluoroscein. The products were run on Genescan (Applied Biosystems) and the ratio of the mutant (108 bp) versus WT (88 bp) product was calculated and compared with known mixtures of WT and GLD DNA (0, 5, 50, 90, 95, and 100% mutant DNA). In addition, to confirm chimerism, blood was taken from mice transplanted with CD45.1 allotype bone marrow and the mice were bled at 10 weeks post transplantation. Red cells were lysed, and Fc receptors were blocked with 2.4G2 and stained with CD45.1 APC and CD45.2 APC. Kidney single-cell suspensions were prepared as previously described.[28] Briefly, kidneys were removed and sliced into six pieces using a scalpel, followed by digestion with DNase I 100 and 0.5 μg/ml Collagenase D (Roche Diagnostics, Burgess Hill, UK). Kidneys were mashed and filtered through a 100-μm nylon mesh. Kidney suspensions were incubated with 2.4G2 (eBiosciences) to block Fc receptors, and then stained with the following antibodies obtained from eBiosciences: APC-CD45.1, PE-CD45.2, fluorescein isothiocyanate F4/80, and PerCP Cy5.5 CD11c. Flow cytometry was performed using a FACScalibur flow cytometer and analyzed using the FlowJo (TreeStar, Ashland, OR) software.

### Mesangial cell cultures

Glomeruli were collected from WT and GLD kidneys and digested with collagenase as previously described.[29] Mesangial cells were cultured in RPMI containing 20% fetal calf serum, and passaged 8–12 times before use. Mesangial cells were characterized as anti-myosin positive, CD11b, and pancytokeratin negative, with characteristic stellate morphology. Briefly, $10^6$ cells/well were cultured in a six-well plate (Nunc, Rochester, NY) for 24 h, after which the cells were serum-starved overnight. Cells were stimulated with 10 ng/ml IL-1β, TNF-α, or left unstimulated in serum-free mesangial media for 24 h. Supernatant MCP-1 levels were analyzed by ELISA according to the manufacturer's instructions (eBioscience). Cytokine levels were corrected for cell numbers and were compared with the end of the experiment using the MTT assay according to the manufacturer's instructions (Sigma). There tended to be more cells in the GLD wells at the termination of the experiments, possibly because of reduced apoptosis in these cells.

### Mesangial cell FasL expression

Mesangial cells were cultured in the presence of 10 μmol/l GM6001 (Sigma) for 24 h before collecting (protease inhibitor to prevent cleavage of membrane-bound FasL). Cells were collected using Cell Dissociation Solution (Sigma), and nonspecific binding was blocked using 10% normal mouse serum. A measure of 1 μg FasFc conjugate (Sigma) was added to $0.5 \times 10^6$ cells, followed by washing in phosphate-buffered saline/1% fetal calf serum. Bound FasFc was detected using fluorescein isothiocyanate-conjugated antihuman IgG (Sigma). Flow cytometry was performed using a FACSCalibur flow cytometer and analyzed using the FlowJo (TreeStar) software.

### Statistics

Results are quoted as median (interquartile range), unless otherwise stated. Lines on graphs represent median value. For comparing two groups, the Mann–Whitney *U*-test was used, and for three or more groups a one-way analysis of variance with Bonferroni's post test was used. GraphPad Prism (GraphPad Software, San Diego, CA) was used to analyze the data. Differences were considered significant when $P < 0.05$.

## DISCLOSURE

All the authors declared no competing interests.

## ACKNOWLEDGMENTS

We thank Mr John Meek, Clinical Chemistry Department, Hammersmith Hospital, for taking the serum urea, creatinine, and urine creatinine measurements, and Mr Phillip Muckett and Ms Nicole Clark for providing technical help. RMT thanks Professor Dorian Haskard for his helpful advice. This work was funded by the Arthritis Research UK and the Nan Dimond Trust. Part of this work was presented in abstract form at the American Society of Nephrology meeting 2009.

## SUPPLEMENTARY MATERIAL

**Figure S1.** Histology from unmanipulated WT and GLD mice at 2 months and 4 months of age.
**Figure S2.** Functional and histological parameters at Day 8 after induction of NTN in wild-type (WT) and GLD mice.

**Figure S3.** A-B: Flow cytometry of blood and kidney leukocytes 10 weeks post bone marrow transplantation, to demonstrate the degree of chimerism.
Supplementary material is linked to the online version of the paper at http://www.nature.com/ki

## REFERENCES


1. Nagata S, Golstein P. The Fas death factor. *Science* 1995; **267**: 1449–1456.
2. Roths JB, Murphy ED, Eicher EM. A new mutation, gld, that produces lymphoproliferation and autoimmunity in C3H/HeJ mice. *J Exp Med* 1984; **159**: 1–20.
3. Boyle JJ. Human macrophages kill human mesangial cells by Fas-L-induced apoptosis when triggered by antibody via CD16. *Clin Exp Immunol* 2004; **137**: 529–537.
4. Wajant H, Pfizenmaier K, Scheurich P. Non-apoptotic Fas signaling. *Cytokine Growth Factor Rev* 2003; **14**: 53–66.
5. Peter ME, Budd RC, Desbarats J *et al.* The CD95 receptor: apoptosis revisited. *Cell* 2007; **129**: 447–450.
6. Dupont PJ, Warrens AN. Fas ligand exerts its pro-inflammatory effects via neutrophil recruitment but not activation. *Immunology* 2007; **120**: 133–139.
7. Seino K, Iwabuchi K, Kayagaki N *et al.* Chemotactic activity of soluble Fas ligand against phagocytes. *J Immunol* 1998; **161**: 4484–4488.
8. Letellier E, Kumar S, Sancho-Martinez I *et al.* CD95-ligand on peripheral myeloid cells activates Syk kinase to trigger their recruitment to the inflammatory site. *Immunity* 2010; **32**: 240–252.
9. Altemeier WA, Zhu X, Berrington WR *et al.* Fas (CD95) induces macrophage proinflammatory chemokine production via a MyD88-dependent, caspase-independent pathway. *J Leukoc Biol* 2007; **82**: 721–728.
10. Ma Y, Liu H, Tu-Rapp H *et al.* Fas ligation on macrophages enhances IL-1R1-Toll-like receptor 4 signaling and promotes chronic inflammation. *Nat Immunol* 2004; **5**: 380–387.
11. Fuss IJ, Strober W, Dale JK *et al.* Characteristic T helper 2 T cell cytokine abnormalities in autoimmune lymphoproliferative syndrome, a syndrome marked by defective apoptosis and humoral autoimmunity. *J Immunol* 1997; **158**: 1912–1918.
12. Tsukinoki T, Sugiyama H, Sunami R *et al.* Mesangial cell Fas ligand: upregulation in human lupus nephritis and NF-kappaB-mediated expression in cultured human mesangial cells. *Clin Exp Nephrol* 2004; **8**: 196–205.
13. Lorz C, Ortiz A, Justo P *et al.* Proapoptotic Fas ligand is expressed by normal kidney tubular epithelium and injured glomeruli. *J Am Soc Nephrol* 2000; **11**: 1266–1277.
14. Takahashi T, Tanaka M, Brannan CI *et al.* Generalized lymphoproliferative disease in mice, caused by a point mutation in the Fas ligand. *Cell* 1994; **76**: 969–976.
15. Izui S, Kelley VE, Masuda K *et al.* Induction of various autoantibodies by mutant gene lpr in several strains of mice. *J Immunol* 1984; **133**: 227–233.
16. Heinzelmann F, Jendrossek V, Lauber K *et al.* Irradiation-induced pneumonitis mediated by the CD95/CD95-ligand system. *J Natl Cancer Inst* 2006; **98**: 1248–1251.
17. Neff TA, Guo RF, Neff SB *et al.* Relationship of acute lung inflammatory injury to Fas/FasL system. *Am J Pathol* 2005; **166**: 685–694.
18. Waldner H, Sobel RA, Howard E *et al.* Fas- and FasL-deficient mice are resistant to induction of autoimmune encephalomyelitis. *J Immunol* 1997; **159**: 3100–3103.
19. Wahlsten JL, Gitchell HL, Chan CC *et al.* Fas and Fas ligand expressed on cells of the immune system, not on the target tissue, control induction of experimental autoimmune uveitis. *J Immunol* 2000; **165**: 5480–5486.
20. Huang XR, Tipping PG, Shuo L *et al.* Th1 responsiveness to nephritogenic antigens determines susceptibility to crescentic glomerulonephritis in mice. *Kidney Int* 1997; **51**: 94–103.
21. Chakour R, Allenbach C, Desgranges F *et al.* A new function of the Fas-FasL pathway in macrophage activation. *J Leukoc Biol* 2009; **86**: 81–90.
22. O'Reilly LA, Tai L, Lee L *et al.* Membrane-bound Fas ligand only is essential for Fas-induced apoptosis. *Nature* 2009; **461**: 659–663.
23. Sabelko-Downes KA, Cross AH, Russell JH. Dual role for Fas ligand in the initiation of and recovery from experimental allergic encephalomyelitis. *J Exp Med* 1999; **189**: 1195–1205.
24. Linkermann A, Himmerkus N, Rolver L *et al.* Renal tubular Fas ligand mediates fratricide in cisplatin-induced acute kidney failure. *Kidney Int* 2011; **79**: 169–178.
25. Farley SM, Dotson AD, Purdy DE *et al.* Fas ligand elicits a caspase-independent proinflammatory response in human keratinocytes: implications for dermatitis. *J Invest Dermatol* 2006; **126**: 2438–2451.
26. Viedt C, Dechend R, Fei J *et al.* MCP-1 induces inflammatory activation of human tubular epithelial cells: involvement of the transcription factors, nuclear factor-kappaB and activating protein-1. *J Am Soc Nephrol* 2002; **13**: 1534–1547.
27. Tarzi RM, Davies KA, Robson MG *et al.* Nephrotoxic nephritis is mediated by Fcgamma receptors on circulating leukocytes and not intrinsic renal cells. *Kidney Int* 2002; **62**: 2087–2096.
28. Hochheiser K, Engel DR, Hammerich L *et al.* Kidney dendritic cells become pathogenic during crescentic glomerulonephritis with proteinuria. *J Am Soc Nephrol* 2011; **22**: 306–316.
29. Chavele KM, Martinez-Pomares L, Domin J *et al.* Mannose receptor interacts with Fc receptors and is critical for the development of crescentic glomerulonephritis in mice. *J Clin Invest* 2010; **120**: 1469–1478.

Molecular Immunology 50 (2012) 49–56

Contents lists available at SciVerse ScienceDirect

Molecular Immunology

journal homepage: www.elsevier.com/locate/molimm

# Increased incidence of anti-GBM disease in Fcgamma receptor 2b deficient mice, but not mice with conditional deletion of Fcgr2b on either B cells or myeloid cells alone

Phoebe E.H. Sharp[a,1], Javier Martin-Ramirez[b,1], Peter Boross[b,3], Sara M. Mangsbo[b,4], John Reynolds[a], Jill Moss[a], Charles D. Pusey[a], H. Terence Cook[a], Ruth M. Tarzi[a,*,2], J. Sjef Verbeek[b,2]

[a] Division of Immunity and Inflammation, Department of Medicine, Imperial College London, W12 0NN, UK
[b] Department of Human Genetics, Leiden University Medical Center, 2333 ZA Leiden, The Netherlands

ARTICLE INFO

*Article history:*
Received 1 December 2011
Accepted 7 December 2011
Available online 14 January 2012

*Keywords:*
Anti-glomerular basement membrane antibody disease
Goodpasture's disease
Mouse
Fcgamma receptor
Conditional gene deletion

ABSTRACT

Fcgamma receptor 2b (Fcgr2b) is the only inhibitory Fcgamma receptor in both humans and mice, and is implicated in both antibody production and effector responses to antibody complexes. Reduced function of Fcgr2b has previously been associated with anti-glomerular basement membrane antibody (anti-GBM) disease in mice. However, the mice used had 129 genetic elements flanking the deleted Fcgr2b gene, which are known to increase susceptibility to autoimmunity. In order to confirm a role for Fcgr2b in protection from anti-GBM disease, wild type (WT) mice, mice lacking Fcgr2b on a pure C57BL/6 background, or mice lacking Fcgr2b on a C57BL/6 background with 129 flanking sequences, were immunized with the recombinant NC1 domain of alpha 3 Type IV collagen. Twenty two weeks after immunization, there was a higher incidence of crescentic glomerulonephritis, macrophage infiltration and renal dysfunction in both groups of Fcgr2b−/− mice, indicating an important role of Fcgr2b in regulating the development of anti-GBM disease, on both genetic backgrounds. In order to determine the cellular origin of the Fcgr2b-associated effect, disease was induced in mice with deficiency of Fcgr2b on either B cells alone (CD19Cre), or a subset of myeloid cells (LysozymeMCre). Neither B cell nor myeloid specific knockout mice developed crescentic glomeruonephritis with higher incidence than WT mice indicating that Fcgr2b deficiency on either B cells or a subset of myeloid cells alone is not sufficient to increase susceptibility to anti-GBM disease, but that a combination of cell types, or deficiency of Fcgr2b in a different cell type, is also required.



## 1. Introduction

Fcgamma receptor 2b (Fcgr2b) is the only inhibitory Fc receptor for IgG found in humans and mice. It has a role in regulating antibody production (Takai et al., 1996) via its expression on B cells, and in effector responses via its expression on cells such as neutrophils, monocytes and macrophages. We have recently shown that in mice Fcgr2b acts as a modifier of autoimmune diseases such as lupus (Boross et al., 2011). Loss of Fcgr2b on a pure C57BL/6 background is not sufficient to induce the development of lupus. However, in a previously studied Fcgr2b knockout mouse model, generated by gene targeting in 129 derived embryonic stem cells and backcrossed into C57BL/6 background, (Bolland and Ravetch, 2000) epistatic interactions between the FcgRIIb allele and autoimmune susceptibility loci present in the 129 derived genomic flanking region result in high incidence of lupus (Boross et al., 2011). Wandstrat et al. (2004) have identified the highly polymorphic SLAM/CD2 cluster within the 129 genome Fcgr2b flanking region which has a regulatory function in both innate and adaptive immunity and is associated with B and T cell tolerance.

Goodpasture's syndrome or anti-glomerular basement membrane antibody disease (anti-GBM disease) is caused by loss of tolerance to the NC1 domain of the alpha 3 chain of Type IV collagen (α3(IV)NC1) leading to the deposition of antibodies in a

*Abbreviations:* Fcgr2b−/−, Fcgamma receptor 2b deficient mice; Fcgr2b−/−(129), Fcgamma receptor 2b deficient mice created using 129 embryonic stem cells and extensively back-crossed to C57BL/6; Fcgr2b−/−(B6), Fcgamma receptor 2b deficient mice created on a pure C57BL/6 background; Fcgr2b−/−/CD19cre, Fcgr2b−/− mice expressing CD19 Cre-recombinase; Fcgr2b−/−(LysMCre), Fcgr2b−/− mice expressing Lysozyme M Cre recombinase; WT, wild type.

* Corresponding author at: Department of Medicine, 9th Floor, Commonwealth Building, Du Cane Road, Imperial College London, W12 0NN, UK.
Tel.: +44 208 383 3152; fax: +44 208 383 2162.
*E-mail address:* r.tarzi@imperial.ac.uk (R.M. Tarzi).
[1] These authors contributed equally to the work.
[2] These authors contributed equally to the work.
[3] Current address: Department of Immunology, University Medical Center Utrecht, 3584 EA Utrecht, The Netherlands.
[4] Current address: Department of Immunology, Genetics and Pathology, Uppsala University, 75181 Uppsala, Sweden.

0161-5890/$ – see front matter © 2012 Elsevier Ltd. All rights reserved.
doi:10.1016/j.molimm.2011.12.007

linear fashion on the glomerular basement membrane and crescentic glomerulonephritis (Salama and Pusey, 2002; Wieslander et al., 1987). Models of anti-GBM disease have been established in the Wistar Kyoto rat by a single immunization with bovine or rat glomerular basement membrane extract (Naito and Sado, 1989; Reynolds et al., 2003) or the recombinant protein of rat α3(IV)NC (Ryan et al., 2001). Mouse models have been developed with immunization of recombinant human α3(IV)NC1 (Hopfer et al., 2003). In addition, Fcgr2b−/− mice created on a 129 background and backcrossed to C57BL/6 developed anti-GBM disease when immunized with bovine Type IV collagen whilst WT C57BL/6 mice did not (Nakamura et al., 2000). As an explanation for this, there was loss of tolerance to murine Type IV collagen in the Fcgr2b−/− mice to a greater degree than WT mice.

In order to definitively determine whether loss of Fcgr2b rather than flanking 129 elements was responsible for the increased incidence of anti-GBM disease, we have used mice lacking Fcgr2b created on a pure C57BL/6 background. The relative contribution of Fcgr2b on B cells compared with myeloid effector cells to protection from anti-GBM disease is not known. We have used mice with conditional deletion of Fcgr2b on B cells and a subset of myeloid cells to investigate this question.

## 2. Materials and methods

### 2.1. Mice

The Fcgr2b−/−(129) mice were a gift of Dr. Toshi Takai (Department of Experimental Immunology, Institute of Development, Ageing and Cancer, Tohoku University, Sendai, Japan) (Takai et al., 1996), and were backcrossed in Leiden University Medical Center onto C57BL/6J for eight generations. The Fcgr2b−/−(B6) mice were generated in Leiden University Medical Center as previously described (Boross et al., 2011). CD19Cre mice were kindly provided by Dr. Ari Waisman (Cologne) (Rickert et al., 1997) and were on a C57BL/6 background. The Lysozyme MCre mice were kindly provide by Dr. Bjorn Clausen (Amsterdam) (Clausen et al., 1999) and were on a C57BL6 background. Littermate WT controls were used. Mice were bred and housed in the animal facility, Leiden University Medical Center, Leiden, The Netherlands. Experiments were performed in accordance with the regulations of the ethics committee at Leiden University Medical Center. Production of antigen, and analysis of serology and histology was performed at Imperial College London, UK.

### 2.2. Cloning, expression and purification of recombinant α3(IV)NC1

The recombinant NC1 domain of alpha3 Type IV collagen (α3(IV)NC1) conjugated to a Flag tag, was expressed in human embryonic kidney cells, as previously described (Reynolds et al., 2005). The amino acid sequence was of rat α3(IV)NC1, which has a high homology to mouse α3(IV)NC1 (Ryan et al., 1998). The recombinant α3(IV)NC1 was purified from the supernatant by affinity chromatography using an anti-FLAG-M2 affinity column (Sigma–Aldrich). The protein was quantitated by spectrophotometry and was characterized by Western blotting as previously described (Reynolds et al., 2005).

### 2.3. Immunization protocol and induction of disease

Age-matched male mice were used for the experiments. The mice were housed in a pathogen free environment, with free access to food and water. The immunization protocol was modified from that of Hopfer et al. (2003). On Day 0, mice were immunized with 25 μg recombindant α3(IV)NC1 emulsified in complete Freund's adjuvant, subcutaneously. At Weeks 1–3, mice were immunized subcutaneously with 25 μg r-α3(IV)NC1 emulsified in incomplete Freund's adjuvant. Mice were bled at Day 28 and at the termination of the experiment for assessment of the immune response. One mouse in the Fcgr2b−/−(B6) group died at Week 17 and tissues were not obtained.

### 2.4. Histology and immunohistochemistry

Glomerular crescents were scored on samples fixed in Bouin's fixative and stained with PAS. Histological samples were assessed by an observer blinded to the experimental group. Crescents were defined as having two or more layers of cells in Bowman's space, and fifty glomeruli were scored per kidney and the percentage of crescents was calculated for each mouse.

For immunofluorescence, frozen kidney sections of 5 μm were fixed in acetone. Glomerular mouse and sheep IgG were visualized using FITC-conjugated goat anti-mouse IgG (Fc-specific) (Sigma) and FITC-conjugated monoclonal mouse anti-sheep IgG clone GT34 (Sigma). To quantitate immunofluorescence, sections were examined at ×40 magnification using an Olympus BX4 fluorescence microscope (Olympus Optical, London, UK) and a Photonic Science Colour Coolview camera (Photonic Science, Robertsbridge, UK). Samples from each experiment were stained on the same occasion and measured together. The total pixel intensity for each glomerulus was measured and averaged for 20 glomeruli per section.

For cell markers, kidneys were fixed in periodate lysine paraformaldehyde as previously described (Tarzi et al., 2002). Sections were stained for macrophages with FA11 (monoclonal rat anti-mouse CD68, Serotec, Oxford, UK) or CD4 cells (GK1.5, BDPharmingen), and developed using the Polink-2 plus HRP rat detection kit (Newmarket Scientific, UK).

### 2.5. Renal function and proteinuria

Serum urea and urinary creatinine were measured in the Department of Clinical Chemistry, Imperial College Healthcare NHS Trust. Serum albumin was measured using the AssayMax mouse albumin ELISA kit (AssayPro, UK). Albuminuria was assessed by radial immunodiffusion against a rabbit anti-mouse albumin (Biogenesis, Poole, UK), as previously described (Tarzi et al., 2002), and proteinuria was semi-quantitatively measured using Siemens Multistix SG.

### 2.6. Assessment of immune response to α3(IV)NC1 and murine Type IV collagen

In order to determine the immune response to α3(IV)NC1, 96 well plates were coated with 5 mcg/ml $\alpha_3$(IV)NC1 in carbonate buffer. Plates were blocked with 3% BSA for 1 h at 37 °C, washed and incubated with diluted serum. Secondary antibody used was goat anti-mouse IgG conjugated to alkaline phosphatase (1:1000), and samples were developed using p-nitrophenyl phosphate buffer and read on an ELISA plate reader at 405 nm.

Antibodies to mouse Type IV collagen were detected by the use of the BIOCOAT® cellware mouse C-IV 96-well plate assay, as previously described (Nakamura et al., 2000) (Becton Dickinson Labware). The diluted serum (1:200–1:400) was added at 50 μl/well and allowed to react overnight at 4 °C. The wells were washed three times with PBS containing 0.05% Tween 20, incubated with 50 μl of a 1:200 dilution of goat anti–mouse IgG conjugated to alkaline phosphatase (Sigma Chemical Co.) at 4 °C for 2 h, washed three times with PBS containing 0.05% Tween 20, developed at room temperature for 30 min with p-nitrophenyl phosphate buffer, and read on an ELISA plate reader at 405 nm.

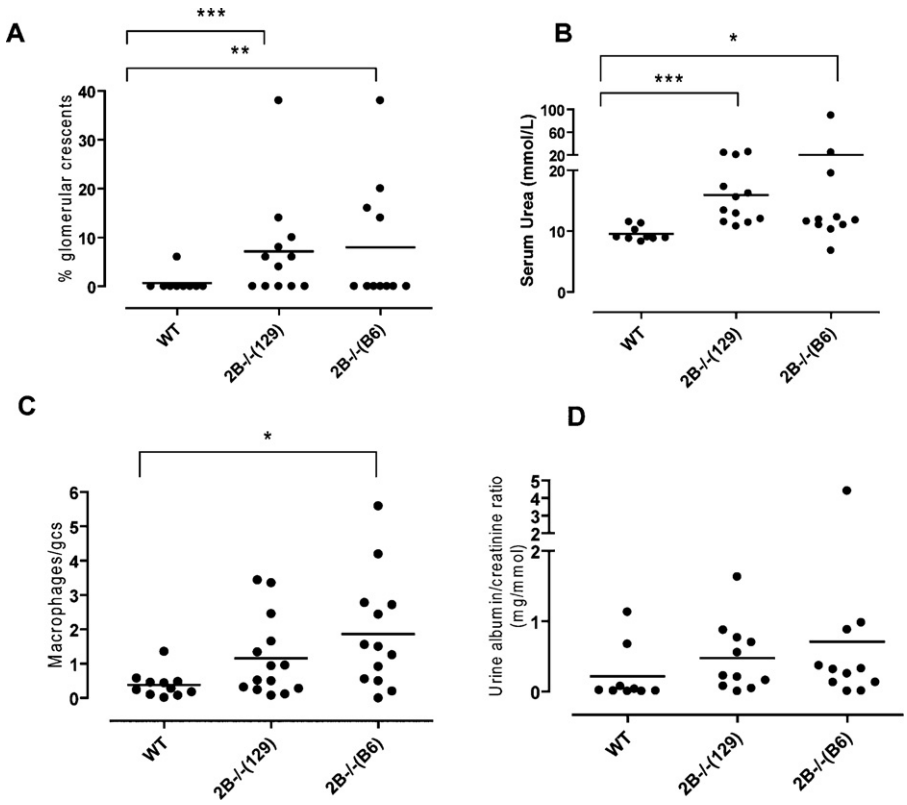


**Fig. 1.** Histological and renal parameters 22 weeks after first immunization with recombinant α3(IV)NC1. WT = wild type C57BL/6, 2B−/−(129) = Fcgr2b−/− mice generated using 129 embryonic stem cells and backcrossed to C57BL/6 for eight generations; 2B−/−(B6) = Fcgr2b−/− mice generated on a pure C57BL/6 background. (A) Percentage glomerular crescents, (B) serum urea mmol/l, (C) glomerular macrophages/glomerular cross section and (D) urinary albumin/creatinine ratio (mg/mmol). (A) Chi-squared test used to compared incidence of crescentic GN and (B–D) one way ANOVA.

For electron microscopy, pieces of kidney were cut into 1 $mm^3$ cubes, and fixed for 4 h in 3% glutaradehyde in 0.1 M cacodylate buffer. The fixed kidney pieces were washed in cacodylate buffer, dehydrated through graded alcohols and embedded in Spurr's resin. Ultra-thin sections were stained with uranyl acetate and Reynold's lead citrate. Sections were imaged using a Hitachi H-7650 transmission electron microscope.

### 2.7. Flow cytometry

Heparinised whole blood was obtained and stained for CD11b, CD19, Gr-1 (BD Pharmingen) and Fcgr2b (clone Ly17.2) expression. Spleen was digested with Liberase TL (Roche) in order to release resident macrophages and dendritic cells from connective tissue. Single cell suspensions were prepared and cells were stained for CD11b, F4/80, CD11c, CD19 and Fcgr2b expression. Blood and spleen were obtained from Fcgr2b−/− mice, Fcgr2b−/−(CD19Cre), Fcgr2b−/−(LysMCre) and WT mice. In blood, B cells were gated as lymphocytes in FSC/SSC and further as CD19+ CD11b− cells. Blood monocytes were gated as $SSC^{low}$, CD11b+ and granulocytes as $SSC^{high}$ Gr1+ cells. Resident macrophages were gated as CD11b+ F4/80+ CD11c− cells. Samples were acquired using a FACSCalibur (BD Biosciences) and data analysis was performed with FlowJo software (Tree Star).

### 2.8. Statistical analysis

Non-parametric statistics were employed, except the flow cytometry analysis, where unpaired *t*-tests were performed. Groups of two were compared by Mann–Whitney *U* test, and groups of three or more were compared by one-way ANOVA. In comparing the incidence of crescentic glomerulonephritis, a chi-squared test was used. Results were significant if $p < 0.05$.

## 3. Results

### 3.1. Fcgr2b−/− mice had a higher incidence of crescentic glomerulonephritis after immunization with α3(IV)NC1 than WT mice

Mice were immunized on four occasions at weekly intervals with recombinant α3(IV)NC1. The disease patterns in Fcgr2b−/− mice on a full C57BL/6 background (FcgRIIb−/− (B6) were compared with Fcgr2b−/− mice generated with 129 embryonic stem cells and extensively backcrossed to C57BL/6 (Fcgr2b−/−(129)), and WT C57BL/6 mice. Mice were sacrificed 22 weeks after initial immunization (Figs. 1 and 2). At the termination of the experiment, 1/9 (11%) WT mice developed glomerular crescents, compared to 7/12 (58%) Fcgr2b−/−(129) mice and 4/11 (36%) Fcgr2b−/−(B6) mice (chi-squared test $p < 0.001$ for Fcgr2b−/−(129) vs WT and $p < 0.01$ for Fcgr2b−/−(B6) vs WT (Fig. 1a). One additional Fcgr2b−/−(B6) mouse died at Week 17, and no tissues were obtained. This mouse was excluded from the analysis. The serum urea was significantly higher in both Fcgr2b−/− groups than WT mice at the termination of the experiment ($p < 0.05$, one way ANOVA) (Fig. 1B). There were significantly more glomerular macrophages in the Fcgr2b−/− mice than WT (Fig. 1C). However, proteinuria was not a significant feature of the disease and there was no overall difference in urinary albumin:creatinine ratio between the groups (Fig. 1D). The experiment shown is representative of two experiments performed, demonstrating an increased incidence of glomerulonephritis in both groups of Fcgr2b−/− mice compared with WT mice.

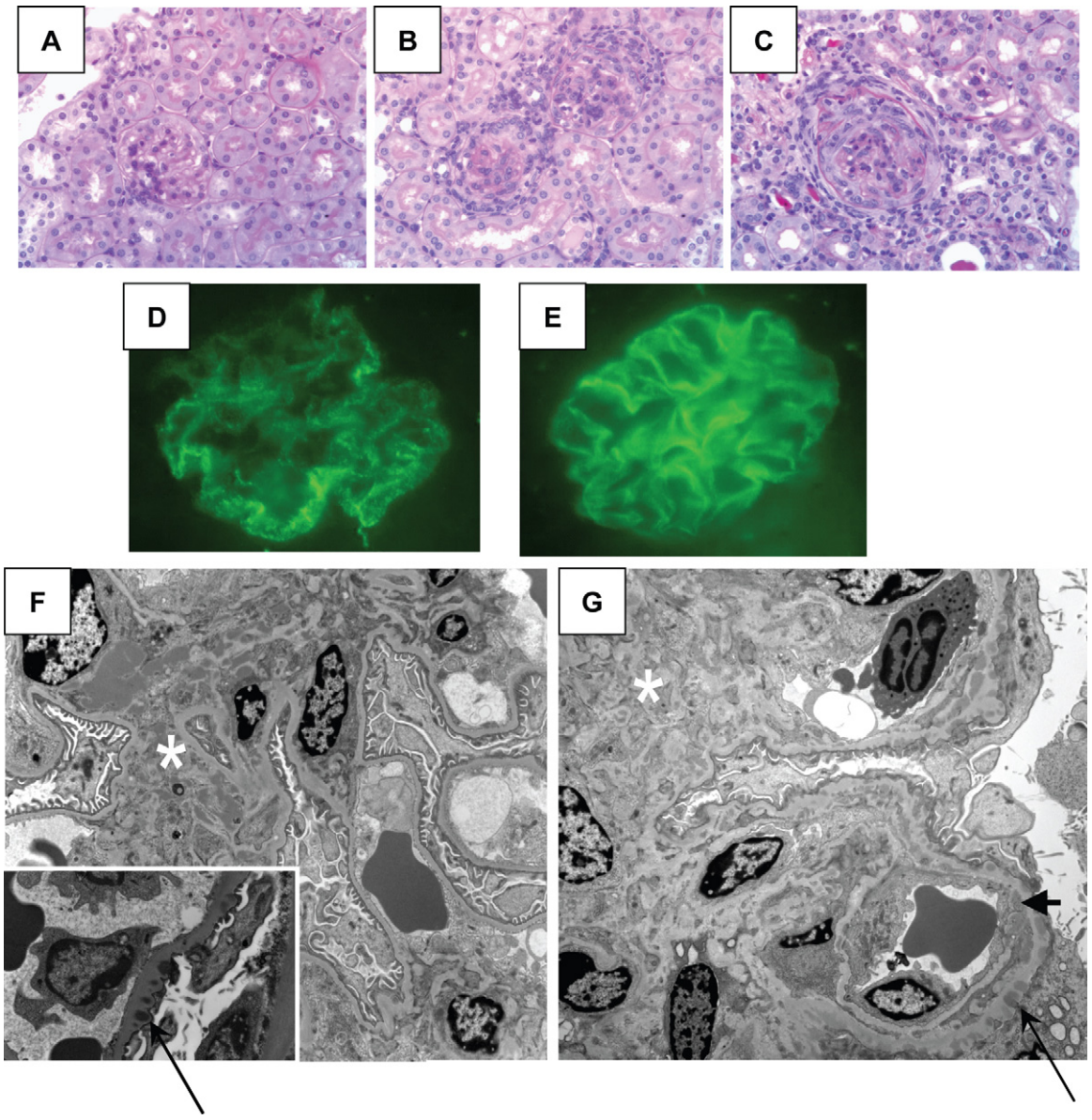


**Fig. 2.** (A–C) PAS-stained kidney sections, 22 weeks after first immunization with α3(IV)NC1. (A) WT C57BL/6 kidney showing preserved glomerular architecture; (B) Fcgr2b−/−(129) kidney showing glomerular crescent; (C) Fcgr2b−/−(B6) kidney showing glomerular crescent. (D) immunofluorescence of glomerulus for IgG showing granular immune complex deposition, (E) immunofluorescence for glomerular IgG showing predominantly linear IgG deposition, (F) electron micrograph of WT kidney; (G) electron micrograph of Fcgr2b−/−(B6) kidney. There was increased mesangial matrix, more marked in Fcgr2b−/− (white stars). (F) WT shows scanty subepithelial deposits (inset arrow). (G) Fcgr2b−/−(B6) shows mesangial deposits (star) as well as extensive subendothelial deposits (arrow head) and subepithelial deposits (long arrow).

### 3.2. Analysis of immune response

ELISA for circulating IgG against the α3(IV)NC1 protein immunogen, showed a tendency to higher levels of antigen specific IgG in both groups of Fcgr2b−/− mice compared to WT, although the range was large, and this did not reach statistical significance (Fig. 3A). Circulating IgG against mouse Type IV collagen (whole molecule) was also assessed (Fig. 3B). This showed a similar tendency to higher antibody titres in the Fcgr2b−/− mice as was seen to the recombinant antigen, with significantly higher levels in the Fcgr2b−/−(129) mice than WT mice. These results are not unexpected, as B cell Fcgr2b is involved in the regulation of antibody production.

The fluorescence patterns for deposited glomerular IgG ranged from linear to mixed linear/granular and granular (Fig. 2D and E). There was no overall difference in the fluorescence intensity between WT, Fcgr2b−/−(129) and Fcgr2b−/−(B6) (not shown), although there was a greater tendency for linear rather than mesangial staining patterns in the Fcgr2b−/− mice. Electron microscopy was performed on 3 WT mice and 2 Fcgr2b−/−(B6) mice. In the WT mice, deposits were more scanty and predominantly localized to the mesangium, whereas in the Fcgr2b−/−(B6) mice, there were deposits in subendothelial, subepithelial and mesangial areas, and increased mesangial matrix (Fig. 2F and G).

### 3.3. Unlike Fcgr2b−/− mice, conditional deletion of Fcgr2b on a subset of myeloid cells (Lysozyme MCre) or B cells (CD19Cre) alone did not significantly increase susceptibility to crescentic glomerulonephritis

Mice with conditional deletion of Fcgr2b on monocytes/macrophages and B cells were created by crossing floxed Fcgr2b−/−(B6) mice with heterozygous expression of Cre recombinase under the control of the LysozymeM promoter

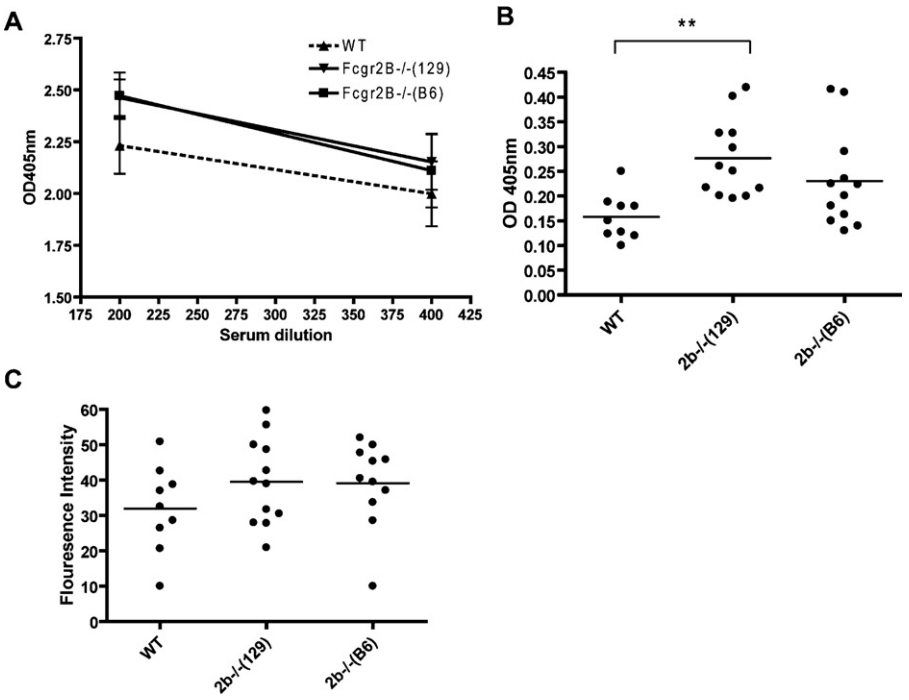


**Fig. 3.** (A) serum IgG against α3(IV)NC1, determined on serum taken at Day 28 after immunization. (B) Serum IgG against mouse Type IV collagen whole molecule taken at Day 28 after immunization (dilution 1:400). (C) Quantitative immunofluorescence for deposited glomerular IgG, 22 weeks after first immunization with α3(IV)NC1.

(monocyte/macrophages) or the CD19 promoter (B cells). The resultant mice were compared with littermate floxed controls, not expressing Cre, and Fcgr2b−/−(B6) mice. Expression of Fcgr2b on various cell types in the conditional knockout mice was assessed by flow cytometry (Fig. 4). There was excellent deletion of Fcgr2b from B cells in the Fcgr2b−/−/CD19Cre mice (Fig. 4A), with no off-target effects (Fig. 4B–D). In Fcgr2b−/−/LysMCre mice there was a 50% reduction in expression of Fcgr2b on circulating monocytes (Fig. 4B), and there was a small reduction of expression on splenic macrophages ($p < 0.05$, Fig. 4D). The expression levels of Fcgr2b on neutrophils were low (Fig. 4C) and not significantly different between WT and Fcgr2b−/−/LysMCre mice. Of note, there was no reduction in Fcgr2b expression on CD11c$^{high}$, CD11b+/− splenic dendritic cells in the Fcgr2b−/−(LysMCre) mice (not shown). The analyses shown in Fig. 4 were taken on healthy mice. As disease-induced mice may display a different phenotype to healthy mice, we also characterized expression of Fcgr2b on granulocytes and monocytes in Fcgr2b−/−/LysMCre mice at 22 weeks after immunization with α3(IV)NC1. The expression levels were similar to untreated Fcgr2b−/−/LysMCre mice (Supplementary Fig. 1).

Mice were sacrificed 22 weeks after induction of disease. 1/12 (8%) Fcgr2b−/−LysMCre mice developed crescentic glomerulonephritis, compared with 1/9 (11%) WT mice, $p$ = NS, chi-squared test. For the CD19-Cre mice, the incidence of crescentic glomerulonephritis was 2/9 (22%) mice ($p$ = NS compared to WT, chi-squared test), Fig. 5A. One Fcgr2b−/−(B6) mouse died at 17 weeks and was excluded from the analysis. Of the remainder, 4/11 (36%) developed crescentic glomerulonephritis ($p < 0.01$ when compared with WT, chi-squared test) (Fig. 5A). In addition to the glomerular crescents, there were significantly more glomerular macrophages in the Fcgr2b−/−(B6) mice than the WT littermate controls or the Fcgr2b−/−CD19Cre mice (Fig. 5B), $p < 0.05$). The serum urea was higher in the Fcgr2b−/−(B6) mice than the WT mice, but there was no significant difference in renal function between WT mice and either of the conditional knockout groups (Fig. 5C). Proteinuria was not a prominent feature in this model, and there was no overall difference between the groups.

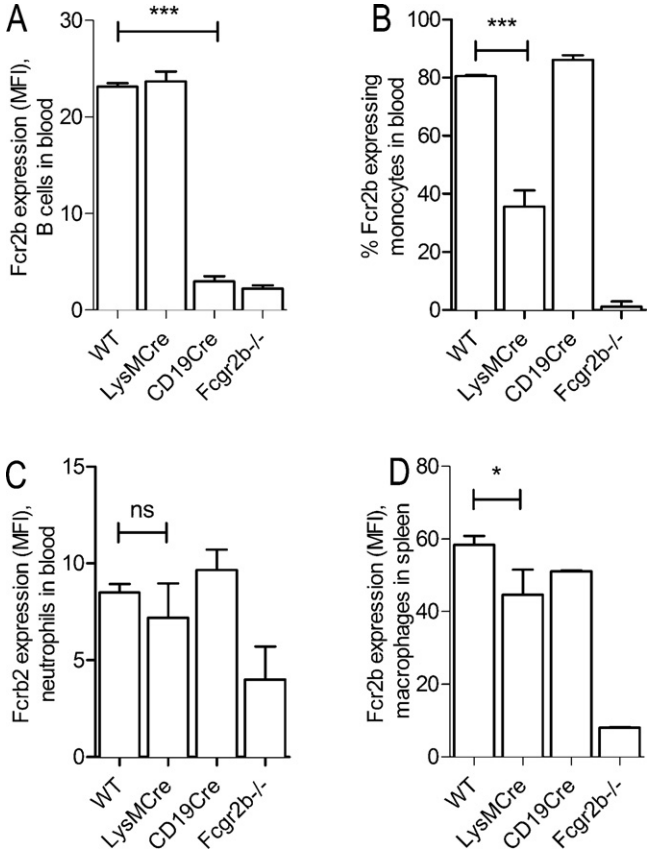


**Fig. 4.** Flow cytometry of blood and spleen cells for Fcg2b expression in the conditional knockout mice. (A) Fcgr2b expression on B cells in blood showing good deletion in Fcgr2b−/−/CD19Cre mice ($p < 0.001$ compared to WT), (B) % circulating monocytes (CD11b+, Gr1+) expressing Fcgr2b, (C) Fcgr2b expression on neutrophils in blood (CD11b−, Gr1+), and (D) Fcgr2b expression on splenic macrophages (CD11b+/CD11c−). LysMCre = Fcgr2b−/−/LysozymeMCre mice; CD19Cre = Fcgr2b−/−/CD19Cre mice. Bars represent standard deviation, $n$ = 3–4/group, representative of 3 replicates.

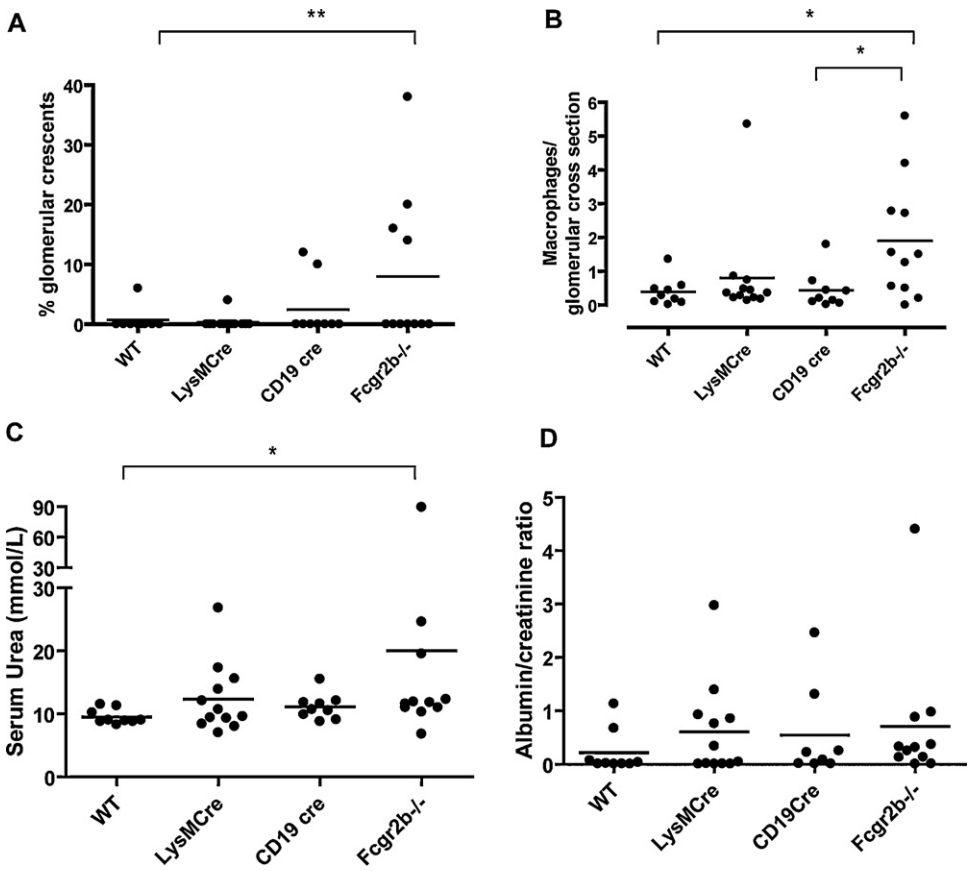


**Fig. 5.** Histological and functional parameters 22 weeks after immunization with α3(IV)NC1. (A) Percentage glomerular crescents; (B) macrophages/glomerular cross section; (C) serum urea (mmol/l); (D) urinary albumin/creatinine ratio (mg/mmol). One of the Fcgr2b null mice died before the end of the experiment and was excluded from the analysis. WT = wild type littermate control mouse (C57BL/6), LysMCre = Fcgr2b−/−/LysMCre mouse, CD19Cre = Fcgr2b−/−/CD19Cre mouse, and Fcgr2b−/− = Fcgr2b−/− (B6).

The mouse anti-α3(IV)NC1 (Fig. 6A) and mouse anti-mouse Type IV collagen IgG responses (Fig. 6B) were determined. As expected, a proportion of the Fcgr2b−/− mice and the Fcgr2b−/−(CD19Cre) mice had higher titres of specific IgG than WT mice, but the overall differences were not statistically significant, due to large differences between individual mice.

## 4. Discussion

These results demonstrate that after immunization with recombinant α3(IV)NC1 protein there is a significantly higher incidence of glomerulonephritis in Fcgr2b−/− mice than WT mice, both in terms of glomerular crescents, macrophage infiltration and renal dysfunction highlighting the importance of Fcgr2b in the pathogenesis of this disease. Previous work has demonstrated that Fcgr2b−/− mice with 129 Chromosome 1 flanking segments have increased susceptibility to anti-GBM disease after immunization with bovine Type IV collagen (Nakamura et al., 2000). We have confirmed these findings, using a different immunogen, and also in mice on a pure C57BL/6 background, demonstrating that it is not solely an effect of the 129 genes on Chromosome 1 related to the creation of the knockout mouse strain using 129 embryonic stem cells. In humans, a polymorphism of Fcgr2b (I232T), associated with low function of the receptor, was demonstrated to be a risk factor for the development of anti-GBM disease in a Chinese population (Zhou et al., 2010b) and increased copy number of the activatory Fcgamma receptor 3A was also associated with anti-GBM disease. Taken together, Fcgr2b is strongly implicated in protection from anti-GBM disease.

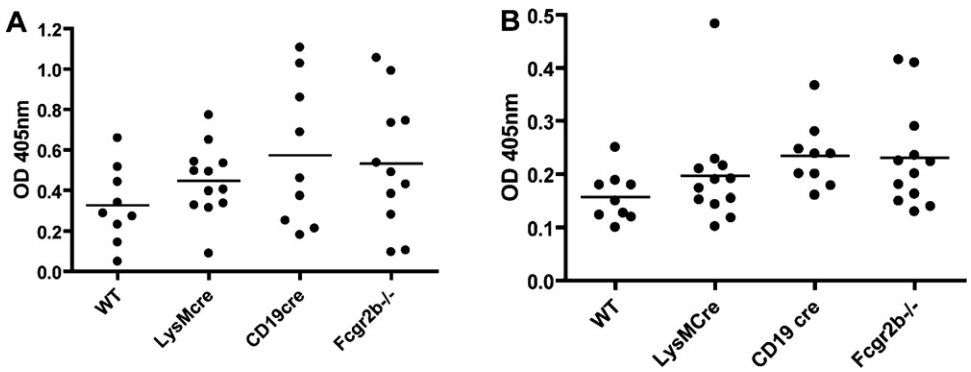


**Fig. 6.** Serum IgG levels in mice, 28 days after immunization with α3(IV)NC1 protein (A) serum IgG mouse anti-α3(IV)NC1 protein (1:400 dilution) and (B) serum IgG anti-collagen Type IV IgG (1:400 dilution).

Secondly, we have used mice with conditional deletion of Fcgr2b on B cells or a subset of myeloid cells to investigate the cellular basis for these effects. Despite a very effective deletion of Fcgr2b from B cells, the Fcgr2b−/−/CD19Cre mice did not have an increased incidence of anti-GBM disease over WT mice, indicating that deficiency on other cell types, or more than one cell type is required.

We have used a new model of anti-GBM disease in mice, by immunizing with recombinant α3(IV)NC1. This model was modified from that of Hopfer et al. (2003), where recombinant human α3(IV)NC1 was used. The use of a recombinant protein antigen as an immunogen has the advantage of reproducibility when compared to bovine collagen Type IV, or other crude extracts. As the recombinant protein used is almost identical to mouse α3(IV)NC1, it also has the advantage that it is a true auto-immune model, rather than being induced using a foreign antigen. However, in contrast to the model used by Nakamura et al. (2000), we did not see pulmonary haemorrhage. This may relate to the differences in the immunogen or the health status of the mice.

Both Fcgrb−/− mice with 129 genetic elements flanking Fcgr2b and Fcgr2b−/− mice on a pure C57BL/6 background had an increased incidence of glomerulonephritis after immunization with α3(IV)NC1. There was no significant difference in the incidence of disease between the groups, suggesting that the deficiency of Fcgr2b itself is the major factor. However, there was a trend to an increase in the incidence of disease in the Fcgr2b−/−(129) mice. We also saw higher antibody titres to collagen Type IV in these mice, although not to the α3(IV)NC1 peptide. Genes of 129 origin in that location are known to be autoimmune susceptibility factors associated with B and T cell tolerance, which may explain this trend (Wandstrat et al., 2004).

Previous work in Dr. Verbeek's laboratory has shown that female Fcgr2b−/− mice with 129 elements flanking the Fcgr2b deleted gene did develop autoantibodies and a degree of spontaneous SLE at one year of age, however this was not see in Fcgr2b−/−(B6) mice (Bolland and Ravetch, 2000; Boross et al., 2011). We used male mice in these experiments, which are less susceptible to SLE-like syndromes. In addition, we saw macrophage influx, glomerulonephritis and renal impairment in both Fcgr2b−/−(129) and Fcgr2b−/−(B6) mice, whilst our previous work has shown a higher incidence of SLE only in Fcgr2b−/−(129) mice (Boross et al., 2011). In addition, we did not see splenomegaly in the Fcgr2b−/− mice (data not shown), and therefore we do not believe that spontaneous SLE is a major contributor to the glomerulonephritis seen in this model.

Loss of Fcgr2b on B cells alone or on a subset of monocytes/macrophages was not sufficient to increase the incidence of crescentic glomerulonephritis over WT littermate controls. This was despite very effective deletion of Fcgr2b from B cells in the Fcgr2b−/−/CD19cre mice. Fcgr2b is involved in regulating the production of antibody by cells of the B cell lineage, and may have a role in B cell tolerance (Boross et al., 2011). We did see a tendency to increased antibody titres in these mice and mice with full deletion of Fcgr2b. However, we only saw increased incidence of glomerulonephritis in mice with a full deletion of Fcgr2b on all cell types. This result implies that loss of Fcgr2b on B cells alone is not sufficient to increase susceptibility to anti-GBM disease but that dysfunction of Fcgr2b on other cell types is also required.

Mice with conditional deletion of Fcgr2b on monocytes/macrophages were induced by using Cre under control of the LysozymeM promoter. The deletion was not complete, especially on resident macrophages. However, there was a significant reduction in the expression of Fcgr2b on circulating monocytes and a smaller reduction on splenic macrophages but no visible reduction on splenic dendritic cells. Nevertheless, modest effects on the levels of expression of Fcgr2b on myeloid cells have previously been shown to have clinical effects in models of infection, and therefore these reductions are likely to be clinically relevant (Brownlie et al., 2008). We did not see an increased incidence of glomerulonephritis amongst the Fcgr2b−/−/LysMcre mice compared to WT mice. This may be either because the deletion was not effective enough, or a combination of defects is required, in multiple cell types, leading for example to enhanced loss of tolerance and increased effector responses. Another factor to consider is that Fcgr2b expression has been demonstrated on cultured mesangial cells (Radeke et al., 2002), and expression of Fcgr2b on intrinsic renal cells may also play a role in anti-GBM disease.

## 5. Conclusions

In conclusion, Fcgr2b−/− mice were more susceptible to crescentic glomerulonephritis induced by α3(IV)NC1 than WT mice. Deletion of Fcgr2b on B cells was insufficient to demonstrate the phenotype, indicating that enhanced antibody production alone is not sufficient to induce disease, but that reduced function of Fcgr2b on effector cells is also required, either from myeloid cells, or intrinsic renal cells. Given that Fc receptors have also been shown to be important in human anti-GBM disease (Zhou et al., 2010a,b), it is likely that these results also have relevance for the human condition.

## Authors' contributions

RT, JSV and TC designed the study. PS, JM-R performed the experiments and collected the data, SM performed and analysed the flow cytometry, JR generated and characterized the recombinant protein, JM performed and analysed the electron microscopy, PB generated the Fgr2bfloxed mice, RT wrote the paper, and CP, JSV and TC assisted in writing the manuscript.

## Acknowledgements

We would like to acknowledge the help of Dr. John Meek, Clinical Chemistry Department, Hammersmith Hospital, for measuring urinary creatinine and serum urea levels. Dr. Tarzi was funded by an Arthritis Research UK Clinician Scientist Fellowship and J. Martin Ramirez by the Dutch Arthritis Association.

## Appendix A. Supplementary data

Supplementary data associated with this article can be found, in the online version, at doi:10.1016/j.molimm.2011.12.007.

## References

Bolland, S., Ravetch, J.V., 2000. Spontaneous autoimmune disease in Fc(gamma)RIIB deficient mice results from strain-specific epistasis. Immunity 13, 277–285.

Boross, P., Arandhara, V.L., Martin-Ramirez, J., Santiago-Raber, M.L., Carlucci, F., Flierman, R., van der Kaa, J., Breukel, C., Claassens, J.W., Camps, M., Lubberts, E., Salvatori, D., Rastaldi, M.P., Ossendorp, F., Daha, M.R., Cook, H.T., Izui, S., Botto, M., Verbeek, J.S., 2011. The inhibiting Fc receptor for IgG, Fcgamma RIIB, is a modifier of autoimmune susceptibility. Journal of Immunology 187, 1304–1313.

Brownlie, R.J., Lawlor, K.E., Niederer, H.A., Cutler, A.J., Xiang, Z., Clatworthy, M.R., Floto, R.A., Greaves, D.R., Lyons, P.A., Smith, K.G., 2008. Distinct cell-specific control of autoimmunity and infection by FcgammaRIIb. The Journal of Experimental Medicine 205, 883–895.

Clausen, B.E., Burkhardt, C., Reith, W., Renkawitz, R., Forster, I., 1999. Conditional gene targeting in macrophages and granulocytes using LysMcre mice. Transgenic Research 8, 265–277.

Hopfer, H., Maron, R., Butzmann, U., Helmchen, U., Weiner, H.L., Kalluri, R., 2003. The importance of cell-mediated immunity in the course and severity of autoimmune anti-glomerular basement membrane disease in mice. FASEB Journal 17, 860–868.

Naito, I., Sado, Y., 1989. Early changes of rat experimental autoimmune glomerulonephritis induced with the nephritogenic antigen from bovine renal basement membranes. Journal of Clinical & Laboratory Immunology 28, 187–193.

Nakamura, A., Yuasa, T., Ujike, A., Ono, M., Nukiwa, T., Ravetch, J.V., Takai, T., 2000. Fcgamma receptor IIB-deficient mice develop Goodpasture's syndrome upon immunization with type IV collagen: a novel murine model for autoimmune glomerular basement membrane disease. The Journal of Experimental Medicine 191, 899–906.

Radeke, H.H., Janssen-Graalfs, I., Sowa, E.N., Chouchakova, N., Skokowa, J., Loscher, F., Schmidt, R.E., Heeringa, P., Gessner, J.E., 2002. Opposite regulation of type II and III receptors for immunoglobulin G in mouse glomerular mesangial cells and in the induction of anti-glomerular basement membrane (GBM) nephritis. The Journal of Biological Chemistry 277, 27535–27544.

Reynolds, J., Moss, J., Duda, M.A., Smith, J., Karkar, A.M., Macherla, V., Shore, I., Evans, D.J., Woodrow, D.F., Pusey, C.D., 2003. The evolution of crescentic nephritis and alveolar haemorrhage following induction of autoimmunity to glomerular basement membrane in an experimental model of Goodpasture's disease. The Journal of Pathology 200, 118–129.

Reynolds, J., Prodromidi, E.I., Juggapah, J.K., Abbott, D.S., Holthaus, K.A., Kalluri, R., Pusey, C.D., 2005. Nasal administration of recombinant rat alpha3(IV)NC1 prevents the development of experimental autoimmune glomerulonephritis in the WKY rat. Journal of the American Society of Nephrology: JASN 16, 1350–1359.

Rickert, R.C., Roes, J., Rajewsky, K., 1997. B lymphocyte-specific, Cre-mediated mutagenesis in mice. Nucleic Acids Research 25, 1317–1318.

Ryan, J.J., Katbamna, I., Mason, P.J., Pusey, C.D., Turner, A.N., 1998. Sequence analysis of the 'Goodpasture antigen' of mammals. Nephrology, Dialysis, Transplantation: Official Publication of the European Dialysis and Transplant Association—European Renal Association 13, 602–607.

Ryan, J.J., Reynolds, J., Norgan, V.A., Pusey, C.D., 2001. Expression and characterization of recombinant rat alpha 3(IV)NC1 and its use in induction of experimental autoimmune glomerulonephritis. Nephrology, Dialysis, Transplantation: Official Publication of the European Dialysis and Transplant Association—European Renal Association 16, 253–261.

Salama, A.D., Pusey, C.D., 2002. Immunology of anti-glomerular basement membrane disease. Current Opinion in Nephrology and Hypertension 11, 279–286.

Takai, T., Ono, M., Hikida, M., Ohmori, H., Ravetch, J.V., 1996. Augmented humoral and anaphylactic responses in Fc gamma RII-deficient mice. Nature 379, 346–349.

Tarzi, R.M., Davies, K.A., Robson, M.G., Fossati-Jimack, L., Saito, T., Walport, M.J., Cook, H.T., 2002. Nephrotoxic nephritis is mediated by Fcgamma receptors on circulating leukocytes and not intrinsic renal cells. Kidney International 62, 2087–2096.

Wandstrat, A.E., Nguyen, C., Limaye, N., Chan, A.Y., Subramanian, S., Tian, X.H., Yim, Y.S., Pertsemlidis, A., Garner Jr., H.R., Morel, L., Wakeland, E.K., 2004. Association of extensive polymorphisms in the SLAM/CD2 gene cluster with murine lupus. Immunity 21, 769–780.

Wieslander, J., Kataja, M., Hudson, B.G., 1987. Characterization of the human Goodpasture antigen. Clinical and Experimental Immunology 69, 332–340.

Zhou, X.J., Lv, J.C., Bu, D.F., Yu, L., Yang, Y.R., Zhao, J., Cui, Z., Yang, R., Zhao, M.H., Zhang, H., 2010a. Copy number variation of FCGR3A rather than FCGR3B and FCGR2B is associated with susceptibility to anti-GBM disease. International Immunology 22, 45–51.

Zhou, X.J., Lv, J.C., Yu, L., Cui, Z., Zhao, J., Yang, R., Han, J., Hou, P., Zhao, M.H., Zhang, H., 2010b. FCGR2B gene polymorphism rather than FCGR2A, FCGR3A and FCGR3B is associated with anti-GBM disease in Chinese. Nephrology, Dialysis, Transplantation: Official Publication of the European Dialysis and Transplant Association—European Renal Association 25, 97–101.

# FcγRIIb on Myeloid Cells and Intrinsic Renal Cells Rather than B Cells Protects from Nephrotoxic Nephritis

**Phoebe E. H. Sharp,*[,1] Javier Martin-Ramirez,[†,2] Sara M. Mangsbo,[†,3] Peter Boross,[†,4] Charles D. Pusey,* Ivo P. Touw,[‡] H. Terence Cook,* J. Sjef Verbeek,[†,5] and Ruth M. Tarzi*[,5]**

**FcγRIIb is the sole inhibitory FcR for IgG in humans and mice, where it is involved in the negative regulation of Ab production and cellular activation. FcγRIIb-deficient mice show exacerbated disease following the induction of nephrotoxic nephritis (NTN). In this study, we determined the cellular origin of the FcγRIIb-knockout phenotype by inducing NTN in mice with a deficiency of FcγRIIb on either B cells alone (FcγRIIB$^{fl/fl}$/CD19Cre$^{+}$) or myeloid cells (FcγRIIB$^{fl/fl}$/CEBPαCre$^{+}$). Deletion of FcγRIIb from B cells did not increase susceptibility to NTN, compared with wild-type (WT) mice, despite higher Ab titers in the FcγRIIB$^{fl/fl}$/CD19Cre$^{+}$ mice compared with the WT littermate controls. In contrast, mice lacking FcγRIIb on myeloid cells had exacerbated disease as measured by increased glomerular thrombosis, glomerular crescents, albuminuria, serum urea, and glomerular neutrophil infiltration when compared with WT littermate controls. The role for FcγRIIb expression on radioresistant intrinsic renal cells in the protection from NTN was then investigated using bone marrow chimeric mice. FcγRIIb$^{-/-}$ mice transplanted with FcγRIIb$^{-/-}$ bone marrow were more susceptible to NTN than WT mice transplanted with FcγRIIb$^{-/-}$ bone marrow, indicating that the presence of WT intrinsic renal cells protects from NTN. These results demonstrate that FcγRIIb on myeloid cells plays a major role in protection from NTN, and therefore, augmentation of FcγRIIb on these cells could be a therapeutic target in human Ab-mediated glomerulonephritis. Where there was a lack of FcγRIIb on circulating myeloid cells, expression of FcγRIIb on intrinsic renal cells provided an additional level of protection from Ab-mediated glomerulonephritis.** ***The Journal of Immunology*****, 2013, 190: 340–348.**

FcγRIIb is a low-affinity FcR for the constant part of IgG and the sole inhibitory FcγR in both humans and mice. It is the most broadly expressed, being found on most cells of myeloid lineage, and it is the only FcγR found on B cells. On B cells, cross-linking of FcγRIIb and the BCR activates a distinct pathway that inhibits cell proliferation, maturation, and the production of cytokines (1); however, cross-linking of FcγRIIb in the absence of the BCR initiates a bim-dependent apoptosis pathway (2). Reduced expression of FcγRIIb is associated with enhanced activation and proliferation of B cells and plasma cells (3), as well as increased Ab production to T-dependent Ags (3, 4) and increased macrophage activation by immune complexes (4–6).

Reduced functionality of FcγRIIb has been associated with systemic lupus erythematosus in humans (7), and several autoimmune strains of mice have a polymorphism in the promoter region of the FcγRIIb gene that is associated with reduced cell-surface expression on macrophages and activated B cells (5). When combined with other autoimmune susceptibility genes, mice deficient in FcγRIIb develop systemic lupus erythematosus, whereas on a pure C57BL/6 background, they do not develop severe autoimmunity, indicating that FcγRIIb is a modifier of autoimmune susceptibility determined by other genetic loci. However, C57BL/6 FcγRIIb$^{-/-}$ mice do show enhanced Ab responses and are highly susceptible to anti–glomerular basement membrane Ab disease and nephrotoxic nephritis (NTN) (8–10). This could be due to increased Ab production by FcγRIIb-deficient B cell lineages or, alternatively, due to increased myeloid cell activation. Mesangial cells have also been shown to express FcγRIIb (11, 12), adding another possible checkpoint in the prevention of severe Ab-mediated glomerulonephritis.

The model of NTN (accelerated NTN) used in this study is a well-characterized disease model that closely resembles human Ab-mediated glomerulonephritis. The animals are preimmunized against sheep IgG. Five days later, the mice are injected i.v. with polyclonal sheep anti-mouse glomerular basement membrane Ab, which is then planted on the mouse glomerular basement membrane. As the mice are presensitized to sheep IgG, this results in

*Division of Immunity and Inflammation, Department of Medicine, Imperial College London, London W12 0NN, United Kingdom; [†]Department of Human Genetics, Leiden University Medical Center, 2333 ZA Leiden, The Netherlands; and [‡]Department of Hematology, Erasmus Medical Center, 3015 GE Rotterdam, The Netherlands

[1]Current address: College of Medicine, Veterinary and Life Sciences, University of Glasgow, Glasgow, Scotland, U.K.

[2]Current address: Sanquin, Research Department, Plasma Proteins, Amsterdam, The Netherlands.

[3]Current address: Department of Immunology, Genetics and Pathology, Uppsala University, Uppsala, Sweden.

[4]Current address: Department of Immunology, University Medical Center Utrecht, Utrecht, The Netherlands.

[5]J.S.V. and R.M.T. contributed equally to this work.

Received for publication August 10, 2012. Accepted for publication September 27, 2012.

This work was supported by a Clinician Scientist Fellowship from Arthritis Research UK (to R.M.T.). J.M.-R. was supported by FP6 Marie Curie Research Training Network Immune Deficient Mice MRTN-CT-2004-005632 and a grant from the Dutch Arthritis Association (Nationaal Reumafonds). I.P.T. was supported by a TOP program grant from The Netherlands Organisation for Scientific Research, and S.M.M. was supported by Dutch Technology Foundation Project 10412.

Address correspondence and reprint requests to Dr. Ruth M. Tarzi, Renal Section, Division of Immunity and Inflammation, Department of Medicine, Imperial College London, Hammersmith Hospital, London W12 0NN, U.K. E-mail address: r.tarzi@imperial.ac.uk

Abbreviations used in this article: gcs, glomerular cross-section; IVIG, i.v. Ig; NTN, nephrotoxic nephritis; NTS, nephrotoxic serum; PAS, periodic acid-Schiff; WT, wild-type.



www.jimmunol.org/cgi/doi/10.4049/jimmunol.1202250

immediate generation and deposition of mouse anti-sheep Ig in the glomerulus, which progresses over several days and leads to cellular infiltration of neutrophils, followed by macrophages, proteinuria, glomerular injury, glomerular crescents, and, in severe cases, progressive uremia. Previous studies of murine NTN have highlighted roles for the involvement of many immune effectors in glomerulonephritis, including macrophages, FcγR, Th1 and Th17 cells, complement, and intrinsic renal cells.

In order to determine the role of FcγRIIb on specific cell types in NTN, we have crossed floxed FcγRIIb mice on a C57BL/6 background with mice expressing Cre recombinase either under control of the human CD19 promoter to delete FcγRIIb in only B cell lineages or under control of the CEBPα promoter to delete FcγRIIb in myeloid lineages. The cell-type–specific FcγRIIb-knockout offspring have been compared with littermate controls. Because a Cre-transgenic strain that expresses Cre under control of a mesangial cell–specific promoter was not available, we have created bone marrow chimeras to determine the role of FcγRIIb on radioresistant cells in the kidney.

## Materials and Methods

### *Mice*

The FcγRIIb$^{-/-}$ (C57BL/6) mice were generated in Leiden University Medical Center as previously described (4). CD19Cre mice were kindly provided by Ari Waisman (Cologne, Germany) (13). CEBPαCre mice were kindly provided by Dr. Ivo Touw (Rotterdam, The Netherlands) (14). All mice were on a C57BL/6 background. Littermate wild-type (WT) controls were used. Mice were bred and housed in the animal facility at Leiden University Medical Centre (Leiden, The Netherlands). Experiments were performed in accordance with the regulations of the ethics committee at Leiden University Medical Center. Analysis of serology and histology was performed at Imperial College London. For experiments involving bone marrow–transplanted mice, FcγRIIb$^{-/-}$ (C57BL/6) mice were bred at the Biological Services Unit, Hammersmith Hospital (London, U.K.). Control age- and sex-matched C57BL/6 WT mice were purchased from Charles River Laboratories. All mice were housed with free access to food and water and kept in a specific pathogen-free environment, according to institutional guidelines. Experiments were performed under the terms of a license issued by the UK Home Office. All mice used in this study were between 6 and 15 wk of age.

### *Phenotyping expression of FcγRIIb by flow cytometry*

Heparinized whole blood was obtained and stained for CD11b, CD19, Gr-1 (BD Pharmingen), and FcγRIIb (clone Ly17.2). Spleen was digested with liberase TL to release resident macrophages from connective tissue. Single-cell suspensions were prepared, and cells were stained for CD11b, F4/80, CD11c, CD19, and FcγRIIb. Blood and spleen were obtained from FcγRIIb$^{-/-}$ mice, FcγRIIb$^{fl/fl}$/CD19Cre$^{+}$, FcγRIIb$^{fl/fl}$/CEBPαCre$^{+}$, and WT C57BL/6 mice.

### *Induction of accelerated nephrotoxic nephritis*

Sheep anti-mouse nephrotoxic globulin was prepared as described previously (15). Mice were preimmunized i.p. with 0.2 mg sheep IgG in a 50:50 mix of saline and CFA (Sigma-Aldrich, Dorset, U.K.). Five days later, mice were injected i.v. with 0.2 ml nephrotoxic globulin via the tail vein. Mice were monitored clinically by using dipstick for detection of proteinuria and hematuria, and the experiments were terminated if the mice showed signs of ill health.

### *Histology and immunohistochemistry*

Glomerular crescents and thrombosis were scored on samples fixed in Bouin's solution and stained with periodic acid-Schiff (PAS) reagent. Histological samples were assessed by an observer blinded to the experimental group. Crescents were defined as two or more layers of cells in the Bowman's space. Glomerular thrombosis was assessed by scoring individual glomeruli for PAS-positive material: grade 0, no PAS-positive material; grade 1, 0–25% of the glomerular section PAS positive; grade 2, 25–50%; grade 3, 50–75%; and grade 4, 75–100%. Fifty glomeruli were scored for crescents and thrombosis for each kidney, and a mean was calculated.

Glomerular mouse and sheep IgG were visualized by direct immunofluorescence staining on 5-μm frozen kidney sections fixed in acetone for 10 min using FITC-conjugated goat anti-mouse IgG (Fc-specific) (Sigma-Aldrich) and FITC-conjugated monoclonal mouse anti-sheep IgG clone GT34 (Sigma-Aldrich). To quantitate immunofluorescence, sections were examined at ×40 original magnification using an Olympus BX4 fluorescence microscope (Olympus Optical, London, U.K.) and a Photonic Science Color Coolview camera (Photonic Science, Robertsbridge, U.K.). Samples from each experiment were stained on the same occasion and measured together. Images of the sections were captured using Image Pro (MediaCybernetics, Bethesda, MD), and the total pixel intensity for each glomerulus was measured and averaged for 20 glomeruli per section.

For cell markers, kidneys were fixed in periodate-lysine-paraformaldehyde. Sections of 5 μm were stained for macrophages with FA11 (monoclonal rat anti-mouse CD68; Serotec, Oxford, U.K.) and neutrophils with Gr-1 (monoclonal rat anti-mouse; Serotec) and developed using the Polink-2 plus HRP rat detection kit (Newmarket Scientific, Newmarket, U.K.). Macrophages and neutrophils in 50 glomeruli/sample were counted and averaged to obtain cells/glomerular cross-section (gcs).

### *Renal function and proteinuria*

Urinary creatinine was measured in the Department of Clinical Chemistry, Imperial College Healthcare NHS Trust. Serum albumin was measured using the AssayMax mouse albumin ELISA kit (AssayPro, St. Charles, MO). Serum urea was measured using the Urea/Ammonia ultraviolet-method kit (R-Biopharm, Darmstadt, Germany). Albuminuria was assessed by radial immunodiffusion against a rabbit anti-mouse albumin (Biogenesis, Poole, U.K.), as previously described (15).

### *Bone marrow chimeras*

Chimeric mice were made by irradiation with a dose of 8 Gy and reconstituted with $10 \times 10^6$ donor bone marrow cells. Nephritis experiments were conducted at 10 wk posttransplant. Confirmation of chimerism was obtained using PCR on DNA extracted from 0.1 ml blood obtained at the terminal bleed, as previously described (4).

### *Mesangial cell cultures*

Kidneys from WT and FcγRIIb$^{-/-}$ mice were homogenized with a syringe plunger and forced through a series of sterile sieves with successively smaller pore sizes of 150, 106, and 45 μm. Glomeruli retained on the 45-μm sieve were retrieved, washed in ice-cold PBS, and spun down at 1000 rpm for 5 min. Glomeruli were digested with 380 U/ml collagenase (Sigma-Aldrich) for 30 min at 37°C, spun down 1200 rpm for 5 min, and resuspended in RPMI 1640 (Invitrogen) supplemented with 20% FCS (Biosera), 100 U/ml penicillin, 100 g/ml streptomycin (Invitrogen), and 1% insulin/selenium/transferrin growth supplement (Sigma-Aldrich). Mesangial cells were characterized as anti-myosin positive and pancytokeratin negative, with characteristic stellate morphology.

### *Mesangial cell FcγRIIb expression*

Expression of FcγRIIb on mesangial cells was confirmed by direct immunofluorescence on cytospin preparations. Briefly, cytospin slides were prepared, air-dried, and cells fixed in acetone for 10 min and stained with FITC-conjugated anti-FcγRIIb Ab (clone Ly17.2). Immunofluorescence was visualized at ×40 original magnification using an Olympus BX4 fluorescence microscope (Olympus Optical) and a Photonic Science Color Coolview camera (Photonic Science, Robertsbridge, U.K.). Images of the sections were captured using Image Pro (MediaCybernetics, Bethesda, MD).

Quantitative real-time PCR was performed as previously described (16) using FcγRIIb-specific primers (12) and normalizing to GAPDH.

### *Statistics*

Results are quoted as median (interquartile range), unless otherwise stated. Lines on graphs represent median values. For comparing two groups, the Mann–Whitney *U* test was used, and for three or more groups, the Kruskal-Wallis test was used, with Dunn's multiple comparisons test ($p$ values given are from Dunn's test). GraphPad Prism (GraphPad Software, San Diego, CA) was used to analyze the data. Differences were considered significant when $p < 0.05$.

## Results

### *Phenotype of FcγRIIb conditional knockouts*

Mice with deletion of FcγRIIb on either myeloid cells or B cells were created by crossing FcγRIIb$^{fl/fl}$ (pure C57BL/6 background) mice with transgenic mice expressing Cre recombinase under the

control of the CEBPα promoter or the CD19 promoter. The resultant mice were compared with littermate FcγRIIb$^{fl/fl}$ controls and FcγRIIb$^{-/-}$ (C57BL/6) mice. Expression of FcγRIIb on various cell types was assessed by flow cytometry (Fig. 1). There was excellent deletion of FcγRIIb from B cells in the FcγRIIb$^{fl/fl}$/CD19Cre$^{+}$ mice with no reduction of expression of FcγRIIb on monocytes or granulocytes in blood or macrophages in the spleen (Fig. 1A). In FcγRIIb$^{fl/fl}$/CEBPαCre$^{+}$ mice, there was excellent deletion from circulating monocytes and granulocytes and partial deletion from splenic macrophages and dendritic cells, with no effect on B cell expression of FcγRIIb (Fig. 1B).

*Mice lacking FcγRIIb on B cells did not have enhanced susceptibility to NTN compared with WT mice*

NTN was induced in preimmunized FcγRIIb$^{-/-}$ mice, FcγRIIb$^{fl/fl}$/CD19Cre$^{+}$ mice, and WT littermate controls. Nephrotoxic serum (NTS) was administered at a 1:20 dilution. Mice were monitored clinically and killed at day 5 after induction of NTN, because the mice with the full deletion of FcγRIIb started to show serious disease symptoms including severe proteinuria and hematuria. At this time point, there was no increase in injury in the FcγRIIb$^{fl/fl}$/CD19Cre$^{+}$ mice compared with the WT mice (Fig. 2A–D). The FcγRIIb$^{fl/fl}$/CD19Cre$^{+}$ mice had more deposited glomerular mouse IgG than the WT mice (Fig. 2F), whereas there was a large range in the circulating anti-sheep IgG titers and no overall difference between WT and FcγRIIb$^{fl/fl}$/CD19Cre$^{+}$ mice.

This was in marked contrast with the FcγRIIb$^{-/-}$ mice that showed a strongly increased susceptibility to disease compared with WT littermate controls (Fig. 2). The FcγRIIb$^{-/-}$ mice had significantly more glomerular thrombosis ($p < 0.001$ compared with WT mice and $p < 0.01$ compared with FcγRIIb$^{fl/fl}$/CD19Cre$^{+}$ mice), increased glomerular macrophage infiltration (median: FcγRIIb$^{-/-}$ 8.3 CD68-positive cells/gcs [interquartile range 7.3–11]; WT: 2.1 [1.8–4.2] [$p < 0.001$]; and FcγRIIb$^{fl/fl}$/CD19Cre$^{+}$ 3.3 [2.4–5.6] [$p < 0.05$]), increased serum urea ($p < 0.01$), and increased albuminuria ($p < 0.05$) than WT or FcγRIIb$^{fl/fl}$/CD19Cre$^{+}$ mice (Fig. 2A–D).

These results demonstrate that lack of FcγRIIb on B cells alone was not sufficient to worsen NTN compared with WT mice, whereas mice with the full deletion of FcγRIIb under the same conditions (5 d after the induction of NTN) had markedly increased disease. This suggests the involvement of FcγRIIb on cell types other than B cells in the protection from NTN.

*Mice lacking FcγRIIb on myeloid cells were more susceptible to NTN than WT*

As myeloid cells such as monocytes, neutrophils, and macrophages infiltrate the kidney abundantly in glomerulonephritis and are known to express FcγRIIb, we then investigated the role of FcγRIIb on these cell types in NTN. For this purpose, FcγRIIb$^{fl/fl}$/CEBPαCre$^{+}$ mice were used and compared with FcγRIIb$^{fl/fl}$/CD19Cre$^{+}$ mice and WT littermate controls. On this occasion, full FcγRIIb$^{-/-}$ mice were not used, which allowed us to use a higher dose of NTS (1:10 dilution) and maintain the mice for a longer period after injection of NTS. One FcγRIIb$^{fl/fl}$/CEBPαCre$^{+}$ mouse was sacrificed at day 5 due to clinical signs of disease, and all other mice were sacrificed day 7 post–NTS injection. Although the FcγRIIb$^{fl/fl}$/CEBPαCre$^{+}$ mice showed clinical signs of disease,

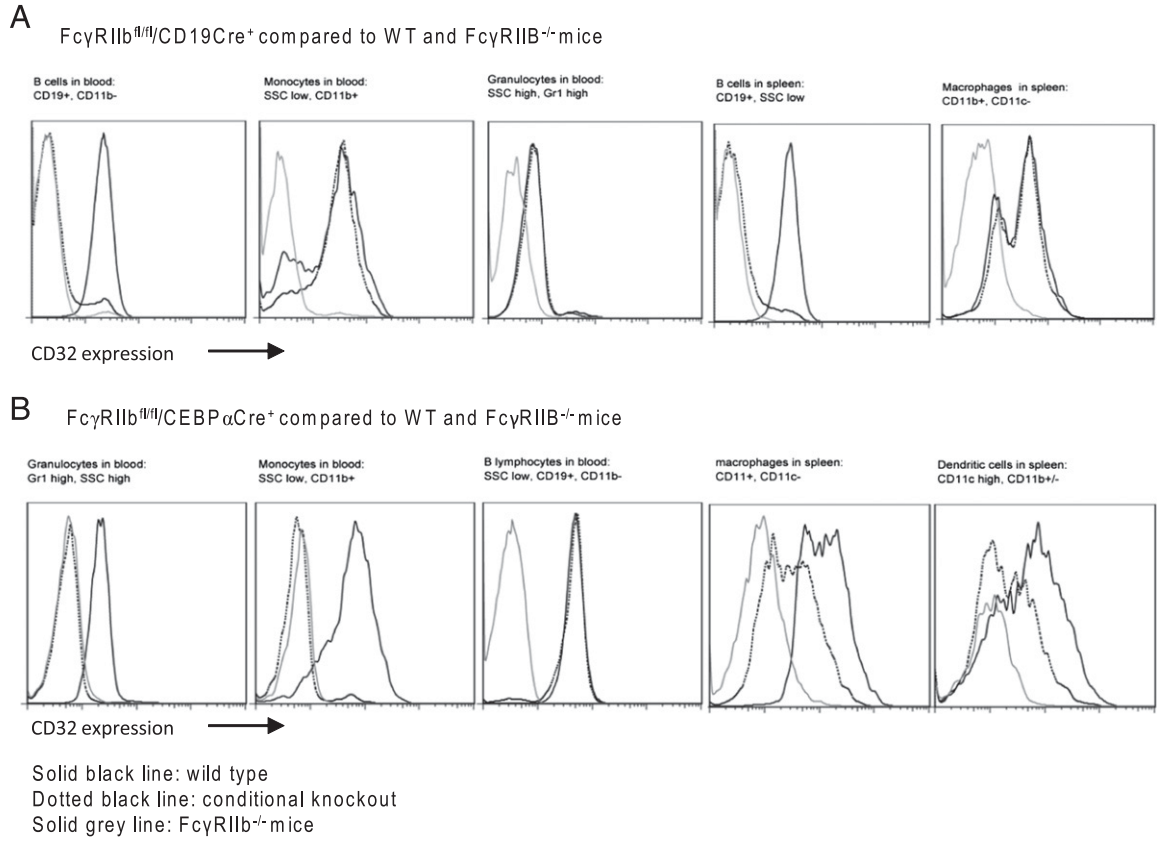


**FIGURE 1.** Flow cytometry to demonstrate specificity of conditional Cre deletion. (**A**) FcγRIIb$^{fl/fl}$/CD19Cre$^{+}$ showing deletion on circulating and splenic B cells but not granulocytes, monocytes, or macrophages. (**B**) FcγRIIb$^{fl/fl}$/CEBPαCre$^{+}$ showing full deletion in circulating monocytes and granulocytes and partial deletion in splenic macrophages and dendritic cells. SSC, Side scatter.

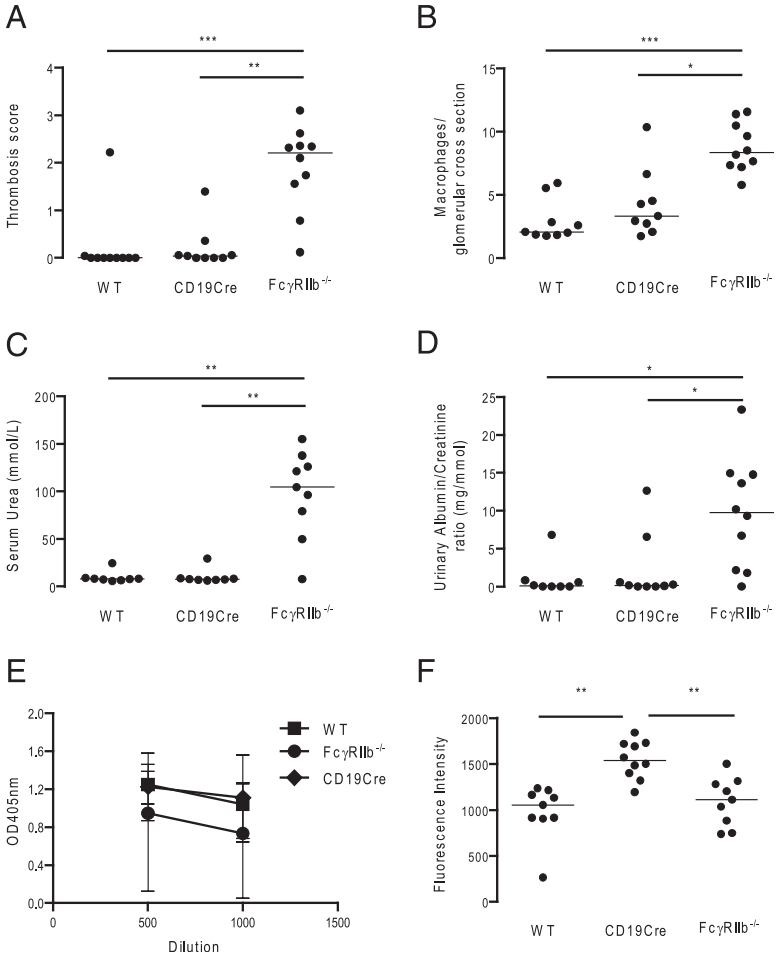


**FIGURE 2.** Functional and histological parameters at day 5 after induction of NTN. (**A**) Glomerular thrombosis score. (**B**) CD68-positive macrophages/gcs. (**C**) Serum urea (mmol/L). (**D**) Urinary albumin/creatinine ratio (mg/mmol). (**E**) ELISA for serum anti-sheep IgG. (**F**) Quantitative immunofluorescence for deposited glomerular mouse IgG. CD19Cre, FcγRIIb$^{fl/fl}$/CD19Cre$^{+}$ mouse ($n = 9$); FcγRIIb$^{-/-}$, FcγRIIb$^{-/-}$ mice generated on a pure C57BL/6 background ($n = 10$); WT, WT littermate control mouse (C57BL/6) ($n = 9$). If not marked, differences were not statistically significant. $*p < 0.05$, $**p < 0.01$, $***p < 0.001$.

the WT and FcγRIIb$^{fl/fl}$/CD19Cre$^{+}$ mice remained well. Analysis of the histology showed that FcγRIIb$^{fl/fl}$/CEBPαCre$^{+}$ mice had increased incidence of glomerular thrombosis compared with WT mice ($p < 0.05$) and FcγRIIb$^{fl/fl}$/CD19Cre$^{+}$ mice ($p < 0.01$) (Figs. 3A, 4A–C), increased levels of albuminuria ($p < 0.05$ when compared with WT mice and $p < 0.01$ when compared with FcγRIIb$^{fl/fl}$/CD19Cre$^{+}$ mice), and increased serum urea ($p < 0.05$ when compared with FcγRIIb$^{fl/fl}$/CD19Cre$^{+}$ mice) (Fig. 3B, 3C). Surprisingly, there was no significant difference in glomerular macrophage infiltration among WT, FcγRIIb$^{fl/fl}$/CD19Cre$^{+}$, and FcγRIIb$^{fl/fl}$/CEBPαCre$^{+}$ mice (medians 1.3, 1.9, and 2.0 CD68-positive cells/gcs, respectively), although this may have been masked by increased glomerular thrombosis in the FcγRIIb$^{fl/fl}$/CEBPαCre$^{+}$ mice (Figs. 3D, 4D–F). However, FcγRIIb$^{fl/fl}$/CEBPαCre$^{+}$ mice did have increased glomerular neutrophil infiltration compared with WT mice (median WT: 0.62 [interquartile range 0.36–0.88], FcγRIIb$^{fl/fl}$/CD19Cre$^{+}$: 0.59 [0.37–1.1], FcγRIIb$^{fl/fl}$/CEBPαCre$^{+}$: 1.5 [1.2–1.6], $p < 0.05$) (Figs. 3E, 4G–I).

Circulating mouse anti-sheep total IgG titers were measured in all mice. Despite the fact that FcγRIIb$^{fl/fl}$/CD19Cre$^{+}$ mice had less disease than FcγRIIb$^{fl/fl}$/CEBPαCre$^{+}$ mice, they had higher circulating anti-sheep Ab titers ($p < 0.05$, 2-way ANOVA). These results clearly demonstrate the importance of FcγRIIb on myeloid cells in vivo in immune complex glomerulonephritis and show that increased mouse anti-sheep IgG titers are not the main determining factor of the heightened susceptibility of FcγRIIb$^{-/-}$ mice to NTN.

### *Role of FcγRIIb in intrinsic renal cells*

Although FcγRIIb$^{fl/fl}$/CEBPαCre$^{+}$ mice had increased NTN compared with WT mice, their disease susceptibility was not as marked as mice with a full deletion of FcγRIIb, as they were able to tolerate a higher dose of NTS and be maintained longer than mice with the full deletion of FcγRIIb. In addition, it was possible to titrate the dose of NTS down such that FcγRIIb$^{fl/fl}$/CEBPαCre$^{+}$ mice developed little disease, whereas mice with a full deletion of FcγRIIb continued to have increased susceptibility to disease compared with WT controls (data not shown). This may be due to the fact that the deletion of FcγRIIb from myeloid cells in the conditional knockout was not absolutely complete (Fig. 1B). However, expression of FcγRIIb on intrinsic renal cells has previously been reported (11), and an FcγRIIb on intrinsic renal cells was suggested by experiments in which a blocking anti-FcγRIIb Ab was injected under the kidney capsule (17). We therefore sought to determine whether there was a contribution of disease susceptibility from intrinsic renal cells to explain the slightly increased susceptibility to disease in the full FcγRIIb$^{-/-}$ mice compared with FcγRIIb$^{fl/fl}$/CEBPαCre$^{+}$ mice.

### *Expression of FcγRIIb by mesangial cells*

Expression of FcγRIIb by cultured mesangial cells was assessed by real-time quantitative PCR. Transcripts were detected in WT mesangial cells, and stimulation with LPS increased the expression, although not significantly. No transcripts were detected in FcγRIIb-deficient mesangial cells (data not shown). We also assessed

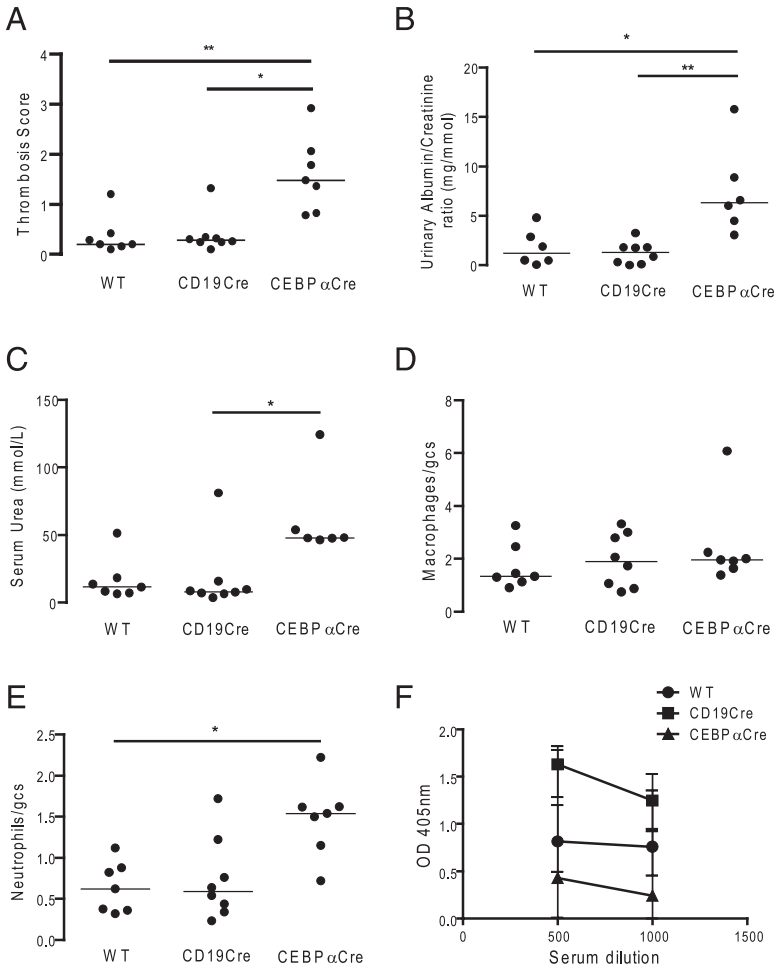


**FIGURE 3.** Functional and histological parameters at day 7 after induction of NTN. (**A**) Glomerular thrombosis score. (**B**) Urinary albumin/creatinine ratio (mg/mmol). (**C**) Serum urea (mmol/L). (**D**) CD68-positive macrophages/gcs. (**E**) Gr-1–positive neutrophils/gcs. (**F**) ELISA for serum anti-sheep IgG. $*p < 0.05$ for CD19Cre versus CEBPαCre. CD19Cre, FcγRIIb$^{fl/fl}$/CD19Cre$^{+}$ mouse ($n$ = 8); CEBPα-Cre, FcγRIIb$^{fl/fl}$/CEBPαCre$^{+}$ mouse ($n$ = 7); WT, WT littermate control mouse (C57BL/6) ($n$ = 7). $*p < 0.05$, $**p < 0.01$.

expression of FcγRIIb on cultured mesangial cells by immunofluorescence staining using an mAb. Cytospins of WT and FcγRIIb$^{-/-}$ mesangial cells were incubated with an FITC-labeled anti-FcγRIIb Ab (Ly 17.2 clone). WT mesangial cells were found to express FcγRIIb, whereas FcγRIIb$^{-/-}$ mesangial cells were negative (Fig. 5).

*Expression of FcγRIIb on radioresistant cells in the kidney induced relative protection from NTN compared with mice with a full deletion of FcγRIIb*

Unfortunately, a mouse with mesangial cell–specific Cre-recombinase expression is not available. We therefore used bone marrow chimeric mice to investigate the role of FcγRIIb on radioresistant intrinsic renal cells. By transplanting CD45.1 allogeneic bone marrow into CD45.2 mice and using flow cytometry of blood and dissociated kidney cells, our previous studies have shown that our method of bone marrow transplantation results in 95% replacement of resident renal CD68-positive macrophages and CD11c-positive dendritic cells, as well as excellent chimerism of circulating neutrophils, monocytes, and B cells (16).

First, WT mice transplanted with FcγRIIb$^{-/-}$ bone marrow were compared with FcγRIIb$^{-/-}$ mice transplanted with FcγRIIb$^{-/-}$ bone marrow using male mice. Mild disease was induced with a low dose of NTS (1:20 dilution), as otherwise the effect of the lack of myeloid FcγRIIb may have masked any protection from FcγRIIb on intrinsic renal cells. The mice were maintained to day 14 after induction of nephritis. FcγRIIb$^{-/-}$ mice transplanted with FcγRIIb$^{-/-}$ bone marrow developed more disease than WT mice transplanted with FcγRIIb$^{-/-}$ bone marrow. FcγRIIb$^{-/-}$ male mice with FcγRIIb$^{-/-}$ bone marrow had significantly more glomerular thrombosis ($p < 0.0001$), glomerular crescents ($p < 0.01$), albuminuria ($p < 0.001$), and glomerular macrophage infiltration ($p < 0.01$) than WT mice transplanted with FcγRIIb$^{-/-}$ bone marrow (Fig. 6A–D).

These results cannot be explained by differences in Ab titer between the groups, as the FcγRIIb$^{-/-}$ mice transplanted with FcγRIIb$^{-/-}$ bone marrow had lower circulating and deposited Ab titers compared with WT mice transplanted with FcγRIIb$^{-/-}$ bone marrow (deposited mouse IgG; $p < 0.05$) (Fig. 6E, 6F). These results suggest that, in addition to the role of myeloid FcγRIIb in protection from immune complex glomerulonephritis, FcγRIIb on intrinsic renal cells may also play a role in protection from disease.

Subsequently, the reciprocal experiment was performed to determine whether the lack of FcγRIIb on intrinsic renal cells alone was sufficient to increase susceptibility to NTN. Mild disease was again induced with a low dose of NTS, and the mice were maintained to day 14 after injection of NTS. The disease induced in both groups was mild, and there was no overall difference in glomerular crescents and thrombosis. The degree of albuminuria in both groups was minimal in most animals, but there was a statistically significant increase in the FcγRIIb$^{-/-}$ mice transplanted with WT bone marrow compared with WT mice transplanted with WT bone marrow ($p < 0.01$) (Fig 7C). There were also more glomerular infiltrating macrophages in the FcγRIIb$^{-/-}$ mice transplanted with WT bone marrow than the WT mice transplanted with WT bone marrow (Fig. 7D, $p <$

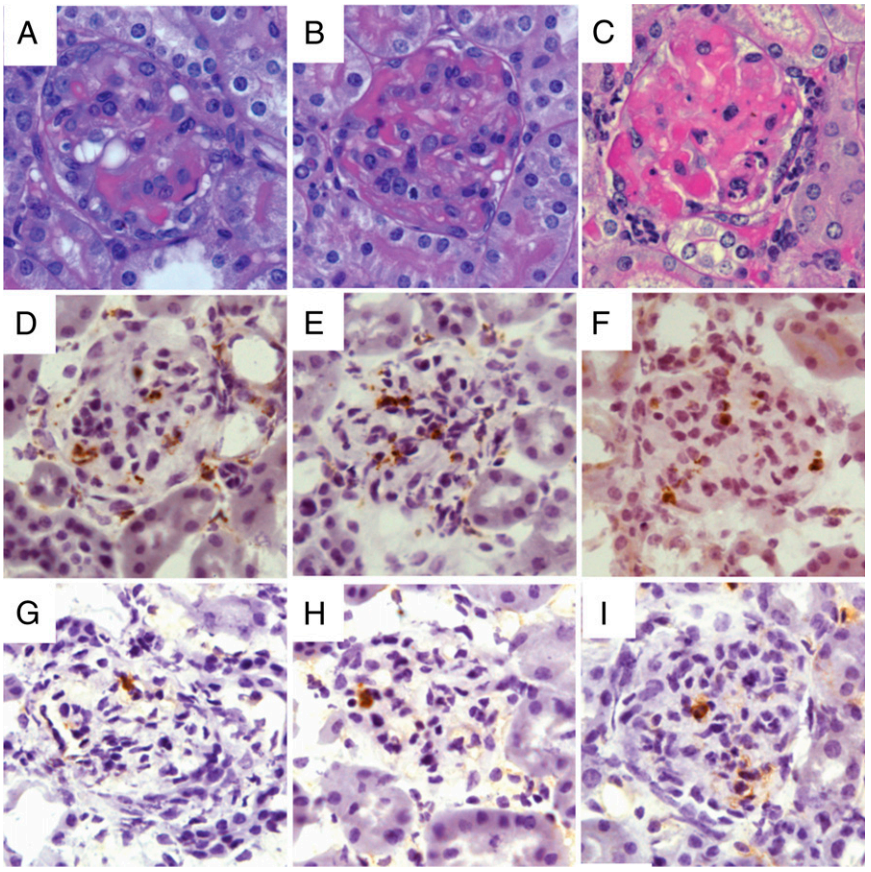


**FIGURE 4.** Histology at day 7 after the induction of NTN. (**A–C**) PAS-stained kidney sections. (A) WT littermate control C57BL/6 kidney showing mild thrombosis. (B) FcγRIIb$^{fl/fl}$/CD19Cre$^{+}$ mice showing mild thrombosis. (C) FcγRIIb$^{fl/fl}$/CEBPαCre$^{+}$ mice showing severe thrombosis. Immunoperoxidase staining for CD68 showing similar glomerular macrophage infiltration among WT kidney (**D**), FcγRIIb$^{fl/fl}$/CD19Cre$^{+}$ kidney (**E**), and FcγRIIb$^{fl/fl}$/CEBPα-Cre$^{+}$ kidney (**F**). Immunoperoxidase staining for Gr-1 showing similar glomerular neutrophil infiltration between WT kidney (**G**) and FcγRIIb$^{fl/fl}$/CD19Cre$^{+}$ kidney (**H**) and increased glomerular neutrophil infiltration in FcγRIIb$^{fl/fl}$/CEBPαCre$^{+}$ kidney (**I**). Original magnification ×20.

0.01). There was no significant difference in deposited glomerular mouse IgG or circulating anti-sheep IgG between the two groups (Fig. 7E, 7F).

## Discussion

Despite a good deletion of FcγRIIb from B cells, the FcγRIIb$^{fl/fl}$/CD19Cre$^{+}$ mice did not show increased susceptibility to NTN compared with WT mice. However, mice with FcγRIIb deleted from their myeloid cells had increased susceptibility to NTN compared with WT littermate controls. This is important direct evidence of a role of myeloid rather than B cell FcγRIIb in protection from glomerulonephritis. Additionally, we have confirmed expression of FcγRIIb on cultured mesangial cells, and our results would suggest that in addition to myeloid cell expression, local expression of FcγRIIb on intrinsic renal cells contributes to protection from injury in NTN.

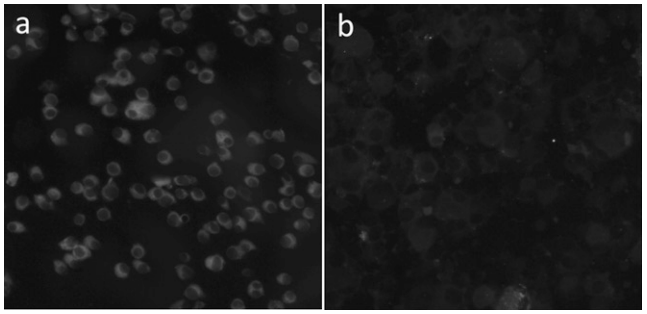


**FIGURE 5.** FcγRIIB expression on mesangial cells. Immunofluorescence staining showing expression of FcγRIIb on mesangial cells: WT mesangial cells (**a**) and FcγRIIb$^{-/-}$ mesangial cells (**b**). Original magnification ×10.

These results support our previous work looking at a model of experimental autoimmune glomerulonephritis in FcγRIIb-deficient mice on a pure C57BL/6 background, where we also found that loss of FcγRIIb on B cells alone was not sufficient to exacerbate experimental autoimmune glomerulonephritis (10). In contrast, transgenic overexpression of FcγRIIb on B cells was found to reduce the severity of collagen-induced arthritis in mice as well as lower the level of anti-collagen Abs (18). Our results suggest that in glomerulonephritis, B cell expression of FcγRIIb is not the sole determinant of protection from injury.

Deletion of FcγRIIb on B cells results in hyperreactive B cells that produce increased Ab titers in response to both thymus-dependent and -independent Ags (3). We did see a wide range of anti-sheep Ab titers in our experiments, and the results were also complicated by the presence of renal disease and proteinuria. Nevertheless, we did see increased levels of deposited murine IgG in mice lacking FcγRIIb on B cells, supporting the presence of increased levels of Ab throughout the disease course. Full FcγRIIb$^{-/-}$ mice had slightly lower levels of circulating anti-sheep total IgG than WT mice, for unknown reasons, possibly due to heavy proteinuria (Fig. 2E).

FcγRIIb$^{fl/fl}$/CEBPαCre$^{+}$ mice showed good deletion of FcγRIIb on myeloid cells, with complete deletion from circulating monocytes and neutrophils and partial deletion on tissue-resident macrophages and dendritic cells. FcγRIIb$^{fl/fl}$/CEBPαCre$^{+}$ mice had significantly more renal injury in terms of albuminuria, glomerular thrombosis, crescent formation, and serum urea than WT mice, highlighting the importance of myeloid FcγRIIb in protection from severe injury in glomerulonephritis. FcγRIIb$^{fl/fl}$/CEBPαCre$^{+}$

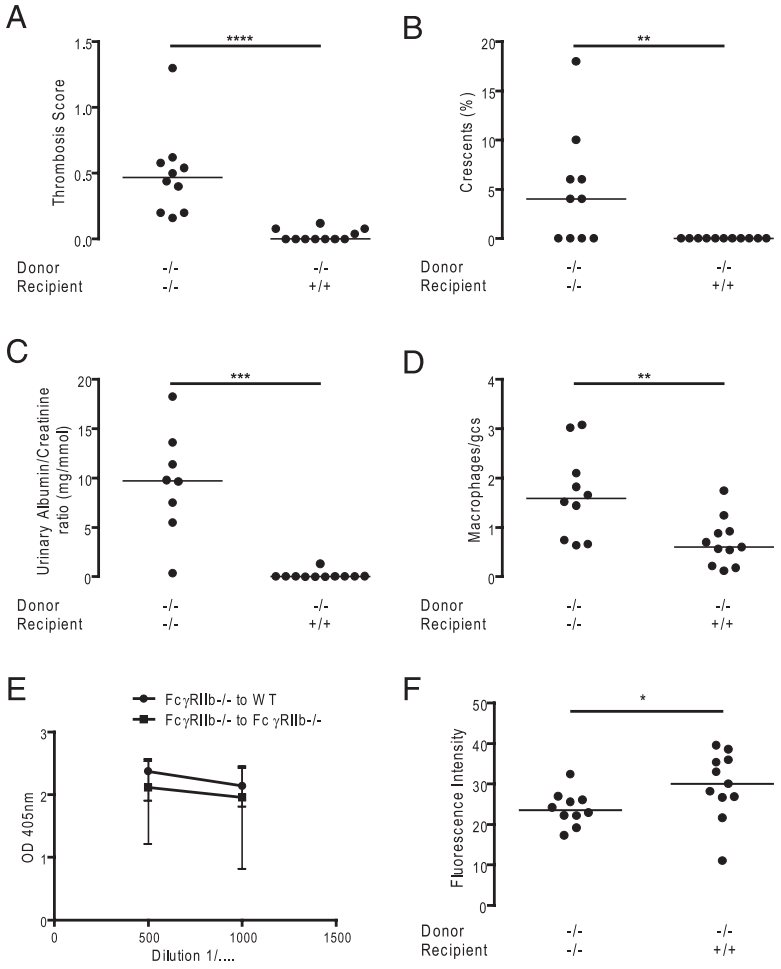


**FIGURE 6.** Functional and histological parameters in male bone marrow–transplanted mice at day 12 post-induction of nephrotoxic nephritis. (**A**) Glomerular thrombosis score. (**B**) Percentage of glomerular crescents. (**C**) Urinary albumin/creatinine ratio (mg/mmol). (**D**) Macrophages/gcs. (**E**) ELISA for serum anti-sheep IgG. (**F**) Quantitative immunofluorescence for deposited glomerular mouse IgG. $^{+/+}$, WT littermate control mice; $^{-/-}$, FcγRIIb$^{-/-}$ mice. $^{-/-}$ transplanted into $^{-/-}$ ($n = 10$), $^{-/-}$ transplanted into $^{+/+}$ ($n = 11$). $^{*}p < 0.05$, $^{**}p < 0.01$, $^{***}p < 0.001$, $^{****}p < 0.0001$.

mice had more infiltrating glomerular neutrophils than WT and FcγRIIb$^{fl/fl}$/CD19Cre$^{+}$ mice. FcγR are known to play a role in neutrophil recruitment. FcRγ$^{-/-}$ and FcγRIII$^{-/-}$ mice both display strongly abrogated recruitment of neutrophil effector cells during heterologous anti-glomerular basement membrane disease (17), suggesting FcγRIIb may play a role in the negative regulation of neutrophil recruitment.

Surprisingly, there was no significant difference in glomerular macrophage infiltration between the WT mice and myeloid cell knockouts. FcγRIIb clearly plays a role in the recruitment of macrophages to the glomerulus, as the FcγRIIb-deficient mice had significantly greater macrophage infiltration than WT mice. This suggests that expression of FcγRIIb on macrophages is not critical for their recruitment. This is supported by previous work looking at the role of activating FcγR in NTN. There was no significant difference in glomerular macrophage infiltration among WT mice, WT mice transplanted with FcRγ$^{-/-}$ bone marrow, and FcRγ$^{-/-}$ mice transplanted with FcRγ$^{-/-}$ bone marrow (15). Despite similar numbers of infiltrating macrophages among the three groups of mice, FcγRIIb$^{fl/fl}$/CEBPαCre$^{+}$ mice had increased disease. This could be explained by the fact that the macrophages are likely to show enhanced activation. Reduced surface expression of FcγRIIb on macrophages was associated with heightened responses following activatory FcγR cross-linking, including increased intracellular calcium flux, superoxide production, and proinflammatory cytokine release (5, 6, 19). On the contrary, administration of i.v. Ig (IVIG) in accelerated NTN was found to upregulate FcγRIIb on effector macrophages in the kidney and protected mice from fatal disease (20). Indeed, IVIG was not effective in protecting FcγRIIb$^{-/-}$ mice from NTN, indicating that this is an important mechanism of action for IVIG (20). Th2 cytokines, such as IL-4, are known to increase myeloid expression of FcγRIIb (21). Recently, it has been determined that the sialylated IgG component of human IVIG binds to a lectin receptor dendritic cell–specific intracellular adhesion molecule 3–grabbing nonintegrin on dendritic cells, leading to the secretion of IL-33, which upregulates IL-4 secretion by basophils and leads to the increased expression of FcγRIIb on myeloid cells (22). Taken together with our results, these findings offer insights into the mechanism of action of IVIG for the treatment of human autoimmune disease, specifically the critical importance of FcγRIIb expression on myeloid cells in the protection from Ab-mediated injury (23).

We have confirmed expression of FcγRIIb on mesangial cells in culture. However, due to the absence of a mesangial cell–specific Cre, bone marrow chimeras were used to investigate the role of FcγRIIb on radioresistant cells, and therefore, we are not able categorically to determine the radioresistant cell type involved. WT mice transplanted with FcγRIIb$^{-/-}$ bone marrow were not as susceptible to NTN as FcγRIIb$^{-/-}$ mice transplanted with FcγRIIb$^{-/-}$ bone marrow. PCR of blood-derived DNA demonstrated that at least 95% of circulating DNA was of donor origin, in addition to our previous work showing that there is a similar high degree of chimerism of resident macrophages and dendritic cells in the kidney (16). Bone marrow–derived cells of recipient origin are therefore unlikely to explain the significant differences

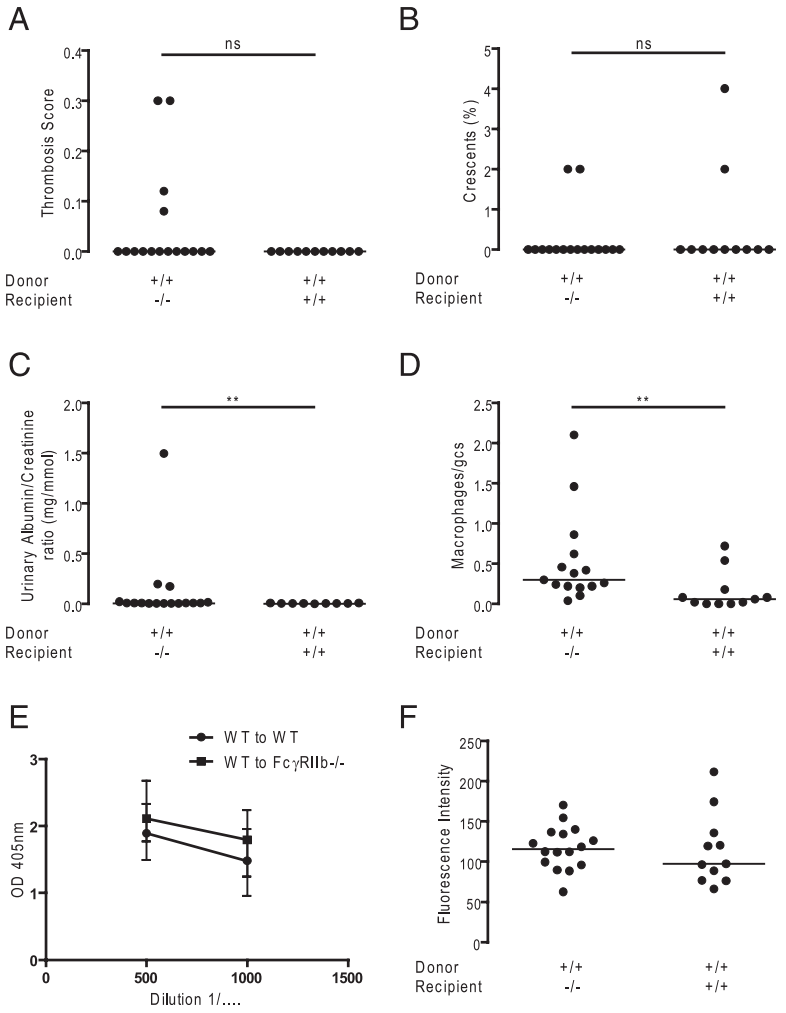


**FIGURE 7.** Functional and histological parameters in male bone marrow–transplanted mice at day 14 post-induction of NTN. (**A**) Glomerular thrombosis score. (**B**) Percentage glomerular crescents. (**C**) Urinary albumin/creatinine ratio (mg/mmol). (**D**) Macrophages/gcs. (**E**) ELISA for serum anti-sheep IgG. (**F**) Quantitative immunofluorescence for deposited glomerular mouse IgG. $^{+/+}$, WT littermate control mice; $^{-/-}$, FcγRIIb$^{-/-}$ mice. $^{+/+}$ transplanted into $^{-/-}$ ($n = 16$); $^{+/+}$ transplanted into $^{+/+}$ ($n = 11$). $^{**}p < 0.01$.

between these two groups, and it is likely that FcγRIIb on radioresistant intrinsic renal cells plays a part in protecting from immune complex glomerulonephritis. In the converse experiment, in which WT bone marrow was transplanted to FcγRIIb mice and compared with WT mice transplanted with WT marrow, the evidence for lack of FcγRIIb on intrinsic renal cells alone to exacerbate NTN significantly was weaker. We did see an increase in the glomerular macrophage infiltration in the FcγRIIb$^{-/-}$ mice transplanted with WT bone marrow compared with WT controls, but other renal parameters were not significantly different. Therefore, the presence of FcγRIIb on intrinsic renal cells was sufficient to afford some protection from NTN, but the lack of FcγRIIb on radioresistant cells alone was not sufficient to exacerbate disease significantly.

Although expression of FcγRIIb on radioresistant cells, possibly mesangial cells, did appear to afford some protection from NTN, we did not see protection from disease in mice lacking activatory FcγR from intrinsic renal cells in our previous work (15). These data suggest FcγRIIb may be interacting with an alternative receptor on mesangial cells. For instance, a negative regulatory interaction between FcγRIIb and the C5a receptor has been implicated in a recently published study (24).

Interestingly, in both of the transplant experiments, mice lacking FcγRIIb on their intrinsic renal cells had more glomerular macrophage influx than mice with WT intrinsic renal cells. Taken with the observations that mice completely lacking FcγRIIb also had increased glomerular macrophage infiltration compared with WT mice, but mice with FcγRIIb only deleted from myeloid cells did not, this suggests that FcγRIIb expression by intrinsic renal cells, such as mesangial cells, acts to downregulate recruitment of macrophages to the glomerulus. It also appears that macrophage recruitment can be uncoupled from macrophage activation, as there was only an increase in disease when FcγRIIb was not expressed on the macrophages themselves rather than the intrinsic renal cells.

In summary, deletion of FcγRIIb on B cells alone was not sufficient to exacerbate NTN, indicating that enhanced Ab production does not contribute to disease in this model. However, deletion of FcγRIIb on myeloid cells did increase susceptibility to renal injury in the mice, confirming the important regulatory function of this inhibiting FcγR on myeloid cells in Ab-mediated inflammatory diseases. Therapeutic means to enhance the expression of FcγRIIb on myeloid cells have the potential to be of importance in the treatment of human glomerulonephritis.

## Acknowledgments

We thank Marijke Valkhof for technical support in creating the CEBPαCre mice, John Meek (Clinical Chemistry Department, Hammersmith Hospital) for taking the serum urea, serum creatinine, and urine creatinine measurements, and Nicole Clark for providing technical help.

## Disclosures

The authors have no financial conflicts of interest.

## References


1. Phillips, N. E., and D. C. Parker. 1984. Cross-linking of B lymphocyte Fc gamma receptors and membrane immunoglobulin inhibits anti-immunoglobulin-induced blastogenesis. *J. Immunol.* 132: 627–632.
2. Xiang, Z., A. J. Cutler, R. J. Brownlie, K. Fairfax, K. E. Lawlor, E. Severinson, E. U. Walker, R. A. Manz, D. M. Tarlinton, and K. G. Smith. 2007. FcgammaRIIb controls bone marrow plasma cell persistence and apoptosis. *Nat. Immunol.* 8: 419–429.
3. Takai, T., M. Ono, M. Hikida, H. Ohmori, and J. V. Ravetch. 1996. Augmented humoral and anaphylactic responses in Fc gamma RII-deficient mice. *Nature* 379: 346–349.
4. Boross, P., V. L. Arandhara, J. Martin-Ramirez, M. L. Santiago-Raber, F. Carlucci, R. Flierman, J. van der Kaa, C. Breukel, J. W. Claassens, M. Camps, et al. 2011. The inhibiting Fc receptor for IgG, FcγRIIB, is a modifier of autoimmune susceptibility. *J. Immunol.* 187: 1304–1313.
5. Pritchard, N. R., A. J. Cutler, S. Uribe, S. J. Chadban, B. J. Morley, and K. G. Smith. 2000. Autoimmune-prone mice share a promoter haplotype associated with reduced expression and function of the Fc receptor FcgammaRII. *Curr. Biol.* 10: 227–230.
6. Clatworthy, M. R., and K. G. Smith. 2004. FcgammaRIIb balances efficient pathogen clearance and the cytokine-mediated consequences of sepsis. *J. Exp. Med.* 199: 717–723.
7. Kyogoku, C., H. M. Dijstelbloem, N. Tsuchiya, Y. Hatta, H. Kato, A. Yamaguchi, T. Fukazawa, M. D. Jansen, H. Hashimoto, J. G. van de Winkel, et al. 2002. Fcgamma receptor gene polymorphisms in Japanese patients with systemic lupus erythematosus: contribution of FCGR2B to genetic susceptibility. *Arthritis Rheum.* 46: 1242–1254.
8. Nakamura, A., T. Yuasa, A. Ujike, M. Ono, T. Nukiwa, J. V. Ravetch, and T. Takai. 2000. Fcgamma receptor IIB-deficient mice develop Goodpasture's syndrome upon immunization with type IV collagen: a novel murine model for autoimmune glomerular basement membrane disease. *J. Exp. Med.* 191: 899–906.
9. Suzuki, Y., I. Shirato, K. Okumura, J. V. Ravetch, T. Takai, Y. Tomino, and C. Ra. 1998. Distinct contribution of Fc receptors and angiotensin II-dependent pathways in anti-GBM glomerulonephritis. *Kidney Int.* 54: 1166–1174.
10. Sharp, P. E., J. Martin-Ramirez, P. Boross, S. M. Mangsbo, J. Reynolds, J. Moss, C. D. Pusey, H. T. Cook, R. M. Tarzi, and J. S. Verbeek. 2012. Increased incidence of anti-GBM disease in Fcgamma receptor 2b deficient mice, but not mice with conditional deletion of Fcgr2b on either B cells or myeloid cells alone. *Mol. Immunol.* 50: 49–56.
11. Radeke, H. H., I. Janssen-Graalfs, E. N. Sowa, N. Chouchakova, J. Skokowa, F. Löscher, R. E. Schmidt, P. Heeringa, and J. E. Gessner. 2002. Opposite regulation of type II and III receptors for immunoglobulin G in mouse glomerular mesangial cells and in the induction of anti-glomerular basement membrane (GBM) nephritis. *J. Biol. Chem.* 277: 27535–27544.
12. Ichii, O., A. Konno, N. Sasaki, D. Endoh, Y. Hashimoto, and Y. Kon. 2008. Altered balance of inhibitory and active Fc gamma receptors in murine autoimmune glomerulonephritis. *Kidney Int.* 74: 339–347.
13. Buch, T., F. L. Heppner, C. Tertilt, T. J. Heinen, M. Kremer, F. T. Wunderlich, S. Jung, and A. Waisman. 2005. A Cre-inducible diphtheria toxin receptor mediates cell lineage ablation after toxin administration. *Nat. Methods* 2: 419–426.
14. Wölfler, A., A. A. Danen-van Oorschot, J. R. Haanstra, M. Valkhof, C. Bodner, E. Vroegindeweij, P. van Strien, A. Novak, T. Cupedo, and I. P. Touw. 2010. Lineage-instructive function of C/EBPα in multipotent hematopoietic cells and early thymic progenitors. *Blood* 116: 4116–4125.
15. Tarzi, R. M., K. A. Davies, M. G. Robson, L. Fossati-Jimack, T. Saito, M. J. Walport, and H. T. Cook. 2002. Nephrotoxic nephritis is mediated by Fcgamma receptors on circulating leukocytes and not intrinsic renal cells. *Kidney Int.* 62: 2087–2096.
16. Tarzi, R. M., P. E. Sharp, J. P. McDaid, L. Fossati-Jimack, P. E. Herbert, C. D. Pusey, H. T. Cook, and A. N. Warrens. 2012. Mice with defective Fas ligand are protected from crescentic glomerulonephritis. *Kidney Int.* 81: 170–178.
17. Coxon, A., X. Cullere, S. Knight, S. Sethi, M. W. Wakelin, G. Stavrakis, F. W. Luscinskas, and T. N. Mayadas. 2001. Fc gamma RIII mediates neutrophil recruitment to immune complexes. a mechanism for neutrophil accumulation in immune-mediated inflammation. *Immunity* 14: 693–704.
18. Brownlie, R. J., K. E. Lawlor, H. A. Niederer, A. J. Cutler, Z. Xiang, M. R. Clatworthy, R. A. Floto, D. R. Greaves, P. A. Lyons, and K. G. Smith. 2008. Distinct cell-specific control of autoimmunity and infection by FcgammaRIIb. *J. Exp. Med.* 205: 883–895.
19. Jiang, Y., S. Hirose, M. Abe, R. Sanokawa-Akakura, M. Ohtsuji, X. Mi, N. Li, Y. Xiu, D. Zhang, J. Shirai, et al. 2000. Polymorphisms in IgG Fc receptor IIB regulatory regions associated with autoimmune susceptibility. *Immunogenetics* 51: 429–435.
20. Kaneko, Y., F. Nimmerjahn, M. P. Madaio, and J. V. Ravetch. 2006. Pathology and protection in nephrotoxic nephritis is determined by selective engagement of specific Fc receptors. *J. Exp. Med.* 203: 789–797.
21. Pricop, L., P. Redecha, J. L. Teillaud, J. Frey, W. H. Fridman, C. Sautès-Fridman, and J. E. Salmon. 2001. Differential modulation of stimulatory and inhibitory Fc gamma receptors on human monocytes by Th1 and Th2 cytokines. *J. Immunol.* 166: 531–537.
22. Anthony, R. M., T. Kobayashi, F. Wermeling, and J. V. Ravetch. 2011. Intravenous gammaglobulin suppresses inflammation through a novel T(H)2 pathway. *Nature* 475: 110–113.
23. Anthony, R. M., F. Nimmerjahn, D. J. Ashline, V. N. Reinhold, J. C. Paulson, and J. V. Ravetch. 2008. Recapitulation of IVIG anti-inflammatory activity with a recombinant IgG Fc. *Science* 320: 373–376.
24. Karsten, C. M., M. K. Pandey, J. Figge, R. Kilchenstein, P. R. Taylor, M. Rosas, J. U. McDonald, S. J. Orr, M. Berger, D. Petzold, et al. 2012. Anti-inflammatory activity of IgG1 mediated by Fc galactosylation and association of FcγRIIB and dectin-1. *Nat. Med.* 18: 1401–1409.